

Bloodstain Pattern Analysis: Developing quantitative methods  
of crime scene reconstruction through the interpretation and  
analysis of environmentally altered bloodstains

**Candidate:** Miss Hester F. Miles

**Institution:** University College London (UCL)

**Degree:** Ph.D Forensic Science

## **Declaration**

I, Hester Frances Miles confirm that the work presented in this thesis is my own. Where information has been derived from other sources, I confirm that this has been indicated in the thesis.

**Signed.....**

**Miss Hester F. Miles**

**June 2014**

## Acknowledgements

This research was funded by the Engineering and Physical Sciences Research Council of the U.K. through the Security Science Doctoral Research Training Centre (UCL SECRiT) based at University College London (EP/G037264/1).

I would like to acknowledge and express my gratitude for the guidance and support I have received during the completion of my research. In particular I would like to acknowledge my supervisors, Dr Ruth Morgan (UCL) and Dr David Lagnado (UCL) and thank them for their supervision and academic guidance. I would also like to acknowledge the input of Jo Millington (Manlove Forensics Ltd) who has provided me with an invaluable insight into the practical aspects of Bloodstain Pattern Analysis (BPA). I gratefully acknowledge the assistance of Professor Robert Speller (UCL) for the provision of laboratory space and the assistance of Mr Steven Hudziak (UCL) during AFM analysis of materials.

I am extremely grateful to my friends and family for all their encouragement, support and love during the completion of this thesis and beyond. In particular, to Eddy, Al & JMM: Thank You and to Madre: I cannot possibly put into words how grateful I am for the immense support and love you have given me. Thank you. Finally, thank you to my wonderful G.Pa, who I'm sure can be the only possible source of any scientific bones in my body!

Hester Miles, June 2014

## **Abstract**

The thesis presents experimental work conducted on environmentally altered bloodstains over four distinct experimental stages. Bloodstains that have been exposed to and altered by the environment are frequently encountered in crime scene analysis and developing accurate methods of quantitatively identifying, interpreting and analyzing them is important for crime scene reconstruction. Over the course of the four experimental stages bloodstains were progressively exposed to a range of environmental conditions and their responses to this exposure recorded.

During the first stage stains were dried at a range of temperatures between -10 and 50°C in order to establish the influence of temperature on stain appearance. In the second stage stains were longitudinally exposed to natural environmental fluctuations over the course of a 6-month experimental period. In the third stage stains were exposed to a variety of extreme environmental conditions, including fire, freezing, freeze-thaw and extreme heat, in order to establish the influence of these conditions on stain appearance and behavior. In the final experimental stage the influence of environmental conditions on stain drying time was examined.

During the course of stain analysis a new quantitative method for digitally capturing and measuring bloodstain colour was designed.

The findings of the experimental work conducted represent the first empirical confirmation of relationships between the environmental conditions explored and bloodstain appearance and behavior. Quantitative confirmation of these relationships has direct implications for developing methods of spatial and temporal crime scene reconstruction from bloodstain pattern analysis.



# Contents

Title page	1
Declaration	2
Abstract	4
Contents page	5
List of figures	15

## **Section 1**

### **Chapter 1 Introduction**

1.1. Forensic Science	38
1.2 Development of trace evidence analysis	40
1.2.1 Locard's exchange principle	
1.2.2 Source level evidence	
1.2.3 Evidence dynamics	
1.2.4 Activity level evidence	
1.2.5 Source and activity level analyses	
1.3 Extrapolation of techniques to crime scene reconstruction	48
1.4 Crime scene reconstruction in the case of Bloodstain Pattern Analysis (BPA)	50
1.4.1 Source level analysis of Bloodstain Pattern evidence	
1.4.2 Activity level analysis of Bloodstain Pattern evidence	
1.5 Limitations in forensic science and BPA	55
1.6 The future of forensic science and BPA	57
1.7 Outline of content	58

### **Chapter 2 Literature review**

2.1 Blood and Bloodstain Pattern Analysis	62
2.1.1 Blood	
2.2.2 Blood in a forensic context	
2.2.3 Bloodstain Pattern Analysis	
2.2 Development of basic Bloodstain Pattern Analysis	66

2.2.1 Determining horizontal origin, impact angle and vertical origin of a stain	
2.2.2 Pattern Identification	
2.3 Development of methods for advanced Bloodstain Pattern Analysis	79
2.3.1 Formation of spines and satellites	
2.3.2 Angled impacts	
2.3.3 Secondary change mechanisms and Physically Altered Bloodstains (PABs)	
2.4 Crime Scene Reconstruction	85
2.4.1 Analysis of blood as a spatial indicator	
2.4.2 Analysis of blood as a temporal indicator	
2.5 The importance of experimental studies to Bloodstain Pattern Analysis	90
2.6 Outlining the research project	93
2.6.1 Identification of bloodstains	
2.6.2 Secondary change mechanisms & PABs	
2.6.2.1 Environmentally forced secondary change mechanisms	
2.6.2.2 Anthropogenically forced secondary change mechanisms	
2.6.3 Influence of surface characteristics on stain morphology and behaviour	
<b>Chapter 3 Materials &amp; Methods</b>	<b>114</b>
3.1 Outlining specific areas for research	114
3.1.1 Environmental influences on visual and chemical identification of bloodstains	
3.1.2 Environmental influences on bloodstain drying time	
3.1.3 Influence of surface characteristics on bloodstains	
3.2 Experimental overview and formation of hypotheses	119
3.2.1 Experimental overview	
3.2.2 Formation of hypotheses	
3.2.2.1 Hypothesis group A	

3.2.2.2 Hypothesis group B	
3.2.2.3 Hypothesis group C	
3.3 Developing a methodology	125
3.4 Sourcing generic experimental materials	126
3.4.1 Sourcing blood	
3.4.1.1 Blood sampling considerations	
3.4.2 Ethical considerations surrounding use of animal blood	
3.4.3 Chemical tests	
3.4.4 The Kastle-Meyer (KM) presumptive test for blood	
3.4.5 The Hemastix presumptive test for blood	
3.4.6 The Bluestar presumptive test for blood	
3.4.7 Quantitative methods of visual identification of stains	
<b><u>Section 2</u></b>	143
<b>Chapter 4 Experimental stage 1 – Methodology</b>	144
4.1 Overview	144
4.2 Materials	144
4.3 Methodology	145
4.3.1 Temperature	
4.3.2 Stain sets	
4.3.3 Pre-experimental fridge set-up	
4.3.4 Stain generation	
<b>Chapter 5 Experimental stage 1 – Results &amp; Analysis</b>	153
5.1 Stain generation checklist & results of chemical identification tests	153
5.2 Images of stains generated	153
5.3 Stain colour analysis	173
5.3.1 Stains generated on paper	
5.3.2 Stains generated on glass	
5.3.3 Stains generated on denim	
5.4 Stain colour analysis – surface comparison	207

5.4.1 Colour ribbon comparison	
5.4.2 Comparison of RGB totals between surfaces	
5.4.3 Comparison of ratios of R, G and B values between surfaces	
5.4.4 Exploring relationships between RGB totals for all surfaces, temperature and humidity	
5.4.5 Statistical test of distribution	
<b>Chapter 6 Experimental stage 2 – Methodology</b>	<b>218</b>
6.1 Overview	218
6.2 Materials	219
6.3 Methodology	219
6.3.1 Climatic conditions at experimental site	
6.3.2 Stain sets	
6.3.2.1 Longitudinal samples	
6.3.2.2 Monthly samples	
6.3.3 Experimental set-up	
6.3.3.1 Shelving unit	
6.3.3.2 Unit set-up within experimental site	
6.3.4 Sampling phases	
6.3.4.1 Longitudinal sampling method	
6.3.4.2 Monthly sampling method	
6.3.5 Sample sets and replicate stains	
6.3.6 Stain generation	
6.3.7 Analysis of stains	
<b>Chapter 7 Experimental stage 2 – Results &amp; Analysis</b>	<b>235</b>
7.1 Stain generation checklist & results of chemical identification tests	235
7.2 Longitudinal sample sets	236
7.2.1 Images of longitudinal sample sets	
7.2.2 Longitudinal stain colour analysis	

7.2.2.1 Stains generated in longitudinal denim sample sets	
7.2.2.2 Stains generated in longitudinal paper sample sets	
7.2.2.3 Stains generated in longitudinal glass sample sets	
7.2.3 Longitudinal stain colour analysis – surface comparison	
7.2.3.1 Colour ribbon comparison	
7.2.3.2 Comparison of RGB totals between surfaces	
7.2.3.3 Comparison of ratios of R, G and B values between surfaces	
7.3 Monthly sample sets	283
7.3.1 Images of monthly sample sets	
7.3.2 Monthly stain colour analysis	
7.3.2.1 Stains generated in monthly denim sample sets	
7.3.2.2 Stains generated in monthly paper sample sets	
7.3.2.3 Stains generated in monthly glass sample sets	
7.3.3 Monthly stain colour analysis – surface comparison	
7.3.3.1 Colour ribbon comparison	
7.3.3.2 Comparison of RGB totals between surfaces	
7.3.3.3 Comparison of ratios of R, G and B values between surfaces	
<b>Chapter 8 Experimental stage 3 – Methodology</b>	<b>330</b>
8.1 Overview	330
8.2 Materials	332
8.3 Methodologies	332
8.4 Exposure of stains to snow	333
8.4.1 Establishing experimental conditions	
8.4.2 Method 1 stain generation	
8.4.3 Method 2 stain generation	
8.4.4 Method 3 stain generation	
8.4.5 Methodological limitations	
8.5 Exposure of stains to freeze-thaw	339
8.5.1 Establishing experimental conditions	
8.5.2 Stain generation	

8.5.3 Methodological limitations	
8.6 Exposure of stains to freezing conditions	341
8.6.1 Establishing experimental conditions	
8.6.2 Method 1 stain generation	
8.6.3 Method 2 stain generation	
8.6.4 Method 3 stain generation	
8.6.5 Methodological limitations	
8.7 Exposure to high temperatures	347
8.7.1 Establishing experimental conditions	
8.7.2 Method 1 stain generation	
8.7.3 Method 2 stain generation	
8.7.4 Methodological limitations	
8.8 Exposure to fire (burning)	351
8.8.1 Establishing experimental conditions	
8.8.2 Stain generation	
8.8.3 Methodological limitations	
<b>Chapter 9 Experimental stage 3 – Results &amp; Analysis</b>	355
9.1 Responses of samples to chemical identification tests	355
9.2 Environmental condition A (stains exposed to snow)	358
9.2.1 Images of stains generated	
9.2.1.1 Method 1	
9.2.1.2 Method 2	
9.2.1.3 Method 3	
9.3 Environmental condition B (stains exposed to freeze-thaw)	369
9.3.1 Images of stains generated	
9.4 Environmental condition C (stains exposed to freezing)	371
9.4.1 Images of stains generated	
9.4.2 Stain colour analysis	
9.4.3 Staining method 1	
9.4.4 Staining method 2	
9.4.5 Statistical tests of comparison	
9.4.5.1 Comparison of means between staining methods 1	

& 2	
9.4.5.2 Comparison of means between surfaces	
9.4.6 Staining method 3	
9.5 Environmental condition D (stains exposed to high temperatures)	383
9.5.1 Images of stains generated	
9.5.2 Stain colour analysis	
9.5.3 Staining method 1	
9.5.4 Staining method 2	
9.5.5 Comparison of stains between surfaces and staining methods	
9.5.5.1 Comparison of means between staining methods 1 & 2	
9.5.5.2 Comparison of means between surfaces	
9.6 Environmental condition E (stains exposed to fire)	403
9.6.1 Images of stains generated	
9.6.2 Stain colour analysis	
<b>Chapter 10 Synthesis of results of experimental stages 1, 2 &amp; 3</b>	408
10.1 Calculation of mean R, G, B values and RGB total values	408
10.2 Comparison of mean R, G, B and RGB total values	409
<b>Chapter 11 Experimental stage 4 – Methodology</b>	414
11.1 Overview	414
11.2 Materials	414
11.3 Methodology	415
11.3.1 Pre-experimental fridge set-up	
11.3.2 Controlling stained surface characteristics	
11.3.3 Controlling temperature	
11.3.4 Controlling humidity	
11.3.5 Controlling blood drop volume	
11.3.6 Controlling stain size	

11.3.7 Stain sets	
11.3.8 Stain generation	
11.3.9 Stain generation order	
11.3.10 Drying time measurement	
11.4 Methodological limitations	427
<b>Chapter 12 Experimental stage 4 – Results &amp; Analysis</b>	429
12.1 Results tables	429
12.1.1 Mean drying time results for 10µl stains (1 <sup>st</sup> experimental run)	
12.1.2 Mean drying time results for 10µl stains (2 <sup>nd</sup> experimental run)	
12.1.3 Mean drying time results for 10µl stains (3 <sup>rd</sup> experimental run)	
12.1.4 Mean drying time results for 10µl stains (4 <sup>th</sup> experimental run)	
12.1.5 Mean drying time results for 10µl stains (5 <sup>th</sup> experimental run)	
12.1.6 Mean drying time results for 45µl stains (1 <sup>st</sup> experimental run)	
12.1.7 Mean drying time results for 45µl stains (2 <sup>nd</sup> experimental run)	
12.2 Descriptive statistics	437
12.2.1 10µl stains on Denim	
12.2.2 10µl stains on Glass	
12.2.3 10µl stains on Paper	
12.2.4 45µl stains on Denim	
12.2.5 45µl stains on Glass	
12.2.6 45µl stains on Paper	
12.3 Exploration of relationships between variables	447
12.3.1 Temperature and drying time	
12.3.2 Humidity and drying time	



- 12.3.3 Age of blood and drying time
- 12.3.4 Volume of blood and drying time
- 12.3.5 Surface type and drying time
  - 12.3.5.1 AFM images of surfaces for comparison of surface roughness
- 12.3.6 Temperature and humidity

### **Section 3** 462

## **Chapter 13 Discussion** 463

### 13.1 Answering experimental hypotheses 463

- 13.1.1 Group A
  - 13.1.1.1 Source level interpretations of Bloodstain Pattern evidence
  - 13.1.1.2 Temperature and source level interpretations of Bloodstain Pattern evidence
  - 13.1.1.3 Temperature and activity level interpretations of Bloodstain Pattern evidence
- 13.1.2 Group B
  - 13.1.2.1 Exposure to environmental conditions and source level interpretations of Bloodstain Pattern evidence
  - 13.1.2.2 Exposure to environmental conditions and activity level interpretations of Bloodstain Pattern evidence
- 13.1.3 Group C
  - 13.1.3.1 Influence on activity level interpretations of drying time
  - 13.1.3.2 Temperature and activity level interpretations of drying time
  - 13.1.3.3 Humidity and activity level interpretations of drying time
  - 13.1.3.4 Surface characteristics and activity level interpretations of drying time

13.1.3.5 Stain volume and activity level interpretations of drying time	
13.2 Implications of results for Bloodstain Pattern Analysis (BPA)	478
13.2.1 Implications of results for analysis of stain appearance	
13.2.2 Implications of results for analysis of stain behaviour	
13.3 Limitations of results	
13.4 The “path forward” for BPA research	
<b>Chapter 14 Conclusions</b>	<b>487</b>
14.1 Summary of research	487
14.2 Empirical observations	488
I. Environmental influences on stain appearance	488
I.i Temperature and stain appearance	
I.ii Longitudinal exposure to climatic variations and stain appearance	
I.iii Extreme environmental conditions and stain appearance	
II. Environmental influences on stain behaviour	490
III. Extrapolation of observations to the identification, interpretation and analysis of PABs	490
III.i Identification of Physically Altered Bloodstains (PABs)	
III.ii Interpretation and analysis of Physically Altered Bloodstains (PABs)	
14.3 Conclusion	493
References	495
Appendices	516

## List of figures

Figure number	Description	Page
1	Illustration of the ‘forensic process’	38
2	Trace material decay-curve demonstrating persistence of particles over time	41
3	Example of “painted fibres” (A) on fabric, formed away from main body of stain	46
4	Identification of 4 distinct evidentiary input streams to the process of crime scene reconstruction	49
5	Sketch diagram of three-dimensional reconstruction of bloodstain origins from two-dimensional stains	54
6	Schematic diagram of the human circulatory system	62
7	Spherical drop of blood in cross-section indicating forces of surface tension (black arrows) and internal cohesion (yellow arrows)	63
8	Sketch diagram of the different stages of collapse mechanics of a blood drop impacting a surface at an angle	67
9	Narrowing of stains to form directional characteristics: tail (left), scallops (middle) and satellite stains (right)	68
10	Images of stains generated at a range of impact angles demonstrating elongation of stain body and emergence of clear directional characteristics	68
11	Illustration of major and minor axis of two stains with different directional characteristics	68
12	Image illustrating elongation of a stain into a tail and indication of direction of travel through alignment with the major axis (length)	69
13	Collective stain pattern comprised of multiple stains, with yellow arrows indicative of general directionality of pattern	69
14	Photograph identifying an area of string convergence, (circled in yellow), for multiple stains within a collective stain pattern	70
15	Calculation of impact angle from stain length and width measurements with trigonometric Sine function	71

16	Photograph of area of convergence with addition of vertical (green) strings running back from leading edges of stains, at impact angles, to the area of convergence, to give vertical origins of stains	72
17	Example of physical stringing technique for multiple stain patterns generated on vertical surfaces	73
18	Illustration of relationship between point or area of convergence (C/POC), distance to the leading edge of a stain (D) and vertical area of origin (AO)	74
19	Right-angled triangle drawn between leading edge of stain, point/area of convergence (C/POC) and vertical area of origin (AO) with distance between stain and point/area of convergence (D), impact angle (i) and height of vertical area of origin (H) also labelled	74
20	Taxonomic classification system for spatter stains	76
21	Taxonomic classification system for non-spatter stains	77
22	Description of generation mechanisms or source events generally associated with different classifications of bloodstain patterns	78
23	High-speed photography of a blood droplet impacting with smooth cardboard displaying transfer of momentum from the vertical to the horizontal direction	80
24	Illustration of spines formed in a bloodstain on paper	81
25	Sketch illustrations comparing a non-disrupting impact on a smooth surface (a) and a disrupting impact on a rough surface (b) and dissipation of satellite drops	82
26	Examples (circled) of satellite stains generated as part of a bloodstain on fabric	82
27	Table outlining currently available and commonly used bloodstain identification methods	96
28	Experimental overview, outlining general focus of experimental enquiry ('Exposure of bloodstains to a range of environmental conditions and variables'), desired experimental outcome (increased accuracy of analysis of environmentally altered bloodstains), three distinct groups of hypothesis (A, B & C) and the outcomes associated with each	119
29	Division of experimental methodology into four distinct experimental stages	126
30	Description of experimental stages, outlining the environmental	126

	conditions stains were exposed to in each, stained surfaces, independent and dependent variables	
31	Photograph of 100ml ovine (sheep) blood mixed in solution with Alsevers solution	128
32	Kastle-Meyer test kit containing 25ml KM reagent and 25ml Hydrogen Peroxide	132
32.a	Photographs from L to R illustrating bloodstain pre-testing (L), filter paper which has been rubbed over a stain and had KM solution added to it (M) and the filter paper following addition of Hydrogen Peroxide solution indicating a presumptive positive reaction for blood	132
33	Hemastix test strips	133
33.a	Photographs from L to R illustrating bloodstain pre-testing (L), indication of a presumptive positive reaction for blood through dark-green colouration of the test strip (M) and of association of different colours to varying concentrations of blood (R)	134
34	Bluestar forensic test kit	134
35	Illustration of the reaction of luminol in the presence of blood	135
36	Illustration of process of digitally scanning stains	136
37	Screenshot of GIMP version 2.8 user interface	137
38	Expression of RGB triplet (R215, G075, B050)	138
39	Conversion process of RGB value (R005, G158, B243) to Hex value #059EF3	139
40	Scanned image of blood stains generated on paper at -10°C opened in GIMP software and displayed via the user-interface	140
41	Bloodstains enlarged to 100% magnification	140
42	Eyedropper tool options	141
43	‘Information window’ for sample analysed indicating average R, G and B values, number of pixels represented by each colour and hexadecimal value	141
44	Completed GIMP software colour analysis of bloodstains generated on paper at -10°C	142
45	Table of materials used in experimental stage 1	144
46	Image of portable laboratory refrigerator	145

47	Image of portable laboratory refrigerator	145
48	Matrix of 9 stain sets	146
49	Sketches of 6 replicate stains on a) paper slips b) glass slides & c) denim fabric	147
50	Illustrated breakdown of generation of 702 stains during experimental stage 1	147
51	Photograph of fridge set up on end with horizontal polystyrene shelves prior to experimentation	148
52	Order in which all stains in experimental stage 1 were generated	149
53	Digital data logger displaying temperature	150
54	Digital data logger displaying relative humidity	150
55	Surfaces to be stained prepared for experimentation	150
56	Fixed volume pipette set to deliver drops of 10µl volume	151
57	Six separate replicate stains generated on paper	151
58	Stains generated on surfaces prior to drying (paper, glass, denim)	151
59	Checklist of number of stains (including replicates) generated across 13 temperature intervals & 3 different surfaces and the results of different chemical tests for these stains	153
60	Stains generated on paper at -10°C	154
61	Stains generated on glass at -10°C	154
62	Stains generated on denim fabric at -10°C	155
63	Stains generated on paper at -5°C	155
64	Stains generated on glass at -5°C	156
65	Stains generated on denim fabric at -5°C	156
66	Stains generated on paper at 0°C	157
67	Stains generated on glass at 0°C	157
68	Stains generated on denim at 0°C	158
69	Stains generated on paper at 5°C	158
70	Stains generated on glass at 5°C	159
71	Stains generated on denim fabric at 5°C	159
72	Stains generated on paper fabric at 10°C	160

73	Stains generated on glass at 10°C	160
74	Stains generated on denim fabric at 10°C	161
75	Stains generated on paper at 15°C	161
76	Stains generated on glass at 15°C	162
77	Stains generated on denim fabric at 15°C	162
78	Stains generated on paper at 20°C	163
79	Stains generated on glass at 20°C	163
80	Stains generated on denim fabric at 20°C	164
81	Stains generated on paper at 25°C	164
82	Stains generated on glass at 25°C	165
83	Stains generated on denim fabric at 25°C	165
84	Stains generated on paper at 30°C	166
85	Stains generated on glass at 30°C	166
86	Stains generated on denim fabric at 30°C	167
87	Stains generated on paper at 35°C	167
88	Stains generated on glass at 35°C	168
89	Stains generated on denim fabric at 35°C	168
90	Stains generated on paper at 40°C	169
91	Stains generated on glass at 40°C	169
92	Stains generated on denim fabric at 40°C	170
93	Stains generated on paper at 45°C	170
94	Stains generated on glass at 45°C	171
95	Stains generated on denim fabric at 45°C	171
96	Stains generated on paper at 50°C	172
97	Stains generated on glass at 50°C	172
98	Stains generated on denim fabric at 50°C	173
99	Table of measurements recorded for stains generated on paper surfaces from -10°C to 20°C	175
100	Table of measurements recorded for stains generated on paper surfaces from 20°C to 50°C	176

101	Table of measurements recorded for stains generated on paper surfaces from -10°C to 50°C	177
102	Descriptive statistics recorded for stains generated on paper surfaces from -25°C to 50°C	178
103	Average R, G and B values for all stains generated on paper	179
104	Table of descriptive statistics recorded for stains generated according to relative humidity values	180
105	Box plot distributions of R values for stains generated on paper at temperature intervals between -10°C and 50°C	181
106	Box plot distributions of G values for stains generated on paper at temperature intervals between -10°C and 50°C	182
107	Box plot distributions of B values for stains generated on paper at temperature intervals between -10°C and 50°C	183
108	Box plot distributions of R, G and B values for stains generated on paper at temperature intervals between -10°C and 50°C	184
109	R, G and B values for stains generated on paper at humidity intervals recorded during experimental stage 1	185
110	Table of measurements recorded for stains generated on glass surfaces from -10°C to 20°C	186
111	Table of measurements recorded for stains generated on glass surfaces from 25°C to 50°C	187
112	Table of measurements recorded for stains generated on glass surfaces from -10°C to 50°C	188
113	Descriptive statistics recorded for stains generated on glass surfaces from -25°C to 50°C	190
114	Average R, G and B values for all stains generated on glass	190
115	Table of descriptive statistics recorded for stains generated according to relative humidity values	191
116	Box plot distributions of R values for stains generated on glass at temperature intervals between -10°C and 50°C	192
117	Box plot distributions of G values for stains generated on glass at temperature intervals between -10°C and 50°C	193
118	Box plot distributions of B values for stains generated on glass at temperature intervals between -10°C and 50°C	194



119	Box plot distributions of R, G and B values for stains generated on glass at temperature intervals between -10°C and 50°C	195
120	R, G and B values for stains generated on glass at humidity intervals recorded during experimental stage 1	196
121	Table of measurements recorded for stains generated on denim surfaces from -10°C to 20°C	197
122	Table of measurements recorded for stains generated on denim surfaces from 25°C to 50°C	198
123	Table of measurements recorded for stains generated on denim surfaces from -10°C to 50°C	199
124	Descriptive statistics recorded for stains generated on denim surfaces from -25°C to 50°C	200
125	Average R, G and B values for all stains generated on denim	201
126	Table of descriptive statistics recorded for stains generated according to relative humidity values	202
127	Box plot distributions of R values for stains generated on denim at temperature intervals between -10°C and 50°C	203
128	Box plot distributions of G values for stains generated on denim at temperature intervals between -10°C and 50°C	204
129	Box plot distributions of B values for stains generated on denim at temperature intervals between -10°C and 50°C	205
130	Box plot distributions of R, G and B values for stains generated on denim at temperature intervals between -10°C and 50°C	206
131	R, G and B values for stains generated on denim at humidity intervals recorded during experimental stage 1	207
132	Longitudinal colour ribbons for stains generated on paper, glass and denim between -10°C and 50°C. Images of six replicate stains are included for each temperature interval.	209
133	Descriptive statistics for RGB totals calculated from all stains generated on denim, glass and paper	211
134	Box-plot demonstrating the range of RGB totals recorded for denim, glass and paper surfaces.	211
135	Representation of average ratios of R to G and B values for paper stains	212
136	Average R, G and B values for all stains generated on paper	212

137	Representation of average ratios of R to G and B values for glass stains	213
138	Average R, G and B values for all stains generated on glass	213
139	Representation of average ratios of R to G and B values for denim stains	213
140	Average R, G and B values for all stains generated on denim	214
141	Box plot distributions of RGB totals for stains generated on paper, glass and denim at temperature intervals between -10°C and 50°C	215
142	Box plot distributions of RGB totals for stains generated on paper, glass and denim at humidity intervals recorded during experimental stage 1	216
143	Independent Kruskal-Wallis tests for distributions of R, G, B values and RGB totals across categories of surface	217
144	Table of materials used in experimental stage 2	219
145	Climatic information recorded from experimental site (ES) and independent weather station (WS) over experimental period (2012/2013)	220
146	Division of longitudinal samples into 7 sample sets, each consisting of 8 replicate stains generated on each of three surfaces (paper, glass and denim)	221
147	Illustration of respective lengths of seven longitudinal samples	221
148	Illustration of arrangement of six monthly samples in relation to each other	222
149	Division of monthly samples into 7 sample sets, each consisting of 8 replicate stains generated on each of three surfaces (paper, glass and denim)	223
150	Open-sided shelving unit used to house stains	224
151	Sketch map of experimental site (garden) and location of experimental unit/equipment within site	226
152	Sketch diagram of location of box net on terracotta stands and placement of shelving unit in net	227
153	Arrangement of box mosquito net and tie around shelving unit	227
154	Breathable fabric tent placed over experimental unit	228
155	Final experimental set-up within experimental site	228
156	Sketch of A4 sheet of paper with marked areas, set up for generation of 8 stains on paper	229
157	Sketch of arrangement of 8 microscope slides, secured by sellotape, on	230

	A4 sheet of paper	
158	Sketch of arrangement of denim fabric swatch, secured by sellotape, on A4 sheet of paper	230
159	Eight replicate stains generated in demarcated boxes on paper	231
160	Arrangement of maximum number of longitudinal and monthly sample sets in 24-partitioned shelving unit	232
161	Shelving columns vertically housing different surfaces, from L-R: paper, glass, denim, which are secured to shelves with duct tape	232
162	Sheets and samples secured in open-sided shelving unit	233
163	Outline of order of sample removals	234
164	Results of presumptive chemical tests for stains generated as longitudinal samples	235
165	Checklist of results of presumptive chemical tests for stains generated as monthly samples	236
166	Stains generated on denim in longitudinal sample set L1	237
167	Stains generated on glass in longitudinal sample set L1	237
168	Stains generated on paper in longitudinal sample set L1	238
169	Stains generated on denim in longitudinal sample set L2	238
170	Stains generated on glass in longitudinal sample set L2	239
171	Stains generated on paper in longitudinal sample set L2	239
172	Stains generated on denim in longitudinal sample set L3	240
173	Stains generated on glass in longitudinal sample set L3	240
174	Stains generated on paper in longitudinal sample set L3	241
175	Stains generated on denim in longitudinal sample set L4	241
176	Stains generated on glass in longitudinal sample set L4	242
177	Stains generated on paper in longitudinal sample set L4	242
178	Stains generated on denim in longitudinal sample set L5	243
179	Stains generated on glass in longitudinal sample set L5	243
180	Stains generated on paper in longitudinal sample set L5	244
181	Stains generated on denim in longitudinal sample set L6	244
182	Stains generated on glass in longitudinal sample set L6	245

183	Stains generated on paper in longitudinal sample set L6	245
184	Stains generated on denim in longitudinal sample set L7	246
185	Stains generated on glass in longitudinal sample set L7	246
186	Stains generated on paper in longitudinal sample set L7	247
187	Table of measurements recorded for stains generated on denim surfaces in longitudinal sample sets	248
188	Descriptive statistics recorded for stains generated on denim surfaces in longitudinal sample sets	249
189	Average R, G and B values for all longitudinal stains generated on denim	250
190	Box plot distributions of R values for stains generated on denim surfaces across longitudinal sample sets	251
191	Box plot distributions of RGB totals for stains generated on denim surfaces across longitudinal sample sets	252
192	Box plot distributions of R values for stains generated on denim surfaces at cumulatively averaged temperatures	253
193	Box plot distributions of RGB Totals for stains generated on denim surfaces at cumulatively averaged temperatures	253
194	Box plot distributions of R values for stains generated on denim surfaces at cumulatively averaged humidity values	254
195	Box plot distributions of RGB totals for stains generated on denim surfaces at cumulatively averaged humidity values	254
196	Box plot distributions of R values for stains generated on denim surfaces and exposed to cumulative volumes of precipitation	255
197	Box plot distributions of RGB totals for stains generated on denim surfaces and exposed to cumulative volumes of precipitation	256
198	Table of measurements recorded for stains generated on paper surfaces in longitudinal sample sets	258
199	Descriptive statistics recorded for stains generated on paper surfaces in longitudinal sample sets	259
200	Average R, G and B values for all longitudinal stains generated on paper	260
201	Box plot distributions of R values for stains generated on paper surfaces across longitudinal sample sets	261
202	Box plot distributions of RGB totals for stains generated on paper	262

	surfaces across longitudinal sample sets	
203	Box plot distributions of R values for stains generated on paper surfaces at cumulatively averaged temperatures	263
204	Box plot distributions of RGB Totals for stains generated on paper surfaces at cumulatively averaged temperatures	263
205	Box plot distributions of R values for stains generated on paper surfaces at cumulatively averaged humidity values	263
206	Box plot distributions of RGB totals for stains generated on paper surfaces at cumulatively averaged humidity values	264
207	Box plot distributions of R values for stains generated on paper surfaces and exposed to cumulative volumes of precipitation	265
208	Box plot distributions of RGB totals for stains generated on paper surfaces and exposed to cumulative volumes of precipitation	266
209	Table of measurements recorded for stains generated on glass surfaces in longitudinal sample sets	267
210	Descriptive statistics recorded for stains generated on glass surfaces in longitudinal sample sets	268
211	Average R, G and B values for all longitudinal stains generated on glass	269
212	Box plot distributions of R values for stains generated on glass surfaces across longitudinal sample sets	270
213	Box plot distributions of RGB totals for stains generated on glass surfaces across longitudinal sample sets	271
214	Box plot distributions of R values for stains generated on glass surfaces at cumulatively averaged temperatures	272
215	Box plot distributions of RGB Totals for stains generated on glass surfaces at cumulatively averaged temperatures	272
216	Box plot distributions of R values for stains generated on glass surfaces at cumulatively averaged humidity values	272
217	Box plot distributions of RGB totals for stains generated on glass surfaces at cumulatively averaged humidity values	273
218	Box plot distributions of R values for stains generated on glass surfaces and exposed to cumulative volumes of precipitation	274
219	Box plot distributions of RGB totals for stains generated on glass surfaces and exposed to cumulative volumes of precipitation	275

220	Colour ribbons for stains generated on denim, paper and glass and exposed to a temperate climate across 7 different longitudinal periods	277
221	Descriptive statistics for RGB totals calculated from all stains generated on denim, glass and paper	278
222	Box plot distributions of average RGB totals for stains generated on denim, glass and paper surfaces	279
223	Trends in average RGB totals for stains generated on denim, glass and paper surfaces across longitudinal sample sets	279
224	Average R, G and B values for all stains generated in longitudinal sample sets on denim, glass and paper	280
225	Representation of average ratios of R to G and B values for denim stains	281
226	Representation of average ratios of R to G and B values for glass stains	281
227	Representation of average ratios of R to G and B values for paper stains	281
228	Kruskal-Wallis test for comparison between distribution of R, G, B values and RGB totals across number of months	282
229	Kruskal-Wallis test for comparison between distribution of R, G, B values and RGB totals across different surfaces (denim, paper, glass)	282
230	Stains generated on denim in monthly sample set M1	283
231	Stains generated on glass in monthly sample set M1	284
232	Stains generated on paper in monthly sample set M1	284
233	Stains generated on denim in monthly sample set M2	285
234	Stains generated on glass in monthly sample set M2	285
235	Stains generated on paper in monthly sample set M2	286
236	Stains generated on denim in monthly sample set M3	286
237	Stains generated on glass in monthly sample set M3	287
238	Stains generated on paper in monthly sample set M3	287
239	Stains generated on denim in monthly sample set M4	288
240	Stains generated on glass in monthly sample set M4	288
241	Stains generated on paper in monthly sample set M4	289
242	Stains generated on denim in monthly sample set M5	289
243	Stains generated on glass in monthly sample set M5	290

244	Stains generated on paper in monthly sample set M5	290
245	Stains generated on denim in monthly sample set M6	291
246	Stains generated on glass in monthly sample set M6	291
247	Stains generated on paper in monthly sample set M6	292
248	Table of measurements recorded for stains generated on denim surfaces in monthly sample sets	293
249	Descriptive statistics recorded for stains generated on denim surfaces in monthly sample sets	294
250	Average R, G and B values for all monthly stains generated on denim	295
251	Box plot distributions of R values for stains generated on denim surfaces across monthly sample sets	295
252	Box plot distributions of RGB totals for stains generated on denim surfaces across monthly sample sets	296
253	Box plot distributions of R values for stains generated on denim surfaces exposed to different temperature averages	297
254	Box plot distributions of RGB Totals for stains generated on denim surfaces exposed to different temperature averages	298
255	Box plot distributions of R values for stains generated on denim surfaces exposed to different humidity averages	299
256	Box plot distributions of RGB totals for stains generated on denim surfaces exposed to different humidity averages	299
257	Box plot distributions of R values for stains generated on denim surfaces and exposed to different volumes of precipitation	300
258	Box plot distributions of RGB totals for stains generated on denim surfaces and exposed to different volumes of precipitation	301
259	Table of measurements recorded for stains generated on paper surfaces in monthly sample sets	302
260	Descriptive statistics recorded for stains generated on paper surfaces in monthly sample sets	303
261	Average R, G and B values for all monthly stains generated on paper	304
262	Box plot distributions of R values for stains generated on paper surfaces across monthly sample sets	304
263	Box plot distributions of RGB totals for stains generated on paper	305

	surfaces across monthly sample sets	
264	Box plot distributions of R values for stains generated on paper surfaces exposed to different temperature averages	306
265	Box plot distributions of RGB Totals for stains generated on paper surfaces exposed to different temperature averages	307
266	Box plot distributions of R values for stains generated on paper surfaces exposed to different humidity averages	307
267	Box plot distributions of RGB totals for stains generated on paper surfaces exposed to different humidity averages	308
268	Box plot distributions of R values for stains generated on paper surfaces and exposed to different volumes of precipitation	309
269	Box plot distributions of G values for stains generated on paper surfaces and exposed to different volumes of precipitation	310
270	Box plot distributions of B values for stains generated on paper surfaces and exposed to different volumes of precipitation	311
271	Box plot distributions of RGB totals for stains generated on paper surfaces and exposed to different volumes of precipitation	312
272	Table of measurements recorded for stains generated on glass surfaces in monthly sample sets	313
273	Descriptive statistics recorded for stains generated on glass surfaces in monthly sample sets	314
274	Average R, G and B values for all monthly stains generated on glass	315
275	Box plot distributions of R values for stains generated on glass surfaces across monthly sample sets	315
276	Box plot distributions of RGB totals for stains generated on glass surfaces across monthly sample sets	316
277	Box plot distributions of R values for stains generated on glass surfaces exposed to different temperature averages	317
278	Box plot distributions of RGB Totals for stains generated on glass surfaces exposed to different temperature averages	317
279	Box plot distributions of R values for stains generated on glass surfaces exposed to different humidity averages	318
280	Box plot distributions of RGB totals for stains generated on glass surfaces exposed to different humidity averages	319



281	Box plot distributions of R values for stains generated on glass surfaces and exposed to different volumes of precipitation	320
282	Box plot distributions of RGB totals for stains generated on glass surfaces and exposed to different volumes of precipitation	321
283	Colour ribbons for stains generated on denim, paper and glass and exposed to a temperate climate across 6 different monthly periods	323
284	Descriptive statistics for RGB totals calculated from all stains generated on denim, glass and paper	325
285	Box plot distributions of average RGB totals for stains generated on denim, glass and paper surfaces	326
286	Average R, G and B values for all stains generated across monthly sample sets on denim, glass and paper	326
287	Representation of average ratios of R to G and B values for M1 stains	327
288	Representation of average ratios of R to G and B values for M2 stains	327
289	Representation of average ratios of R to G and B values for M3 stains	328
290	Representation of average ratios of R to G and B values for M4 stains	328
291	Representation of average ratios of R to G and B values for M5 stains	328
292	Representation of average ratios of R to G and B values for M6 stains	329
293	Table of materials used in experimental stage 3	332
294	Table listing the extreme conditions stains were exposed to during experimental stage 3, broadly categorised between extremes of cold/hot, and descriptive overviews of each condition	333
295	Clean area of snow for experimentation	334
296	24 single-drop replicate stains generated on snow	335
297	Clean area of snow for experimentation	336
298	12 replicate stains generated on glass microscope slides, on snow	336
299	Clean area of snow for experimentation	337
300	Multi-drop stain generated on snow	337
301	Digital temperature and humidity data logger, attached at experimental site	339
302	Stains generated on glass microscope slides, on brick wall at experimental site, located next to digital temperature and humidity data	340

	logger	
303	Portable freezer	341
304	Plastic tub filled with water to a depth of 3cm	342
305	Bloodstains generated on paper (top left), glass microscope slides (right) and denim fabric (bottom left) surfaces, which were then placed on top of a frozen ice surface after generation	342
306	Plastic tub filled with ice (to an approximate depth of 3cm) containing swatches of paper, denim fabric and glass microscope slides following 24 hours exposure to freezing conditions	344
307	18 bloodstains generated onto frozen surfaces (paper, glass, denim) from a height of 10cm	344
308	Plastic tub filled with ice (to a depth of approximately 3cm)	345
309	24 bloodstains generated directly onto ice from a height of 10cm	345
310	Glass microscope slides mounted on white record cards	348
311	Stains on middle shelf of fan-assisted oven	349
312	Eight glass microscope slides arranged on mesh grill of unlit charcoal barbecue (slide circled in photo on left)	352
313	Eight bloodstains generated on glass microscope slides from a height of 10cm	352
314	Blood-stained slides on the barbecue, immediately after charcoal was ignited	352
315	Tray barbecue following completion of the ignition process, when charcoal throughout the tray was alight	353
316	Checklist of responses recorded for stains generated across five different extreme environmental conditions (& multiple methods) to presumptive chemical tests	355
317	Hemastix test for stain on glass	356
318	Kastle-Meyer test for stain on denim	356
319	Stains pictured following application of Kastle-Meyer solution	356
320	Stains pictured following application of Hydrogen Peroxide solution	356
321	Stains pictured in normal light	357
322	Stains pictured following application of Bluestar Luminol solution (in darkness)	357

323	Stains pictured in normal light	357
324	Stains pictured following application of Bluestar Luminol solution (in darkness)	357
325	Overall images of 24 single drop stains generated directly onto snow taken at time intervals of +00:05, +00:15, +00:30, +00:45 and +01:00 hours	359
326	Images of one particular single drop stain generated directly onto snow taken at time intervals of +00:05, +00:15, +00:30, +00:45 and +01:00 hours	361
327	Average R, G, B values and RGB totals for single drop stains generated directly onto snow	363
328	Overall images of single drop stains generated onto glass slides on snow taken at time intervals of +00:15, +00:30, +00:45 and +01:00 hours	363
329	Images of one particular single drop stain generated onto glass slides on snow taken at time intervals of +00:15, +00:30, +00:45 and +01:00 hours	365
330	Average R, G, B values and RGB totals for single drop stains generated directly onto snow	366
331	Images of multi-drop stain generated directly onto snow taken at time intervals of +00:05, +00:15, +00:30, +00:45 and +01:00 hours	367
332	Average R, G, B values and RGB totals for single drop stains generated directly onto snow	368
333	Overall images of stains generated onto glass slides and exposed to freeze-thaw mechanisms	370
334	Two stains generated on a glass slide and exposed to identical environmental conditions	371
335	Images of stains generated on room temperature denim, paper and glass surfaces and exposed to freezing conditions	373
336	Table of measurements recorded for stains generated and exposed to environmental condition C via staining method 1	374
337	Average R, G, B values and RGB Totals for denim, paper and glass stains exposed to condition C via staining method 1	375
338	Images of stains generated on frozen denim, paper and glass surfaces and exposed to freezing conditions	376
339	Table of measurements recorded for stains generated exposed to	377

	environmental condition C via staining method 2	
340	Average R, G, B values and RGB Totals for denim, paper and glass stains exposed to condition C via staining method 2	378
341	Kruskal-Wallis test comparing distributions of R, G, B values and RGB totals between staining methods 1 and 2	379
342	Kruskal-Wallis test comparing distributions of R, G, B values and RGB totals between surfaces	380
343	Images of stains generated directly onto ice and exposed to freezing conditions	381
344	R, G, B values and RGB totals calculated for stains (n = 24) generated directly on ice and exposed to freezing conditions.	382
345	Images of stains generated on denim, paper and glass surfaces and exposed to temperatures of 100°C, 150°C, 200°C and 250°C	384
346	Table of measurements recorded for stains generated on denim surfaces from 100°C to 250°C	385
347	Descriptive statistics recorded for stains generated on denim surfaces from 100°C to 250°C	386
348	Table of measurements recorded for stains generated on paper surfaces from 100°C to 250°C	387
349	Descriptive statistics recorded for stains generated on paper surfaces from 100°C to 250°C	388
350	Table of measurements recorded for stains generated on glass surfaces from 100°C to 250°C	389
351	Descriptive statistics recorded for stains generated on glass surfaces from 100°C to 250°C	390
352	Images of stains generated on denim, paper and glass surfaces and exposed to temperatures of 100°C, 150°C, 200°C and 250°C	391
353	Table of measurements recorded for stains generated on denim surfaces from 100°C to 250°C	392
354	Descriptive statistics recorded for stains generated on denim surfaces from 100°C to 250°C	393
355	Table of measurements recorded for stains generated on paper surfaces from 100°C to 250°C	394
356	Descriptive statistics recorded for stains generated on paper surfaces	395

	from 100°C to 250°C	
357	Table of measurements recorded for stains generated on glass surfaces from 100°C to 250°C	396
358	Descriptive statistics recorded for stains generated on glass surfaces from 100°C to 250°C	397
359	Longitudinal colour ribbons for stains generated on denim, paper and glass between 100°C and 250°C ( <b>staining method 1</b> )	399
360	Longitudinal colour ribbons for stains generated on denim, paper and glass between 100°C and 250°C ( <b>staining method 2</b> )	400
361	Mann Whitney test comparing distributions of R, G, B values and RGB totals between staining methods 1 and 2	401
362	Kruskal-Wallis test comparing distributions of R, G, B values and RGB totals between surfaces	402
363	Images of stains exposed to environmental condition E	404
364	Table of measurements recorded for stains generated on glass slides and exposed to environmental condition E (fire)	405
365	Average ratio of R to G to B values for stains exposed to fire	406
366	Table of mean R, G, B and RGB total values calculated	408
367	Comparison of mean R, G, B and RGB total values calculated for stains according to environmental exposure, including 'Temperature' (stain code A), 'Natural Climate' (stain code B), 'Snow' (stain code C), 'Freezing' (stain code D), 'Ice' (stain code E), 'High temperatures' (stain code F) and 'Fire' (stain code G)	412
368	Kruskal-Wallis test for comparison between distributions of R, G, B and RGB total values for 'stain codes' (categories of stains exposed to different environmental conditions)	413
369	Table of materials used in experimental stage 4	415
370	Photograph of experimental fridge set-up	416
371	Sketch diagram of AFM set-up	417
372	Images of portable laboratory refrigerator	418
373	Sketches of 6 replicate stains on a) paper slips b) glass slides & c) denim fabric (L-R) generated for drying at each temperature interval	420
374	1170 individual bloodstains generated from 10µl drops	421

375	468 individual bloodstains generated from 45µl drops	422
376	Surfaces to be stained prepared for experimentation (Paper/Glass/Denim from L-R)	423
377	Fixed volume pipette set to deliver drops of 10µl volume	423
378	Table outlining age of blood (in days) used to generate stains at each temperature interval, across the 5 experimental runs completed for 10µl volume stains and the 2 experimental runs completed for 45µl volume stains	425
379	Mean drying time results for 10µl stains ( <b>1<sup>st</sup> experimental run</b> )	430
380	Mean drying time results for 10µl stains ( <b>2<sup>nd</sup> experimental run</b> )	431
381	Mean drying time results for 10µl stains ( <b>3<sup>rd</sup> experimental run</b> )	432
382	Mean drying time results for 10µl stains ( <b>4<sup>th</sup> experimental run</b> )	433
383	Mean drying time results for 10µl stains ( <b>5<sup>th</sup> experimental run</b> )	434
384	Mean drying time results for 45µl stains ( <b>1<sup>st</sup> experimental run</b> )	435
385	Mean drying time results for 45µl stains ( <b>2<sup>nd</sup> experimental run</b> )	436
386	Results for 10µl stains on denim, averaged from replicates (n = 30) at each temperature interval and across 5 experimental runs	438
387	Calculation of minimum, maximum and mean drying time for 10µl stains on denim	438
388	Results for 10µl stains on glass, averaged from replicates (n = 30) at each temperature interval and across 5 experimental runs	439
389	Calculation of minimum, maximum and mean drying time for 10µl stains on glass	440
390	Results for 10µl stains on paper, averaged from replicates (n = 30) at each temperature interval and across 5 experimental runs	441
391	Calculation of minimum, maximum and mean drying time for 10µl stains on paper	441
392	Results for 45µl stains on denim, averaged from replicates (n = 30) at each temperature interval and across 2 experimental runs	443
393	Calculation of minimum, maximum and mean drying time for 45µl stains on denim	443
394	Results for 45µl stains on glass, averaged from replicates (n = 30) at each temperature interval and across 2 experimental runs	444

395	Calculation of minimum, maximum and mean drying time for 45µl stains on glass	445
396	Results for 45µl stains on paper, averaged from replicates (n = 30) at each temperature interval and across 2 experimental runs	446
397	Calculation of minimum, maximum and mean drying time for 45µl stains on paper	446
398	Relationship between temperature (°C) and stain drying time (minutes) for all stains	448
399	Kruskal-Wallis test for comparison between distributions of drying time across temperature intervals	449
400	Relationship between humidity (%) and stain drying time (minutes) for all stains	452
401	Relationship between age of blood (days) and stain drying time (minutes) for all stains	453
402	Relationship between volume of blood (µl) and drying time (minutes) for all stains	454
403	Mann-Whitney test for comparison between distributions of drying time across temperature intervals	455
404	Relationship between stain type and drying time (minutes)	456
405	Distributions of drying time (minutes) for denim, glass and paper surfaces, combined for 10µl and 45µl volume stains	456
406	Kruskal-Wallis test for comparison between distributions of drying time and stain type	457
407	AFM images of denim surfaces generated during calculation of surface roughness average (Ra)	459
408	AFM images of glass surfaces generated during calculation of surface roughness average (Ra)	459
409	AFM images of paper surfaces generated during calculation of surface roughness average (Ra)	459
410	Relationship between temperature intervals and humidity recorded during experimental stage 4	460
411	Image of bloodstains observed in a cold environment that were initially misidentified as brain tissue on account of their pink puffy appearance	466
412	Mock-up of possible smartphone application designed for rapid	480





## **Section 1**

# 1. Introduction

## 1.1 Forensic Science

Forensic science is a multidisciplinary approach applied to evidence associated with a crime event. It incorporates scientifically proven methods from a range of scientific disciplines in order to interpret and present physical evidence within a legal context. The progression of physical evidence from crime scene to courtroom occurs through a series of distinct stages, which can be illustrated holistically as a forensic ‘process’ (figure 1).

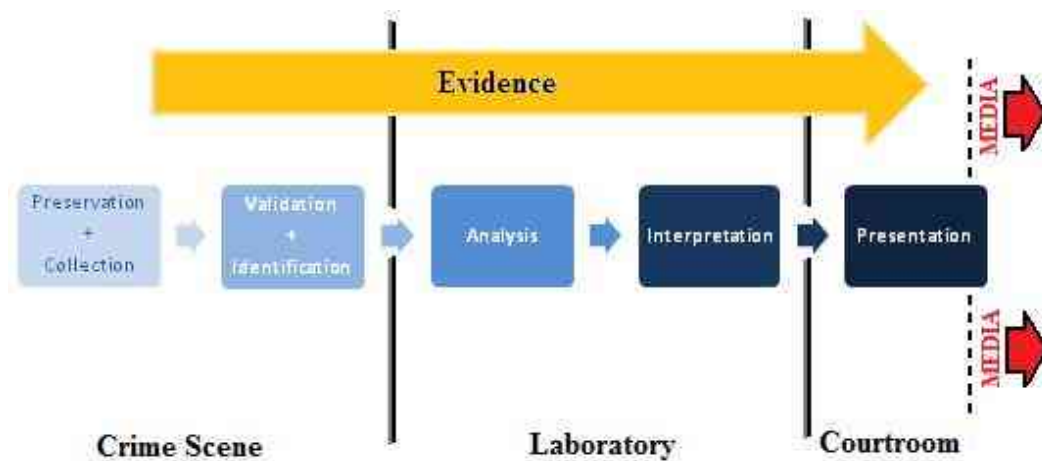


Figure 1 Illustration of the ‘forensic process’ (Source: Author. 2010)

Facilitating the progression of physical evidence through this process is the domain of the forensic scientist. As evidence progresses from preservation and collection, through validation and identification to laboratory analysis and interpretation, a series of inferences about it can be made, relating to the origins and circumstances surrounding its generation and presence at a scene (Chisum. Turvey. 2000. Baryamureeba. Tushabe. 2004:2). Inferences which identify the likely sources of physical evidence and activities which led to its deposition at a scene can allow investigators to reconstruct the events immediately prior to, during and following a crime event.

There are many types of physical evidence that may be encountered at a crime scene. Strands of hair, both natural and man-made fibres, fragments of glass or paint,

gunshot residue (GSR) and bodily fluids are examples of some of the most commonly encountered physical evidences (*Evetts. 1987: 1*), known generically as trace materials or evidence on account of the often small, fragmented or even microscopic volumes in which they are usually encountered.

Fluid trace evidence and specifically blood trace evidence is often encountered by forensic investigators, particularly in violent crimes involving fatalities where surviving eyewitness testimonies are absent (*James et al. 2005: 1*). The value of developing accurate methods of identifying, analysing and interpreting fluid evidence, in the case of blood through the forensic sub-discipline of Blood Pattern Analysis (BPA), is therefore significant.

The development of techniques for identification, analysis and interpretation of all types of evidence should be conducted with respect to the entire forensic process, as the different stages evidence progresses through (in a robust forensic investigation) are relevant to and dependent upon each other. As evidence progresses through preservation and collection, to validation, identification, analysis, interpretation and finally presentation for evaluation by a lay jury, the importance of ensuring continuity and integrity in the handling of evidence at each of these stages is vital to allow the meaningful progression of evidence through the whole process, from crime scene to courtroom.

For example, when presenting physical evidence in a courtroom, it could be considered that certain presentation methods might be more persuasive than probative, or indeed more persuasive than others. Making considerations towards the methods of presentation of evidence in a courtroom, where the probative value of any opinions regarding the evidence collected is assessed, are therefore ultimately an equally vital part of forensic science as original stages of evidence collection or handling.

Despite this, in many discussions of developing forensic techniques, including the body of BPA research published thus far, little attempt has been made to identify or confront courtroom issues that specifically affect the presentation of evidence or its interpretation by a layperson jury.

## **1.2 Development of trace evidence analysis**

In the field of trace evidence analysis the development of two particular forensic theories have supplied the fundamental philosophies underpinning trace evidence analysis and its use in crime scene reconstruction. These are Locard's exchange principle (*Locard. 1930*) and the principles of Evidence Dynamics (*Chisum. Turvey. 2000*).

### **1.2.1 Locard's exchange principle**

The relationship between physical evidence and its original source was first summarised by Edmond Locard and his exchange principle, which stipulates, "every contact leaves a trace" (*attributed to Locard. 1930 in Houck. 2001*). The implications of this are that when two surfaces (A&B) come into contact with each other a two-way transfer of material takes place. Traces of surface A will be deposited on surface B and vice versa. The volume of traces exchanged depends on the extent and length of contact between the surfaces and surface characteristics of A and B (*Houck. 2001*). Following contact, a quantity of trace materials exchanged will remain on each surface to bear "*mute witness*" (*Kirk. 1974*) to contact having occurred. Examination of traces exchanged can indicate the provenance, or source and in certain instances the nature and extent of any exchange may additionally be indicative of specific actions (*Cwiklik. 1999*).

A secondary tenet of Locard's principle relates to the persistence of trace materials on a surface. Over time exchanged traces will be naturally shed by the surface according to a natural decay curve over time, a typical illustration of which is given in *figure 2*. The persistence of traces varies according to a series of variables, which include characteristics of the parent material and target surfaces as well as any deliberate actions taken by a suspect to attempt to remove trace materials, for example by washing or brushing. Experimental studies have demonstrated however that some trace materials are capable of significant periods of persistence on surfaces. Both tulip and daffodil pollen particles for example, were recoverable from fabric up to 168 hours after pollen particles had been deposited on it (*Bull et al. 2006*).

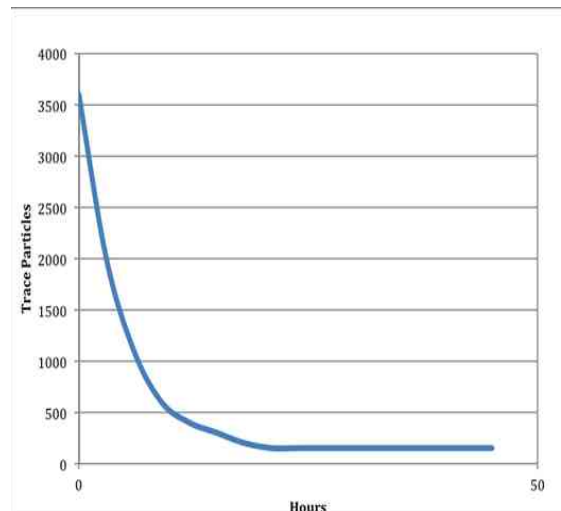


Figure 2 Trace material decay-curve demonstrating persistence of particles over time

(Author. 2010)

Using methods of identifying trace evidence, presence of evidence on a surface or at scene can be interpreted as evidence of a contact having taken place between two specific surfaces. This evidence is described as source level evidence.

### 1.2.2 Source level evidence

Source level evidence can be broadly understood as evidence that purely by its presence gives investigators some indication of events; what has happened or “where the incident occurred” (Boonkhong *et al.* 2010: 169).

For example gunshot residue (GSR) evidence recovered from a glove might suggest that contact was made between that glove and a gun/gun cartridge at some point or blood pattern evidence observed on the garments of a suspect may indicate that they came into contact with a bleeding victim. In these cases source level evidence may be incriminating in itself by attesting to the presence of exchanged trace materials in a crime scene and allowing some additional inferences regarding the nature and extent of exchange to be made. In most instances however the presence, alone, of a trace material on a surface is often not sufficient or powerful evidence to implicate the wearer of the glove, for example, with handling a weapon or indeed firing it. In the case of blood evidence, presence of blood on a suspects garment is certainly suspicious but it alone does not imply the suspect was definitely present or involved during a bloodletting attack on a victim. Without further information it could be reasonable to argue that the bloodstaining of the suspect had occurred following the victims attack, perhaps as the suspect went to their aid. Empirical studies on the

persistence of different trace materials on a variety of surfaces (*Pounds. Smalldon. 1975. Robertson. Grieve. 1999. Houck. 2001*) and evidence of the presence of secondary (*Lowrie. Jackson. 1994. Houck. 2001*), tertiary and further (*Taupin. 1996. French et al. 2012*) levels of indirect transfers of trace materials have shown that source level evidence is vulnerable to being explained away by innocent indirect contact at some point with the trace materials, in exactly this way.

These studies illustrate that a limitation exists if using source level evidence in isolation for crime scene reconstruction, in that it relies heavily on an assumption of evidential integrity (*Chisum. Turvey. 2000*). This is an assumption that evidence collected at a crime scene is pristine and has not been altered, either intentionally or unintentionally, prior to or during its collection. This assumption is not always accurate and failing to incorporate the possibility of evidence having been altered is problematic.

Interpretation of source level evidence is an undoubtedly important stage in crime scene reconstruction. It assists investigators in identifying the presence of exchanged trace materials in a crime scene, and may allow some inferences regarding the nature and extent of exchange to be made, which in itself can be probative. In order to establish the significance of the presence of trace materials however, an understanding of the second fundamental philosophy of trace evidence analysis: evidence dynamics, is also necessary.

### **1.2.3 Evidence Dynamics**

Evidence dynamics refers to any activities or “any influence that changes, relocates, obscures, or obliterates physical evidence, regardless of intent” (*Chisum. Turvey. 2000*) between the initial point of evidence exchange and transfer and the ultimate conclusion of the investigation. These influences often complicate the process of interpreting and analysing traces of evidence for the purposes of contextualising their presence at a crime scene. Developing an understanding of evidence dynamics affords investigators a theoretical basis from which to incorporate any pertinent evidentiary influences into the process of crime scene reconstruction.

There are many different types and sources of potential influence to consider. Influences can include an individual's actions either during or post-event. An offender may be motivated, for example, to attempt to conceal their involvement with an event, their identity or indeed any evidence of the crime having taken place at all (*Turvey. 1999*). Actions of a victim prior to, during and after a crime may also influence physical evidence at a scene. If a victim suffers an accidental bloodletting event such as a cut finger, for example, immediately prior to an event, observation of the resulting blood spatter evidence during a subsequent investigation of the scene could be interpreted as resulting from the crime event, despite its innocent origin – if evidence dynamics are not considered. Other animate parties such as any witnesses, emergency services, investigating officers, animals or even insects at a crime scene during or after an event can also be responsible for influencing physical evidence present. At a relatively simple level movement of these parties in and around a crime scene can lead to evidence being transported around or even away from the scene, unwittingly, by footwear.

Environmental conditions at a crime scene should be included in discussions on evidence dynamics as they too can act on evidence at a scene. Precipitation, wind, snow and more extreme features like fire can all obscure or completely destroy traces. In an instance of fire occurring, either intentionally or otherwise, the effects any fire suppression efforts employed may have had must also be considered as they may have caused alterations on top of the effects of fire.

One of the most delicate areas of evidence dynamics concerns secondary transfer. During an initial exchange material is transferred from a source to a surface. Secondary transfer refers to the onwards transfer of that material to other surfaces, through contacts following the initial exchange (*Houck. 2001*). Secondary transfer becomes problematic when objects or surfaces involved in secondary exchanges are not associated with the original exchange event. During analysis, presence of traces on these surfaces could be misinterpreted as evidence of the surfaces' presence or involvement with the initial exchange event. The likelihood of this interpretation being made is almost guaranteed if investigators only apply Locard's exchange principle to the analysis of trace evidence.

Incorporating considerations of the issue of secondary transfer as well as influences other activities exert on evidence into the analysis of a crime scene is essential to avoid these kinds of possible misinterpretations of evidence. The principles of evidence dynamics assist with this by interpreting and explaining the possible activities surrounding generation of evidence. An understanding of evidence dynamics allows investigators to infer whether the presence of evidence on a surface could be the result of certain mechanisms and activities having surrounded the generation of evidence. This evidence is described as activity level evidence.

#### **1.2.4 Activity level evidence**

Activity level evidence is evidence that explains the circumstances of evidence generation, i.e. through what mechanisms physical trace evidence has been deposited at a site. It achieves this by applying principles of evidence dynamics to the interpretation of source level trace evidence.

Following a discussion of evidence dynamics, the limitations and possibilities for misinterpretation that may result from conducting source level analysis alone becomes clear. Two examples of source level evidence were outlined (1.2.2) in which GSR particles were observed on a glove and blood pattern evidence was observed on a suspect's garments. Source level analysis in these two examples is limited to indicating that the materials are present on both the glove and garments and does not offer any propositions as to the investigative significance of their presence. If the evidence is then analysed at activity level however, investigators can begin to make propositions about the context surrounding and significance of the evidence. Activity level evidence in the example of GSR recovered from a glove might be an observation that GSR particles on the glove are present in a quantity that has been empirically established to be typical of direct contact transfer. In the example of blood pattern evidence observed on a suspect's garments, activity level evidence could be derived from an observation that blood patterns observed are consistent with the suspect having been exposed to a particular blood spatter mechanism. For example standing in close proximity to an impact event. Both examples illustrate, albeit fairly basically, the investigative value activity level interpretations of evidence can provide, in combination with source level analysis.



Activity level evidence analysis is not without its limitations however, in certain instances differences in interpretations of activity level propositions from trace evidence can occur, particularly when empirical knowledge regarding certain evidence generation mechanisms is lacking or limited, as the following case examples: *R v Jenkins* (1998) and *State of Indiana v. Camm* (2002) demonstrate. Both cases show how activity level propositions relating to certain aspects of blood pattern evidence can differ and how those differences became pertinent to crime scene reconstruction.

In *R v Jenkins* (1998) the case centred on the murder of 13 year old Billie-Jo Jenkins on the 15<sup>th</sup> February 1997 and the subsequent discovery of 158 microscopic bloodstains on the upper clothing of her foster father, Siôn Jenkins (*Gibson. 2006*). At the original trial (1998) blood pattern analysts testified to these stains being consistent only with the garment having been in close proximity to the victim during an impact spatter event, for example whilst the victim was being violently beaten by the garment wearer (*Thorne. 2006. Woffinden. Jenkins. 2008*). This testimony was based on the classification of stains according to certain criteria, including size; morphology and distribution, as impact spatter stains. An understanding of the relationship between size of stain and distance travelled was also applied during analysis. Blood drops of small volume lack sufficient mass to travel any significant distance from the impact site they have originated from (*Bevel. Gardner. 2008*) and observation of microscopic impact spatter stains on a surface is therefore usually indicative of the surface's close proximity to the original impact. Knowledge of this assisted experts with their interpretation of the blood evidence, resulting in their activity level proposition of the stains being consistent with impact spatter. Jenkins was subsequently convicted. Following two retrials the conviction was quashed, in no small part due to expert disagreements with the activity level propositions posited in the initial trial. During retrial other blood pattern analysts disputed that stains observed were 'typical' of impact spatter and suggested they were more likely to be exhaled stains, generated by the victim suddenly breathing or coughing out trapped blood in the presence of her father (*Gibson. 2006*). In this staining scenario, the proximity of her father to her was explicable through the innocent act of going to his daughter's aid, post bloodletting event, and moving her – unwittingly providing a release for the trapped blood. With medical examiners reports testifying to the

presence of a blockage in Billie-Jo's airway and presence of blood in her throat (Laville. 2006), this new activity level proposition could not be excluded from consideration. Siôn Jenkins was released.

In *State of Indiana v Camm* (2002) the case centred on charges brought against David Camm for the murders of his wife Kim Camm, son Bradley Camm and daughter Jill Camm (Kozarovich. 2009). Kim was found on the floor of the family garage with a single fatal gunshot wound, whilst Bradley and Jill were found shot in the backseat of the family car. In the original trial prosecutors drew particular attention to eight microscopic bloodstains identified in a small section ('Area 30') of the shirt David Camm was wearing on the night of the murders. The blood was identified as Jill's. During the course of the trial, expert blood pattern analysts for the prosecution and defence differed in opinion over the activity level propositions they proffered, regarding the most probable stain generating mechanism for 'Area 30'. Prosecution experts testified that stains were consistent in size, morphology and distribution, with spatter stains that would have been generated if David Camm shot Jill from a distance of no more than 4 feet, concluding that 'Area 30 specifically was in range of a gunshot wound in which backspatter was created' (Bevel. 2013, cited in Kircher. 2013b). The defence disagreed; arguing that the stains were in fact consistent with contact stains transferred from Jill's bloody hair to Camm's t-shirt as he leant into and across the backseat of the car to pull Bradley's body out of the car (Goetz. 2013, cited in Kircher. 2013a). The defence experts claimed that the presence of "painted fibres" supported their activity level proposition and excluded the possibility of the prosecutions (Bevel. Gardner. 2008: 265).

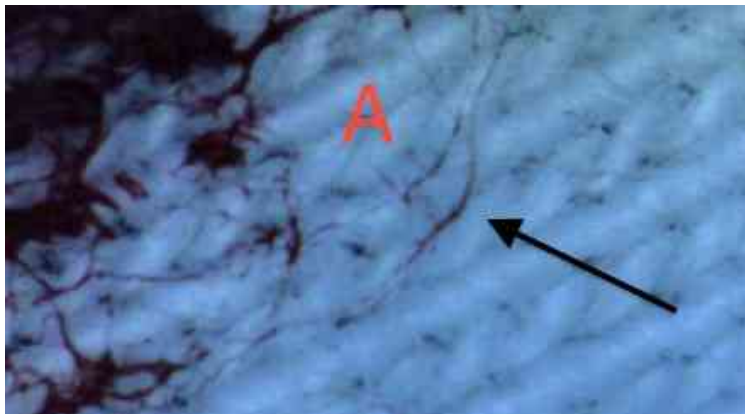


Figure 3 Example of "painted fibres" (A) on fabric, formed away from main body of stain (Author. 2013)

The defence described “Painted fibers” as fibres that appear coated in blood despite being separate to the main body of a fabric stain (*figure 3*) and claimed they are a unique feature to contact stains. The defence’s discussion of “painted fibers” was considered highly contentious, given that prior to the Camm case the term and characteristics of “painted fibers” had never been heard, or even discussed, within the blood pattern analysis discipline. As such no experimental research had been conducted or subject to peer review on these “fibers”. In fact, simple experimentation carried out following this first use of the term has since shown that “painted fibers” occur in both contact and spatter events. This suggests the probative value of them, in this case at least, is insignificant (*Bevel. Gardner. 2008*). Following consideration of all evidence presented, David Camm was found guilty and sentenced to 195 years in prison.

Issues with blood pattern evidence presented in the Camm case continued to be contended by prosecution and defence analysts beyond the initial trial, as the case has been brought to appeal (*Camm v State 2004, Camm v State 2009*) and retrial (*State v Camm 2006, State v Camm 2013*) several times since. Amongst other points of contention, the bloodstains in ‘Area 30’ continue to be one of the most problematic pieces of evidence, dividing the expert blood pattern analysis community between the prosecution and defence’s activity level propositions.

Both the Jenkins and Camm case highlight several issues regarding the interpretation of activity level evidence and it’s interpretation alongside source level evidence. The cases provide examples of the importance of conducting activity level evidence analysis and the role it fulfils in crime scene reconstruction. By incorporating an appreciation of the role of evidence dynamics into interpretation of physical traces, activity level analysis significantly develops the conclusions of source level analysis, establishing a context for evidence generation and inferring the significance of traces present.

The limitations of activity level analysis are also highlighted. As a secondary level of evidence analysis, activity level analysis is fundamentally reliant on accurate completion of source level analysis preceding it. Without this, activity level analysis is likely to be misinformed, inaccurate or even incomplete. Even in cases where

source level analysis is conducted robustly, activity level analysis may still experience limitations. In both cases, opposing analysts experienced difficulties in agreeing on a singular activity level proposition amongst themselves. This was in large part due to a lack of available empirical understanding of the particular propositions being discussed, in the context of the exact case-specific scenarios presented, which limited the ability to ultimately dismiss or accept one activity level interpretation over another. Lack of empirical research, sufficient to justify activity level propositions, leaves activity level analysis vulnerable to this limitation.

### **1.2.5 Source and activity level analyses**

Source and activity level analyses are not mutually exclusive and it is prudent to approach them as aspects of joint importance in trace evidence analysis. The significance and accuracy that can be attached to each is somewhat dependent upon the other. Source level analysis provides the initial identification of trace material and association to its origin through an application of the exchange principle. Activity level analysis then provides the context for the presence of a material through an application of the principles of evidence dynamics. Activity analysis is reliant upon source analysis for identification of evidence and source analysis in turn relies upon activity analysis to give probative value to that evidence. Together they allow investigators to identify and explain the presence of trace materials at a crime scene, which assists in the process of crime scene reconstruction.

### **1.3 Extrapolation of techniques to crime scene reconstruction**

By combining source and activity level evidence analyses, a forensic investigator can begin to carry out crime scene reconstruction. Crime scene reconstruction is the process of reconstructing the most probable chain of events that occurred at a crime scene, on the basis of the evidence recovered. In the face of conflicting witness accounts it can provide an ‘objective’ perspective for investigators (*Chisum. Turvey. 2000*). The aim of crime scene reconstruction is to create an accurate and plausible account of the circumstances surrounding the generation of evidence, which will then be produced in a “tangible form” before a judge and jury in the final stage of the ‘forensic process’: a courtroom presentation (*Chisum. Turvey. 2007*).

Findley and Hopkins (1984) provide a deconstructed view of the process of crime scene reconstruction that identifies several distinct phases of it, including the analysis of both source and activity level evidence and logical formulation of theories. Their recognition that the process of crime scene reconstruction extends beyond scientific scene analysis and interpretation of physical evidence is important. Whilst analysis and interpretation of physical evidence recovered from a scene provide the foundation for reconstructing the events surrounding a crime (Saferstein. 1998), crucially, the process of crime scene reconstruction incorporates a systematic study of related information in order to facilitate the logical formulation of a theory or set of theories within the context of the entire scene (Lee. 1994 cited in Chisum. Turvey. 2000). To reinforce this idea of a more holistic crime scene appraisal Findley and Hopkins identified four distinct areas of possible evidentiary input (figure 4), each of which should be considered during any reconstruction.

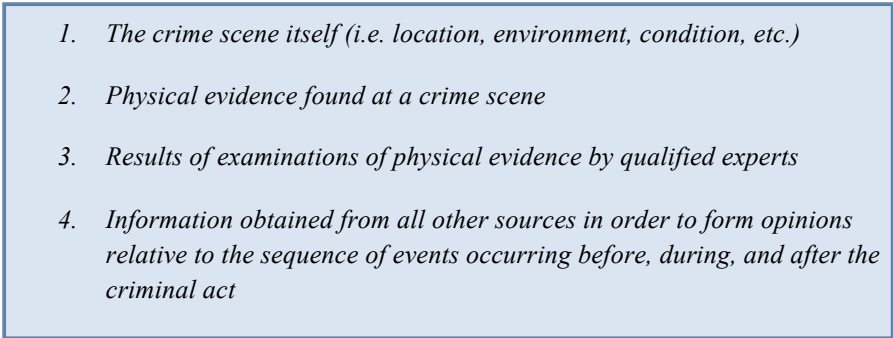
- 
1. *The crime scene itself (i.e. location, environment, condition, etc.)*
  2. *Physical evidence found at a crime scene*
  3. *Results of examinations of physical evidence by qualified experts*
  4. *Information obtained from all other sources in order to form opinions relative to the sequence of events occurring before, during, and after the criminal act*

Figure 4 Identification of four distinct evidentiary input streams to the process of crime scene reconstruction (Findley. Hopkins. 1984)

The separate evidentiary input streams in combination, assist investigators in the processes of both source and activity level analyses. Analysis of the crime scene and physical evidence found at the scene accounts for source level evidence analysis, whilst expert examination of recovered evidence and the formation of opinions relating to events surrounding the criminal act relates to activity level evidence analysis. Emphasis is placed on the importance of underpinning the whole reconstructive process with a combination of logic and scientific principles in order to ensure accuracy and plausibility in crime scene reconstruction presented.

The power of crime scene reconstruction is ultimately reliant upon three things:

- 1) Accuracy and plausibility of reconstructions offered by experts (derived from evidence of the application of logic, scientific principles, training and a certain extent experience to crime scene analysis).
- 2) The existence of scientifically robust, technique specific (for example Blood Pattern Analysis), methods for analysing:
  - a. Source level evidence
  - b. Activity level evidence
- 3) Ability of a jury to accurately appreciate, decipher and critique both the crime scene reconstructions presented to them and the logic or methods experts have employed to arrive at them.

When conducting research aimed at developing specific forensic techniques of crime scene analysis, consideration of these conditions should be incorporated into experimental design and methodologies.

The process of crime scene reconstruction in relation to blood trace evidence specifically will now be discussed.

#### **1.4 Crime Scene reconstruction in the case of Blood Pattern Analysis (BPA)**

Blood is a type of trace evidence. It is therefore subject to the same philosophies of source and activity level interpretation and analysis and extrapolation of the results of these to crime scene reconstruction, as other types of trace evidence.

The analysis of bloodstains, spatters and the patterns formed by bloodletting events at crime scenes is a technique known as Blood Pattern Analysis (BPA). The scientific basis of BPA is in fluid mechanics and physical laws, as blood is a fluid and therefore reacts in predictable ways to certain forces being exerted upon it. Of all fluid evidence presented at a crime scene “*blood is one of the most significant and frequent types of physical evidence*” an investigator may encounter (James *et al.* 2005:1). BPA is the process by which the two-dimensional morphologies of bloodstains are interpreted in the “*aftermath of a blood transfer event*” (Laber *et al.*

2008: 4) to help investigators reconstruct the circumstances under which they were generated, by drawing inferences about the three-dimensional origins of the blood (Raymond et al. 1995. Laber et al. 2008).

Elements of possible crime scene reconstructions from blood pattern analysis range from the fairly simple reconstruction of single bloodstain directionality which roughly *indicates the direction blood was moving at the time of deposition* (SWGSTAIN. 2009), to more complex analyses of a collective stain pattern to “*determine the approximate source in three-dimensional space of those bloodstains*” (Raymond et al 1996: 162). Current analytical techniques available to Blood Pattern Analysts for interpreting both source and activity levels associated with blood evidence, which may be used in crime scene reconstruction are outlined below.

#### **1.4.4 Source level analysis of Blood Pattern evidence**

Source level analysis of blood evidence deals broadly with confirming the presence of blood at a scene as an indicator of injuries sustained and possible location(s) of bloodletting events.

Blood presence is confirmed by a two-step process, 1<sup>st</sup>) visual identification and 2<sup>nd</sup>) chemical identification. Where possible visual identification should be carried out at a crime scene but where this is not possible the process can be done from scene photographs. Visual identification relies on assessment of suspect fluids through an “ABC approach to Bloodstain Verification” where the ABC refers to **A**pppearance, **B**ehaviour and **C**ontext (Wonder. 2001: 11). Appearance indicators rely on the distinctive colour, hue, tint and saturation of blood that investigators learn to recognise with experience. Additionally, as bloodstains age, they progress through a sequence of colour changes that alter their appearance (James et al. 2005).

Behavioural indicators rely on the unique and distinct composition of blood to other fluids, which enables it to clot, separate and haemolyse. Its deformation when drying results in recognizable and unique behaviour. The particulate nature of blood can be observed in a dry stain and a distinct odour resulting from decomposition and biochemical changes is also produced during the drying process. Context indicators relate to the ability to recognize individual stains as part of a pattern, therefore

overcoming the need to individually identify each individual bloodstain (*Wonder. 2001*).

Once visual identification has been conducted chemical identification of bloodstains should be carried out as a confirmatory step. This is necessary due to the experiential basis of visual identification methods. Chemical tests available are either presumptive or confirmatory for blood. Presumptive tests give two possible outcomes; **a)** that a sample is definitely NOT blood or **b)** that the sample probably is blood but it cannot be excluded from being one of a small range of other substances. Presumptive tests are mostly useful for identifying possible areas of interest when dealing with a large crime scene (*Tobe. David. 2007*). Smaller areas highlighted by presumptive tests can then be selected for more focused confirmatory testing.

Examples of presumptive tests for blood include the Kastle-Meyer (Phenolphthalein), Leucomalachite Green (LMG) (*Cox. 1991*), Hemastix, Bluestar and Luminol tests (*Barni et al. 2007*). Once a possible bloodstain has been identified via presumptive testing further laboratory based confirmatory tests can be carried out on the sample. Examples of confirmatory tests include the Hexagon OBTI, Takayama and Teichmann tests.

Through visual and chemical identification of bloodstains at a crime scene investigators are informed that a bloodletting event has taken place, and locations of stains gives an indication of the location of these events. Observations relating to volume of blood found at a scene may give an additional indication of the severity of injuries sustained and extent of blood loss suffered by involved parties. Intrinsic qualities of blood can also contribute to source level evidence where identification of blood type, DNA extraction and species identification can help identify the most likely individual source of the blood, whether there are single or multiple blood sources and in cases where multiple sources are identified they can help distinguish patterns derived from a suspect and victim.

#### **1.4.5 Activity level analysis of Blood Pattern evidence**

Activity level analysis of Blood Pattern evidence builds from the source level identification of bloodstains to interpret stain patterns and infer the mechanisms through which the patterns were generated. This becomes hugely important in



scenarios where the presence of blood at a scene or on a suspect is not disputed but the innocence of its origin is, as demonstrated in the case examples of *R v Jenkins* (1998) and *State v Camm* (2002) (**section 1.2.4**). In both these cases the presence of blood itself was not contended, instead the differing activity level propositions over the circumstances that led to the presence of blood were disputed.

In attempting to reach activity level propositions, analysts are guided by three founding principles. These principles assist with pattern identification and other aspects of activity level analysis and can be broadly defined as [1] the pattern diversity principle, [2] the principle of stain shape and vector correlation and [3] the physically altered bloodstain (PAB) principle (*Gardner. Griffin. 2010*).

In order to identify the bloodletting mechanism responsible for generation of a bloodstain pattern investigators carry out pattern identification in accordance with the pattern diversity principle. A series of ‘*objective criteria*’ (*Wonder. 2001*) help investigators categorize stain patterns into spatter or non-spatter stains and a range of discrete patterns within both of those categories, including: impact spatter, cast-off, drip, spurt, expired, flow, contact and void stains. Each of these pattern types is caused by a distinct mechanism, for example impact spatter patterns are generated by an impact or force acting on pooled blood (*SWGSTAIN. 2009*) whereas contact stains are generated by a blood-soaked surface coming into contact with a clean surface. Identification of the mechanisms responsible for the generation of certain patterns is reliant upon principles of fluid dynamics and informed by fluid responses to a range of different forces.

Following pattern identification, the principle of stain shape and vector correlation can be applied, in activity level analysis of blood pattern evidence, to contribute to crime scene reconstruction (*Gardner. Griffin. 2010*). The principle is based on two experimental observations relating to bloodstain morphology. According to collapse mechanics, stains impacting at angles display scalloping or tail features, which are related to direction of travel at impact (*Piotrowski. 1895*). In addition, the width and length ratio of stains is a direct empirical function of impact angle (*Balthazard et al. 1939*). These two observations allow investigators to establish the directionality and impact angle of stains through the application of associated trigonometric functions.

This allows a three-dimensional reconstruction of the area of stain origin to be carried out (*figure 5*).

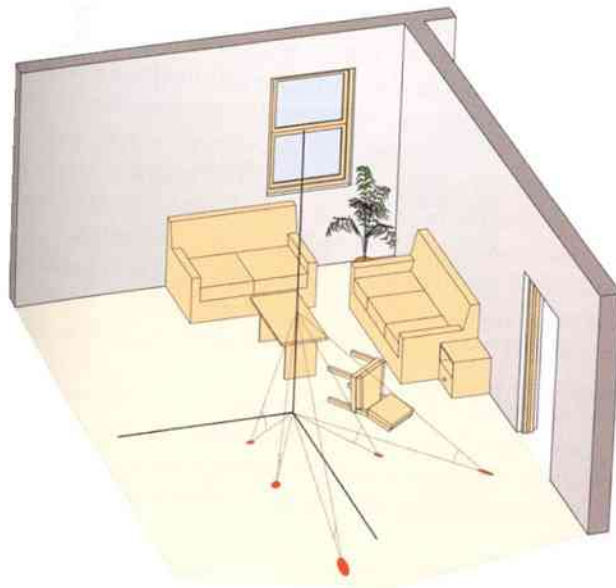


Figure 5 Sketch diagram of three-dimensional reconstruction of bloodstain origins from two-dimensional stains (*James et al. 2005: 219*)

The use of the principle of stain shape and vector is usually restricted to the analysis of spatter stains and in particular, impact spatter. Three-dimensional reconstructions of area of stain origin can be extremely useful when trying to establish the exact area of a crime scene where impact spatter originated. An example of where this might become critical might be in cases where a suspect claims they attacked a victim out of self-defence. By reconstructing the exact position and height of origin of an impact spatter pattern a distinction between the victim having been standing, sitting or lying when attacked may be possible. The inference drawn from victim positioning could be that had a victim been lying down during an attack, it is unlikely that the actions of the suspect were in self-defence. Activity level analysis can be further strengthened by cross-referencing pattern identifications and counts with forensic biological reports from medical examiner's observations of injuries sustained (*pers. comm. Wolson. 2011*).

A final consideration during activity level analysis of blood pattern evidence regards the physically altered bloodstain (PAB) principle (*Gardner. Griffin. 2010*). This recognises that blood, once exposed to environmental conditions, will react to

influences such as temperature, humidity and surface characteristics. These influences will most likely vary on a case-specific basis but may contribute to analysis if they exhibit some known predictability. For example, blood drying or coagulation times for a specific surface at a certain temperature. Whilst research has been conducted in some aspects of PABs, a much more concerted and focused effort is required in order to validate a wider inclusion of them in activity level analysis (Gardner. Griffin. 2010). The importance of this is undoubted, given that the majority of stains analysed will be affected by some environmental fluctuations.

By combining both source and activity level analysis of blood pattern evidence, forensic investigators can make a series of observations about the identity and location of bloodstains origins. The process of making these observations allows them to carry out crime scene reconstruction.

### **1.5 Limitations in forensic science and BPA**

A report published by the National Academy of Science (2009) entitled “Strengthening Forensic Science in the United States: A path forward” singled out many forensic science disciplines, including Blood Pattern Analysis, for critical review. The acknowledgements that “*faulty forensic science has, on occasion, contributed to the wrongful conviction of innocent persons*” (NAS. 2009:42) and that many forensic techniques have never been subjected to stringent scientific scrutiny provided the impetus for the NAS’s report, highlighting current limitations of forensic techniques. Over the course of three pages Blood Pattern Analysis was afforded particular attention. Criticisms were made of the perceived over-reliance on an expert’s personal experience given “*the importance of rigorous and objective hypothesis testing and the complex nature of fluid dynamics*” (NAS. 2009: 178) with the opinions of experts held as more subjective than scientific. The tendency for some experts to extrapolate experimentally established findings for certain blood stain analyses to other more unknown, highly variable situations was also identified by NAS authors as a cause for concern. Both the Jenkins and Camm case are examples of how this sort of extrapolation can become problematic, when the credibility of certain hypotheses proposed has not been experimentally established in a relevant case-specific context. The NAS authors demanded an increased volume of

case-specific experimental work as a necessary step to set about overcoming this trend (NAS. 2009: 178).

The NAS report highlighted general concerns with the state of forensic science at present as well as specifically with blood pattern analysis. As well as drawing attention to the weaker areas of the discipline, the observation of results being extrapolated from better-known areas of the field to less well-researched ones is an important one. It highlights the real need for increasingly scientifically based, case-specific empirical work in the field of blood pattern analysis, the impetus towards which should be driving future research projects.

At present certain aspects of blood pattern analysis remain under-researched and to an extent misunderstood, despite them being aspects which investigators may reasonably encounter on a regular basis. It should be reiterated that this assessment does not extend to the entire discipline and only to certain aspects of BPA and absolutely does not concur with the NAS report's claim that "*The uncertainties associated with bloodstain pattern analysis are enormous*" (NAS. 2009: 179). The aspects referred to include the behaviour of blood on fabric surfaces, methods of visualizing bloodstains on dark surfaces, methods of determining the age of bloodstains, determining the extent of bias in bloodstain pattern analysis, examining the effects of variability in blood composition on resulting bloodstain pattern formation and the effects of environmental variability on identification of bloodstain patterns (SWGSTAIN. 2011: 1-4). By extension, in some of these areas, whilst an accepted level of understanding of certain phenomena may exist amongst the expert practitioner community, relatively little of that understanding may remain documented in peer-reviewed literature (Laber et al. 2008. Gardner. Griffin. 2010).

In order for practitioners to be qualified to give empirically based, objective testimony on these more (at present) ambiguous areas of blood pattern analysis, an experimental body of research into each area needs to be produced and subjected to peer-review. Until this is completed limitations exist to the extent to which Blood Pattern Analysts can produce definitively accurate source and activity analyses and crime scene reconstructions for the entire range of stains encountered.

## 1.6 The future of forensic science and BPA

The response of forensic science, and in particular Blood Pattern Analysis, to the criticisms levelled by the NAS report has to be clearly organised. Whilst orchestrating this response it is important to acknowledge that certain criticisms made by the report appear somewhat contradictory or inaccurate and as such the contents of the report should be digested accordingly. The report ignores the scientifically founded principles of pattern diversity, stain shape and vector and physiologically altered bloodstains on its way to claiming the discipline's emphasis is on '*experience over scientific foundation*' (NAS. 2009: 178) for example. A more general criticism is also made that with the exception of DNA analysis other forensic methods, such as BPA, have '*evolved piecemeal in response to law enforcement needs*' and have never been '*closely scrutinized by the scientific community*' (Frueh. Yeibio. 2009). This is somewhat at odds with the reality that as a forensic discipline BPA has been reported in scientific literature for over a hundred years with its first major developments noted by doctors of forensic medicine, well versed in scientific methods of research (Gardner. Griffin. 2010).

Notwithstanding some of the inaccuracies contained within the NAS report, it does however prompt some necessary and valuable discussions regarding the future direction of the discipline. Where possible, focus needs to continue towards establishing a set of universally accepted objective criteria for source and activity level analysis (Wonder. 2001). Development of such criteria should aim to be conducted through a combination of experimental studies, case-specific analyses and peer-review, in both academic and practitioner-based environments, to ensure scientific robustness of research conclusions (Gardner. Griffin. 2010). Ensuring practising analysts are then proficient and familiar with these criteria is essential.

Areas of the discipline for which objective analytical criteria are lacking, or are in the process of development, should be identified and acknowledged as areas about which activity level propositions and crime scene reconstructions should be very cautiously, if at all, made. For example, the limitations at present of incorporating certain physiologically altered bloodstains (PABs) into analyses should be acknowledged and adhered to.

Throughout, the development of analytical techniques should be conducted with an appreciation of their role within the context of the entire forensic process, which progresses from crime scene to courtroom. The analysis of evidence exists as a stage within the wider processes of crime scene investigation and reconstruction. In order to ensure initial relevance of enquiry, the development of appropriate techniques and proper communication of techniques and results to a layperson jury, the development of analytical techniques therefore should be conducted with a more holistic appreciation of the entire investigative process.

Research in the field of Blood Pattern Analysis should always be conducted with a consideration to its future possible application in crime scene reconstruction. The power of crime scene reconstruction is reliant on several conditions: accuracy and plausibility of reconstructions, existence of scientifically robust methods of analysing source and activity level evidence and the ability of a jury to attach appropriate evidential weight to reconstructions offered. The research outlined in this thesis is concerned majorly with the first two of these conditions, focusing on the development of analytical techniques for interpreting bloodstains that have been exposed to environmental variations. A set of hypotheses, informed by peer-reviewed literature and discussions with practitioners were tested through a series of experiments to ensure the scientific robustness of data collected and associated conclusions drawn from them.

## **1.7 Outline of content**

Content is set out in three sections, each of which consists of a number of chapters. An explanation of the content of each section and chapter follows.

### **1.7.1 Section 1**

In section 1 Bloodstain pattern analysis (BPA) as a forensic technique for crime scene reconstruction is introduced. A literature review for the discipline and existing gaps in related experimental research is presented and experimental hypotheses formulated.

### **1.7.1.1 Chapter 1**

Chapter 1 introduces the forensic discipline of Bloodstain Pattern Analysis (BPA) through discussion of its role in trace evidence analysis. The relevance of Locard's exchange principle and evidence dynamics to the interpretation of Bloodstain Pattern evidence are discussed in the context of interpretation of evidence at source and activity levels during the process of crime scene reconstruction. Case-specific examples of the use of BPA in real forensic scenarios are provided.

### **1.7.1.2 Chapter 2**

Chapter 2 contains a literature review of Bloodstain Pattern Analysis (BPA) and outlines the research project. In depth reviews for the particular areas of research focus (identification of bloodstains, physically altered bloodstains and influence of surface characteristics on stains) are included.

### **1.7.1.3 Chapter 3**

Chapter 3 sets out an experimental overview and the formulation of specific hypotheses for testing by separate experimental stages. The development of a general methodological approach is prescribed and general methodological considerations relevant to all experimental work are outlined.

## **1.7.2 Section 2**

Section 2 sets out all methodologies and results for individual experimental stages.

### **1.7.2.1 Chapter 4**

Chapter 4 provides a methodological overview of experimental stage 1, which examined the effects of controlled environmental variations on bloodstain patterns.

### **1.7.2.2 Chapter 5**

Chapter 5 presents analysis of results from experimental stage 1.

### **1.7.2.3 Chapter 6**

Chapter 6 provides a methodological overview of experimental stage 2, which expands the experimental design of experimental stage 1 to explore the effects of

natural fluctuations in environmental influences on bloodstain identification methods, over longitudinal and monthly timeframes.

#### **1.7.2.4 Chapter 7**

Chapter 7 presents analysis of results from experimental stage 2.

#### **1.7.2.5 Chapter 8**

Chapter 8 provides a methodological overview of experimental stage 3, which examines the influence of extreme environmental conditions on bloodstains.

#### **1.7.2.6 Chapter 9**

Chapter 9 presents analysis of results from experimental stage 3.

#### **1.7.2.7 Chapter 10**

Chapter 10 provides a synthesis of results from experimental stages 1, 2 & 3.

#### **1.7.2.8 Chapter 11**

Chapter 11 provides a methodological overview of experimental stage 4, which examines the influence of environmental variations and surface characteristics on stain drying time.

#### **1.7.2.9 Chapter 12**

Chapter 12 presents analysis of results from experimental stage 4.

### **1.7.3 Section 3**

Section 3 contains a synthesis of experimental results to allow conclusions to be made about the validity of interpreting of environmentally altered bloodstains for the purposes of crime scene reconstruction.

#### **1.7.3.1 Chapter 13**

Chapter 13 presents a discussion of experimental research in the context of implications for source & activity level interpretations of bloodstain pattern evidence and the process of crime scene reconstruction.



### **1.7.3.2 Chapter 14**

Chapter 13 presents a concluding discussion of the main findings and implications of research.

## 2. Literature Review

### 2.1 Blood and Bloodstain Pattern Analysis

#### 2.1.1 Blood

Blood is the circulating fluid tissue found in humans and other vertebrate animals accounting for approximately 8% body weight in humans (*Peschel et al. 2011*). The fluid and formed elements suspended in it circulate in axial laminar flow (*Wonder. 2001: 29*) continually through the body and the circulatory system, the heart, arteries, capillaries and veins (*Stedmans Medical Dictionary. 2005*) (*figure 6*). As an organ blood has two primary functions, it facilitates the transportation of 1) Oxygen and nutritive materials to the tissues and 2) Carbon dioxide and metabolic waste products away from the tissues.

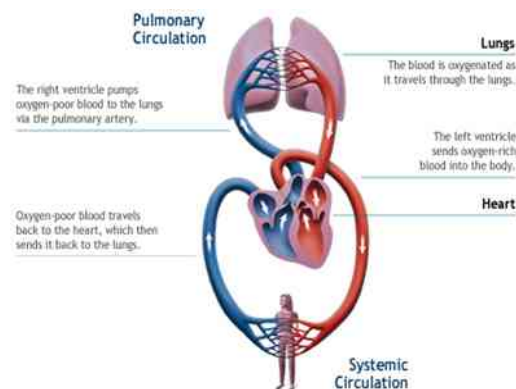


Figure 6 Schematic diagram of the human circulatory system  
(*Tracleer.com*)

The internal composition of blood can be broken down into two component groups; plasma and formed elements. Plasma is the liquid portion of blood, made up of approximately 91% water. The remaining 9% consists of various dissolved materials, such as hormones, metabolic waste products (including urea), carbohydrate food materials (including glucose, amino acids and lipids) and gases (including oxygen, nitrogen and carbon dioxide). The formed elements are the second component group of blood, consisting of everything that is not plasma; erythrocytes (red blood cells),

leucocytes (white blood cells) and platelets (small, cytoplasmic fragments central to process of blood clotting) (*Christman. 1996*).

As a fluid, blood has no shape of its own (*Peschel et al. 2011*). It relies upon the influence of surrounding surfaces as well as internal and external forces acting on it in order to maintain any shape. Whilst inside the body the structural walls of blood vessels enclose the blood and restrict its shape to that of the circulatory system. However, once released from the confines of these vessels, a number of complex mechanisms involving internal and external forces act on the blood, dictating its behaviour and dispersal through space (*Raymond et al. 1995*). This is an important consideration when attempting to interpret the morphology of blood outside of the circulatory system, for example, bloodstains at a crime scene.

Blood, as a fluid, is influenced by internal forces, which include surface tension, internal cohesion and viscosity as well as external forces such as air resistance, gravity and the external application of force (*Bevel. Gardner. 2008*). Internal forces significantly influence the behaviour of all fluids to the extent that they can be categorized according to their properties of surface tension, internal cohesion and viscosity into Newtonian and Non-Newtonian fluids (*Elena. Mohamed. 2009*). Differences in properties between these groups of fluids dictate differences in the ways they behave. The behaviour of Newtonian fluids (for example water) is largely determined by surface tension whereas the behaviour of Non-Newtonian fluids (for example blood) by contrast is dictated more by internal cohesion (*Wonder. 2003*) (*figure 7*).

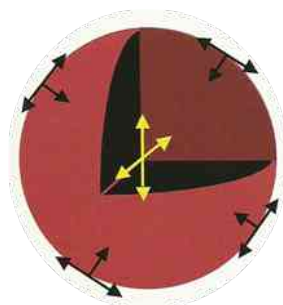


Figure 7 Spherical drop of blood in cross-section indicating forces of surface tension (black arrows) and internal cohesion (yellow arrows)

(*Wonder. 2001: 27*)

Internal cohesion acts throughout a fluid, whereas surface tension acts at the surface of a fluid. This means that blood experiences much greater internal stability than

water, which prevents drop separation. Within the circulatory system this resistance to drop separation is vital to maintaining the constant flow of blood required for circulation. Outside the circulatory system, it means that a much greater force must be applied to blood, in order to overcome internal cohesion acting throughout the blood and generate and disperse it as drops. Once dispersed as flows or drops, this stability is imparted to resulting fluid flows or drops (*Wonder. 2001*), establishing parameters for their behaviour when acted upon by external forces such as gravity, air resistance or the application of force (*Bevel. Gardner. 2008*).

These parameters, dictated by the unique characteristics and Non-Newtonian nature of blood, mean that when a volume of it is dispersed by external forces it results in “*predictable and reproducible patterns*” (*Wonder. 2001: 28*). If sufficiently understood, these patterns can be interpreted as records of the dynamic events responsible for their generation, allowing calculation of forces and mechanisms that have been applied to a mass of blood. The ability to do so makes patterns formed by Non-Newtonian fluids particularly suitable to interpretation (*Raymond et al. 1995*) unlike patterns generated from Newtonian fluids such as water.

### **2.1.2 Blood in a forensic context**

The significance of blood to the forensic scientist is in its association with crime events as physical evidence generated during a bloodletting event or mechanism (*Laber et al. 2008*). Of all physical trace and fluid evidences “*blood is one of the most significant and frequent types of physical evidence associated with the forensic investigation of death and violent crime*” (*James et al. 2005: 1*). As such, bloodstains analysed in the aftermath of a crime event is one of the most important evidence interpreted at a crime scene (*Boonkhong et al. 2010*).

During a crime event, external forces acting on a body bring about injuries that often result in the expulsion of blood as blood drops or flows. Interactions between the internal forces of surface tension, viscosity and internal cohesion and external forces of gravity, air resistance and applications of force determine the manner in which blood is expelled. These interactions determine with certain predictability, the nature

and formation of blood drops, the forces required to disperse blood from a source and how blood behaves upon interaction with external forces.

Following impact with a surface, droplets of blood deform to generate bloodstains. The Non-Newtonian nature of blood dictates that stains will be formed in a predictable manner. With knowledge of blood dynamics therefore the morphology and characteristics of stains can be interpreted to infer the mechanics required to generate them (*Bevel. Gardner. 2008*). This may include estimations of the magnitude, direction and type of force involved in a bloodletting mechanism.

Accurate analysis and interpretation of bloodstains and patterns formed collectively by them allows investigators to establish the nature, locations, directionality and chronology of bloodletting events associated with a crime scene (*Bevel. Gardner. 2008*). The forensic technique of analysing bloodstains and patterns associated with a crime is Bloodstain Pattern Analysis (BPA).

### 2.1.3 Bloodstain Pattern Analysis

*“Bloodstain pattern analysis (BPA) is defined as the examination of the shapes, size, locations and distribution patterns of bloodstains, in order to provide an objective analysis of the physical events that gave rise to their origin by application of concepts of biology, biochemistry, physics and mathematics”*

**IABPA. 2009**

Bloodstain Pattern Analysis (BPA) is a forensic technique concerned with the collection, categorization and interpretation of bloodstains connected with a crime (*Peschel et al. 2011*). It draws heavily on the scientific disciplines of mathematics, fluid dynamics, chemistry, forensic biology, physics and medical science (*Wonder. 2003*) to determine from the size, shape and distribution of bloodstains which activities and mechanisms produced them (*James et al. 2005:1*).

As it is concerned with the interpretation of traces of blood, the technique is an example of trace evidence analysis (*section 1.2*). The fundamental trace evidence analysis concepts of Locard’s exchange principle and evidence dynamics can therefore be applied to analysis of blood traces. This allows bloodstain pattern

analysts to complete source and activity level analyses in their interpretations of blood evidence, identifying where and what bloodletting event has occurred.

Through inferences about source and activity level origins of bloodstains and pattern evidence investigators can contribute to crime scene reconstruction (*section 1.3*), a process of holistically analysing a scene in order to achieve a fuller understanding of a crime event and objective interpretation of the crime dynamics (*Chisum. Turvey. 2000. Fratini et al 2006*). In this regard the practice of BPA can provide a significant contribution to criminal investigations (*Pizzamiglio et al. 2006*).

Areas of the discipline have and continue to be empirically developed in order to enhance the ability of analysts to complete both source and activity levels of analysis. Development of techniques has focused on establishing, through experimental work and an understanding of fluid dynamics, sets of objective criteria and methods through which to analyse stains and patterns. As a result, a range of different methods for the analysis of bloodstain patterns has been developed. A description of the development of these methods and the principles that underpin them is set out in *section 2.2*.

## **2.2 Development of basic Bloodstain Pattern Analysis techniques**

The discipline of BPA draws on many scientific disciplines such as mathematics, physics, biology, chemistry, fluid dynamics and medical science, which provide an underlying framework of knowledge in which it is grounded. The specific theoretical tenets of the discipline have been developed through a process of empirical research, which has resulted in the formation of a set of founding principles of BPA. These principles include the general application of Locard's exchange principle and evidence dynamics but also principles particularly pertinent to the interpretation of bloodstain evidence. These principles include the 1) Principle of stain size and vector, 2) Pattern diversity principle and 3) the Principle of Physically Altered Bloodstains (PABS) (*Gardner. Griffin. 2010*). These three principles act as founding principles from which both basic and advanced techniques of BPA have developed, providing robust guidance to analysts, and were prescribed as the theoretical

fundamentals of the discipline in response to the National Academy of Sciences' 2009 report critiquing the discipline (*Gardner. Griffin. 2010*). The principles are individually, as well as collectively, reliant on perhaps the most fundamental theoretic of BPA – an expectation that blood, acted upon by force, responds in a predictable and reproducible manner (*Wonder. 2001*). The role of these principles in the development of BPA techniques is expanded on in sections 2.2.1, 2.2.2 and 2.3.3.

### 2.2.1 Determining horizontal origin, impact angle and vertical origin of a stain

As a blood drop in flight encounters a surface it deforms on impact in a defined fashion to form a bloodstain (*Bevel. Gardner. 2008*). Stain characteristics are generated as a function of the collapse mechanics of a drop and can be interpreted to calculate direction and angle the drop was travelling in upon impact.

Direction of travel can be determined through an analysis of directionality from characteristics 'of a bloodstain that indicate the direction blood was moving in at the time of deposition' (*SWGSTAIN. 2009*). These characteristics are generated when a drop impacts a surface at an angle (*figure 8*).

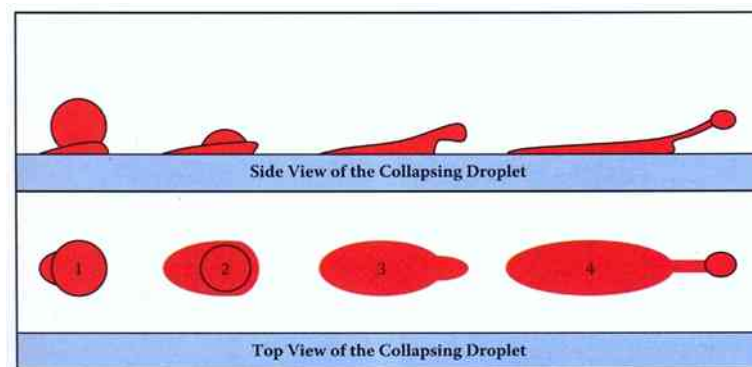


Figure 8 Sketch diagram of the different stages of collapse mechanics of a blood drop impacting a surface at an angle (*Bevel. Gardner. 2008: 151*)

As the drop impacts, a portion of the drop makes contact with the surface first and stops moving, creating the beginning of an ellipse [1] (*Wonder. 2001*). The remainder of the drop continues to travel in the original direction, collapsing as it continues (*Bevel. Gardner. 2008*). As it does so the ellipse generated by the initial contact will widen until approximately half of the drop has collapsed [2]. As mass of

blood decreases following this point, during the second half of this elongated collapse, the stain narrows in the direction of original travel [3] (*Bevel. Gardner. 2008*). The narrowing of the stain may conclude in the formation of characteristics such as a tail, scallops and spines or satellite stains [4] (*figure 9*).



Figure 9 Narrowing of stains to form directional characteristics: tail (left), scallops (middle) and satellite stains (right) (*Bevel. Gardner. 2008: 171*)

As impact angle decreases from close to a  $90^\circ$  perpendicular impact towards a more acutely angled impact of  $10^\circ$ , the elongation of a stain increases and formation of directional characteristics becomes clearer (*figure 10*).

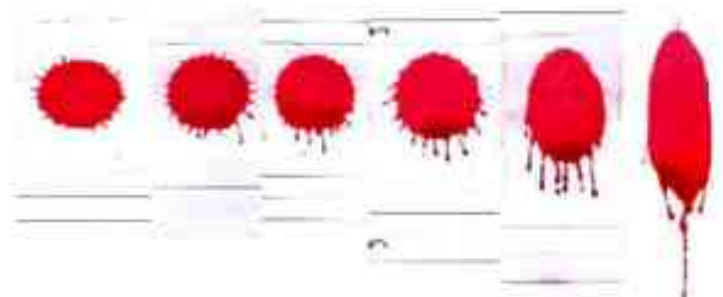


Figure 10 Images of stains generated at a range of impact angles demonstrating elongation of stain body and emergence of clear directional characteristics. Angles of impact for stains, from left to right:  $90^\circ$ ,  $78^\circ$ ,  $62^\circ$ ,  $56^\circ$ ,  $44^\circ$  and  $22^\circ$ . (*Author. 2009*)

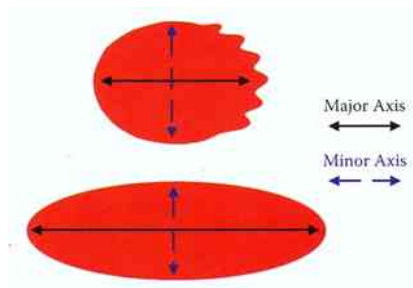


Figure 11 Illustration of major and minor axis of two stains with different directional characteristics

(*Bevel. Gardner. 2008: 171*)



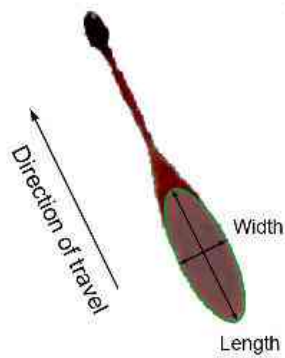


Figure 12 Image illustrating elongation of a stain into a tail and indication of direction of travel through alignment with the major axis (length)

(<http://forensics4fiction.wordpress.com>)

The axis along which a stain collapses and is elongated is labelled the major axis of the stain (*figure 11*). This axis is always aligned to the direction of travel and the elongation of a stain along it can therefore be used to indicate the directionality of an impact (*Bevel. Gardner. 2002. Elena. Mohamed. 2009*) (*figure 12*).

By running a string back along a tail and along the major axis of a stain, opposite to the direction of travel, a line can be drawn back towards the origin of a stain. Use of this technique to identify the horizontal origins of a stain is known as '*stringing method*' (*Bevel. Gardner. 2008*).



Figure 13 Collective stain pattern comprised of multiple stains, with yellow arrows indicative of general directionality of pattern

(*James et al. 2005*)

For certain bloodstain patterns, namely impact spatter patterns, the stringing method can be carried out for multiple stains within a collective stain pattern (*figure 13*) to generate an area of string convergence (*figure 14*). The location of this area will approximately correspond to the source or area of origin for a spatter generating impact (*Pizzola et al. 1986: 37*).

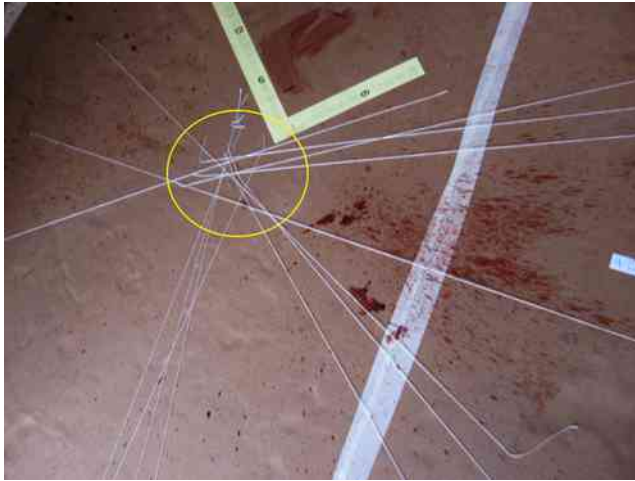


Figure 14 Photograph identifying an area of string convergence, (circled in yellow), for multiple stains within a collective stain pattern

(Author. 2011)

The development of “*stringing methods*” (Bevel et al. 2002) as a method of drawing straight lines back from bloodstains to determine the origin of each stain is based on observations made during the earliest experimental studies in the field of BPA, of the relationships between directionality and tailing of a stain.

In one of the earliest published experimental manuscripts on Bloodstain Pattern Analysis; “*Concerning the origin, shape, direction and distribution of the bloodstains following head wound caused by blows*” (1895) Dr Eduard Piotrowski was the first to comment on the elongation of bloodstains and the layout of collective stain patterns. Having conducted beating experiments on animals he observed that varying the implement and force applied was reflected in stain patterns generated from impacts. As bloodstains impacted at angles he also noted the tendency for them to exhibit tailed stain morphology, aligned to directionality of impact. This manuscript was the first to postulate, “*the formation, shape and distribution of bloodstains follow specific rules*” (Piotrowski. 1895: 32 cited in Bevel. Gardner. 2008: 6). Exploration of the possible investigative applications of these rules was carried out in 1939 by Dr Victor Balthazard, who pioneered the idea of using ‘stringing techniques’ to locate the horizontal origin of multiple stains within a collective pattern (Bevel. Gardner. 2008).

Conducting directionality analysis for a bloodstain pattern assists analysts with the identification of an area of origin for bloodstains on a horizontal plane. As Balthazard recognised however, there are limitations to only being able to estimate the horizontal area of blood origin. Occasionally, he stated, “*it is necessary to find*

out [from a bloodstain] whether a victim, at the moment he was injured, stood on his feet or was lying” (Balthazard et al. 1939: 25 cited in Bevel. Gardner. 2008: 11). In order to infer which position is more likely some method of calculating the vertical origins of a bloodstain is necessary.

Development of a method of identifying the vertical origins of a bloodstain was furthered by Balthazar’s observations that width-to-length ratios of individual stains are a function of impact angle (Balthazard et al. 1939). The angle at which a drop impacts therefore defines the shape of the resulting stain. Circular stains are formed by impacts close to the perpendicular (90°) whilst more elliptical stains are generated by impacts at more acute angles (Bevel. Gardner. 2008). These observations were further refined, until it was established that by entering the width/length ratio of a stain into a specific trigonometric function (the sine function) impact angle could be calculated (Macdonell. 1982 reported in Bevel. Gardner. 2008: 171) (figure 15).

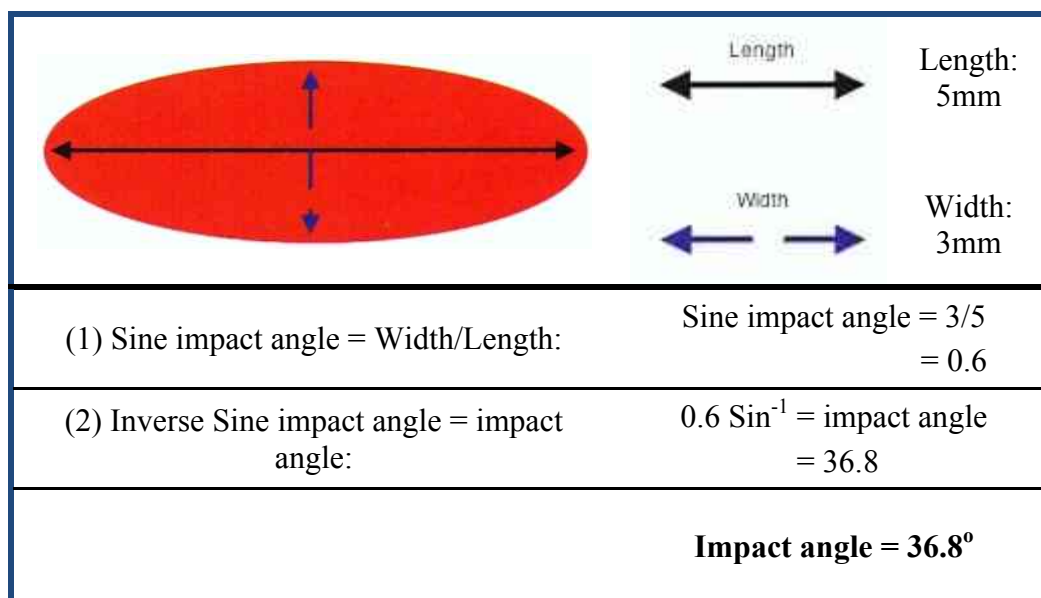


Figure 15 Calculation of Impact angle from stain length and width measurements with trigonometric Sine function (Bevel. Gardner. 2008: 173)

This function allows analysts to give “an estimate of impact angle with an acceptable accuracy” (Balthazard et al. 1939 cited in Bevel. Gardner. 2008), of within 2-7° depending on the stain shape. Impact angles for elliptical stains can generally be calculated with greater precision than impact angles for more circular stains.

Whilst calculations of both directionality and impact angle can be used in the analysis of individual stains, use of them to calculate the vertical origin of a bloodstain is most effective when applied to multiple stains within a collective pattern (*Bevel. Gardner. 2008*). Most specifically, they are used for calculating the vertical origin for stain patterns generated by particular impact spatter mechanisms. The use of them in calculations of vertical origins of blood is therefore restricted to these patterns and impact spatter analysis.

Impact spatter analysis combines methods of establishing an area of convergence (two-dimensional approximation of blood source or origin) with calculations relating to individual stain sizes and shapes to draw an inference about the approximate three-dimensional source of those stains (*Raymond et al. 1996: 162. Laber et al. 2008*). In order to calculate the three-dimensional source of a bloodstain through impact spatter analysis, multiple stains within a pattern must be included in the analysis.

For multiple stains within an impact spatter pattern the process of identifying the vertical area of origin or source is as follows. Directionality analysis is carried out for a number of stains within a pattern and horizontal stringing is completed for these stains in order to identify an area of convergence (*figure 16*). Impact angles are then



Figure 16 Photograph of area of convergence with addition of vertical (green) strings running back from leading edges of stains, at impact angles, to the area of convergence, to give vertical origins of stains

(*Author. 2011*)

calculated from the width to length ratios of each stain. Having calculated the impact angle of each stain, analysts attach a string to the leading edge of each bloodstain and run it back towards the area of convergence at the corresponding angle (*Bevel. Gardner. 2008*).

The point where the vertical string meets the area of convergence is the ‘approximate’ vertical positioning, and point of origin in three-dimensions for each individual stain (*Boonkhong et al. 2010*). The term ‘approximate’ is used because it is rare that bloodstains in a spatter pattern will have emanated from a single point. More commonly a source of blood is an object with three-dimensional area and multiple ‘points of origin’ within that area may emerge for a single spatter pattern as stains within the pattern are analysed. In combination, these points indicate an area of vertical origin. This can be extremely useful to analysts, particularly in cases where it is necessary to identify the upright position of a victim at the point of bloodletting. Stringing carried out for stains generated on vertical surfaces can similarly give indications of vertical positionality of a blood source (*figure 17*).



Figure 17 Example of physical stringing technique for multiple stain patterns generated on vertical surfaces

(*Author. 2011*)

A mathematical ‘tangent’ method can be incorporated into impact spatter analysis, to act as a substitute for the often laborious process of identifying vertical origins of stains through physical stringing (*Bevel. Gardner. 2008*).

In the tangent method, directionality of stains is analysed first to identify a point, or area of convergence (**C/POC**). Once this has been done, for each stain, the distance

(D) from the leading edge of the stain to the point or area of convergence is measured (*figure 18*).

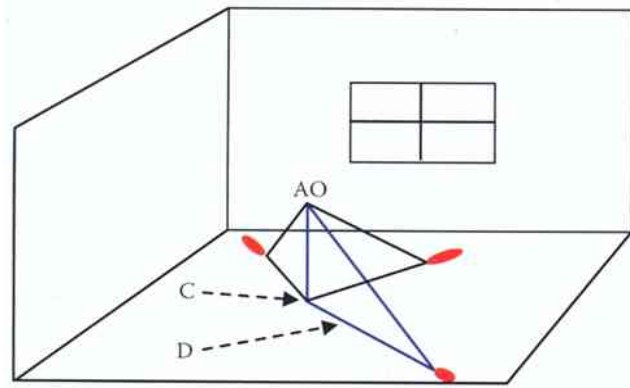


Figure 18 Illustration of relationship between point or area of convergence (C/POC), distance to the leading edge of a stain (D) and vertical area of origin (AO)

(Bevel. Gardner. 2008: 184)

Width and length measurements of individual stains are then used to calculate impact angles (*i*) for individual stains.

The tangent method is based on the known relationship for a right-angled triangle that:  $\tan \theta = \text{opposite side} / \text{adjacent side}$  ( $\theta$ : angle). Once distances (D) and impact angles (*i*) have been calculated, a right-angled triangle is imagined between the three points of (1) leading edge of a stain, (2) point/area of convergence (C/POC) and (3) vertical area of origin (AO) (*figure 19*). The height (H) of the vertical area of origin (AO) represents one side of this triangle. Other known measurements within the triangle can be used to calculate height, which locates the vertical position of origin of blood.

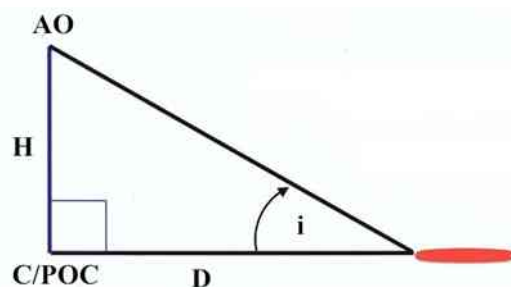


Figure 19 Right-angled triangle drawn between leading edge of stain, point/area of convergence (C/POC) and vertical area of origin (AO) with distance between stain and point/area of convergence (D), impact angle (*i*) and height of vertical area of origin (H) also labelled

(Author. 2013)

As the tangent formula dictates;  $\tan \theta = \text{opposite side} / \text{adjacent side}$  : so  $\tan i = \text{height (H)} / \text{distance (D)}$ . To calculate the unknown H the formula is rearranged so that;  $H = \tan i \times D$  (Bevel. Gardner. 2008).

Techniques developed from the initial observations of Piotrowski and Balthazard allow analysts to calculate the impact angle, horizontal and vertical origins of a bloodstain. These techniques have developed as the basic tools of Bloodstain Pattern Analysis, assisting investigators to achieve an “*accurate interpretation of bloodstain morphology, geometry and directionality [to] allow the calculation of an angle of impact and blood source position within a 3-dimensional space*” (Millington. 2004: 3) from analysis of two-dimensional stain morphologies. By calculating the three-dimensional sources of blood within a crime scene an investigator can establish the positionality of individuals involved during each bloodletting event, the chronology of events and the nature of the bloodletting mechanisms involved.

This allows blood pattern analysts to begin reconstruction of a crime scene on the basis of blood evidence observed at the scene.

In addition they can use more complex tools such as pattern identification to help them build up a more informed reconstruction of a crime scene.

### **2.2.2 Pattern identification**

Pattern identification is based on the expectation that, due to inherent characteristics, blood responds to forces in a predictable and reproducible manner (Wonder. 2001). Variations in volume of blood and forces acting on blood generate a range of reproducible responses, which allows classification of bloodstain patterns according to pattern type. Classification of pattern type therefore corresponds to the nature of the underlying events or mechanisms responsible for stain generation (Bevel. Gardner. 2012. b). Six basic, reproducible, pattern types exist and each type corresponds to a particular underlying blood generation mechanism. The corresponding mechanisms are:

- Ejection of blood from a point source
- Ejection of blood from an object in motion
- Streaming ejections of blood
- Dispersal of blood through air as a function of gravity



- Accumulation of blood on a surface
- Deposition of blood through a transfer

(Bevel. Gardner. 2012. b).

Within each of these basic mechanism types sub-types exist.

Identification and classification of discrete stain patterns relies on the comparison of a set of objective criteria to distinct stain patterns (Wonder. 2001). These criteria relate to the morphology of primary stains, overall stain distribution, the size or range of sizes of individual stains within a pattern, the presence of volume in individual stains, margin characteristics and satellite or spine characteristics (Bevel. Gardner. 2008). A taxonomic classification system can be used to work through objective criteria for stains observed in order to identify pattern types present. The system advocates a top-down approach to pattern identification, which begins with distinction of stains according to broad objective criteria, for example, dividing stain patterns between two groups; spatter (figure 20) and non-spatter (figure 21) stains, according to the circular or elliptical nature of primary stains (Bevel. Gardner. 2012).

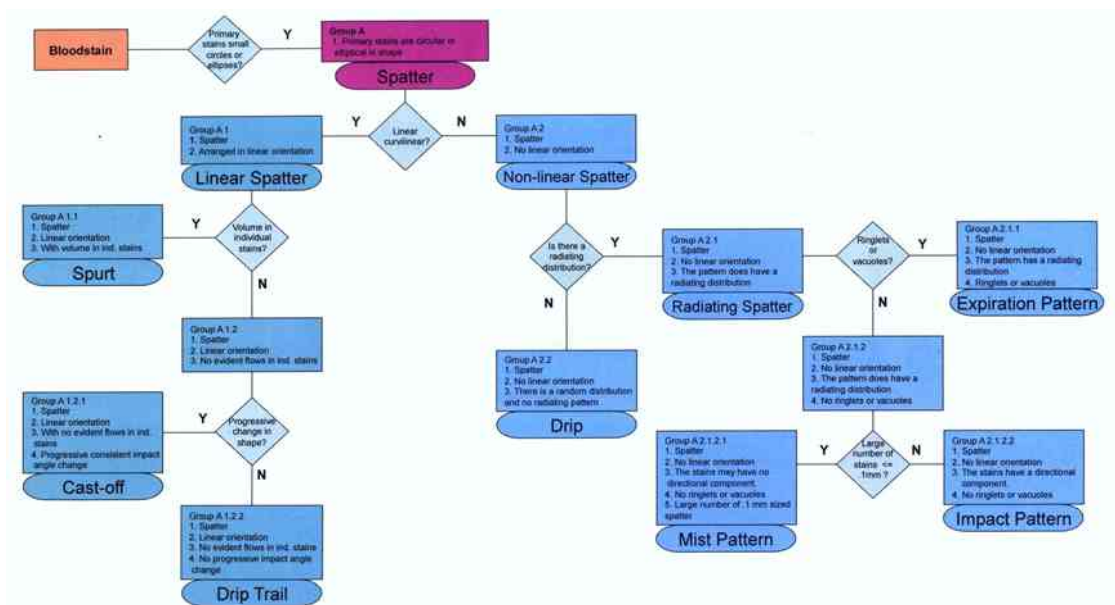


Figure 20 Taxonomic classification system for spatter stains (Bevel. Gardner. 2013)



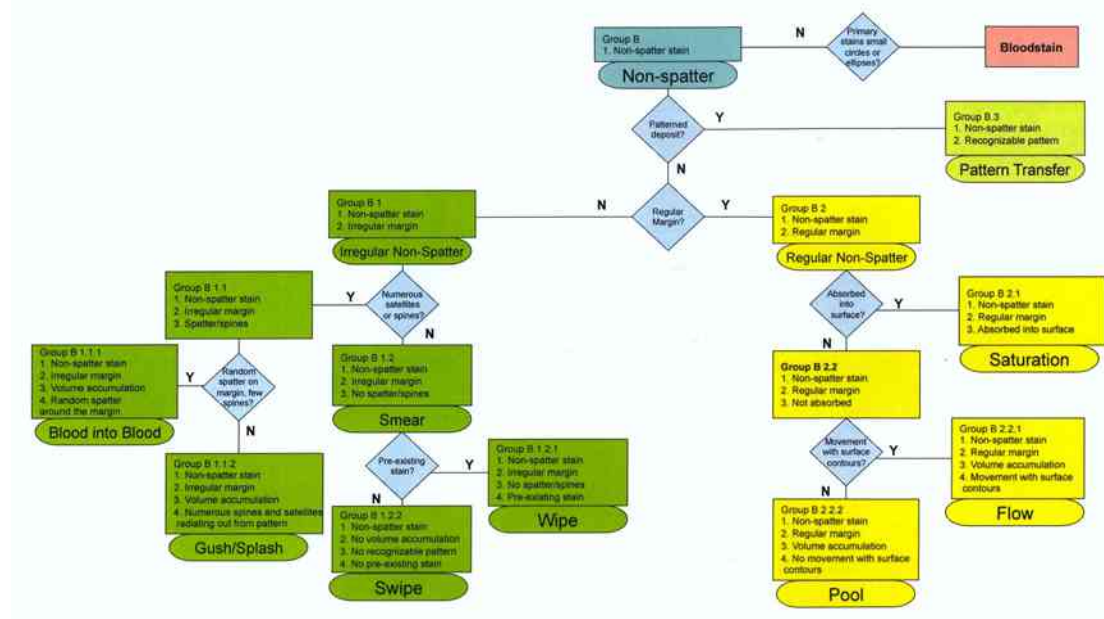


Figure 21 Taxonomic classification system for non-spatter stains (Bevel. Gardner. 2013)

Once patterns have been classified as either spatter or non-spatter stains, further criteria are chronologically applied in order to further classify pattern types (figures 20 & 21). For example, identifying a pattern as an impact pattern would require confirmation of certain criteria, in the following order: spatter stain (Spatter), non linear or curvilinear distribution (Non-linear), radiating distribution (Radiating spatter), no ringlets or vacuoles and a small number of stains sized  $< 0.1\text{mm}$ . By chronologically progressing through the classification systems at any point if further classification is impossible, classifications made up to that point are still valid.

Once discrete patterns have been identified and classified, inferences can be made regarding the generating mechanism or source event for the pattern (James et al. 2005). For example, a pattern identified as an impact spatter pattern will be characterised by circular or elliptical primary stains with a radiating distribution from a central point and a progressive change in the shape and size of stains throughout the pattern. Patterns with these characteristics are associated with the generating mechanism or source event of a '*blood source being broken up at some point by some force*' (Bevel. Gardner. 2012. b:18). Generation mechanisms or source events generally associated with different classifications of patterns (figures 20 & 21) are outlined in figure 22.

Pattern	Spatter	Non-spatter	Generating mechanism or source event
Spurt			Stream of blood escaping under pressure usually from a breach in an artery or the heart showing pressure, pressure fluctuations in a discrete pattern
Cast-off			Blood being flung or projected from an object either in motion, or which suddenly stops some motion
Drip Trail			Deposition of individual bloodstains on a surface, demonstrating movement of the item
Drip			Deposition of an individual bloodstain on a surface
Impact			Breaking up of blood source by application of force
Mist			Breaking up of blood source by application of explosive force
Expiration			Blood being forced from the mouth, nose, or respiratory system under pressure
Blood into blood			Liquid blood dripping into blood or another liquid
Gush/Splash			Large volume of blood escaping under pressure, usually from a breach in an artery or the heart
Smear			Transfer of blood from one object to another through contact involving lateral motion
Swipe			Transfer of blood onto a target by a bloodstained object in motion
Wipe			Movement of an object through a pre-existing stain
Pool			Pooling of liquid blood according to gravity and container characteristics of the pooling area
Saturation			Contact with a significant blood source (pool/flow)
Flow			Movement of fluid blood as a mass under the effect of gravity
Pattern transfer			Transfer of blood from one object to another in which a recognizable image or characteristic is visible in the pattern

Figure 22 Description of generation mechanisms or source events generally associated with different classifications of bloodstain patterns (*Bevel. Gardner. 2012: 15-21*)

Identification and classification of bloodstains according to objective criteria and pattern type allows analysts to interpret bloodstains in the context of a particular source event, or generating mechanism (*Bevel. Gardner. 2008*). This allows them to

infer types of bloodletting events and activities associated with bloodstains at a crime scene.

### **2.3 Development of methods for advanced Bloodstain Pattern Analysis**

The focus of research to date in the field of Bloodstain Pattern Analysis has largely been on developing methods of stain and pattern analysis through experimental observations. Early experimental observations regarding stain shape and size have ultimately led to the development of two principles, which remain key to modern-day bloodstain pattern analysis: the principle of stain size and vector, and the pattern diversity principle. Analysts continue to apply these principles to stain analysis in order to objectively identify horizontal and vertical origins, impact angle and source event or generating mechanism for a bloodstain.

Increasingly however, in recognition of the existence of increasingly complex stain and pattern interactions, the discipline has progressed to developing more complex understanding of the influence of other variables, for example impact surface characteristics and environmental factors on bloodstain analysis. This progression has sought to develop advanced techniques for interpretation and analysis of stains, which go beyond the relatively simple analyses of directionality, width and length measurements or pattern identification (*Hulse-Smith et al. 2005*). Given the extraordinary variability in crime scene circumstances an analyst may encounter, the development of more complex BPA methods for analysing stains within these case-specific circumstances is highly necessary.

A review of the literature, to date, highlights the need for the development of more advanced methods of Bloodstain Pattern Analysis. It identifies several more complex characteristics of bloodstain patterns, the understanding of which is empirically incomplete, that currently place limitations on the ability of an analyst to complete advanced crime scene reconstructions from bloodstains.

### 2.3.1 Formation of spines and satellites

High-speed photography of a blood droplet impacting with a smooth, non-porous surface (in this case cardboard) demonstrates the characteristically sudden transfer of momentum within a falling drop from the vertical to the horizontal upon impact (*Thoroddsen. Sakakibara. 1998: 1359*) (*figure 23*).



**Figure 23** High-speed photography of a blood droplet impacting with smooth cardboard displaying transfer of momentum from the vertical to the horizontal direction (*Laber et al. 2008*)

As the blood collides with the dry, solid surface it impacts with a ring-shaped liquid/solid contact area within which air is trapped to temporarily form a semi-convex bubble of air. As the momentum is transferred to the horizontal the non-contact area of fluid held in the bubble collapses to result in the drop forming a constant contact with the surface (*Fujimoto et al. 2000*). These are the characteristics of a liquid drop impacting with a smooth, dry, solid surface however which can be regarded as fairly ‘ideal’ and perhaps not that commonly observed in realistic forensic scenarios. Impacts occurring under more variable impact conditions generate more complex impact characteristics, such as stain distortion in impacts with rougher surfaces (*Bevel. Gardner. 2008*).

As a liquid drop impacts with a smooth surface it deforms, with momentum shifting from the vertical to horizontal as described above, and dries to form a stain. Impact surface characteristics, which deviate away from this smooth, solid, ‘ideal’ surface exert disruptions on this deformation process. As the roughness of a surface increases the impacting jet of fluid loses axisymmetry leading to the development of undulations in the radial edge of the horizontally expanding stain (*Thoroddsen. Sakakibara. 1998*). These undulating ‘finger-like perturbations’, or spines are a distinctive morphological feature of bloodstains generated on the majority of relatively smooth, flat, non-porous surfaces such as ceramic tiling, linoleum, or stainless steel (*Mehdizadeh et al. 2004*) (*figure 24*).

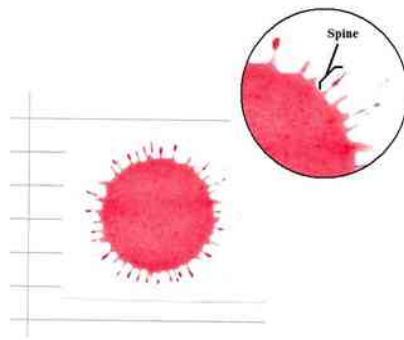


Figure 24 Illustration of spines formed in a bloodstain on paper

(Author. 2009)

Empirical observations of spine formation established that increases in size and number of spines generated in a stain correlate to higher impact velocity and droplet diameter (Mehdizadeh *et al.* 2004:353) as well as surface roughness (Hulse-Smith *et al.* 2005). Hulse-Smith *et al.* (2005) conducted a series of experiments where bloodstains were generated on a range of different surfaces, including glass, steel, plastic and paper to observe the effects of these different surface characteristics on the generation of spines. A range of different surfaces was selected to more realistically mimic the variety of surfaces typically encountered at a crime scene with surfaces deliberately chosen for their relative similarity, all being reasonably smooth and with the exception of paper: non-porous. They concluded that even within this relatively close range of values, surface roughness exerted a significant effect on the morphology of spines generated (Hulse-Smith *et al.* 2005). They later concluded that number of spines generated correlates to both the vertical source (height origin) of a bloodstain as well as drop volume. This conclusion, in theory, could allow investigators to combine directionality analysis, impact angle and spine analysis to calculate the horizontal origin of a stain, the impact angle and vertical origin of a stain. The calculation of either an unknown vertical source or drop volume however requires the other value to be known (*pers. comm. Wolson. 2011*) so their conclusions about the contributions spine analysis can make towards determining drop volume and vertical blood source remain limited at present. Although they experimented with a range of different surfaces, a further limitation of their research was in their focus purely on bloodstains which had been generated at a vertical, 90° impact angle.

If a surface is sufficiently rough the disruption caused to fluid drops upon impact may be substantial enough to cause the tips of expanding spines to break free from

the main stain body and dissipate the parental drop as smaller, individually ineffective satellite drops (Moss. 1989:2) (figure 25).

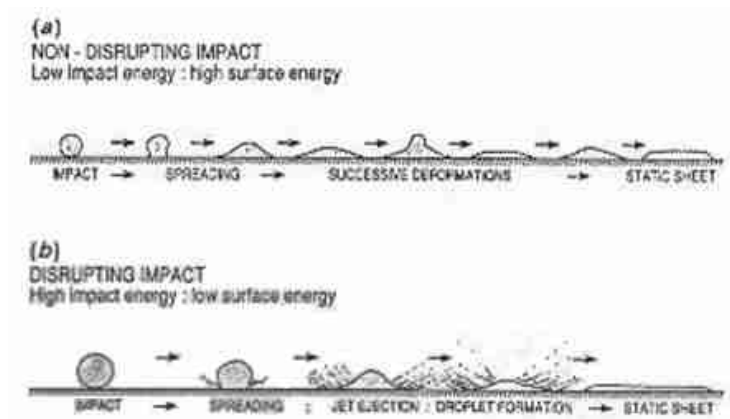


Figure 25 Sketch illustrations comparing a non-disrupting impact on a smooth surface (a) and a disrupting impact on a rough surface (b) and dissipation of satellite drops (Moss. 1989)

These satellite drops then settle and dry to form satellite stains around the main stain body. Satellite stains are commonly observed in stains formed on rougher surfaces such as fabrics (White. 1986. Elena. Mohamed. 2009) (figure 26).

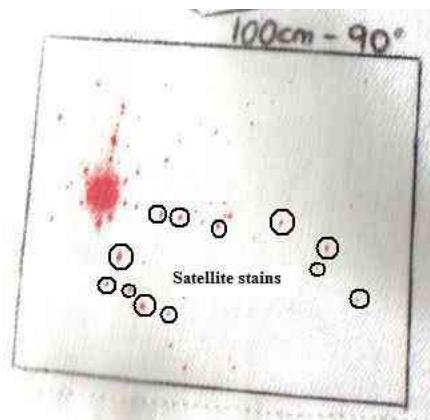


Figure 26 Examples (circled) of satellite stains generated as part of a bloodstain on fabric

(Author. 2009)

Although stains on fabrics have been explored briefly, no empirical assessment of the relationship between the surface roughness of a fabric and the volume of satellite stains generated has been conducted for bloodstains. Observations for water impacts suggest however that there is a direct correlation between surface roughness and volume of satellite spatter generated (Stow. Hadfield. 1981) and preliminary work on proxy blood impacts with fabrics of varying surface roughness confirms this (Miles et al. 2014). Further work needs to be conducted with bloodstains on the exact

influence of surface roughness characteristics on satellite spatter however before there is any possibility of satellite stains being used in BPA in real casework.

### 2.3.2 Angled impacts

Limitations of experimental work conducted on developing methods of analysing bloodstains have included the fact that fluids other than blood have been examined, with observations about their behaviour then extrapolated to the behaviour of blood (*Stow. Hadfield. 1981. Moss. 1989*). Research has also been limited to stains generated on paper, a relatively ‘ideal’ surface (*Karger et al. 1998: 85*) or to 90° impacts (*Hulse-Smith et al. 2005*). The repercussions of such a narrow body of research are that the abilities of analysts in real forensic case scenarios are somewhat limited as a result. For example, accurate interpretation of a bloodstain, generated at an angle on a fabric surface is extremely difficult if no empirical observations of the particular case-specific dynamics involved have ever been made. Without empirical observations it is extremely difficult to rigorously justify and demonstrate the connection made between particular evidence characteristics and specific mechanisms (e.g. angled impact) responsible for generation of evidence (*Mnookin et al. 2011*).

The particular significance of work on impact characteristics being limited largely to 90° impacts is that in the context of realistic forensic scenarios “*droplets usually impact upon a surface obliquely*” (*Kang. Lee. 2000:580*). Despite this tendency however hardly any studies have been conducted on the characteristics of angled droplet impacts (*Knock. Davison. 2007: 1045*). For the purposes of extrapolating conclusions of work on impact characteristics to the more realistic reconstructions required of crime scene analysts, work focused on stain generation from angled impacts is necessary. Some research into angled impacts has been carried out on right-angled corners (*Bussmann et al. 1999*) and inclined slopes (*Kang. Lee. 2000*) but as with research into advanced impact characteristics the work has been largely limited to aqueous drop dynamics and impact characteristics (*Pizzola et al 1986:36*).

Having identified an absence of research into angled impact dynamics for bloodstains Knock and Davison (2007) developed an experimental design with the

aim of establishing whether tentative relationships observed between size of stains, spine characteristics, drop height and impact velocity for stains generated at 90° impact angle applied to stains generated at angled impacts. Bloodstains were generated on paper at a series of different angles ranging from 22.7° up to 90° with stains then analysed to determine stain width, length and number of spines. Results of analysis demonstrated that impact angle has a significant influence on stain morphology, as impact angle was increased (from 22.7° through angles of 43.5°, 56.3°, 61.6°, 78.8° to 90°) stains were observed to shorten whilst the number of spines increased (*Knock. Davison. 2007:1049*). With known impact velocities and drop heights Knock and Davison devised a set of equations incorporating all measurements relating to stain size, spine count, drop height, drop volume, impact angle and impact velocities. In combination their conclusions were that for bloodstains generated on paper, at angles it is possible by measuring the width, length and spine count of a stain to determine the impact velocity and therefore the vertical position of the stain source (*Knock. Davison. 2007: 1049*). As acknowledged by Knock and Davison themselves however, these relationships remain confined to impacts on angled paper surfaces. Surfaces more likely to be encountered by investigators include hardened surfaces such as glass, steel, asphalt, concrete, wood or fabrics, which are all likely to exhibit much higher surface roughness values than paper and a higher degree of variability between themselves as well. Experimental findings must therefore be replicated on such surfaces before any inferences can be made about the possibility of the relationships and analytical possibilities outlined by Knock and Davison (2007) being applicable to other surfaces.

### **2.3.3 Secondary Change Mechanisms and Physically Altered Bloodstains (PABs)**

Secondary change mechanisms are mechanisms that act on a stain after it has been generated, to alter its morphology in some way (*Peschel et al. 2011*). The result is Physically Altered Bloodstains (PABs) (*Bevel. Gardner. 2008*). Mechanisms that alter stains may be either anthropogenic in origin or occur naturally. Examples of anthropogenically forced secondary change mechanisms include attempts by a suspect to obliterate or remove incriminating evidence through flooding or burning of a crime scene (*Paonessa. 2005*), washing (*Spector. Von Gemmingen. 1971*).



*Quickenden et al. 2004*) or possibly bleaching (*Castello et al. 2009*). Examples of alterations to stain appearance or behaviour, which may occur naturally, usually follow exposure to various weather conditions such as precipitation and subsequent surface flow (*Leak. 2010*) freeze thaw cycles (*Lovelock. 1953. Leak. 2006*), degradation over time (*Gurfinkel. Franklin. 1987*) or high levels of humidity (*Brady et al. 2002*) and heat (*Fechner. Gee. 1989*). The likelihood of investigators encountering stain patterns that have been exposed to secondary change mechanisms is reasonably high, particularly when dealing with crime scenes located outdoors, scenes exhibiting a significant lag time between generation and investigation and in light of the increasing forensic awareness of criminals (*Pye. 2004: 2*). Despite the likelihood of having to analyse physically altered bloodstains and patterns that have been subjected to secondary change mechanisms, the area remains under-researched and in need of empirical research.

## **2.4 Crime Scene Reconstruction**

Although it is not uncommon to find blood pattern evidence at the scene of a violent crime, accurate and correct interpretation of the evidence to estimate its probative value depends largely upon crime scene reconstruction (*Raymond et al. 1995: 154. Raymond. 1996*). Crime scene reconstruction, as described in *section 1.3*, is the process of reconstructing chronologically the most probable sequence of events associated with a crime scene, on the basis of source and activity level evidence analysis. Different levels of reconstruction are possible by blood pattern analysts, from relatively simple reconstructions of stain directionality to more complex three-dimensional reconstructions of entire impact spatter patterns. In scenes exhibiting large blood spatter patterns, for example resulting from extremely dynamic, varied and sustained bloodletting events, investigators are often faced with much more ‘complex scenarios’ (*Pizzamiglio et al. 2006:538*). In these instances, conducting crime scene reconstruction integrating bloodstain analysis with other forensic techniques such as DNA analysis is the only way to achieve a full understanding of a complete event and give an ‘exact interpretation to the crime dynamics’ (*Fratini et al. 2006: 537*). The application of crime scene reconstruction as a technique in order to achieve this has developed to such an extent that it is now recognised as an independent step in crime scene investigation.

Methods of reconstruction for bloodstain patterns specifically range from graphically reconstructing a sequence of events, to applying known techniques to reconstruct individual events, to conducting experiments to reproduce characteristics of bloodstain patterns (*Wonder. 2003*). The final approach is usually employed when new and uncharacteristic blood patterns are encountered and investigators must attempt by trial-and-error method to experimentally replicate observed patterns in order to identify the mechanisms that generated them. Experimental reconstructions are a fundamental aspect of crime scene reconstruction, reliant upon intelligence gathered from a crime scene to allow accurate interpretation of evidence in the context of specific scene variables (*Chisum. Turvey. 2007*). Reconstruction allows investigators to scientifically test particular theories or hypotheses about a crime against physical evidence recovered from an individual scene (*Chisum. 2006*). These theories and hypotheses are usually concerned with establishing activity level propositions that explain evidence generation in a specific environment or scenario. Intelligence about evidence recovered, surrounding evidence or the environment at a crime scene all play an important role in ensuring investigators test these propositions in a experimental scenario which mimics the forensic reality in which evidence was recovered as closely as possible. For example, an observation of a bloodstain with an unusual appearance at a particular scene has limited use in inferring the likely cause of its unusual appearance, by itself. Further intelligence gathered from both the stain (colour, physical characteristics) and the scene (temperature, humidity, microclimatic features) however can begin to help investigators in formulating possible hypotheses regarding the cause of the stain's unusual appearance. Intelligence about the environment can then be replicated in the laboratory, for example, to ascertain whether environmental variables may have been a factor. Information about temperature, humidity and other environmental variables at a scene, is not evidentially probative in itself. Neither is purely an observation of a stain's unusual appearance. When incorporated as contextual information in an experimental reconstruction however, they may carry increased evidential weight by supporting or a refuting particular activity level propositions that require certain conditions. Inherent variability in conditions, circumstances and evidence types at crime scenes means that scenes are highly individualized. To accurately contextualize and test hypotheses relating to the generation, presence or nature of evidence at any individual scene, therefore, intelligence about the scene must be

sought to assist in the design and adaptation of a case-specific experimental reconstruction. An illustration of this approach to reconstruction is demonstrated by a case where it was used to help investigators establish whether the cause of death in a case of gunshot trauma was suicide or homicide (*Karger et al. 2002*). In the case in question, spatter was observed on the hands of both a suspect and the victim and investigators sought to determine the origin of each spatter. By determining whether the origin of spatter on the hands was back spatter, impact spatter or derived through contact, investigators could establish positionality of the suspect relative to the victim at the time of weapon discharge (*Karger et al. 1998*). If a suspect has offered an innocent explanation for the presence of blood spatter on their hands, determining positionality may eliminate or confirm the likelihood of their explanations. Other information that could be gained from such an analysis could help indicate likely posture of a victim at time of discharge, shooting distance and possible line of fire.

Limitations in crime scene reconstruction exist, as it is almost impossible to re-create and replicate all of the dynamics and variables associated with a crime exactly without re-enacting the actual crime for example. Continuing development of methods that enhance the analysis and interpretation of bloodstain pattern evidence as spatial and temporal indicators of crime events, for use in crime scene reconstruction, remains necessary however to contribute to the ability of investigators to perform reconstructions.

### **2.2.1 Analysis of blood as a spatial indicator**

Analysis of blood pattern evidence as a spatial indicator is largely based on the development of stain analysis to enable investigators to determine where a bloodletting event has taken place and where blood has originated. Methods of spatial analysis include determination of directionality for a single stain (*Elena. Mohamed. 2009: 78*) and interpretation of a bloodstain pattern's collective morphology, geometry and directionality to calculate impact angles and therefore the position, in three-dimensions, of the pattern's blood source position (*Millington. 2004: 3*). The development of research into deriving spatial reconstructions from bloodstains has been consistently thorough with the outcome that investigators are

able to determine locations of involved individuals and individual bloodletting events relatively comprehensively. By contrast methods of analysing blood as a temporal indicator, to indicate chronology of bloodletting events and individuals movements during and post-event, have remained under-researched.

### **2.2.2 Analysis of blood as a temporal indicator**

The analysis of blood as a temporal indicator allows investigators to reconstruct the chronology of events associated with a crime event. Within a crime event there are a minimum of three events associated with blood spatter sequencing:

- 1) exposure of a blood source,
- 2) distribution of blood following exposure (whilst it is still liquid) and
- 3) discovery of the crime scene (*Wonder. 2003*).

Investigators attempting to reconstruct a crime event need to determine the tightest possible chronology surrounding these events in order to narrowly pinpoint possible windows of activity surrounding evidence generation. This may then allow them to include or discount a suspect from being in the general vicinity or close proximity of the crime scene at a particular time when blood evidence was either generated or altered post-event. Establishing as precisely as possible when exactly biological material such as blood has been deposited is crucial, for example, in cases where victims and suspects share close personal ties and an already therefore significant window for explaining away a sample innocently is increased (*Anderson et al. 2005*).

Determining through blood evidence analysis the chronology of certain events has the advantage that it may also speed up and focus parallel lines of inquiry. For example if faced with a high volume of CCTV footage to review, identifying a narrow window in time when the blood letting events are most likely to have occurred will significantly reduce the workload.

Temporal inferences about bloodstains are somewhat limited at present to rudimentary methods of determining visually the approximate age of stains. As a stain ages it breaks down chemically. This chemical breakdown is characterised by

changes in the chemical make-up of a bloodstain as well as discolouration and sometimes an emission of odour, which may be measured quantitatively. Medical research has led the development of quantitative methods of measuring the age of blood. For example, as a dried bloodstain breaks down it is characterised by a diffusion of chloride towards the edge of the stain to form a black border. This black border increases incrementally every nine months giving a rough indication of time since deposition (*Anderson et al. 2005*). The application of this knowledge in bloodstain pattern analysis is of course limited to bloodstains that are older than 9 months, which depreciates its use in analysis at a majority of crime scenes. Formation of a black-border in stains concurs with an internal breakdown of haemoglobin (the oxygen-carrying component of blood) into bilirubin. This breakdown is characterised by a measurable discolouration of blood from bright red to brown-yellow and finally yellow. In the field of medical physics spectroscopic methods of quantifying this discolouration have been developed for applications in forensic medicine: determining the precise age of bruises associated with child abuse and domestic violence (*Aalders et al. 2010*). The implications to this field of making this technology available are significant, and could be transferable to certain aspects of Bloodstain Pattern Analysis, in measuring much more precisely the colour changes associated with ageing blood than is currently possible through the experienced eyes of an analyst. This could be of significant use in estimating the age of stains and deducing from that time of generation and so occurrence of a bloodletting event. In several other areas of forensic science, technologies for determining the nature of ageing processes associated with criminal acts have been developed for specific scenarios. Infrared imaging has been applied to both skin burns and corpses to assess skin temperature distribution, as a means to approximate the age of a burn, or time of death (*Ammer. Ring. 2005*). This kind of technology may have some possible application to the analysis of bloodstains.

There is a significant lack of published research into methods of ageing bloodstains despite recognition of the investigative strength of being able to objectively determine drying time (age of stain) not only for stains drying under ‘*normal circumstances*’ but also following secondary change mechanisms. Observations of the effects of environmental influences such as extreme temperatures, either negative or positive, and humidity on bloodstain pattern analysis suggest that the

morphological characteristics of stains are unaltered and subsequent pattern analysis of them unaffected (*James. Eckert. 1999*). These conditions do however affect other stain characteristics and behaviour, such as drying time, with drying times significantly lower at higher temperatures (*Brady et al. 2002*). Experiments exposing stains to a relatively limited range of different temperatures (18°C, 71°C, 102°C) also yielded observations that the colour of stains generated differed according to temperature (*Brady et al. 2002*) although the cause or level of colour variation remains unknown.

For the purposes of temporal analysis of bloodstains for crime scene reconstruction, these fledgling observations demonstrate the significant considerations that must be given to environmental influences on drying times, ageing and identification of bloodstains. Environmental influences must be researched in much greater depth however before theories generated about their effects on bloodstains can be utilised in real-case stain analysis, interpretation and crime scene reconstruction. Underlining of the necessity of conducting discipline-specific research is recognition of the increasing importance of establishing empirical data to justify, when challenged, the evidentiary inferences and interpretations made by analysts (*Mnookin et al. 2011*).

## **2.5 The importance of experimental studies to Bloodstain Pattern Analysis**

Despite its importance in generating objective criteria for the analysis of case-specific bloodstains, the depth and breadth of experimental research into BPA in the published literature to date, has been relatively limited. This is problematic given that the level of informed understanding and appreciation of blood related evidence often necessary for proffering an expert opinion is “*only achieved through practical experimentation of simulated blood spatter*” (*Raymond. 1995*). Particularly in light of the criticisms made of BPA in the 2009 NAS report, of its purported over-reliance on subjective expert opinion and experience based logic (*SWGSTAIN. 2011*), the need for robust, scientifically replicable and proven experimental studies to base expert reasoning on has increased.

From an investigative point of view experimental studies may provide the only way of increasing the evidentiary value of trace evidence by differentiating between innocent and guilty explanations of evidence origins (*Karger et al. 1998. Morgan et al. 2009*). As evidence presented in connection with a particular crime is usually case-specific, in order to validate related theories experimental studies must demonstrate ecological validity. They must be designed to incorporate and mimic the exact conditions of a crime scene and event, for example, environmental conditions at a scene (*Peschel et al. 2011*). Experimental design should be two-tiered, with an initial experimental stage dealing with general studies of forensic reality and a second focussing on much more case-specific scenarios where all attempts to replicate the exact conditions in question should be made (*Morgan et al. 2009*). Only by conducting replicable experiments, which adequately mimic real-life scenarios, can specific knowledge of particular phenomenon be attained (*Hicks et al. 2005*). In addition, experimental research gives an indication of error margins that may be associated with the interpretation of particular phenomena and formally validates forensic techniques (*Risinger. 2010*). Information on these margins is increasingly being demanded in association with forensic expert testimony (*NAS. 2009*) and particularly more so following the publication of the NAS report (*Risinger. 2010*).

In BPA the general mechanisms of bloodstain generation are covered in sufficient depth by the body of discipline specific peer-reviewed literature to make source level analysis, for example recognition of a bloodstain pattern as impact spatter, possible. The possibility however of accurately determining the probability of recovering that level or kind of source evidence given a certain activity level proposition, for example “*the victim was beaten with a golf club*” as opposed to “*the victim was beaten with a baseball bat*”, without case-specific experimental testing of opposing propositions within a realistic reconstruction of the event, is unlikely. When it is considered that more often than not it is the activity level propositions, rather than source level analyses, that provide the main evidentiary point of contention, the importance of these case-specific experimental studies is clear.

Although it is not always possible to identically mimic case-specific circumstances associated with an evidentiary enquiry, attempts should be made to provide as accurate as possible a re-creation with comparable proxies. In forensic research, due

to the nature of incidents researchers may be attempting to replicate, the issue of substituting with comparable proxies may be more pertinent than in some other fields. Difficulties in sourcing human blood are commonly encountered and differences in viscosity and surface tension between human blood and more readily available bovine, ovine or avian blood may provide a source of experimental variability (*Illes et al. 2010*). This variability is relatively negligible for the majority of forensic experimental purposes but in certain cases awareness of it, in light of questions being made, may be crucial (*Laurent et al. 1999. Millington. 2004*). In research conducted specifically on examining the nature of bloodstains on fabric a balance was required between meeting financial limitations and achieving accurately a replication of the natural three-dimensional contouring of clothes around a persons' body (*Veldhoen. 2006*). The solution was to employ overalls stuffed with a relatively rigid material, hanging from a coat hanger, with limbs pinned into required positions. Although this approach arguably appears fairly crude, this proxy had the advantages of affordability, disposability and increased validity and weight of experimental results generated in court (*Veldhoen. 2006*). In another instance, knowledge of rates of cadaver decomposition within a heavy clay soil at low seasonal temperatures was required. Replication of the specific climatological and sedimentary conditions in question was achieved by burying pig carcasses (a proxy for human corpses) in heavy clay soil for periods over which the temperature was monitored (*Turner. Wiltshire. 1999*).

Although, as illustrated by the examples given, it is not always possible to identically mimic or recreate the materials and circumstances associated with a specific crime, viable experimental proxies can be sourced and should be used to provide as accurate as possible a re-creation. The importance of doing so was illustrated in a case where a victim had been fatally kicked and beaten around the face and neck and extensive blood spatter patterns on the walls surrounding the victim were observed (*Ristenblatt. Shaler. 1995*). An experimental simulation of the crime was required to establish the level of force required to generate such spatter patterns. This was required to allow investigators to either accept or reject the admission made by a suspect that although he had administered the fatal blows to the victim, he did so out of self-defence and so was only employing reasonable force whilst the victim was standing. A re-creation of “*stomping*” motions was carried out in a room



reconstructed to the exact dimensions of the crime scene (*Ristenblatt. Shaler. 1995*). Using a selection of stains from the real crime scene the approximate location of the head of the victim during the attack was estimated, with spongy Styrofoam serving as a representation of the head. Interpretation of the stains generated in the experimental re-creation of the crime scene concluded that the stains observed at the real crime scene were only consistent with those that had been generated by a forceful “*stomping*” motion being applied to a prostrate victim. This conclusion allowed the prosecution to dismiss the explanations of self-defence offered by the suspect (*Ristenblatt. Shaler. 1995*).

Experiments carrying out crime scene re-creations involving the use of proxies have similarly been successfully conducted in several areas of BPA. These have included the disputed case of a homicidal v. suicidal shooting (*Karger et al. 1996*), experimental determination of proximity of source through backspatter analysis (*Karger et al. 1996. 1997. Yen et al. 2003*), a case disputed for insurance purposes which sought to determine whether the death of a man on a goods loading ramp was accidental or due to negligence (*Burnett et al. 1997*) and a case where the persistence of bleach to act as an evasive agent against the detection of bloodstains was unknown but required by investigators (*Castello et al. 2009*).

In light of the need for increasingly scientifically robust expert BPA testimony the requirement for empirical demonstrations consolidating the conclusions investigators’ present in court is also increasing. Successes in certain areas of BPA have demonstrated that even with the use of proxies, such demonstrations can be conducted to add probative weight to expert opinions. In light of this, the importance of experimental studies to the validity and reputation of BPA is underlined.

## **2.6 Outlining the research project**

The focus of the research design takes into account: the increasing demand for experimental studies of realistic case-inspired scenarios, the importance of locating these studies within the context of crime scene reconstruction and a holistic awareness of the forensic process.

A series of case-specific scenarios to provide the focus of the research were identified following an extensive review of both the body of existing peer-reviewed literature in the discipline and discussion with current practitioners of BPA. At the 2010 European IABPA conference a distinct lack of knowledge of environmental influences on bloodstain analysis was cited as particularly problematic, due to the frequent encountering of environmentally exposed stains by analysts (*Leak. 2006. 2010. Morris. 2010*). The effects of temperature, humidity and surface characteristics as the main influences over bloodstain drying time is generally recognised (*Leak. 2006. 2010. Lovelock. 1953. Brady et al. 2002. Fechner. Gee. 1989*) through a small existing body of research investigating the persistence of stains exposed to limited ranges of environmental conditions. However extensive empirical data on the relationships between each of these influences and bloodstain morphology and drying time, which may affect the methods of their interpretation, has never been produced and certainly not within the context of the holistic forensic process. This research was proposed in order to attempt to redress this oversight.

This thesis focuses on environmentally altered bloodstains, exposing stains to a range of naturally occurring temperature variations as well as more extreme temperature conditions in order to gain some indication of how stains which may have been subjected either accidentally or purposefully to these extremes may differ behaviourally from more ‘*ideal*’ and unaltered stains. The stains were subjected to both visual and chemical identification and measurement of drying times in order to make observations about behavioural responses to environmental fluctuations. As to whether either environmental conditions or surface characteristics exerts the dominant influence over stain characteristics, this was tested by varying the surface characteristics stains were generated on. The significance of experimental findings regarding the behaviour of environmentally altered stains was contextualised within the process of crime scene reconstruction and finally, results discussed in the context of presentation methods for environmentally altered bloodstains in a courtroom.

This thesis therefore has a research focus on:

- Visual and chemical methods of identifying bloodstains
- Environmental and anthropogenic influences on bloodstain

- The influence of surface characteristics on stain morphology and behaviour

A more focused literature review of those specific areas follows.

### **2.6.1 Identification of bloodstains**

*Figure 27* outlines the most commonly used and available methods through which investigators can identify bloodstains. Several methods, which historically proved popular, have been deliberately excluded from consideration. One example is the Benzidine test, the use of which has been discontinued on the basis of concerns surrounding the carcinogenic properties of chemicals involved in its application (*Ingham. 1932*)

Figure 27 Table outlining currently available and commonly used bloodstain identification methods

Test Name	Presumptive	Confirmatory	Method of Application	Observation If Positive	Specificity	Sensitivity in solution	Advantages	Disadvantages
<b>Visual Identification</b>			<i>Examine exhibits in natural light for observable stains. Exhibits can also be examined under 230-269 nm frequency UV light.</i>	Brown/Reddish-Brown stains or powder.	<b>Low</b>	N/A	<i>Inexpensive and easy to conduct.</i>	<i>Subjective. High frequency of false positives. Accuracy reliant on experience levels. Stains must be patent.</i>
<b>Luminol</b>			<i>Spray luminol evenly across suspect area whilst environment is in a darkened state.</i>	Blue-green chemiluminescence.	<b>Low</b>	1: 5,000,000 (Proescher. Moody. 1939. Webb et al. 2006)	<i>Commercially available. Highly sensitive. Can detect latent stains. Non-carcinogenic and safe to use. Highly sensitive, so suited to detection of dried or old stains (Larkin. Gannicliffe. 2007)</i>	<i>Not specific for blood; several substances cause false-positives. Application must be in a darkened environment. Photographing reaction requires training.</i>
<b>Kastle-Meyer (Phenolphthalein)</b>			<i>Swab or rub stains onto filter paper. Add 2-3 drops of KM solution to the paper. If no colour develops add 2-3 drops of 6% Hydrogen Peroxide solution.</i>	Intense pink colour.	<b>Low</b>	1:100,000 (Webb et al. 2006)	<i>Relatively quick results. Considered safe if handled with gloves. Relatively long shelf life. Reaction is well marked and immediate with very few false positives (Glaister. 1926).</i>	<i>Not specific for blood; some substances such as horseradish cause false positives. Hydrogen Peroxide is an irritant.</i>
<b>LMG (Leucomalachite Green)</b>			<i>Apply distilled water to the tip of a sterile swab. Swab the suspected stain. Apply 1-2 drops of LMG reagent. If there is no colour change add 1-2 drops of 3% Hydrogen Peroxide to swab.</i>	Immediate blue-green colour change (after addition of Hydrogen Peroxide)	<b>Low</b>	1: 1,000 (Grodsky et al. 1951. Webb et al. 2006)	<i>Produces rapid results.</i>	<i>Not specific for blood. Prone to false-positives. Suspected carcinogen. Hydrogen Peroxide is an irritant. Not specific for blood.</i>

<b>Hemastix</b>			<i>For an indirect test, rub a moistened swab over the suspected stain and then touch to a moistened reagent strip. For a direct test, swab a small portion of a suspected stain and then touch to a moistened reagent strip.</i>	Strip turns yellow- dark green depending on the concentration of haemoglobin present.	<b>Low</b>	1:1, 000, 000 in dilution (Webb J. L et al. 2006)	<i>Commercially available. Easy to conduct.</i>	<i>Not species specific (Johnston. E et al. 2008).</i>
<b>Bluestar®</b>			<i>Apply Bluestar® on to suspected stains with a spray atomizer from a distance of 50cm whilst environment is in a darkened state.</i>	Blue chemiluminescence.	<b>Low</b>	1: 5,000,000 (Webb. J. L et al. 2006)	<i>Extremely sensitive. Strong and long lasting luminescence. Does not damage DNA. Very long shelf life pre-mixing, Can detect latent stains.</i>	<i>Not specific for blood; several substances cause false-positives. Application must be in a darkened environment. Photographing reaction requires training. Once mixed only lasts few days.</i>
<b>Takayama</b>			<i>Place material to be tested on slide. Add drop of Takayama reagent. Warm slide gently at 65°C for 10-20 seconds. Allow to cool</i>	Appearance of pink needle shaped crystals.	<b>High</b>	1: 1000 in dilution of whole blood (Miller. L. B. 1969)	<i>Confirmatory test for blood.</i>	<i>Requires a significant quantity of a sample (Dixon. 1976). Confirmatory of presence of blood, not species specific.</i>
<b>Teichmann</b>			<i>Place material to be tested on slide. Let reagent flow under cover slip. Warm at 65°C for 10-20 seconds. Allow to cool</i>	Appearance of brown rhombohedrum shaped crystals.	<b>High</b>	1: 1000 in dilution of whole blood (Miller. L. B. 1969)	<i>Confirmatory test for blood.</i>	<i>Confirmatory of presence of blood, not species specific. Less effective than Takayama test.</i>
<b>ABAcad® Hematrace®</b>			<i>Swab suspected bloodstain and then immerse swab in liquid test vial. Shake gently. Dispense 2 drops from vial into sample well of test stick.</i>	Observation of two visual markers.	<b>Very high</b> (although some cross reactivity)	1: 500,000 (Atkinson. C et al. 2003) 1: 10,000,000 in dilution	<i>Quick and easy to conduct. Commercially available. High specificity for human haemoglobin as use anti-</i>	<i>Cross reactivity exists with some 'higher' primates (Reynolds. M. 2004).</i>

						(Swander. Stites. (1998)	human antibodies in detections. Confirmatory test for blood. No false-positives.	
<b>Hexagon OBTI</b>			Swab suspected bloodstain and immerse swab in transport medium (contained in collection tube). Shake gently. Leave for 30 minutes. Dispense 2 drops into sample well of test stick. Wait 10 minutes.	Appearance of both a blue control line and blue secondary 'test' line after approx. 10 minutes.	<b>Very high</b> (although some cross reactivity)	1:1,000,000 in dilution (Johnston et al. 2008)	Quick and easy to conduct. Commercially available. High specificity for human haemoglobin as use anti-human antibodies as detection means. Confirmatory test for blood. No false-positives (Johnston at al. 2008)	Cross reactivity exists with the blood of a few species, which are; primates, ferrets and skunk (Hockmeister et al. 1998. Rowley. 1999).

With all tests a positive control and negative control should be carried out, prior to testing, to demonstrate they are working correctly (Bevel. Gardner. 2008).

In the table a distinction is made between presumptive and confirmatory tests. Presumptive tests are used to indicate the possible presence of blood, as a method to help exclude certain areas and focus further testing on a smaller, more manageable scale (*Garner et al. 1976. Tobe et al. 2007*). They act as a kind of ‘*search tool*’ (*Bevel. Gardner. 2008*). Confirmatory tests in contrast are, by definition, tests that confirm the presence of blood. Once a sample of a possible bloodstain has been identified via presumptive testing, the sample should be submitted for confirmatory testing (*Johnston et al. 2008*). The use of both as a two-step identification method is essential as both have disadvantages that prohibit the use of each exclusively in the identification of bloodstains at a crime scene.

In the context of processing a large crime scene or a scene which is in danger of degrading over time, where speed in pinpointing suspect areas for closer scrutiny is imperative, presumptive tests offer a distinct investigative advantage. Their application is relatively quick and easy and certain tests, for example Luminol and Bluestar® test reagents, are capable of identifying latent stains, i.e. those which are not visible. In cases where attempts have been made by a suspect to clear evidence from a scene this can be of significant use. In this context presumptive tests for blood afford investigators an advantage over both time and resource limitations.

Presumptive tests give two possible outcomes; that a suspect sample is either definitely not blood or that the sample probably is blood but simultaneously cannot be conclusively excluded as being one of a small range of other substances, i.e. a ‘*false positive*’.

#### **2.6.1.1 False Positives**

False positives are caused by substances capable of reacting with the presumptive reagents in a similar way to blood, making it falsely appear that blood is present when in fact it is not. Discussion exists as to the extent to which these substances can truly replicate and mimic the reaction of tests to actual blood, with arguments about the significance of their “*interference*” being dismissed as defence orientated arguments (*Grodsky. 1951*). Experimental studies have examined the veracity of this by testing the ability of commonly encountered household substances, surfaces and chemicals to trigger false positives (*Tobe et al. 2007*). The most comprehensive of

these tested up to 250 commonly encountered household substances, surfaces and materials, to measure the extent to which they were capable of triggering a false positive reaction when subjected to the luminol test (*Creamer et al. 2003*). The wavelength of chemiluminescence given off by each of the substances was compared to the levels of luminescence that would be expected by a luminol reaction to blood and only 9 of the relatively comprehensive catalogue of household substances gave off a level of luminescence realistically comparable to that of blood. These substances were; turnips, parsnips, horseradishes, commercial bleach, copper metal, certain furniture polishes, some enamel paints and some interior fabrics from motor vehicles (*Creamer et al. 2003*). In certain circumstances these substances may very likely be encountered at a crime scene and for that reason the problem of false-positive reactions in presumptive testing remains a significant one.

In order to negate, or overcome, the problem of '*false positives*' a 2-step process of following up presumptive testing with confirmatory testing is recommended. The application of confirmatory tests initially to crime scenes, in place of presumptive tests is not considered a realistic one, given the increased cost, skill and focus required of their application.

### **2.6.2 Secondary change mechanisms & PABs**

Secondary change mechanisms are those that act on a stain to alter it in some way (*Peschel et al. 2010*). The consequence of exposing stains to these mechanisms is the generation of physically altered bloodstains (PABs) (*Bevel. Gardner. 2008*). PABs can be caused by either innocent and intentional human actions, for example bleaching of a bloodstain pattern or washing of a garment to remove incriminating traces of blood, or by exposure to naturally occurring environmental conditions such as precipitation or freeze-thaw temperature cycling. The likelihood of investigators encountering stain patterns that have been exposed to secondary change mechanisms is reasonably high, particularly when dealing with crime scenes located outdoors, scenes exhibiting a significant lag time between generation and investigation and in light of increasing forensic awareness amongst criminals (*Pye. 2004: 2*). Despite, however, the likelihood of encountering stains affected by these mechanisms, they have to a certain extent escaped experimental scrutiny.



Aspects that remain particularly under-researched in the published literature include considerations about the effects of these mechanisms on the ability of identification tests to continue to accurately identify bloodstains and their influence on the behaviour of blood. Exposure over a lengthy period to the environment, evasive cleaning attempts by suspects or extreme events such as fire or freezing, whether intentional or accidental, are all factors that may influence identification of a stain or interpretation of it for the purposes of crime scene reconstruction.

Over time bloodstains naturally degrade, both visually and chemically. The rate and extent of this degradation is influenced by natural conditions and fluctuations in humidity, temperature and precipitation levels (*Cotton et al. 2000*). These influences are environmentally natural and are therefore referred to as ‘environmentally forced secondary change mechanisms’.

As well as environmental alterations to bloodstains, investigators must also consider the effects of secondary change mechanisms originating from deliberate actions employed by perpetrators to obstruct the ability of identification and therefore evidential value of stains. These actions may include washing of stained clothing for example (*Spector. Von Gemmingen. 1971*), burning or flooding a crime scene (*Paonessa. 2005*) or attempted removal of a stain pattern with the aid of cleaning products, for example household bleach. These actions are collectively termed ‘anthropogenically forced secondary change mechanisms’.

#### **2.6.2.1 Environmentally forced secondary change mechanisms**

Environmentally forced secondary change mechanisms are mechanisms that act on a stain after it has been generated to alter it in some way. They occur naturally within the environment surrounding a crime scene and most commonly, although not exclusively, are encountered in the analysis of crime scenes located outdoors (*Cox. 1990*). Investigations dealing with stain analysis in unusual or microclimatic indoor environments, for example in vehicles where temperature and humidity may be artificially inflated or walk-in fridges and cool rooms, may also require an

understanding of the influence of relatively natural ranging environmental conditions on bloodstains.

Outdoor crime scenes may be exposed, for different lengths of time, to a variety of climatic elements, which each may bring about a visual or chemical change in bloodstains generated (*Brady et al. 2002. Lovelock. 1953*). These elements include fluctuations in temperature, to both negative and positive extremes, varying levels of precipitation that may initiate surface run-off over ground stains (*Leak. 2010*), fluctuations in humidity (*Cotton et al. 2000*) and exposure to snow, ice and diurnal freeze-thaw cycles. The possible influences of these conditions on stain analysis are important in light of the fact that whilst some experimental results have demonstrated that blood may be remarkably persistent when exposed to natural temperature variations for significant lengths of time (*Jain. Singh. 1984. Waldoch. 1996. Adair. 2008*) others have identified significant alterations in both the aesthetical appearance and internal structure of stains when exposed to certain environmental conditions (*Brady et al. 2002. Leak. 2006. Morris. 2010*). It is these alterations, which increase the difficulty for investigators to visually as well as chemically identify bloodstains, as colour changes (*Brady et al. 2002*) and internal breakdowns such as haemolysis (*Lovelock. 1953. Fechner. Gee. 1989*) subsequently occur hindering tests that rely upon consistency in chromatographic values and bio-chemical structure.

The effect of temperature, in particular, on Bloodstain Pattern Analysis is one of the main areas requiring further empirical research. The importance of increasing understanding of the effects of temperature on stain analysis is two-fold, firstly concerning the effects of temperature on subsequent stain identification either visually or chemically and secondly in the significance of temperature being a main influence on stain drying time. The three main influences on drying time are temperature, humidity and characteristics of the surface a stain has been generated on (*Peschel et al. 2011*) with drying time being of significant use to investigators attempting to reconstruct a timeline of events associated with a crime scene (*Wonder. 2003*).

Early observations of the effects of temperature on bloodstains identified the possible effects of temperature ‘extremes’ on stain identification, through their effects on

internal stain components. The resulting alterations inhibit identification tests that rely on the detection of stains in their unaltered forms (*Lee. De Forest. 1976*). Observations of this influence of temperature on stains have been largely restricted to examining the effects of extremes of heat, consistent with stain exposure to fire (*Fechner. Gee. 1989*), or extremes of cold, consistent with stains generated on ice or snow in outdoors locations (*Leak. 2006*). Observations of stains generated at sub-zero temperatures remarked upon stain discolouration (*Brady et al. 2002. Leak. 2006*) and argued the possible cause as temperature induced changes within the blood, as cells freeze and haemolyse (*Leak. 2010*). Lovelock hypothesized that as red blood cells were exposed to freeze-thawing, as might reasonably be naturally expected when dealing with a nocturnal or outdoor crime scene, the concentration of electrolytes in and around the cells associated with ice formation causes damage to the internal structure of the cells (*Lovelock. 1953*). This may have repercussions for chemical identification tests reliant on reactions with internal components of blood.

Although temperature is thought to be the cause of these alterations to the visual appearance and bio-chemical structure of bloodstains it is also acknowledged that the limited published empirical research into the effects of temperature on stains means that experts are far from definitively, or even quantitatively linking the two (*Morris. 2010. Leak. 2010*). In addition, empirical work on the possible influence of even relatively benign temperatures on stain analysis is lacking. There is no quantitative knowledge of the critical temperature margins where bloodstain characteristics start undergoing alterations, both visually and chemically. Limitations therefore exist in investigators' knowledge of which identification methods may be most appropriate for stain identification or how bloodstains may appear visually, given the environmental conditions at the scene.

Although limited results have been generated for the success of application of luminol to environmentally altered stains (*Waldoch. 1996. Creamer et al. 2003. Adair et al. 2008. Tontarski et al. 2009*), other chemical tests have not been subjected to similar scrutiny. The reaction of bloodstains to exposure to a range of temperatures, from simulated diurnal variations to more extreme temperatures associated with fire or freezing, remains an important one to establish, particularly in the context of analysing crime scenes located outdoors, in extreme climates or those

which have been intentionally subjected to extreme conditions and associated secondary change mechanisms.

The second main area of the interest in influences of temperature variations on stain analysis is related to stain drying time and its implications for crime scene reconstruction. Drying time fluctuates in accordance with environmental variations in temperature and humidity as well as characteristics of a stained surface (*Peschel. 2010*). As temperature increases for example drying time decreases and stains dry faster (*Brady et al. 2002*). Quantitative knowledge about this relationship could assist crime scene investigators attempting to reconstruct from discovery of a wet stain on glass, for example, what the upper limit of possible deposition time for that stain may have been. The empirical research necessary to allow crime scene investigators to draw reconstructive temporal inferences from the dry versus wet state of a discovered stain however has not yet been completed. The subtleties of influence of temperature over drying time variability therefore remain unknown. Influence of other environmental variables, such as humidity on stain drying time are similarly unquantified in the published literature to date.

A focus on the influence of environmentally forced secondary change mechanisms on bloodstains and lack of research in this field has been outlined. In other forensic disciplines a more significant exploration of the interaction of time and temperature, as environmentally forced secondary change mechanisms, on physical evidence has been undertaken.

The forensic discipline of forensic taphonomy focuses on quantitatively evaluating and interpreting post-mortem alterations to and decomposition of a body in order primarily to estimate a Post-Mortem Interval (PMI) (*SWGANTH. 2013*). Once calculated, PMI can be indicative of time of death and may therefore provide critical intelligence to an investigation (*Simmons. Cross. 2013*). Complications regarding calculations of PMI arise from an acknowledgement that environmentally forced mechanisms such as weathering, freeze-thaw cycling, sun-bleaching and variables such as temperature, humidity, rainfall and elevation all influence rates of decomposition (*SWGANTH. 2013*), largely through their influence on insect and scavenger activity (*Kasper et al. 2012. Dabbs. Martin. 2013*). The possible

interactions of a wide range of environmentally forced mechanisms results in the process of decomposition of human remains being highly volatile and variable (*Parks. 2011*). This, in turn, increases the complexity of calculating accurate temporal reconstructions of PMI from observations of levels of decomposition. Acknowledging the importance of quantifying the influence of environmental variables on rates of decomposition in order to facilitate more accurate, site-specific estimations of PMI, forensic anthropologists have conducted experimental work exploring environmental influences on decomposition. In particular work has examined differential rates of decomposition in geographical locations presenting different climatic conditions. Observations indicated that temperature (*Brown. Peckmann. 2014*), humidity (*Galloway et al. 1989*) and seasonality (*Mann et al. 1990. Komar. 1998*) all exert a significant influence on rates of decomposition and seasonality and reiterate the importance of incorporating a consideration of active scene-specific environmental mechanisms into taphonomic calculations.

The discipline of forensic entomology has also attempted to quantify interactions over time between environmental mechanisms and physical evidence to increase the accuracy of interpretations relating to levels of decomposition. Forensic entomology is the investigation of insect and arthropod species recovered from crime scenes to allow calculations about PMI to be made (*Benecke. 2001*). These calculations are based on the premise that each species has a unique life cycle and rate of development associated with it (*Wolff et al. 2001*) and that identification and evaluation of the stage of development insects are observed at can be used to make inferences regarding the length of time since decomposition and insect activity began, which may be indicative of PMI. The development and life cycle of insects are sensitive however and can be modified by climatological variables such as temperature and humidity (*Wolff et al. 2001*). The potential influence of these environmental variables on insect development therefore needs to be considered during calculations based on stages of insect life.

Current estimates of PMI are largely based on historical observations of insect development and succession made in the late 19<sup>th</sup> to mid 20<sup>th</sup> centuries (*Turchetto. Vanin. 2004*) tested within the geographical limits of the USA and Western Europe (*Myburgh et al. 2013*). There is acknowledgement however that due to the gradual

effects of global warming (*Turchetto. Vanin. 2004*), differences in climate across global regions (*Myburgh et al. 2013*) and site-specific variabilities (*Ames. Turner. 2003*) estimates of PMI based on these historical observations may result in inaccurate calculations of PMI (from entomological inferences) if an assumption is made of their continued and universal relevance. Within the discipline it has been recognised therefore that forensic entomologists must make careful site-specific environmental measurements in order to focus generalised trends towards more accurate, precise and environmentally specific calculations (*Oliveira-Costa. Antunes de Mello-Patiu. 2004*) of PMI.

As outlined, in both disciplines of forensic anthropology and entomology, the necessity of understanding site-specific variables when addressing environmentally forced secondary change mechanisms has been demonstrated. The research outlined in this thesis develops and expands on this by addressing these mechanisms for PABs.

#### **2.6.2.2 Anthropogenically forced secondary change mechanisms**

As well as environmental alterations to bloodstains, investigators must also consider the effects of secondary change mechanisms originating from deliberate actions employed by perpetrators to obstruct the identification and possible evidential value of stains. These actions may include washing bloodstained clothing (*Cox. 1990*), burning or flooding a crime scene (*Paonessa. 2005*) and attempted removal of a stain pattern with the aid of cleaning products, for example household bleach (*Castello et al. 2009*).

Similar to environmentally forced secondary change mechanisms these mechanisms may alter the appearance of blood to the extent that stains no longer are visible to the unaided eye or the internal composition of blood in a manner that inhibits chemical tests applied for the purposes of identification. Additionally some anthropogenically forced mechanisms, such as application of household bleach to stains, have the opposite effect of confusing results by conversely inducing false positives (*Castello et al. 2009*).

These effects have significance for investigative attempts to reconstruct a crime scene in the same way that environmentally forced alterations of stains do. They may prevent investigators from accurately identifying bloodstains at a scene and disrupt the natural drying time of stains, increasing the difficulty in temporally reconstructing events associated with a crime. In this manner, accurate interpretation of the effects of anthropogenically forced secondary change mechanisms can prove a highly valuable investigative tool for crime scene reconstruction.

Anthropogenically forced mechanisms can also provide investigators with an additional evidential consideration. If their influence can be detected it serves as evidence of evasive actions having been purposefully taken, adding weight to the guilt of a suspect. If investigators can definitively distinguish between anthropogenically forced alterations, derived from attempts to destroy incriminating evidence, and those that may possibly have been caused by natural degradation for example the evidential value of that distinction is extremely significant. Despite the investigative interest in developing an understanding of the effects of anthropogenically forced secondary change mechanisms, the area has remained relatively unsupported by empirical evidence (*Brady et al. 2002*).

Some preliminary experimental studies that address the ability of chemical tests to positively identify blood, following its exposure to anthropogenic change mechanisms, have been conducted. Discussions on the efficiency of luminol in detecting traces of blood following different washing techniques demonstrated that washing stains with water only effectively removed about 50% of haemoglobin present in stains (*Quickenden et al. 2004*). The addition of soap to water increased the removal of haemoglobin to approximately 90% but this was still sufficient to gain a positive identification of stains with the luminol reagent (*Jain. Singh. 1984. Quickenden et al. 2004*). The implications of these results aids crime scene reconstruction by inferring whether the washing level an evidential item had been subjected to had been intentional or accidental from the level of activity required (*Cox. 1990*). The ability of luminol to positively identify stains following cleaning methods will vary depending not only on the cleaning mechanisms used on stains but on other variables too, such as composition and characteristics of surfaces stained

(Cox. 1990). The results of such preliminary studies however do strengthen the use of luminol as a stain identification test which can overcome certain anthropogenic change mechanisms (Gross *et al.* 1999).

The use of bleach as an obstacle to identification has also been examined, with results suggesting that bleach is a much more effective ‘*cleaning*’ agent than water and/or a water and soap combination at preventing detection of bloodstains by luminol. It was observed that the ability of bleach to interfere with the detection of bloodstains however, although effective, was restricted to a approximately 8 hours (Creamer *et al.* 2005) for non-porous surfaces included in the experiments (Castello *et al.* 2009). The implication of experimentally observing this, for investigators, is that by waiting a matter of time, for bleach interference levels to decrease, the luminol identification test could be successfully conducted.

Further experimental work aimed at establishing the interference caused to stain identification by burning or freezing also needs to be conducted. As yet, the levels of possible interference by such activities are unknown, despite preliminary suggestions that production of soot associated with burning and haemolysis associated with freezing act as a barrier to positive identification of bloodstains by several chemical tests (Tontarski *et al.* 2009).

### **2.6.3 Influence of surface characteristics on stain morphology and behaviour**

Consideration of the potential influence of the characteristics of a surface on bloodstain morphology or behaviour is highly important given the likelihood of encountering a variety of stained surfaces at a crime scene (Hulse-Smith *et al.* 2005). An analyst may encounter, at a crime scene, stains on wooden, metal, glass, ceramic, lino or textile surfaces such as carpet, clothing and other fabric surfaces. Despite the likelihood of encountering stains formed on different surfaces, relatively little is empirically understood about the influence of surface characteristics on bloodstains formed on them. This limits the use of these stains in bloodstain pattern analysis, and with stains formed on clothing, this is particularly problematic (Elena. Mohamed. 2009). Clothing is the ‘*most commonly examined textile product in forensic science*’



(Grieve. Robertson. 1999 cited in Elena. Mohamed. 2009), passing through police hands on a regular basis (Elena. Mohamed. 2009). The variability of fabric surfaces means patterns formed on fabrics demonstrate less predictability or reproducibility (Wonder. 2003) in comparison to patterns formed on more regular or uniform surfaces. As a result, bloodstained fabrics are often approached with caution, as interpretation is expected to be inherently erroneous (Elena. Mohamed. 2009), risky and difficult (Slemko. 1999 cited in Elena. Mohamed. 2009). This assumption is derived from a relative lack of published experimental work examining the particular nature of stains formed on ranges of surfaces, despite the fact that careful examination of surfaces such as bloodstained fabric in clothing can '*potentially provide information regarding the movements and activities of the wearer*' at a crime scene and during bloodletting events (Holbrook. 2010: 3).

Surfaces differ according to a range of properties including absorbency, permeability, surface roughness and chemical treatment (Elena. Mohamed. 2009). Any one of these properties might exert an influence on the behaviour of blood as well as morphology and characteristics of stains, once generated on surfaces. In order to be capable of analysing and interpreting stains formed on a range of surfaces, analysts need to understand the influence of varying properties of stain morphology and behaviour and how to incorporate interpretations of them into bloodstain pattern analysis.

Some preliminary experimental research has been conducted on examining how stains formed on a variety of surfaces differ or may be affected by surface characteristics. Surface characteristics may affect identification of bloodstains by increasing or decreasing the persistence and tenacity of blood on a surface. This is of particular interest in cases where either innocently or intentionally a stained surface has been exposed to cleaning actions (Cox. 1990). In experiments conducted on bloodstained carpet, lino, wood, concrete and sheet rock the ability of various cleaning methods to completely remove all traces of blood were tested. Luminol was used after cleaning to identify any residual traces. Results showed variable levels of blood detection between different surfaces after cleaning (Gross *et al.* 1999). Perhaps amongst such differing surfaces these results are not entirely surprising. Similar relationships between surface characteristics and the retention of blood were also

observed however for stains generated across a range of much similar surfaces (twelve different fabric types) (Cox 1990). Once stained and subjected to washing a significant difference in stain retention rates was observed across these twelve fabrics, with results suggesting that the retention rates were largely dependent upon fibre compositions of each fabric (Cox. 1990). Even in cases where extreme cleaning methods, such as bleaching of surfaces or a prolonged immersion in water are involved, surface characteristics have an influence on bloodstain persistence. It has been shown it is possible to detect blood on fabrics following immersion in water for up to 20 days (Jain. Singh. 1984). Experimentally it has also been established that in cases where extreme cleaning methods such as bleach are used, for certain porous surfaces, the ability of bleach to mask detection of latent bloodstains is limited (Castello. et al. 2009). This suggests that even when evasive actions are taken by a suspect to remove stains, there may still be an increased chance of recovering evidence from certain surfaces. Results of both experiments support a suggestion that bloodstains generated on absorbent and permeable surfaces and materials are likely to exhibit significant persistence. Further experimental work is required to establish whether persistence is indeed highest for these surfaces and whether absorbency and permeability are important factors in controlling persistence.

Another aspect of interest to analysts regarding the influence of surface characteristics on bloodstains is their influence on stain morphology (Elena. Mohamed. 2009). The influence of surface roughness in particular is of interest due to its perceived role in the generation of 'satellite stains' and control over stain size and shape. Observations of water impacting with soil demonstrated the generation during some impacts, of satellite stains. Satellite stains form as an impacting drop disrupts upon impact and is partially dissipated as numerous, smaller 'satellites' (Moss. 1989). The formation of satellite stains is believed to be a function of surface roughness, with rougher surfaces likely to exhibit a greater presence of satellite stains (Moss. 1989). Observations have been limited however to water droplet impacts. Further experimental work is required to establish whether this proposed relationship is valid for impacts involving blood and whether any relationships between surface roughness and the formation of satellite stains could be usefully incorporated into analysis of bloodstained surfaces, such as clothing where satellite stains are commonly observed. At present, a lack of understanding over the exact

mechanisms and interactions, which lead to the generation of satellite stains, is extremely concerning for continuing interpretation of them. Currently, the extent of bloodstaining observed on a surface is interpreted as an indication of levels of proximity or involvement of that surface with a bloodletting event. If surface roughness has a significant influence on the tendency of impacting drops to disrupt on impact and form numerous stains, surfaces with higher roughness will demonstrate increased levels of staining as a function of surface characteristics rather than involvement with an original blood letting event. Consideration of this alternative needs to be incorporated into the analysis of surfaces exhibiting satellite staining. Until further experimental work on the relationships between surface roughness and satellite stains has been completed, any analysis of these surfaces and suggestion of activity level propositions concerning stains analysed should be conducted with extreme caution.

The influence of surface roughness on stain size and shape in the case of blood impacts has been examined in more depth in the published literature. Physical characteristics such as absorbency and permeability are responsible for the overall appearance of a stain. Experiments conducted for blood impacts on a variety of fabrics indicated that stain size in particular is dependent upon the absorbency of a surface (*Elena. Mohamed. 2009*). Absorbent surfaces lead to the formation of larger stains as blood penetrates the surface further and diffuses within it to a greater extent (*White. 1986*). Absorbency of a surface can also influence stain shape (*White. 1986. Holbrook. 2010*). Highly absorbent surfaces tend to exhibit high levels of distortion to stain shape, limiting the investigative use of analysis of stain shape in these instances (*Slemko. 2003*). The influence of surface characteristics on stain size and shape has consequences for the suitability of extrapolating calculations regarding known relationships between stain width, length, shape, directionality and angle of impact, (observed for stains formed on more regular, uniform surfaces), to surfaces exhibiting high degrees of surface variability (*Slemko. 2003*).

An important further consideration for investigators analysing stains generated on a range of different surfaces is in the influence of surface characteristics on stain drying time. This has potentially major implications when attempting to estimate time of stain deposition and reconstruct the chronological progression of a

bloodletting event. If drying time of blood on a specific surface is known, for example, observation of a wet stain on that surface allows analysts to estimate an upper-limit for time of stain deposition. Depending on an understanding of the nature of particular surface characteristics, these estimations should vary. Fabric surfaces, for example, are likely to exhibit greater absorbency than glass surfaces, which are impermeable. This will influence drying time. When blood impacts with an impermeable surface, upon impact, the blood disrupts and momentum is transferred from a vertical to a horizontal plane – observed through the transformation of an impacting drop from a spherical drop to a disc-like stain.

When blood impacts permeable surfaces, such as fabrics, transfer of momentum from the vertical to horizontal plane is still observed but there is also a continuation of vertical momentum, observed by penetration of blood vertically down through the surface (*Holbrook. 2010*). This means when blood impacts fabric surfaces it is likely to be dissipated both vertically and horizontally through the surface, with the effect of decreasing and distorting the horizontal surface area of a stain generated on fabric compared to a stain generated on an impermeable surface (*Slemko. 2003*). By decreasing the environmentally exposed surface area of the stain, drying time may therefore be increased. A similar effect may also be observed where horizontal surface area of stains generated on different surfaces varies according surface roughness.

Despite the importance of understanding the influence of surface characteristics on stain drying time, very little experimental work has been conducted in the published literature in order to understand these features more quantitatively. Recent criticisms levelled at the discipline of BPA (and forensic science more generally) have focused on the perceived lack of empirical support for inferences and claims made by investigators, following their analysis of evidence. Critics claim in lieu of empirical evidence disciplines have become over-reliant on ‘experience-based’ judgments of expertise. In most instances it is fair to surmise that analysts’ experience-based judgments may in fact be relatively accurate (*Mnookin et al. 2011*). However, in order to reduce the vulnerability of the discipline to such criticisms, it is essential to promote and establish an empirical body of supportive evidence. Further experimental work is therefore required to explore the potential for integrating

interpretations of stain drying times on a range of surfaces into crime scene reconstructions.

### **3. Materials & Methods**

#### **3.1 Outlining specific areas for research**

Following a review of existing literature in the forensic discipline of BPA, three areas were identified to form the focus of experimental research, concerning 1) environmental influences on visual and chemical identification of bloodstains 2) environmental influences on bloodstain drying time and 3) the influence of surface characteristics on bloodstains. To allow the formulation of experimental hypotheses within each area, specific unknowns associated with each were identified.

##### **3.1.1 Environmental influences on visual and chemical identification of bloodstains**

The initial step in bloodstain identification is usually visual identification of areas of interest and suspect stains by an analyst at a crime scene. Early visual identification of potential bloodstains allows analysts to prioritise specific areas of likely interest at a scene, for further scrutiny.

Despite the contribution visual identification of stains can afford the early stages of an investigation use of it remains an arguably subjective technique, reliant upon an analyst's personal experience and opinions. This leaves it as an investigative technique susceptible to certain criticism, particularly in the wake of the 2009 NAS report which widely criticised the reliance of certain forensic disciplines, including elements of BPA, on subjective expert opinions (*National Academies Press. 2009*).

In stain analysis involving physically altered bloodstains (PABs) the technique becomes even more subjective as mechanisms may have altered a stain's appearance dramatically. A limited number of experimental studies and observations have commented on the influence of exposing stains to certain environmental conditions on stain appearance (*Gurfinkel. Franklin. 1987. Brady et al. 2002. Paonessa. 2005. Leak. 2010. Morris. 2010*). These alterations may obscure interpretation or identification of bloodstains, resulting in incomplete evidence recovery following a

bloodletting event. In theory this suggests that evidence recovery from sites that exhibit PABs may be reduced.

An alternative effect of these alterations may lead to misinterpretation of ‘misfit’ stains. ‘Misfit’ stains possess characteristics that are at odds with expected characteristics, given conditions of a crime scene. Accurate identification of “misfit” stains allows distinction between stains exhibiting alterations that might have occurred naturally and those that cannot have, given the environmental conditions known to surround the stains generation. By identifying alterations brought about by unnatural processes investigators may then be able to make inferences about possible attempts by a suspect to remove incriminating evidence.

Given the likelihood of encountering PABs and importance of ensuring they can be accurately identified and analysed very little experimental work has been conducted on them and subjected to peer-review. Developing a set of objective criteria for the identification, interpretation and analysis of a range of PABs however appears essential. The majority of work on PABs to date has focused on the influence of extreme temperatures of stain colour (*Brady et al. 2002. Leak. 2010*). This work suggests that stain discolouration is a function of exposure to extreme temperatures and can occur to such an extent that identification of discoloured stains can become difficult. Observations of stains generated on snow at temperatures of approximately -16°C for example demonstrated a pink discolouration and ‘puffy’ appearance that led investigators to initially identify the stains as brain tissue (*Morris. 2010*). This has obvious implications for visual identification of stains but as yet attempts have not been made to experimentally test this theory, to establish the nature of relationships between temperature and colour at benign as well as extreme temperatures, to establish if alterations in colour are associated with particular temperatures or temperature intervals or to establish the accuracy rates amongst practitioners in identifying significantly discoloured stains.

A major focus for this research therefore was to quantitatively establish relationships between temperature and colour within **a)** a relatively benign temperature range (-10°C to 50°C) which stains could be naturally exposed to on a day to day basis and

**b)** more extreme temperatures which stains could be exposed to in extreme climates or under conditions such as fire or freezing.

Following visual identification of potential bloodstains at a scene the next investigative step is to positively confirm the presence of and species origin of any stains. A range of presumptive and confirmatory chemical tests is available for this purpose (outlined in *section 2.4.1*). The tests work by reacting in a particular way with certain components or chemicals found in blood. There is a possibility however that under exposure to certain conditions, such as extreme cold, heat or contact with bleaching agents that these components may become denatured and remodelled following subsequent degradation of stain (*Lovelock. 1953. Gurfinkel. Franklin. 1987*). These effects might prevent or inhibit chemical tests from reacting positively in the presence of blood, leading to false negatives and potentially misleading investigators in evidence recovery. In order to test this theory experimental work was included in this research on chemical identification of stains that had been subjected to extreme climatic mechanisms: snow, freeze-thaw, freezing, high temperatures and fire.

### **3.1.2 Environmental influences on bloodstain drying time**

In addition to influencing stain appearance and subsequent identification, environmental mechanisms and conditions have an effect on drying time. This has investigative consequences during the process of crime scene reconstruction. The analysis of stains at a scene can assist investigators in establishing time elapsed since deposition, for stains that remain partially wet (*Ramsthaler et al. 2012*). Consider for example the discovery of a wet stain on a certain surface under certain environmental conditions. Knowledge of the time taken for a stain to dry on that certain surface at a certain temperature allows investigators to exclude a depositional timeframe beyond that time and therefore more precisely reconstruct the temporal evolution of bloodletting.

Existing empirical work on stain drying times and how they might be influenced by environmental conditions is extremely limited despite the contribution such knowledge could bring to crime scene reconstruction. It is known that the main



influences over drying time are stain volume, characteristics of the stained surface, temperature and humidity (*Laber. Epstein. 1983. Peschel et al. 2011. Brady et al. 2002*), however detailed quantitative relationships between drying time and each of these influences have yet to be established. Two studies have examined correlations between specific temperature intervals and changes in drying time but in each observations were limited to three temperature intervals. In one, drying time was recorded for stains generated on a range of surfaces, including linoleum, wood, glass, tile and mirror, at temperatures of 15°C, 20°C and 24°C. Results indicated a negative correlation between temperature and drying time with stains exhibiting an average drying time of 75-90 minutes at 15°C, 60-75 minutes at 20°C and 30 minutes at 24°C (*Ramsthaler et al. 2012*). In the other, drying time was recorded for blood deposited on lino at -3°C, 22°C and 45°C. Results again supported a negative correlation between temperature and drying time with stains exhibiting an average drying time of 87 minutes at -3°C and 13 minutes at 45°C (*Brady et al. 2002*). The results for drying time at 22°C however indicated that temperature is perhaps not the sole environmental influence on drying time. At 22°C average drying time was 8 minutes, shorter than drying time at the much colder temperature of -3°C but also shorter than drying time at the higher temperature of 45°C. If temperature is the main influence on drying time this result appears anomalous. Relative humidity readings of 64% at -3°C, 67% at 22°C and 92% at 45°C indicate that humidity at 45°C was very high which may have partially affected the drying process, lengthening drying time at 45°C. In order to establish the true effect of humidity on drying time and the relative strengths of temperature and humidity on drying times, much more detailed experimental work needs to be conducted on environmental influences on bloodstain drying time.

The development of detailed empirical understanding of these influences would assist investigators in establishing more accurately drying times and therefore upper-limits to possible stain deposition times.

### **3.1.3 Influence of surface characteristics on bloodstains**

The influence of surface characteristics on bloodstain morphology and appearance is an important consideration when analysing stains generated across a range of

different surfaces. Despite the likelihood of encountering stains formed on different surfaces, relatively little has been empirically established about the influence of surface characteristics on bloodstains formed on them. In relation to their influence on stain identification and drying time a limited number of experimental studies have been conducted.

In developing a quantitative method for analysing stain colour to infer environmental conditions surrounding stain generation, the influence of surface characteristics on stain colour needs to be established. In existing studies on stain identification, experimental work has largely focused on the persistence of blood on different surfaces following washing or cleaning attempts (*Cox. 1990. Gross et al. 1999*) and the consequences of varying persistence on visual identification. No work has been conducted on the variability of stain colour between stains generated under identical environmental conditions on different surfaces. In developing methods for the analysis of stain colour, this variability needs to be experimentally tested.

Results from experimental work indicated that surface characteristics such as fibre weave, composition, absorbency and permeability influence stain retention rates with surfaces exhibiting high absorbency and permeability supporting higher retention rates. These characteristics may also exert an influence on drying time with implications for estimating time of stain deposition in crime scene reconstructions. Depending on nature of a particular surface, estimations of drying time for stains generated under identical environmental conditions should vary for different surfaces. Increasing awareness of the magnitude and nature of these variations is necessary to allow estimations of drying time to be completed to the highest accuracy possible.

Further experimental work is required to explore the true potential for interpretations of stain drying times on a range of surface in crime scene reconstructions.

## 3.2 Experimental overview and formation of hypotheses

### 3.2.1 Experimental overview

Following identification of existing gaps in certain areas of experimental Bloodstain Pattern Analysis research, an experimental design was developed. Hypotheses relating to the identification of bloodstains, environmental influences on bloodstains and influence of surface characteristics were all incorporated into the experimental design (*figure 28*).

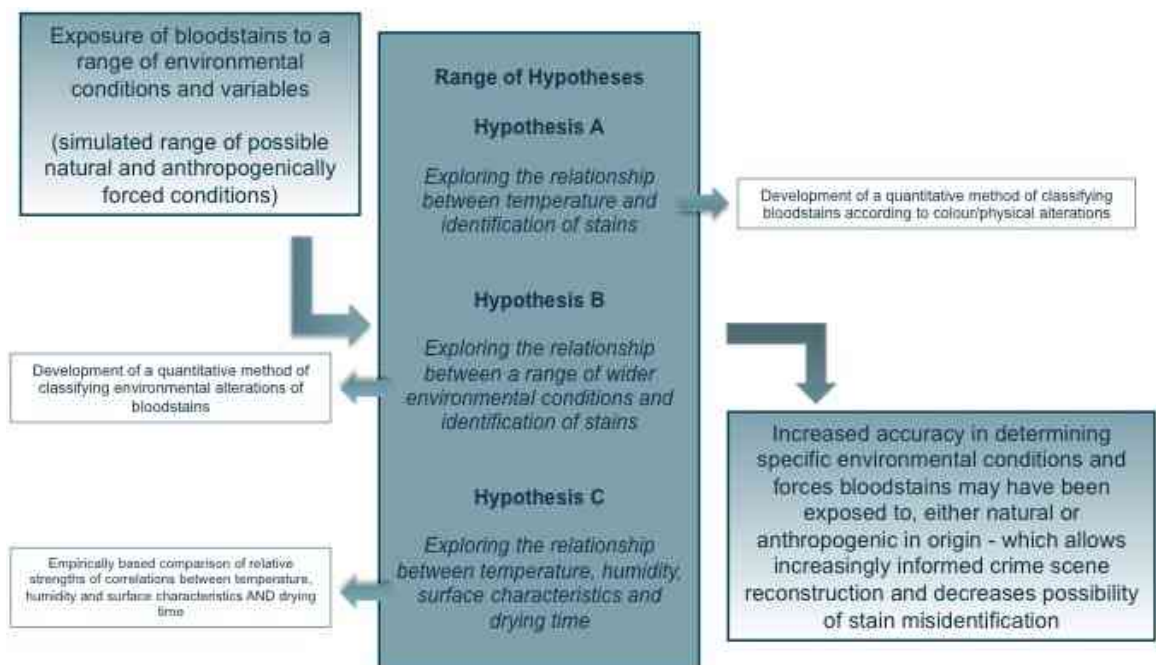


Figure 28 Experimental overview, outlining general focus of experimental enquiry ('Exposure of bloodstains to a range of environmental conditions and variables'), desired experimental outcome (increased accuracy of analysis of environmentally altered bloodstains), three distinct groups of hypothesis (A, B & C) and the outcomes associated with each

Bloodstains generated on different surfaces were exposed to a range of environmental conditions and variables, across a number of experimental stages. Observations and measurements regarding stain responses to these conditions were recorded and then interpreted in the context of the associated environmental conditions. This allowed identification of quantitative relationships existing between certain environmental variables and bloodstain appearance and behaviour.

Observations and measurements were organised to facilitate the exploration of three separate groups of hypotheses, each of which corresponded to a distinct area of experimental enquiry (**A, B & C**). Individual hypotheses within each group were developed from extensive literature review (*chapter 2*) and grouped collectively to focus on **A**) exploring the relationship between temperature and identification of stains **B**) exploring the relationship between a range of wider environmental conditions and identification of stains and **C**) exploring the relationship between temperature, humidity, surface characteristics and drying time.

The overall experimental aim was to increase the accuracy with which Bloodstain Pattern Analysts can approach analysis of physically altered bloodstains (PABs) at a crime scene for the purposes of crime scene reconstruction. The answering of each hypothesis achieved this by providing a basis for the development of quantitative and empirically based methods of stain analysis.

### 3.2.2 Formation of hypotheses

Individual hypotheses were collectively grouped to form three thematic groups of hypotheses (**A, B & C**). Each group was defined according to their relevance to separately distinct areas of experimental enquiry.

#### 3.2.2.1 Hypothesis Group A

Hypothesis group **A** focused on the exploration of the relationship between temperature and identification of bloodstains. Results assisted the development of a quantitative method for classifying stains generated at different temperatures, according to appearance and behaviour, which has implications for crime scene reconstruction. Individual hypotheses tested in group **A** are outlined below.

---

#### Temperature and chemical identification:

<b>H<sup>A</sup></b>	Stains generated at a range of temperature intervals between -10°C & 50°C can be positively identified by a range of presumptive chemical tests.
----------------------	--

Temperature and stain appearance:	
H <sup>A</sup>	At all temperatures, stains exhibit higher R than G or B values. Stains are therefore coloured towards a red hue.
H <sup>A</sup>	Temperature has a significant influence on stain colour (R, G & B values, RGB totals).
H <sup>A</sup>	Temperature has a significant negative correlation to quantitative measures of stain colour (R-values and RGB totals)
H <sup>A</sup>	Stains generated at high temperatures exhibit lower R-values and RGB totals and therefore darker intensities of colour than stains generated at low temperatures.
H <sup>A</sup>	Within the temperature range -10°C to 50°C, significant alterations to quantitative measures of stain colour (R, G & B values, RGB totals) occur at particular temperature intervals.

Answering hypotheses in Group A assisted with the development of a quantitative method for interpretation and analysis of environmentally altered stains, based on the classification of stain colour according to temperature.

### 3.2.2.2 Hypothesis Group B

Hypothesis group **B** focused on exploration of the relationship between a range of environmental conditions and identification of bloodstains. Stains were exposed to naturally variable environmental conditions over longitudinally progressive periods of time or for fixed consecutive periods of time that were characterised by differences in environmental conditions. Other stains were exposed to different environmental extremes: snow, freeze-thaw mechanisms, freezing, high temperatures and fire. Results assisted the development of methods for identifying and analysing different classifications of environmentally altered bloodstains. Individual hypotheses tested in group **B** are outlined below.

Environmental exposure and chemical identification:	
H <sup>A</sup>	Presumptive identification of stains is not inhibited by exposure (either longitudinal or periodic) to naturally variable environmental conditions
H <sup>A</sup>	Presumptive identification of stains is not inhibited by exposure to extreme conditions of freeze-thaw, freezing, high temperatures and fire.

<b>Environmental exposure and stain appearance:</b>	
<b>H<sup>A</sup></b>	Humidity has an influence on stain colour.
<b>H<sup>A</sup></b>	Humidity has significant positive correlation to quantitative measures of stain colour (R value, RGB total).
<b>H<sup>A</sup></b>	Significant alterations to quantitative measures of stain colour (R, G & B values, RGB totals) occur at particular levels of relative humidity.
<b>H<sup>A</sup></b>	Stains exposed to naturally variable environmental conditions exhibit significant differences in colour (R, G, B values & RGB totals) to stains generated in laboratory-controlled conditions.
<b>H<sup>A</sup></b>	Stains exposed to naturally variable environmental conditions for longer longitudinal periods of time exhibit significantly lower R, G, B values and RGB totals than stains exposed for shorter longitudinal periods.
<b>H<sup>A</sup></b>	Stains exposed to naturally variable environmental conditions for longitudinal periods exhibit lighter intensity of colour (lower R, G, B values and RGB totals) than stains exposed for monthly periods.
<b>H<sup>A</sup></b>	Stains exposed to naturally variable environmental conditions for different monthly periods differ significantly according to R, G, B values and RGB totals.
<b>H<sup>A</sup></b>	Stains exposed to snow exhibit significant differences in colour (R, G, B values & RGB total) to stains generated in laboratory-controlled or naturally variable conditions.
<b>H<sup>A</sup></b>	Stains exposed to freeze-thaw conditions exhibit significant differences in colour (R, G, B values & RGB total) to stains generated in laboratory-controlled or naturally variable conditions.
<b>H<sup>A</sup></b>	Stains exposed to freezing exhibit significant differences in colour (R, G, B values & RGB total) to stains generated in laboratory-controlled or naturally variable conditions.
<b>H<sup>A</sup></b>	Stains exposed to high temperatures (100°C, 150°C, 200°C, 25°C) exhibit significant differences in colour (R, G, B values & RGB total) to stains generated in laboratory-controlled (-10°C to 50°C) or naturally variable conditions.
<b>H<sup>A</sup></b>	Stains exposed to burning exhibit significant differences in colour (R, G, B values & RGB total) to stains generated in laboratory-controlled or naturally variable conditions.
<b>Surface characteristics and stain appearance:</b>	
<b>H<sup>A</sup></b>	Stains generated on three different surfaces (paper, glass and denim) all exhibit higher R than G or B values. Stains are coloured towards a red hue.
<b>H<sup>A</sup></b>	Stains generated on different surfaces (paper, glass and denim) differ in intensity of red colouration according to varying ratios of R, G and B values and RGB totals.

Answering hypotheses in Group B determined whether the development of a quantitative method for identification, interpretation and analysis of environmentally

altered stains, based on the classification of stain colour according to temperature and environmental influences, is possible.

### 3.2.2.3 Hypothesis Group C

Hypothesis group C focused on exploration of relationships between a range of variables and drying time. Variables tested by individual hypotheses in group C included temperature, humidity, drop volume, stain diameter, age of blood, surface characteristics. Results assisted in the identification of individual as well as comparative strengths of influence exerted by each variable on stain drying time. From results, a method for quantitative calculation of upper drying time limits for bloodstains generated across different surfaces and environmental conditions could be developed, which has implications for crime scene reconstruction. Individual hypotheses tested in group C are outlined below.

Temperature and drying time:	
H <sup>A</sup>	There is a negative correlation between temperature and drying time.
H <sup>A</sup>	Within the temperature range -10°C to 50°C, significant changes in drying time occur at particular temperature intervals.
Humidity and drying time:	
H <sup>A</sup>	There will be a positive correlation between relative humidity and drying time.
H <sup>A</sup>	Significant changes in drying time are correlated with specific measures of relative humidity.
Drop volume and drying time:	
H <sup>A</sup>	There is a positive correlation between drop volume (10µl or 45µl) and drying time.
Stain diameter and drying time:	
H <sup>A</sup>	There is a negative correlation between stain diameter and drying time.
Age of blood and drying time:	
H <sup>A</sup>	Age of blood has a significant influence on stain drying time.

---

**Surface characteristics and drying time:**

**H<sup>A</sup>** Surface characteristics and type have a significant influence on stain drying time.

**H<sup>A</sup>** There is a positive correlation between surface roughness and stain drying time.

---

Temperature, humidity, drop volume, stain diameter, age of blood and surface characteristics are all variables that exert an influence on bloodstain drying time. Testing of hypotheses focused on the individual influence of each of these variables on drying time are therefore underpinned by an assumption that during testing of each, all other variables were kept constant. This was achieved with the exception of humidity, which due to experimental limitations was not possible to control.

The comparative strengths of individual variables were tested by further hypotheses.

---

**Drying time:**

**H<sup>A</sup>** A correlation exists between temperature and humidity.

**H<sup>A</sup>** Environmental variables (temperature & humidity) exert the greatest influence on stain drying time compared other variables (drop volume, stain diameter, age of blood, surface characteristics).

**H<sup>A</sup>** Surface characteristics exert a more significant influence on stain drying time than drop volume, stain diameter and age of blood.

**H<sup>A</sup>** Quantitative calculation of upper drying limits for bloodstains generated across different surfaces and environmental conditions is possible.

---



### 3.3 Developing a methodology

An experimental, multi-stage methodology was developed as the most suitable approach to testing hypotheses.

Having outlined criticisms of certain aspects of forensic and Bloodstain Pattern Analysis research and highlighted the advantages of shifting the discipline's research-focus towards a more empirical and scientifically robust one (*sections 1.5 – 1.6*) an experimental methodology was considered the only suitable approach towards establishing an objective set of robust and replicable results in previously un-researched aspects of the discipline.

A multi-stage approach was adopted to allow observations and results to be interpreted and tested through progressively more complex and ecologically valid scenarios. Given the limited empirical understanding of environmental influences on bloodstains, it was important that results were initially established in the context of a relatively variable controlled environment. Once established, results could be extrapolated to observations made in more realistic and variable scenarios, more likely to be encountered by forensic investigators. Evidence at a scene is often complex and highly case-specific due to the variable nature of crime scene conditions (*Peschel et al. 2010*). Any experimental development of knowledge or techniques, involving the interpretation or analysis of evidence, needs to be sensitive to this to be relevant across a wide range of possible scenarios. A multi-stage or – tiered approach ensures this, with initial experimental stages dealing with establishing general principles of specific forensic interactions and latter stages with developing and introducing increasing number of variables to create an empirical understanding of more complex, case-specific interactions (*Morgan et al. 2009*).

The methodology was divided into four experimental stages (*figure 29*). Each stage was designed to generate a series of specific observations. In combination, these observations allowed the answering of numerous hypotheses relating to the analysis of environmentally altered bloodstains.

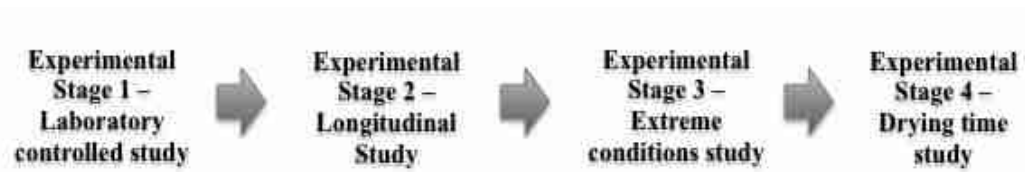


Figure 29 Division of experimental methodology into four distinct experimental stages

Each experimental stage was defined by an individual set of conditions and variables, expected outcomes and limitations (*figure 30*).

	Stage 1	Stage 2	Stage 3	Stage 4
Environmental conditions	Controlled temperature range (-10°C – 50°C).	Natural environment fluctuations over course of 6 months.	Extreme environmental conditions.	Controlled temperature range (-10°C – 50°C).
Surfaces	Glass slides, denim fabric, paper	Glass slides, denim fabric, paper	Glass slides, denim fabric, paper	Glass slides, denim fabric, paper
Independent variable (s)	Surface characteristics. Blood drop volume. Stain diameter. Temperature. Humidity.	Surface characteristics. Blood drop volume. Stain diameter. Temperature. Humidity. Conditions of exposure	Surface characteristics. Blood drop volume. Stain diameter. Climatic conditions.	Surface characteristics. Blood drop volume. Stain diameter. Temperature. Humidity.
Dependent variable (s)	Stain appearance and response to identification tests.	Stain appearance and response to identification tests.	Stain appearance and response to identification tests.	Drying time.

Figure 30 Description of experimental stages, outlining the environmental conditions stains were exposed to in each, stained surfaces, independent and dependent variables

### 3.4 Sourcing generic experimental materials

Certain materials and methods were used generically during the course of all experimental stages, in order to maintain fundamental experimental consistencies. These included type and source of blood, the chemical tests used to identify blood and quantitative methods of visualizing stains. To avoid repetition across the

methodologies of each individual stage, these generic methodological aspects are discussed here.

### **3.4.1 Sourcing blood**

A decision was made to use ovine (sheep) blood for experimentation, with several justifications. The decision to use animal blood rather than human blood satisfied laboratory regulations and ethical concerns regarding the use of human blood.

A combination of considerations including fluid characteristics (*Laurent. 1999*), zoonotic disease capabilities (*Christman. 1996*) and commercial availability of animal bloods led to the decision to source ovine blood. In terms of fluid characteristics such as surface tension, viscosity and fluidity, swine (pig) blood is considered most homogenous to human blood (*Laurent. 1999*). Differentiation of these characteristics between ovine and human blood is however also relatively negligible and considered insignificant for the purposes of the research proposed. The use of ovine rather than swine blood was therefore based on further considerations of zoonotic disease capacities and commercial availability. Swine blood carries a higher risk of zoonotic disease transmission and was more expensive (per volume) than ovine blood. Taking all considerations into account, ovine blood was identified as the most suitable experimental blood.

To facilitate the transportation, storage and extended use of blood, it was necessary for the suppliers to add an anticoagulant or preservative to the whole blood product. Alsevers solution, an isotonic, balanced salt solution, was selected as the preserving agent (*figure 31*). Once mixed in equal volumes with whole blood it has a preservative effect on blood (if stored at refrigerator temperatures) for up to 10 weeks. (*Sigma-Aldrich, Inc. 2011*). In reality, during experimentation, blood was only ever stored (under refrigerated conditions) for a maximum of two weeks.



Figure 31 Photograph of 100ml ovine (sheep) blood mixed in solution with Alsevers solution

(Author. 2012)

### 3.4.1.1 Blood sampling considerations

Experimental work was completed over an extended period meaning it was necessary to source blood throughout the calendar year. The potential effect of seasonal variability on characteristics of sourced blood therefore required consideration.

Hematocrit (or Packed Cell Volume – PCV) is an expression of the volume percentage of red blood cells (erythrocytes) in blood (*Wonder. 2001*) which influences the overall colour of blood, varying the intensity and strength of orientation towards a red hue. The higher the hematocrit, the greater the proportion of total blood volume is comprised of red blood cells and therefore the greater the intensity and strength of red colouring. In humans, variability in hematocritic values exists as a function of age (*Maes et al. 1995*), according to diet, substance use and abuse, general health (*Wonder. 2001*) and to a lesser extent seasonality (*Gallerani et al. 2013*). In animals, hematocritic variability is most commonly a function of age (*Jelinek et al. 1984*), breed (*Shaffer et al. 1981*) and seasonality (*Lane. Campbell. 1969. Dini et al. 2011*). As an expression of red blood cell count, inherent variability in an individual's hematocrit means there is an inherent variability, or source of variability, in the colour of blood. This variability needs to be considered when attempting analysis of blood on the basis of colour.

As blood used in experimentation was sourced from animals, in different batches over the course of 18 months, the potential effects of age, breed and season of

sampling from donor animals on hematocrit values and therefore colour of blood and subsequent colour analysis of stains was considered. For the purposes of experimental work conducted, the potential variability of haematocrit did not need to be incorporated for consideration into the interpretation of results for two reasons. Firstly, the source of experimental blood collected blood into Alsevers solution to engender a preservative effect upon it. As is laboratory practice, all blood collected into Alsevers is then '*adjusted to a standard packed cell volume to ensure product consistency*' (Harlan Laboratories. 2013). This practice ensured that a consistent hematocrit was maintained throughout experimental work. Secondly, studies have observed that seasonal variability in hematocrit is significantly minimised in animals that are being clinically controlled, as the donor animals used for blood sourcing were (Dini et al. 2011).

In forensic reality, the hematocrit of blood encountered is likely to be highly variable. The causes and effects of its variability on any subsequent stain colour analysis must therefore be considered before any conclusions relating to colour analysis can be made.

### **3.4.2 Ethical considerations surrounding the use of animal blood**

The use of blood product requires careful ethical consideration. The use of biological materials from sentient donor creatures engenders two main ethical concerns. The first is with the potential transmission of zoonotic diseases (animal to human transmissions) associated with non-appropriate handling, storage and disposal of animal blood used in experiments. The second is with the sourcing of blood from donor animals, bred and kept specifically for this purpose.

The transmission of zoonotic diseases is an ethical concern given that "*approximately 75% of recently emerging infectious diseases affecting humans are diseases of animal origin*" (Center for Disease Control and Prevention. 2011). Although the magnitude of the consequences of potential transmissions is clearly sizeable, the likelihood of transmission occurring during experimentation was minimised in a number of ways. Blood was sourced from an established UK-based

supplier who only sample biological products from un-diseased animals in accordance with existing UK regulations and restrictions. Many zoonotic diseases are transmitted following regular handling of infected animals and by sourcing whole blood remotely from donor animals the risk of contracting these diseases is entirely mitigated. As a final but nevertheless important precaution, the disposal of animal blood used in experiments was carried out in accordance with designated laboratory procedures for the disposal of biological materials. As the laboratory space being utilised for experimentation is a UCL laboratory, guidelines regarding approved methods of disposing of ‘anatomical waste’ set out by UCL Safety Services were consulted and adhered to.

The sourcing of blood from donor animals, specifically bred for that purpose, raises additional ethical concerns relating to the unnecessary suffering of animals. The Animal Welfare Act (2006) and Animal (Scientific Procedures) Act (1986) were specifically drawn up to guard against this and to establish basic animal welfare rights for animals defined as “protected animals”. This includes any domesticated animals in the British Isles and those either permanently or temporarily under the control of man (*Animal Welfare Act. 2006*). The supplier selected for sourcing blood is regulated by and monitored in accordance with these Acts to ensure the well-being of donor animals, that any unnecessary suffering is minimised and that extraction of donor blood is conducted carefully. Total avoidance of use of animal blood was unrealistic given the experimental demands of the proposed research, however pursuing a policy of; **a)** substitution **b)** reduction and **c)** consistency where possible helped responsibly minimise the use of blood and associated discomfort to donor animals (*Cohen. 1986*). **Substitution** in the case of the proposed research could have been achieved through the use of a proxy artificial blood. For the purposes however of ensuring ecological validity of observations, the use of real blood during experimentation was considered necessary. **Reduction** in the case of proposed research work was achieved by conducting preliminary experiments, designed to familiarise the researcher with experimental methodologies, with artificial proxy blood so as to not unnecessarily waste donor blood. **Consistency** in the use of animal donors as a blood source refers to consistency between personal and professional ethics in relation to the use of animals in scientific research (*Macklin. 1997*). An individuals’ holding of personal objections to the use of animals in scientific

research, for example, is arguably undermined and inconsistent if they simultaneously condone the killing of animals for other purposes, for example as food or clothing materials. Proponents of this argument suggest that the welfare of animals destined for the abattoir and methods of killing employed therein are likely to cause much more distress and discomfort to animals than suffered by those used in scientific research (*Cohen. 1986*).

Adopting a policy of substitution, reduction and consistency where possible somewhat mitigated ethical objections to the use of animal blood in experimental work.

### **3.4.3 Chemical tests**

Chemical identification tests are conducted on suspect stains in order to identify whether or not the stains are likely to be blood and if so, what species they originate from. Several different chemical tests are available to investigators, each presenting their own advantages or disadvantages in terms of practicality, cost, sensitivities, environmental application and limitations (*section 2.4.1*). The main distinction between chemical tests is whether they are presumptive or confirmatory in nature. Presumptive tests, such as Luminol, Kastle-Meyer, LMG, Hemastix and Bluestar®, are used to indicate the potential presence of blood in a suspect stain. They can however give false-positives and their use is therefore limited to providing indicative identification methods, which allow investigators to then focus further confirmatory testing on a smaller scale. Confirmatory tests, such as Hematrace® and Hexagon OBTI, can then be used to confirm the presence of blood and also give an indication of the species of blood origin.

A range of commercially available and commonly used chemical tests was selected for experimental work. Tests selected included the Kastle-Meyer, Hemastix, Bluestar® and Hexagon OBTI tests. The Kastle-Meyer, Hemastix and Bluestar® tests are all examples of presumptive tests and were therefore considered appropriate tests for use on animal bloodstains. The Hexagon OBTI test, as an example of a confirmatory test, only yields positive results in the presence of human blood. As

sheep blood was used in all experiments the ultimate exclusion of the Hexagon OBTI test from chemical testing was justified (explanation of the application of the Hexagon OBTI confirmatory test is provided in *appendix 1*).

Explanations of the tests used (Kastle-Meyer, Hemastix & Bluestar<sup>®</sup>), their methods of application and guidelines for use are outlined below.

#### 3.4.4 The Kastle-Meyer (KM) presumptive test for blood



Figure 32 Kastle-Meyer test kit containing 25ml KM reagent and 25ml Hydrogen Peroxide

(SceneSafe.co.uk)

##### 3.4.4.1 Product description:

The Kastle-Meyer test relies upon the oxidation of colourless phenolphthalin (in KM reagent) to pink phenolphthalein. Oxidation is promoted in the presence of both the iron element of haemoglobin and hydrogen peroxide.



Figure 32.a Photographs from L to R illustrating bloodstain pre-testing (L), filter paper which has been rubbed over a stain and had KM solution added to it (M) and the filter paper following addition of Hydrogen Peroxide solution indicating a presumptive positive reaction for blood (Author. 2011)

##### 3.4.4.2 Application method:

A small, clean, dry piece of filter paper was gently rubbed across a suspected stain. 1 to 2 drops of KM solution were then deposited onto the paper. Following a period of



5-10 seconds, if no colour had developed, the test was continued by adding 1 to 2 drops of 6% Hydrogen Peroxide solution to the paper. Observation of an immediate pink colouration following addition of Hydrogen Peroxide indicates a presumptive positive reaction for blood. The test solutions naturally oxidize over time, bringing about pink colouration, so only reactions occurring ‘immediately’ (within 30 seconds) were considered presumptive positive for blood (*Bevel. Gardner. 2008*).

#### 3.4.4.3 Guidelines for use:

Prior to testing test kits and components were checked to ensure they were within their expiry date and that the KM reagent did not show any signs of oxidation (pink colouration). Whilst conducting the tests protective gloves, clothing and eyewear were worn, due to the irritable, flammable and corrosive nature of reagents (*SceneSafe. 2011*).

#### 3.4.5 The Hemastix® presumptive test for blood



Figure 33 Hemastix® test strips

(*SceneSafe.co.uk*)

##### 3.4.5.1 Product description:

Hemastix® strips were originally designed for the detection of blood traces in urine. By slight adaptation of the method of application however, the test strips can be used as a presumptive test for blood. Test strips contain two compounds **1)** *diisopropylbenzene dihydroperoxide* and **2)** *tetramethylbenzidine*. The peroxidase-like activity of haemoglobin, present in blood, catalyses a reaction converting the reduced colourless form of *tetramethylbenzidine* to an oxidized coloured form. The catalysis of this reaction is demonstrated by colouration of the pad on the end of test

strips from orange to green (and in the presence of high concentrations of blood to blue) (*Siemens Healthcare Diagnostics Inc. 2008*).

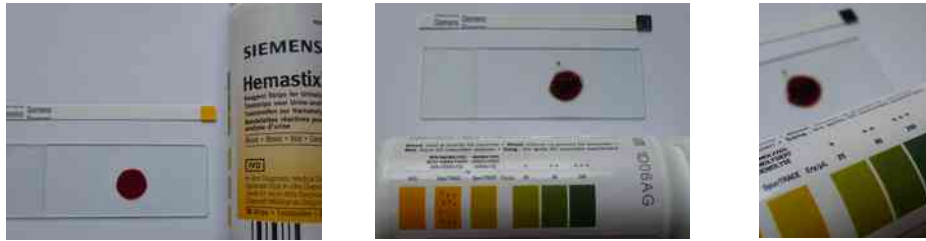


Figure 33.a Photographs from L to R illustrating bloodstain pre-testing (L), indication of a presumptive positive reaction for blood through dark-green colouration of the test strip (M) and of association of different colours to varying concentrations of blood (R) (*Author. 2011*)

#### 3.4.5.2 Application method:

2 to 3 drops of distilled water were applied to the pad-end of a Hemastix® test strip. The dampened pad was then gently rubbed across a suspect stain. The strip was then left for approximately 60 seconds and then observed for any colour changes. A colour change through orange to green or dark-blue was interpreted as a presumptive positive reaction for blood (*Bevel. Gardner. 2008*).

#### 3.4.5.3 Guidelines for use:

Prior to testing, test strips were checked to ensure they were within their expiry date. Whenever test strips were not in use they were stored in a tightly closed container, containing desiccant.

#### 3.4.6 The Bluestar® presumptive test for blood



Figure 34 Bluestar® forensic test kit (*SceneSafe.co.uk*)

##### 3.4.6.1 Product description:

Bluestar® is a luminol-based reactive agent. Luminol is a chemical compound that exhibits chemiluminescent properties in the presence of an oxidizing agent. In order

to prepare the agent for use the luminol must be activated with an oxidant (usually Hydrogen Peroxide).

When this luminol & oxidant solution is exposed to blood, iron present in Haemoglobin acts as a catalyst, speeding up the reaction between luminol and hydrogen peroxide to produce the strong chemiluminescent property of luminol, demonstrated through the emission of a blue light (*Bluestar® Forensics Ltd. 2012*).

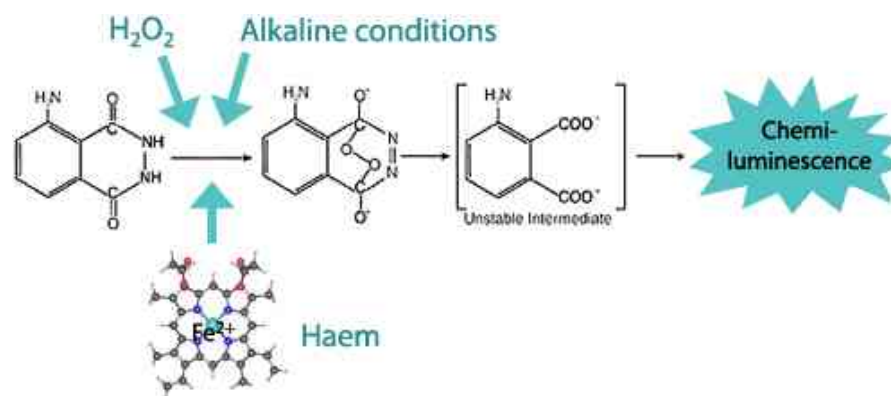


Figure 35 Illustration of the reaction of luminol in the presence of blood. The compound to the left of the reaction is luminol (a compound consisting of nitrogen, hydrogen, oxygen and carbon). It is activated by the addition of Hydrogen Peroxide ( $H_2O_2$ ) and their reaction is catalysed in the presence of the iron in haemoglobin. During catalysis the luminol loses nitrogen and hydrogen atoms and gains oxygen atoms. This creates a new compound from the former luminol which is highly charged. Extra charge is therefore emitted as light. (*Bluestar® Forensics Ltd. 2012*)

#### 3.4.6.2 Application method:

Three oxidizing tablets were added to 500ml bottle of Bluestar® Forensic chemiluminescent solution which was sealed with a spray-applicator head. The bottle was then gently moved in a circular motion for approximately 1 to 2 minutes to ensure contents were evenly mixed. Once prepared, the solution was sprayed, from a distance of approximately 50cm, towards suspect stains in a horizontal, sweeping motion (*Bluestar® Forensic Ltd. 2006*).

Observations of intense light-blue chemiluminescence were interpreted as presumptive positive reactions for blood (*Bevel. Gardner. 2008*).

#### 3.4.6.3 Guidelines for use:

The Bluestar® solution promotes chemiluminescence in the presence of blood and conditions had to be manipulated in order to allow detection of this luminescence,

the intensity of which can vary according to the strength of reaction. To ease observations suspect stains were always tested indoors, in a completely darkened room, allowing time for eyes to adjust to darkness before conducting detection with Bluestar®. In accordance with guidelines, once mixed, Bluestar® solution was used within a 24-hour period.

### 3.4.7 Quantitative methods of visual identification of stains

Visual identification of stains is currently reliant upon an expert's knowledge of likely appearance and colour of bloodstains.

In order to provide a quantitative method for identifying and comparing stains generated at different temperatures, a method of digitally capturing and analysing the colour of stains was designed.

Immediately following removal from the experimental fridge, stains were digitally scanned, using a HP Scanjet flatbed scanner (*figure 36*) – with 2400 x 4800 dpi (dots per square inch) resolution. Stains were placed face down in the centre of the glass bed of the scanner. The scanner lid was then lowered and a box placed around the scanner, to ensure variations in ambient light levels did not influence stain imaging.



Figure 36 Illustration of process of digitally scanning stains (*Author. 2012*)

Once captured in a digital format (*figure 36*), quantitative information about stain appearance was extracted through application of colour analysis software to images of stains.

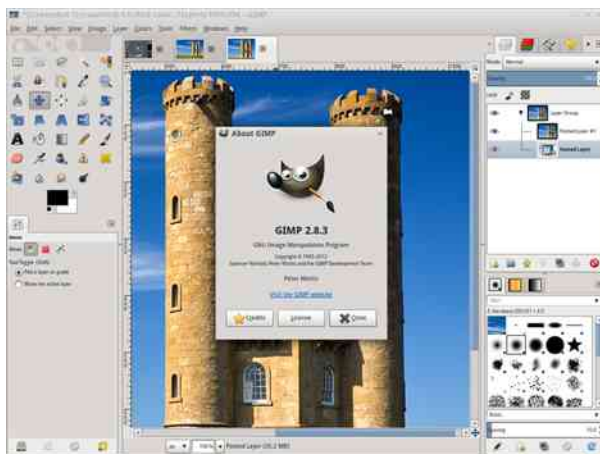


Figure 37 Screenshot of GIMP version 2.8 User interface

(<http://en.wikipedia.org/wiki/GIMP>)

The colour analysis software used was the GNU Image Manipulation Program (GIMP), freely available software capable of analysing and editing images (*figure 37*). Once an image had been opened in GIMP an eyedropper tool allowed selection of a certain area of an image. Once a selection had been made, colour analysis of the selected area was then carried out. Colour analysis is the process of evaluating an image or unknown colour according to known colour references. There are several measures through which this evaluation can be conceived. For the purposes of experimentation two particular measures were used: RGB values and hexadecimal values.

#### 3.4.4.1 RGB values

To form a colour, three separate beams of light are superimposed: red (R), green (G) and blue (B). The beams are emitted at varying intensities, depending upon the colour being represented. The RGB model is an additive colour model. This means it expresses the intensity of the three R, G and B components required in combination to produce a certain colour's spectrum.

The intensity of each R, G or B component is expressed as a 3-digit number, for example: R 105. This number can range from 000 to a maximum value of 255. 000 represents the darkest intensity of colour (considered '*black*') and 255 the lightest intensity of colour (considered '*white*'). When the numerical expressions of each of the three components are combined an RGB triplet is produced, for example: (R102, G204, B153). This 9-digit RGB triplet corresponds to a particular colour.

An RGB triplet of (R000, G000, B000) appears as black, whilst an RGB triplet of (R255, G255, B255) appears as white. If all intensities within the triplet are equal, for example R113, G113, B113, the colour produced appears a shade of grey. When the intensities expressed are different, a colourized hue, tending towards the most intense component is produced. For example, an RGB triplet of (R215, G075, B050) will be strongly orientated towards a red colouring (*figure 38*).

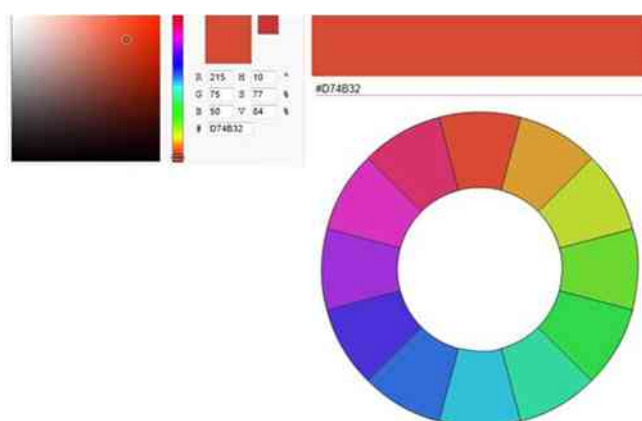


Figure 38 Expression of RGB triplet (R215, G075, B050)

([www.colorsfire.com](http://www.colorsfire.com))

The strength of orientation is determined by the difference between the strongest component (R215) and the weakest components (G075 & B050). The greater the difference, the stronger the expression towards one component, in this case: towards red, rather than green or blue.

The RGB model is used in computer monitors and other digital screens employing light, and therefore was deemed the most appropriate measure for analysing the colour of digital images. It also has the advantage of being a relatively simple and accessible method of quantifying colour.

### 3.4.4.2 Hexadecimal values

Hexadecimal values refer, as RGB values do, to colours used primarily in computing and digital screen formats.

Hexadecimal (or hex) values are expressed as 6-digit numbers, which broken down, consist of two digits coding for each of the levels of red, green and blue components present in a single colour. This 6-digit number is known as a hex triplet. Within the triplet the first two digits represent the red value, the middle two digits represent the green value and the final two digits represent the blue value (RRGGBB).

To generate a hex triplet (RRGGBB), RGB value triplets (RRRGGGBBB) have to be converted into 6-digit hexadecimal format, by dividing each RGB value (ranging from 000-255) by 16. The number of times 16 divides as a whole into each value becomes the first hexadecimal digit. The remainder is then used to derive the second hexadecimal digit. Hexadecimal digits used range from 0-F: (0, 1, 2, 3, 4, 5, 6, 7, 8, 9, A (10), B (11), C (12), D (13), E (14), F (15)), i.e. letters A-F are used to represent the numbers 10 to 15.

Using these conversion rules therefore, a RGB colour value of (R005, G158, B243) would be presented as 059EF3 in hexadecimal notation (*figure 39*).

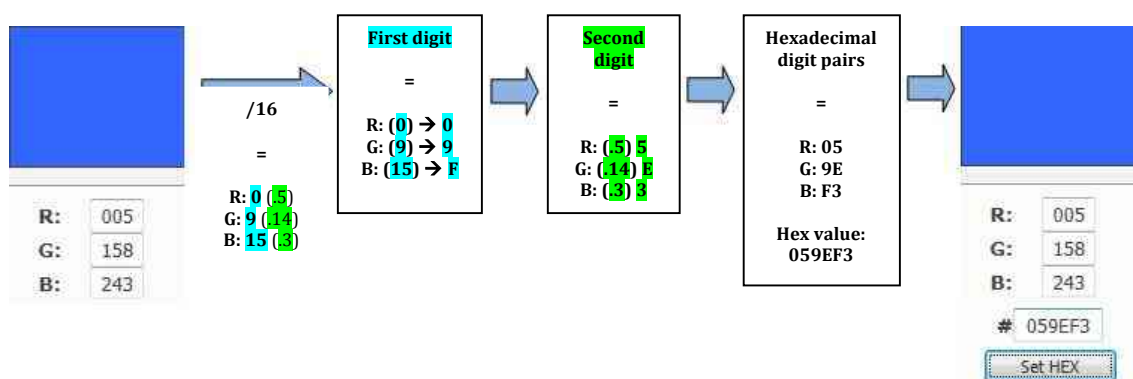


Figure 39 Conversion process of RGB value (R005, G158, B243) to Hex value #059EF3

In hexadecimal notation, digit pair's range from 00 to FF. 00 represents the lowest intensity possible and FF the highest intensity possible for a coloured component.



### 3.4.4.3 Colour analysis using GIMP software package

Using GIMP and RGB and Hexadecimal values generated, quantitative colour analysis of stains was possible. The process of conducting this analysis through the software was as follows. Scanned images of stains were opened in the GIMP software package (*figure 40*).

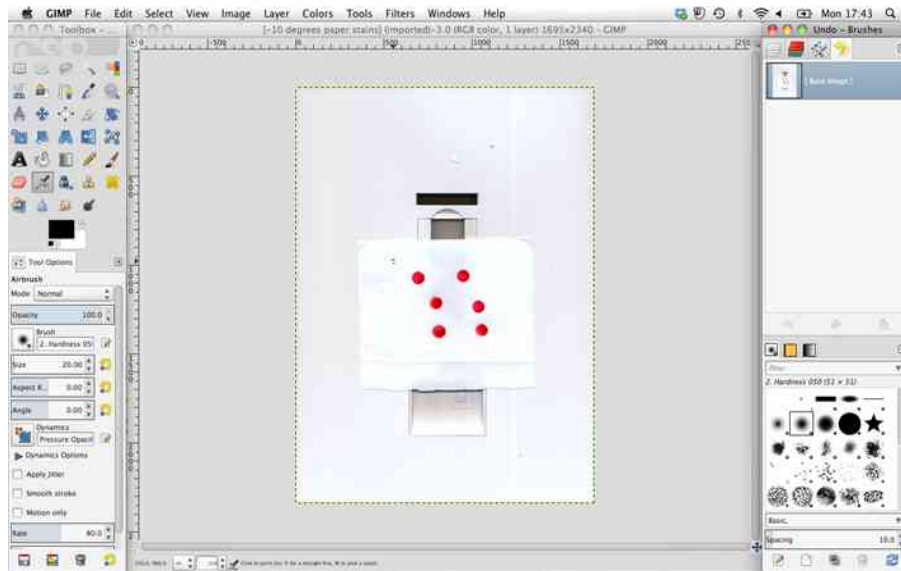


Figure 40 Scanned image of blood stains generated on paper at -10°C opened in GIMP software and displayed via the user-interface (GIMP software. 2012)

Stains were enlarged to 100% zoom magnification (*figure 41*). This allowed selection of the greatest area possible per individual stain and therefore the most thorough method of colour analysis.

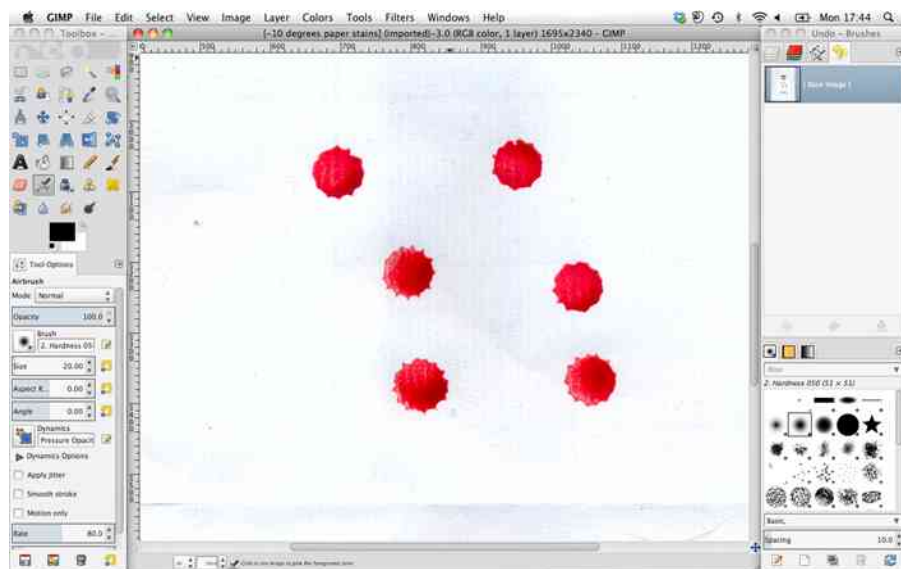


Figure 41 Bloodstains enlarged to 100% magnification (GIMP software. 2012)



An ‘eyedropper’ tool (*figure 42*) was used to select areas of individual stains to sample colour from. Under tool options several criteria were outlined prior to area sampling. The ‘Sample Average’ option was chosen, to instruct the eyedropper to compute an average colour value for the whole area of a stain sampled. The radius option allowed adjustment of the size of area to be sampled. This varied for each different surface, as stain size varied from surface to surface. The radius sizes for the different surfaces were: paper (24), glass (26) and denim fabric (30). Radius size was determined by the size of stains on different surfaces, so that for each stain the maximum area was included in computing an average colour. Finally, the option of using an ‘information window’ (*figure 43*) was checked, which generated a visible output when sample averages were calculated.

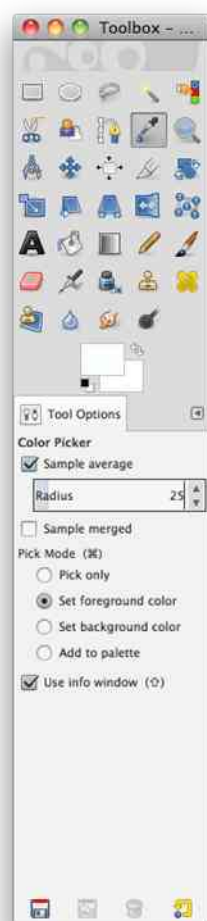


Figure 42 (Left) Eyedropper tool options

(GIMP software. 2012)



Figure 43 (Above) ‘Information window’ for sample analysed, indicating average R, G and B values, number of pixels represented by each colour and hexadecimal value

(GIMP software. 2012)

RGB and hexadecimal values were then recorded for comparative and interpretative purposes.

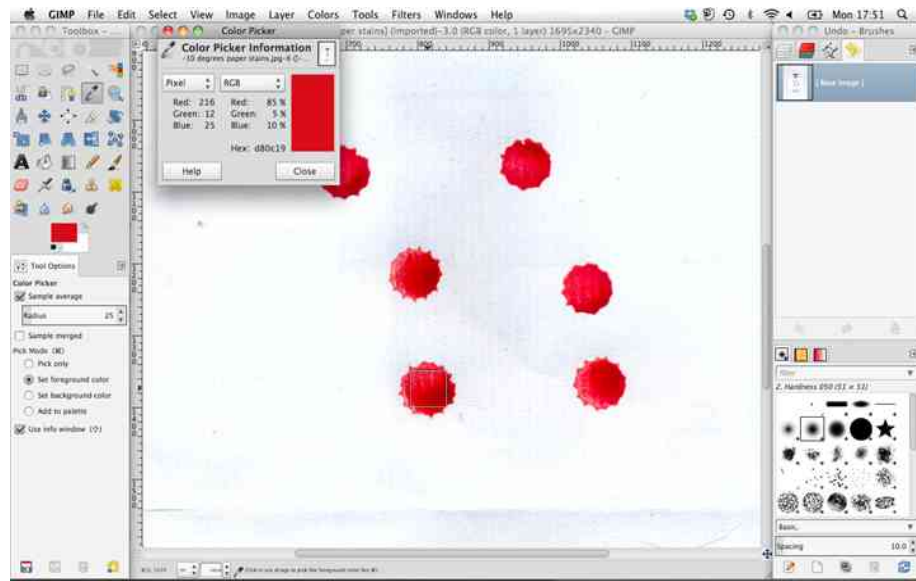


Figure 44 Completed GIMP software colour analysis of bloodstains generated on paper at  $-10^{\circ}\text{C}$   
(GIMP software. 2012)

## **Section 2**

## 4. Experimental Stage 1 – Exploration of environmental influences on bloodstain identification (laboratory controlled conditions)

### 4.1 Overview

Experimental stage 1 consisted of a series of drying experiments. Bloodstains, on a variety of surfaces, were dried at a range of different temperatures. Temperature was the main independent variable. Once stains had been dried they were subjected to observations about visual appearance (discolouration/translucency) and presumptive chemical tests. The primary objective of stage 1 was to establish whether visual or chemical identification of bloodstains, dried within a certain range of temperatures, was influenced by temperature.

### 4.2 Materials

The materials utilised for the experimental work in this chapter are set out in figure 45.

Experimental equipment	Additional specifications
<b>100ml whole Ovine blood</b>	With Alsever's solution
<b>MESM Portable laboratory refrigerator</b>	With temperature range -10°C to 60°C
<b>Temperature &amp; relative humidity data logger</b>	Ebro. VWR. EBI 20-TH1
<b>Paper</b>	Ryman's A4 white laid paper, 100 gm <sup>2</sup>
<b>Glass microscope slides</b>	CellPath. 90° ground edges. 25.4 x 76.2 mm. Thickness 1.0-1.2mm
<b>White denim cloth</b>	100% cotton. Weight: 345g/metre
<b>Plain white record cards</b>	Ryman's Silvine 127x77mm
<b>Thermo Scientific Finnpiptette® F1 Variable Volume Single Channel Pipette</b>	Volume range between 1-10µl
<b>Biological waste disposal unit</b>	
<b>Kastle-Meyer testing kit</b>	SceneSafe. Product code K160
<b>Hemastix® testing kit</b>	SceneSafe. Product code K162
<b>Bluestar testing kit</b>	SceneSafe. Product code K285
<b>Digital scanner</b>	HP Scanjet G2710

Figure 45 Table of materials used in experimental stage 1 (Author. 2012)

Justification for the selection of presumptive tests is provided in *section 3.4.3*.

## 4.3 Methodology

### 4.3.1 Temperature

During the experiment single blood drops, of a fixed 10 $\mu$ l volume, were deposited onto three different surfaces (paper, glass, denim fabric). Three surfaces were chosen to allow comparison of stains generated across surfaces exhibiting different characteristics in addition to being surfaces that are representative of a range of surfaces, with each readily available and commonly encountered in case work. Stains generated were then dried at a range of temperatures, chosen to mirror temperature ranges selected in previous experimental studies on the influence of temperature on bloodstains (*Ramsthaler et al. 2012. Brady et al. 2002*). The chosen range minimum was -10°C and the maximum was 50°C. Experimental temperatures were incrementally increased between the minimum (-10°C) and maximum temperature (50°C) through 5-degree intervals. This generated a set of stains dried at the following temperatures: -10°C, -5°C, 0°C, 5°C, 10°C, 15°C, 20°C, 25°C, 30°C, 35°C, 40°C, 45°C and 50°C. Temperature was increased by incremental intervals in order to facilitate the identification of any critical temperature margins where discolourations of stains or differential responses to chemical tests were observed. If, or once, any margin of change was identified, stains could be dried at 1°C intervals within that margin, to determine more precisely at what exact temperature changes were likely to occur at.

Temperature was controlled throughout experimentation by drying stains in a MESM portable laboratory refrigerator (*figures 46 & 47*), chosen for its ability to individually reach and sustain all designated temperature intervals within the chosen experimental range (-10°C to 50°C).



Figures 46 (L) and 47 (R) Images of portable laboratory refrigerator (*Author. 2011*)

### 4.3.2 Stain Sets

At each temperature interval a series of stain sets were generated. This allowed stains to be generated at each interval across the three different surfaces (paper, glass, denim fabric), in sufficient number to allow testing of each with 3 chemical presumptive tests. In total, at each temperature interval, 9 distinct stain sets were generated. A matrix (*figure 48*) outlines the parameters defining each stain set.

Paper	Glass	Denim Fabric	
AAA	BBB	CCC	Kastle-Meyer
AAA	BBB	CCC	Hemastix
AAA	BBB	CCC	Bluestar

*Figure 48 Matrix of 9 stain sets*

In the matrix 3 letters are used (A, B & C) to indicate stain sets formed on paper, glass & denim fabric respectively.

Stain sets formed on each surface were subjected to Kastle-Meyer, Hemastix and Bluestar presumptive chemical tests. In order to avoid any possible cross-contaminations, false-positives or negatives, a decision was made to conduct each presumptive chemical test on a previously untested stain set. Therefore, three separate stain sets were generated on each surface (AAA, BBB & CCC), under the same environmental conditions to allow for separate chemical testing.

Each of the 9 stain sets generated at each temperature interval was comprised of 6 replicate stains (*figure 49*). This allowed for repeat testing and identification of any possible errors across chemical testing results.

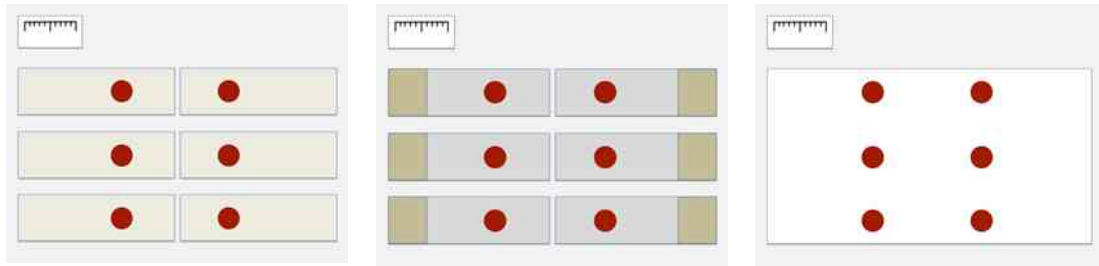


Figure 49 Sketches of 6 replicate stains on a) paper slips b) glass slides & c) denim fabric (L-R)  
(Author. 2012)

In total 702 individual bloodstains were generated, accounted for by 9 sets of 6 replicate stains at 13 temperature intervals (*figure 50*). The order in which they were generated was primarily arranged by temperature interval. Stain sets at the range minimum ( $-10^{\circ}\text{C}$ ) were generated first and stains sets at the range minimum ( $50^{\circ}\text{C}$ ) last. In between the range minimum and maximum, the order of staining ran sequentially in line with increases in temperature intervals.

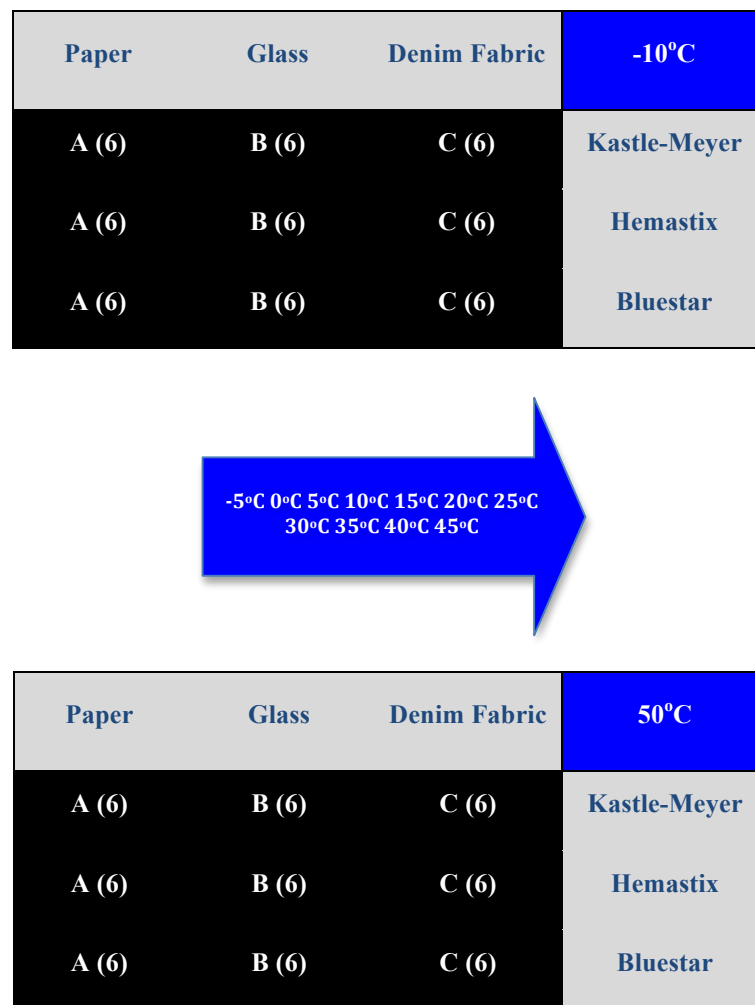


Figure 50 Illustrated breakdown of generation of 702 stains during experimental stage 1

### 4.3.3 Pre-experimental Fridge Set-Up

Prior to experimentation, the fridge was placed on its end, with the door opening towards the experimenter. This arrangement allowed horizontal shelves to be fixed within the fridge (*figure 51*), in order to maximise the number of stain sets that could be simultaneously placed in the fridge. Pieces of polystyrene, cut to size, were used as shelves. The decision to use polystyrene was due to its insulating nature, which would ensure the shelves maintained a more stable temperature in comparison to the metallic interior of the fridge.



Figure 51 Photograph of fridge set up on end with horizontal polystyrene shelves prior to experimentation

(*Author. 2012*)

With the addition of shelves, the fridge could house 3 stain sets at a time. Having determined a primary staining order which ran according to increases in temperature intervals, taking into account the capacity of the fridge, a decision was made to order the experimental run further, according to surfaces to be stained. For example, the 3 stain sets generated on paper at  $-10^{\circ}\text{C}$  were stained first, followed by all 3 stain sets generated on glass at  $-10^{\circ}\text{C}$  and finally all 3 stain sets generated on denim fabric at  $-10^{\circ}\text{C}$ . The complete order in which all stains were generated is shown in *figure 52*.



-10°C	<ul style="list-style-type: none"> <li>• AAA (Paper stains) (18)</li> <li>• BBB (Glass stains) (18)</li> <li>• CCC (Denim fabric stains) (18)</li> </ul>
-5°C	<ul style="list-style-type: none"> <li>• AAA (Paper stains) (18)</li> <li>• BBB (Glass stains) (18)</li> <li>• CCC (Denim fabric stains) (18)</li> </ul>
0°C	<ul style="list-style-type: none"> <li>• AAA (Paper stains) (18)</li> <li>• BBB (Glass stains) (18)</li> <li>• CCC (Denim fabric stains) (18)</li> </ul>
5°C	<ul style="list-style-type: none"> <li>• AAA (Paper stains) (18)</li> <li>• BBB (Glass stains) (18)</li> <li>• CCC (Denim fabric stains) (18)</li> </ul>
10°C	<ul style="list-style-type: none"> <li>• AAA (Paper stains) (18)</li> <li>• BBB (Glass stains) (18)</li> <li>• CCC (Denim fabric stains) (18)</li> </ul>
15°C	<ul style="list-style-type: none"> <li>• AAA (Paper stains) (18)</li> <li>• BBB (Glass stains) (18)</li> <li>• CCC (Denim fabric stains) (18)</li> </ul>
20°C	<ul style="list-style-type: none"> <li>• AAA (Paper stains) (18)</li> <li>• BBB (Glass stains) (18)</li> <li>• CCC (Denim fabric stains) (18)</li> </ul>
25°C	<ul style="list-style-type: none"> <li>• AAA (Paper stains) (18)</li> <li>• BBB (Glass stains) (18)</li> <li>• CCC (Denim fabric stains) (18)</li> </ul>
30°C	<ul style="list-style-type: none"> <li>• AAA (Paper stains) (18)</li> <li>• BBB (Glass stains) (18)</li> <li>• CCC (Denim fabric stains) (18)</li> </ul>
35°C	<ul style="list-style-type: none"> <li>• AAA (Paper stains) (18)</li> <li>• BBB (Glass stains) (18)</li> <li>• CCC (Denim fabric stains) (18)</li> </ul>
40°C	<ul style="list-style-type: none"> <li>• AAA (Paper stains) (18)</li> <li>• BBB (Glass stains) (18)</li> <li>• CCC (Denim fabric stains) (18)</li> </ul>
45°C	<ul style="list-style-type: none"> <li>• AAA (Paper stains) (18)</li> <li>• BBB (Glass stains) (18)</li> <li>• CCC (Denim fabric stains) (18)</li> </ul>
50°C	<ul style="list-style-type: none"> <li>• AAA (Paper stains) (18)</li> <li>• BBB (Glass stains) (18)</li> <li>• CCC (Denim fabric stains) (18)</li> </ul>

Figure 52 Order in which all stains in experimental stage 1 were generated (*Author. 2012*)

To complete the fridge set-up, a digital temperature & relative humidity data logger was placed within the fridge (*figures 53 & 54*). The addition of a data logger served three main experimental purposes. First, it offered a real-time indication of when a target temperature interval had been reached and therefore when stain generation for that temperature could commence. Secondly, the data logger provided a monitor of relative humidity during the experiment. It was not possible to control humidity during the experiment and so a method of measuring and monitoring levels of humidity was essential, in order to allow it to be taken into consideration as a variable. Finally, it recorded any fluctuations in temperature or relative humidity whilst stains were drying. As these fluctuations may have been possible causes of

any erroneous results, monitoring and recording them was important. The data logger was placed on the middle shelf of the fridge.



Figure 53 Digital data logger displaying temperature (Author. 2012)



Figure 54 Digital data logger displaying relative humidity (Author. 2012)

#### 4.3.4 Stain generation

To generate the first set of stains the temperature of the fridge was adjusted to the first experimental temperature ( $-10^{\circ}\text{C}$ ). A thin piece of insulating material was placed into the open side of the inner compartment of the fridge. The door was then shut and the fridge left for approximately 2 hours to adjust to the target temperature. In the meantime, the surfaces to be stained were prepared for staining. This involved cutting to size and mounted onto white record cards where appropriate, as in *figure 55*. White record cards were chosen, as a visual colour-based analysis of stains was later carried out and the white card provided a measure of controlled background colour.

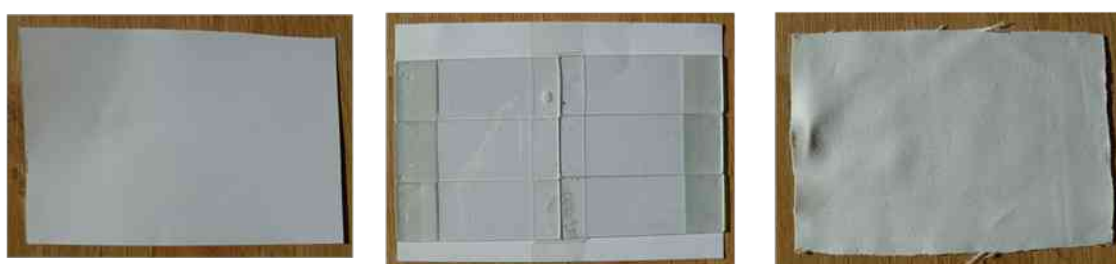


Figure 55 Surfaces to be stained prepared for experimentation (Paper/Glass/Denim from L-R) (Author. 2012)

After 2 hours, the fridge was re-opened and the data logger checked to ascertain that the target temperature interval had been reached. Stains could then be generated. Whilst preparing the stains, the fridge was reclosed, to prevent any alteration in temperature.



Figure 56 Fixed volume pipette set to deliver drops of 10µl volume (Author. 2012)

Using a fixed volume pipette (*figure 56*), a series of Ovine blood drops were deposited onto paper to form six separate replicate stains (*figure 57*). This process repeated on two other pieces of paper in order to make up the 3 stain sets generated on paper at -10°C, required for chemical testing. The fixed drop volume was 10µl. Once bloodstains had been generated, the blood was returned to storage at a refrigerated 4°C.

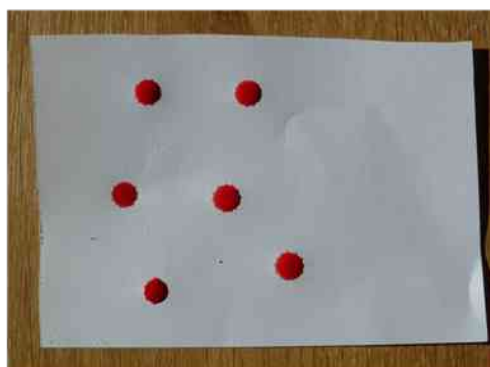


Figure 57 Six separate replicate stains generated on paper (Author. 2012)

All 3 paper stain sets were then placed in the experimental fridge and left to dry. Once dry, stains were removed from the refrigerator and immediately subjected to visual and chemical identification tests as set out in *sections 3.4.4 – 3.4.7*.

With the fridge temperature still set at -10°C, the process was then replicated to generate 3 sets, (each of 6 replicate stains), for the second target surface: glass microscope slides and then finally for the third target surface: denim fabric (*figure 58*).

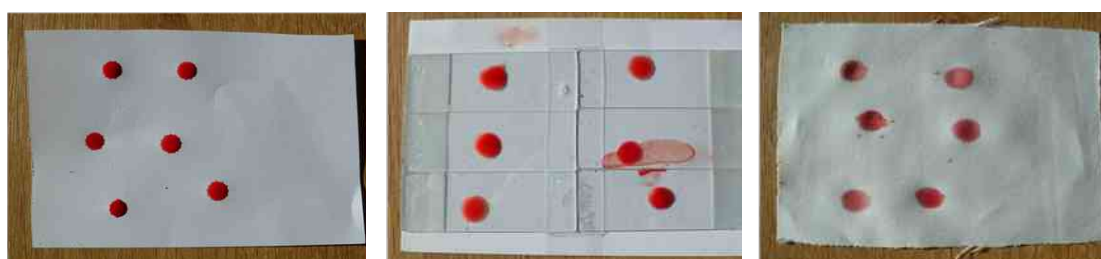


Figure 58 Stains generated on surfaces prior to drying (Paper/Glass/Denim, L-R) (Author. 2012)

Once stain sets had been generated for all 3 target surfaces at -10°C, the refrigerator was adjusted to the next experimental temperature (-5 °C) and left for 2 hours to reach that temperature throughout. Once the temperature had been achieved, the process of stain generation was then repeated. This process was repeated to generate stain sets at all experimental temperature intervals: -10°C, -5°C, 0°C, 5°C, 10°C, 15°C, 20°C, 25°C, 30°C, 35°C, 40°C, 45°C and 50°C.

Once stains were dry they were removed from the experimental unit and digitally scanned for visual analysis. Once scanned, stains were subjected to chemical testing. Of the 18 replicate stains generated on each surface, at each temperature interval, 6 replicates were subjected to Hemastix testing, 6 replicates were subjected to Kastle-Meyer testing and 6 replicates were subjected to Bluestar testing.

## 5. Experimental Stage 1 – Results

### 5.1 Stain generation checklist & results of chemical identification tests

Figure 59 presents the results of presumptive chemical identification tests on bloodstains dried at temperatures between -10°C and 50°C, at 5-degree intervals. The results of the tests for all 702 stains generated are shown in *figure 59* and indicate that all stains generated tested presumptive positive for blood. This suggests that exposing and drying blood at temperatures within the range: -10°C to 50°C has no adverse effect on chemical identification of bloodstains.

Temperature °C	Glass Microscope Slides			Paper Slips			Denim Strips		
	Hemastix	Kastle-Meyer	Bluestar	Hemastix	Kastle-Meyer	Bluestar	Hemastix	Kastle-Meyer	Bluestar
-10	6 +ive	6 +ive	6 +ive	6 +ive	6 +ive	6 +ive	6 +ive	6 +ive	6 +ive
-5	6 +ive	6 +ive	6 +ive	6 +ive	6 +ive	6 +ive	6 +ive	6 +ive	6 +ive
0	6 +ive	6 +ive	6 +ive	6 +ive	6 +ive	6 +ive	6 +ive	6 +ive	6 +ive
5	6 +ive	6 +ive	6 +ive	6 +ive	6 +ive	6 +ive	6 +ive	6 +ive	6 +ive
10	6 +ive	6 +ive	6 +ive	6 +ive	6 +ive	6 +ive	6 +ive	6 +ive	6 +ive
15	6 +ive	6 +ive	6 +ive	6 +ive	6 +ive	6 +ive	6 +ive	6 +ive	6 +ive
20	6 +ive	6 +ive	6 +ive	6 +ive	6 +ive	6 +ive	6 +ive	6 +ive	6 +ive
25	6 +ive	6 +ive	6 +ive	6 +ive	6 +ive	6 +ive	6 +ive	6 +ive	6 +ive
30	6 +ive	6 +ive	6 +ive	6 +ive	6 +ive	6 +ive	6 +ive	6 +ive	6 +ive
35	6 +ive	6 +ive	6 +ive	6 +ive	6 +ive	6 +ive	6 +ive	6 +ive	6 +ive
40	6 +ive	6 +ive	6 +ive	6 +ive	6 +ive	6 +ive	6 +ive	6 +ive	6 +ive
45	6 +ive	6 +ive	6 +ive	6 +ive	6 +ive	6 +ive	6 +ive	6 +ive	6 +ive
50	6 +ive	6 +ive	6 +ive	6 +ive	6 +ive	6 +ive	6 +ive	6 +ive	6 +ive

Figure 59 Checklist of number of stains (including replicates) generated across 13 temperature intervals & 3 different surfaces and the results of different chemical tests for these stains

### 5.2 Images of stains generated

Images of individual stains generated in experimental stage 1 are set out in section 5.2. Images were generated by digitally scanning stains immediately following their removal from the experimental unit. Stains are presented in groups of six, representing individual groups of 6 replicate stains generated on three different surfaces (paper, glass, denim) at each of thirteen different temperature intervals (-10°C, 5°C, 0°C, 5°C, 10°C, 15°C, 20°C, 25°C, 30°C, 35°C, 40°C, 45°C and 50°C). Images are accompanied by an indication of the surface and temperature stains correspond to. These images formed the basis for digital colour analysis of stains.

Figure 60 Stains generated on paper at -10°C

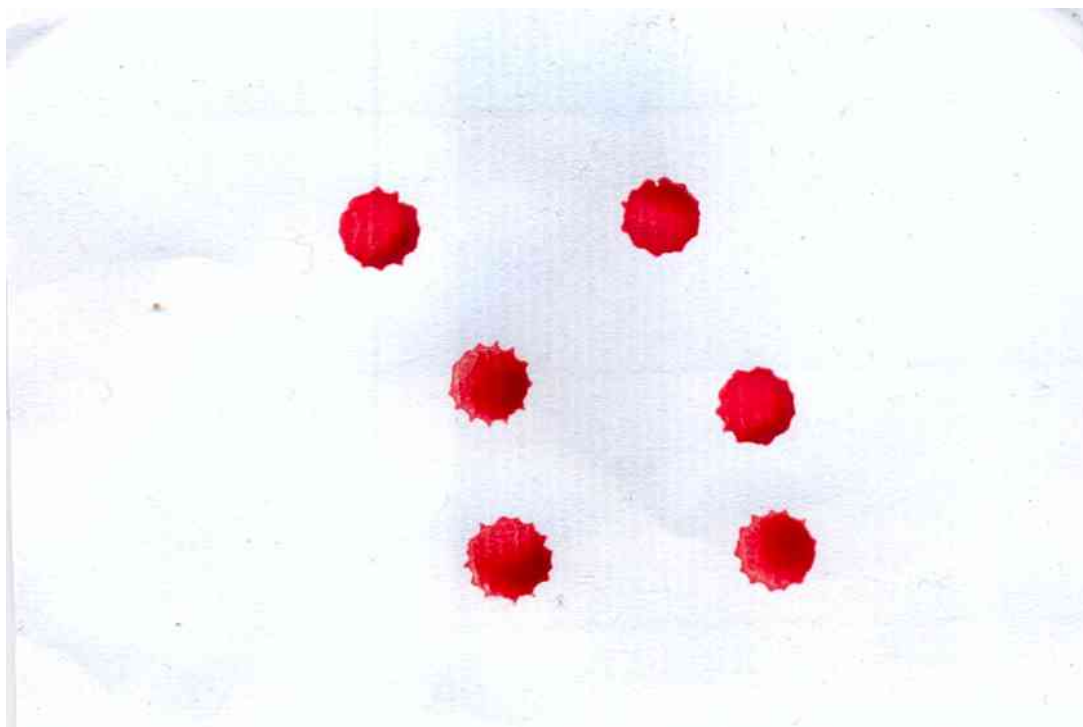


Figure 61 Stains generated on glass at -10°C

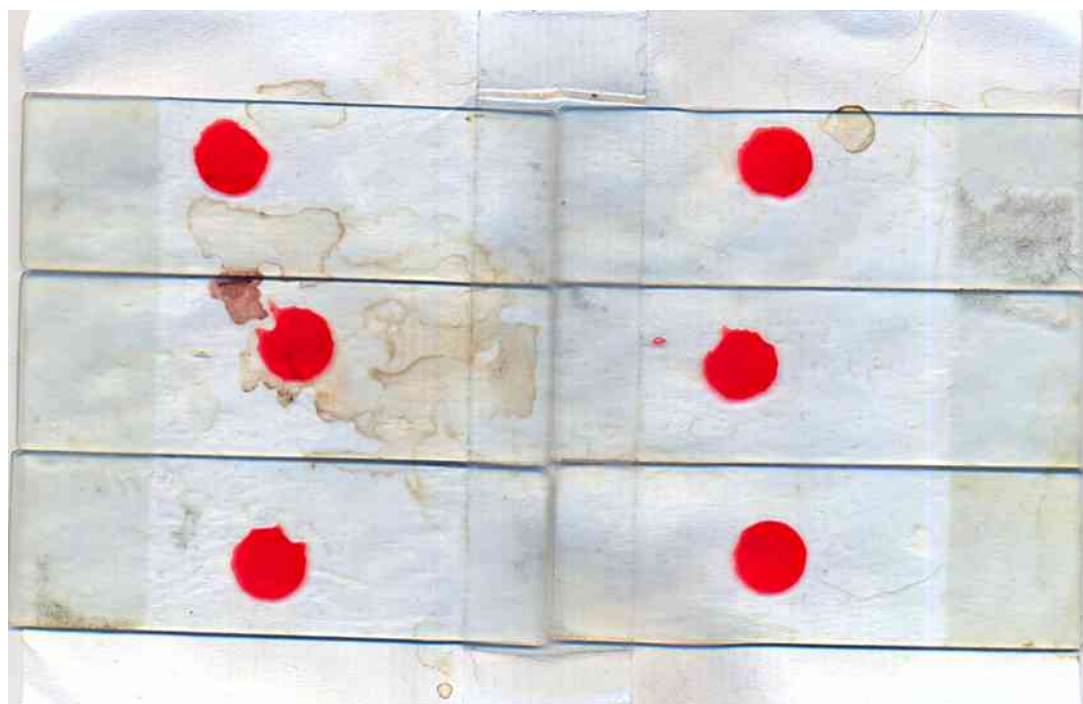




Figure 62 Stains generated on denim fabric at -10°C

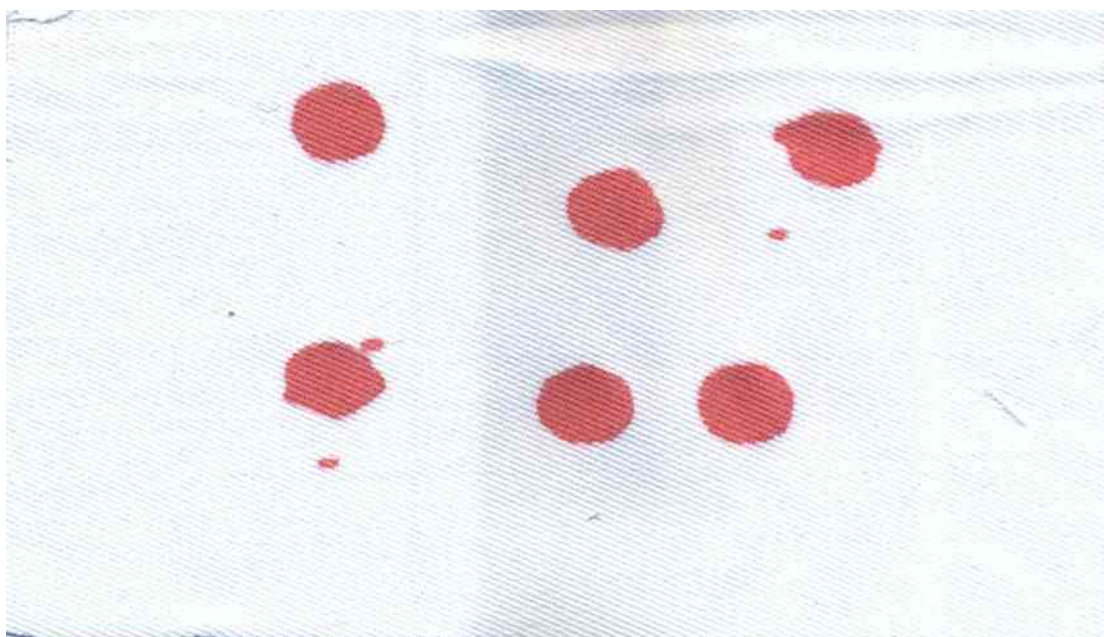


Figure 63 Stains generated on paper at -5°C

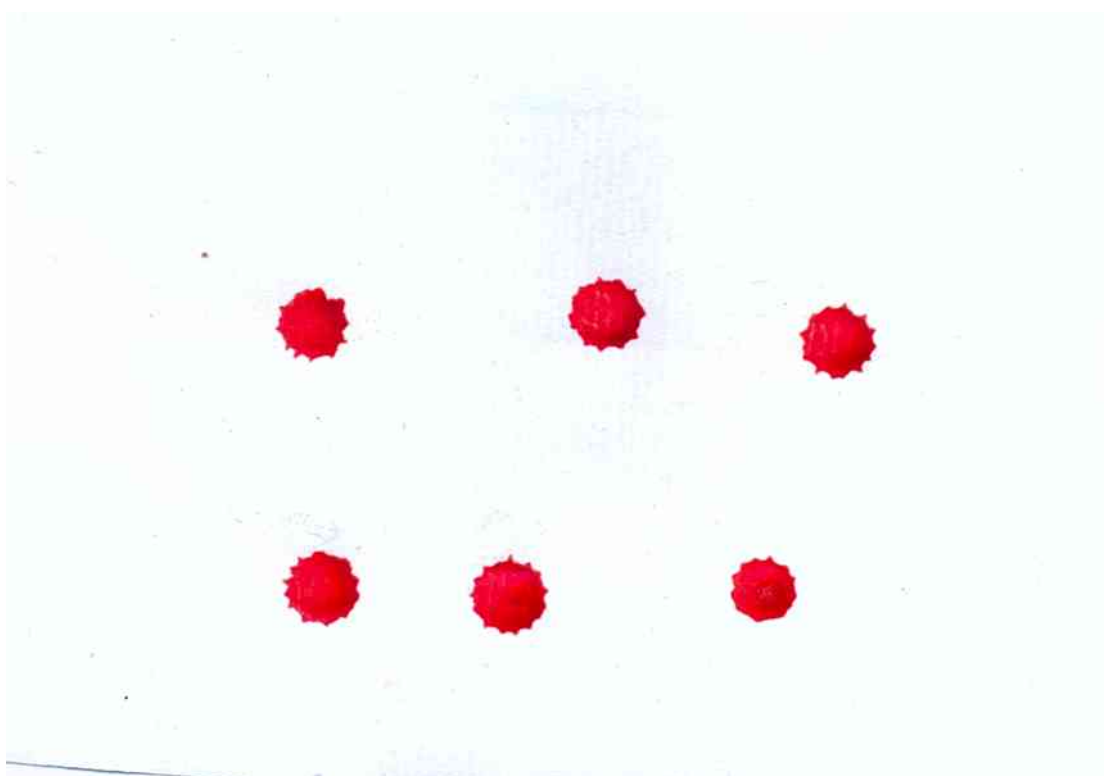


Figure 64 Stains generated on glass at -5°C

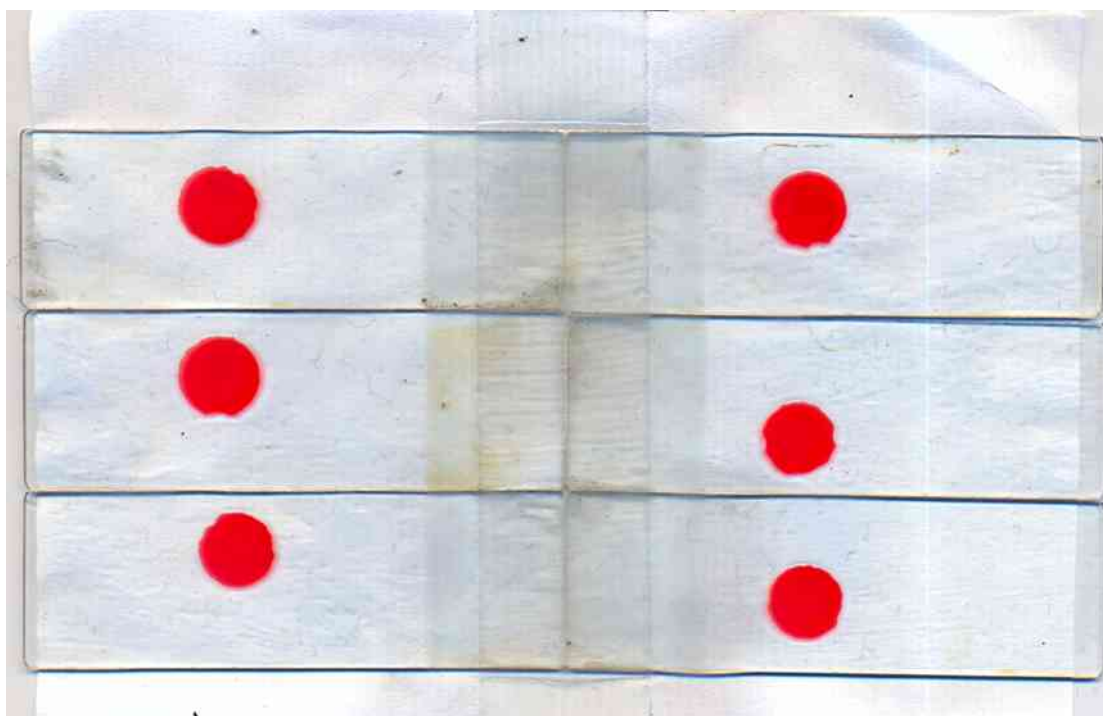


Figure 65 Stains generated on denim fabric at -5°C

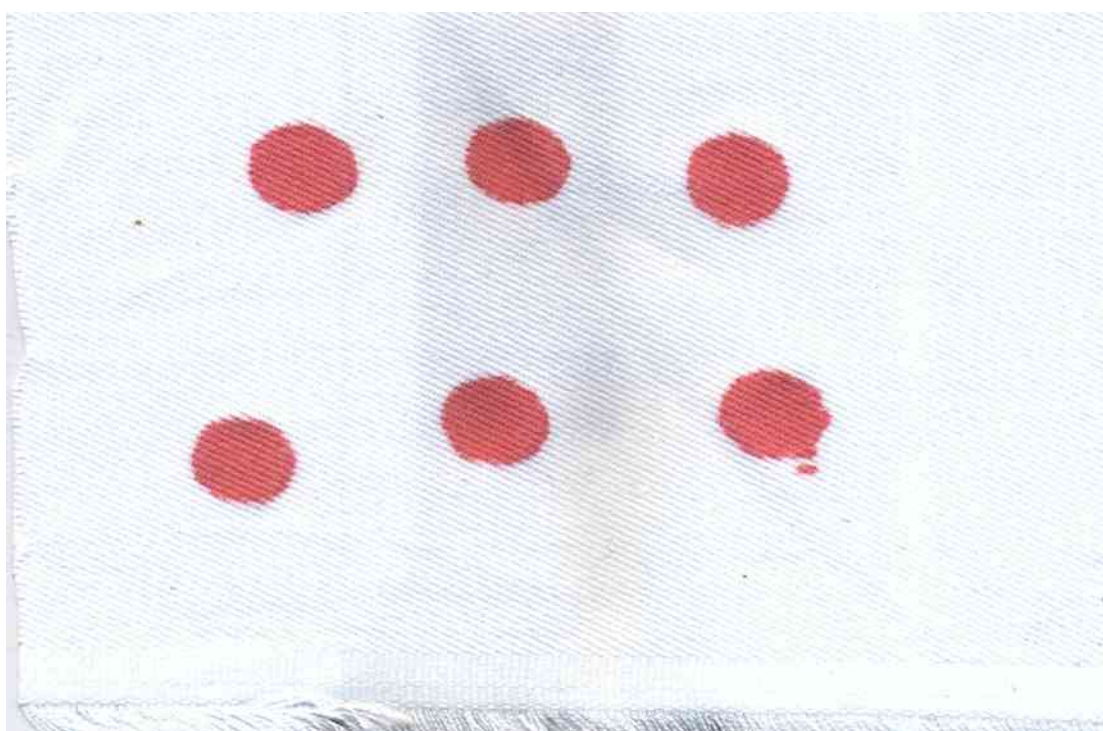




Figure 66 Stains generated on paper at 0°C

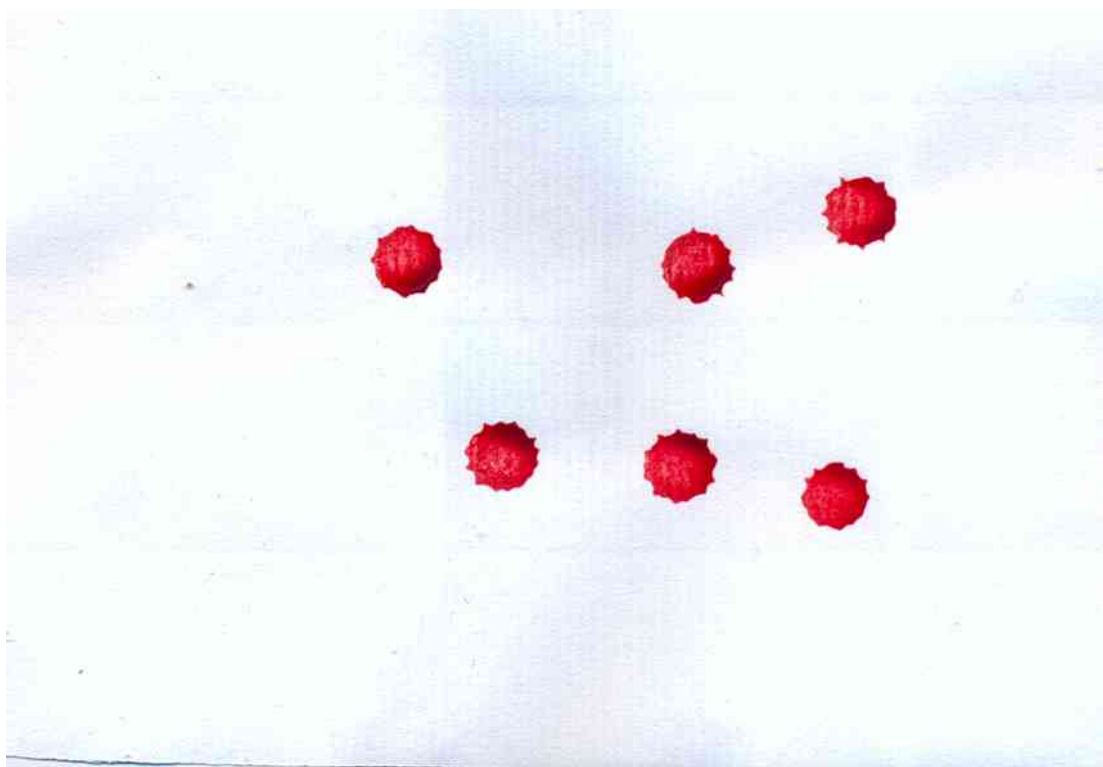


Figure 67 Stains generated on glass at 0°C

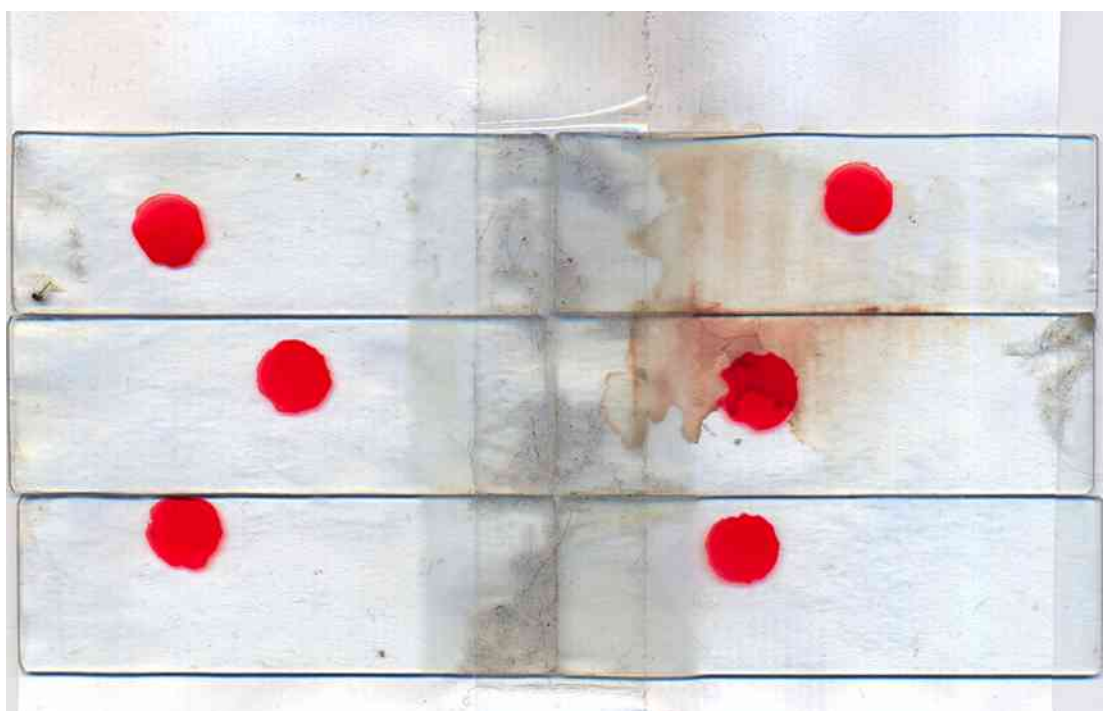


Figure 68 Stains generated on denim at 0°C

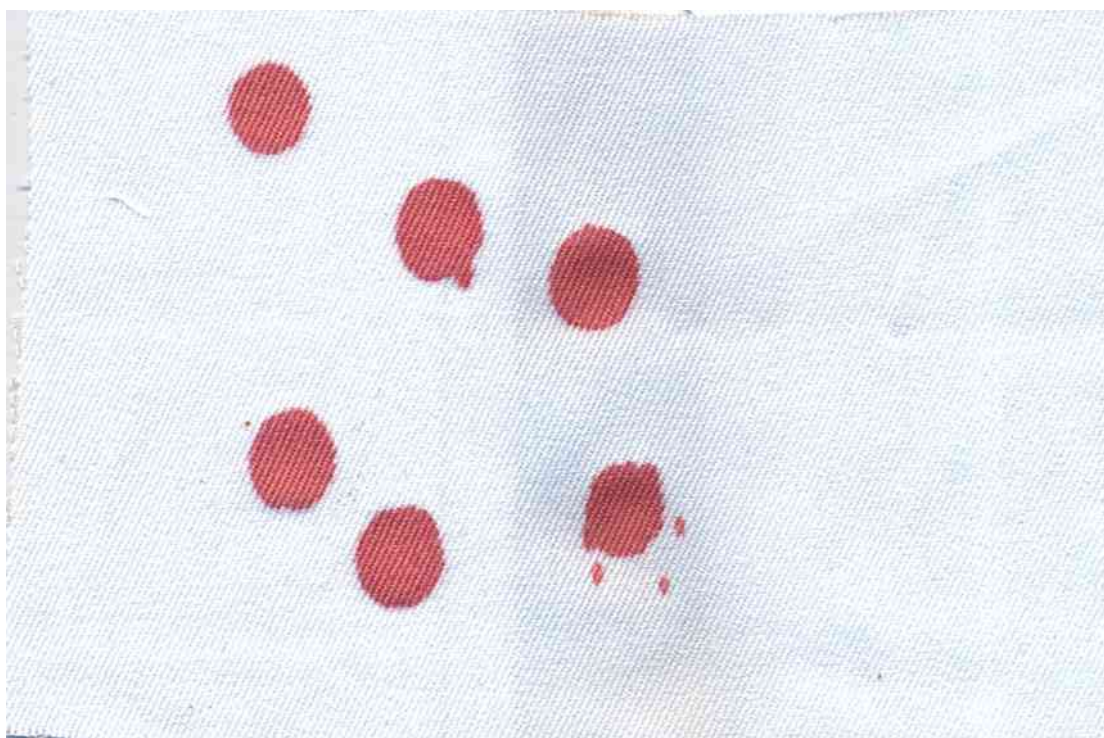


Figure 69 Stains generated on paper at 5°C

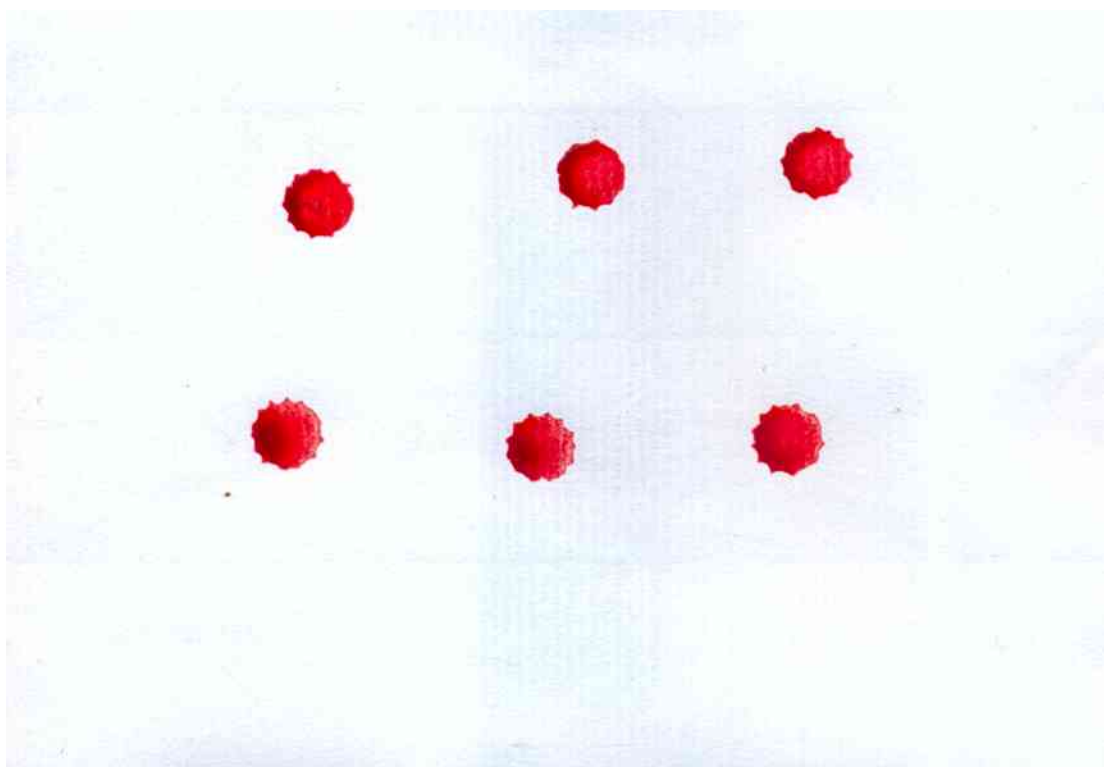


Figure 70 Stains generated on glass at 5°C

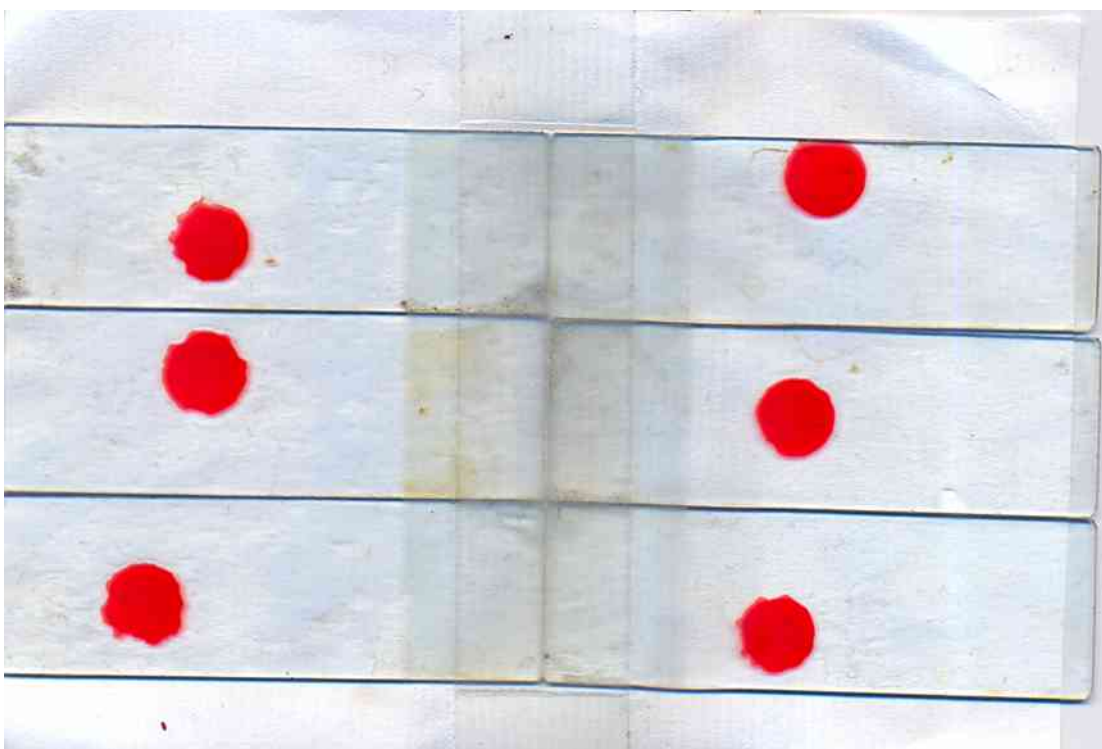


Figure 71 Stains generated on denim fabric at 5°C

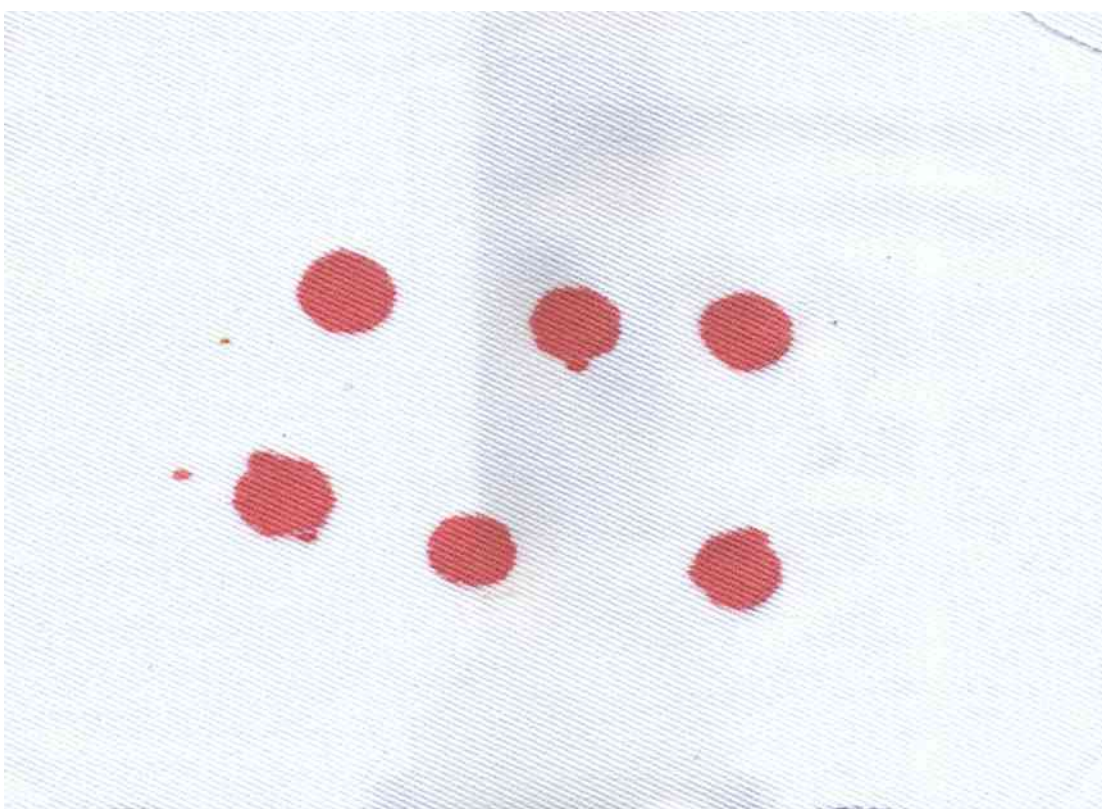




Figure 72 Stains generated on paper at 10°C

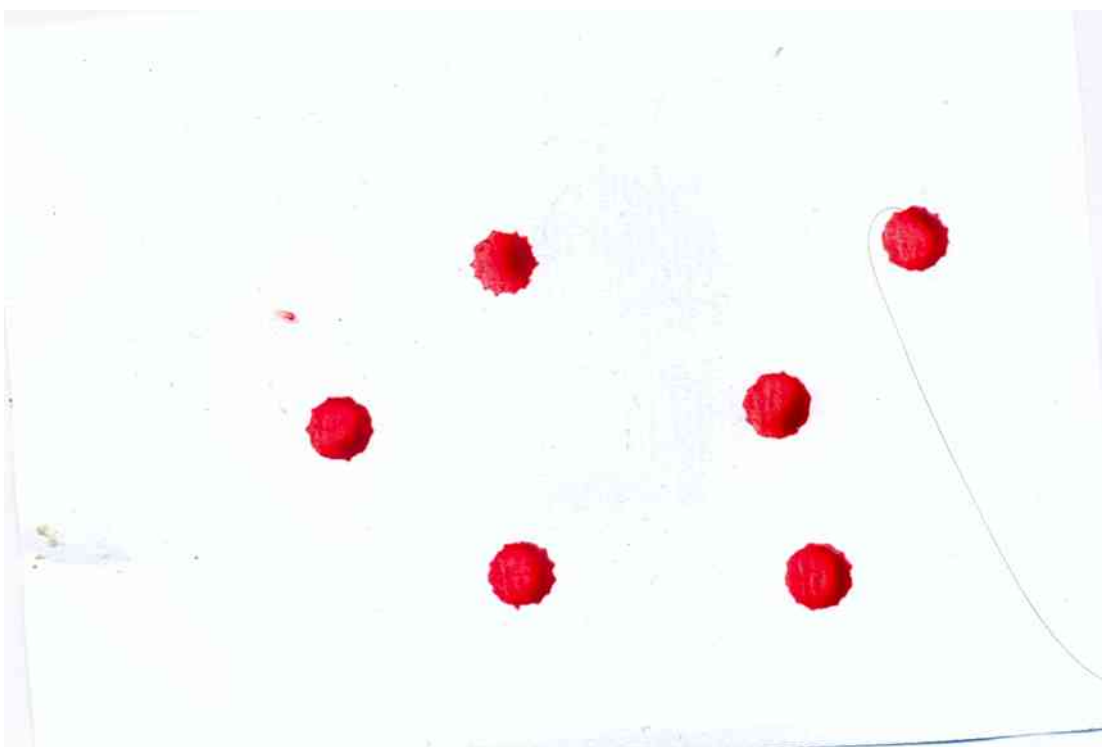


Figure 73 Stains generated on glass at 10°C

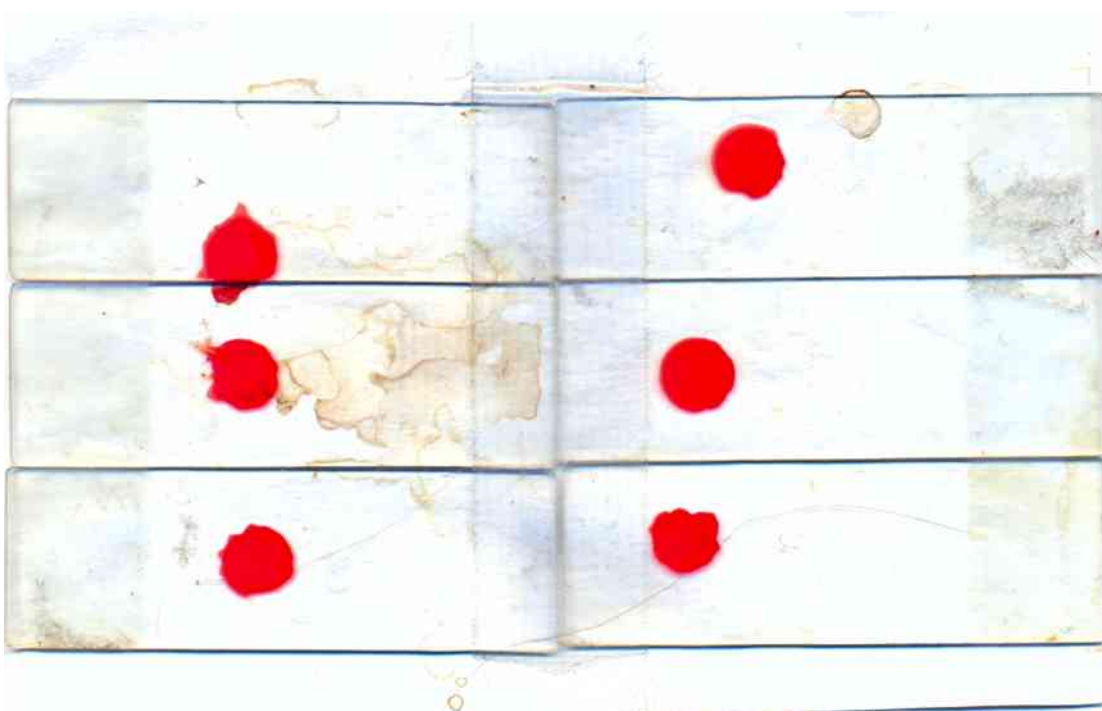


Figure 74 Stains generated on denim fabric at 10°C

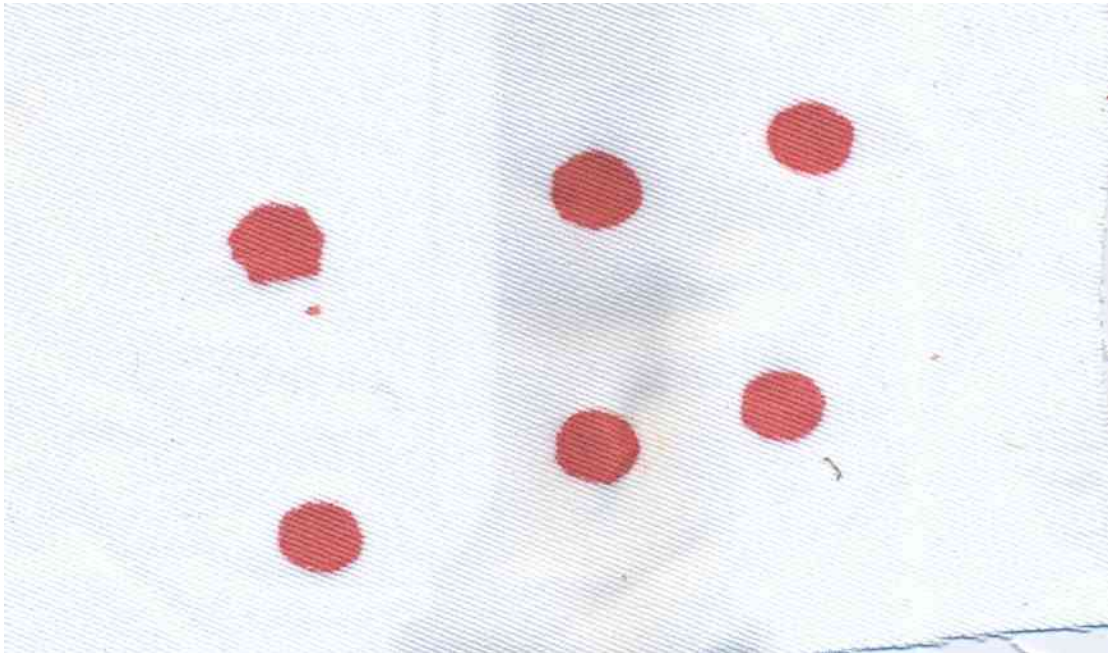


Figure 75 Stains generated on paper at 15°C

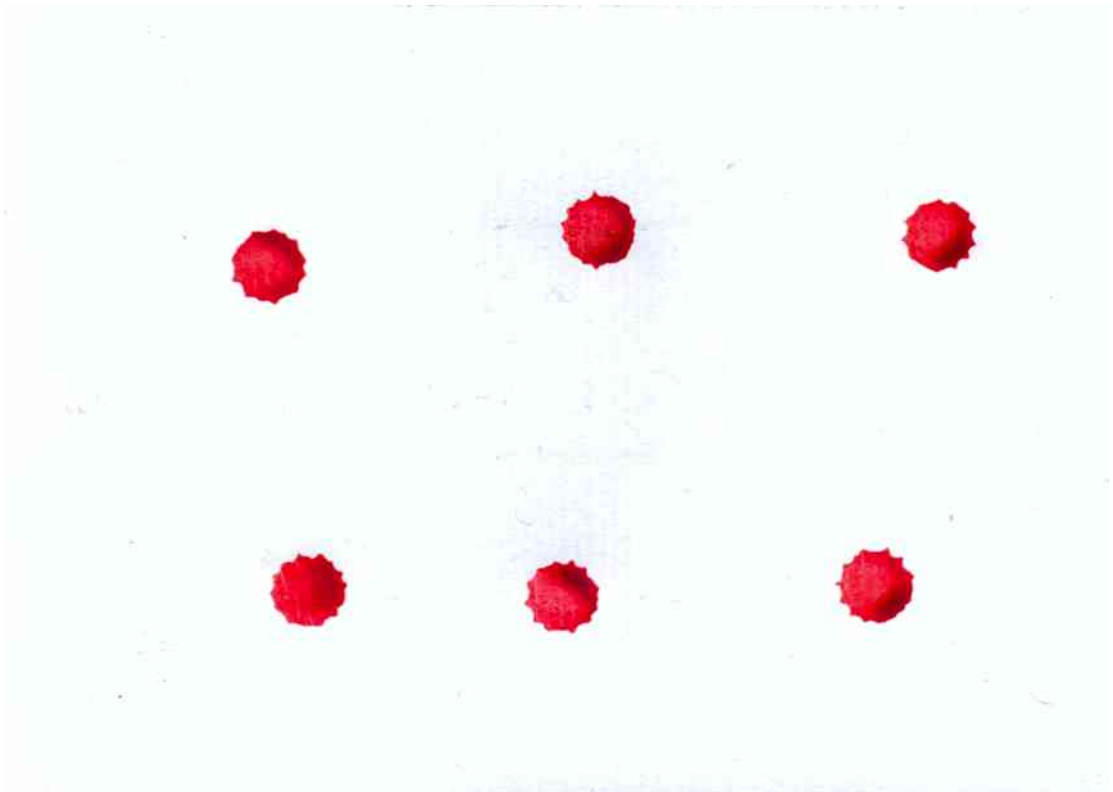


Figure 76 Stains generated on glass at 15°C

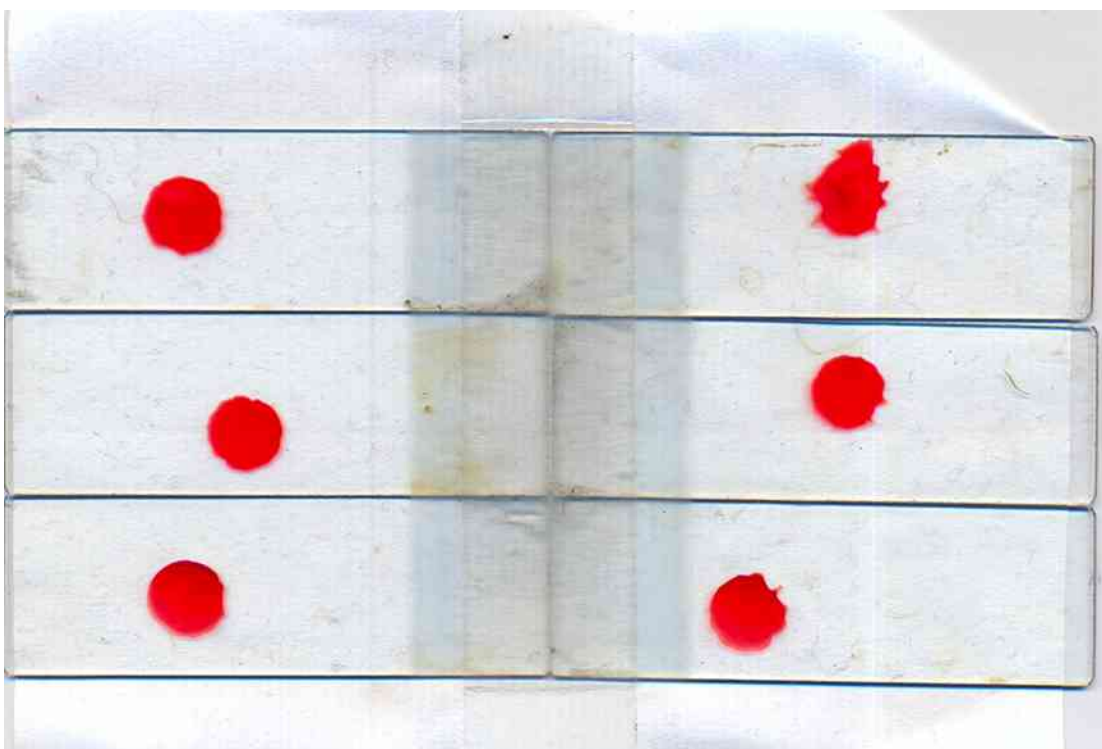


Figure 77 Stains generated on denim fabric at 15°C

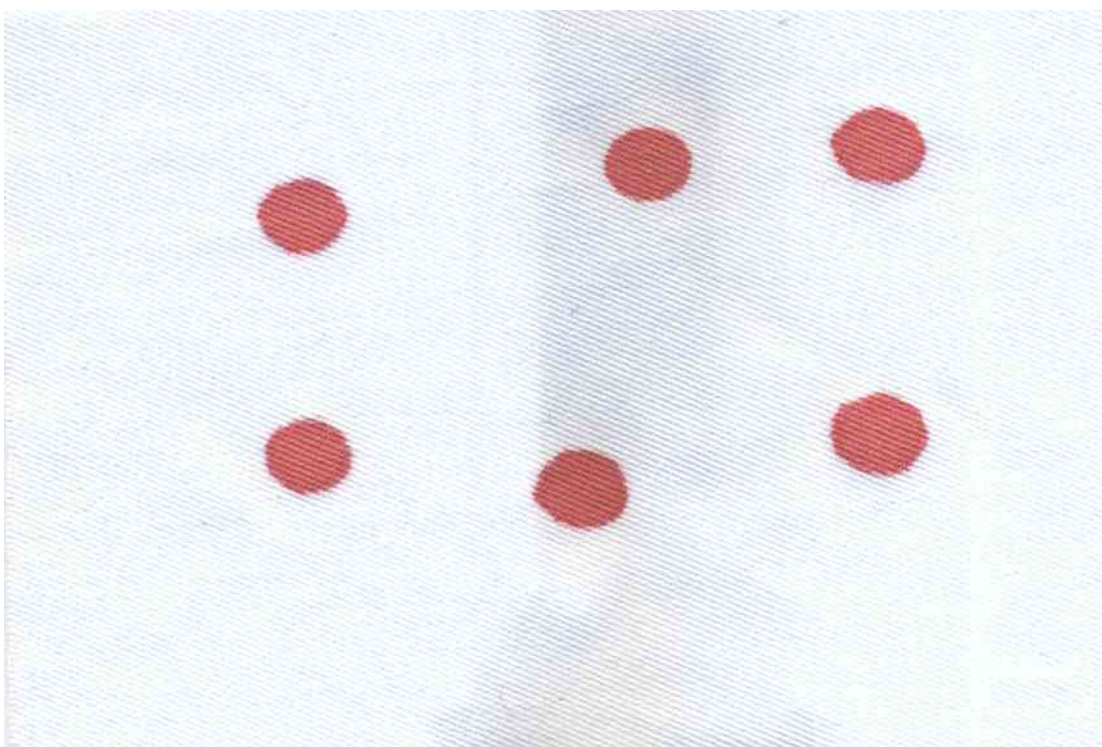


Figure 78 Stains generated on paper at 20°C

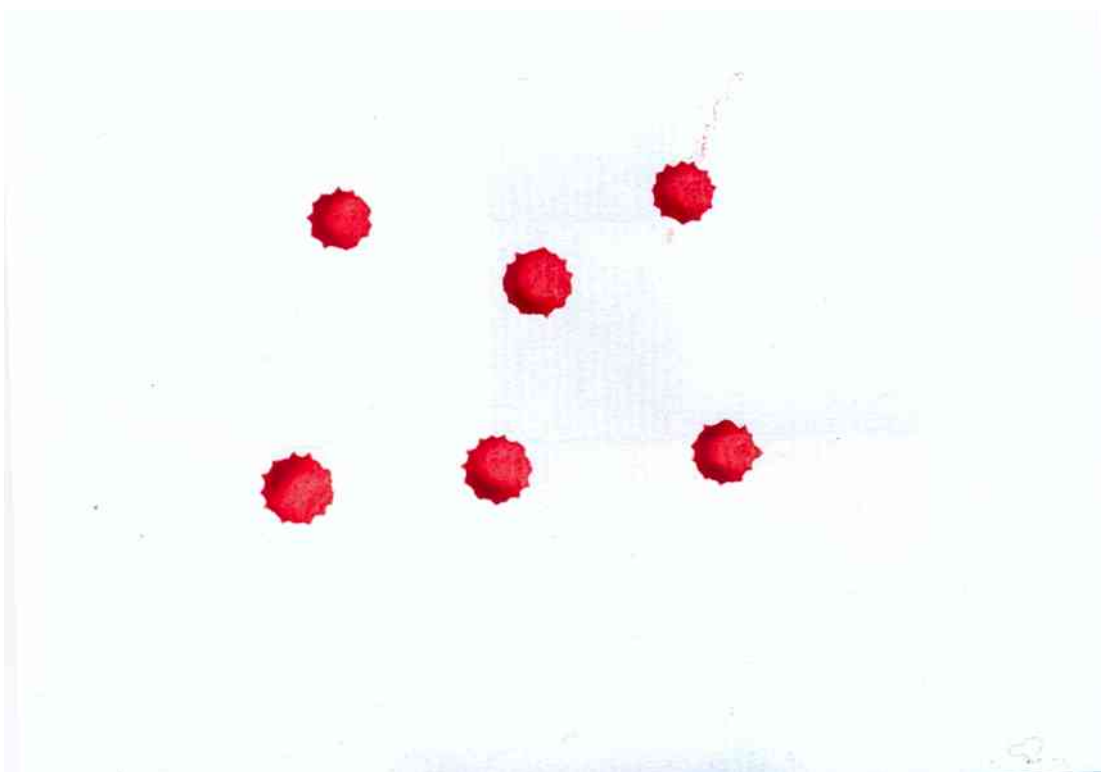


Figure 79 Stains generated on glass at 20°C

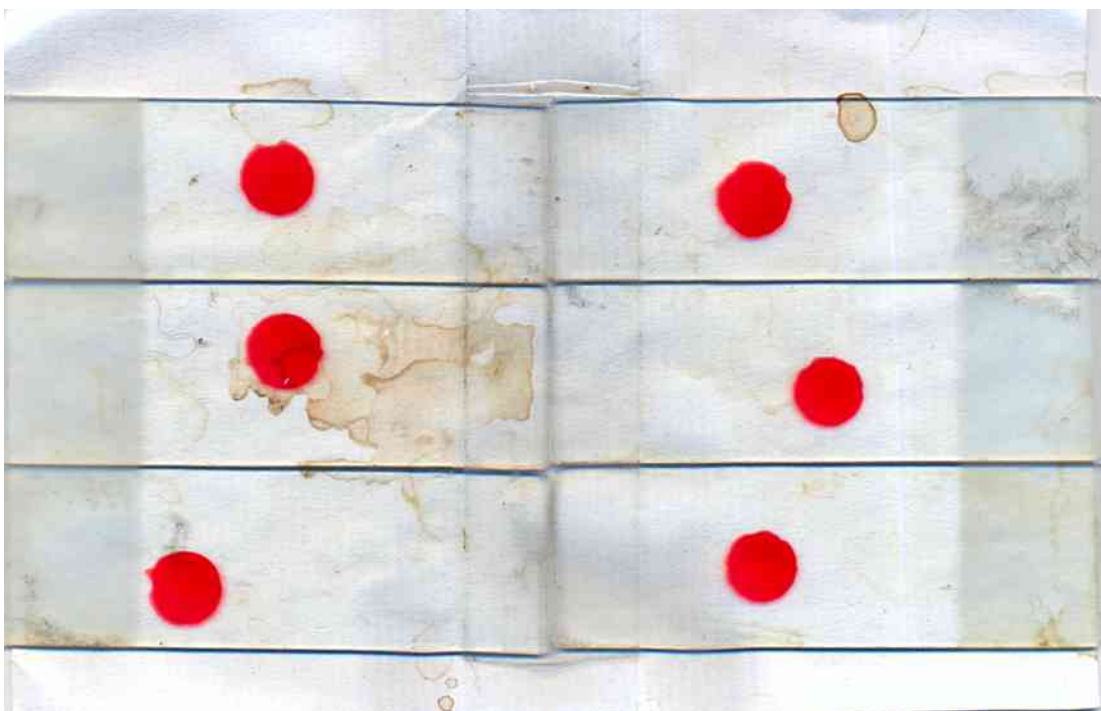




Figure 80 Stains generated on denim fabric at 20°C

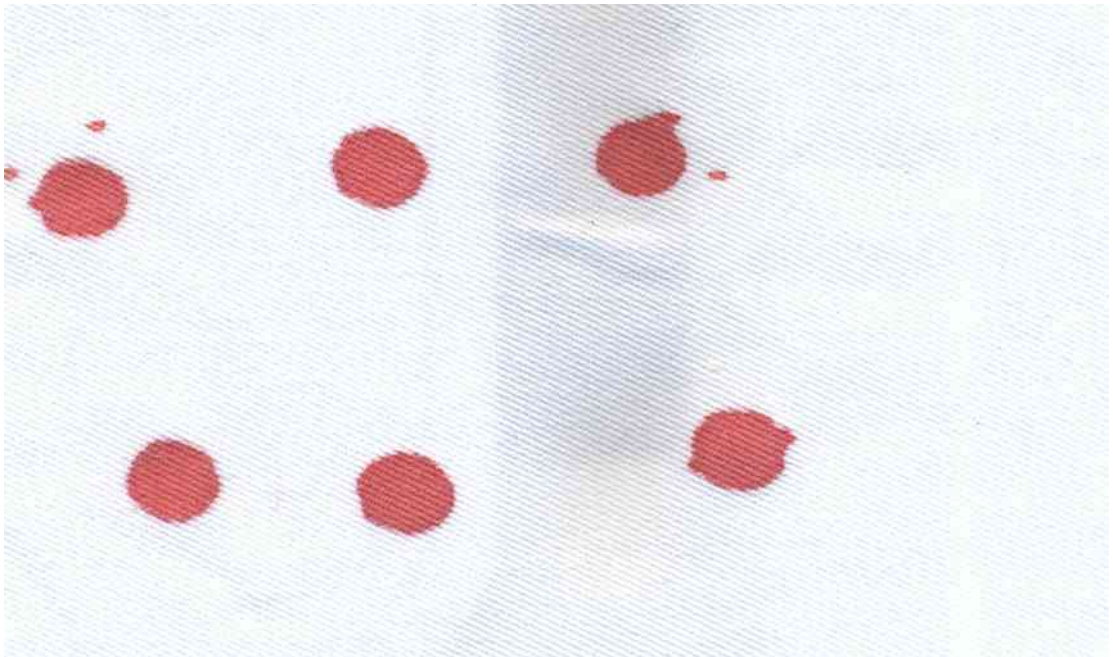


Figure 81 Stains generated on paper at 25°C

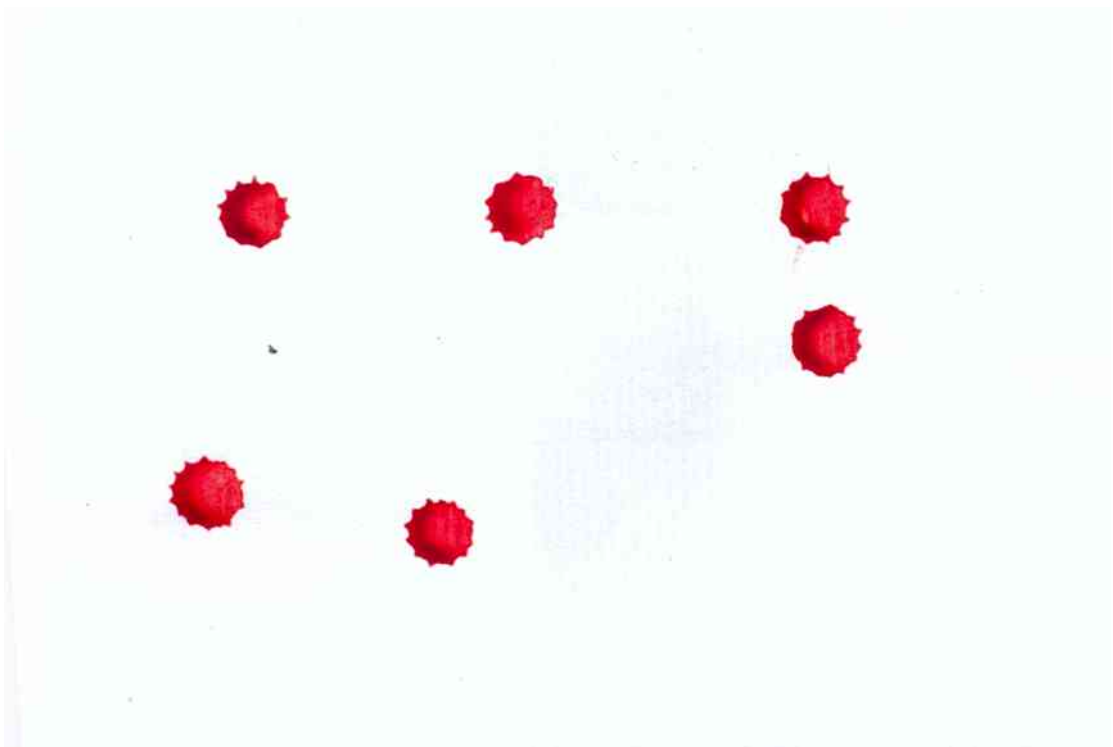




Figure 82 Stains generated on glass at 25°C

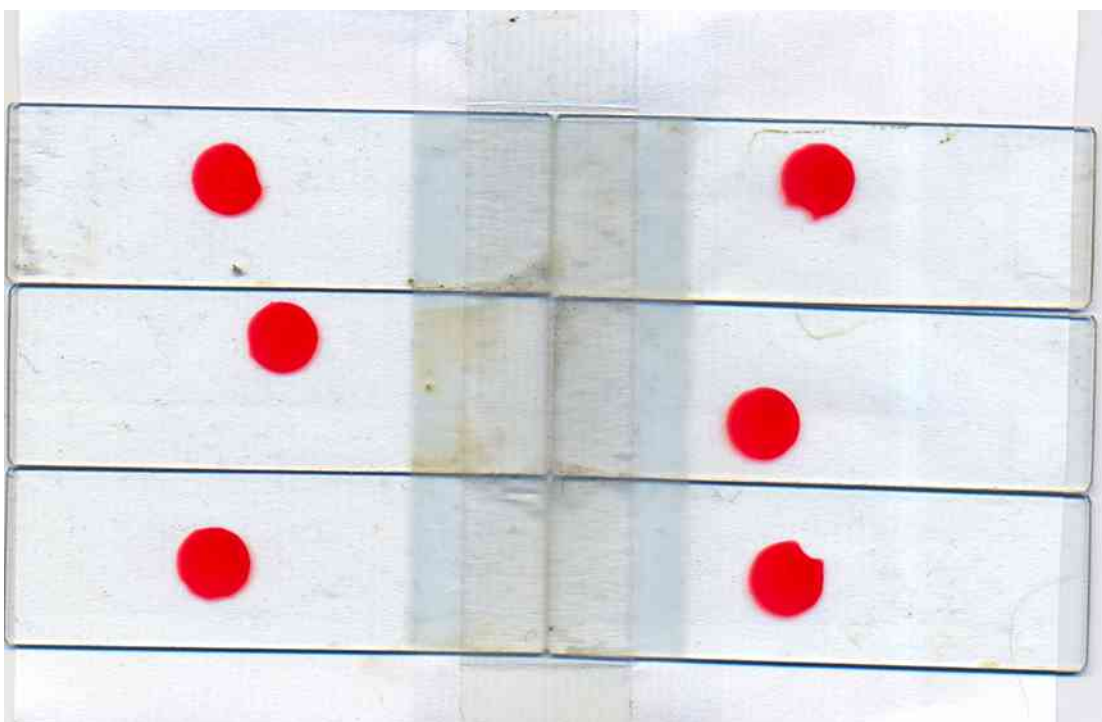


Figure 83 Stains generated on denim fabric at 25°C

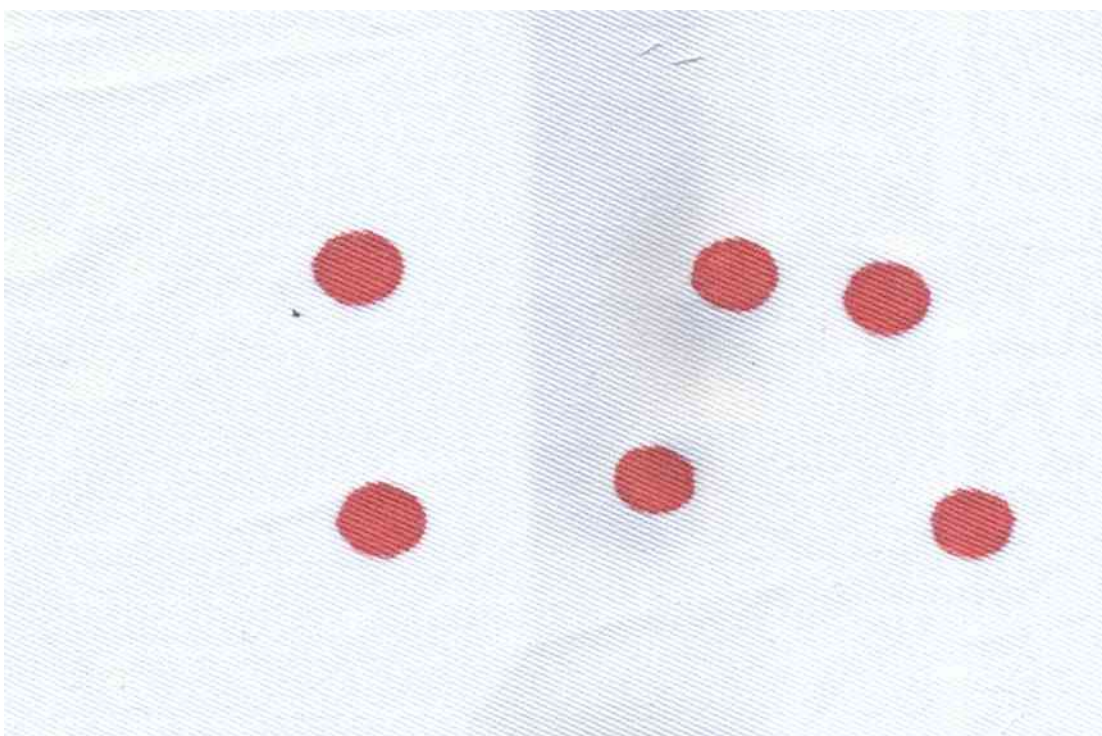


Figure 84 Stains generated on paper at 30°C

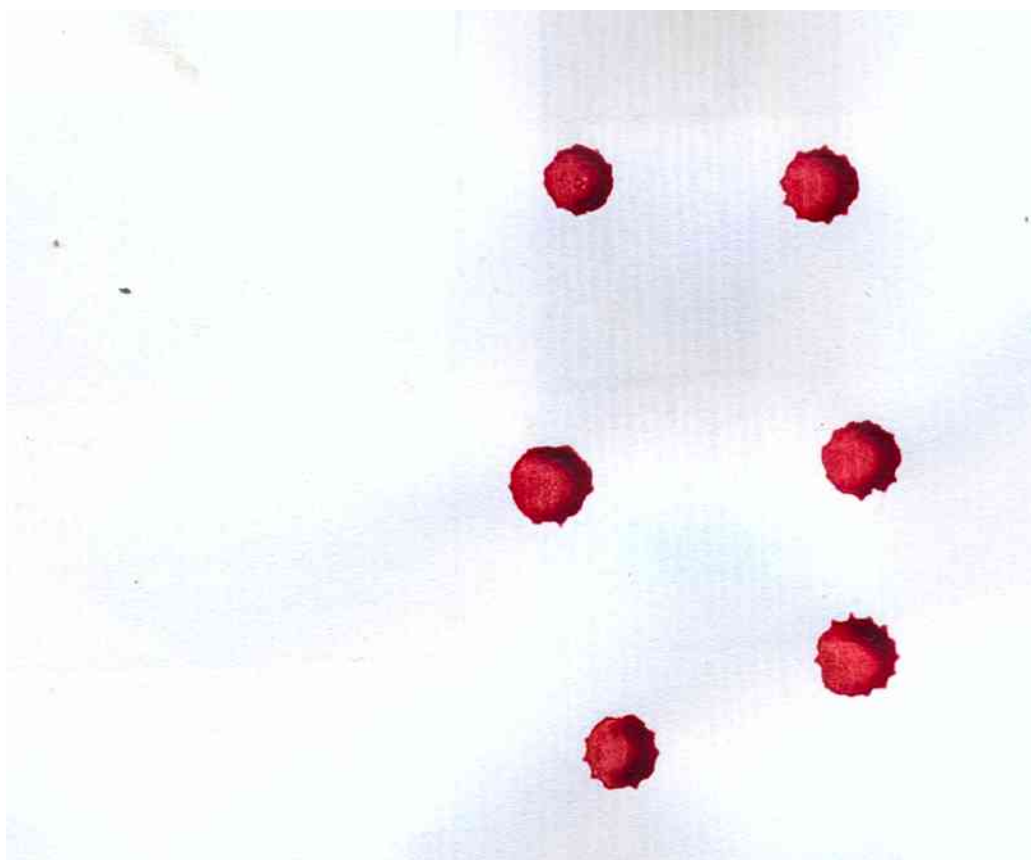


Figure 85 Stains generated on glass at 30°C

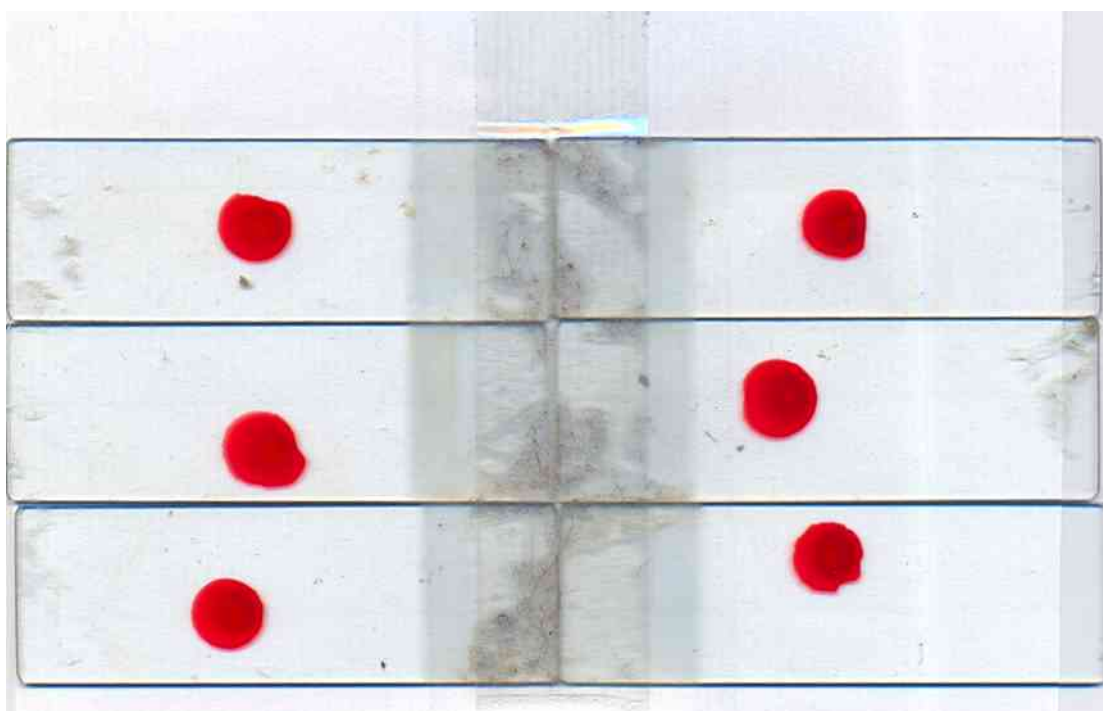


Figure 86 Stains generated on denim fabric at 30°C

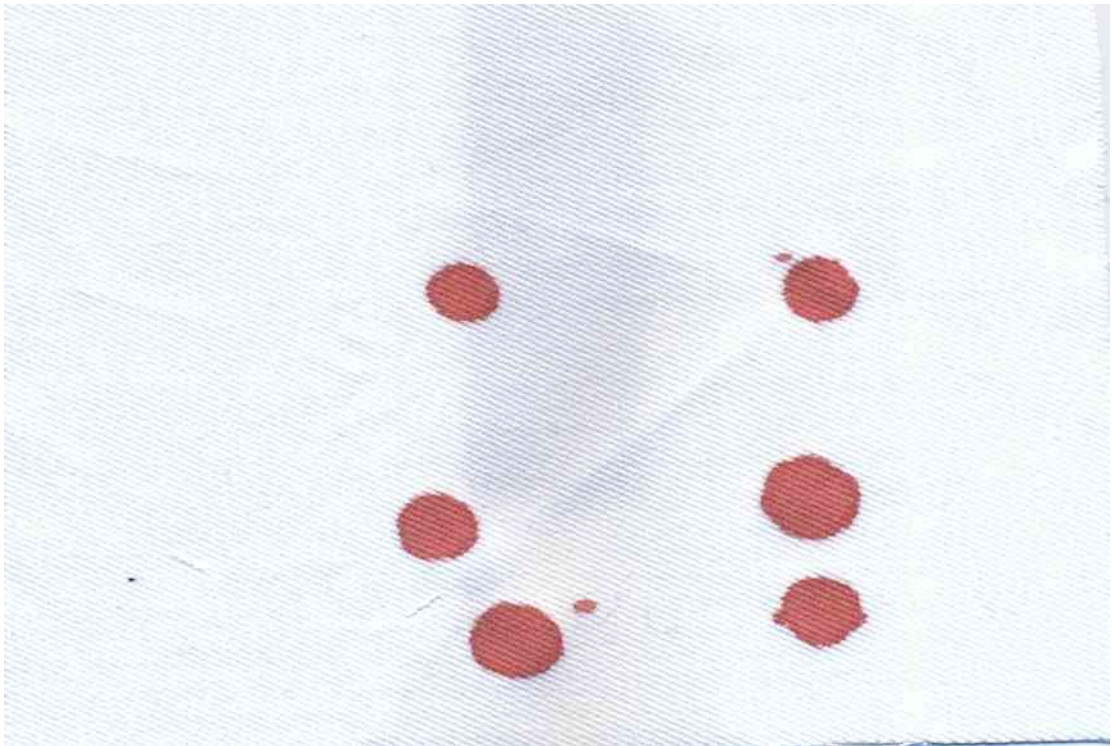


Figure 87 Stains generated on paper at 35°C

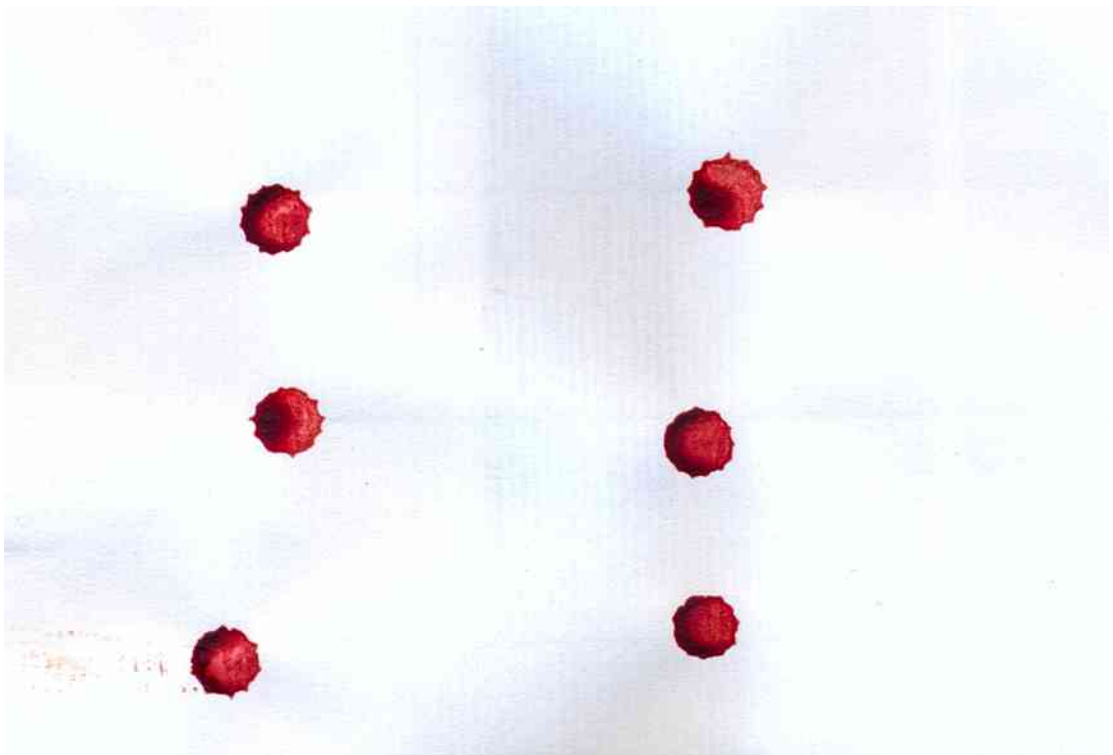




Figure 88 Stains generated on glass at 35°C

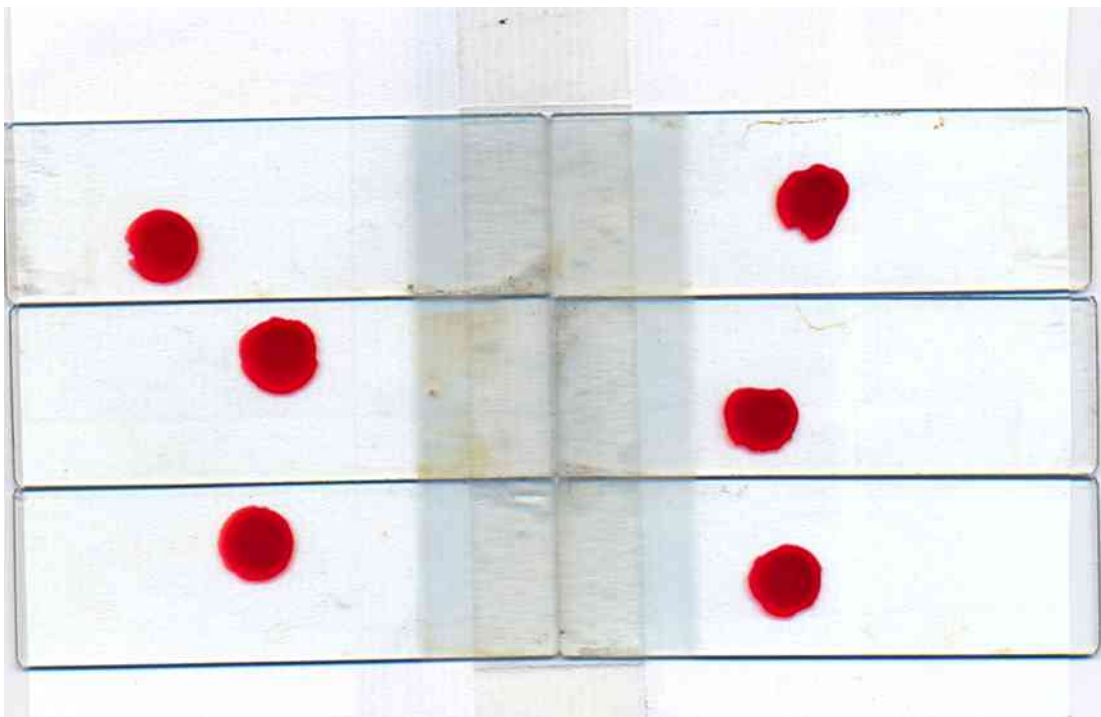


Figure 89 Stains generated on denim fabric at 35°C

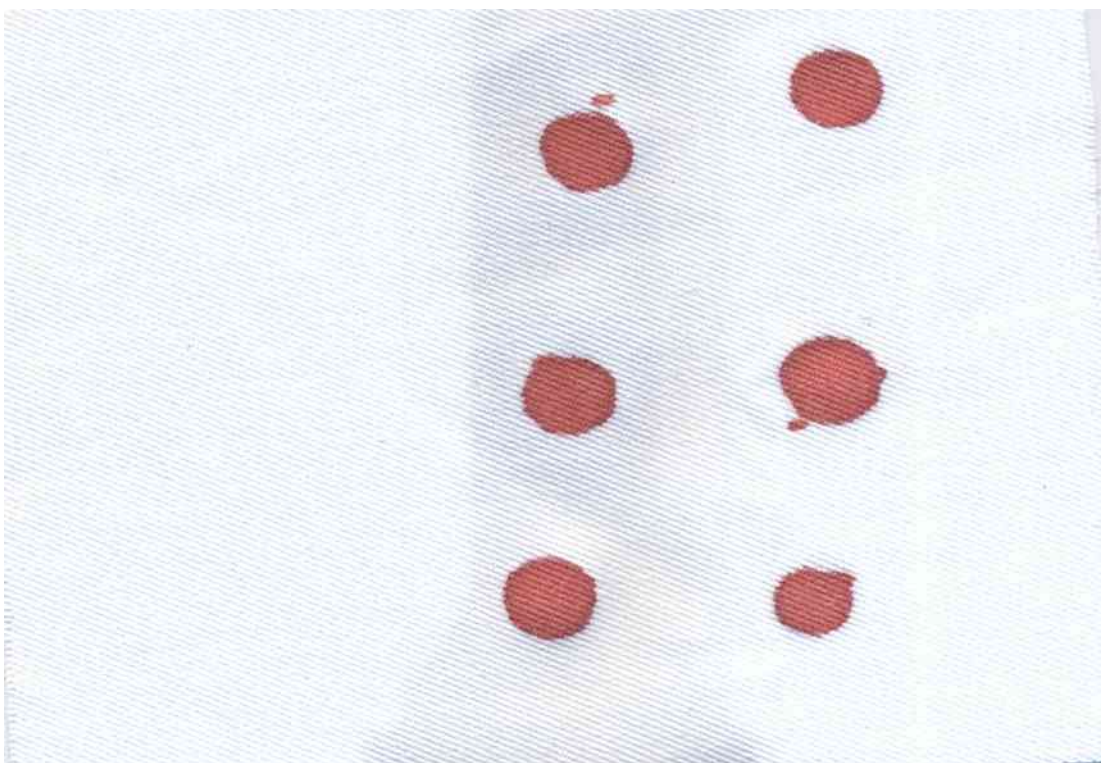


Figure 90 Stains generated on paper at 40°C

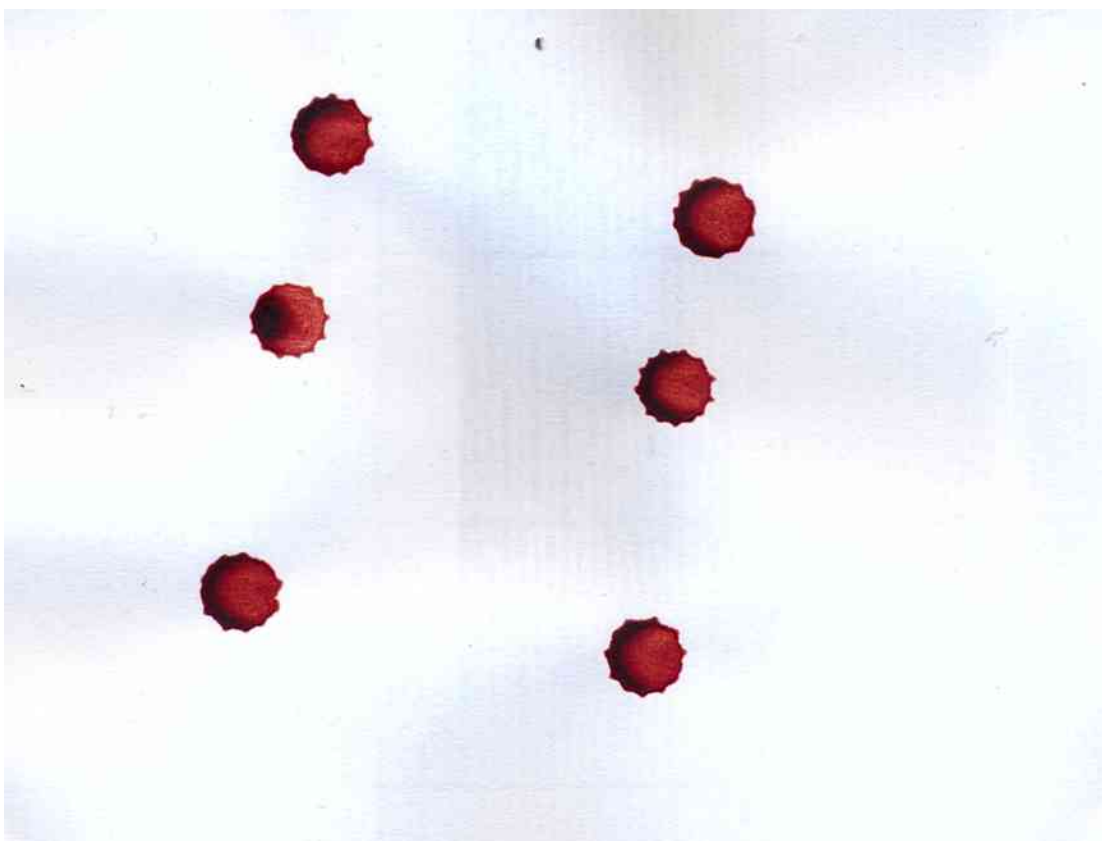


Figure 91 Stains generated on glass at 40°C

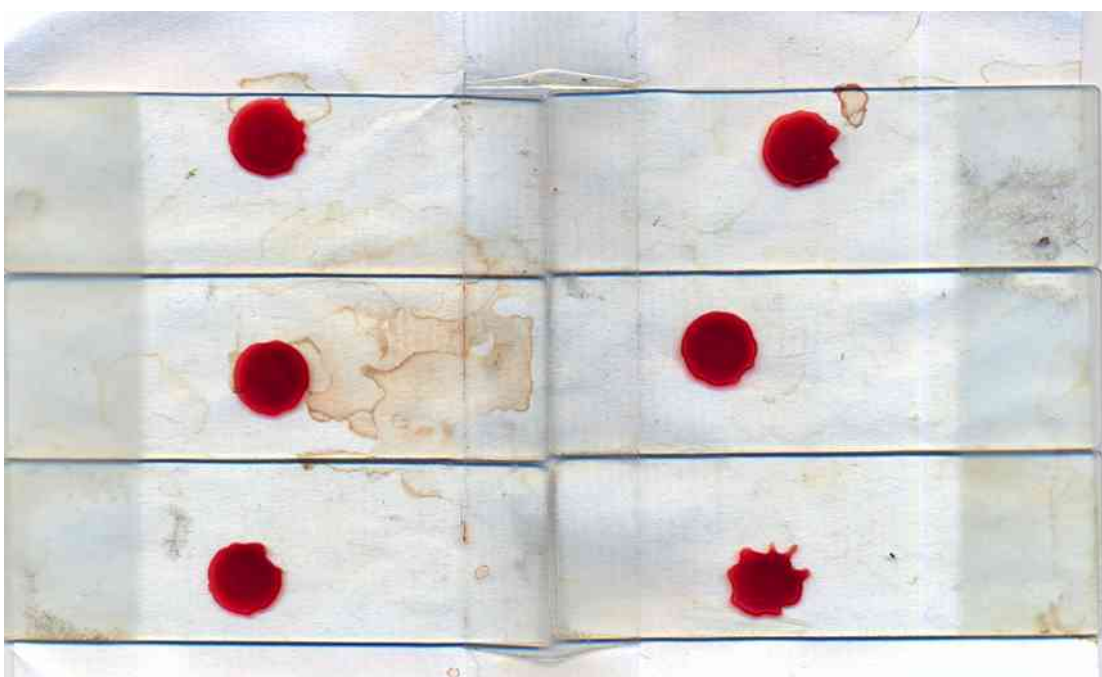


Figure 92 Stains generated on denim fabric at 40°C

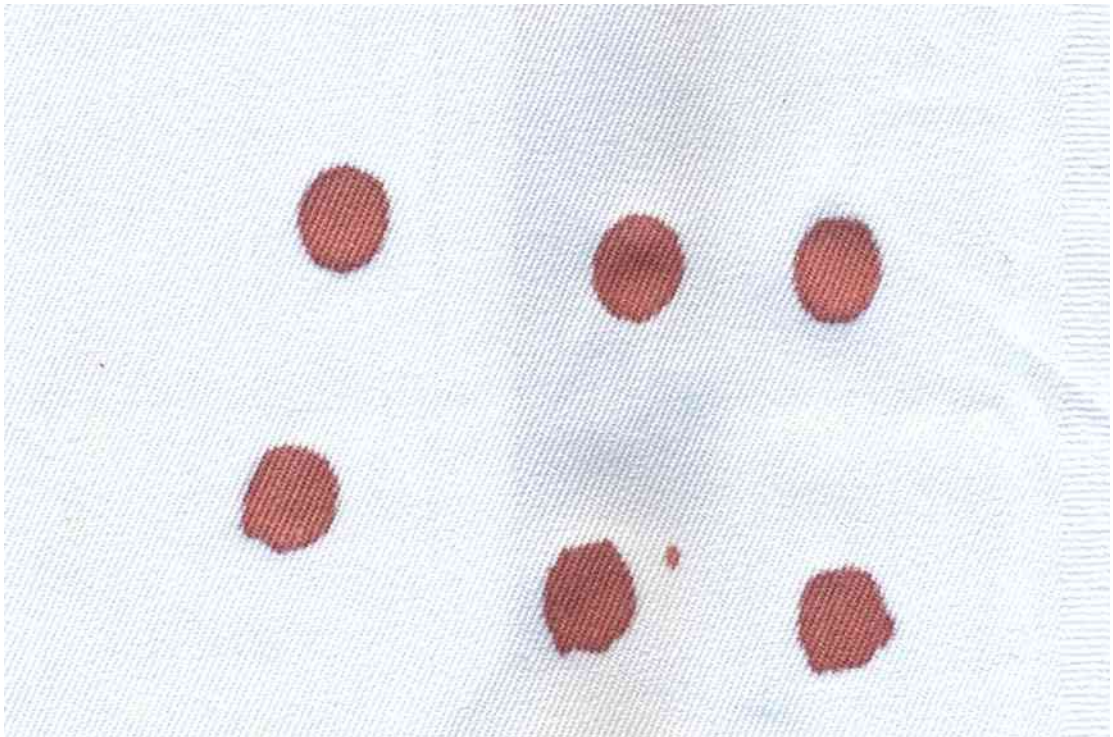


Figure 93 Stains generated on paper at 45°C

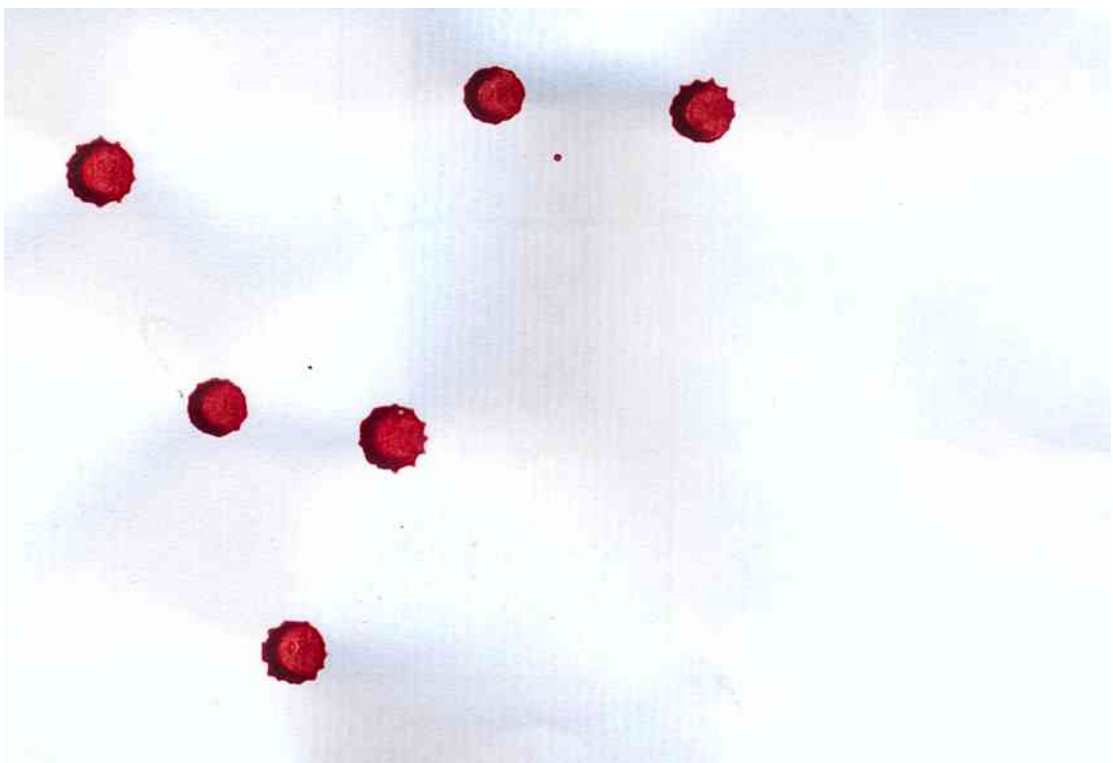




Figure 94 Stains generated on glass at 45°C

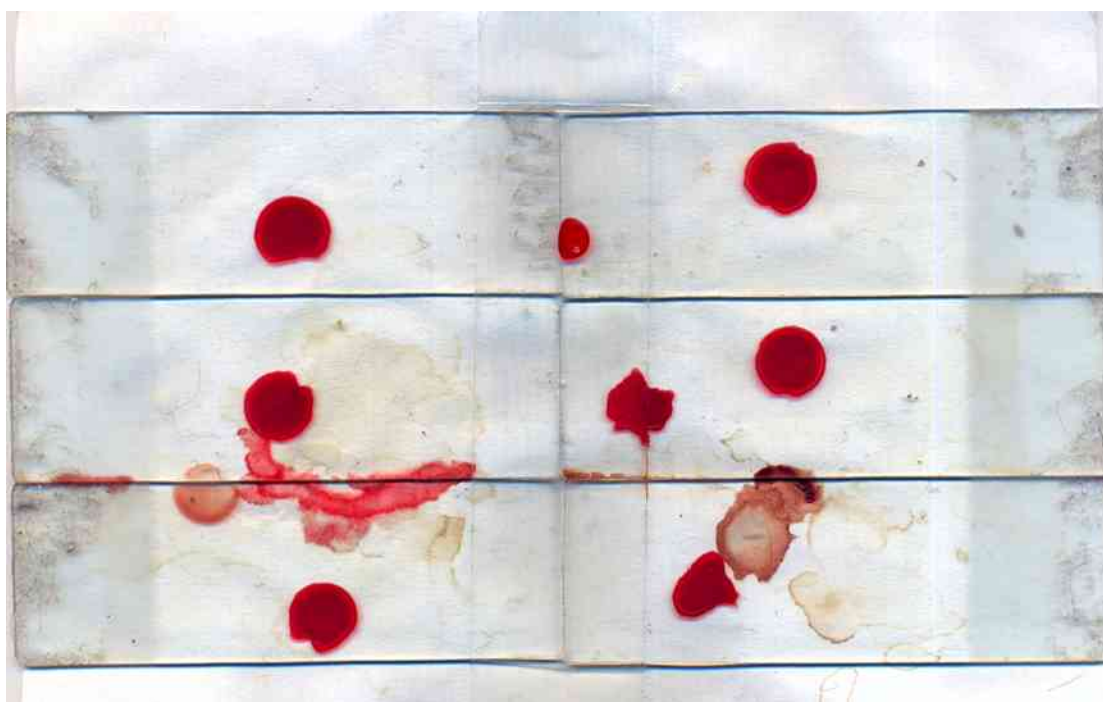


Figure 95 Stains generated on denim fabric at 45°C

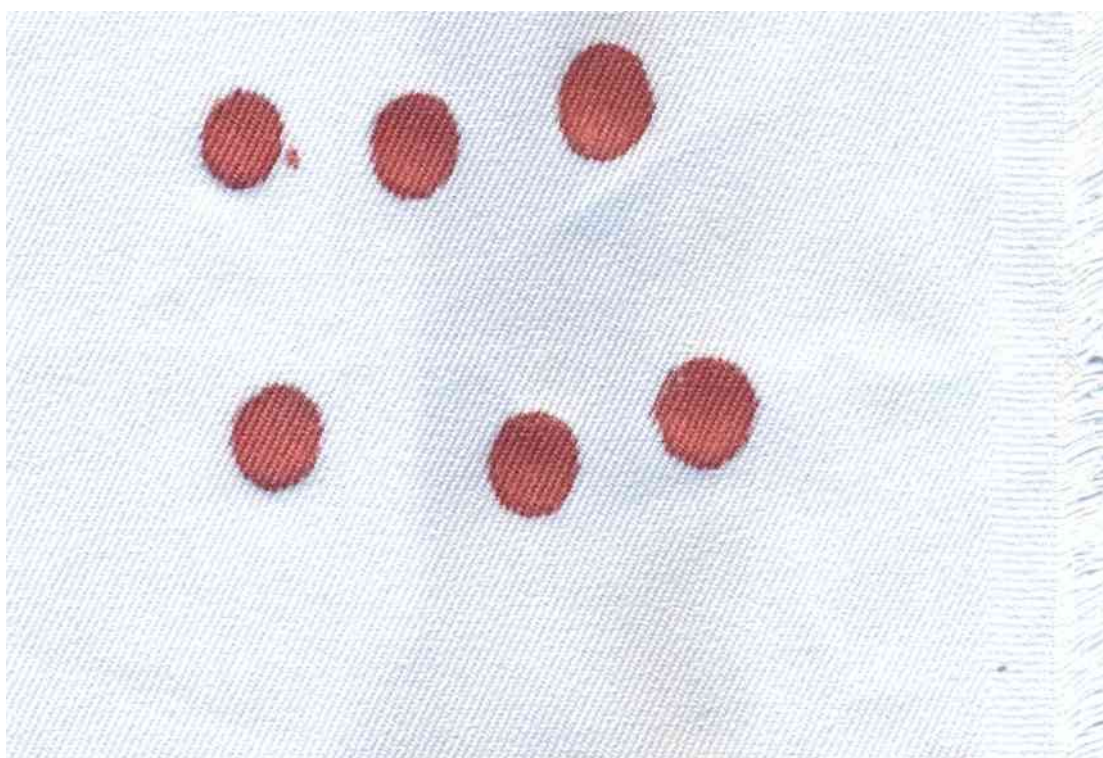


Figure 96 Stains generated on paper at 50°C



Figure 97 Stains generated on glass at 50°C

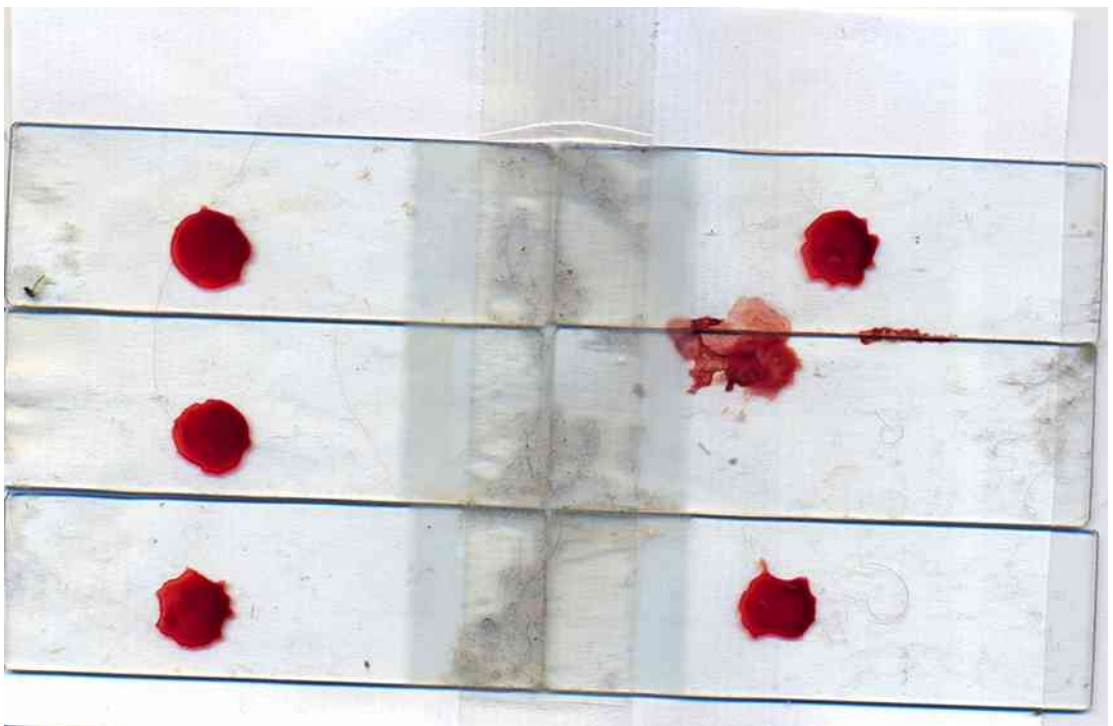
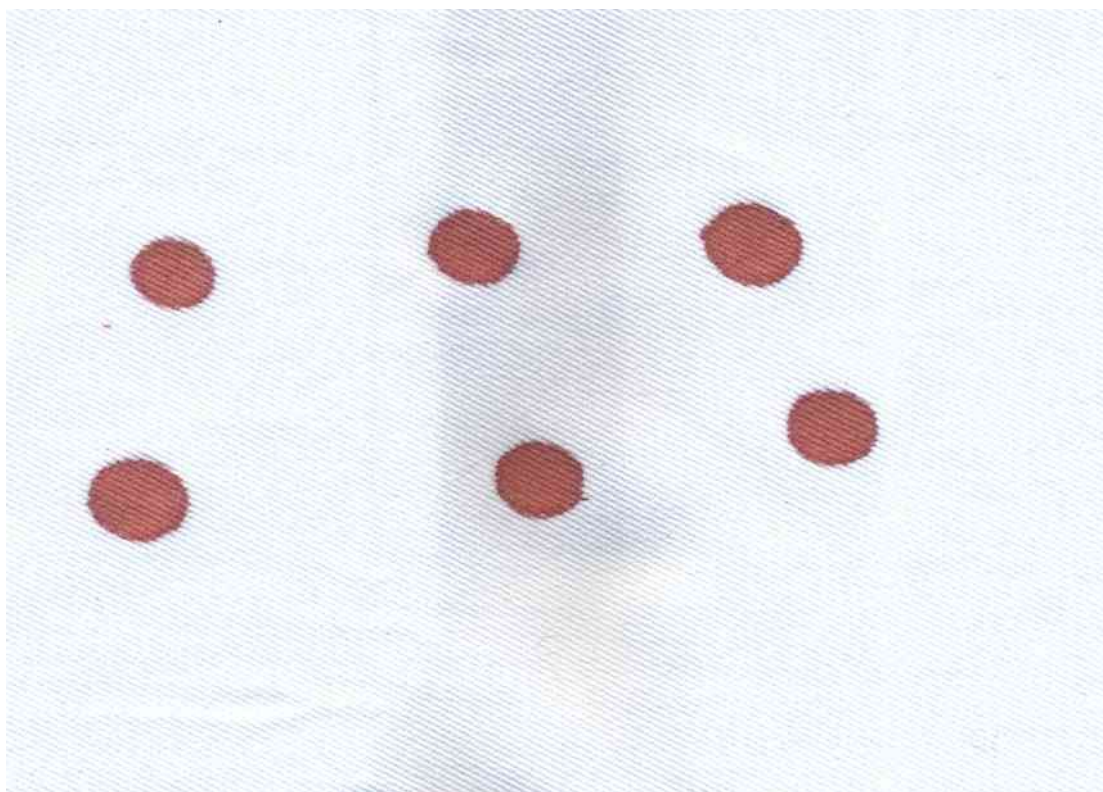




Figure 98 Stains generated on denim fabric at 50°C



### 5.3 Stain colour analysis

Once stains had been scanned and captured in a digital format, images were imported into colour analysis software to extract quantitative information about stain colour from the images. Each stain was analysed individually. An ‘eyedropper’ tool was used to select as large an area of each stain as possible for analysis and the calculation of several measurements of colour for each stain, from this selected area, was requested. These measurements are set out in *figures 99-101, 110-112 & 121-123*. Particular columns correspond to measurements of colour recorded for each stain. ‘R value’ is a measure of intensity of the red component of colour, ‘G value’ is a measure of intensity of the green component of colour and ‘B value’ is a measure of intensity of the blue component of colour. The higher these values are, the lighter (i.e. closer to white) the intensity of that colour component is. ‘RGB total’ is an overall measure of colour intensity, calculated by addition of R, G and B values and the ‘Hex’ column indicates the hexadecimal value of each stain’s colour. Images of












































individual stains analysed to derive measurements are included alongside measurements as well as blocks of the hexadecimal colour of each stain.

Descriptive statistics and box-plots of the results of stain colour analysis are discussed for each surface individually to assist the identification of trends between temperature, humidity and stain colour. The comparison of trends and results between surfaces is then presented.

































### **5.3.1 Stains generated on paper**

The measurements for stains derived on paper surfaces from -10 to 50°C are presented in figures 99-101. The descriptive statistics are then presented in *figures 102 and 103*.

**Figure 99** Table of measurements recorded for stains generated on paper surfaces from -10°C to 20°C

Stain ID	Surface	Temperature /oC	Average Humidity	R Value	G Value	B Value	RGB total	Hex	
A001	Paper	-10	89.7	244	15	54	313	f40f36	
A002	Paper	-10	89.7	227	6	36	269	e30624	
A003	Paper	-10	89.3	212	7	16	235	d40710	
A004	Paper	-10	89.3	241	8	48	297	f10830	
A005	Paper	-10	89.3	219	9	24	252	db0918	
A006	Paper	-10	89.3	221	9	21	251	dd0915	
A007	Paper	-5	84.1	240	6	50	296	f00632	
A008	Paper	-5	84.1	240	19	58	317	f0133a	
A009	Paper	-5	84.1	241	12	49	302	f10c31	
A010	Paper	-5	84.1	243	7	39	289	f30727	
A011	Paper	-5	85.9	242	11	44	297	f20b2c	
A012	Paper	-5	85.9	237	12	42	291	ed0c2a	
A013	Paper	0	91.5	227	35	64	326	e32340	
A014	Paper	0	91.5	223	30	56	309	df1e38	
A015	Paper	0	91.5	232	32	63	327	e8203f	
A016	Paper	0	91.5	222	35	67	324	de2343	
A017	Paper	0	91.5	227	28	63	318	e31c3f	
A018	Paper	0	91.5	235	23	58	316	eb173a	
A019	Paper	5	89.1	237	9	29	275	ed091d	
A020	Paper	5	89.1	232	15	40	287	e80f28	
A021	Paper	5	89.5	236	16	50	302	ec1032	
A022	Paper	5	89.5	225	17	35	277	e11123	
A023	Paper	5	89.5	219	19	46	284	db132e	
A024	Paper	5	90.0	229	12	52	293	e50c34	
A025	Paper	10	96.0	228	23	49	300	e41731	
A026	Paper	10	96.0	241	39	66	346	f12742	
A027	Paper	10	96.0	239	20	56	315	ef1438	
A028	Paper	10	96.0	229	24	42	295	e5182a	
A029	Paper	10	96.0	240	21	54	315	f01536	
A030	Paper	10	96.0	241	17	44	302	f1112c	
A031	Paper	15	96.5	237	22	59	318	ed163b	
A032	Paper	15	96.5	222	21	50	293	de1532	
A033	Paper	15	96.5	231	27	52	310	e71b34	
A034	Paper	15	96.6	230	8	45	283	e6082d	
A035	Paper	15	96.6	232	35	67	334	e82343	
A036	Paper	15	96.6	236	33	61	330	ec213d	
A037	Paper	20	87.2	232	29	62	323	e81d3e	
A038	Paper	20	88.0	237	29	59	325	ed1d3b	
A039	Paper	20	88.0	228	23	54	305	e41736	
A040	Paper	20	88.0	243	50	79	372	f3324f	
A041	Paper	20	88.3	239	42	71	352	ef2a47	
A042	Paper	20	88.3	229	35	65	329	e52341	
A043	Paper	25	84.2	224	28	60	312	e01c3c	

**Figure 100** Table of measurements recorded for stains generated on paper surfaces from 20°C to 50°C

A044	Paper	25	84.2	235	24	58	317	eb183a		
A045	Paper	25	84.2	230	23	52	305	e61734		
A046	Paper	25	84.2	237	30	58	325	ed1e3a		
A047	Paper	25	84.2	229	18	54	301	e51236		
A048	Paper	25	84.2	231	28	62	321	e71c3e		
A049	Paper	30	69.3	177	29	56	262	b11d38		
A050	Paper	30	69.3	193	34	60	287	c1223c		
A051	Paper	30	69.3	195	40	66	301	c32842		
A052	Paper	30	69.3	195	39	64	298	c32740		
A053	Paper	30	69.3	177	35	56	268	b12338		
A054	Paper	30	69.3	210	49	72	331	d23148		
A055	Paper	35	65.7	185	45	64	294	bd2d40		
A056	Paper	35	65.7	179	46	64	289	b32e40		
A057	Paper	35	65.7	179	40	61	280	b3283d		
A058	Paper	35	64.4	174	36	56	266	ae2438		
A059	Paper	35	64.4	187	48	66	301	bb3042		
A060	Paper	35	64.4	172	31	53	256	ac1f35		
A061	Paper	40	60.0	156	42	53	251	9c2a35		
A062	Paper	40	60.0	161	45	53	259	a12d35		
A063	Paper	40	60.0	152	53	60	265	98353c		
A064	Paper	40	60.0	150	42	50	242	962a32		
A065	Paper	40	60.0	154	38	49	241	9a2631		
A066	Paper	40	60.0	153	41	52	246	992934		
A067	Paper	45	51.7	180	36	55	271	b42437		
A068	Paper	45	48.5	165	32	50	247	a52032		
A069	Paper	45	48.5	170	35	52	257	aa2334		
A070	Paper	45	48.5	177	31	51	259	b11f33		
A071	Paper	45	48.5	185	28	52	265	b91c34		
A072	Paper	45	48.5	175	36	55	266	af2437		
A073	Paper	50	44.3	163	53	64	280	a33540		
A074	Paper	50	44.3	161	53	62	276	a1353e		
A075	Paper	50	44.9	164	52	61	277	a4343d		
A076	Paper	50	44.9	164	49	58	271	a4313a		
A077	Paper	50	44.9	155	39	52	246	9b2734		
A078	Paper	50	44.9	164	51	59	274	a4333b		



**Figure 101** Table of measurements recorded for stains generated on paper surfaces from -10°C to 50°C

Stain ID	Surface	Temperature /°C	Average Humidity	R Value	G Value	B Value	RGB total	Hex
A001	Paper	-10	89.7	244	15	54	313	f80f36
A002	Paper	-10	89.7	227	6	36	269	e30624
A003	Paper	-10	89.3	212	7	16	235	d40710
A004	Paper	-10	89.3	241	8	48	297	f10830
A005	Paper	-10	89.3	219	9	24	252	db0918
A006	Paper	-10	89.3	221	9	21	251	db0915
A007	Paper	-5	84.1	240	6	50	296	f00632
A008	Paper	-5	84.1	240	19	58	317	f0133a
A009	Paper	-5	84.1	241	12	49	302	f10c31
A010	Paper	-5	84.1	243	7	39	289	f30727
A011	Paper	-5	85.9	242	11	44	297	f20b2c
A012	Paper	-5	85.9	237	12	42	291	e00c2a
A013	Paper	0	91.5	227	35	64	326	e32340
A014	Paper	0	91.5	223	30	56	309	df1a38
A015	Paper	0	91.5	232	32	63	327	e8203f
A016	Paper	0	91.5	222	35	67	324	de2343
A017	Paper	0	91.5	227	28	63	318	e31c3f
A018	Paper	0	91.5	235	23	58	316	eb173a
A019	Paper	5	88.1	237	9	29	275	e0091d
A020	Paper	5	88.1	232	15	40	287	e80f28
A021	Paper	5	89.5	236	16	50	302	ec1032
A022	Paper	5	89.5	225	17	35	277	e11129
A023	Paper	5	89.5	219	19	46	284	de132e
A024	Paper	5	90.0	229	12	52	293	e50c34
A025	Paper	10	96.0	228	23	49	300	e41731
A026	Paper	10	96.0	241	39	66	346	f22742
A027	Paper	10	96.0	239	20	56	315	ef1438
A028	Paper	10	96.0	229	24	42	295	e5182a
A029	Paper	10	96.0	240	21	54	315	f01536
A030	Paper	10	96.0	241	17	44	302	f1112c
A031	Paper	15	96.5	237	22	59	318	ed163b
A032	Paper	15	96.5	222	21	50	293	de1532
A033	Paper	15	96.5	231	27	52	310	e71b34
A034	Paper	15	96.6	230	8	45	283	e6082d
A035	Paper	15	96.6	232	35	67	334	e82343
A036	Paper	15	96.6	236	33	61	330	ec213d
A037	Paper	20	87.2	232	29	62	323	e81d3e
A038	Paper	20	88.0	237	29	59	325	ed1d3b
A039	Paper	20	88.0	228	23	54	305	e41736
A040	Paper	20	88.0	243	50	79	372	f32a4f
A041	Paper	20	88.3	239	42	71	352	ef2a47
A042	Paper	20	88.3	229	35	65	329	e52341
A043	Paper	25	84.2	234	28	60	312	e01c3c
A044	Paper	25	84.2	235	24	58	317	eb183a
A045	Paper	25	84.2	230	23	52	305	e61734
A046	Paper	25	84.2	237	30	58	325	ed1a3a
A047	Paper	25	84.2	229	18	54	301	e51236
A048	Paper	25	84.2	231	28	62	321	e71c3e
A049	Paper	30	68.3	177	29	56	262	b11d38
A050	Paper	30	68.3	193	34	60	287	c1223c
A051	Paper	30	69.3	195	40	66	301	c32842
A052	Paper	30	69.3	195	39	64	298	c32740
A053	Paper	30	69.3	177	35	56	268	b12338
A054	Paper	30	69.3	210	49	72	331	d31148
A055	Paper	35	65.7	185	45	64	294	b62d40
A056	Paper	35	65.7	179	46	64	289	b32e40
A057	Paper	35	65.7	179	40	61	280	b3283d
A058	Paper	35	64.4	174	36	56	266	ae2438
A059	Paper	35	64.4	187	48	66	301	bb3042
A060	Paper	35	64.4	172	31	53	256	ae1735
A061	Paper	40	60.0	156	42	53	251	9c2a35
A062	Paper	40	60.0	161	45	53	259	a12d35
A063	Paper	40	60.0	152	53	60	265	98353c
A064	Paper	40	60.0	150	42	50	242	962a32
A065	Paper	40	60.0	154	38	49	241	9a2631
A066	Paper	40	60.0	153	41	52	246	992934
A067	Paper	45	51.7	180	36	55	271	b42437
A068	Paper	45	48.5	165	32	50	247	e52032
A069	Paper	45	48.5	170	35	52	257	ae2334
A070	Paper	45	48.5	177	31	51	259	b11f33
A071	Paper	45	48.5	185	28	52	265	b01c34
A072	Paper	45	48.5	175	36	55	266	af2437
A073	Paper	50	44.3	163	53	64	280	a33540
A074	Paper	50	44.3	161	53	62	276	a1353e
A075	Paper	50	44.9	164	52	61	277	a0343d
A076	Paper	50	44.9	164	49	58	271	a0313a
A077	Paper	50	44.9	155	39	52	246	9b2734
A078	Paper	50	44.9	164	51	59	274	a0333b

Figure 102 outlines average R, G and B values calculated from 6 replicate stains at each temperature interval. At each temperature interval R-values for stains were higher than G and B-values. Stains therefore appear coloured towards a red rather than green or blue hue. For temperatures  $-10^{\circ}\text{C}$  to  $25^{\circ}\text{C}$  R-values were in excess of 200, with the highest value of 240.5 recorded at  $-5^{\circ}\text{C}$ . For temperatures  $30^{\circ}\text{C}$  to  $50^{\circ}\text{C}$  R-values were lower than 200. This suggests that as temperature increased from  $-10^{\circ}\text{C}$  to  $50^{\circ}\text{C}$  levels of R decreased overall. A decrease in R of 65.5 between  $-10^{\circ}\text{C}$  (R-value: 227.3) and  $50^{\circ}\text{C}$  (R-value: 161.8) confirms this. The most significant decrease (39.8) in R-value between two temperature intervals occurred between  $25^{\circ}\text{C}$  and  $30^{\circ}\text{C}$ . The colour change associated with this decrease can be observed between these intervals in *figure 101*.

Levels of G and B values increased between  $-10^{\circ}\text{C}$  (G-value 9.0, B-value 33.2) and  $50^{\circ}\text{C}$  (G-value 49.5, B-value 59.3) although higher B-values were recorded at  $0^{\circ}\text{C}$  (61.8)  $20^{\circ}\text{C}$  (65.0),  $30^{\circ}\text{C}$  (62.3) and  $35^{\circ}\text{C}$  (60.7).

**Figure 102** Descriptive statistics recorded for stains generated on paper surfaces from  $-25^{\circ}\text{C}$  to  $50^{\circ}\text{C}$

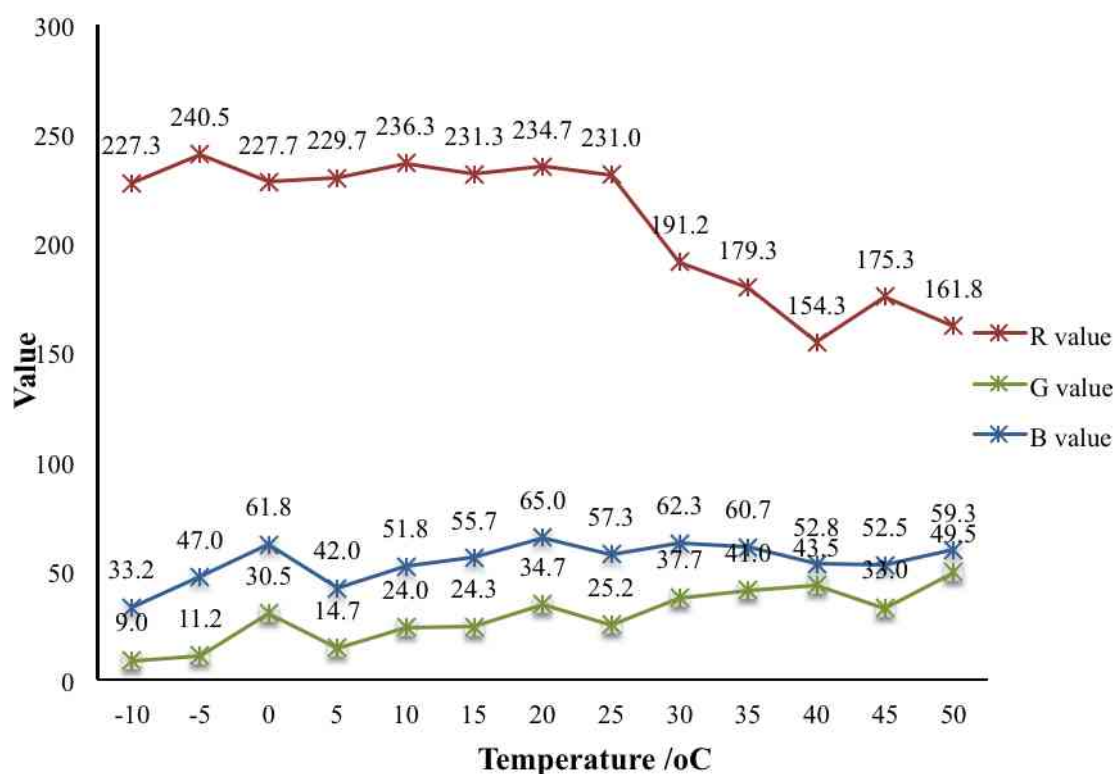


Figure 103 outlines mean colour values for all paper stains. Average R, G and B values were calculated between all replicate stains at all temperature intervals. Values for stains generated on paper were R (209.27), G (29.09) and B (53.95). Stains therefore exhibit a higher ratio of R colour components, to G and B colour components. This means stains are coloured towards a red rather than green or blue hue. G and B values were significantly lower than R values, the average G value was 180.18 points lower and the average B value was 155.32 points lower than the average R value. This indicates stains generated on paper were very strongly coloured towards an intense red.

**Figure 103** Average R, G and B values for all stains generated on paper

	N	Minimum	Maximum	Mean	Std. Deviation
R Value	78	150	244	209.27	31.288
G Value	78	6	53	29.09	13.377
B Value	78	16	79	53.96	11.074
Valid N (listwise)	78				

Figure 104 outlines average R, G and B values according to relative humidity intervals recorded during experimental stage 1. Comparison of R, G and B values between the lowest (44.3 rH) and highest (96.6 rH) recorded humidity levels appears to indicate the possibility of trends in each. Average R-values increased from 162.0 (44.3 rH) to 232.7 (96.6 rH), average G values decreased from 53.0 (44.3 rH) to 25.3 (96.6 rH) and average B values decreased from 63.0 (44.3 rH) to 57.7 (96.6 rH). Although comparisons between the lowest (44.3 rH) and highest (96.6 rH) humidity levels could be interpreted as evidence of possible overall correlations between humidity and R, G and B values, the variability of values occurring between lowest and highest humidity levels meant that no overall trends could be confirmed. These results suggest the relationship between humidity and stain colour is not a strongly correlated one.

**Figure 104** Table of descriptive statistics recorded for stains generated according to relative humidity values

Humidity /rH		R Value	G Value	B Value
44.3	Mean	162.0	53.0	63.0
	Std. Deviation	1.4	0.0	1.4
44.9	Mean	161.8	47.8	57.5
	Std. Deviation	4.5	6.0	3.9
48.5	Mean	174.4	32.4	52.0
	Std. Deviation	7.5	3.2	1.9
51.7	Mean	180.0	36.0	55.0
	Std. Deviation	.	.	.
60	Mean	154.3	43.5	52.8
	Std. Deviation	3.8	5.2	3.9
64.4	Mean	177.7	38.3	58.3
	Std. Deviation	8.1	8.7	6.8
65.7	Mean	181.0	43.7	63.0
	Std. Deviation	3.5	3.2	1.7
69.3	Mean	191.2	37.7	62.3
	Std. Deviation	12.6	6.8	6.3
84.1	Mean	241.0	11.0	49.0
	Std. Deviation	1.4	5.9	7.8
84.2	Mean	231.0	25.2	57.3
	Std. Deviation	4.6	4.4	3.7
85.9	Mean	239.5	11.5	43.0
	Std. Deviation	3.5	0.7	1.4
87.2	Mean	232.0	29.0	62.0
	Std. Deviation	.	.	.
88	Mean	236.0	34.0	64.0
	Std. Deviation	7.6	14.2	13.2
88.3	Mean	234.0	38.5	68.0
	Std. Deviation	7.1	5.0	4.2
89.1	Mean	234.5	12.0	34.5
	Std. Deviation	3.5	4.2	7.8
89.3	Mean	223.3	8.3	27.3
	Std. Deviation	12.4	1.0	14.2
89.5	Mean	226.7	17.3	43.7
	Std. Deviation	8.6	1.5	7.8
89.7	Mean	235.5	10.5	45.0
	Std. Deviation	12.0	6.4	12.7
90	Mean	229.0	12.0	52.0
	Std. Deviation	.	.	.
91.5	Mean	227.7	30.5	61.8
	Std. Deviation	5.0	4.6	4.1
96	Mean	236.3	24.0	51.8
	Std. Deviation	6.1	7.7	8.8
96.5	Mean	230.0	23.3	53.7
	Std. Deviation	7.6	3.2	4.7
96.6	Mean	232.7	25.3	57.7
	Std. Deviation	3.1	15.0	11.4

Figure 105 outlines the distributions of individual R-values for replicate stains generated at each temperature interval as a box-plot. At each temperature interval the median, minimum, maximum and interquartile ranges (IQRs) for R-values are identified. Two clear trends in distribution can be identified for stains generated between -10°C and 25°C and stains generated between 30°C and 50°C. The first group of stains, generated between -10°C and 25°C, are characterized by higher medians and IQRs than the second group, between 30°C and 50°C. There is no overlap between the minimum value in the first group (212) and the maximum value in the second group (210) (*figure 101*). In the first group medians and overall distributions of R-values are horizontally aligned across temperature intervals indicating relative consistency in R-values and distributions for stains in this group. In the second group medians and overall distributions are more variably arranged and with the exception of results at 40°C appear to be inversely related to further increases in temperature. These results suggest that R-values are consistent in stains



exposed to temperatures between -10°C and 25°C and then decrease as stains are exposed to temperatures between 30°C and 50°C. Despite this decrease, observations indicate that stains generated on paper across all temperatures between -10°C and 50°C exhibit significant levels of R-values.

Stains generated at 30°C exhibited the largest range between maximum and minimum R-values (33) at any temperature interval (*figure 105*). They had a significantly greater range (r) than other sets of stains in the second group at 35°C (r.15), 40°C (r.11), 45°C (r.20) and 50°C (r.9). They also exhibited a significantly greater range than stains in the first group at -5°C (r.6), 0°C (r.13), 5°C (r.18), 10°C (r.13), 15°C (r.15), 20°C (r.15) and 25°C (r.13). This suggests that the greatest variability and change in R-values occurs around 30°C and supports the suggestion that there are observable differences in R-value distributions between temperatures above and below this temperature.

**Figure 105** Box plot distributions of R values for stains generated on paper at temperature intervals between -10°C and 50°C

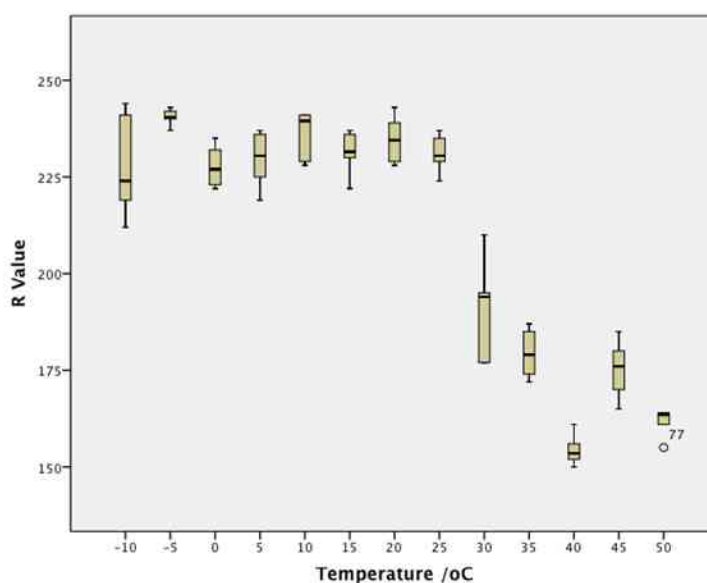


Figure 106 outlines the distributions of individual G-values for replicate stains generated at each temperature interval as a box-plot. At each temperature interval the median, minimum, maximum and interquartile ranges (IQRs) for G-values are identified. A clear positive relationship between temperature and G-value distribution is illustrated by the box-plot. For stains generated on paper, as temperature increases G-values also increase. This contrasts with the relationship

observed between temperature and R-values, which decrease with increases in temperature. This indicates the difference between R and G values of stains narrows as temperature increases.

**Figure 106** Box plot distributions of G values for stains generated on paper at temperature intervals between -10°C and 50°C

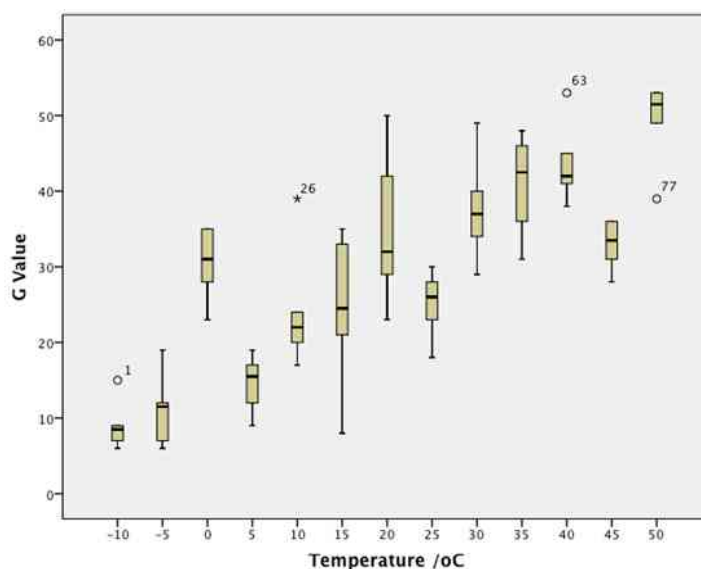


Figure 107 outlines the distributions of individual B-values for replicate stains generated at each temperature interval as a box-plot. At each temperature interval the median, minimum, maximum and interquartile ranges (IQRs) for B-values are identified. Trends in B-value distributions can be broadly separated into two phases, the first of which concerns distributions between -10°C and 20°C and the second of which concerns distributions between 25°C and 50°C. As temperature increases between -10°C and 20°C B-values increase. Medians increased from 30.0 (-10°C) to 63.5 (20°C). From 25°C to 50°C B-values appear to plateau between a median low of 52.0 (45°C) and a median high of 62.5 (35°C). These observations indicate that B-values increase with temperature increases. This increase continues until around 20°C, where after they remain high. As with observations of the relationship between G-values and temperature increases, this observation for B-values contrasts with the relationship observed between temperature and R-values, in which increases in temperature are associated with lower R-values. This indicates that the difference between R and B values of stains narrows as temperature increases. Observations from figures 106 and 107 demonstrate that as temperature increases and R-values

decrease, G and B values increase, decreasing the dominance of R-values in paper stains.

As temperature increases ranges of B-value distributions at each temperature appear to generally decrease, from a range of 38 at  $-10^{\circ}\text{C}$  to a range of 12 at  $50^{\circ}\text{C}$ . This indicates that B-values are less variable at higher temperatures. This trend was also observed for G-values, which appear less variable at higher temperatures, whilst R-values appear to exhibit a consistent variability across all temperature intervals.

**Figure 107** Box plot distributions of B values for stains generated on paper at temperature intervals between  $-10^{\circ}\text{C}$  and  $50^{\circ}\text{C}$

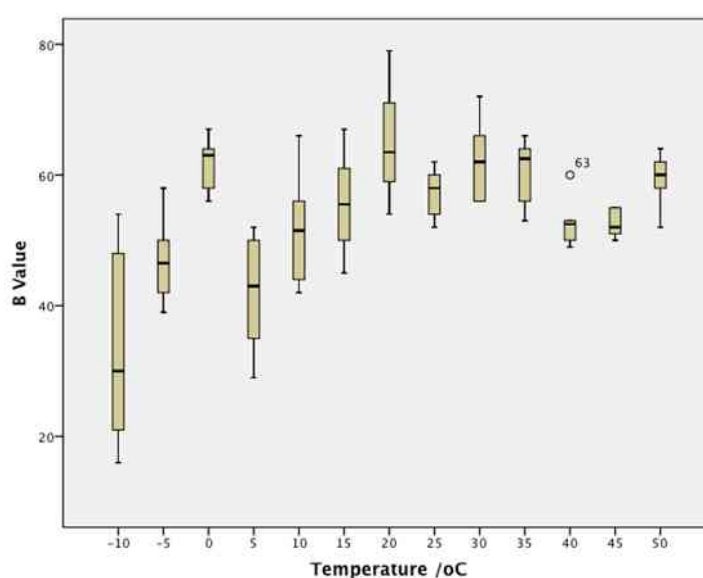


Figure 108 outlines the distributions of individual R, G and B-values for replicate stains generated at each temperature interval in comparison to each other in a box-plot. The trends in each appear relative to each other. Trends in R-values appear clearer than trends in G and B values. R-values represent the highest colour values at every temperature interval, all recorded between 150 ( $40^{\circ}\text{C}$ ) and 243 ( $-10^{\circ}\text{C}$ ). G and B-values are represented by much lower values at each temperature interval, all recorded between a 6 (G-values at  $-10^{\circ}\text{C}$  &  $-5^{\circ}\text{C}$ ) and 79 (B-value at  $20^{\circ}\text{C}$ ). These results indicate stains generated on paper between  $-10^{\circ}\text{C}$  and  $50^{\circ}\text{C}$  exhibited an intense red, rather than green or blue, colour. The intensity of the colouring is affected by the combination of high levels of R values and low levels of G and B values. The intensity of this red colour is altered between  $25^{\circ}\text{C}$  and  $30^{\circ}\text{C}$ .

**Figure 108** Box plot distributions of R, G and B values for stains generated on paper at temperature intervals between -10°C and 50°C

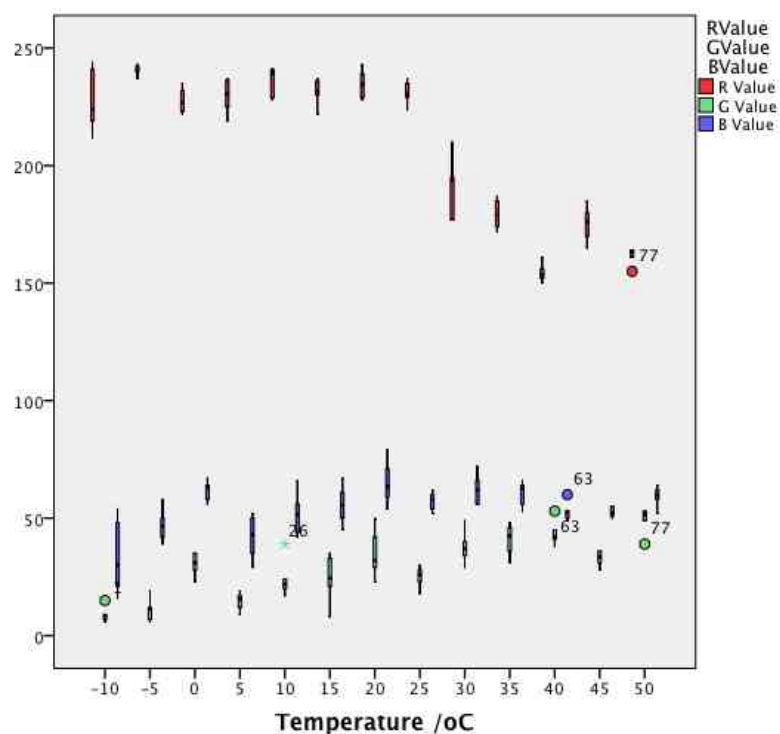
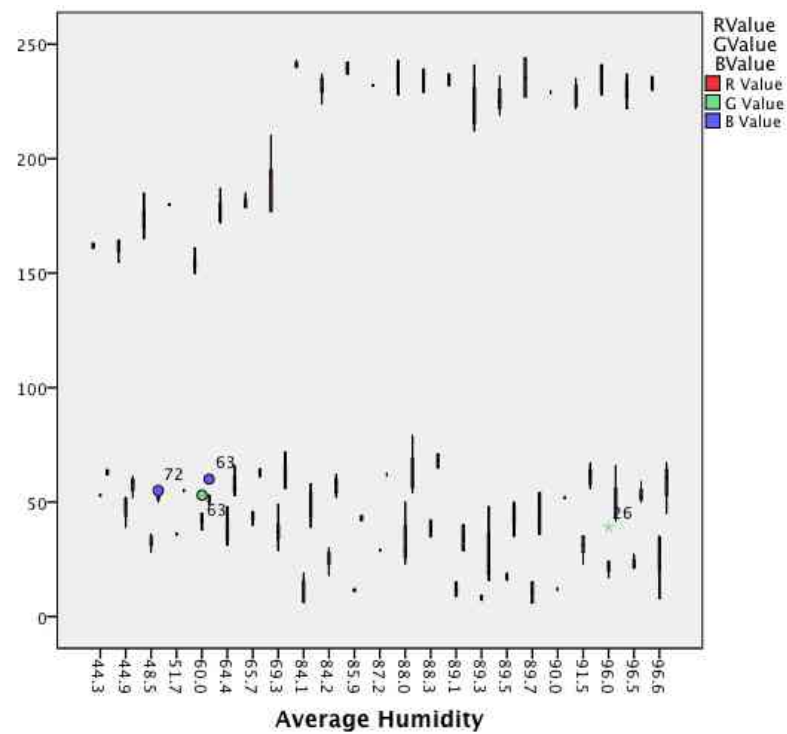


Figure 109 outlines the distributions of R, G and B-values for stains generated at humidity intervals recorded during experimental stage 1 in comparison to each other. As humidity increased from the lowest measure of 44.3 rH (relative humidity) to the highest of 96.6 R-values increase. R-values increased up to a humidity level of 84.1 rH where after R-values appeared to plateau and remain at a high level. G and B values appeared at a constant level across humidity levels. These results suggest that stains generated at higher levels of humidity will exhibit higher levels of R-value than stains generated at lower levels of humidity. As G and B values remained constant across humidity intervals, increases in R-values at higher levels of humidity increased the difference between R, G and B values at each interval, which should result in stains at higher humidity intervals exhibiting a lighter intensity of colour.

Although a relationship between R-values and humidity does appear to be supported by results presented in *figure 109*, humidity is influenced by temperature and it is difficult therefore to determine what influence humidity alone exerts on R-values.

**Figure 109** R, G and B values for stains generated on paper at humidity intervals recorded during experimental stage 1







































### 5.3.2 Stains generated on glass

The measurements for stains derived on glass surfaces from -10 to 50°C are presented in *figures 110-112*. The descriptive statistics are then presented in *figures 113 and 114*.

**Figure 110** Table of measurements recorded for stains generated on glass surfaces from -10°C to 20°C

Stain ID	Surface	Temperature /oC	Average Humidity	R Value	G Value	B Value	RGB total	Hex
A079	Glass	-10	88.0	241	0	35	276	f10023
A080	Glass	-10	88.0	246	1	37	284	f60125
A081	Glass	-10	88.0	233	0	37	270	e90025
A082	Glass	-10	88.0	237	0	37	274	ed0025
A083	Glass	-10	88.0	243	0	37	280	f30025
A084	Glass	-10	88.0	245	0	36	281	f50024
A085	Glass	-5	85.6	247	0	37	284	f70025
A086	Glass	-5	85.6	243	1	10	254	f3010a
A087	Glass	-5	85.6	245	0	34	279	f50022
A088	Glass	-5	85.6	247	2	26	275	f7021a
A089	Glass	-5	84.1	246	1	37	284	f60125
A090	Glass	-5	84.1	248	1	33	282	f80121
A091	Glass	0	94.0	241	3	40	284	f10328
A092	Glass	0	94.0	242	5	44	291	f2052c
A093	Glass	0	94.0	242	0	38	280	f20026
A094	Glass	0	94.0	213	0	33	246	d50021
A095	Glass	0	94.0	244	0	36	280	f40024
A096	Glass	0	94.0	237	1	37	275	ed0125
A097	Glass	5	88.9	241	2	34	277	f10222
A098	Glass	5	88.9	246	0	18	264	f60012
A099	Glass	5	88.9	242	0	32	274	f20020
A100	Glass	5	88.9	241	0	21	262	f10015
A101	Glass	5	89.0	243	0	22	265	f30016
A102	Glass	5	89.0	242	1	26	269	f2011a
A103	Glass	10	94.3	254	2	41	297	fe0229
A104	Glass	10	94.3	254	2	13	269	fe020d
A105	Glass	10	94.3	253	2	35	290	fd0223
A106	Glass	10	94.3	254	1	13	268	fe010d
A107	Glass	10	94.3	254	1	34	289	fe0122
A108	Glass	10	94.3	253	1	20	274	fd0114
A109	Glass	15	96.4	243	0	9	252	f30009
A110	Glass	15	96.4	245	1	18	264	f50112
A111	Glass	15	96.4	245	0	4	249	f50004
A112	Glass	15	96.4	247	2	7	256	f70207
A113	Glass	15	96.4	243	2	15	260	f3020f
A114	Glass	15	96.4	246	3	19	268	f60313
A115	Glass	20	87.2	242	1	24	267	f20118
A116	Glass	20	87.2	240	2	23	265	f00217
A117	Glass	20	87.2	233	0	19	252	e90013
A118	Glass	20	88.0	245	2	21	268	f50215
A119	Glass	20	88.0	244	1	26	271	f4011a
A120	Glass	20	88.0	244	1	25	270	f40119
A121	Glass	25	84.2	246	3	20	269	f60314

**Figure 111** Table of measurements recorded for stains generated on glass surfaces from 25°C to 50°C

A122	Glass	25	84.2	240	2	27	269	f0021b		
A123	Glass	25	84.2	246	1	22	269	f60116		
A124	Glass	25	84.2	245	1	26	272	f5011a		
A125	Glass	25	84.2	245	1	25	271	f50119		
A126	Glass	25	84.2	246	2	31	279	f6021f		
A127	Glass	30	69.2	218	0	26	244	da001a		
A128	Glass	30	69.2	207	1	30	238	cf011e		
A129	Glass	30	69.2	222	0	30	252	de001e		
A130	Glass	30	69.2	208	0	30	238	d0001e		
A131	Glass	30	69.2	216	0	25	241	d80019		
A132	Glass	30	69.2	204	0	27	231	cc001b		
A133	Glass	35	65.7	196	1	29	226	c4011d		
A134	Glass	35	65.7	181	3	30	214	b5031e		
A135	Glass	35	65.7	192	0	27	219	c0001b		
A136	Glass	35	65.7	186	1	29	216	ba011d		
A137	Glass	35	65.7	193	2	33	228	c10221		
A138	Glass	35	65.7	185	1	31	217	b9011f		
A139	Glass	40	63.6	157	2	32	191	9d0220		
A140	Glass	40	63.6	149	3	34	186	950322		
A141	Glass	40	63.6	143	1	30	174	8f011e		
A142	Glass	40	63.6	142	2	33	177	8e0221		
A143	Glass	40	63.6	153	4	32	189	990420		
A144	Glass	40	63.6	151	4	34	189	970422		
A145	Glass	45	48.5	163	1	37	201	a30125		
A146	Glass	45	48.5	169	2	37	208	a90225		
A147	Glass	45	48.5	164	2	37	203	a40225		
A148	Glass	45	48.5	164	1	39	204	a40127		
A149	Glass	45	48.5	167	1	38	206	a70126		
A150	Glass	45	48.5	159	2	38	199	9f0226		
A151	Glass	50	44.3	144	3	32	179	900320		
A152	Glass	50	44.3	147	9	36	192	930924		
A153	Glass	50	44.3	146	5	32	183	920520		
A154	Glass	50	44.9	153	38	52	243	992634		
A155	Glass	50	44.9	153	8	34	195	990822		
A156	Glass	50	44.9	146	5	34	185	920522		



**Figure 112** Table of measurements recorded for stains generated on glass surfaces from -10°C to 50°C

Stain ID	Surface	Temperature /oC	Average Humidity	R Value	G Value	B Value	RGB total	Hex
A079	Glass	-10	88.0	241	0	35	276	f10023
A080	Glass	-10	88.0	246	1	37	284	f60125
A081	Glass	-10	88.0	233	0	37	270	e90025
A082	Glass	-10	88.0	237	0	37	274	e90025
A083	Glass	-10	88.0	243	0	37	280	f30025
A084	Glass	-10	88.0	245	0	36	281	f50024
A085	Glass	-5	85.6	247	0	37	284	f70025
A086	Glass	-5	85.6	243	1	10	254	f3010a
A087	Glass	-5	85.6	245	0	34	279	f50022
A088	Glass	-5	85.6	247	2	26	275	f7021a
A089	Glass	-5	84.1	246	1	37	284	f60125
A090	Glass	-5	84.1	248	1	33	282	f80121
A091	Glass	0	94.0	241	3	40	284	f10328
A092	Glass	0	94.0	242	5	44	291	f2052c
A093	Glass	0	94.0	242	0	38	280	f20026
A094	Glass	0	94.0	213	0	33	246	d50021
A095	Glass	0	94.0	244	0	36	280	f40024
A096	Glass	0	94.0	237	1	37	275	e80125
A097	Glass	5	88.9	241	2	34	277	f10222
A098	Glass	5	88.9	246	0	18	264	f60012
A099	Glass	5	88.9	242	0	32	274	f20020
A100	Glass	5	88.9	241	0	21	262	f10015
A101	Glass	5	89.0	243	0	22	265	f30016
A102	Glass	5	89.0	242	1	26	269	f2011a
A103	Glass	10	94.3	254	2	41	297	fe0229
A104	Glass	10	94.3	254	2	13	269	fe020a
A105	Glass	10	94.3	253	2	35	290	f60223
A106	Glass	10	94.3	254	1	13	268	fe010a
A107	Glass	10	94.3	254	1	34	289	fe0122
A108	Glass	10	94.3	233	1	20	274	f60114
A109	Glass	15	96.4	243	0	9	252	f30009
A110	Glass	15	96.4	245	1	18	264	f50112
A111	Glass	15	96.4	245	0	4	249	f50004
A112	Glass	15	96.4	247	2	7	256	f70207
A113	Glass	15	96.4	243	2	15	260	f3020f
A114	Glass	15	96.4	246	3	19	268	f60313
A115	Glass	20	87.2	242	1	24	267	f20118
A116	Glass	20	87.2	240	2	23	265	f00217
A117	Glass	20	87.2	233	0	19	252	e90013
A118	Glass	20	88.0	245	2	21	268	f50215
A119	Glass	20	88.0	244	1	26	271	f4011a
A120	Glass	20	88.0	244	1	25	270	f40119
A121	Glass	25	84.2	246	3	20	269	f60314
A122	Glass	25	84.2	240	2	27	269	f0021b
A123	Glass	25	84.2	246	1	22	269	f60116
A124	Glass	25	84.2	245	1	26	272	f5011a
A125	Glass	25	84.2	245	1	25	271	f50119
A126	Glass	25	84.2	246	2	31	279	f6021f
A127	Glass	30	69.2	218	0	26	244	d6001a
A128	Glass	30	69.2	207	1	30	238	c7011e
A129	Glass	30	69.2	222	0	30	252	d6001e
A130	Glass	30	69.2	208	0	30	238	d0001e
A131	Glass	30	69.2	216	0	25	241	d80019
A132	Glass	30	69.2	204	0	27	231	cc001b
A133	Glass	35	65.7	196	1	29	226	c4011d
A134	Glass	35	65.7	181	3	30	214	b5031e
A135	Glass	35	65.7	182	0	27	219	c0001b
A136	Glass	35	65.7	186	1	29	216	ba011d
A137	Glass	35	65.7	183	2	33	228	c10221
A138	Glass	35	65.7	185	1	31	217	b9011f
A139	Glass	40	63.6	157	2	32	191	9d0220
A140	Glass	40	63.6	149	3	34	186	950322
A141	Glass	40	63.6	143	1	30	174	8f011e
A142	Glass	40	63.6	142	2	33	177	8e0221
A143	Glass	40	63.6	153	4	32	189	990420
A144	Glass	40	63.6	151	4	34	189	970422
A145	Glass	45	48.5	163	1	37	201	a30125
A146	Glass	45	48.5	169	2	37	208	a90225
A147	Glass	45	48.5	164	2	37	203	a40225
A148	Glass	45	48.5	164	1	39	204	a40127
A149	Glass	45	48.5	167	1	38	206	a70126
A150	Glass	45	48.5	159	2	38	199	980226
A151	Glass	50	44.3	144	3	32	179	900320
A152	Glass	50	44.3	147	9	36	192	930924
A153	Glass	50	44.3	146	5	32	183	920520
A154	Glass	50	44.9	153	38	52	243	992634
A155	Glass	50	44.9	153	8	34	195	990822
A156	Glass	50	44.9	146	5	34	185	920522



Figure 113 outlines average R, G and B values calculated from 6 replicate stains at each temperature interval. At each temperature interval R-values for stains were higher than G and B-values. Stains therefore appear coloured towards a red rather than green or blue hue. For temperatures -10°C to 30°C R-values were in excess of 200, with a highest value of 253.7 recorded at 10°C. The maximum a possible R-value can be is 255 so an R-value of 253.7 for a stain indicates the stain is an extremely intense colour of red. Several stains have very high R-values, approaching 255, including at -5°C (246.0), 5°C (242.5), 15°C (244.8), 20°C (241.3) and 25°C (244.7). This indicates several stains generated on glass exhibit intense red colourations. For temperatures 35°C to 50°C R-values were lower than 200. This suggests that as temperature increased from -10°C to 50°C levels of R decreased overall. A decrease in R of 92.6 between -10°C (R-value: 240.8) and 50°C (R-value: 148.2) confirms this. The most significant decrease (39.6) in R-value between two temperature intervals occurred between 35°C and 40°C. Another significant decrease (32.2) in R-value between two temperature intervals occurred between 25°C and 30°C. Significant colour changes associated with these decreases occurred over these intervals. This observation of a significant decrease in R-values between 25°C and 30°C for glass stains mirrors observations of the same trend in stains generated on paper.

Levels of G values increased slightly between -10°C (0.2) and 50°C (11.3) but this was not considered significant as G values were no higher than 2.7 for the 11 temperature intervals between -10°C and 50°C. Levels of G values in glass stains were considered relatively constant. Levels of B values also appeared relatively constant between -10°C (36.5) and 50°C (36.7).

**Figure 113** Descriptive statistics recorded for stains generated on glass surfaces from -25°C to 50°C

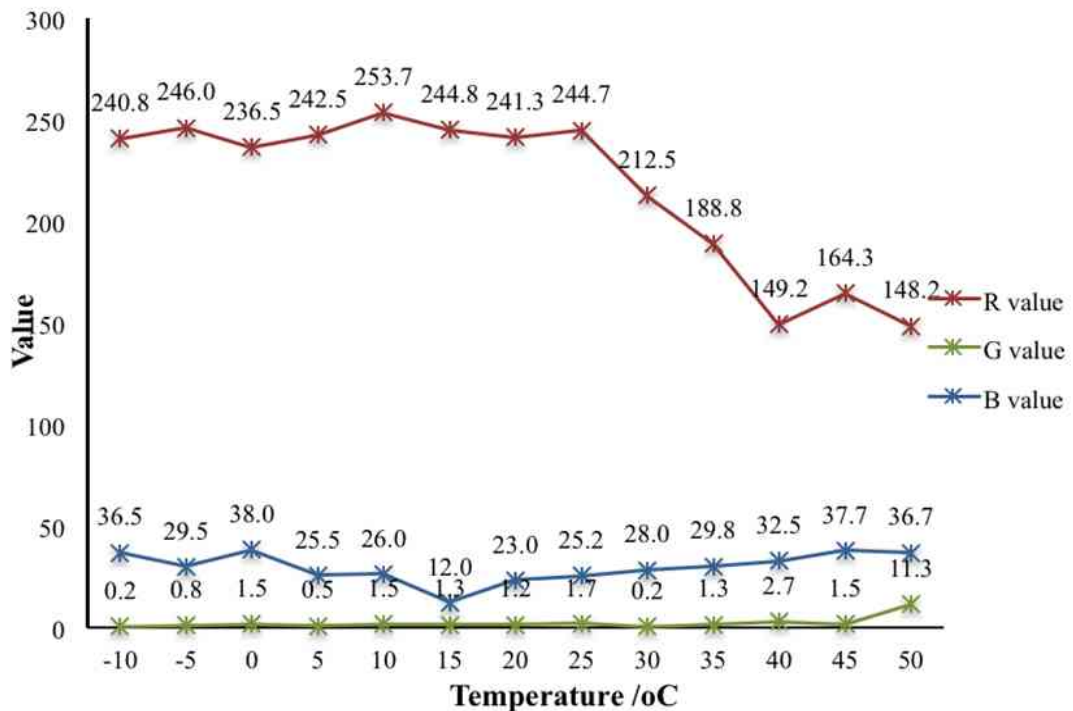


Figure 114 outlines average colour values for all glass stains. Average R, G and B values were calculated between all replicate stains at all temperature intervals. Values for stains generated on glass were R (218.41), G (1.97) and B (29.26). Stains therefore exhibit a higher ratio of R colour components, to G and B colour components. This means stains are coloured towards a red rather than green or blue hue. G and B values were significantly lower than R values, the average G value was 214.44 points lower and the average B value was 187.15 points lower than the average R value. This indicates stains generated on glass were very strongly coloured towards an intense red. Comparison of R, G and B values recorded for glass stains and paper stains indicate that glass stains, on average, exhibit slightly higher R-values and lower G and B values. This means stains generated on glass exhibited a lighter intensity and brighter red colour than stains generated on paper.

**Figure 114** Average R, G and B values for all stains generated on glass

	N	Minimum	Maximum	Mean	Std. Deviation
R Value	78	142	254	216.41	38.602
G Value	78	0	38	1.97	4.469
B Value	78	4	52	29.26	8.891
Valid N (listwise)	78				

Figure 115 outlines average R, G and B values according to relative humidity intervals recorded during experimental stage 1. Comparison of R, G and B values between the lowest (44 rH) and highest (96 rH) recorded levels of humidity appears to indicate the possibility of trends in each. Average R values increased from 145.67 (44 rH) to 244.83 (96 rH), average G values decreased from 5.67 (44 rH) to 1.33 (96 rH) and average B values decreased from 33.33 (44 rH) to 12 (96 rH). Although comparisons between R, G and B values at the lowest (44 rH) and highest (96 rH) levels of humidity could be interpreted as evidence of possible overall correlations between humidity and R, G and B values, no correlation appears to be supported in progressions through intermediate humidity values. These results suggest the relationship between humidity and stain colour is not a strongly correlated one.

**Figure 115** Table of descriptive statistics recorded for stains generated according to relative humidity values

Humidity /rH		R Value	G Value	B Value
44	Mean	145.67	5.67	33.33
	Std. Deviation	1.528	3.055	2.309
45	Mean	150.67	17	40
	Std. Deviation	4.041	18.248	10.392
49	Mean	164.33	1.5	37.67
	Std. Deviation	3.445	0.548	0.816
64	Mean	149.17	2.67	32.5
	Std. Deviation	5.811	1.211	1.517
66	Mean	188.83	1.33	29.83
	Std. Deviation	5.707	1.033	2.041
69	Mean	212.5	0.17	28
	Std. Deviation	7.148	0.408	2.28
84	Mean	247	1	35
	Std. Deviation	1.414	0	2.828
84	Mean	244.67	1.67	25.17
	Std. Deviation	2.338	0.816	3.869
86	Mean	245.5	0.75	26.75
	Std. Deviation	1.915	0.957	12.093
87	Mean	238.33	1	22
	Std. Deviation	4.726	1	2.646
88	Mean	242	0.56	32.33
	Std. Deviation	4.33	0.726	6.423
89	Mean	242.5	0.5	26.25
	Std. Deviation	2.38	1	7.932
89	Mean	242.5	0.5	24
	Std. Deviation	0.707	0.707	2.828
94	Mean	236.5	1.5	38
	Std. Deviation	11.743	2.074	3.742
94	Mean	253.67	1.5	26
	Std. Deviation	0.516	0.548	12.198
96	Mean	244.83	1.33	12
	Std. Deviation	1.602	1.211	6.197

Figure 116 outlines the distributions of individual R-values for replicate stains generated at each temperature interval as a box-plot. At each temperature interval the median, minimum, maximum and interquartile ranges (IQRs) for R-values are identified. Two clear trends in distribution can be identified for stains generated between  $-10^{\circ}\text{C}$  and  $25^{\circ}\text{C}$  and stains generated between  $30^{\circ}\text{C}$  and  $50^{\circ}\text{C}$ . The first group of stains, generated between  $-10^{\circ}\text{C}$  and  $25^{\circ}\text{C}$ , are characterized by higher medians and IQRs than the second group, between  $30^{\circ}\text{C}$  and  $50^{\circ}\text{C}$ . Medians in the first group range from a lowest of 241.5 ( $0^{\circ}\text{C}$ ) to a high of 254.0 ( $10^{\circ}\text{C}$ ). In the second group medians range from the highest of 212.0 ( $30^{\circ}\text{C}$ ) to a low of 146.5 ( $50^{\circ}\text{C}$ ). Despite this decrease, observations indicate that stains generated on glass across all temperatures between  $-10^{\circ}\text{C}$  and  $50^{\circ}\text{C}$  exhibit significant levels of R-values.

Stains generated at  $0^{\circ}\text{C}$  exhibited the largest range between maximum and minimum R-values (31) at any temperature interval (*figure 112*). The presence of one extreme R-value of 213 has however, contributed to this range. The second largest range between maximum and minimum values for stains at a single temperature interval occurred at  $30^{\circ}\text{C}$  (18). This suggests that the greatest variability and change in R-values occurs around  $30^{\circ}\text{C}$  and supports the idea of division of R-value distribution trends at this temperature.

**Figure 116** Box plot distributions of R values for stains generated on glass at temperature intervals between  $-10^{\circ}\text{C}$  and  $50^{\circ}\text{C}$

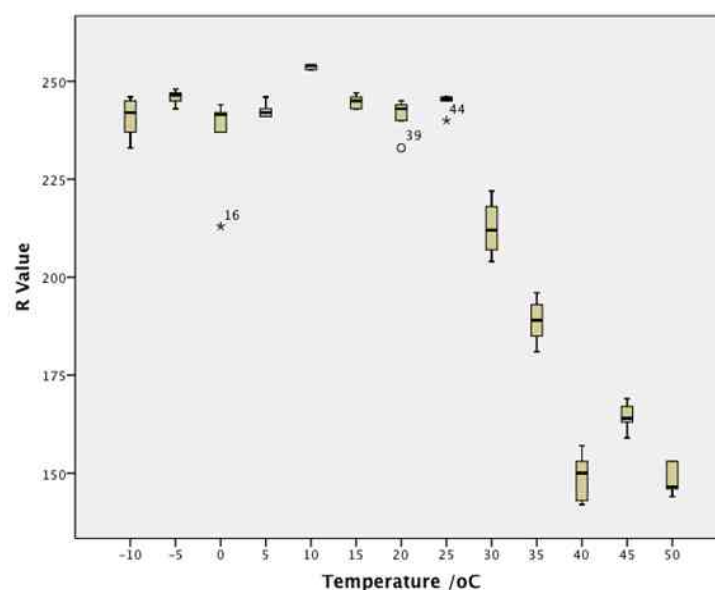


Figure 117 outlines the distributions of individual G-values for replicate stains generated at each temperature interval as a box-plot. At each temperature interval the median, minimum, maximum and interquartile ranges (IQRs) for G-values are identified. G-values for glass stains were consistently, extremely low across all temperature intervals. Medians ranged from a low of 0.00 (-10°C & 5°C) to a high of 6.5 (50°C). One extreme G-value of 38 was recorded at 50°C. When viewed alongside other G-values recorded however it appears to be an anomaly. For stains generated on glass, G-values are extremely low and no relationship between temperature and G-value for these stains is apparent. This observation is quite a contrast to the clear relationship observed between increases in temperature and decreases in R-values.

**Figure 117** Box plot distributions of G values for stains generated on glass at temperature intervals between -10°C and 50°C

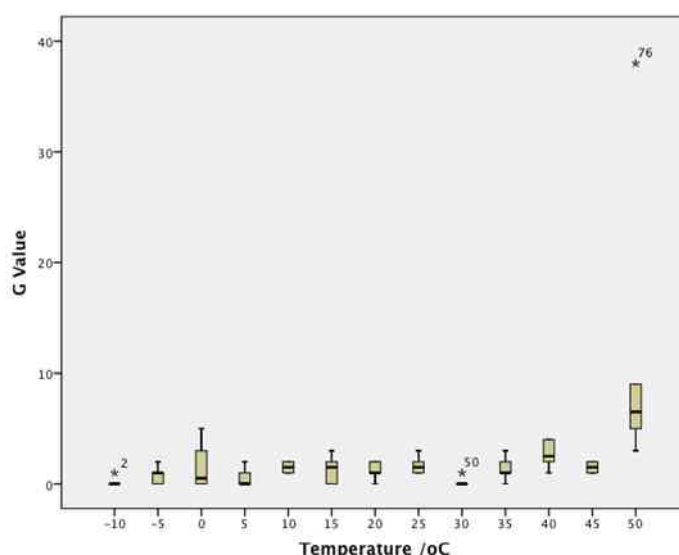


Figure 118 outlines the distributions of individual B-values for replicate stains generated at each temperature interval as a box-plot. At each temperature interval the median, minimum, maximum and interquartile ranges (IQRs) for B-values are identified. Trends in B-value distributions can be broadly separated into two phases, the first of which concerns distributions between -10°C and 15°C and the second of which concerns distributions between 20°C and 50°C. As temperature increases between -10°C and 15°C B-values decreased. Medians decreased from 37.0 (-10°C) to 12.0 (15°C). From 20°C to 50°C, B-value medians appear to increase from a low of 23.5 (20°C) to a high of 37.5 (45°C) and 34.0 (50°C). These observations indicate

no clear relationship between temperature and B-values for stains generated on glass. This contrasts with the clear relationship observed between increases in temperature and R-values. Comparison of B-values for glass stains and B-values for paper stains indicate that B-values for paper stains are higher than for glass stains and the difference between R and B values are smaller for paper stains than glass stains. This suggests stains on glass are more strongly orientated towards R-values than B-values, compared to paper stains and are therefore characterized by stronger and brighter shades of red.

**Figure 118** Box plot distributions of B values for stains generated on glass at temperature intervals between -10°C and 50°C

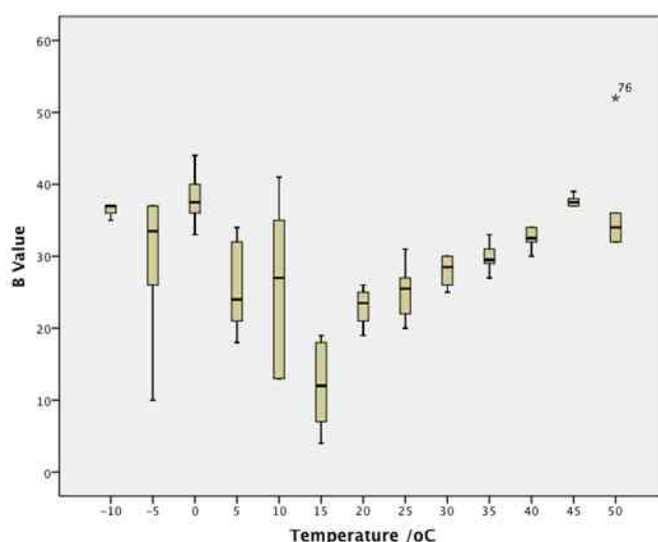


Figure 119 outlines the distributions of individual R, G and B-values for replicate stains generated at each temperature interval in comparison to each other in a box-plot. The trends in each appear relative to each other. Trends in R-values appear more significantly than trends in G and B values. R-values represent the highest colour values at every temperature interval, all recorded between 142 (40°C) and 247 (15°C). G and B-values are represented by much lower values at each temperature interval, all recorded between 0 and 52 (B-value at 50°C). These results indicate stains generated on glass between -10°C and 50°C exhibited an intense red, rather than green or blue, colour. The intensity of the colouring is affected by the combination of high levels of R values and low levels of G and B values. The intensity of this red colour is altered between 25°C and 30°C, an observation that was also made for stains generated on paper.

**Figure 119** Box plot distributions of R, G and B values for stains generated on glass at temperature intervals between -10°C and 50°C

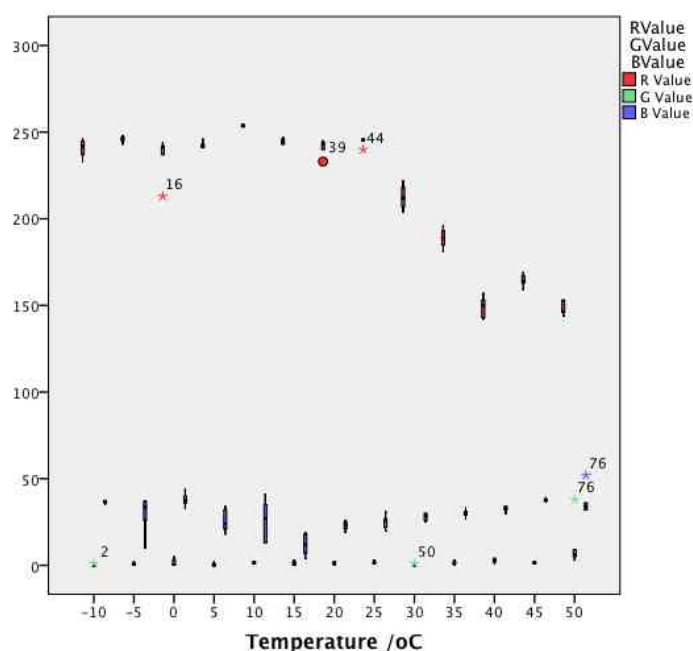
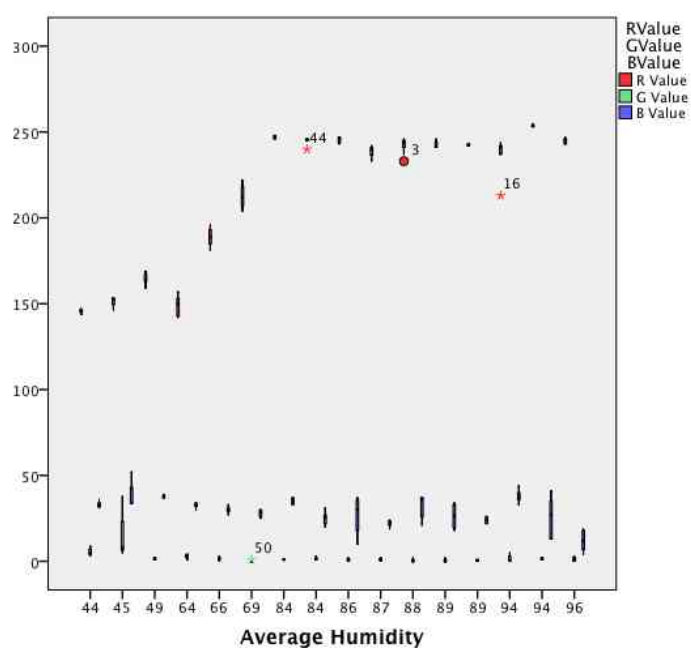


Figure 120 outlines the distributions of R, G and B-values for stains generated at humidity intervals recorded during experimental stage 1 in comparison to each other. As humidity increased from the lowest measure of 44 rH (relative humidity) to the highest of 96, R-values increased. R-values increased up to a humidity level of 84 rH where after R-values appeared to plateau and remain at a high level. G and B values appeared at a constant level across humidity levels. These results suggest that stains generated at higher levels of humidity will exhibit higher levels of R-value than stains generated at lower levels of humidity. As G and B values remained constant across humidity intervals, increases in R-values at higher levels of humidity increased the difference between R, G and B values at each interval, which should result in stains at higher humidity intervals exhibiting a lighter intensity of colour.

Although a relationship between R-values and humidity does appear to be supported by results presented in figure 120, humidity is influenced by temperature and it is difficult therefore to determine what influence humidity alone exerts on R-values.

**Figure 120** R, G and B values for stains generated on glass at humidity intervals recorded during experimental stage 1














































### 5.3.2 Stains generated on denim

The measurements for stains derived on denim surfaces from -10 to 50°C are presented in *figures 121-123*. The descriptive statistics are then presented in *figures 124 and 125*.



**Figure 121** Table of measurements recorded for stains generated on denim surfaces from -10°C to 20°C

Stain ID	Surface	Temperature /oC	Average Humidity	R Value	G Value	B Value	RGB total	Hex	
A157	Denim	-10	83.9	222	121	125	468	de797d	
A158	Denim	-10	83.9	216	119	122	457	d8777a	
A159	Denim	-10	83.9	224	120	123	467	e0787b	
A160	Denim	-10	83.9	222	123	127	472	de7b7f	
A161	Denim	-10	83.9	211	114	116	441	d37274	
A162	Denim	-10	83.9	221	119	122	462	dd777a	
A163	Denim	-5	82.7	224	119	124	467	e0777c	
A164	Denim	-5	82.7	208	111	113	432	d06f71	
A165	Denim	-5	82.7	222	118	123	463	de767b	
A166	Denim	-5	82.7	223	121	125	469	df797d	
A167	Denim	-5	82.7	213	113	116	442	d57174	
A168	Denim	-5	82.7	225	119	124	468	e1777c	
A169	Denim	0	93.4	218	123	128	469	da7b80	
A170	Denim	0	93.4	217	118	125	460	d9767d	
A171	Denim	0	93.4	193	103	109	405	c1676d	
A172	Denim	0	93.4	215	119	125	459	d7777d	
A173	Denim	0	93.4	215	117	124	456	d7757c	
A174	Denim	0	93.4	190	103	109	402	be676d	
A175	Denim	5	89.4	222	121	124	467	de797c	
A176	Denim	5	89.4	208	115	115	438	d07373	
A177	Denim	5	89.4	217	120	122	459	d9787a	
A178	Denim	5	89.4	223	120	123	466	df787b	
A179	Denim	5	89.4	216	118	120	454	d87678	
A180	Denim	5	89.4	217	120	122	459	d9787a	
A181	Denim	10	98.5	219	123	123	465	db7b7b	
A182	Denim	10	98.5	203	113	112	428	cb7170	
A183	Denim	10	98.5	219	122	123	464	db7a7b	
A184	Denim	10	98.5	218	124	125	467	da7c7d	
A185	Denim	10	98.5	211	117	117	445	d37575	
A186	Denim	10	98.5	223	127	127	477	df7f7f	
A187	Denim	15	96.3	216	126	127	469	d87e7f	
A188	Denim	15	96.3	206	119	118	443	ce777d	
A189	Denim	15	96.3	221	129	129	479	dd8181	
A190	Denim	15	96.3	216	125	125	466	d87d7d	
A191	Denim	15	96.3	204	117	114	435	cc7572	
A192	Denim	15	96.3	219	128	127	474	db807f	
A193	Denim	20	86.9	223	123	124	470	df7b7c	
A194	Denim	20	86.9	222	121	124	467	de797c	
A195	Denim	20	86.9	200	110	109	419	c86e6d	
A196	Denim	20	86.9	222	122	124	468	de7a7c	
A197	Denim	20	86.9	219	121	122	462	db797a	
A198	Denim	20	86.9	219	122	124	465	db7a7c	
A199	Denim	25	84.4	218	121	124	463	da797c	

**Figure 122** Table of measurements recorded for stains generated on denim surfaces from 25°C to 50°C

A200	Denim	25	84.4	217	121	122	460	d9797a	
A201	Denim	25	84.4	217	120	122	459	d9787a	
A202	Denim	25	84.4	219	120	122	461	db787a	
A203	Denim	25	84.4	212	119	120	451	d47778	
A204	Denim	25	84.4	220	124	127	471	dc7c7f	
A205	Denim	30	67.1	202	120	119	441	ca7877	
A206	Denim	30	67.1	204	121	121	446	cc7979	
A207	Denim	30	67.1	208	124	124	456	d07c7c	
A208	Denim	30	67.1	209	125	124	458	d17d7c	
A209	Denim	30	69.2	204	122	121	447	cc7a79	
A210	Denim	30	69.2	209	124	123	456	d17c7b	
A211	Denim	35	66.5	196	117	115	428	c47573	
A212	Denim	35	66.5	204	121	120	445	cc7978	
A213	Denim	35	66.5	195	117	115	427	c37573	
A214	Denim	35	66.5	210	126	124	460	d27e7c	
A215	Denim	35	66.5	204	121	120	445	cc7978	
A216	Denim	35	66.5	205	127	127	459	cd7f7f	
A217	Denim	40	63.0	198	129	127	454	c6817f	
A218	Denim	40	63.0	179	114	113	406	b37271	
A219	Denim	40	63.0	200	130	127	457	c8827f	
A220	Denim	40	63.0	196	127	124	447	c47f7c	
A221	Denim	40	63.0	178	111	109	398	b26f6d	
A222	Denim	40	63.0	192	123	122	437	c07b7a	
A223	Denim	45	55.4	198	114	116	428	c67274	
A224	Denim	45	55.4	189	107	109	405	bd6b6d	
A225	Denim	45	55.4	193	112	111	416	c1706f	
A226	Denim	45	55.4	203	119	120	442	cb7778	
A227	Denim	45	55.4	184	106	107	397	b86a6b	
A228	Denim	45	55.4	195	112	112	419	c37070	
A229	Denim	50	55.5	196	123	122	441	c47b7a	
A230	Denim	50	55.5	183	113	111	407	b7716f	
A231	Denim	50	55.5	191	119	116	426	bf7774	
A232	Denim	50	55.5	179	109	104	392	b36d68	
A233	Denim	50	55.5	179	109	104	392	b36d68	
A234	Denim	50	55.5	190	118	115	423	be7673	

**Figure 123** Table of measurements recorded for stains generated on denim surfaces from -10°C to 50°C

Stain ID	Surface	Temperature /oC	Average Humidity	R Value	G Value	B Value	RGB total	Hex
A157	Denim	-10	83.9	222	121	125	468	de797d
A158	Denim	-10	83.9	216	119	122	457	d8777a
A159	Denim	-10	83.9	224	120	123	467	e0787b
A160	Denim	-10	83.9	223	123	127	472	de7b7f
A161	Denim	-10	83.9	211	114	116	441	d37274
A162	Denim	-10	83.9	221	119	122	462	dd777a
A163	Denim	-5	82.7	224	119	124	467	e0777c
A164	Denim	-5	82.7	208	111	113	432	d06f71
A165	Denim	-5	82.7	222	118	123	463	de767b
A166	Denim	-5	82.7	223	121	125	469	df797d
A167	Denim	-5	82.7	213	113	116	442	d57174
A168	Denim	-5	82.7	225	119	124	468	e1777c
A169	Denim	0	93.4	218	123	128	469	da7b80
A170	Denim	0	93.4	217	118	125	460	d9767d
A171	Denim	0	93.4	193	103	109	405	c1676d
A172	Denim	0	93.4	215	119	125	459	d7777d
A173	Denim	0	93.4	215	117	124	456	d7757c
A174	Denim	0	93.4	190	103	109	402	be676d
A175	Denim	5	89.4	222	121	124	467	de797c
A176	Denim	5	89.4	208	115	115	438	d07373
A177	Denim	5	89.4	217	120	122	459	d9787a
A178	Denim	5	89.4	223	120	123	466	df787b
A179	Denim	5	89.4	216	118	120	454	d8767b
A180	Denim	5	89.4	217	120	122	459	d9787a
A181	Denim	10	98.5	219	123	123	465	db7b7b
A182	Denim	10	98.5	203	113	112	428	cb7170
A183	Denim	10	98.5	219	122	123	464	db7a7b
A184	Denim	10	98.5	218	124	125	467	da7c7d
A185	Denim	10	98.5	211	117	117	445	d37575
A186	Denim	10	98.5	223	127	127	477	df7ff7
A187	Denim	15	96.3	216	126	127	469	db7e7f
A188	Denim	15	96.3	206	119	118	443	ce777d
A189	Denim	15	96.3	221	129	129	479	dd8181
A190	Denim	15	96.3	216	125	125	466	db7d7d
A191	Denim	15	96.3	204	117	114	435	cc7572
A192	Denim	15	96.3	219	128	127	474	db807f
A193	Denim	20	86.9	223	123	124	470	df7b7c
A194	Denim	20	86.9	222	121	124	467	de797c
A195	Denim	20	86.9	200	110	109	419	c86e6d
A196	Denim	20	86.9	222	122	124	468	de7a7c
A197	Denim	20	86.9	219	121	122	462	db797a
A198	Denim	20	86.9	219	122	124	465	db7a7c
A199	Denim	25	84.4	218	121	124	463	da797c
A200	Denim	25	84.4	217	121	122	460	d9797a
A201	Denim	25	84.4	217	120	122	459	d9787a
A202	Denim	25	84.4	219	120	122	461	db787a
A203	Denim	25	84.4	212	119	120	451	d47778
A204	Denim	25	84.4	220	124	127	471	dc7c7f
A205	Denim	30	67.1	202	120	119	441	ca7877
A206	Denim	30	67.1	204	121	121	446	cc7979
A207	Denim	30	67.1	208	124	124	456	dd7c7c
A208	Denim	30	67.1	209	125	124	458	d17d7c
A209	Denim	30	69.2	204	122	121	447	cc7a79
A210	Denim	30	69.2	209	124	123	456	d17c7b
A211	Denim	35	66.5	196	117	115	428	ca7573
A212	Denim	35	66.5	204	121	120	445	cc7978
A213	Denim	35	66.5	195	117	115	427	c87573
A214	Denim	35	66.5	210	126	124	460	d27e7c
A215	Denim	35	66.5	204	121	120	445	cc7978
A216	Denim	35	66.5	205	127	127	459	cd777f
A217	Denim	40	63.0	198	129	127	454	ca817f
A218	Denim	40	63.0	179	114	113	406	b37271
A219	Denim	40	63.0	200	130	127	457	c8827f
A220	Denim	40	63.0	196	127	124	447	ca7f7c
A221	Denim	40	63.0	178	111	109	398	b2696d
A222	Denim	40	63.0	192	123	122	437	c07b7a
A223	Denim	45	55.4	198	114	116	428	ca7274
A224	Denim	45	55.4	189	107	109	405	ba6b6d
A225	Denim	45	55.4	193	112	111	416	c1706f
A226	Denim	45	55.4	203	119	120	442	cb7778
A227	Denim	45	55.4	184	106	107	397	b86a6b
A228	Denim	45	55.4	195	112	112	419	c37070
A229	Denim	50	55.5	196	123	122	441	ca7b7a
A230	Denim	50	55.5	183	113	111	407	b7716f
A231	Denim	50	55.5	191	119	116	426	ba7774
A232	Denim	50	55.5	179	109	104	392	b36d68
A233	Denim	50	55.5	179	109	104	392	b36d68
A234	Denim	50	55.5	190	118	115	423	ba7673

Figure 124 outlines average R, G and B values calculated from 6 replicate stains at each temperature interval. At each temperature interval R-values for stains were higher than G and B-values. Stains therefore appear coloured towards a red rather than green or blue hue. For temperatures -10 to 35°C R-values were in excess of 200. For 40°C, 45°C and 50°C R-values were 190.5, 193.7 and 186.3 respectively. This suggests that as temperature increased from -10°C to 50°C levels of R decreased overall. A decrease in R of 33 between -10°C (R-value: 219.3) and 50°C (R-value: 186.3) confirms this. Levels of G and B values also decreased between -10°C (G-value 119.3, B-value 122.5) and 50°C (G-value 115.2, B-value 112.0), with observable decreases of 10.6 (G-value) and 7.8 (B-value) occurring between 40°C and 45°C. This observation of trends in R-values for denim stains contrasted with observations of trends in R-values for both paper and glass stains, which exhibited sizeable decreases in R-values between 25°C and 30°C. R-values for denim stains by contrast appeared to vary little across temperature intervals.

**Figure 124** Descriptive statistics recorded for stains generated on denim surfaces from -25°C to 50°C

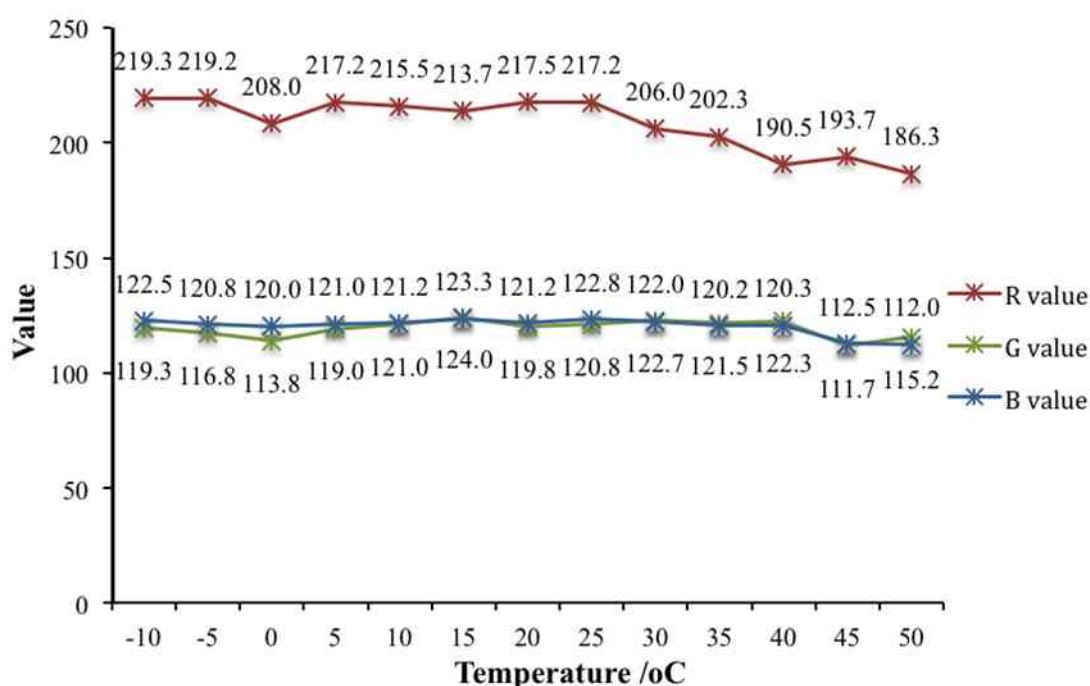


Figure 125 outlines average colour values for all denim stains. Average R, G and B values were calculated between all replicate stains at all temperature intervals. Values for stains generated on denim were R (208.18), G (119.08) and B (119.99).

Stains therefore exhibit a higher ratio of R colour components, to G and B colour components. This means stains are coloured towards a red rather than green or blue hue. G and B values were equally represented (119.08 and 119.99). On average, G values were 89.1 points lower than R values and B values were 88.19 points lower than R values. Comparison of R, G and B values recorded for denim and paper and glass stains indicates that denim stains, on average, exhibit similar R-values but much higher G and B values. This meant that stains generated on denim exhibited the lowest intensity of red colour compared to stains generated on paper and glass. This was supported by observations of a pinker colour for denim stains (*figure 123*) than the red colours displayed by paper (*figure 101*) and glass (*figure 112*) stains.

**Figure 125** Average R, G and B values for all stains generated on denim

	N	Minimum	Maximum	Mean	Std. Deviation
R Value	78	178	225	208.18	13.049
G Value	78	103	130	119.08	5.808
B Value	78	104	129	119.99	6.115
Valid N (listwise)	78				

Figure 126 outlines average R, G and B values according to relative humidity intervals recorded during experimental stage 1. Comparison of R, G and B values at the lowest recorded humidity (55.4 rH) with R, G and B values at the highest recorded humidity (98.5 rH) appears to indicate that R, G and B values increased as humidity increased. Average R values increased from 193.7 (55.4 rH) to 215.5 (98.5 rH), G values increased from 111.7 (55.4 rH) to 121.0 (98.5 rH) and B values increased from 112.5 (55.4 rH) to 121.1 (98.5 rH). Although an increase between values at 55.4 rH and 98.5 rH were observed, values at humidity levels in between are higher than those recorded at 98.5 rH. For R values for example, a value of 215.5 is calculated at 98.5 rH but the highest value of 219.3 is recorded at 83.9 rH. For G values, a value of 121.0 is recorded at 98.5 rH with the highest value of 124.0 at 96.3 rH. For B values, a value of 121.2 is recorded at 98.5 rH with the highest value of 123.3 at 96.3. These results suggest the relationship between humidity and stain colour is unclear and weaker perhaps than the relationship between stain colour and other influences.

**Figure 126** Table of descriptive statistics recorded for stains generated according to relative humidity values

Humidity /rH		R Value	G Value	B Value
55.4	Mean	193.7	111.7	112.5
	Std. Deviation	6.7	4.8	4.8
55.5	Mean	186.3	115.2	112.0
	Std. Deviation	7.0	5.7	7.1
63	Mean	190.5	122.3	120.3
	Std. Deviation	9.7	8.0	7.6
66.5	Mean	202.3	121.5	120.2
	Std. Deviation	5.8	4.3	4.8
67.1	Mean	205.8	122.5	122.0
	Std. Deviation	3.3	2.4	2.4
69.2	Mean	206.5	123.0	122.0
	Std. Deviation	3.5	1.4	1.4
82.7	Mean	219.2	116.8	120.8
	Std. Deviation	7.0	3.9	5.0
83.9	Mean	219.3	119.3	122.5
	Std. Deviation	4.9	3.0	3.7
84.4	Mean	217.2	120.8	122.8
	Std. Deviation	2.8	1.7	2.4
86.9	Mean	217.5	119.8	121.2
	Std. Deviation	8.7	4.9	6.0
89.4	Mean	217.2	119.0	121.0
	Std. Deviation	5.3	2.2	3.2
93.4	Mean	208.0	113.8	120.0
	Std. Deviation	12.9	8.6	8.6
96.3	Mean	213.7	124.0	123.3
	Std. Deviation	7.0	4.9	6.0
98.5	Mean	215.5	121.0	121.2
	Std. Deviation	7.3	5.1	5.6

Figure 127 outlines the distributions of individual R-values for replicate stains generated at each temperature interval as a box-plot. At each temperature interval the median, minimum, maximum and interquartile ranges (IQRs) for R-values are identified. Two trends in distribution can be identified for stains generated between -10°C and 20°C and stains generated between 25°C and 50°C. The first group of stains, generated between -10°C and 20°C, are characterized by higher medians than the second group, between 25°C and 50°C. In the first group medians of R-values are roughly horizontally aligned across temperature intervals suggesting there is a relative consistency amongst R-values for stains in this group. In the second group medians are negatively correlated to further increases in temperature. These results suggest that R-values are broadly consistent in stains exposed to temperatures between -10°C and 20°C and decrease as stains are exposed to temperatures between 25°C and 50°C. Despite this decrease, observations indicate that stains generated on denim across all temperatures between -10°C and 50°C exhibit significant levels of R-values. Observation of the greatest decrease in R-values occurring between 25°C



and 30°C mirrors observations of the same trend in paper and glass stains.

At several temperature intervals R-values are distributed over significant ranges, 17 (-5°C), 28 (0°C), 20 (10°C), 17 (15°C), 22 (40°C), 19 (45°C) and 17 (50°C). The presence of significant ranges of R-values at multiple temperatures supports the suggestion that R-values are extremely variable for stains generated on denim.

**Figure 127** Box plot distributions of R values for stains generated on denim at temperature intervals between -10°C and 50°C

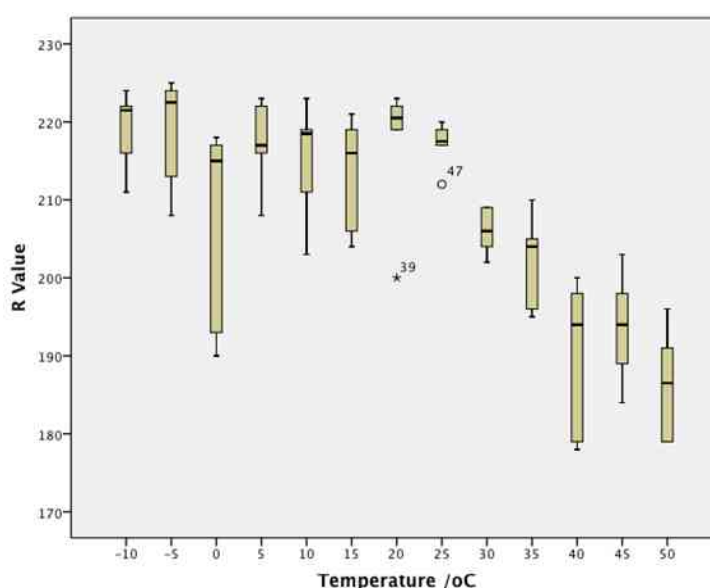


Figure 128 outlines the distributions of individual G-values for replicate stains generated at each temperature interval as a box-plot. At each temperature interval the median, minimum, maximum and interquartile ranges (IQRs) for G-values are identified. G-values for denim stains appeared consistently high across all temperature intervals, with medians ranging between a low of 112.0 (45°C) and a high of 125.5 (15°C). These observations indicate that stains generated on denim exhibit high levels of G-values. G-values observed for denim stains were much higher, by comparison, to G values recorded for paper or glass stains.

At two temperature intervals G-values are distributed over significant ranges of 20 (0°C) and 19 (40°C). This suggests G-values are variable for stains generated on denim. Variability of G-values was similar to variability of R and B values for

denim stains. Compared to stains generated on other surfaces, G-values for denim were more variable than glass but similar to the variability observed for paper stains.

**Figure 128** Box plot distributions of G values for stains generated on denim at temperature intervals between -10°C and 50°C

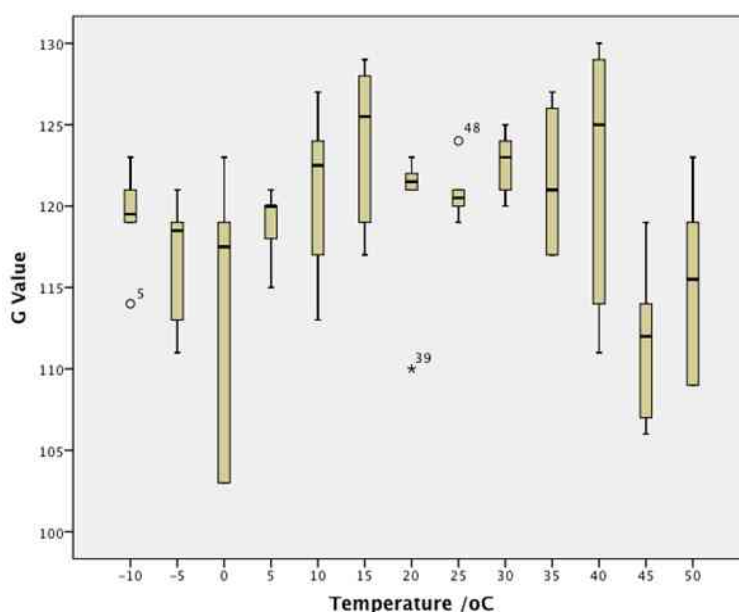


Figure 129 outlines the distributions of individual B-values for replicate stains generated at each temperature interval as a box-plot. At each temperature interval the median, minimum, maximum and interquartile ranges (IQRs) for B-values are identified. B-values for denim stains appeared consistently high across all temperature intervals between -10°C and 40°C, with medians ranging between a low of 120.0 (30°C) and a high of 126.0 (15°C). Medians for B-values of stains at 45°C (111.5) and 50°C (113.0) appear noticeably lower than B-values between -10°C and 40°C but still remain high. These observations indicate that stains generated on denim exhibit high levels of B-values. B-values observed for denim stains were higher, by comparison, to B values recorded for paper or glass stains.

At two temperature intervals B-values are distributed over significant ranges of 19 (0°C) and 18 (40°C). This suggests B-values are variable for stains generated on denim. Variability of B-values was similar to variability of R and G values for denim stains. Variability of B-values for denim stains was greater than variability of values



observed in paper and glass stains.

**Figure 129** Box plot distributions of B values for stains generated on denim at temperature intervals between -10°C and 50°C

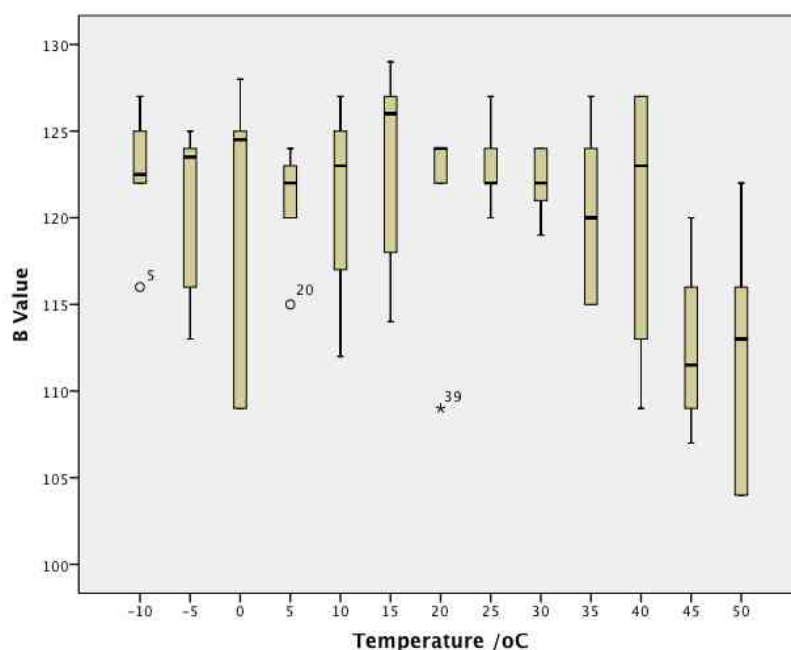


Figure 130 outlines the distributions of individual R, G and B-values for replicate stains generated at each temperature interval in comparison to each other in a box-plot. The trends in each appear relative to each other. R-values represent the highest colour values at every temperature interval, all recorded between 178 (40°C) and 225 (-5°C). G and B-values are represented by lower values at each temperature interval, all recorded between a 103 (G-value at 0°C) and 130 (G-value at 40°C). The differences between R, G and B values at each temperature interval are not significantly large, for example the difference between minimum R-value (178) and maximum G-value (130) at 40°C is only 48. These results indicate that stains generated on denim between -10°C and 50°C exhibited high levels of R, G and B values. R-values are dominant and stains will therefore be coloured closer to a red, rather than green or blue, hue. The strength of orientation in denim stains towards a red colouring will not be strong, as levels of green and blue colours are also high. Compared to paper and glass stains, denim stains demonstrate the lowest intensity of red colour as they exhibit the smallest differences between R, G and B values across all temperature intervals.

**Figure 130** Box plot distributions of R, G and B values for stains generated on denim at temperature intervals between -10°C and 50°C

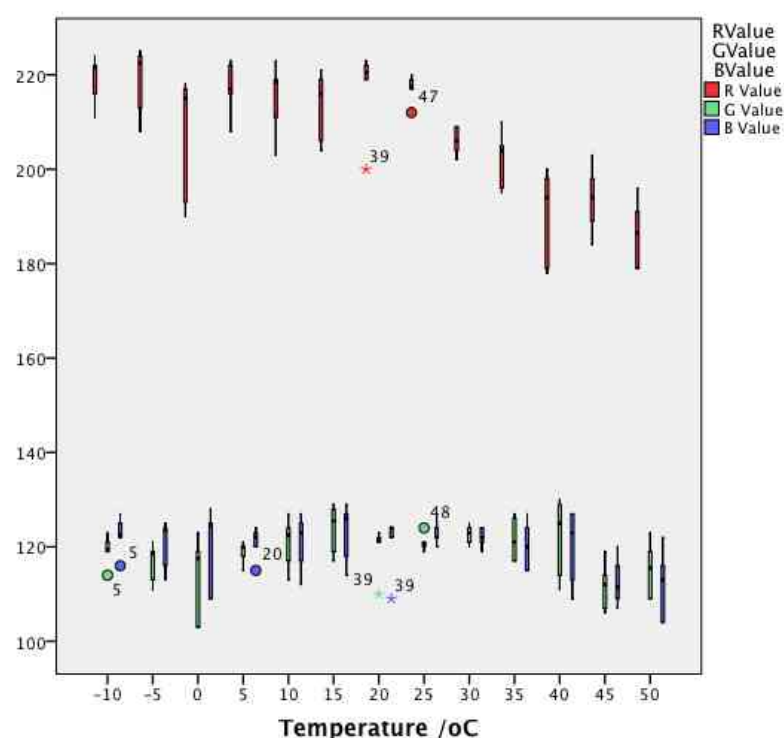
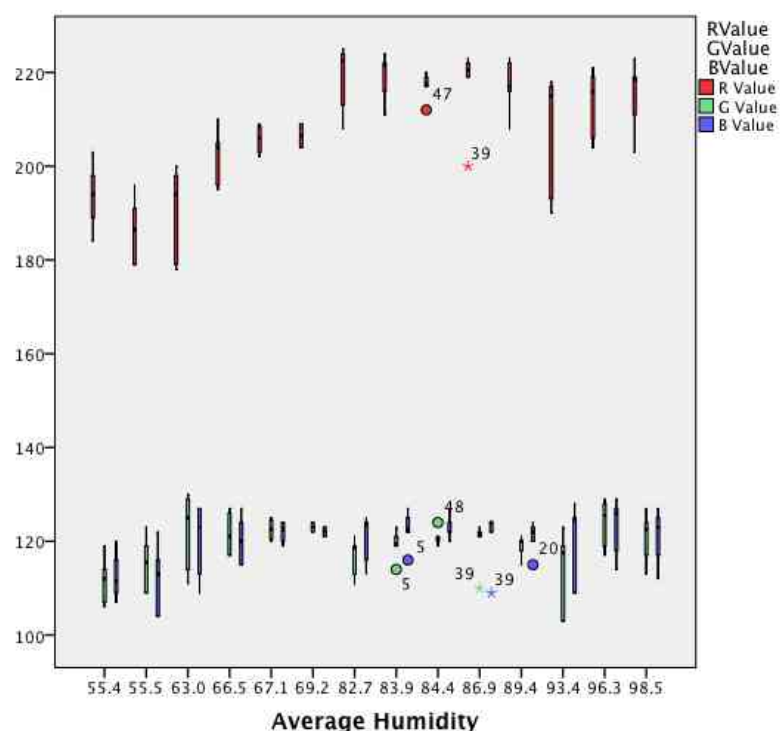


Figure 131 outlines the distributions of R, G and B-values for stains generated at humidity intervals recorded during experimental stage 1 in comparison to each other. As humidity increased from the lowest measure of 55.4 rH (relative humidity) to the highest of 98.5, R-values increased. G and B values appeared at a relatively constant level across humidity levels. These results suggest that stains generated at higher levels of humidity will exhibit higher levels of R-value than stains generated at lower levels of humidity. As G and B values remained constant across humidity intervals, increases in R-values at higher levels of humidity increased the difference between R, G and B values at each interval, which should result in stains at higher humidity intervals exhibiting a lighter intensity of colour.

Although a positive relationship between R-values and humidity does appear to be supported by results presented in *figure 131*, humidity is influenced by temperature and it is difficult therefore to determine what influence humidity alone exerts on R-values.

**Figure 131** R, G and B values for stains generated on denim at humidity intervals recorded during experimental stage 1



## 5.4 Stain colour analysis – surface comparison

Having identified the trends for each surface, the trends and results observed for all three surfaces were compared in more depth. Such a comparison enables the identification of both similarities and differences observed between stains generated under the same conditions, on different surfaces. Thus, the colours of stains generated on the three different surfaces (paper, glass and denim) were compared visually and through quantitative analysis.

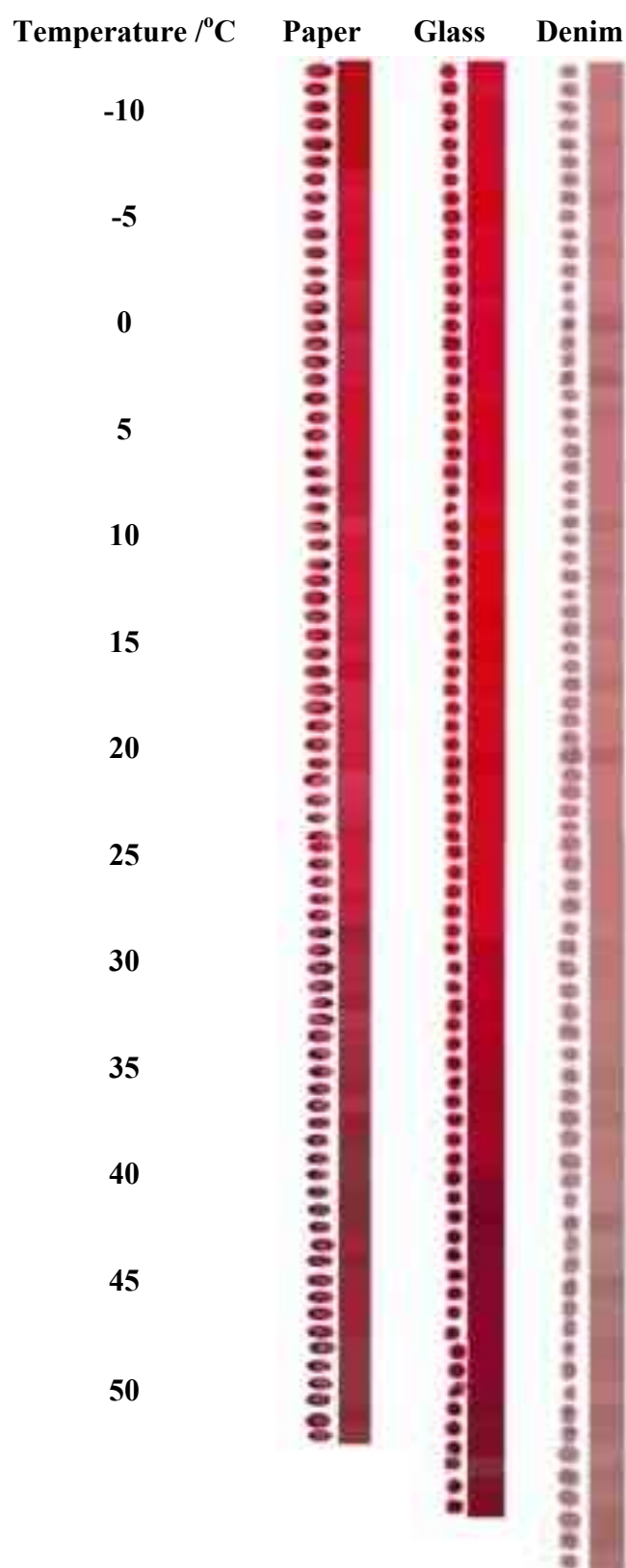
### 5.4.1 Colour ribbon comparison

To facilitate visual comparison of colours of stains generated at different temperatures, colour ribbons were compiled. Images of individual stains and blocks of hexadecimal colour corresponding to each stain were organised into longitudinal ribbons according to temperature. Colour ribbons for all three surfaces (paper, glass and denim) are shown in *figure 132* alongside each other.

Figure 132 provides a quick visual overview of changes in stain colour between -10°C and 50°C for each surface and how colours of stains compare between paper, glass and denim overall. Comparison of colour ribbons allows several observations to be made regarding the colour of stains formed at different temperatures on different surfaces. An initial observation was made regarding visible difference in colours of stains between surfaces. Stains at each temperature interval were generated on all three surfaces under the same conditions and from the same blood. A reasonable expectation follows that stains would therefore be generally similar in colour. Denim stains however appear more pink and grey than paper and glass stains, which are red or red-brown in colour. A quantitative confirmation of this difference is set out in 5.4.2 and 5.4.3 through comparisons of mean RGB totals (*denim: 306.9, glass: 314.1, paper: 306.8*) and ratios of R, G and B values.

A secondary observation related to gradual alterations in bloodstain colour as temperature stains are generated at progresses from -10°C to 50°C. Although alterations in colour occur gradually, comparison of stain colour at -10°C (top of ribbons) and 50°C (bottom of ribbons) indicate the effect of this gradual change over the course of the entire temperature range is observable. This alteration appears more prominently in paper and glass stains and to a lesser extent in denim stains. Visual observations were confirmed and explored further through a quantitative analysis of measures of colour recorded for stains.

**Figure 132** Longitudinal colour ribbons for stains generated on paper, glass and denim between -10°C and 50°C. Images of six replicate stains are included for each temperature interval.



### 5.4.2 Comparison of RGB totals between surfaces

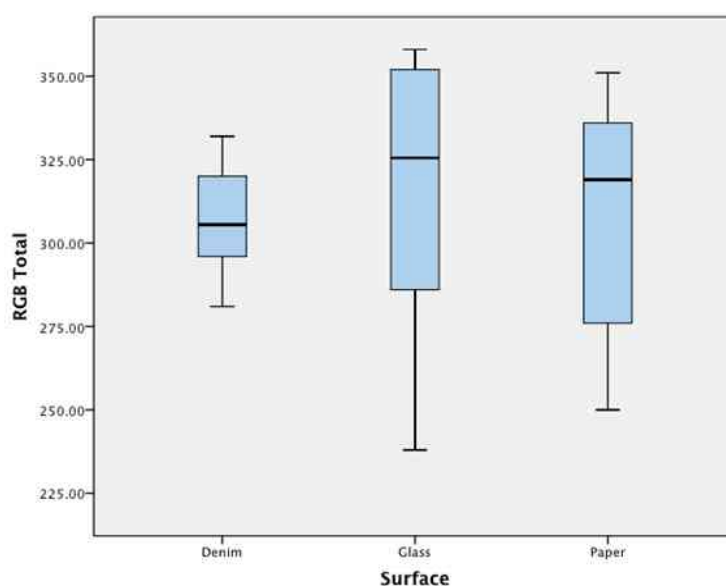
RGB totals were calculated by adding R, G and B values recorded for individual replicate stains at each temperature interval. Totals were then averaged between replicate stains and temperature intervals to generate an overall average RGB total for each surface. This was completed separately for each surface. The results are presented in *figure 133*.

Figure 133 outlines descriptive statistics for RGB totals calculated from all stains generated on denim, glass and paper. RGB totals are associated with an indication of overall intensity of a colour. The lightest intensity of colour, 'white', is characterised by (R255, G255, B255) and the darkest intensity of colour, 'black', is characterised by (R000, G000, B000). A comparison of mean RGB totals indicates that stains generated on glass exhibited higher RGB totals (314.13) than stains generated on denim (306.92) or paper (306.86). This suggests that either glass stains have the highest R-values, which contributes to higher RGB totals, or that glass stains have higher levels of G and B values contributing to higher RGB totals. Comparison of *figures 103, 114 and 125* indicate the former, that glass stains exhibit higher R-values (216.41) on average than denim stains (208.18) and paper stains (209.27). Observations that glass stains exhibit the highest RGB totals supports the suggestion that glass stains are characterised by a lighter intensity than denim and paper stains, which will be characterised by darker intensities.

**Figure 133** Descriptive statistics for RGB totals calculated from all stains generated on denim, glass and paper

Surface		Statistic	Std. Error
RGB Total	Denim	Mean	1.67017
		Median	
		Std. Deviation	
		Minimum	
		Maximum	
		Range	
	Glass	Mean	4.48843
		Median	
		Std. Deviation	
		Minimum	
		Maximum	
		Range	
	Paper	Mean	3.71919
		Median	
		Std. Deviation	
		Minimum	
		Maximum	
		Range	

Comparison of the range of RGB totals calculated for denim, glass and paper stains demonstrates that denim stains display the smallest range of RGB totals (51) with glass and paper stains exhibiting larger ranges of 120 and 101 respectively (*figure 134*).



**Figure 134** Box-plot demonstrating the range of RGB totals recorded for denim, glass and paper surfaces.

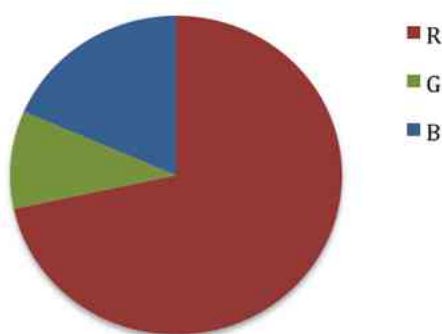
The significance of comparisons of ranges of RGB totals is in the association of ranges with levels of variability of stain colour. Results set out in *figures 133 and 134* suggest that denim stains exhibit a smaller range and therefore variability in colour, across all stains sampled, than glass or paper stains. This supports the observation that between -10°C and 50°C glass and paper stains demonstrated a clearly visible alteration in colour, which denim stains did not (*figure 132*).

### 5.4.3 Comparison of ratios of R, G and B values between surfaces

RGB totals give a measure of intensity of overall stain colour but ratios of R to G and B values give an indication of the significance or strength of colour orientation towards a particular component. Average RGB totals for stains were broken down to calculate average ratios of R, G and B values to allow comparison of the red colouration of stains between surfaces.

Figure 135 illustrates the ratio of R to G and B values for paper stains. The ratio was weighted towards R-values (209.27), then B-values (53.96) and lastly G-values (29.09) (figures from figure 136). This indicates paper stains were strongly orientated towards a red colour.

**Figure 135** Representation of average ratios of R to G and B values for paper stains



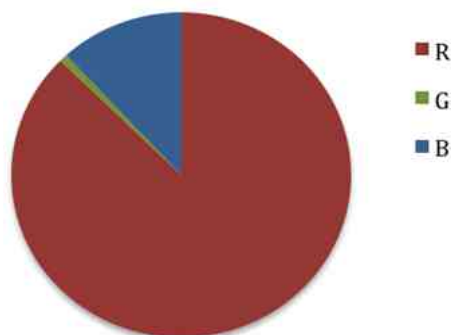
**Figure 136** Average R, G and B values for all stains generated on paper

	N	Minimum	Maximum	Mean
R Value	78	150	244	209.27
G Value	78	6	53	29.09
B Value	78	16	79	53.96
Valid N (listwise)	78			



Figure 137 illustrates the ratio of R to G and B values for glass stains. The ratio was weighted very heavily towards R-values (216.41), then B-values (29.26) and lastly to an extremely small representation of G-values (1.97) (figures from figure 138). This indicates glass stains were very strongly orientated towards a red colour.

**Figure 137** Representation of average ratios of R to G and B values for glass stains

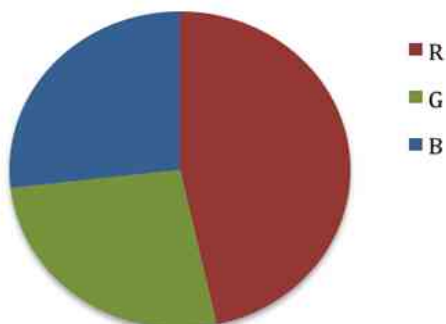


**Figure 138** Average R, G and B values for all stains generated on glass

	N	Minimum	Maximum	Mean
R Value	78	142	254	216.41
G Value	78	0	38	1.97
B Value	78	4	52	29.26
Valid N (listwise)	78			

Figure 139 illustrates the ratio of R to G and B values for denim stains. The largest single component of RGB totals for denim stains was R-values, however R-values accounted for less than half of RGB totals. Levels of G and B values are sizeable in combination making up over half the components of RGB totals. This indicates denim stains are slightly orientated towards a red colour but that high levels of G and B values will introduce a grey hue to the final colour.

**Figure 139** Representation of average ratios of R to G and B values for denim stains



**Figure 140** Average R, G and B values for all stains generated on denim

	N	Minimum	Maximum	Mean
R Value	78	178	225	208.18
G Value	78	103	130	119.08
B Value	78	104	129	119.99
Valid N (listwise)	78			

Comparison of ratios of R to G and B values in stains generated across paper, glass and denim indicated that glass stains were most strongly orientated towards a red colour, followed by paper stains and then denim stains. Under 50% of RGB totals for denim stains was contributed by R-values, which caused denim stains to appear less red and more pinky-grey than paper and glass stains. This was reflected in comparisons of colour ribbons (*figure 132*) where denim stains appear more pink and grey than the red and reddy-brown colours of paper and glass stains.

#### **5.4.4 Exploring relationships between RGB totals for all surfaces, temperature and humidity**

To establish whether common relationships between temperature, humidity and RGB totals exist for all surfaces, RGB totals for all surfaces were plotted against temperature (*figure 141*) and humidity (*figure 142*).

Figure 141 outlines the general correlation between temperature and RGB totals demonstrated by stains across all three surfaces (paper, glass and denim). Two clear trends in distribution between temperature and RGB totals can be identified for stains generated between -10°C and 25°C and stains generated between 30°C and 50°C. The first group of stains, generated between -10°C and 25°C, are characterized by higher medians than the second group, between 30°C and 50°C. The first group appeared to demonstrate a positive correlation between temperature and RGB totals whilst the second group appeared to demonstrate a negative correlation between temperature and RGB totals.

Observations support the suggestion that RGB totals for stains increase for temperatures between -10°C and 25°C and at 30°C there is a significant drop in RGB totals, which continue to decrease from 30°C to 50°C. Stains generated above 25°C

are therefore likely to be characterized by a darker intensity of colour than stains generated below 25°C. These trends apply to stains generated on any of the surfaces tested.

**Figure 141** Box plot distributions of RGB totals for stains generated on paper, glass and denim at temperature intervals between -10°C and 50°C

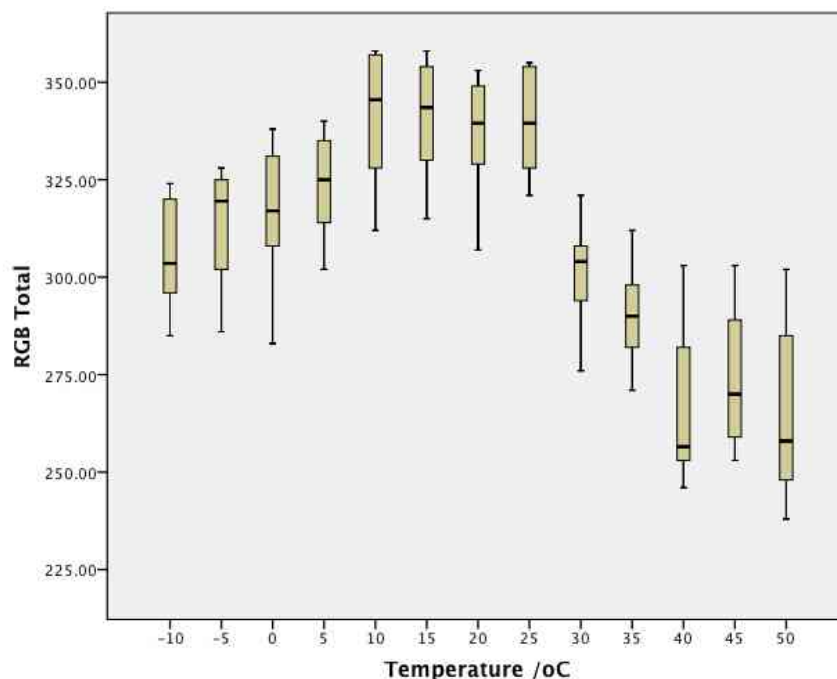
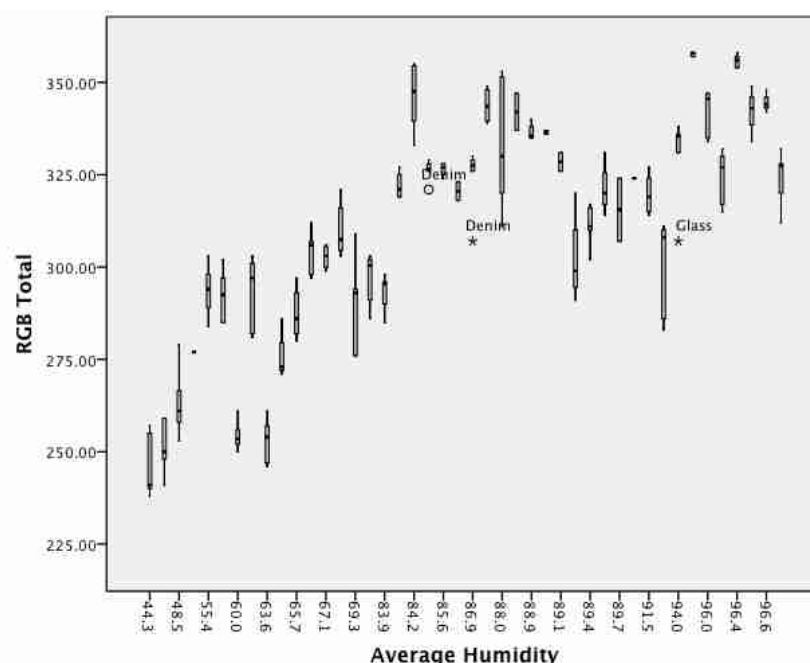


Figure 142 outlines the distributions of RGB totals for stains generated at humidity intervals recorded during experimental stage 1. As humidity increased from the lowest measure of 44.3 rH (relative humidity) to the highest of 96.6, RGB totals increased. These results suggest that stains generated at higher levels of humidity will exhibit higher RGB totals than stains generated at lower levels of humidity. This should mean that stains generated at higher humidity intervals exhibit a lighter intensity of colour.

Although a positive relationship between RGB totals and humidity does appear to be supported by *figure 142*, humidity is influenced by temperature and it is difficult therefore to determine what influence humidity alone exerts on RGB totals.

**Figure 142** Box plot distributions of RGB totals for stains generated on paper, glass and denim at humidity intervals recorded during experimental stage 1



### 5.4.5 Statistical test of distribution

Statistical tests were conducted to establish the significance of differences in distributions of R, G, B values and RGB totals between surfaces. Normality tests indicated that data was not normally distributed. This may have been due to small sample sizes (6 replicate stains on each surface per temperature) and therefore, non-parametric tests were used.

The Kruskal-Wallis test is a non-parametric test used to compare means of multiple independent groups of data. It was used to compare medians of R, G, B values and RGB totals recorded, grouped according to surface type (*Laerd statistics. 2013*).

When R, G, B and RGB totals for each surface are not averaged from replicate stains generated at each temperature interval it is possible to reject the null hypotheses. There is therefore a significant difference between the R, G, B and RGB-values recorded between the different surfaces at the 99% significance level ( $p = 0.000 < 0.01$ ) as *figure 143* shows.

Hypothesis Test Summary			
	Null Hypothesis	Test	Sig.
1	The distribution of R Value is the same across categories of Surface.	Independent-Samples Kruskal-Wallis Test	.000
2	The distribution of G Value is the same across categories of Surface.	Independent-Samples Kruskal-Wallis Test	.000
3	The distribution of B Value is the same across categories of Surface.	Independent-Samples Kruskal-Wallis Test	.000
4	The distribution of RGB Total is the same across categories of Surface.	Independent-Samples Kruskal-Wallis Test	.017

Asymptotic significances are displayed. The significance level is .05.

Figure 143 Kruskal-Wallis test comparing distributions of R, G, B values and RGB totals across surfaces (paper, denim, glass) stained in experimental stage 1

RGB totals and R-values act indicators, respectively, of intensity of colour and significance of orientation towards one particular colour (red). Results of the Kruskal-Wallis test demonstrate that intensity and strength of red colour varied significantly between stains generated on paper, glass and denim surfaces. Stains generated on glass exhibited the brightest intensity and strength of red colour, compared to stains generated on paper and denim. Denim stains by contrast were characterized by the lowest intensities and strength of red colour, appearing pink as a result. Results also indicated that temperature had a significant effect on stain colour, regardless of surface type. Stains generated at higher temperatures were characterized by darker intensities of colour than stains generated at low temperatures.

Variations in intensity and strength of red colouring may affect the interpretation of bloodstain evidence by affecting the ease with which analysts identify stains generated across different surfaces. This has implications for the analysis of bloodstains at a crime scene, where it is likely that stains will be encountered on a range of different surfaces. The implications of results of experimental stage 1 for bloodstain pattern analysis and the subsequent process of crime scene reconstruction are discussed in *chapter 13*.

## **6. Experimental Stage 2 – Exploration of environmental influences on bloodstain identification (longitudinal conditions)**

### **6.1 Overview**

Experimental stage 2 consisted of a series of stain drying experiments carried out in a progressively more ecologically valid forensic scenario than in experimental stage 1. Bloodstains, on a variety of surfaces, were housed in a semi-protected environment (located outdoors) and allowed to dry naturally according to ambient climatic conditions. After stains had dried they were left in situ and exposed to the natural climatic environment for varying periods of time. This was designed to mimic a forensic scenario where stained surfaces in outdoors or environmentally exposed locations, are discovered some length of time after they were generated. Temperature and humidity fluctuations over the experimental period were recorded and treated as the main independent variables.

Over the course of 6-7 months, stains were exposed to natural climatic fluctuations for one of two conditions; 1) cumulative lengths of time or 2) separate periods within the overall experimental timeframe. Once stains had been exposed to the natural climatic environment for distinct experimental periods they were subjected to visual and chemical identification methods.

The primary objective of stage 2 was to establish whether visual or chemical identification of bloodstains, exposed for varying lengths of time to variable climatic conditions, was influenced by these climatic fluctuations and whether stains generated at different experimental periods could therefore be distinguished from each other. The implications of this objective for crime scene reconstruction are in improving the ability of investigators to identify stains that have been exposed to a range of climatic fluctuations and estimate approximate time of deposition for these stains. A secondary objective was to draw comparisons between the results of experimental stage 1 and stage 2 – stains generated under different environmental conditions. The implications of this objective for crime scene reconstruction are in establishing how stains analysed immediately after deposition differ from stains

analysed some time after deposition, which have been exposed to a range of environmental conditions in the interim.

## 6.2 Materials

The materials utilised for the experimental work in this chapter are set out in *figure 144*.

Experimental equipment	Additional specifications
100ml whole Ovine blood	With Alsever's solution
Open-sided shelving unit	21 compartments
Rainproof, breathable cover for shelving unit	Children's play tent
Mosquito net	Lifesystems box single mosquito net
Temperature & relative humidity data logger	Ebro. VWR. EBI 20-THI
Paper	Ryman's A4 white laid paper, 100gm <sup>2</sup>
Glass microscope slides	CellPath. 90° ground edges. 25.4 x 76.2 mm. Thickness 1.0-1.2mm
White denim cloth	100% cotton. Weight: 345g/metre
Duct tape & sellotape	
Thermo Scientific Finnpiptette® F1 Variable Volume Single Channel Pipette	Volume range between 1-10µl
Biological waste disposal unit	
Kastle-Meyer testing kit	SceneSafe. Product code K160
Hemastix® testing kit	SceneSafe. Product code K162
Bluestar testing kit	SceneSafe. Product code K285
Digital scanner	HP Scanjet G2710

Figure 144 Table of materials used in experimental stage 2 (Author. 2012)

Justification for the selection of presumptive tests is provided in *section 3.4.3*.

## 6.3 Methodology

### 6.3.1 Climatic conditions at experimental site

The experiment required samples to be sited in an outdoors location for the duration of experimentation, so that they could be exposed to natural climatic conditions. During the experiment, one experimental site was used as the location for all sampling. This was in order to ensure a fair comparison could be made between sample sets and the environmental conditions they had been exposed to. The experimental site was set up outdoors in a garden, in an East London location (*London, E2, 51°531'494"N, -0°071'669"W*) chosen for its accessibility and

proximity to other experimental sites. The site was located in a temperate climatic zone.

Climate conditions at the experimental site (ES) were measured and recorded with a digital temperature and relative humidity data logger. The logger was placed in the middle of the experimental unit and pre-programmed to record temperature and humidity values every 15 minutes, for the duration of the experiment (6-7 months). In addition measurements of precipitation, wind speed and direction were recorded from an independent weather station (WS) located 800m from the experimental site. These measurements provided a more detailed record of temporal climatic variations at the site (*figure 145*).

#### Climatic summary from experimental site (ES) and weather station (WS)

Month	Temperature			Humidity	Precipitation	Wind	
	Average Temperature /°C	High Temperature /°C	Low Temperature /°C	Average Humidity /%	Total Precipitation /mm	Average Wind speed /mph	Average Wind Direction
	ES	ES	ES	ES	WS	WS	WS
X	7.2	13.0	-0.5	81	57.2	4.0	SW
X	5.2	16.9	-6.2	78	19.7	3.4	W
X	9.6	21.5	2.6	75	15.9	2.8	W
X	8.9	17.4	0.8	75	128.6	4.0	WSW
X	13.8	26.8	5.2	74	65.2	3.5	NNW
0*	15.3	27.8	7.3	74	193.7	4.1	SW
1**	17.4	30.8	11.1	73	129.0	2.6	SW
2**	19.3	30.6	8.0	70	35.9	2.4	SW
3**	15.3	28.0	6.6	70	60.2	2.6	WSW
4**	11.3	17.4	1.7	83	112	2.5	WSW
5**	8.6	15.4	0.3	86	100.8	2.8	SW
6**	6.5	13.5	-2.6	85	142	3.7	WSW
7*	6.7	13.9	0.0	81	44.4	5.2	SW
* Experimental Months							

Figure 145 Climatic information recorded from experimental site (ES) and independent weather station (WS) over experimental period (2012/2013)

#### 6.3.2 Stain sets

Stains were exposed to the environment for varying periods of time according to one of two categorical conditions: ‘longitudinal’ or ‘monthly’ sampling methods.



### 6.3.2.1 Longitudinal samples

Longitudinal samples were exposed to environmental conditions for longitudinally progressive periods of time. For each surface (paper, glass, denim) 7 different sample sets, each containing 8 replicate stains, were generated (*figure 146*).

	Paper	Glass	Denim
Longitudinal sample set 1 (L1)	8 replicate stains	8 replicate stains	8 replicate stains
Longitudinal sample set 2 (L2)	8 replicate stains	8 replicate stains	8 replicate stains
Longitudinal sample set 3 (L3)	8 replicate stains	8 replicate stains	8 replicate stains
Longitudinal sample set 4 (L4)	8 replicate stains	8 replicate stains	8 replicate stains
Longitudinal sample set 5 (L5)	8 replicate stains	8 replicate stains	8 replicate stains
Longitudinal sample set 6 (L6)	8 replicate stains	8 replicate stains	8 replicate stains
Longitudinal sample set 7 (L7)	8 replicate stains	8 replicate stains	8 replicate stains

Figure 146 Division of longitudinal samples into 7 sample sets, each consisting of 8 replicate stains generated on each of three surfaces (paper, glass and denim)

All samples were generated at the outset of the experimental period and simultaneously housed within the experimental shelving unit. The experiment then ran for a total period of seven consecutive months, with one set of longitudinal samples being removed at the end of each month.

This sampling method resulted in the generation of seven different sample sets, which had been exposed to the environment for cumulative amounts of time (*figure 147*). The generated stain sets reflected: one month, two months, three months, four months, five months, six months and seven months concurrent exposure to environmental conditions.

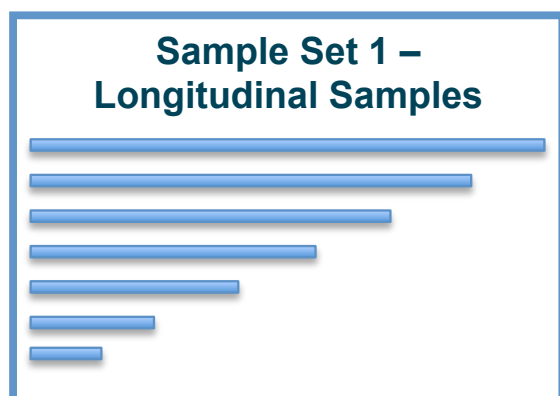


Figure 147 Illustration of respective lengths of seven longitudinal samples

The first sample set, for example, contained stains that were only exposed to the environment for the 1<sup>st</sup> experimental month (L1). The second sample set contained stains that were exposed to the environment for the 1<sup>st</sup> and 2<sup>nd</sup> experimental months (L2). The third sample set contained stains exposed for the 1<sup>st</sup>, 2<sup>nd</sup> and 3<sup>rd</sup> experimental months (L3), and so on, up to the seventh and final sample set taken, which contained stains exposed to the environment from the 1<sup>st</sup> through to 7<sup>th</sup> experimental months (L7). Each sample set contained 8 replicate stains on each of 3 surfaces (24 stains). Across seven separate samples (L1, L2, L3, L4, L5, L6, L7) this generated a total of 168 ‘longitudinal’ stains. Generation of longitudinal sample sets allowed comparisons to be made between stain appearance and progressive length of time exposed to the environment.

### 6.3.2.2 Monthly samples

Monthly samples were exposed to environmental conditions for separate but consecutive periods of time, each lasting a month in length (*figure 148*).



Figure 148 Illustration of arrangement of six monthly samples in relation to each other

For each surface (paper, glass, denim) 6 different sample sets, each containing 8 replicate stains, were generated (*figure 149*). New sample sets were generated on the first day of each experimental month, housed in the experimental unit for the rest of that month and then removed on the first day of the next experimental month. This sampling process continued for the duration of 6 months, generating a series of stain sets that individually had been exposed to environmental conditions for separate monthly periods collectively spanning the course of 6 months.

	Paper	Glass	Denim
Monthly sample set 1 (M1)	8 replicate stains	8 replicate stains	8 replicate stains
Monthly sample set 2 (M2)	8 replicate stains	8 replicate stains	8 replicate stains
Monthly sample set 3 (M3)	8 replicate stains	8 replicate stains	8 replicate stains
Monthly sample set 4 (M4)	8 replicate stains	8 replicate stains	8 replicate stains
Monthly sample set 5 (M5)	8 replicate stains	8 replicate stains	8 replicate stains
Monthly sample set 6 (M6)	8 replicate stains	8 replicate stains	8 replicate stains

Figure 149 Division of monthly samples into 7 sample sets, each consisting of 8 replicate stains generated on each of three surfaces (paper, glass and denim)

The first sample set contained stains exposed to the environment for the 1<sup>st</sup> experimental month (M1), the second for stains exposed for the 2<sup>nd</sup> experimental month (M2) and so on, until stains had also been generated for experimental months 3 (M3), 4 (M4), 5 (M5) and 6 (M6). Each sample set contained 8 replicate stains on each of 3 surfaces (24 stains). Across six separate samples (M1, M2, M3, M4, M5, M6) this generated a total of 144 ‘monthly’ stains.

Generation of monthly sample sets allowed comparisons to be made between stains exposed for different months, characterised by different climatic conditions.

Generation of both sample sets: longitudinal (L) and monthly (M) samples, allowed further comparisons to be made between both sample sets.

### 6.3.3 Experimental set up

The primary objective of the experimental stage was to expose stains to a variety of climatic conditions and observe the effects of exposure on stain appearance and internal composition (measured through visual and chemical analyses). Observations contributed towards establishing an empirical basis for future interpretations of environmentally altered stains, which will subsequently enhance crime scene reconstructions of scenes where they are encountered. A certain level of stain preservation was therefore necessary in order to allow observations to be made, without undermining the experimental objective of examining the influence of environment on bloodstains.

Stains were housed in a semi-protected environment in order to prevent removal of stains through exposure to precipitation, or more extreme climatic mechanisms. The main independent variables were temperature and humidity. Priority was therefore given to ensuring as natural as possible exposure to temperature and humidity fluctuations, whilst protecting stains from other climatic variables and removal mechanisms. Several design features were incorporated into the experimental set up in order to create this semi-protected, whilst still experimentally valid, experimental environment.

#### **6.3.3.1 Shelving unit**

Stains were housed at the experimental site in an open-sided shelving unit (*figure 150*). This afforded them some necessary protection from precipitation whilst continuing to allow free-flow of air around the stains. Prior to experimentation the back wall of the unit was removed to further increase the flow of air through the unit. The open-sides also ensured stains were more sensitized to any temperature and humidity variations.

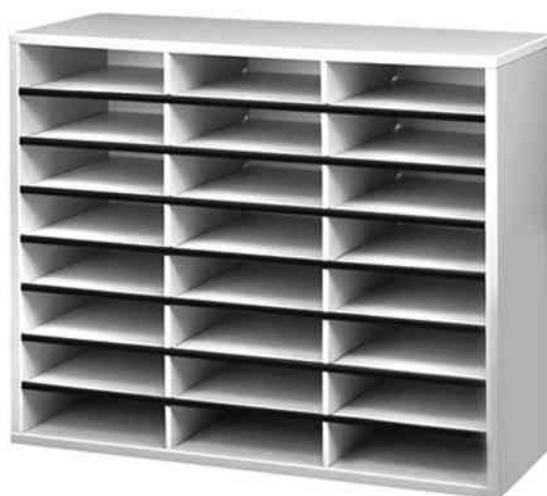


Figure 150 Open-sided shelving unit used to house stains ([www.viking-direct.co.uk](http://www.viking-direct.co.uk))

The shelving unit consisted of three vertical columns and seven horizontal shelves, dividing the unit into 24 partitioned sections. A shelving unit of these dimensions and divisions was purposefully chosen for experimental reasons. The three vertical columns allowed easy separation of samples according to each of the three surface types used in experimentation: paper, glass and denim fabric. Columns, from left to right, housed glass, paper and denim surfaces respectively. Each column was separated into 8 horizontal platforms by 7 horizontal shelves. Each platform was of

sufficient size (300mm x 225mm) to house an A4 piece of paper; upon which individual stains within a sample set could be collectively mounted.

The arrangement of the shelving unit's partitions meant that at any one time during the experiment a maximum of 8 sample sets *for each surface* could be accommodated in the shelving unit. As monthly samples ran sequentially to one another, only one monthly sample set (for each surface) was housed in the shelving unit at any time. Longitudinal samples were all generated at the outset of the experimental period and therefore all needed to be housed in the unit from the start. For each surface, there were seven different longitudinal sample sets.

Taking into account the longitudinal and monthly sampling methods, the absolute maximum number of sample sets, for each surface, in the shelving unit at any one time – was 8 (1 monthly sample set, 7 longitudinal sample sets). This equated to 24 sample sets across the 3 surfaces. With 24 partitioned platforms, the shelving unit chosen was therefore naturally suitable for accommodating all stains during the experiment.

#### **6.3.3.2 Unit set-up within experimental site**

Once the back wall of the shelving unit had been removed the unit was positioned within the experimental site. The experimental site was a garden, bounded on all four sides by walls, so naturally sheltered. The North, East and South wall were each in excess of 10 feet tall and the West wall was 5 feet tall.

In order to maintain the necessary semi-protected experimental conditions the unit was placed in a corner (Northwest) of the site, so that surrounding walls could provide some additional sheltering from climatic extremes (*figure 151*).

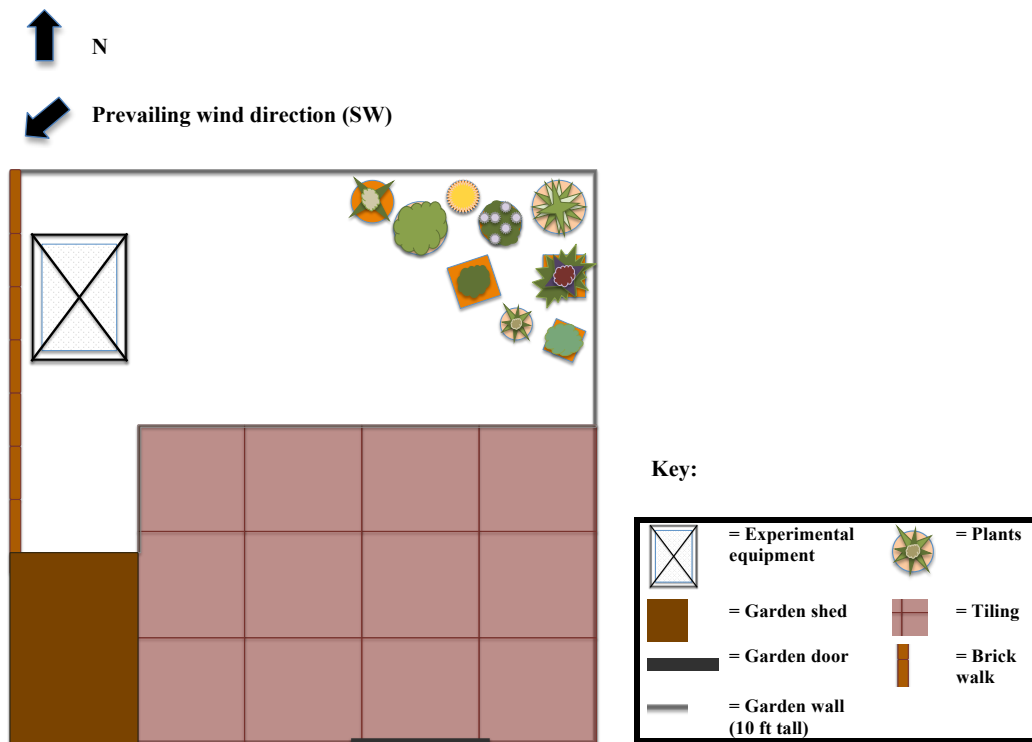


Figure 151 Sketch map of experimental site (garden) and location of experimental unit/equipment within site (*Author. 2013*)

In order to prevent any groundwater flow through the lower levels of the unit the unit was raised off the ground by placing terracotta stands underneath the unit. As stains were located outdoors it was assumed that various insects and other small animals might be attracted to the presence of blood. Therefore to avoid external influences in and around stains which could alter or obscure subsequent observations being made regarding the influence of environmental conditions on bloodstains, a method of deterring or preventing insects and animals from accessing stains, which continued to ensure free-flow circulation of air through the unit and prevent a build-up for humidity, therefore had to be incorporated into the experimental set-up. The experimental unit was enclosed in a mosquito net to achieve this. Mosquito nets consist of tightly woven mesh that is tight enough to prevent penetration by small insects but loose enough to interfere minimally with ventilation and airflow, thus providing a breathable, physical barrier.

A box mosquito net was arranged around the unit during set-up. The net was rotated 90° onto its side so that its opening, formerly at the base of the net, was orientated vertically to the side. This meant the net could be accessed from the side.

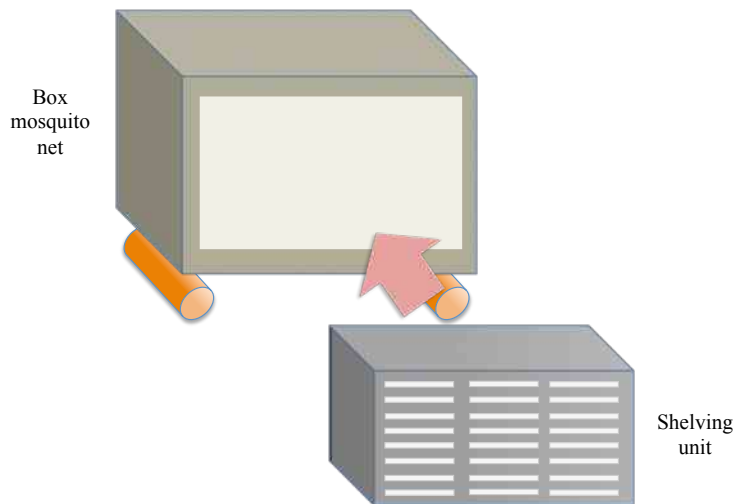


Figure 152 Sketch diagram of location of box net on terracotta stands and placement of shelving unit in net (Author. 2013)

The net was placed on top of the terracotta stands, with the net opening into the experimental site. The shelving unit was then placed into the box net through the side opening (*figure 152*). The weight of the unit was used to help secure the netting for the duration of the experiment by anchoring the netting between the terracotta stands and the base of the shelving unit. The open side of the net was then tied to fully enclose the shelving unit (*figure 153*).



Figure 153 Arrangement of box mosquito net and tie around shelving unit (Author. 2012)

As a final consideration to the set up of the unit, a breathable fabric tent was placed over the entire unit (*figures 154 & 155*). This provided some protection for the mosquito net against becoming saturated with precipitation but maintained some level of exposure to the elements which was necessary to mimic real life stain exposure.



Figure 154 Breathable fabric tent placed over experimental unit (*Author. 2012*)



Figure 155 Final experimental set-up within experimental site (*Author. 2012*)

### 6.3.4 Sampling phases

Generation of stain samples was separated into two distinct phases. The first phase was completed prior to the start of the experiment and involved the generation of all longitudinal sample sets and the first monthly sample set. The second phase continued throughout the experiment and involved the generation of new sample sets at the beginning of each month.

#### 6.3.4.1 Longitudinal sampling method

On day 1 of the experiment all longitudinal samples were generated. For each of the three surfaces (paper, glass, denim fabric) stained, seven different longitudinal sample sets were taken. Each sample set contained 8 replicate stains.

#### 6.3.4.2 Monthly sampling method

On day 1 of the experiment the first monthly sample was generated. For each of the three surfaces (paper, glass, denim fabric) stained, one sample set was taken. Each sample set contained 8 replicate stains. Monthly samples were then generated on the first day of each experimental month until six different monthly sample sets had been taken. Each sample set contained 8 replicate stains.

All stains in both phases were generated according to the same method.



### 6.3.5 Sample sets and replicate stains

Within each sample set 8 replicate stains were generated. These replicate stains were collectively mounted on a single sheet of A4 paper. Mounting replicate stains on a single sheet of paper eased both processes of accessing and securing samples within the unit during experimentation. As there was free air-flow through the unit throughout the experimental period, without this, samples may have been significantly affected through movement by wind. Samples were secured within the unit in two ways.

Firstly, before replicate stains were generated, the surfaces they were to be generated on were securely attached to sheets of A4 paper. In the case of stains generated on paper, the A4 paper itself served as the target surface. Instead of attaching any other surface to the paper therefore a marker was used to outline 8 different boxes on the sheet, each of which was to contain one replicate stain (*figure 156*).

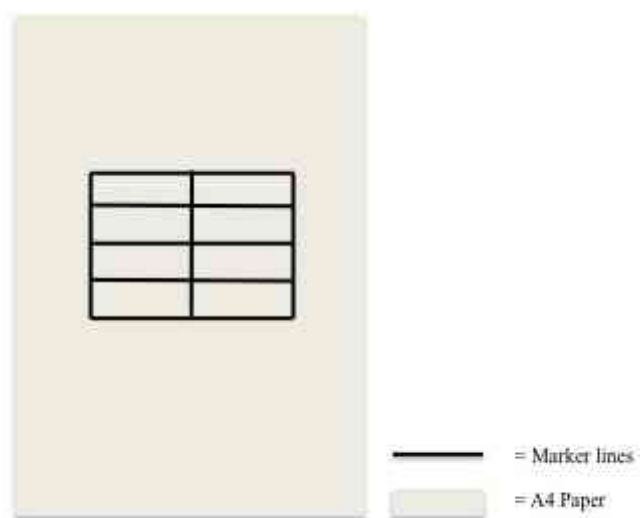


Figure 156 Sketch of A4 sheet of paper with marked areas, set up for generation of 8 stains on paper

(Author. 2012)

For stains generated on glass, 8 glass microscope slides were aligned grid-like on top of the paper. Sellotape strips were then used to attach the slides to the paper at both ends so no movement of the slides was possible (*figure 157*).

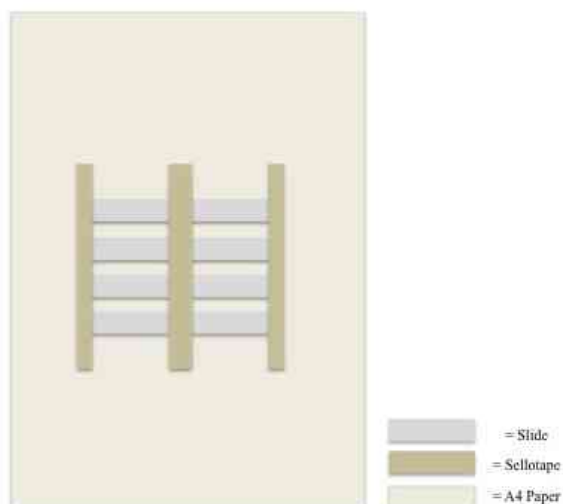


Figure 157 Sketch of arrangement of 8 microscope slides, secured by sellotape, on A4 sheet of paper

(Author. 2012)

For stains generated on denim, a swatch of denim fabric, was mounted onto paper. Sellotape strips were used to attach the fabric to the paper on all sides, so it was firmly attached (*figure 158*). Fabric swatches were of sufficient size to allow for the generation of 8 separate stains on each individual swatch. Once replicate stain surfaces had been attached, or outlined, on A4 sheets of paper they were then stained. As a second method of securing samples within the unit; once sample sets had been generated, A4 sheets were placed on horizontal shelves in the unit and secured in situ by lengths of duct tape at each end.

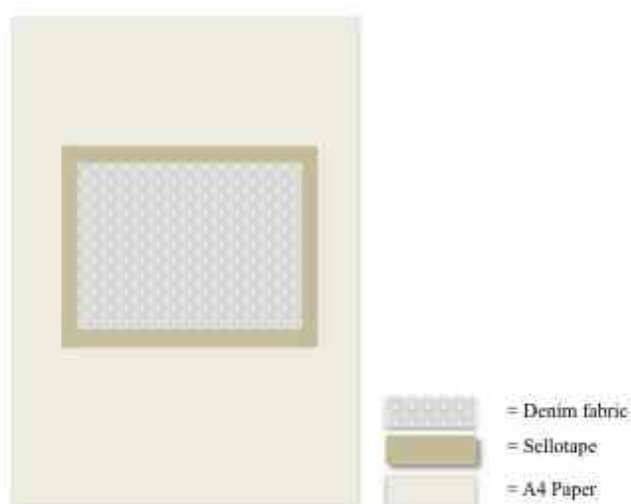


Figure 158 Sketch of arrangement of denim fabric swatch, secured by sellotape, on A4 sheet of paper

(Author. 2012)

### 6.3.6 Stain generation

Using a fixed 10µl volume pipette, a series of Ovine blood stains were deposited from a height of 10cm onto paper to form eight separate replicate stains. Each stain

was generated within an individual, previously demarcated box on the paper (*figure 159*). This process was then replicated and repeated 7 further times to generate a total of 8 paper sample sets. These sets represented 1 monthly and 7 longitudinal sample sets.

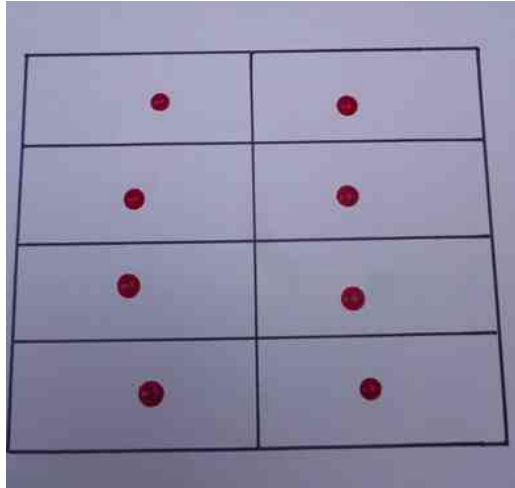


Figure 159 Eight replicate stains generated in demarcated boxes on paper

(Author. 2012)

The entire stain generation process, outlined above, was then replicated for both glass and denim surfaces. Glass stains were each generated on individual microscope slides, mounted on paper. Denim stains were generated separately on a denim swatch mounted on paper.

Once stain sets had been generated on paper, glass and denim surfaces, for each surface there were 8 sample sets, each containing 8 replicate stains. The sample sets represented 7 longitudinal sample sets and the 1<sup>st</sup> monthly sample set for each surface. Each sample set was mounted on an A4 sheet, meaning there was a total of 24 A4 sheets to be housed in the experimental shelving unit. Each sheet was placed on a separate shelf within the unit. The alignment of sheets (and therefore sample sets) within the unit was vertically according to surface and horizontally according to sample set type and number (*figure 160*).

	Left Column Paper Surfaces	Centre Column Glass Surfaces	Right Column Denim Surfaces
Top	Monthly sample set (M1)	Monthly sample set (M1)	Monthly sample set (M1)
	Longitudinal sample set (L1)	Longitudinal sample set (L1)	Longitudinal sample set (L1)
	Longitudinal sample set (L2)	Longitudinal sample set (L2)	Longitudinal sample set (L2)
	Longitudinal sample set (L3)	Longitudinal sample set (L3)	Longitudinal sample set (L3)
	Longitudinal sample set (L4)	Longitudinal sample set (L4)	Longitudinal sample set (L4)
	Longitudinal sample set (L5)	Longitudinal sample set (L5)	Longitudinal sample set (L5)
	Longitudinal sample set (L6)	Longitudinal sample set (L6)	Longitudinal sample set (L6)
Bottom	Longitudinal sample set (L7)	Longitudinal sample set (L7)	Longitudinal sample set (L7)

Figure 160 Arrangement of maximum number of longitudinal and monthly sample sets in 24-partitioned shelving unit



Figure 161 Shelving columns vertically housing different surfaces, from L-R: paper, glass, denim, which are secured to shelves with duct tape (Author. 2012)

Sheets were secured to the shelf at each end with a length of duct tape (*figure 161*). Once sheets and samples had been securely housed in the unit (*figure 162*), the mosquito netting was secured over the open side of the unit. The breathable fabric tent was then placed over the entire unit.



Figure 162 Sheets and samples secured in open-sided shelving unit (*Author. 2012*)

The unit was left undisturbed, at the experimental site, for the duration of one month. This period represented the first experimental month. At the end of the month the tent was lifted off the unit and the mosquito netting over the side untied, to allow access to the unit from the site. Certain sets of samples were then removed from the experimental unit. Samples removed from the unit at the end of the first experimental month were the 1<sup>st</sup> monthly samples (M1) and 1<sup>st</sup> longitudinal samples (L1). These samples were removed from the unit and then set aside for analysis.

Before the unit could be resealed and left for the next experimental month a new set of monthly samples (M2) were generated for paper, glass and denim surfaces and securely placed into the unit. The new sets were generated through exactly the same process as previous stain sets and secured to shelves in the same way with lengths of duct tape at each end. M2 sample sets were placed in the shelves that had previously been occupied by M1 sample sets. All longitudinal samples had been generated at the start of the 1<sup>st</sup> experimental month, so no further longitudinal sample sets were generated. The mosquito netting was then secured again and the tent placed back over the unit. Analysis of samples that had been removed (M1 & L1) was conducted immediately.

The process, as outlined above, of removing certain sets of both monthly and longitudinal samples and generating new monthly sample sets at the end of every month was repeated throughout the experiment for the 1<sup>st</sup>, 2<sup>nd</sup>, 3<sup>rd</sup>, 4<sup>th</sup>, and 5<sup>th</sup> months. At the end of the 6<sup>th</sup> month the monthly sample set (M6) was removed but a

new one was not generated to replace it. During the 7<sup>th</sup> month therefore there was only one longitudinal sample set (L7) housed in the unit. Figure 163 outlines the order of removal and generation of sample sets across all months.

Month Number	Samples in unit	Samples removed at end of month	Samples generated at end of month
1	M1, L1, L2, L3, L4, L5, L6, L7	M1, L1	M2
2	M2, L2, L3, L4, L5, L6, L7	M2, L2	M3
3	M3, L3, L4, L5, L6, L7	M3, L3	M4
4	M4, L4, L5, L6, L7	M4, L4	M5
5	M5, L5, L6, L7	M5, L5	M6
6	M6, L6, L7	M6, L6	
7	L7	L7	

Figure 163 Outline of order of sample removals

### 6.3.7 Visual and chemical analysis of Stains

All sample sets of stains were analysed immediately after they had been removed from the experimental unit. Stains were subjected to both visual and chemical identification analysis as outlined in *sections 3.4.4 – 3.4.7*. Results of both analyses were recorded for comparative and interpretative purposes.

## 7. Experimental Stage 2 – Results

### 7.1 Stain generation checklist & results of chemical identification tests

Figures 164 and 165 present the results of chemical identification tests conducted on bloodstains exposed to environmental fluctuations during experimental stage 2 as longitudinal and monthly sample sets (*chapter 6*). Presumptive tests including the Hemastix, Kastle-Meyer and Bluestar tests were conducted on stains in each sample set (*as outlined in chapter 3, sections 3.4.4 – 3.4.6*). After each sample set had been removed from the experimental unit it was immediately digitally scanned for visual analysis (*as outlined in chapter 3, section 3.4.7*). Once scanned, stains within each sample set were subjected to chemical testing. The results of the tests for stains generated are set out in *figures 164 and 165*.

Longitudinal sample set	Glass Microscope Slides			Paper Slips			Denim Strips		
	Hemastix	Kastle-Meyer	Bluestar	Hemastix	Kastle-Meyer	Bluestar	Hemastix	Kastle-Meyer	Bluestar
L1	+ive	+ive	+ive	+ive	+ive	+ive	+ive	+ive	+ive
L2	+ive	+ive	+ive	+ive	+ive	+ive	+ive	+ive	+ive
L3	+ive	+ive	+ive	+ive	+ive	+ive	+ive	+ive	+ive
L4	+ive	+ive	+ive	+ive	+ive	+ive	+ive	+ive	+ive
L5	+ive	+ive	+ive	+ive	+ive	+ive	+ive	+ive	+ive
L6	+ive	+ive	+ive	+ive	+ive	+ive	+ive	+ive	+ive
L7	+ive	+ive	+ive	+ive	+ive	+ive	+ive	+ive	+ive

Figure 164 Results of presumptive chemical tests for stains generated as longitudinal samples

The results of tests conducted on stains in all longitudinal and monthly sample sets are shown in *figures 164 and 165*. Results indicate that all stains in these sample sets tested presumptive positive for blood. This indicates that exposing bloodstains to a naturally variable temperate climate for longitudinal periods of between 1 to 7 months, and to a naturally variable temperate climate for monthly periods characterised by different climatic conditions does not inhibit positive chemical identification of stains with presumptive tests.

Monthly sample set	Glass Microscope Slides			Paper Slips			Denim Strips		
	Hemastix	Kastle-Meyer	Bluestar	Hemastix	Kastle-Meyer	Bluestar	Hemastix	Kastle-Meyer	Bluestar
M1	+ive	+ive	+ive	+ive	+ive	+ive	+ive	+ive	+ive
M2	+ive	+ive	+ive	+ive	+ive	+ive	+ive	+ive	+ive
M3	+ive	+ive	+ive	+ive	+ive	+ive	+ive	+ive	+ive
M4	+ive	+ive	+ive	+ive	+ive	+ive	+ive	+ive	+ive
M5	+ive	+ive	+ive	+ive	+ive	+ive	+ive	+ive	+ive
M6	+ive	+ive	+ive	+ive	+ive	+ive	+ive	+ive	+ive

Figure 165 Checklist of results of presumptive chemical tests for stains generated as monthly samples

## 7.2 Longitudinal sample sets

The images captured of individual stains generated in longitudinal sample sets are set out in sections 7.2. Longitudinal stains are presented in groups of eight, representing individual groups of 8 replicate stains generated on three different surfaces (denim, glass, paper) in each sample set (L1, L2, L3, L4, L5, L6 & L7).



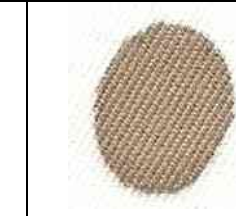



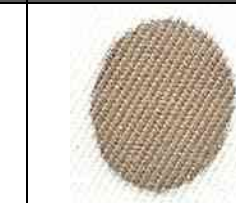
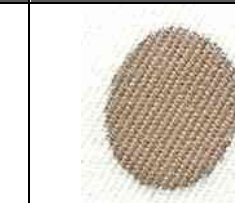
### 7.2.1 Images of longitudinal sample sets

Images are accompanied by an indication of sample set and surface they correspond to. Underneath each image a ‘stain ID’ is listed, for example B001, this ID refers to a numbering of individual stains for ease of identification. The results of digital measurements of colour for each stain are also given as R, G and B values listed sequentially and a ‘hex code’ that identifies the hexadecimal colour of each stain.







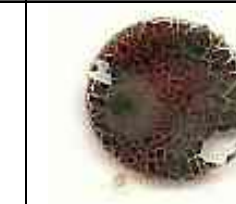
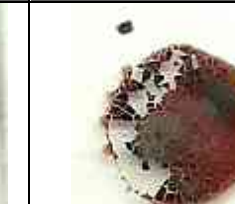


### 7.2.1.1 Images of longitudinal sample set L1 (Months: 0 to 1)

7.2.1.1.1 Figure 166 Stains generated on denim

			
<b>B001</b> RGB 174, 149, 123 Hex: ae967b	<b>B002</b> RGB 177, 153, 126 Hex: b1997e	<b>B003</b> RGB 174, 150, 124 Hex: ae967c	<b>B004</b> RGB 177, 156, 130 Hex: b19c81
			
<b>B005</b> RGB 169, 145, 120 Hex: a99178	<b>B006</b> RGB 169, 146, 120 Hex: a99278	<b>B007</b> RGB 173, 151, 125 Hex: ad977e	<b>B008</b> RGB 171, 148, 123 Hex: ab947b

7.2.1.1.2 Figure 167 Stains generated on glass



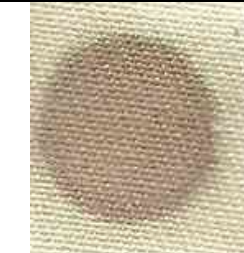
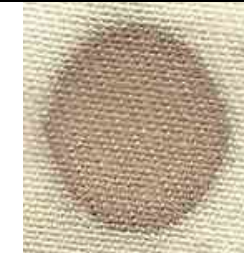



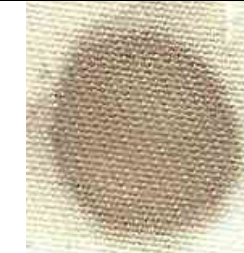
			
<b>B009</b> RGB 86, 59, 40 Hex: 563e2d	<b>B010</b> RGB 78, 60, 48 Hex: 4e3b2f	<b>B011</b> RGB 91, 69, 57 Hex: 5b4539	<b>B012</b> RGB 98, 66, 55 Hex: 624236
			
<b>B013</b> RGB 89, 78, 68 Hex: 594e43	<b>B014</b> RGB 75, 57, 46 Hex: 4b392d	<b>B015</b> RGB 81, 61, 52 Hex: 513e35	<b>B016</b> RGB 101, 67, 56 Hex: 654338

7.2.1.1.3 Figure 168 Stains generated on paper





			
<b>B017</b> RGB 71, 70, 62 Hex: 47463e	<b>B018</b> RGB 85, 82, 72 Hex: 555248	<b>B019</b> RGB 91, 89, 77 Hex: 5b594d	<b>B020</b> RGB 85, 84, 73 Hex: 555449
			
<b>B021</b> RGB 84, 77, 64 Hex: 544d40	<b>B022</b> RGB 75, 74, 66 Hex: 4b4a42	<b>B023</b> RGB 54, 42, 35 Hex: 362a23	<b>B024</b> RGB 23, 20, 16 Hex: 171410

## 7.2.1.2 Images of longitudinal sample set L2 (Months: 0 to 2)

7.2.1.2.1 Figure 169 Stains generated on denim

			
<b>B025</b> RGB 171, 147, 123 Hex: ab937b	<b>B026</b> RGB 167, 144, 120 Hex: a79078	<b>B027</b> RGB 169, 147, 123 Hex: a9937b	<b>B028</b> RGB 174, 151, 125 Hex: ae977d
			
<b>B029</b> RGB 165, 142, 116 Hex: a58e74	<b>B030</b> RGB 172, 150, 124 Hex: ac967c	<b>B031</b> RGB 166, 144, 118 Hex: a69076	<b>B032</b> RGB 170, 150, 124 Hex: aa967c

7.2.1.2.2 Figure 170 Stains generated on glass

			
<b>B033</b> RGB 216, 210, 192 Hex: d8d2c0	<b>B034</b> RGB 138, 124, 104 Hex: 8a7c68	<b>B035</b> RGB 141, 114, 83 Hex: 8d7253	<b>B036</b> RGB 115, 95, 81 Hex: 735f51
			
<b>B037</b> RGB 117, 87, 68 Hex: 755744	<b>B038</b> RGB 105, 90, 79 Hex: 6a5a4f	<b>B039</b> RGB 107, 89, 74 Hex: 6b594a	<b>B040</b> RGB 111, 87, 71 Hex: 6f5747









7.2.1.2.3 Figure 171 Stains generated on paper

			
<b>B041</b> RGB 61, 60, 54 Hex: 3d3c36	<b>B042</b> RGB 52, 45, 38 Hex: 342d26	<b>B043</b> RGB 49, 50, 42 Hex: 31322a	<b>B044</b> RGB 65, 48, 41 Hex: 413029
			
<b>B045</b> RGB 46, 34, 26 Hex: 2e221a	<b>B046</b> RGB 61, 43, 34 Hex: 3d2b22	<b>B047</b> RGB 56, 46, 38 Hex: 382e26	<b>B048</b> RGB 48, 34, 26 Hex: 30221a







### 7.2.1.3 Images of longitudinal sample set L3 (Months: 0 to 3)




#### 7.2.1.3.1 Figure 172 Stains generated on denim

			
<b>B049</b> RGB 177, 155, 129 Hex: b19b81	<b>B050</b> RGB 178, 156, 130 Hex: b29c82	<b>B051</b> RGB 173, 151, 126 Hex: ad977e	<b>B052</b> RGB 178, 155, 127 Hex: b29b7f
			
<b>B053</b> RGB 170, 148, 122 Hex: aa947a	<b>B054</b> RGB 182, 160, 133 Hex: b6a085	<b>B055</b> RGB 176, 155, 128 Hex: b09b80	<b>B056</b> RGB 170, 147, 119 Hex: aa9377

#### 7.2.1.3.2 Figure 173 Stains generated on glass




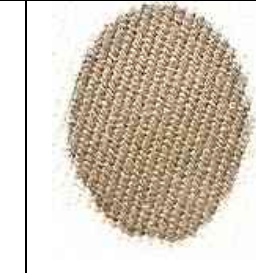



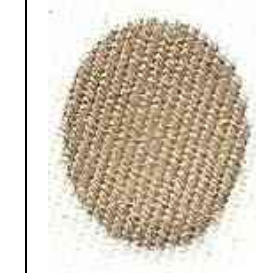
			
<b>B057</b> RGB 101, 68, 52 Hex: 654434	<b>B058</b> RGB 105, 70, 50 Hex: 694632	<b>B059</b> RGB 117, 71, 46 Hex: 75472e	<b>B060</b> RGB 134, 79, 38 Hex: 864f26
			
<b>B061</b> RGB 117, 69, 48 Hex: 754530	<b>B062</b> RGB 107, 71, 58 Hex: 6b473a	<b>B063</b> RGB 102, 90, 82 Hex: 665a52	<b>B064</b> RGB 108, 69, 48 Hex: 6c4530

7.2.1.3.3 Figure 174 Stains generated on paper









			
<b>B065</b> RGB 68, 61, 43 Hex: 443d2b	<b>B066</b> RGB 91, 68, 55 Hex: 5b4437	<b>B067</b> RGB 72, 67, 56 Hex: 484338	<b>B068</b> RGB 59, 40, 31 Hex: 3b281f
			
<b>B069</b> RGB 91, 75, 60 Hex: 5b4b3c	<b>B070</b> RGB 52, 21, 10 Hex: 34150a	<b>B071</b> RGB 82, 57, 44 Hex: 52392c	<b>B072</b> RGB 63, 33, 21 Hex: 3f2115

7.2.1.4 Images of longitudinal sample set L4 (Months: 0 to 4)

7.2.1.4.1 Figure 175 Stains generated on denim

			
<b>B073</b> RGB 179, 157, 127 Hex: b39d7f	<b>B074</b> RGB 184, 163, 132 Hex: b8a384	<b>B075</b> RGB 172, 150, 120 Hex: ac9678	<b>B076</b> RGB 176, 154, 123 Hex: b09a7b
			
<b>B077</b> RGB 175, 153, 122 Hex: af997a	<b>B078</b> RGB 177, 156, 125 Hex: b19c7d	<b>B079</b> RGB 184, 163, 132 Hex: b8a384	<b>B080</b> RGB 179, 158, 126 Hex: b39e7e

7.2.1.4.2 Figure 176 Stains generated on glass

			
<b>B081</b> RGB 142, 112, 89 Hex: 8e7059	<b>B082</b> RGB 128, 110, 88 Hex: 806e58	<b>B083</b> RGB 90, 66, 54 Hex: 5a4236	<b>B084</b> RGB 90, 70, 59 Hex: 5a463b
			
<b>B085</b> RGB 67, 54, 46 Hex: 43362e	<b>B086</b> RGB 84, 71, 63 Hex: 54473f	<b>B087</b> RGB 93, 72, 59 Hex: 5d483b	<b>B088</b> RGB 97, 68, 52 Hex: 614434








7.2.1.4.3 Figure 177 Stains generated on paper

			
<b>B089</b> RGB 84, 79, 66 Hex: 544f42	<b>B090</b> RGB 85, 75, 61 Hex: 554b3d	<b>B091</b> RGB 63, 41, 27 Hex: 3f291b	<b>B092</b> RGB 79, 58, 45 Hex: 4f3a2d
			
<b>B093</b> RGB 82, 67, 54 Hex: 524336	<b>B094</b> RGB 61, 35, 23 Hex: 3d2317	<b>B095</b> RGB 63, 43, 31 Hex: 3f2b1f	<b>B096</b> RGB 65, 47, 34 Hex: 412f22







### 7.2.1.5 Images of longitudinal sample set L5 (Months: 0 to 5)

#### 7.2.1.5.1 Figure 178 Stains generated on denim

			
<b>B097</b> RGB 169, 147, 118 Hex: a99376	<b>B098</b> RGB 174, 154, 124 Hex: ae9a7c	<b>B099</b> RGB 190, 169, 140 Hex: bea98c	<b>B100</b> RGB 186, 165, 136 Hex: baa588
			
<b>B101</b> RGB 172, 149, 120 Hex: ac9578	<b>B102</b> RGB 185, 164, 135 Hex: b9a487	<b>B103</b> RGB 185, 164, 134 Hex: b9a486	<b>B104</b> RGB 189, 169, 138 Hex: bda98a

#### 7.2.1.5.2 Figure 179 Stains generated on glass

			
<b>B105</b> RGB 174, 171, 151 Hex: aeab97	<b>B106</b> RGB 96, 84, 59 Hex: 60543b	<b>B107</b> RGB 153, 145, 116 Hex: 999174	<b>B108</b> RGB 111, 98, 68 Hex: 6f6244
			
<b>B109</b> RGB 134, 126, 106 Hex: 867e6a	<b>B110</b> RGB 76, 63, 42 Hex: 4c3f2a	<b>B111</b> RGB 76, 64, 46 Hex: 4c402e	<b>B112</b> RGB 66, 49, 32 Hex: 423120

### 7.2.1.5.3 Figure 180 Stains generated on paper

			
<b>B113</b> RGB 51, 25, 20 Hex: 331914	<b>B114</b> RGB 64, 51, 42 Hex: 40332a	<b>B115</b> RGB 46, 34, 22 Hex: 2e2216	<b>B116</b> RGB 48, 39, 29 Hex: 30271d
			
<b>B117</b> RGB 57, 45, 35 Hex: 392d23	<b>B118</b> RGB 50, 38, 28 Hex: 32261c	<b>B119</b> RGB 41, 27, 15 Hex: 291a0f	<b>B120</b> RGB 54, 39, 28 Hex: 36271c









### 7.2.1.6 Images of longitudinal sample set L6 (Months: 0 to 6)

#### 7.2.1.6.1 Figure 181 Stains generated on denim

			
<b>B121</b> RGB 243, 240, 216 Hex: f3f0d8	<b>B122</b> RGB 242, 240, 217 Hex: f2f0d9	<b>B123</b> RGB 235, 232, 210 Hex: ebe8d2	<b>B124</b> RGB 223, 217, 184 Hex: dfd9b8
			
<b>B125</b> RGB 230, 226, 195 Hex: e6e2c3	<b>B126</b> RGB 229, 224, 191 Hex: e5e0bf	<b>B127</b> RGB 180, 166, 132 Hex: b4a684	<b>B128</b> RGB 149, 123, 97 Hex: 957b61



7.2.1.6.2 Figure 182 Stains generated on glass









			
<b>B129</b> RGB 99, 61, 42 Hex: 633d2a	<b>B130</b> RGB 132, 102, 71 Hex: 846647	<b>B131</b> RGB 238, 236, 208 Hex: eeced0	<b>B132</b> RGB 113, 81, 48 Hex: 715130
			
<b>B133</b> RGB 174, 127, 90 Hex: ae7f5a	<b>B134</b> RGB 129, 109, 82 Hex: 816d52	<b>B135</b> RGB 116, 94, 73 Hex: 745e49	<b>B136</b> RGB 197, 168, 141 Hex: c5a88d

7.2.1.6.3 Figure 183 Stains generated on paper









			
<b>B137</b> RGB 59, 50, 43 Hex: 3b322b	<b>B138</b> RGB 55, 41, 31 Hex: 37291f	<b>B139</b> RGB 53, 17, 11 Hex: 35110b	<b>B140</b> RGB 72, 54, 42 Hex: 48362a
			
<b>B141</b> RGB 40, 31, 20 Hex: 281f14	<b>B142</b> RGB 37, 33, 24 Hex: 252118	<b>B143</b> RGB 57, 45, 36 Hex: 392d24	<b>B144</b> RGB 46, 36, 26 Hex: 2e241a

### 7.2.1.7 Images of longitudinal sample set L7 (Months: 0 to 7)

7.2.1.7.1 Figure 184 Stains generated on denim

			
<b>B145</b> RGB 183, 165, 134 Hex: b7a586	<b>B146</b> RGB 182, 163, 133 Hex: b6a385	<b>B147</b> RGB 184, 165, 135 Hex: b8a587	<b>B148</b> RGB 184, 164, 134 Hex: b8a486
			
<b>B149</b> RGB 180, 160, 130 Hex: b4a082	<b>B150</b> RGB 185, 164, 135 Hex: b9a487	<b>B151</b> RGB 180, 159, 131 Hex: b49f83	<b>B152</b> RGB 186, 166, 136 Hex: baa688

7.2.1.7.2 Figure 185 Stains generated on glass

			
<b>B153</b> RGB 125, 103, 79 Hex: 7d674f	<b>B154</b> RGB 148, 122, 87 Hex: 947a57	<b>B155</b> RGB 112, 81, 59 Hex: 70513b	<b>B156</b> RGB 96, 72, 57 Hex: 604839
			
<b>B157</b> RGB 93, 60, 43 Hex: 5d3c2b	<b>B158</b> RGB 95, 65, 49 Hex: 5f4131	<b>B159</b> RGB 82, 61, 48 Hex: 523d30	<b>B160</b> RGB 93, 78, 68 Hex: 5d4e44

**7.2.1.7.3 Figure 186 Stains generated on paper**

			
<b>B161</b> RGB 42, 28, 17 Hex: 2a1c11	<b>B162</b> RGB 45, 37, 28 Hex: 2d251c	<b>B163</b> RGB 48, 33, 23 Hex: 302117	<b>B164</b> RGB 68, 40, 30 Hex: 44281e
			
<b>B165</b> RGB 45, 32, 23 Hex: 2d2017	<b>B166</b> RGB 55, 26, 14 Hex: 371a0e	<b>B167</b> RGB 33, 25, 15 Hex: 21190f	<b>B168</b> RGB 49, 30, 21 Hex: 311e15

## 7.2.2 Longitudinal stain colour analysis

Once stains had been scanned and captured in a digital format, images were imported into colour analysis software to extract quantitative information about stain colour from the images. Each stain was analysed individually. Descriptive statistics were calculated and box-plots of the results of stain colour analysis are provided for each surface individually to assist in the identification of trends between climatic conditions and stain colour. Once results were outlined for each surface, it was possible to make a comparison of the trends and results between surfaces. For longitudinal stains generated on all surfaces and monthly stains generated on denim and glass surfaces, trends across sample sets, average temperatures, average humidity levels and cumulative volumes of precipitation in distributions of R, G, B values and RGB totals approximately mirrored each other. For the purposes of analysis, discussion for these stains was therefore limited to R-value distribution (an indication of orientation towards a red colour) and RGB total distribution (an indication of overall colour intensity). Discussion of G and B-value distributions is included in *appendix 2*. Distribution of R, G, B values and RGB totals for paper stains across volumes of precipitation differed from each other and these were discussed individually.

### 7.2.2.1 Stains generated in longitudinal denim sample sets

The measurements derived for stains on denim surfaces from longitudinal sample sets are presented in *figure 187*. Descriptive statistics are then presented in *figures 188* and *189*.

Figure 187 Table of measurements recorded for stains generated on denim surfaces in longitudinal sample sets

Stain ID	Surface	Months	Average temperature /°C	Average humidity /%	Total precipitation /mm	Number of Months	R Value	G Value	B Value	Hex	Hex Colour
B001	Denim	0 to 1	15.3	74.0	193.7	1	174	149	123	ae967b	
B002	Denim	0 to 1	15.3	74.0	193.7	1	177	153	126	b1997e	
B003	Denim	0 to 1	15.3	74.0	193.7	1	174	150	124	ae967c	
B004	Denim	0 to 1	15.3	74.0	193.7	1	177	156	130	b19c81	
B005	Denim	0 to 1	15.3	74.0	193.7	1	169	145	120	a99178	
B006	Denim	0 to 1	15.3	74.0	193.7	1	169	146	120	a99278	
B007	Denim	0 to 1	15.3	74.0	193.7	1	173	151	125	ad977e	
B008	Denim	0 to 1	15.3	74.0	193.7	1	171	148	123	ab947b	
B025	Denim	0 to 2	16.4	73.5	322.7	2	171	147	123	ab937b	
B026	Denim	0 to 2	16.4	73.5	322.7	2	167	144	120	a79078	
B027	Denim	0 to 2	16.4	73.5	322.7	2	169	147	123	a9937b	
B028	Denim	0 to 2	16.4	73.5	322.7	2	174	151	125	ae977d	
B029	Denim	0 to 2	16.4	73.5	322.7	2	165	142	116	a58e74	
B030	Denim	0 to 2	16.4	73.5	322.7	2	172	150	124	ac967c	
B031	Denim	0 to 2	16.4	73.5	322.7	2	166	144	118	a69076	
B032	Denim	0 to 2	16.4	73.5	322.7	2	170	150	124	aa967c	
B049	Denim	0 to 3	17.3	72.3	358.6	3	177	155	129	b19b81	
B050	Denim	0 to 3	17.3	72.3	358.6	3	178	156	130	b29c82	
B051	Denim	0 to 3	17.3	72.3	358.6	3	173	151	126	ad977e	
B052	Denim	0 to 3	17.3	72.3	358.6	3	178	155	127	b29b7f	
B053	Denim	0 to 3	17.3	72.3	358.6	3	170	148	122	aa947a	
B054	Denim	0 to 3	17.3	72.3	358.6	3	182	160	133	b6a085	
B055	Denim	0 to 3	17.3	72.3	358.6	3	176	155	128	b09b80	
B056	Denim	0 to 3	17.3	72.3	358.6	3	170	147	119	aa9377	
B073	Denim	0 to 4	16.8	72.0	418.8	4	179	157	127	b39d7f	
B074	Denim	0 to 4	16.8	72.0	418.8	4	184	163	132	b8a384	
B075	Denim	0 to 4	16.8	72.0	418.8	4	172	150	120	ac9678	
B076	Denim	0 to 4	16.8	72.0	418.8	4	176	154	123	b09a7b	
B077	Denim	0 to 4	16.8	72.0	418.8	4	175	153	122	af997a	
B078	Denim	0 to 4	16.8	72.0	418.8	4	177	156	125	b19c7d	
B079	Denim	0 to 4	16.8	72.0	418.8	4	184	163	132	b8a384	
B080	Denim	0 to 4	16.8	72.0	418.8	4	179	158	126	b39e7e	
B097	Denim	0 to 5	15.7	74.0	530.8	5	169	147	118	a99376	
B098	Denim	0 to 5	15.7	74.0	530.8	5	174	154	124	ae9a7c	
B099	Denim	0 to 5	15.7	74.0	530.8	5	190	169	140	bea98c	
B100	Denim	0 to 5	15.7	74.0	530.8	5	186	165	136	baa588	
B101	Denim	0 to 5	15.7	74.0	530.8	5	172	149	120	ac9578	
B102	Denim	0 to 5	15.7	74.0	530.8	5	185	164	135	b9a487	
B103	Denim	0 to 5	15.7	74.0	530.8	5	185	164	134	b9a486	
B104	Denim	0 to 5	15.7	74.0	530.8	5	189	169	138	bda98a	
B121	Denim	0 to 6	14.5	76.0	631.6	6	243	240	216	f3f0d8	
B122	Denim	0 to 6	14.5	76.0	631.6	6	242	240	217	f2f0d9	
B123	Denim	0 to 6	14.5	76.0	631.6	6	235	232	210	ebe8d2	
B124	Denim	0 to 6	14.5	76.0	631.6	6	223	217	184	dfd9b8	
B125	Denim	0 to 6	14.5	76.0	631.6	6	230	226	195	e6e2c3	
B126	Denim	0 to 6	14.5	76.0	631.6	6	229	224	191	e5e0bf	
B127	Denim	0 to 6	14.5	76.0	631.6	6	180	166	132	b4a684	
B128	Denim	0 to 6	14.5	76.0	631.6	6	149	123	97	957b61	
B145	Denim	0 to 7	13.4	77.3	773.6	7	183	165	134	b7a586	
B146	Denim	0 to 7	13.4	77.3	773.6	7	182	163	133	b6a385	
B147	Denim	0 to 7	13.4	77.3	773.6	7	184	165	135	b8a587	
B148	Denim	0 to 7	13.4	77.3	773.6	7	184	164	134	b8a486	
B149	Denim	0 to 7	13.4	77.3	773.6	7	180	160	130	b4a082	
B150	Denim	0 to 7	13.4	77.3	773.6	7	185	164	135	b9a487	
B151	Denim	0 to 7	13.4	77.3	773.6	7	180	159	131	b49f83	
B152	Denim	0 to 7	13.4	77.3	773.6	7	186	166	136	baa688	



Figure 188 outlines mean R, G, B values and RGB totals calculated from 8 replicate stains in each of 7 longitudinal sample sets. In each longitudinal sample set R-values were greater than G and B-values. G and B-values recorded for each sample set were also high however, which meant for some sample sets R-values were only slightly higher than G and B values. For example, in the L6 sample set the average R-value was 216.4, average G-value was 209.0 and average B-value was 180.3.

R-values for all sample sets fell between a low of 169.3 (L2) and a highest value of 216.4 observed for the L6 sample set. G-values across all sample sets fell between a recorded low of 147.0 (L2) and a high of 209.0 (L6). B-values were recorded between a low of 122.0 (L2) and a high of 180.3 (L6). Results demonstrate that whilst R, G and B-values were represented in similar levels in each sample set, for each sample set R-values represented the highest colour component, followed by G-values and finally B-values which represented the lowest individual colour component. The slight dominance of R-values suggests stains generated on denim and exposed to a range of longitudinal periods are all coloured towards red, rather than green or blue hues of colour. Observations of similarly high levels of R, G and B values support observations of a tan-brown colour of stains (*figure 187*). An RGB triplet for a light tan-brown colour are typically represented by similar figures in each of R, G and B values, approximately half-way between 000 (black) and 255 (white), for example RGB (R210, G180, B140).

Figure 188 Descriptive statistics recorded for stains generated on denim surfaces in longitudinal sample sets

Sample Set		R Value	G Value	B Value	RGB Total
<b>L1</b>	Mean	173.0	150.0	124.0	447.0
	Std. Deviation	3.2	4.0	3.3	10.0
<b>L2</b>	Mean	169.3	147.0	122.0	438.0
	Std. Deviation	3.1	3.3	3.3	10.0
<b>L3</b>	Mean	175.5	153.4	127.0	456.0
	Std. Deviation	4.2	4.4	4.5	13.0
<b>L4</b>	Mean	178.3	157.0	126.0	461.0
	Std. Deviation	4.2	4.6	4.4	13.2
<b>L5</b>	Mean	181.3	160.1	131.0	472.0
	Std. Deviation	8.2	9.0	8.6	26.0
<b>L6</b>	Mean	216.4	209.0	180.3	605.1
	Std. Deviation	34.0	42.0	43.3	119.0
<b>L7</b>	Mean	183.0	163.3	134.0	480.0
	Std. Deviation	2.2	2.5	2.1	7.0

*Figure 189* outlines average colour values for all denim stains. Average R, G and B values were calculated between all replicate stains in all longitudinal sample sets. Values for stains generated on denim were R (182.38), G (162.66) and B (134.64). Stains exhibit a higher ratio of R to G and B colour components. This means stains were coloured towards a red rather than green or blue hue. Levels of R, G and B values were approximately halfway between values of 000 (black) and 255 (white), which corresponds to the medium intensity observed in longitudinal stains generated on denim (*figure 187*). The combination of a slight orientation towards red hues of colour and a medium intensity of colour indicate that stains generated on denim, on average, were characterised by a light brown or tan colouring. For six stains generated in sample set L6 (B121, B122, B123, B124, B125 & B126) R, G and B values were particularly high. Average values for these stains were R234, G230, B202, which is close to (R255, G255, B255) an RGB triplet that corresponds to the colour white.

Figure 189 Average R, G and B values for all longitudinal stains generated on denim

	N	Minimum	Maximum	Mean	Std. Deviation
R Value	56	149	243	182.38	19.407
G Value	56	123	240	162.66	25.035
B Value	56	97	217	134.64	24.961
Valid N (listwise)	56				

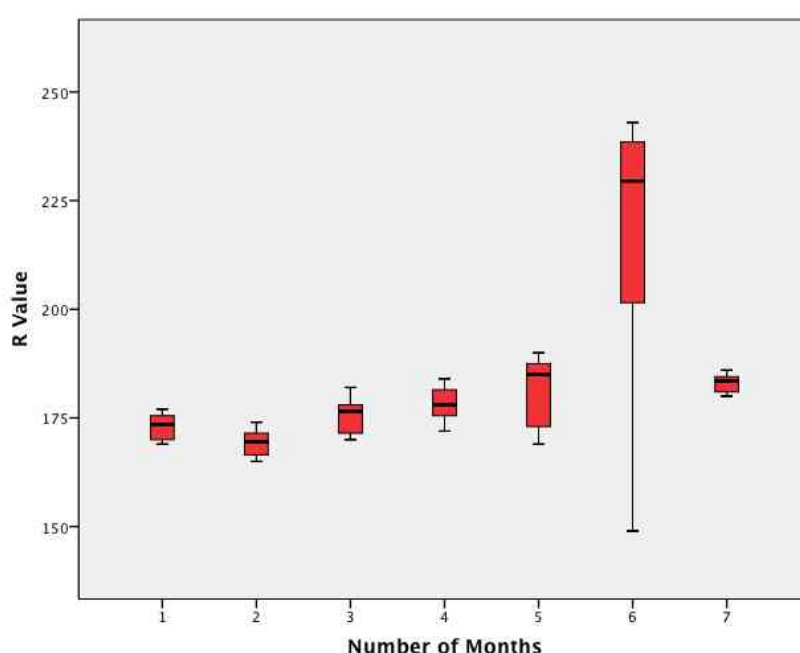
#### **7.2.2.1.a Sample Sets**

*Figures 190 & 191* outline distributions of R-values and RGB totals for stains generated on denim surfaces across longitudinal sample sets.

*Figure 190* outlines the distribution of R-values for replicate stains (n = 8) generated in each of 7 longitudinal sample sets. Across sample sets distributions of recorded R-values appeared generally similar. Stains exposed for 1 month (sample set L1), 2 months, 3 months (L3), 4 months (L4), 5 months (L5) and 7 months (L7) exhibited similar median R-values of 173.5 (L1), 169.5 (L2), 176.5 (L3), 178.0 (L4), 185.0 (L5) and 183.5 (L7), which all fell within a small range of 15.5. An anomaly to this trend appeared in R-values recorded for stains exposed for 6 months (L6), which exhibited a median R-value of 229.5.

Comparison of ranges exhibited by each sample set, between minimum and maximum R-values recorded, confirms the anomalous nature of stains exposed for 6 months (L6). Ranges between minimum and maximum R-values for sample sets L1 (8), L2 (9), L3 (12), L4 (12), L5 (21) and L7 (6) calculated from *figure 187* are small and support an observation that stains generated on denim exhibit minimal variability when exposed for varying longitudinal periods (*figure 187*). Stains exposed for 6 months (L6) once again appear anomalous to the general trend observed for R-value distributions across sample set. The range between minimum and maximum R-values for L6 was 94. The general presence of minimal ranges suggests that R-value distributions for denim stains are not significantly variable across sample sets. This supports an observation that as length of exposure increases, stains generated on denim surfaces do not exhibit observable changes in colour.

Figure 190 Box plot distributions of R values for stains generated on denim surfaces across longitudinal sample sets

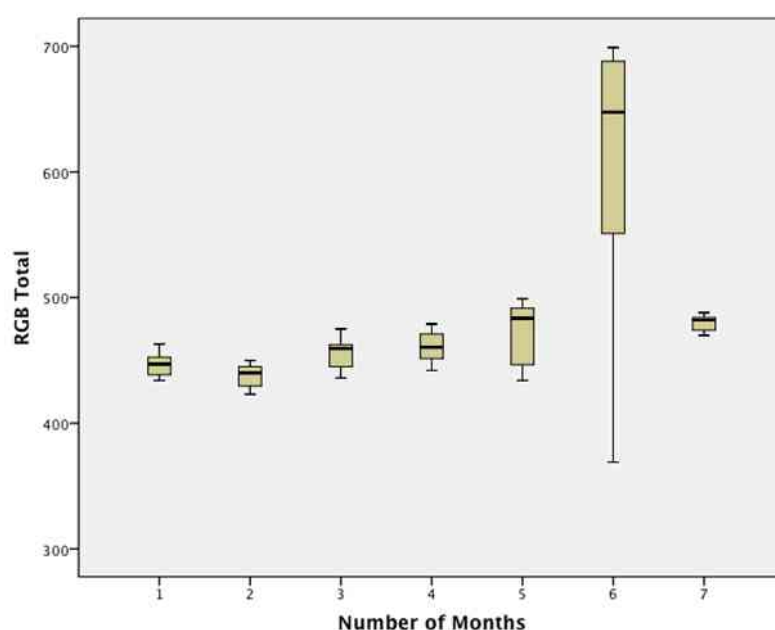


*Figure 191* outlines the distribution of RGB totals for replicate stains ( $n = 8$ ) generated in each of 7 longitudinal sample sets. Across sample sets distributions of recorded RGB totals appeared generally similar. Stains exposed for 1 month (sample set L1), 2 months, 3 months (L3), 4 months (L4), 5 months (L5) and 7 months (L7) exhibited similar median RGB totals of 447.0 (L1), 440.0 (L2), 459.5 (L3), 460.5

(L4), 483.5 (L5) and 482.0 (L7), which all fell within a small range of 43.5. An anomaly to this trend appeared in RGB totals recorded for stains exposed for 6 months (L6), which exhibited a median RGB total of 647.5.

Comparison of ranges exhibited by each sample set, between minimum and maximum RGB totals recorded, confirms the anomalous nature of stains exposed for 6 months (L6). Ranges for sample sets L1 (29), L2 (27), L3 (39), L4 (37), L5 (65) and L7 (18) calculated from *figure 187* are small and support an observation that stains generated on denim exhibit minimal variability when exposed for varying longitudinal periods (*figure 187*). Stains exposed for 6 months (L6) once again appear anomalous to the general trend observed for RGB total distributions across sample set. The range between minimum and maximum RGB totals for L6 was 330. The general presence of minimal ranges suggests that RGB total distributions for denim stains are not significantly variable across sample sets. This supports an observation that as length of exposure increases, stains generated on denim surfaces do not exhibit significant changes in colour.

Figure 191 Box plot distributions of RGB totals for stains generated on denim surfaces across longitudinal sample sets



Across all distributions a general trend can be identified between length of time (number of months) stains were exposed to temperate climatic variations for and R,



G, B values and RGB totals. As length of time increased from 1 to 7 months, R-values (*figure 190*), G-values (*appendix 2*), B-values (*appendix 2*) and RGB totals (*figure 191*) did not considerably vary. This suggests that for denim stains, length of environmental exposure did not influence stain colour.

#### **7.2.2.1.b Temperature**

*Figures 192 & 193* outline distribution of R-values and RGB totals for stains generated on denim surfaces across cumulatively averaged temperatures.

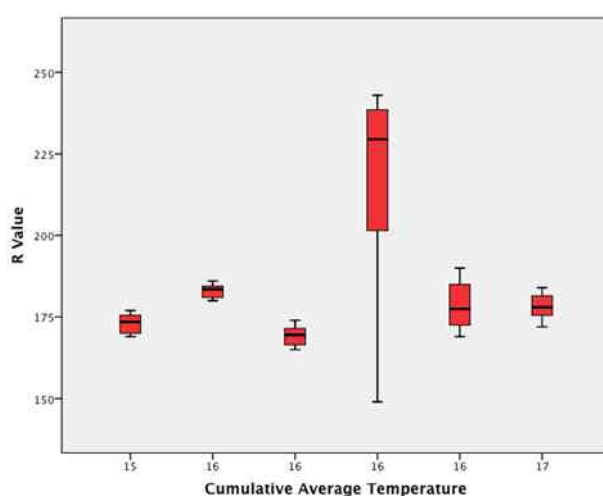


Figure 192 Box plot distributions of R values for stains generated on denim surfaces at cumulatively averaged temperatures

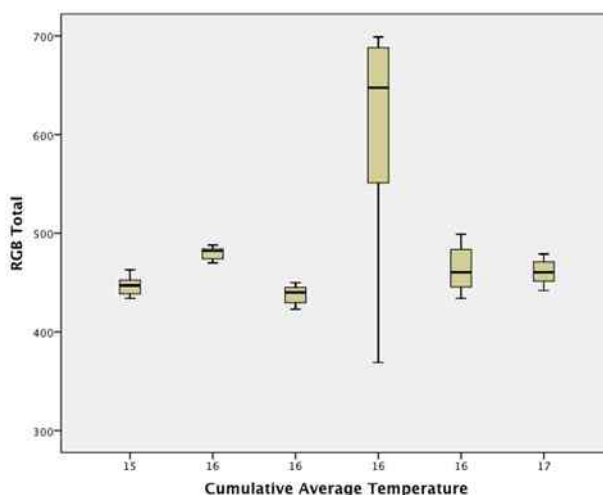


Figure 193 Box plot distributions of RGB Totals for stains generated on denim surfaces at cumulatively averaged temperatures

#### **7.2.2.1.c Humidity**

*Figures 194 & 195* outline distribution of R-values and RGB totals for stains generated on denim surfaces across cumulatively averaged humidity values.

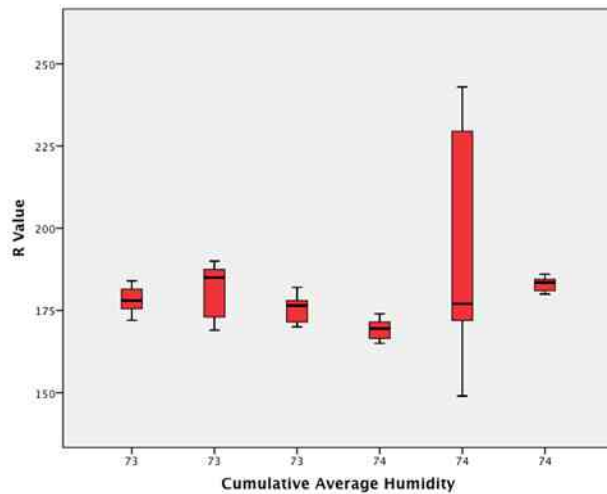


Figure 194 Box plot distributions of R values for stains generated on denim surfaces at cumulatively averaged humidity values

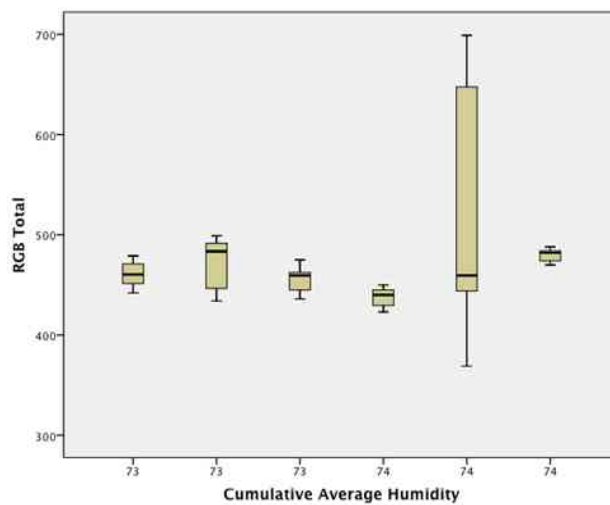


Figure 195 Box plot distributions of RGB totals for stains generated on denim surfaces at cumulatively averaged humidity values

Across all distributions, trends between average temperature, R, G, B values and RGB totals and average humidity, R, G, B values and RGB totals were not identified. Observations indicated average temperature only varied by 2°C and humidity values only varied by 1%. This was not a significant enough variation or range of variations to determine any influence of temperature or humidity over longitudinal periods on stains generated on denim surfaces.

#### **7.2.2.1.d Precipitation**

*Figures 196 & 197* outline distribution of R-values and RGB totals for stains generated on denim surfaces exposed to cumulative volumes of precipitation across longitudinal sample sets.

Figure 196 outlines the distribution of R-values for replicate stains generated in longitudinal sample sets that were exposed to cumulative volumes of precipitation.

Across cumulative volumes of precipitation R-values appeared generally similar. Stains exposed to 194mm (sample set L1), 323mm (L2), 359mm (L3), 419mm (L4), 531mm (L5) and 774mm (L7) exhibited similar median R-values of 173.5 (L1), 169.5 (L2), 176.5 (L3), 178.0 (L4), 185.0 (L5) and 183.5 (L7), which all fell within a small range of 15.5. An anomaly to this trend appeared in R-values recorded for stains exposed to 632mm (L6), which exhibited a median R-value of 229.5.

Comparison of ranges exhibited by each sample set, between minimum and maximum R-values recorded, confirms the anomalous nature of stains exposed to 632mm precipitation (L6). Ranges for sample sets of 8 (L1), 9 (L2), 12 (L3), 12 (L4), 21 (L5) and 6 (L7) are small and support an observation that stains generated on denim exhibit minimal variability when exposed to cumulative volumes of precipitation (*figure 187*). Stains exposed to 632mm (L6) once again appear anomalous to the general trend observed for R-value distributions across sample set. The range between minimum and maximum R-values for L6 was 94. The general presence of minimal ranges suggests that R-value distributions for denim stains exhibited minimal variability across sample sets. This supports an observation that as volume of precipitation stains are exposed to increases, stains generated on denim surfaces do not exhibit observable changes in colour.

Figure 196 Box plot distributions of R values for stains generated on denim surfaces and exposed to cumulative volumes of precipitation

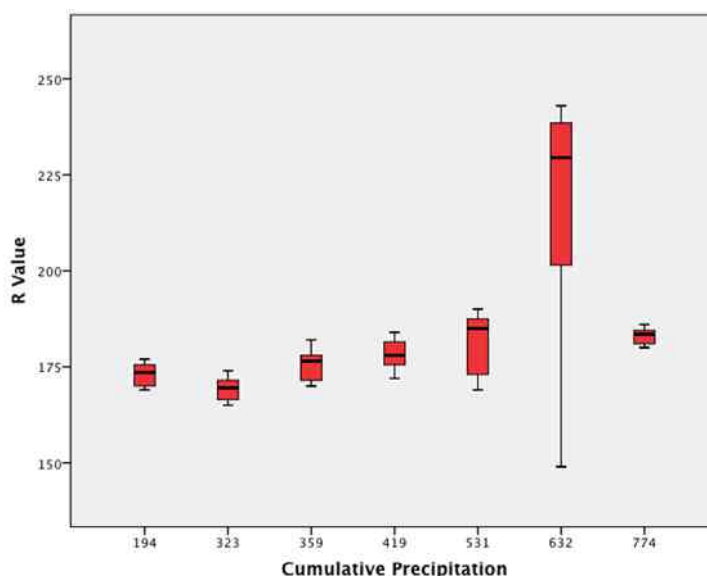
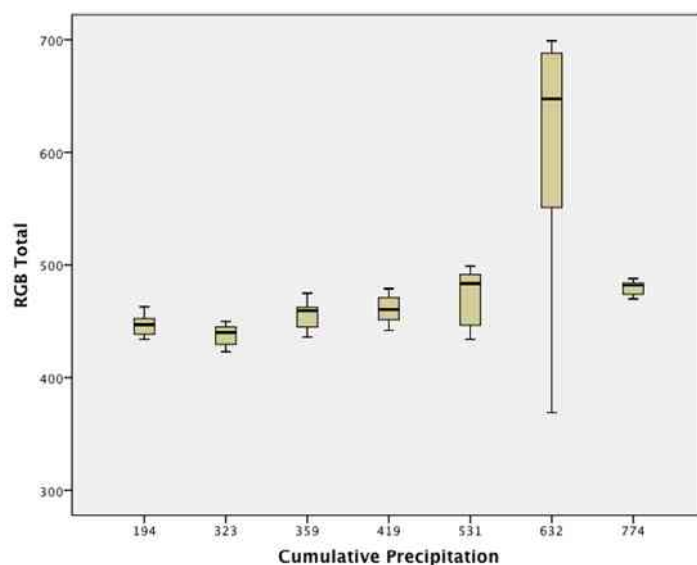


Figure 197 outlines the distribution of RGB totals for replicate stains generated in longitudinal sample sets that were exposed to cumulative volumes of precipitation. Across cumulative volumes of precipitation RGB totals appeared generally similar. Stains exposed to 194mm (sample set L1), 323mm (L2), 359mm (L3), 419mm (L4), 531mm (L5) and 774mm (L7) exhibited similar median RGB totals of 447.0 (L1), 440.0 (L2), 459.5 (L3), 460.5 (L4), 483.5 (L5) and 482.0 (L7), which all fell within a small range of 43.5. An anomaly to this trend appeared in RGB totals recorded for stains exposed to 632mm (L6), which exhibited a median RGB total of 647.5.

Comparison of ranges exhibited by each sample set, between minimum and maximum RGB totals recorded, confirms the anomalous nature of stains exposed to 632mm precipitation (L6). Ranges for sample sets of 29 (L1), 27 (L2), 39 (L3), 37 (L4), 65 (L5) and 18 (L7) are small and support an observation that stains generated on denim exhibit minimal variability when exposed to cumulative volumes of precipitation (*figure 187*). Stains exposed to 632mm (L6) once again appear anomalous to the general trend observed for RGB total distributions across sample set. The range between minimum and maximum RGB totals for L6 was 330. The general presence of minimal ranges suggests that B-value distributions for denim stains are not significantly variable across sample sets. This supports an observation that as volume of precipitation stains are exposed to increases, stains generated on denim surfaces do not exhibit significant changes in colour.

Figure 197 Box plot distributions of RGB totals for stains generated on denim surfaces and exposed to cumulative volumes of precipitation



Across all distributions a general trend can be identified between cumulative volumes of precipitation (number of months) and R, G, B values and RGB totals. As levels of precipitation increased from 194mm to 774mm, R-values (*figure 196*), G-values (*appendix 2*), B-values (*appendix 2*) and RGB totals (*figure 197*) did not considerably vary. This suggests that for denim stains, volume of precipitation stains were exposed to did not influence stain colour.

#### **7.2.2.2 Stains generated in longitudinal paper sample sets**

The measurements derived for stains on paper surfaces from longitudinal sample sets are presented in *figure 198*. Descriptive statistics are then presented in *figures 199* and *200*.

Figure 198 Table of measurements recorded for stains generated on paper surfaces in longitudinal sample sets

Stain ID	Surface	Months	Average temperature /°C	Average humidity /%	Total precipitation /mm	Number of Months	R Value	G Value	B Value	Hex	Hex Colour
B017	Paper	0 to 1	15.3	74.0	193.7	1	71	70	62	47463e	
B018	Paper	0 to 1	15.3	74.0	193.7	1	85	82	72	555248	
B019	Paper	0 to 1	15.3	74.0	193.7	1	91	89	77	5b594d	
B020	Paper	0 to 1	15.3	74.0	193.7	1	85	84	73	555449	
B021	Paper	0 to 1	15.3	74.0	193.7	1	84	77	64	544d40	
B022	Paper	0 to 1	15.3	74.0	193.7	1	75	74	66	4b4a42	
B023	Paper	0 to 1	15.3	74.0	193.7	1	54	42	35	362a23	
B024	Paper	0 to 1	15.3	74.0	193.7	1	23	20	16	171410	
B041	Paper	0 to 2	16.4	73.5	322.7	2	61	60	54	3d3c36	
B042	Paper	0 to 2	16.4	73.5	322.7	2	52	45	38	342d26	
B043	Paper	0 to 2	16.4	73.5	322.7	2	49	50	42	31322a	
B044	Paper	0 to 2	16.4	73.5	322.7	2	65	48	41	413029	
B045	Paper	0 to 2	16.4	73.5	322.7	2	46	34	26	2e221a	
B046	Paper	0 to 2	16.4	73.5	322.7	2	61	43	34	3d2b22	
B047	Paper	0 to 2	16.4	73.5	322.7	2	56	46	38	382e26	
B048	Paper	0 to 2	16.4	73.5	322.7	2	48	34	26	30221a	
B065	Paper	0 to 3	17.3	72.3	358.6	3	68	61	43	443d2b	
B066	Paper	0 to 3	17.3	72.3	358.6	3	91	68	55	5b4437	
B067	Paper	0 to 3	17.3	72.3	358.6	3	72	67	56	484338	
B068	Paper	0 to 3	17.3	72.3	358.6	3	59	40	31	3b281f	
B069	Paper	0 to 3	17.3	72.3	358.6	3	91	75	60	5b4b3c	
B070	Paper	0 to 3	17.3	72.3	358.6	3	52	21	10	34150a	
B071	Paper	0 to 3	17.3	72.3	358.6	3	82	57	44	52392c	
B072	Paper	0 to 3	17.3	72.3	358.6	3	63	33	21	3f2115	
B089	Paper	0 to 4	16.8	72.0	418.8	4	84	79	66	544f42	
B090	Paper	0 to 4	16.8	72.0	418.8	4	85	75	61	554b3d	
B091	Paper	0 to 4	16.8	72.0	418.8	4	63	41	27	3f291b	
B092	Paper	0 to 4	16.8	72.0	418.8	4	79	58	45	4f3a2d	
B093	Paper	0 to 4	16.8	72.0	418.8	4	82	67	54	524336	
B094	Paper	0 to 4	16.8	72.0	418.8	4	61	35	23	3d2317	
B095	Paper	0 to 4	16.8	72.0	418.8	4	63	43	31	3f2b1f	
B096	Paper	0 to 4	16.8	72.0	418.8	4	65	47	34	412f22	
B113	Paper	0 to 5	15.7	74.0	530.8	5	51	25	20	331914	
B114	Paper	0 to 5	15.7	74.0	530.8	5	64	51	42	40332a	
B115	Paper	0 to 5	15.7	74.0	530.8	5	46	34	22	2e2216	
B116	Paper	0 to 5	15.7	74.0	530.8	5	48	39	29	30271d	
B117	Paper	0 to 5	15.7	74.0	530.8	5	57	45	35	392d23	
B118	Paper	0 to 5	15.7	74.0	530.8	5	50	38	28	32261c	
B119	Paper	0 to 5	15.7	74.0	530.8	5	41	27	15	291a0f	
B120	Paper	0 to 5	15.7	74.0	530.8	5	54	39	28	36271c	
B137	Paper	0 to 6	14.5	76.0	631.6	6	59	50	43	3b322b	
B138	Paper	0 to 6	14.5	76.0	631.6	6	55	41	31	37291f	
B139	Paper	0 to 6	14.5	76.0	631.6	6	53	17	11	35110b	
B140	Paper	0 to 6	14.5	76.0	631.6	6	72	54	42	48362a	
B141	Paper	0 to 6	14.5	76.0	631.6	6	40	31	20	281f14	
B142	Paper	0 to 6	14.5	76.0	631.6	6	37	33	24	252118	
B143	Paper	0 to 6	14.5	76.0	631.6	6	57	45	36	392d24	
B144	Paper	0 to 6	14.5	76.0	631.6	6	46	36	26	2e241a	
B161	Paper	0 to 7	13.4	77.3	773.6	7	42	28	17	2a1c11	
B162	Paper	0 to 7	13.4	77.3	773.6	7	45	37	28	2d251c	
B163	Paper	0 to 7	13.4	77.3	773.6	7	48	33	23	302117	
B164	Paper	0 to 7	13.4	77.3	773.6	7	68	40	30	44281e	
B165	Paper	0 to 7	13.4	77.3	773.6	7	45	32	23	2d2017	
B166	Paper	0 to 7	13.4	77.3	773.6	7	55	26	14	371a0e	
B167	Paper	0 to 7	13.4	77.3	773.6	7	33	25	15	21190f	
B168	Paper	0 to 7	13.4	77.3	773.6	7	49	30	21	311e15	

Figure 199 outlines mean R, G, B values and RGB totals calculated from 8 replicate stains in each of 7 longitudinal sample sets. In each longitudinal sample set R-values were greater than G and B-values. G and B-values recorded for each sample set were also high however, which meant for some sample sets R-values were only slightly higher than G and B values. For example, in the L1 sample set the average R-value was 71.0, average G-value was 67.3 and average B-value was 58.1.

R-values for all sample sets fell between a low of 51.4 (L5) and a highest value of 73.0 observed for the L4 sample set. G-values across all sample sets fell between a recorded low of 31.4 (L6) and a high of 67.3 (L1). B-values were recorded between a low of 21.4 (L6) and a high of 58.1 (L1). Results demonstrate that whilst R, G and B-values were represented in similar levels in each sample set, for each sample set R-values represented the highest colour component, followed by G-values and finally B-values. The slight dominance of R-values suggests stains generated on paper and exposed to a range of longitudinal periods are all coloured towards red, rather than green or blue hues of colour. Observations of similarly low levels of R, G and B values support observations of a dark-brown or grey-black colour of stains (figure 198). An RGB triplet for the darkest hues of grey ('dark slate grey') are typically represented by low, similar figures of R, G and B values, for example RGB (R79, G76, B47). The colour black corresponds to an RGB triplet of (R0, G0, B0).

Figure 199 Descriptive statistics recorded for stains generated on paper surfaces in longitudinal sample sets

Sample Set		R Value	G Value	B Value	RGB Total
<b>L1</b>	Mean	71.0	67.3	58.1	196.4
	Std. Deviation	22.6	24.0	21.4	68.0
<b>L2</b>	Mean	55.0	45.0	37.4	137.1
	Std. Deviation	7.0	9.0	9.1	23.0
<b>L3</b>	Mean	72.3	53.0	40.0	165.0
	Std. Deviation	15.0	19.2	18.0	50.2
<b>L4</b>	Mean	73.0	56.0	43.0	171.0
	Std. Deviation	11.0	17.0	16.3	43.3
<b>L5</b>	Mean	51.4	37.3	27.4	116.0
	Std. Deviation	7.1	9.0	9.0	23.4
<b>L6</b>	Mean	52.4	38.4	29.1	120.0
	Std. Deviation	11.3	12.0	11.1	31.4
<b>L7</b>	Mean	48.1	31.4	21.4	101.0
	Std. Deviation	10.2	5.2	6.0	19.0

Figure 200 outlines average colour values for all paper stains. Average R, G and B values were calculated between all replicate stains in all longitudinal sample sets.

Values for stains generated on paper were R (60.38), G (46.80) and B (36.57). Stains exhibit a marginally higher ratio of R to G and B colour components. This means stains were slightly coloured towards a red rather than green or blue hue. Levels of R, G and B values were all low which corresponds to the dark intensity observed in longitudinal stains generated on paper (*figure 198*). The combination of a slight orientation towards red hues of colour and a dark intensity indicate that stains generated on paper, on average, were characterised by a very dark grey or brown colouring. For some individual stains, for example B024 (R23, G20, B16) had such low R, G and B values they were close to (R000, G000, B000) an RGB triplet that corresponds to the colour black.

Figure 200 Average R, G and B values for all longitudinal stains generated on paper

	N	Minimum	Maximum	Mean	Std. Deviation
R Value	56	23	91	60.38	15.971
G Value	56	17	89	46.80	18.176
B Value	56	10	77	36.57	17.353
Valid N (listwise)	56				

#### **7.2.2.2.a Sample Sets**

*Figures 201 & 202* outline distribution of R-values and RGB totals for stains generated on paper surfaces across longitudinal sample sets.

*Figure 201* outlines the distribution of R-values for replicate stains ( $n = 8$ ) generated in each of 7 longitudinal sample sets. Stains exposed for 1 month (sample set L1), 3 months (L3) and 4 months (L4) exhibited median R-values of 79.5, 70.0 and 72.0 respectively, which were the highest median R-values recorded across sample sets. Stains exposed for 5 months (L5), 6 months (L6) and 7 months (L7) exhibited median R-values of 50.5, 54.0 and 46.5 respectively, which were the lowest median R-values recorded across sample sets. These results suggest that as length of exposure increases for stains generated on paper surfaces, R-values of stains decrease. Stains exposed for 2 months (sample set L2) are the only stains that do not support this general trend. They exhibited a median R-value of 54.0, which appears anomalous alongside the R-values of 79.5 (L1), 70.0 (L3) and 72.0 (L4) of stains exposed for shorter lengths of time.

Significant ranges were exhibited by all sample sets between minimum and



maximum R-values. The largest range of 68 was observed for stains exposed for 1 month (L1) and the smallest range of 19 was observed for stains exposed for 2 months (L2). The presence of significant ranges suggests that R-value distributions for paper stains are variable across sample sets.

Figure 201 Box plot distributions of R values for stains generated on paper surfaces across longitudinal sample sets

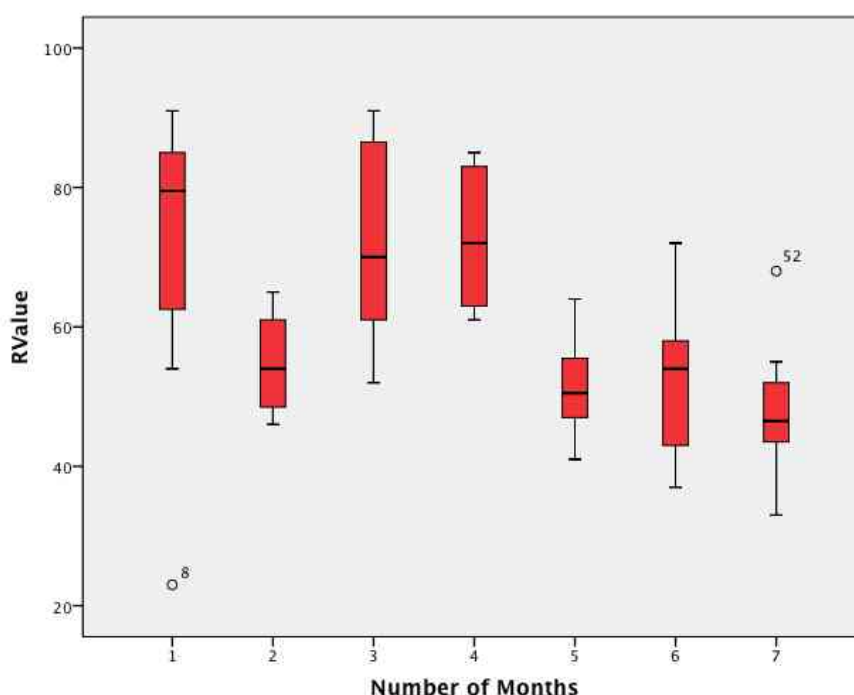
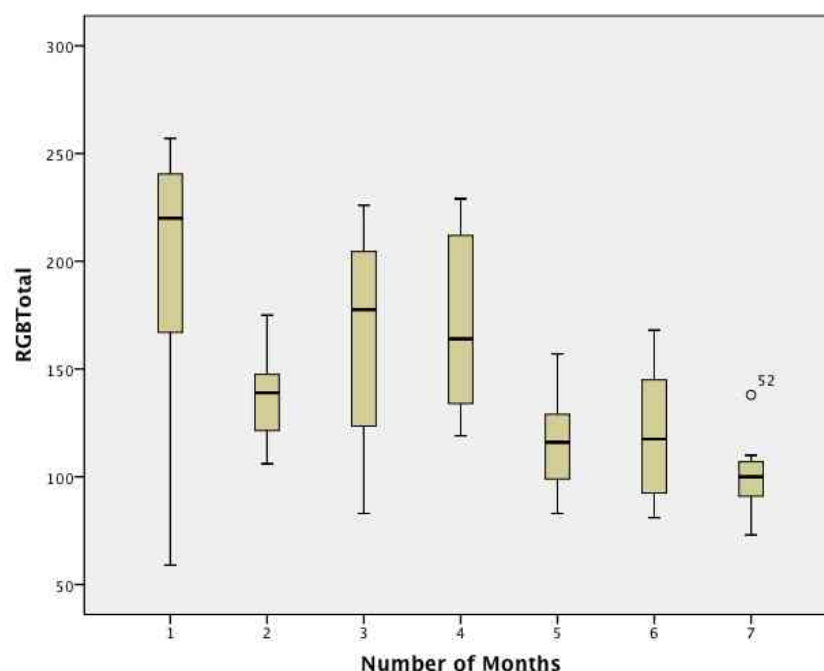


Figure 202 outlines the distribution of RGB totals for replicate stains ( $n = 8$ ) generated in each of 7 longitudinal sample sets. Stains exposed for 1 month (sample set L1), 3 months (L3) and 4 months (L4) exhibited median RGB totals of 220.0, 177.5 and 164.0.0 respectively, which were the three highest median RGB totals recorded across sample sets. Stains exposed for 5 months (L5), 6 months (L6) and 7 months (L7) exhibited median RGB totals of 116.0, 117.5 and 100.0 respectively, which were the lowest median RGB totals recorded across sample sets. These results suggest that as length of exposure increases for stains generated on paper surfaces, RGB totals of stains decrease. This supports an observation of darker intensities of stain colour as length of exposure to temperate climatic variations increases (*figure 198*). Stains exposed for 2 months (sample set L2) are the only stains that do not support this general trend. They exhibited a median RGB total of 139.0, which appears anomalous as this total was higher than the RGB total exhibited by stains in sample set L3 (177.5).

Significant ranges were exhibited by all sample sets between minimum and maximum RGB totals. The largest range of 198 was observed for stains exposed for 1 month (L1) and the smallest range of 65 was observed for stains exposed for 7 months (L7). The presence of significant ranges suggests that RGB totals distributions for paper stains are variable across sample sets.

Figure 202 Box plot distributions of RGB totals for stains generated on paper surfaces across longitudinal sample sets



Across all distributions a general trend can be identified between length of time (number of months) stains were exposed to temperate climatic variations for and R, G, B values and RGB totals. As length of time increased from 1 to 7 months, R-values (*figure 201*), G-values (*appendix 2*), B-values (*appendix 2*) and RGB totals (*figure 202*) decreased. R-values decreased from 71 (L1) to 64 (L7). G-values decreased from 90 (L1) to 42 (L7). B-values decreased from 78 (L1) to 29 (L7) and RGB totals decreased from 239 (L1) to 135 (L7). This suggests that for paper stains, length of environmental exposure did influence stain colour.

#### **7.2.2.2.b Temperature**

*Figures 203 & 204* outline distribution of R-values and RGB totals for stains generated on paper surfaces across cumulatively averaged temperatures.

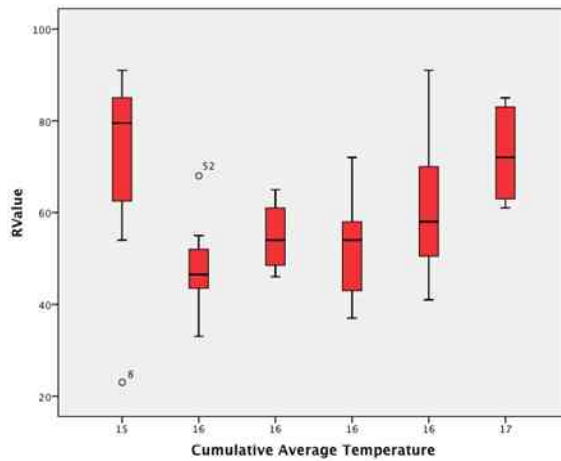


Figure 203 Box plot distributions of R values for stains generated on paper surfaces at cumulatively averaged temperatures

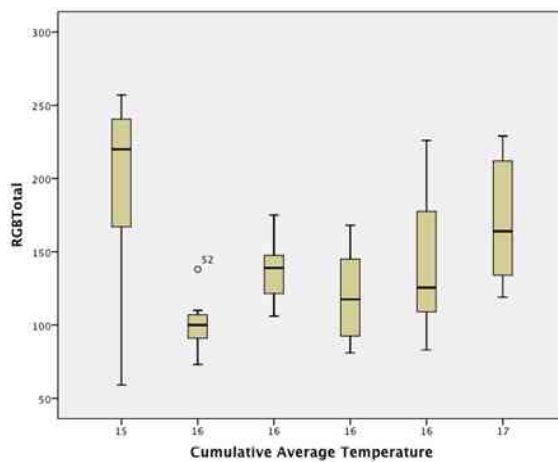


Figure 204 Box plot distributions of RGB Totals for stains generated on paper surfaces at cumulatively averaged temperatures

### 7.2.2.2.c Humidity

Figures 205 & 206 outline distribution of R-values and RGB totals for stains generated on paper surfaces across cumulatively averaged humidity values.

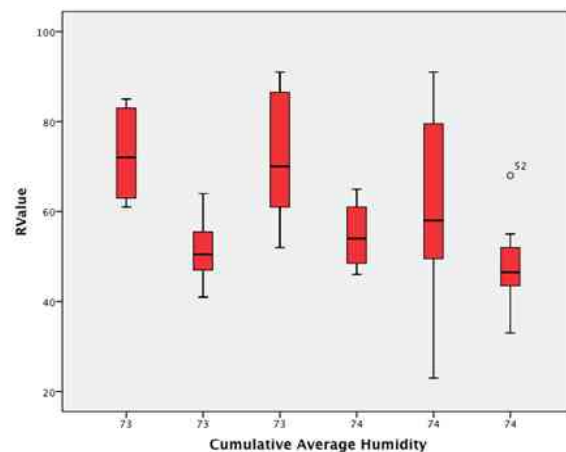


Figure 205 Box plot distributions of R values for stains generated on paper surfaces at cumulatively averaged humidity values

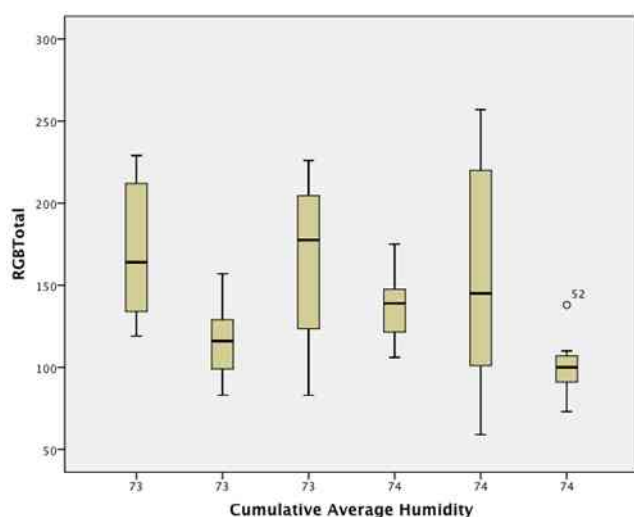


Figure 206 Box plot distributions of RGB totals for stains generated on paper surfaces at cumulatively averaged humidity values

Across all distributions, trends between average temperature, R, G, B values and RGB totals and average humidity, R, G, B values and RGB totals were not identified. Observations indicated average temperature only varied by 2°C and humidity values only varied by 1%. This was not a significant enough variation or range of variations to determine any influence of temperature or humidity over longitudinal periods on stains generated on paper surfaces.

#### **7.2.2.2.d Precipitation**

*Figures 207 & 208* outline distribution of R-values and RGB totals for stains generated on paper surfaces exposed to cumulative volumes of precipitation across longitudinal sample sets.

*Figure 207* outlines the distribution of R-values for replicate stains generated in longitudinal sample sets that were exposed to cumulative volumes of precipitation. Stains exposed to the lowest volume of precipitation (194mm) exhibited the highest median R-value of 79.5. Stains exposed to the highest cumulative volume of precipitation (774mm) exhibited the lowest median R-value of 46.5. This supports a suggestion that as volume of precipitation stains generated on paper are exposed to increases, R-values of stains generally decrease. R-values recorded for stains exposed to 323mm precipitation appear slightly anomalous to this general trend. They exhibited a median R-value of 54.0, which appears anomalous alongside R-values of 70.0 (359mm) and 72.0 (419mm) recorded for stains exposed to higher cumulative levels of precipitation.

Figure 207 Box plot distributions of R values for stains generated on paper surfaces and exposed to cumulative volumes of precipitation

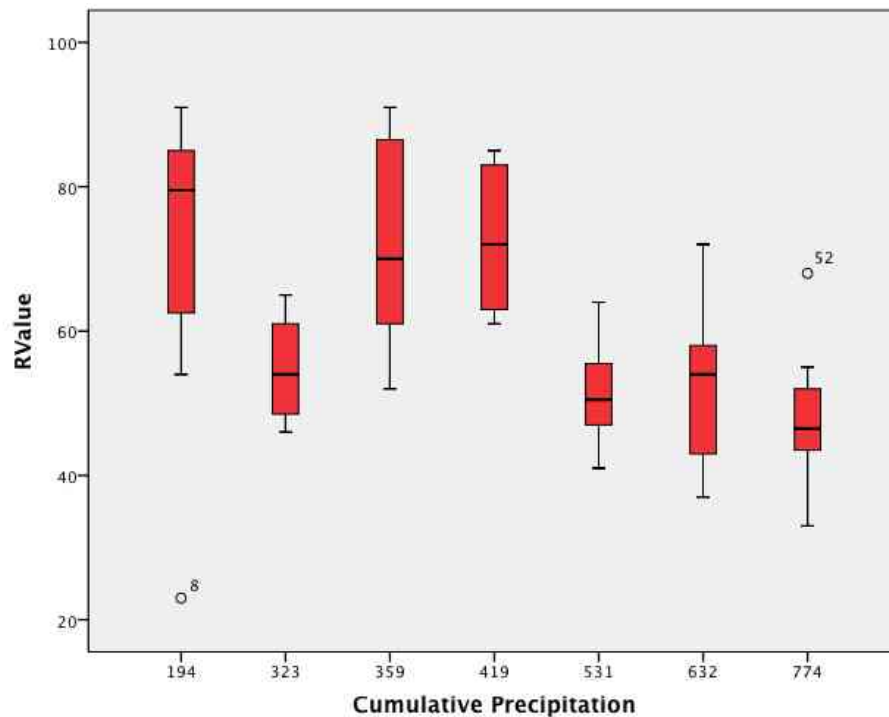
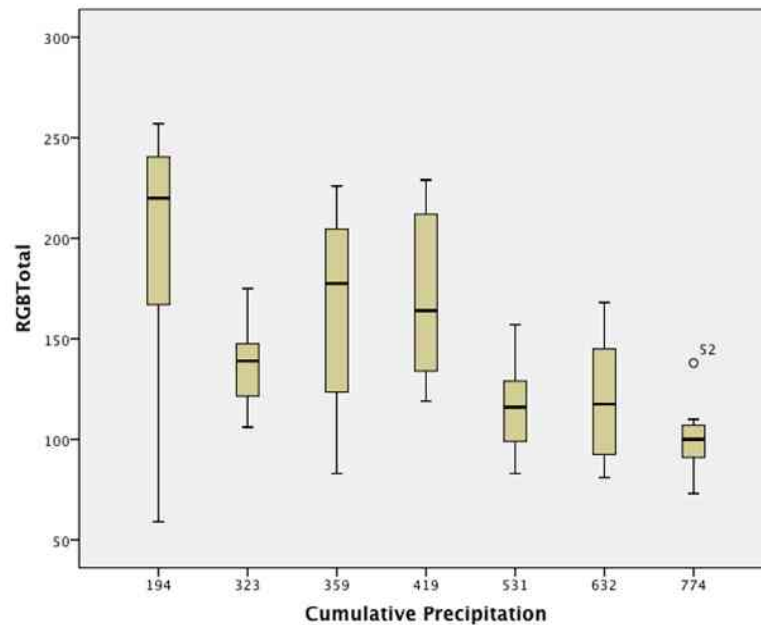


Figure 208 outlines the distribution of RGB totals for replicate stains generated in longitudinal sample sets that were exposed to cumulative volumes of precipitation. Stains exposed to the lowest volume of precipitation (194mm) exhibited the highest median RGB total of 220.0. Stains exposed to the highest cumulative volume of precipitation (774mm) exhibited the lowest median RGB-value of 100.0. This supports a suggestion that as volume of precipitation stains generated on paper are exposed to increases, RGB totals of stains generally decrease. RGB totals recorded for stains exposed to 323mm precipitation appear slightly anomalous to this general trend. They exhibited a median RGB total of 139.0, which appears anomalous alongside RGB totals of 177.5 (359mm) and 164.0 (419mm) recorded for stains exposed to higher cumulative levels of precipitation.

Figure 208 Box plot distributions of RGB totals for stains generated on paper surfaces and exposed to cumulative volumes of precipitation



Across all distributions general trends can be identified between cumulative volumes of precipitation and R, G, B values and RGB totals. As levels of precipitation increased from 194mm to 774mm, R-values (*figure 207*), G-values (*appendix 2*), B-values (*appendix 2*) and RGB totals (*figure 208*) decreased. This suggests that for paper stains, cumulative volume of precipitation stains were exposed to did influence stain colour.

### 7.2.2.3 Stains generated in longitudinal glass sample sets

The measurements derived for stains on glass surfaces from longitudinal sample sets are presented in *figure 209*. Descriptive statistics are then presented in *figures 210* and *211*.

Figure 209 Table of measurements recorded for stains generated on glass surfaces in longitudinal sample sets

Stain ID	Surface	Months	Average temperature /°C	Average humidity /%	Total precipitation /mm	Number of Months	R Value	G Value	B Value	Hex	Hex Colour
B009	Glass	0 to 1	15.3	74.0	193.7	1	86	59	40	563e2d	
B010	Glass	0 to 1	15.3	74.0	193.7	1	78	60	48	4e3b2f	
B011	Glass	0 to 1	15.3	74.0	193.7	1	91	69	57	5b4539	
B012	Glass	0 to 1	15.3	74.0	193.7	1	98	66	55	624236	
B013	Glass	0 to 1	15.3	74.0	193.7	1	89	78	68	594e43	
B014	Glass	0 to 1	15.3	74.0	193.7	1	75	57	46	4b392d	
B015	Glass	0 to 1	15.3	74.0	193.7	1	81	61	52	513e35	
B016	Glass	0 to 1	15.3	74.0	193.7	1	101	67	56	654338	
B033	Glass	0 to 2	16.4	73.5	322.7	2	216	210	192	d8d2c0	
B034	Glass	0 to 2	16.4	73.5	322.7	2	138	124	104	8a7c68	
B035	Glass	0 to 2	16.4	73.5	322.7	2	141	114	83	8d7253	
B036	Glass	0 to 2	16.4	73.5	322.7	2	115	95	81	735f51	
B037	Glass	0 to 2	16.4	73.5	322.7	2	117	87	68	755744	
B038	Glass	0 to 2	16.4	73.5	322.7	2	105	90	79	6a5a4f	
B039	Glass	0 to 2	16.4	73.5	322.7	2	107	89	74	6b594a	
B040	Glass	0 to 2	16.4	73.5	322.7	2	111	87	71	6f5747	
B057	Glass	0 to 3	17.3	72.3	358.6	3	101	68	52	654434	
B058	Glass	0 to 3	17.3	72.3	358.6	3	105	70	50	694632	
B059	Glass	0 to 3	17.3	72.3	358.6	3	117	71	46	75472e	
B060	Glass	0 to 3	17.3	72.3	358.6	3	134	79	38	864f26	
B061	Glass	0 to 3	17.3	72.3	358.6	3	117	69	48	754530	
B062	Glass	0 to 3	17.3	72.3	358.6	3	107	71	58	6b473a	
B063	Glass	0 to 3	17.3	72.3	358.6	3	102	90	82	665a52	
B064	Glass	0 to 3	17.3	72.3	358.6	3	108	69	48	6c4530	
B081	Glass	0 to 4	16.8	72.0	418.8	4	142	112	89	8e7059	
B082	Glass	0 to 4	16.8	72.0	418.8	4	128	110	88	806e58	
B083	Glass	0 to 4	16.8	72.0	418.8	4	90	66	54	5a4236	
B084	Glass	0 to 4	16.8	72.0	418.8	4	90	70	59	5a463b	
B085	Glass	0 to 4	16.8	72.0	418.8	4	67	54	46	43362e	
B086	Glass	0 to 4	16.8	72.0	418.8	4	84	71	63	54473f	
B087	Glass	0 to 4	16.8	72.0	418.8	4	93	72	59	5d483b	
B088	Glass	0 to 4	16.8	72.0	418.8	4	97	68	52	614434	
B105	Glass	0 to 5	15.7	74.0	530.8	5	174	171	151	aeab97	
B106	Glass	0 to 5	15.7	74.0	530.8	5	96	84	59	60543b	
B107	Glass	0 to 5	15.7	74.0	530.8	5	153	145	116	999174	
B108	Glass	0 to 5	15.7	74.0	530.8	5	111	98	68	6f6244	
B109	Glass	0 to 5	15.7	74.0	530.8	5	134	126	106	867e6a	
B110	Glass	0 to 5	15.7	74.0	530.8	5	76	63	42	4c3f2a	
B111	Glass	0 to 5	15.7	74.0	530.8	5	76	64	46	4c402e	
B112	Glass	0 to 5	15.7	74.0	530.8	5	66	49	32	423120	
B129	Glass	0 to 6	14.5	76.0	631.6	6	99	61	42	633d2a	
B130	Glass	0 to 6	14.5	76.0	631.6	6	132	102	71	846647	
B131	Glass	0 to 6	14.5	76.0	631.6	6	238	236	208	eeecd0	
B132	Glass	0 to 6	14.5	76.0	631.6	6	113	81	48	715130	
B133	Glass	0 to 6	14.5	76.0	631.6	6	174	127	90	ae7f5a	
B134	Glass	0 to 6	14.5	76.0	631.6	6	129	109	82	816d52	
B135	Glass	0 to 6	14.5	76.0	631.6	6	116	94	73	745e49	
B136	Glass	0 to 6	14.5	76.0	631.6	6	197	168	141	c5a88d	
B153	Glass	0 to 7	13.4	77.3	773.6	7	125	103	79	7d674f	
B154	Glass	0 to 7	13.4	77.3	773.6	7	148	122	87	947a57	
B155	Glass	0 to 7	13.4	77.3	773.6	7	112	81	59	70513b	
B156	Glass	0 to 7	13.4	77.3	773.6	7	96	72	57	604839	
B157	Glass	0 to 7	13.4	77.3	773.6	7	93	60	43	5d3c2b	
B158	Glass	0 to 7	13.4	77.3	773.6	7	95	65	49	5f4131	
B159	Glass	0 to 7	13.4	77.3	773.6	7	82	61	48	523d30	
B160	Glass	0 to 7	13.4	77.3	773.6	7	93	78	68	5d4e44	

Figure 210 outlines mean R, G, B values and RGB totals calculated from 8 replicate stains in each of 7 longitudinal sample sets. In each longitudinal sample set R-values were greater than G and B-values. G and B-values recorded for each sample set were also high however, which meant for some sample sets R-values were only slightly higher than G and B values. For example, in the L5 sample set the average R-value was 111.0, average G-value was 100.0 and average B-value was 78.0.

R-values for the majority of sample sets (L2, L3, L5, L6 and L7) were above 100.0, with R-values below 100.0 only being observed for L1 and L4 sample sets. G-values across all sample sets fell between a recorded low of 65.0 (L1) and 122.3 (L6) and for all sample sets B-values were recorded below 100.0. Results demonstrate that whilst R, G and B-values were observed in similar levels in each sample set, for each sample set R-values represented the highest colour component, followed by G-values and finally B-values. The slight dominance of R-values suggests stains generated on glass and exposed to a range of longitudinal periods are all coloured towards red, rather than green or blue hues of colour. Observation of similar levels of R, G and B values support observations of a predominantly brown or grey colour of stains (figure 209). An RGB triplet for a grey colour are typically represented by an equal figure in each of R, G and B values, approximately half-way between 000 (black) and 255 (white), for example RGB (R138, G138, B138). RGB triplets for brown colours are typically represented by a dominance of R-values to significant levels of G and B-values, for example (R160, G82, B45).

Figure 210 Descriptive statistics recorded for stains generated on glass surfaces in longitudinal sample sets

Sample Set		R Value	G Value	B Value	RGB Total
<b>L1</b>	Mean	87.4	65.0	53.0	205.0
	Std. Deviation	9.2	7.0	8.4	21.4
<b>L2</b>	Mean	131.3	112.0	94.0	337.3
	Std. Deviation	37.0	42.0	41.1	119.1
<b>L3</b>	Mean	111.4	73.4	53.0	238.0
	Std. Deviation	11.0	7.5	13.1	17.4
<b>L4</b>	Mean	99.0	78.0	64.0	241.0
	Std. Deviation	24.3	21.2	16.1	61.0
<b>L5</b>	Mean	111.0	100.0	78.0	288.3
	Std. Deviation	40.0	43.5	42.2	125.1
<b>L6</b>	Mean	150.0	122.3	94.4	367.0
	Std. Deviation	48.4	56.0	55.0	158.1
<b>L7</b>	Mean	106.0	80.3	61.3	247.0
	Std. Deviation	22.0	22.0	16.0	58.0



*Figure 211* outlines average colour values for all glass stains. Average R, G and B values were calculated between all replicate stains in all longitudinal sample sets. Values for stains generated on paper were R (113.55), G (90.05) and B (70.91). Stains exhibit a higher ratio of R to G and B colour components. This means stains were coloured towards a red rather than green or blue hue. Levels of R-values were approximately halfway between values of 000 (black) and 255 (white) and indicated a medium intensity of R-values, whilst G and B values were lower than 100 and much closer therefore to a value of 000 (black). Overall, this corresponds to the medium intensity observed in longitudinal stains generated on glass (*figure 209*). The combination of an orientation towards red hues of colour and a dark intensity of colour indicate that stains generated on glass, on average, were characterised by a brown or dark-grey colouring.

Figure 211 Average R, G and B values for all longitudinal stains generated on glass

	N	Minimum	Maximum	Mean	Std. Deviation
R Value	56	66	238	113.55	34.784
G Value	56	49	236	90.05	37.411
B Value	56	32	208	70.91	34.668
Valid N (list wise)	56				

#### **7.2.2.3.a Sample Sets**

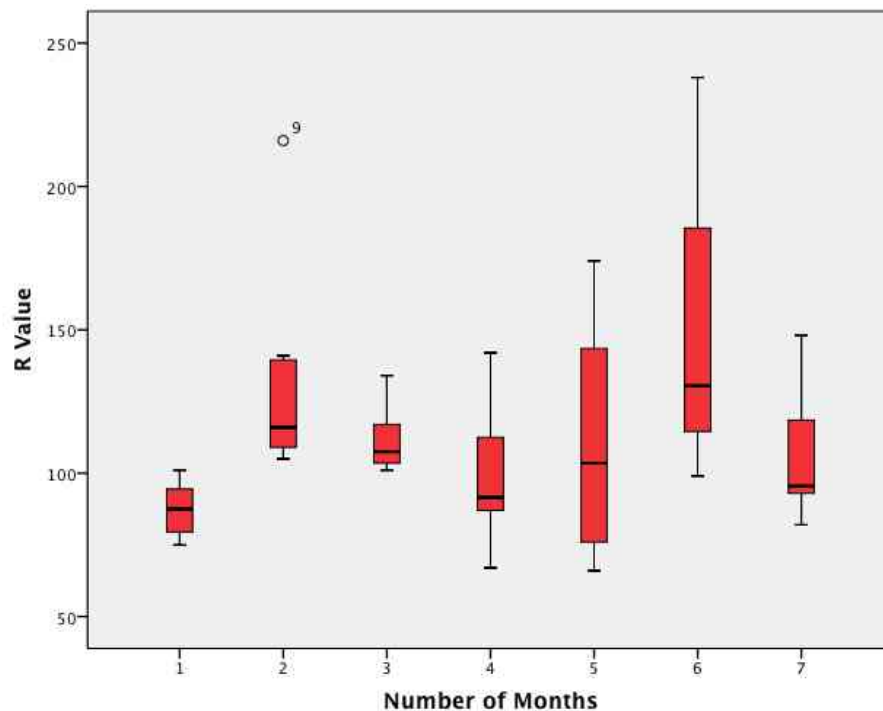
*Figures 212 & 213* outline distribution of R-values and RGB totals for stains generated on glass surfaces across longitudinal sample sets.

*Figure 212* outlines the distribution of R-values for replicate stains (n = 8) generated in each of 7 longitudinal sample sets. Across sample sets distributions of recorded R-values varied but there was no clear relationship between variations in R-value distributions and increasing length of time stains were exposed for. Stains exposed for 1 month (sample set L1), 2 months, 3 months (L3), 4 months (L4), 5 months (L5), 6 months (L6) and 7 months (L7) exhibited median R-values of 87.5 (L1), 116.0 (L2), 107.5 (L3), 91.5 (L4), 103.5 (L5), 130.5 (L6) and 95.5 (L7).

Ranges exhibited by each sample set, between minimum and maximum R-values, also varied but there was no clear relationship between variations in range and length

of time stains were exposed for. Ranges for sample sets of 26 (L1), 111 (L2), 33 (L3), 75 (L4), 108 (L5), 139 (L6) and 66 (L7) support an observation that stains generated on glass exhibit variability in R-value distributions following exposure to longitudinally variable climates (*figure 209*).

Figure 212 Box plot distributions of R values for stains generated on glass surfaces across longitudinal sample sets

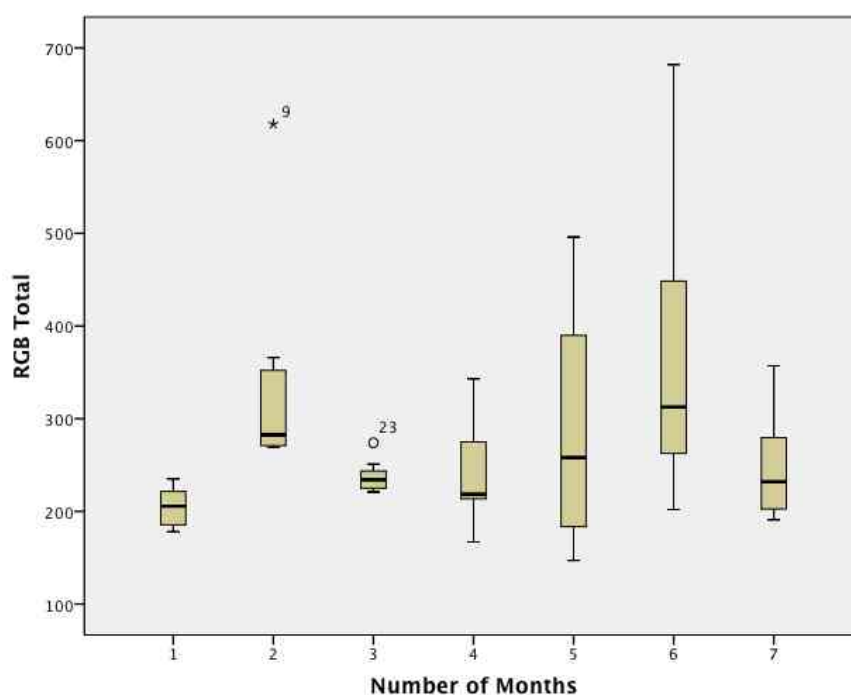


*Figure 213* outlines the distribution of RGB totals for replicate stains ( $n = 8$ ) generated in each of 7 longitudinal sample sets. Across sample sets distributions of recorded RGB totals varied but there was no clear correlation between variations in RGB total distributions and increasing length of time stains were exposed for. Stains exposed for 1 month (sample set L1), 2 months, 3 months (L3), 4 months (L4), 5 months (L5), 6 months (L6) and 7 months (L7) exhibited median RGB totals of 205.5 (L1), 282.5 (L2), 234.0 (L3), 218.5 (L4), 258.0 (L5), 312.5 (L6) and 232.0 (L7).

Ranges exhibited by each sample set, between minimum and maximum RGB totals, also varied but there was no clear correlation between variations in range and lengths of time stains were exposed for. Ranges for sample sets of 57 (L1), 349 (L2), 53 (L3), 176 (L4), 349 (L5), 480 (L6) and 166 (L7) support an observation that stains

generated on glass exhibit variability in RGB total distribution when exposed to temperate climatic variations over a range of longitudinal periods (*figure 209*).

Figure 213 Box plot distributions of RGB totals for stains generated on glass surfaces across longitudinal sample sets



Across all distributions a general trend can be identified between length of time (number of months) stains were exposed to temperate climatic variations for and R, G, B values and RGB totals. As length of time increased from 1 to 7 months, R-values (*figure 212*), G-values (*appendix 2*), B-values (*appendix 2*) and RGB totals (*figure 213*) did not significantly vary. This suggests that for glass stains, length of environmental exposure did not significantly influence stain colour. Particular features of relationships between length of time (number of months) and R, G, B values and RGB totals are set out for each.

### **7.2.2.3.b Temperature**

*Figures 214 & 215* outline the distribution of R-values and RGB totals for stains generated on glass surfaces across cumulatively averaged temperatures.

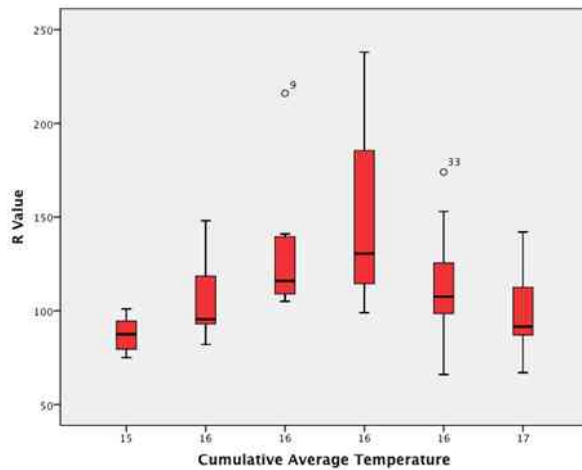


Figure 214 Box plot distributions of R values for stains generated on glass surfaces at cumulatively averaged temperatures

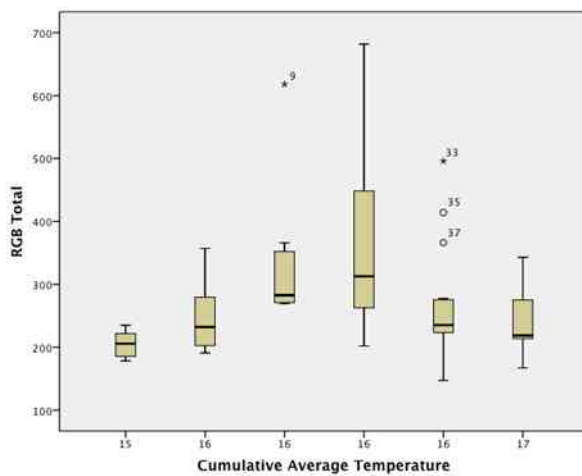


Figure 215 Box plot distributions of RGB Totals for stains generated on glass surfaces at cumulatively averaged temperatures

### 7.2.2.3.c Humidity

Figures 216 & 217 outline distribution of R-values and RGB totals for stains generated on glass surfaces across cumulatively averaged humidity values.

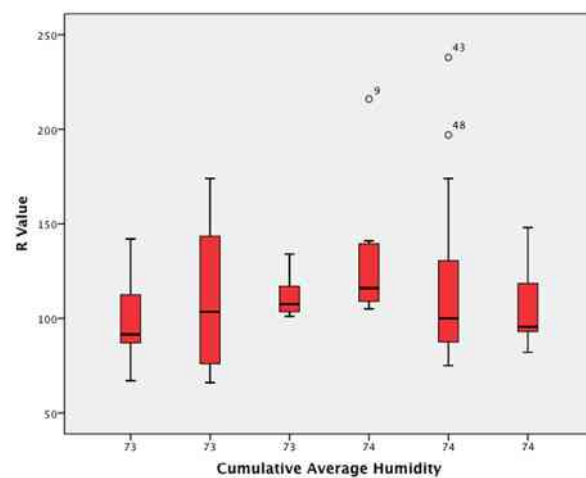


Figure 216 Box plot distributions of R values for stains generated on glass surfaces at cumulatively averaged humidity values

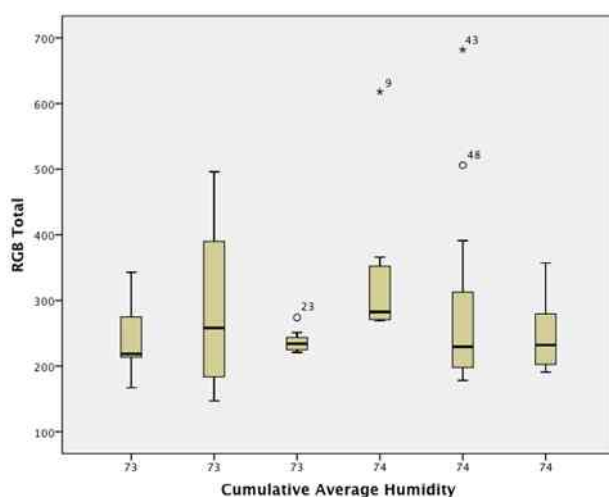


Figure 217 Box plot distributions of RGB totals for stains generated on glass surfaces at cumulatively averaged humidity values

Across all distributions, trends between average temperature, R, G, B values and RGB totals and average humidity, R, G, B values and RGB totals were not identified. Observations indicated average temperature only varied by 2°C and humidity values only varied by 1%. This was not a significant enough variation or range of variations to determine any influence of temperature or humidity over longitudinal periods on stains generated on glass surfaces.

#### **7.2.2.3.d Precipitation**

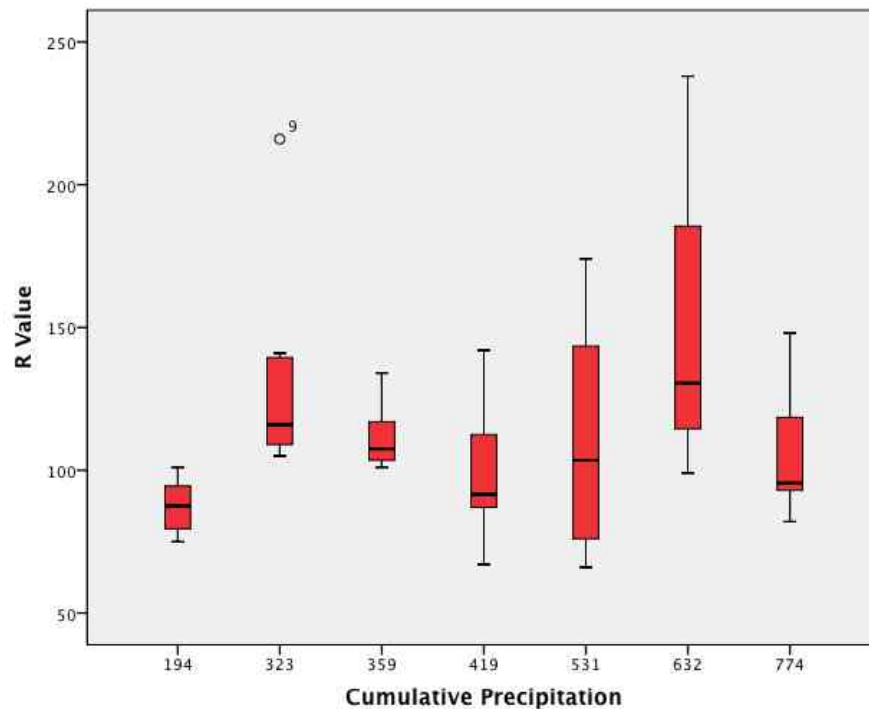
*Figures 218 & 219* outline distribution of R-values and RGB totals for stains generated on glass surfaces exposed to cumulative volumes of precipitation across longitudinal sample sets.

*Figure 218* outlines the distribution of R-values for replicate stains generated in longitudinal sample sets that were exposed to cumulative volumes of precipitation. Across sample sets distributions of recorded R-values varied but there was no clear correlation between variations in R-value distributions and increasing length of time stains were exposed for. Stains exposed for 1 month (sample set L1), 2 months, 3 months (L3), 4 months (L4), 5 months (L5), 6 months (L6) and 7 months (L7) exhibited median R-values of 87.5 (L1), 116.0 (L2), 107.5 (L3), 91.5 (L4), 103.5 (L5), 130.5 (L6) and 95.5 (L7).

Ranges exhibited by each sample set, between minimum and maximum R-values, also varied but there was no clear correlation between variations in range and length of time stains were exposed for. Ranges for sample sets of 26 (L1), 111 (L2), 33

(L3), 75 (L4), 108 (L5), 139 (L6) and 66 (L7) support an observation that stains generated on glass exhibit variability in R-value distribution when exposed to temperate climatic variations over a range of longitudinal periods (*figure 209*).

Figure 218 Box plot distributions of R values for stains generated on glass surfaces and exposed to cumulative volumes of precipitation

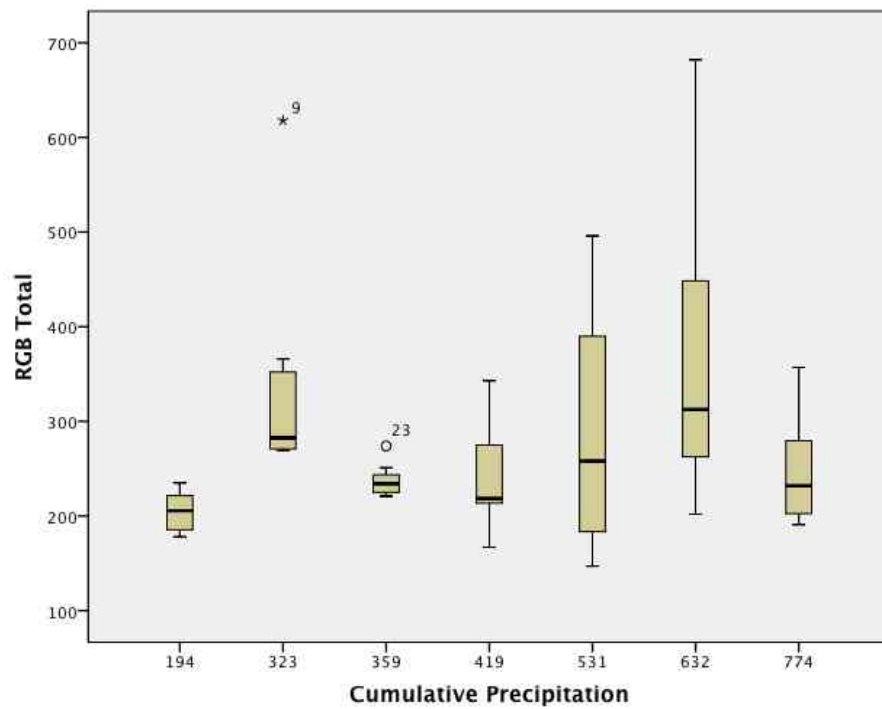


*Figure 219* outlines the distribution of RGB totals for replicate stains generated in longitudinal sample sets that were exposed to cumulative volumes of precipitation. Across sample sets distributions of recorded RGB totals varied but there was no clear correlation between variations in RGB total distributions and increasing length of time stains were exposed for. Stains exposed for 1 month (sample set L1), 2 months, 3 months (L3), 4 months (L4), 5 months (L5), 6 months (L6) and 7 months (L7) exhibited median RGB totals of 205.5 (L1), 282.5 (L2), 234.0 (L3), 218.5 (L4), 258.0 (L5), 312.5 (L6) and 232.0 (L7).

Ranges exhibited by each sample set, between minimum and maximum RGB totals, also varied but there was no clear relationship between variations in range and lengths of time stains were exposed for. Ranges for sample sets of 57 (L1), 349 (L2), 53 (L3), 176 (L4), 349 (L5), 480 (L6) and 166 (L7) support an observation that stains generated on glass exhibit variability in RGB total distribution when exposed to

temperate climatic variations over a range of longitudinal periods (*figure 209*).

Figure 219 Box plot distributions of RGB totals for stains generated on glass surfaces and exposed to cumulative volumes of precipitation



Across all distributions a general trend can be identified between cumulative volumes of precipitation and R, G, B values and RGB totals. As levels of precipitation increased from 194mm to 774mm, R-values (*figure 218*), G-values (*appendix 2*), B-values (*appendix 2*) and RGB totals (*figure 219*) did not appear to vary considerably.

### **7.2.3 Longitudinal stain colour analysis – surface comparison**

This section provides a comparison between the trends and results observed for the three surfaces in order to identify both similarities and differences between stains generated under the same conditions, on different surfaces. Both visual and quantitative analysis of the colours of stains generated on the three different surfaces (paper, glass and denim) are presented.

#### **7.2.3.1 Colour ribbon comparison**

To facilitate visual comparison of colours of stains exposed to a temperate climate for different longitudinal periods, colour ribbons were compiled for all three surfaces (denim, paper and glass) (*figure 220*). Blocks of hexadecimal colour corresponding to individual stain were aligned into longitudinal ribbons according to length of stain exposure.

*Figure 220* provides a visual overview of changes in stain colour between lengths of longitudinal exposure for each surface and how colours of stains compare between denim, paper and glass overall. As all surfaces were stained under the same conditions at the beginning of the 1<sup>st</sup> experimental month and from the same blood source, a reasonable expectation follows that stains might therefore be generally similar in colour. Observations from *figure 220* indicated however that stains generated on denim, paper and glass surfaces vary in colour. Stains generated on denim surfaces generally appear a light tan-brown or beige colour. Stains generated on paper surfaces generally appear much darker hues of brown, grey and even black. Stains generated on glass surfaces generally appear a more varied range of colours, including hues of beige, grey, brown and khaki. A quantitative confirmation of this difference is set out in 7.4.2 and 7.4.3 through comparisons of R, G, B values and RGB totals for all three surfaces. It is also clear that there is no observable trend of colour alteration over time (1-7 months) for the three surfaces (denim, paper, glass) (*figure 220*).



Figure 220 Colour ribbons for stains generated on denim, paper and glass and exposed to a temperate climate across 7 different longitudinal periods. Each individual colour block represents the hexadecimal colour of one replicate stain (total **n** for each surface = 56)



### 7.2.3.2 Comparison of RGB totals between surfaces

Mean RGB totals for each surface are presented in *figures 221 and 222*.

*Figures 221 and 222* outline descriptive statistics for RGB totals calculated from all stains generated on denim, glass and paper. A comparison of mean RGB totals indicates the comparative intensity of stains between denim, glass and paper surfaces, following exposure to a temperate climate for periods of up to 7 months. Stains generated on denim exhibit higher RGB totals (479.86) than those generated on glass (274.57) or paper (143.71), thus denim stains are characterised by lighter intensities of colour than glass and paper stains, as shown in the colour ribbons (*figure 220*).

Figure 221 Descriptive statistics for RGB totals calculated from all stains generated on denim, glass and paper

Surface		Statistic	Std. Error
RGB Total	Denim	Mean	479.86
		Median	21.536
		Std. Deviation	
		Minimum	438
		Maximum	605
		Range	167
	Glass	Mean	274.57
		Median	22.094
		Std. Deviation	
		Minimum	205
		Maximum	366
		Range	161
	Paper	Mean	143.71
		Median	13.031
		Std. Deviation	
		Minimum	101
		Maximum	196
		Range	95

Figure 222 Box plot distributions of average RGB totals for stains generated on denim, glass and paper surfaces

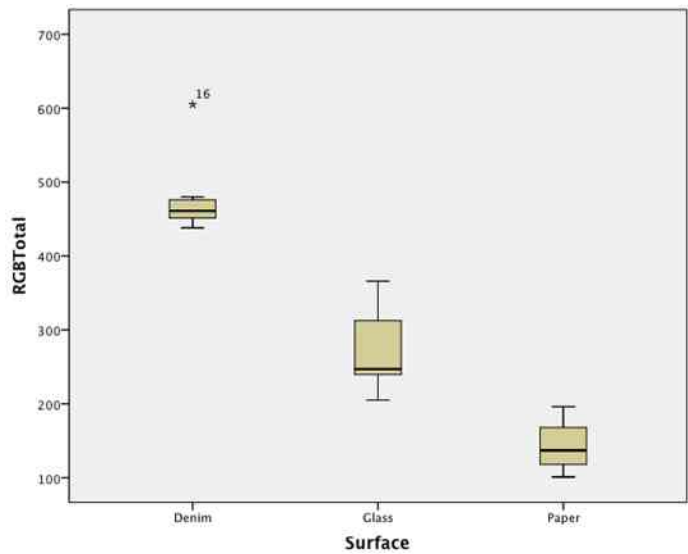
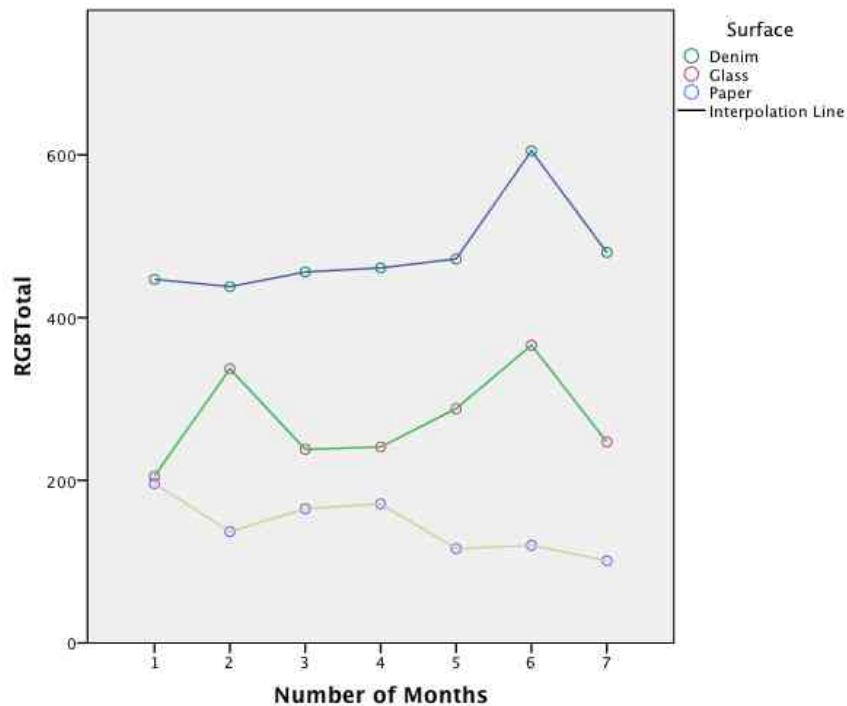


Figure 223 comparatively demonstrates the trends in average RGB totals for stains generated on denim, glass and paper surfaces across all 7 longitudinal sample sets. A slight trend in decreasing RGB totals as length of exposure increases can be identified for paper stains. RGB totals for glass and denim stains by contrast appear to gradually increase as length of exposure increases.

Figure 223 Trends in average RGB totals for stains generated on denim, glass and paper surfaces across longitudinal sample sets



### 7.2.3.3 Comparison of ratios of R, G and B values between surfaces

RGB totals give a measure of intensity of overall stain colour but ratios of R to G and B values give an indication of the significance or strength of colour orientation towards a particular component. Average RGB totals for stains were broken down to calculate average ratios of R, G and B values (*figure 224*) to allow comparison of the colouration of stains between surfaces.

Figure 224 Average R, G and B values for all stains generated in longitudinal sample sets on denim, glass and paper

	N	R Value	G Value	B Value
Denim	56	182.4	163.0	135.0
Glass	56	114.0	90.1	71.0
Paper	56	60.4	47.0	37.0

*Figure 225* illustrates the ratio of average R to G and B values for denim stains. The largest single component of RGB totals for denim stains was R-values (182), however R-values accounted for less than half (38.0%) of RGB totals. Levels of G (163) and B (135) values were significant, making up 34.0% and 28.0% of RGB totals respectively.

*Figure 226* illustrates the ratio of average R to G and B values for glass stains. The largest single component of RGB totals for glass stains was R-values (114), however R-values accounted for less than half (41.5%) of RGB totals. Levels of G (90) and B (71) values were significant, making up 32.7% and 25.8% of RGB totals respectively.

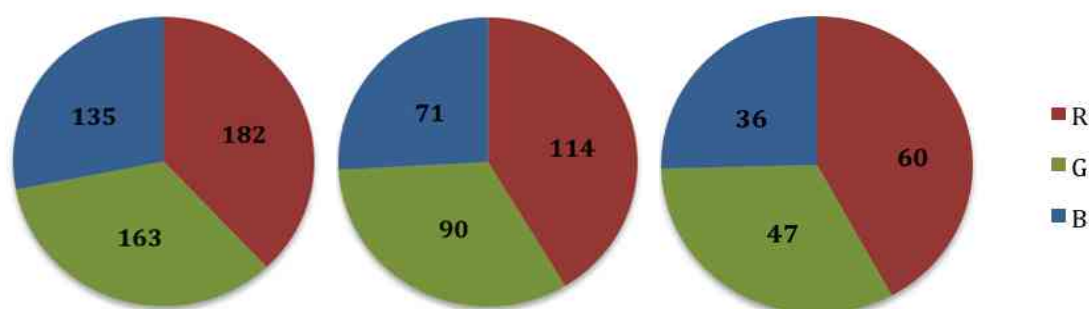
*Figure 227* illustrates the ratio of average R to G and B values for paper stains. The largest single component of RGB totals for paper stains was R-values (60), however R-values accounted for less than half (42.0%) of RGB totals. Levels of G (47) and B (36) values are significant, making up 33.0% and 25.0% of RGB totals respectively.

### Representation of average ratios of R to G and B values for stains

Figure 225 Denim stains

Figure 226 Glass stains

Figure 227 Paper stains



Figures 225-227 demonstrate that longitudinal stains generated on denim, glass and paper surfaces all exhibit balanced ratios of R to G and B values. On average R-values accounted for between 38 - 42%, G-values accounted for between 32.7 – 34% and B-values accounted for between 25 – 28% of RGB totals. This suggests that longitudinal stains on any surface are characterised by even representations of R, G and B values with very slight orientations towards red hues of colour. This will be reflected in observations of grey and brown hues of stain colour for longitudinal stains, confirmed in stain images and colour ribbons in *figure 220*.

Figure 228 presents the results of a Kruskal-Wallis test carried out on longitudinal stains. The Kruskal-Wallis test is a non-parametric statistical method that tests a null hypothesis that three or more unrelated (independent) sets of data have the same distribution (*Laerd Statistics. 2013*). A non-parametric test was used as normality tests conducted on data from experimental stage 2 indicated that datasets were not normally distributed. Results of the test indicated whether the number of months stains were exposed for had a significant effect on R, G, B values and RGB totals. The results (*figure 228*) indicated that the null hypotheses should be retained ( $p > 0.05$  for each test), which meant that distributions of R, G, B values and RGB totals of stains exposed for different longitudinal periods were statistically similar. This confirmed that length of longitudinal exposure did not have a significant influence on stain colour, for stains generated as longitudinal stains in experimental stage 2.

Figure 228 The Kruskal-Wallis test for comparison between distribution of R, G, B values and RGB totals across number of months

	Null Hypothesis	Test	Sig.	Decision
1	The distribution of R Value is the same across categories of Number of Months.	Independent-Samples Kruskal-Wallis Test	.861	Retain the null hypothesis.
2	The distribution of G Value is the same across categories of Number of Months.	Independent-Samples Kruskal-Wallis Test	.943	Retain the null hypothesis.
3	The distribution of B Value is the same across categories of Number of Months.	Independent-Samples Kruskal-Wallis Test	.953	Retain the null hypothesis.
4	The distribution of RGB Total is the same across categories of Number of Months.	Independent-Samples Kruskal-Wallis Test	.959	Retain the null hypothesis.

Asymptotic significances are displayed. The significance level is .05.

Figure 229 presents the results of a Kruskal-Wallis test carried out on longitudinal stains to assess whether there was a significant effect of the surface on the R, G, B and RGB totals. Results indicated that the null hypotheses should be rejected. There is therefore a significant difference between the R, G, B and RGB-values recorded between different surfaces at the 99% significance level ( $p=0.000 < 0.01$ ).

Figure 229 The Kruskal-Wallis test for comparison between distribution of R, G, B values and RGB totals across different surfaces (denim, paper, glass)

	Null Hypothesis	Test	Sig.	Decision
1	The distribution of R Value is the same across categories of Surface.	Independent-Samples Kruskal-Wallis Test	.000	Reject the null hypothesis.
2	The distribution of G Value is the same across categories of Surface.	Independent-Samples Kruskal-Wallis Test	.000	Reject the null hypothesis.
3	The distribution of B Value is the same across categories of Surface.	Independent-Samples Kruskal-Wallis Test	.000	Reject the null hypothesis.
4	The distribution of RGB Total is the same across categories of Surface.	Independent-Samples Kruskal-Wallis Test	.000	Reject the null hypothesis.

Asymptotic significances are displayed. The significance level is .05.

## 7.3 Monthly sample sets


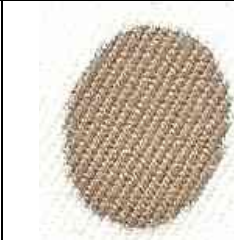
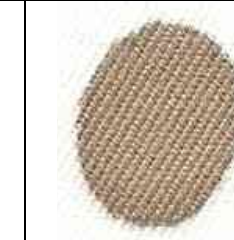

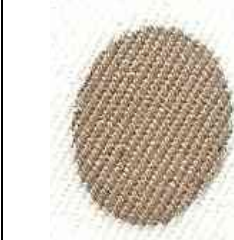
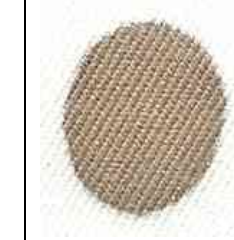

The images captured of individual stains generated in monthly sample sets are set out in section 7.3. Monthly stains are presented in groups, representing individual groups of replicate stains generated on three different surfaces (denim, glass, paper) in each sample set (M1, M2, M3, M4, M5 & M6).

### 7.3.1 Images of monthly sample sets

Images are accompanied by an indication of sample set and surface they correspond to. Underneath each image a ‘stain ID’ is listed, for example C001, this ID refers to a numbering of individual stains for ease of identification. The results of digital measurements of colour for each stain are also given as R, G and B values listed sequentially and a ‘hex code’ that identifies the hexadecimal colour of each stain.








#### 7.3.1.1 Images of monthly sample set M1 (Month 1)

##### 7.3.1.1.1 Figure 230 Stains generated on denim

			
<b>C001</b> RGB 174, 149, 123 Hex: ae967b	<b>C002</b> RGB 177, 153, 126 Hex: b1997e	<b>C003</b> RGB 174, 150, 124 Hex: ae967c	<b>C004</b> RGB 177, 156, 130 Hex: b19c81
			
<b>C005</b> RGB 169, 145, 120 Hex: a99178	<b>C006</b> RGB 169, 146, 120 Hex: a99278	<b>C007</b> RGB 173, 151, 125 Hex: ad977e	<b>C008</b> RGB 171, 148, 123 Hex: ab947b



7.3.1.1.2 Figure 231 Stains generated on glass

			
<b>C009</b> RGB 86, 59, 40 Hex: 563e2d	<b>C010</b> RGB 78, 60, 48 Hex: 4e3b2f	<b>C011</b> RGB 91, 69, 57 Hex: 5b4539	<b>C012</b> RGB 98, 66, 55 Hex: 624236
			
<b>C013</b> RGB 89, 78, 68 Hex: 594e43	<b>C014</b> RGB 75, 57, 46 Hex: 4b392d	<b>C015</b> RGB 81, 61, 52 Hex: 513e35	<b>C016</b> RGB 101, 67, 56 Hex: 654338

7.3.1.1.3 Figure 232 Stains generated on paper

			
<b>C017</b> RGB 71, 70, 62 Hex: 47463e	<b>C018</b> RGB 85, 82, 72 Hex: 555248	<b>C019</b> RGB 91, 89, 77 Hex: 5b594d	<b>C020</b> RGB 85, 84, 73 Hex: 555449
			
<b>C021</b> RGB 84, 77, 64 Hex: 544d40	<b>C022</b> RGB 75, 74, 66 Hex: 4b4a42	<b>C023</b> RGB 54, 42, 35 Hex: 362a23	<b>C024</b> RGB 23, 20, 16 Hex: 171410



### 7.3.1.2 Images of monthly sample set M2 (Month 2)





#### 7.3.1.2.1 Figure 233 Stains generated on denim

			
<b>C025</b> RGB 149, 131, 109 Hex: 95836d	<b>C026</b> RGB 189, 171, 147 Hex: bdab93	<b>C027</b> RGB 167, 149, 126 Hex: a7957e	<b>C028</b> RGB 179, 161, 137 Hex: b3a189
			
	<b>C029</b> RGB 160, 142, 120 Hex: a08e78	<b>C030</b> RGB 161, 143, 121 Hex: a18f79	

#### 7.3.1.2.2 Figure 234 Stains generated on glass


			
<b>C031</b> RGB 228, 227, 200 Hex: e4e3c8	<b>C032</b> RGB 238, 239, 214 Hex: eeefd6	<b>C033</b> RGB 231, 230, 204 Hex: e7e6cc	<b>C034</b> RGB 197, 191, 158 Hex: c5bf9e
			
<b>C035</b> RGB 244, 247, 230 Hex: f4f7e6	<b>C036</b> RGB 241, 244, 222 Hex: flf4e0	<b>C037</b> RGB 227, 225, 197 Hex: e3e1c5	<b>C038</b> RGB 250, 251, 237 Hex: eeedd8

### 7.3.1.2.3 Figure 235 Stains generated on paper



			
<b>C039</b> RGB 58, 52, 44 Hex: 3a342c	<b>C040</b> RGB 93, 88, 77 Hex: 5d584d	<b>C041</b> RGB 54, 54, 49 Hex: 363631	<b>C042</b> RGB 97, 91, 79 Hex: 615b4f
			
	<b>C043</b> RGB 96, 71, 50 Hex: 604732	<b>C044</b> RGB 96, 89, 78 Hex: 60594e	

### 7.3.1.3 Images of monthly sample set M3 (Month 3)

#### 7.3.1.3.1 Figure 236 Stains generated on denim

			
<b>C045</b> RGB 179, 158, 135 Hex: b39e87	<b>C046</b> RGB 151, 131, 110 Hex: 97836e	<b>C047</b> RGB 144, 124, 103 Hex: 907c67	<b>C048</b> RGB 170, 149, 125 Hex: aa957d
			
<b>C049</b> RGB 169, 150, 127 Hex: a9967f	<b>C050</b> RGB 166, 147, 124 Hex: a6937c	<b>C051</b> RGB 174, 155, 130 Hex: ae9b82	<b>C052</b> RGB 168, 148, 125 Hex: a8947d

7.3.1.3.2 Figure 237 Stains generated on glass

			
<b>C053</b> RGB 120, 63, 57 Hex: 783f39	<b>C054</b> RGB 107, 64, 60 Hex: 6b403c	<b>C055</b> RGB 110, 58, 54 Hex: 6e3a36	<b>C056</b> RGB 102, 54, 50 Hex: 663632
			
<b>C057</b> RGB 119, 64, 59 Hex: 77403b	<b>C058</b> RGB 94, 57, 53 Hex: 5e3935	<b>C059</b> RGB 107, 60, 56 Hex: 6b3e38	<b>C060</b> RGB 112, 62, 57 Hex: 703e39

7.3.1.3.3 Figure 238 Stains generated on paper

			
<b>C061</b> RGB 98, 47, 39 Hex: 622f27	<b>C062</b> RGB 73, 52, 39 Hex: 493427	<b>C063</b> RGB 138, 96, 70 Hex: 8a6046	<b>C064</b> RGB 100, 42, 32 Hex: 642a20
			
<b>C065</b> RGB 45, 37, 31 Hex: 2d251f	<b>C066</b> RGB 54, 29, 24 Hex: 361d18	<b>C067</b> RGB 98, 40, 32 Hex: 622820	<b>C068</b> RGB 105, 75, 58 Hex: 694b3a










### 7.3.1.4 Images of monthly sample set M4 (Month 4)

#### 7.3.1.4.1 Figure 239 Stains generated on denim

			
<b>C069</b> RGB 179, 155, 127 Hex: b39b7f	<b>C070</b> RGB 179, 155, 127 Hex: b39b7f	<b>C071</b> RGB 179, 157, 128 Hex: b39d80	<b>C072</b> RGB 178, 156, 128 Hex: b29c80
			
<b>C073</b> RGB 175, 152, 124 Hex: af987c	<b>C074</b> RGB 177, 156, 127 Hex: b19c7f	<b>C075</b> RGB 173, 151, 123 Hex: ad977b	<b>C076</b> RGB 174, 153, 125 Hex: ae997d

#### 7.3.1.4.2 Figure 240 Stains generated on glass

			
<b>C077</b> RGB 125, 71, 44 Hex: 7d472c	<b>C078</b> RGB 103, 44, 21 Hex: 672c15	<b>C079</b> RGB 163, 130, 106 Hex: a3826a	<b>C080</b> RGB 136, 82, 45 Hex: 88522d
			
<b>C081</b> RGB 174, 135, 97 Hex: ae8761	<b>C082</b> RGB 164, 126, 85 Hex: a47e55	<b>C083</b> RGB 206, 188, 159 Hex: cebc9f	<b>C084</b> RGB 180, 152, 116 Hex: b49874

7.3.1.4.3 Figure 241 Stains generated on paper









			
<b>C085</b> RGB 120, 73, 46 Hex: 78492e	<b>C086</b> RGB 100, 53, 32 Hex: 643520	<b>C087</b> RGB 103, 49, 31 Hex: 67311f	<b>C088</b> RGB 113, 56, 32 Hex: 713820
			
<b>C089</b> RGB 126, 71, 41 Hex: 7e4729	<b>C090</b> RGB 142, 93, 58 Hex: 8e5d3a	<b>C091</b> RGB 95, 45, 29 Hex: 5f2d1d	<b>C092</b> RGB 105, 66, 45 Hex: 69422d

7.3.1.5 Images of monthly sample set M5 (Month 5)

7.3.1.5.1 Figure 242 Stains generated on denim

			
<b>C093</b> RGB 170, 146, 119 Hex: aa9277	<b>C094</b> RGB 168, 141, 114 Hex: a88d72	<b>C095</b> RGB 176, 152, 123 Hex: b0987b	<b>C096</b> RGB 170, 143, 116 Hex: aa8f74
			
<b>C097</b> RGB 170, 148, 120 Hex: aa9478	<b>C098</b> RGB 165, 140, 112 Hex: a58c70	<b>C099</b> RGB 171, 147, 119 Hex: ab9377	<b>C100</b> RGB 161, 135, 107 Hex: a1876b

7.3.1.5.2 Figure 243 Stains generated on glass

			
<b>C101</b> RGB 113, 83, 69 Hex: 715345	<b>C102</b> RGB 105, 62, 43 Hex: 693e2b	<b>C103</b> RGB 117, 73, 49 Hex: 754931	<b>C104</b> RGB 144, 104, 69 Hex: 906845
			
<b>C105</b> RGB 114, 58, 36 Hex: 723a24	<b>C106</b> RGB 115, 71, 50 Hex: 734732	<b>C107</b> RGB 126, 88, 63 Hex: 7e583f	<b>C108</b> RGB 129, 78, 52 Hex: 814e34






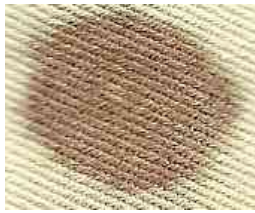


7.3.1.5.3 Figure 244 Stains generated on paper

			
<b>C109</b> RGB 120, 78, 57 Hex: 784e39	<b>C110</b> RGB 71, 51, 39 Hex: 473327	<b>C111</b> RGB 120, 71, 49 Hex: 784731	<b>C112</b> RGB 120, 78, 55 Hex: 784e37
			
<b>C113</b> RGB 113, 70, 53 Hex: 714635	<b>C114</b> RGB 108, 65, 44 Hex: 6c412c	<b>C115</b> RGB 92, 76, 66 Hex: 5c4c42	<b>C116</b> RGB 132, 103, 72 Hex: 846748



### 7.3.1.6 Images of monthly sample set M6 (Month 6)

#### 7.3.1.6.1 Figure 245 Stains generated on denim

			
<b>C117</b> RGB 162, 136, 106 Hex: a2886a	<b>C118</b> RGB 174, 154, 124 Hex: ae9a7c	<b>C119</b> RGB 158, 131, 103 Hex: 9e8367	<b>C120</b> RGB 161, 135, 105 Hex: a18769
			
<b>C121</b> RGB 152, 120, 93 Hex: 98785d	<b>C122</b> RGB 156, 126, 97 Hex: 9c7e61	<b>C123</b> RGB 151, 119, 93 Hex: 97775d	<b>C124</b> RGB 153, 122, 95 Hex: 997a5f

#### 7.3.1.6.2 Figure 246 Stains generated on glass

			
<b>C125</b> RGB 79, 26, 16 Hex: 4f1a10	<b>C126</b> RGB 84, 25, 16 Hex: 541910	<b>C127</b> RGB 80, 27, 17 Hex: 501b11	<b>C128</b> RGB 79, 26, 16 Hex: 4f1a10
			
<b>C129</b> RGB 76, 22, 13 Hex: 4c160d	<b>C130</b> RGB 77, 30, 21 Hex: 4d1e15	<b>C131</b> RGB 81, 29, 19 Hex: 511d13	<b>C132</b> RGB 82, 31, 22 Hex: 521f16

**7.3.1.6.3** Figure 247 Stains generated on paper

			
<b>C133</b> RGB 77, 44, 36 Hex: 4d2c24	<b>C134</b> RGB 97, 55, 40 Hex: 613728	<b>C135</b> RGB 83, 43, 36 Hex: 532b24	<b>C136</b> RGB 83, 50, 43 Hex: 53322b
			
<b>C137</b> RGB 77, 41, 34 Hex: 4d2922	<b>C138</b> RGB 81, 43, 35 Hex: 512b23	<b>C139</b> RGB 93, 38, 25 Hex: 5d2619	<b>C140</b> RGB 100, 49, 38 Hex: 643126

## 7.3.2 Monthly stain colour analysis

Once stains had been scanned and captured in a digital format, stain images were imported into colour analysis software and quantitative information about stain colour was extracted from the images as outlined in 7.2.2.

### 7.3.2.1 Stains generated in monthly denim sample sets

The measurements derived for stains on denim surfaces from monthly sample sets are presented in *figure 248*. Descriptive statistics are then presented in *figures 249* and *250*.



Figure 248 Table of measurements recorded for stains generated on denim surfaces in monthly sample sets

Stain ID	Surface	Month	Average Temperature /°C	Average Humidity /%	Total Precipitation /mm	R Value	G Value	B Value	RGB Total	Hex	Hex Colour
C001	Denim	1	17.4	73	129.0	174	149	123	446	ae967b	
C002	Denim	1	17.4	73	129.0	177	153	126	456	b1997e	
C003	Denim	1	17.4	73	129.0	174	150	124	448	ae967c	
C004	Denim	1	17.4	73	129.0	177	156	130	463	b19c81	
C005	Denim	1	17.4	73	129.0	169	145	120	434	a99178	
C006	Denim	1	17.4	73	129.0	169	146	120	435	a99278	
C007	Denim	1	17.4	73	129.0	173	151	125	449	ad977e	
C008	Denim	1	17.4	73	129.0	171	148	123	442	ab947b	
C025	Denim	2	19.3	70	35.9	149	131	109	389	95836d	
C026	Denim	2	19.3	70	35.9	189	171	147	507	bdab93	
C027	Denim	2	19.3	70	35.9	167	149	126	442	a7957e	
C028	Denim	2	19.3	70	35.9	179	161	137	477	b3a189	
C029	Denim	2	19.3	70	35.9	160	142	120	422	a08e78	
C030	Denim	2	19.3	70	35.9	161	143	121	425	a18f79	
C045	Denim	3	15.3	70	60.2	179	158	135	472	b39e87	
C046	Denim	3	15.3	70	60.2	151	131	110	392	97836e	
C047	Denim	3	15.3	70	60.2	144	124	103	371	907c67	
C048	Denim	3	15.3	70	60.2	170	149	125	444	aa957d	
C049	Denim	3	15.3	70	60.2	169	150	127	446	a9967f	
C050	Denim	3	15.3	70	60.2	166	147	124	437	a6937c	
C051	Denim	3	15.3	70	60.2	174	155	130	459	ae9b82	
C052	Denim	3	15.3	70	60.2	168	148	125	441	a8947d	
C069	Denim	4	11.3	83	112.0	179	155	127	461	b39b7f	
C070	Denim	4	11.3	83	112.0	179	155	127	461	b39b7f	
C071	Denim	4	11.3	83	112.0	179	157	128	464	b39d80	
C072	Denim	4	11.3	83	112.0	178	156	128	462	b29c80	
C073	Denim	4	11.3	83	112.0	175	152	124	451	af987c	
C074	Denim	4	11.3	83	112.0	177	156	127	460	b19c7f	
C075	Denim	4	11.3	83	112.0	173	151	123	447	ad977b	
C076	Denim	4	11.3	83	112.0	174	153	123	450	ae997d	
C093	Denim	5	8.6	86	100.8	170	146	119	435	aa9277	
C094	Denim	5	8.6	86	100.8	168	141	114	423	a88d72	
C095	Denim	5	8.6	86	100.8	176	152	123	451	b0987b	
C096	Denim	5	8.6	86	100.8	170	143	116	429	aa8f74	
C097	Denim	5	8.6	86	100.8	170	148	120	438	aa9478	
C098	Denim	5	8.6	86	100.8	165	140	112	417	a58c70	
C099	Denim	5	8.6	86	100.8	171	147	119	437	ab9377	
C100	Denim	5	8.6	86	100.8	161	135	107	403	a1876b	
C117	Denim	6	6.5	85	142.0	162	136	106	404	a2886a	
C118	Denim	6	6.5	85	142.0	174	154	124	452	ae9a7c	
C119	Denim	6	6.5	85	142.0	158	131	103	392	9e8367	
C120	Denim	6	6.5	85	142.0	161	135	105	401	a18769	
C121	Denim	6	6.5	85	142.0	152	120	93	365	98785d	
C122	Denim	6	6.5	85	142.0	156	126	97	379	9c7e61	
C123	Denim	6	6.5	85	142.0	151	119	93	363	97775d	
C124	Denim	6	6.5	85	142.0	153	122	95	370	996a5f	

Figure 249 outlines mean R, G, B values and RGB totals calculated from replicate stains (n = 8) in each of 6 monthly sample sets. In each monthly sample set R-values were greater than G and B-values. G and B-values recorded for each sample set were also high however, which meant for some sample sets R-values were only slightly higher than G and B values. For example, in the M3 sample set the average R-value was 165.3, average G-value was 145.3 and average B-value was 122.3.

R-values for all sample sets fell between a low of 158.4 (M6) and a highest value of 177.0 observed for the M4 sample set. G-values across all sample sets fell between a recorded low of 130.4 (M6) and a high of 154.4 (M4). B-values were recorded between a low of 102.0 (M6) and a high of 126.6 (M2). There was no overlap between ranges of R, G and B values recorded. Results demonstrate that whilst R, G and B-values were sometimes represented in similar levels in each sample set, for each sample set R-values represented the highest colour component, followed by G-values and finally B-values which represented the lowest individual colour component. The dominance of R-values suggests stains generated on denim and exposed to a range of monthly periods are all coloured towards red, rather than green or blue hues of colour. Observations of similarly high levels of R, G and B values support observations of a tan-brown colour of stains (*figure 248*). An RGB triplet for a light tan-brown colour are typically represented by similar figures in each of R, G and B values, approximately half-way between 000 (black) and 255 (white), for example RGB (R210, G180, B140).

Figure 249 Descriptive statistics recorded for stains generated on denim surfaces in monthly sample sets

Sample Set		R Value	G Value	B Value	RGB Total
<b>M1</b>	Mean	173.0	150.0	124.0	447.0
	Std. Deviation	3.2	4.0	3.3	10.0
<b>M2</b>	Mean	167.5	149.5	126.6	443.6
	Std. Deviation	14.4	14.4	13.5	42.3
<b>M3</b>	Mean	165.3	145.3	122.4	432.8
	Std. Deviation	11.7	11.7	10.6	34.0
<b>M4</b>	Mean	177.0	154.4	126.0	457.0
	Std. Deviation	2.4	2.1	4.4	6.5
<b>M5</b>	Mean	169.0	144.0	116.3	429.1
	Std. Deviation	4.4	5.3	5.1	14.7
<b>M6</b>	Mean	158.4	130.4	102.0	390.8
	Std. Deviation	7.5	11.6	10.3	29.3

Figure 250 sets out average colour values for all denim stains. Average R, G and B values were calculated between all replicate stains in all monthly sample sets.

Average values for stains generated on denim were R (168.30), G (145.37) and B (119.20). Stains exhibit a higher ratio of R to G and B colour components indicating that stains were coloured towards a red rather than green or blue hue. Levels of R, G and B values were approximately halfway between values of 000 (black) and 255 (white), which corresponds to the medium intensity observed in monthly stains generated on denim (*figure 248*). The combination of a slight orientation towards red hues of colour and a medium intensity of colour indicate that stains generated on denim, on average, were characterised by a light brown or tan colouring.

Figure 250 Average R, G and B values for all monthly stains generated on denim

	N	Minimum	Maximum	Mean	Std. Deviation
R Value	46	144	189	168.30	9.736
G Value	46	119	171	145.37	11.523
B Value	46	93	147	119.20	32.227
Valid N (listwise)	46				

### 7.3.2.1.a Sample Sets

*Figures 251 & 252* outline the distribution of R-values and RGB totals for stains generated on denim surfaces across monthly sample sets. Distributions across monthly sample sets were compared to establish whether there were any differences between stains exposed to months characterised by different climatic characteristics (temperature, humidity and precipitation).

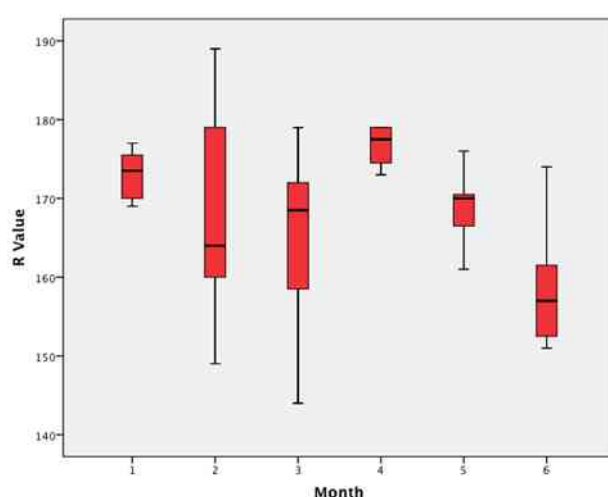


Figure 251 Box plot distributions of R values for stains generated on denim surfaces across monthly sample sets

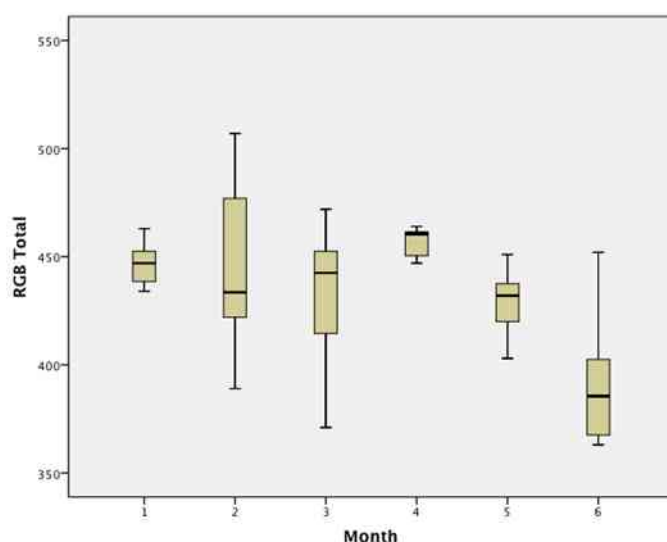


Figure 252 Box plot distributions of RGB totals for stains generated on denim surfaces across monthly sample sets

Results indicated that R (*figure 251*), G (*appendix 2*), B values (*appendix 2*) and RGB totals (*figure 252*) demonstrated minimal variability between all monthly sets, with a maximum range of 19 (mean R-values), 19.6 (mean G-values), 24.6 (mean B-values) and 66.2 (mean RGB total) between all monthly sets. This suggests that for denim stains, monthly variations in climatic characteristics (over the course of experimental stage 2) did not significantly influence stain colour, which was supported by observations of stain colours in *figure 248*. To determine whether variability observed in R, G, B values and RGB totals was linked to individual climatic characteristics (temperature, humidity, precipitation), the influence of each of these characteristics on stain colour was also examined.

### **7.3.2.1.b Temperature**

*Figures 253 & 254* outline distribution of R-values and RGB totals for stains generated on denim surfaces, which were exposed to different temperatures according to monthly sample set.

*Figure 253* outlines the distribution of R-values for replicate stains ( $n = 8$ ) generated in each monthly sample set and exposed to different mean monthly temperatures. Stains exposed to the lowest temperature ( $7^{\circ}\text{C}$ ) exhibited the lowest median R-value of 157.0. As temperature increased to  $11^{\circ}\text{C}$ , median R-values increased to a high of 177.5. From  $15^{\circ}\text{C}$  to  $19^{\circ}\text{C}$  median R-values decreased slightly and then remained relatively consistent: 168.5 ( $15^{\circ}\text{C}$ ), 173.5 ( $17^{\circ}\text{C}$ ) and 164.0 ( $19^{\circ}\text{C}$ ). This supports a suggestion that as temperature increases from  $7^{\circ}\text{C}$  to  $11^{\circ}\text{C}$ , R-values of stains

generated on denim generally increase. At higher temperatures (15°C to 19°C) R-values for stains generated on denim decrease and appear to plateau.

Significant ranges between minimum and maximum R-values were exhibited by sample sets exposed to temperatures of 7°C (23), 15°C (35) and 19°C (40). The presence of significant ranges suggests that R-value distributions for denim stains are variable across sample sets.

Figure 253 Box plot distributions of R values for stains generated on denim surfaces exposed to different temperature averages

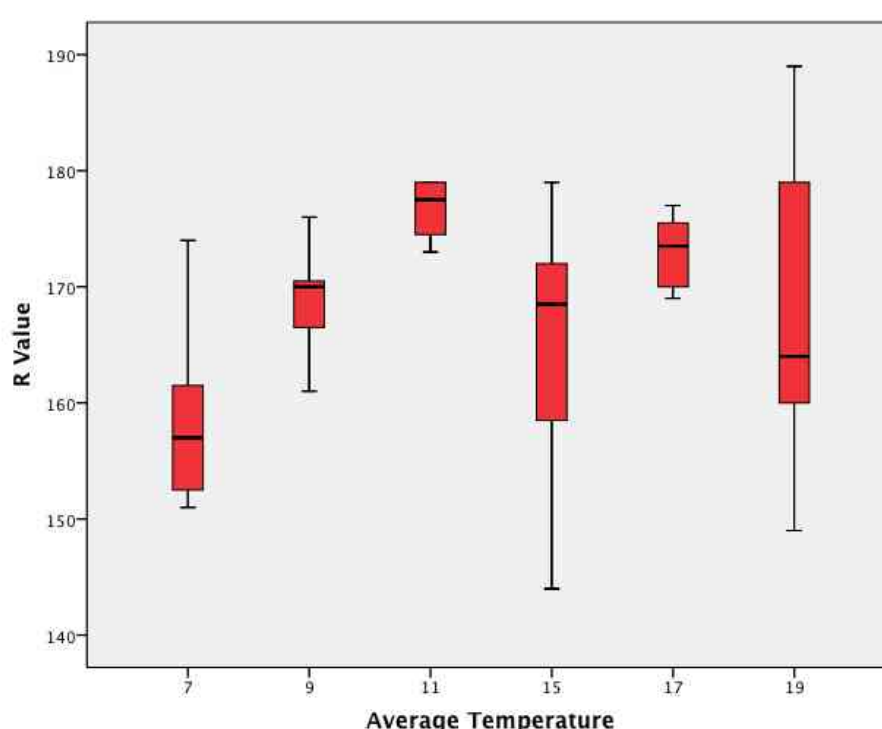
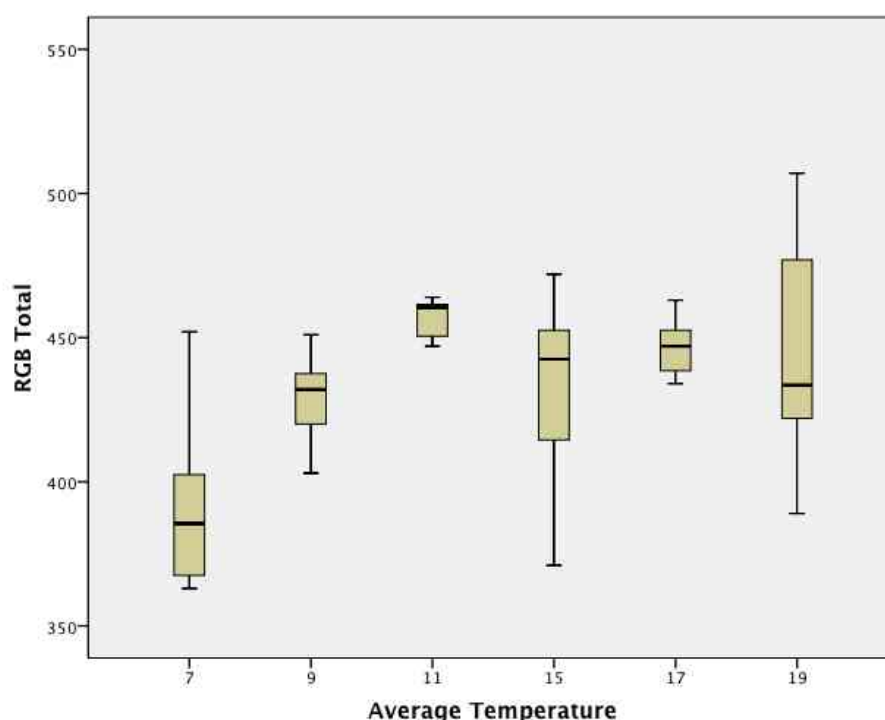


Figure 254 outlines the distribution of RGB totals for replicate stains ( $n = 8$ ) generated in each monthly sample set and exposed to different average temperatures. Stains exposed to the lowest temperature (7°C) exhibited the lowest median RGB total of 385.5. As temperature increased to 11°C, median RGB totals increased to a high of 460.5. From 15°C to 19°C median RGB totals decreased slightly and then remained relatively consistent: 442.5 (15°C), 447.0 (17°C) and 433.5 (19°C). This supports a suggestion that as temperature increases from 7°C to 11°C, RGB totals of stains generated on denim generally increase. At higher temperatures (15°C to 19°C) RGB totals for stains generated on denim decrease and appear to plateau.

Significant ranges between minimum and maximum RGB totals were exhibited by sample sets exposed to temperatures of 7°C (89), 15°C (101) and 19°C (118). The presence of significant ranges suggests that RGB total distributions for denim stains are variable across sample sets.

Figure 254 Box plot distributions of RGB Totals for stains generated on denim surfaces exposed to different temperature averages



Across all four distributions a general trend between average temperature, R, G, B values and RGB totals was identified. As temperature increased from 7°C to 11°C, R-values (*figure 253*), G-values (*appendix 2*), B-values (*appendix 2*) and RGB totals (*figures 254*) increased. As temperatures increased from 11°C to 19°C values stopped increasing and appeared to plateau.

### **7.3.2.1.c Humidity**

*Figures 255 & 256* outline distribution of R-values and RGB totals for stains generated on denim surfaces exposed to different average humidity levels across monthly sample sets.

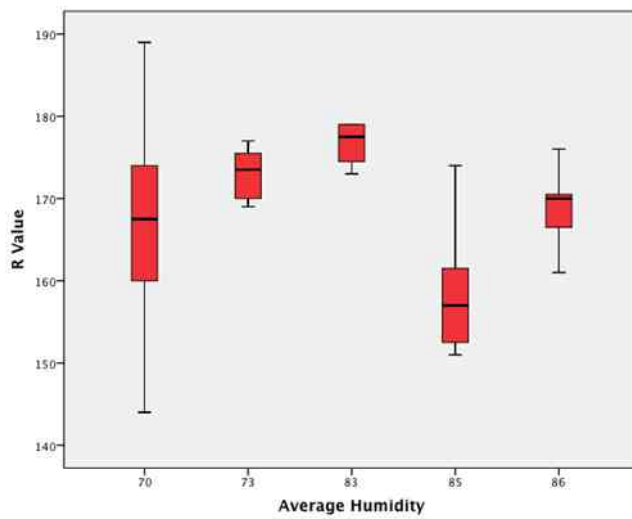


Figure 255 Box plot distributions of R values for stains generated on denim surfaces exposed to different humidity averages

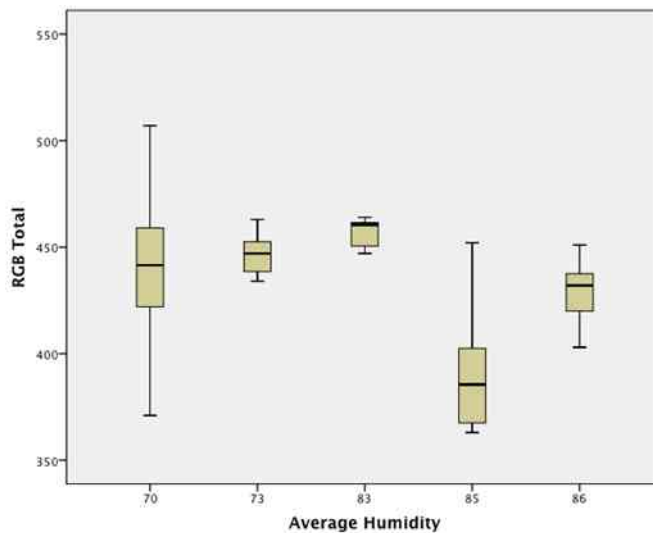


Figure 256 Box plot distributions of RGB totals for stains generated on denim surfaces exposed to different humidity averages

Across all box-plots, trends between increases in average humidity and R-values (figure 255), G-values (appendix 2), B-values (appendix 2) and RGB totals (figure 256) were not identified.

#### **7.3.2.1.d Precipitation**

Figures 257 & 258 outline distribution of R-values and RGB totals for stains generated on denim surfaces exposed to different volumes of precipitation across monthly sample sets.

Figure 257 outlines the distribution of R-values for replicate stains exposed to different volumes of precipitation. Across sample sets, distributions of recorded R-values varied but there was no clear relationship between variations in R-value

distributions and increasing levels of precipitation stains were exposed to. Stains exposed to precipitation totals of 36mm, 60mm, 101mm, 112mm, 129mm and 142mm exhibited median R-values of 164.0 (36mm), 168.5 (60mm), 170.0 (101mm), 177.5 (112mm), 173.5 (129mm) and 157.0 (142mm).

Ranges exhibited by each sample set, between minimum and maximum R-values, also varied but there was no clear relationship between variations in range and total volume of precipitation stains were exposed to. Ranges for sample sets of 35 (36mm), 35 (60mm), 15 (101mm), 6 (112mm), 8 (129mm) and 23 (142mm) support an observation that stains generated on denim exhibit variability in R-value distribution when exposed to different volumes of precipitation over a range of monthly periods.

Figure 257 Box plot distributions of R values for stains generated on denim surfaces and exposed to different volumes of precipitation

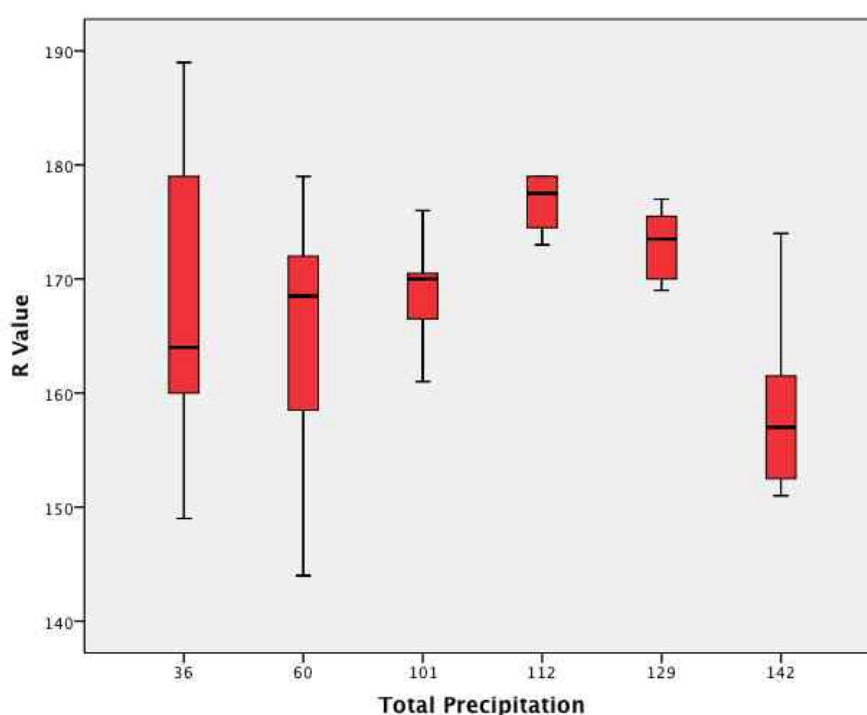


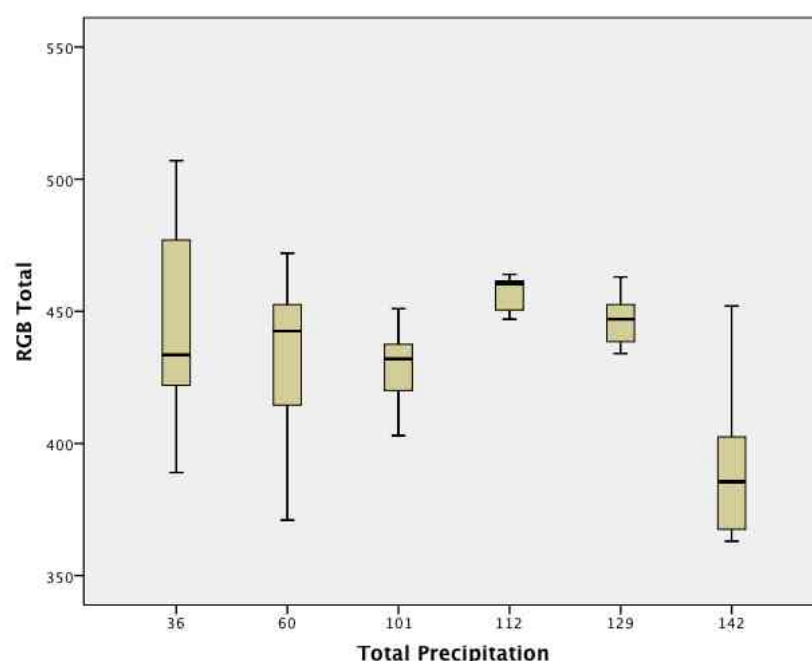
Figure 258 outlines the distribution of RGB totals for replicate stains exposed to different volumes of precipitation. Across sample sets distributions of recorded RGB totals varied but there was no clear correlation between variations in RGB total distributions and increasing levels of precipitation stains were exposed to. Stains exposed to precipitation totals of 36mm, 60mm, 101mm, 112mm, 129mm and



142mm exhibited median RGB totals of 433.5 (36mm), 442.5 (60mm), 432.0 (101mm), 460.5 (112mm), 477.0 (129mm) and 385.5 (142mm).

Ranges exhibited by each sample set, between minimum and maximum RGB totals, also varied but there was no clear relationship between variations in range and total volume of precipitation stains were exposed to. Ranges for sample sets of 118 (36mm), 101 (60mm), 48 (101mm), 17 (112mm), 29 (129mm) and 89 (142mm) support an observation that stains generated on denim exhibit variability in RGB total distribution when exposed to different volumes of precipitation over a range of monthly periods.

Figure 258 Box plot distributions of RGB totals for stains generated on denim surfaces and exposed to different volumes of precipitation



As levels of precipitation increased from 36mm to 142mm, R-values (*figure 257*), G-values (*appendix 2*), B-values (*appendix 2*) and RGB totals (*figure 258*) did not significantly vary.

### 7.3.2.2 Stains generated in monthly paper sample sets

The measurements derived for stains on paper surfaces from monthly sample sets are presented in *figure 259*. Descriptive statistics are then presented in *figures 260* and *261*.

Figure 259 Table of measurements recorded for stains generated on paper surfaces in monthly sample sets

Stain ID	Surface	Month	Average Temperature /oC	Average Humidity /%	Total Precipitation /mm	R Value	G Value	B Value	RGB Total	Hex	Hex Colour
C017	Paper	1	17.4	73	129.0	71	70	62	203	47463e	
C018	Paper	1	17.4	73	129.0	85	82	72	239	555248	
C019	Paper	1	17.4	73	129.0	91	89	77	257	5b594d	
C020	Paper	1	17.4	73	129.0	85	84	73	242	555449	
C021	Paper	1	17.4	73	129.0	84	77	64	225	544d40	
C022	Paper	1	17.4	73	129.0	75	74	66	215	4b4a42	
C023	Paper	1	17.4	73	129.0	54	42	35	131	362a23	
C024	Paper	1	17.4	73	129.0	23	20	16	59	171410	
C039	Paper	2	19.3	70	35.9	58	52	44	154	3a342c	
C040	Paper	2	19.3	70	35.9	93	88	77	258	5d584d	
C041	Paper	2	19.3	70	35.9	54	54	49	157	363631	
C042	Paper	2	19.3	70	35.9	97	91	79	267	615b4f	
C043	Paper	2	19.3	70	35.9	96	71	50	217	604732	
C044	Paper	2	19.3	70	35.9	96	89	78	263	60594e	
C061	Paper	3	15.3	70	60.2	98	47	39	184	622f27	
C062	Paper	3	15.3	70	60.2	73	52	39	164	493427	
C063	Paper	3	15.3	70	60.2	138	96	70	304	8a6046	
C064	Paper	3	15.3	70	60.2	100	42	32	174	642a20	
C065	Paper	3	15.3	70	60.2	45	37	31	113	2d251f	
C066	Paper	3	15.3	70	60.2	54	29	24	107	361d18	
C067	Paper	3	15.3	70	60.2	98	40	32	170	622820	
C068	Paper	3	15.3	70	60.2	105	75	58	238	694b3a	
C085	Paper	4	11.3	83	112.0	120	73	46	239	78492e	
C086	Paper	4	11.3	83	112.0	100	53	32	185	643520	
C087	Paper	4	11.3	83	112.0	103	49	31	183	67311f	
C088	Paper	4	11.3	83	112.0	113	56	32	201	713820	
C089	Paper	4	11.3	83	112.0	126	71	41	238	7e4729	
C090	Paper	4	11.3	83	112.0	142	93	58	293	8e5d3a	
C091	Paper	4	11.3	83	112.0	95	45	29	169	5f2d1d	
C092	Paper	4	11.3	83	112.0	105	66	45	216	69422d	
C109	Paper	5	8.6	86	100.8	120	78	57	255	784e39	
C110	Paper	5	8.6	86	100.8	71	51	39	161	473327	
C111	Paper	5	8.6	86	100.8	120	71	49	240	784731	
C112	Paper	5	8.6	86	100.8	120	78	55	253	784e37	
C113	Paper	5	8.6	86	100.8	113	70	53	236	714635	
C114	Paper	5	8.6	86	100.8	108	65	44	217	6c412c	
C115	Paper	5	8.6	86	100.8	92	76	66	234	5c4c42	
C116	Paper	5	8.6	86	100.8	132	103	72	307	846748	
C133	Paper	6	6.5	85	142.0	77	44	36	157	4d2c24	
C134	Paper	6	6.5	85	142.0	97	55	40	192	613728	
C135	Paper	6	6.5	85	142.0	83	43	36	162	532b24	
C136	Paper	6	6.5	85	142.0	83	50	43	176	53322b	
C137	Paper	6	6.5	85	142.0	77	41	34	152	4d2922	
C138	Paper	6	6.5	85	142.0	81	43	35	159	512b23	
C139	Paper	6	6.5	85	142.0	93	38	25	156	5d2619	
C140	Paper	6	6.5	85	142.0	100	49	38	187	643126	

Figure 260 outlines mean R, G, B values and RGB totals calculated from replicate stains (n = 8) in each of 6 monthly sample sets. In each monthly sample set R-values were greater than G and B-values. G and B-values recorded for each sample set were also high however, which meant for some sample sets R-values were only slightly higher than G and B values. For example, in the M1 sample set the average R-value was 71.0, average G-value was 67.3 and average B-value was 58.1.

R-values for all sample sets ranged between a low of 71.0 (M1) and a highest value of 113.0 observed for the M4 sample set. G-values across all sample sets fell between a recorded low of 52.3 (M3) and a high of 74.2 (M2). B-values were recorded between a low of 39.3 (M4) and a high of 62.8 (M2). Results demonstrate that whilst R, G and B-values were sometimes represented in similar levels in each sample set, for each sample set R-values represented the highest colour component, followed by G-values and finally B-values which represented the lowest individual colour component. The dominance of R-values suggests stains generated on paper and exposed to a range of monthly periods are all coloured towards red, rather than green or blue hues of colour. Observations of similarly high levels of R, G and B values with an orientation towards red hues of colour support observations of grey or brown colours of stains (*figure 259*).

Figure 260 Descriptive statistics recorded for stains generated on paper surfaces in monthly sample sets

Sample Set		R Value	G Value	B Value	RGB Total
<b>M1</b>	Mean	71.0	67.3	58.1	196.4
	Std. Deviation	22.6	23.8	21.4	68.0
<b>M2</b>	Mean	82.3	74.2	62.8	219.3
	Std. Deviation	20.5	18.0	16.8	53.0
<b>M3</b>	Mean	89.0	52.3	40.6	182.0
	Std. Deviation	30.1	22.3	15.5	64.3
<b>M4</b>	Mean	113.0	63.3	39.3	215.5
	Std. Deviation	15.7	15.8	10.1	40.4
<b>M5</b>	Mean	109.5	74.0	54.4	237.8
	Std. Deviation	19.4	14.7	11.0	40.8
<b>M6</b>	Mean	86.4	45.4	36.0	167.6
	Std. Deviation	9.0	5.5	5.3	15.3

Figure 261 sets out mean colour values for all paper stains. Average R, G and B values were calculated between all replicate stains in all monthly sample sets. Average values for stains generated on paper were R (92.26), G (62.22) and B (47.89). Stains exhibit a higher ratio of R to G and B colour components indicating

that stains were coloured towards a red rather than green or blue hue. Levels of R, G and B values were low (below 100), which corresponds to the dark intensities of colour in monthly stains generated on denim (*figure 259*). For one stain (C024) R, G and B values recorded were so low (R23, G20, B16) the stain appeared black. The combination of a slight orientation towards red hues of colour and dark intensities of colour indicate that, on average, stains generated on paper were characterised by a dark brown or grey colouring.

Figure 261 Average R, G and B values for all monthly stains generated on paper

	N	Minimum	Maximum	Mean	Std. Deviation
R Value	46	23	142	92.26	24.651
G Value	46	20	103	62.22	19.883
B Value	46	16	79	47.89	16.802
Valid N (listwise)	46				

### 7.3.2.2.a Sample Sets

*Figures 262 & 263* outline distributions of R-values and RGB totals for stains generated on paper surfaces across monthly sample sets. Distributions across monthly sample sets were compared to establish whether there were any differences between stains exposed to months characterised by different climatic characteristics (temperature, humidity and precipitation).

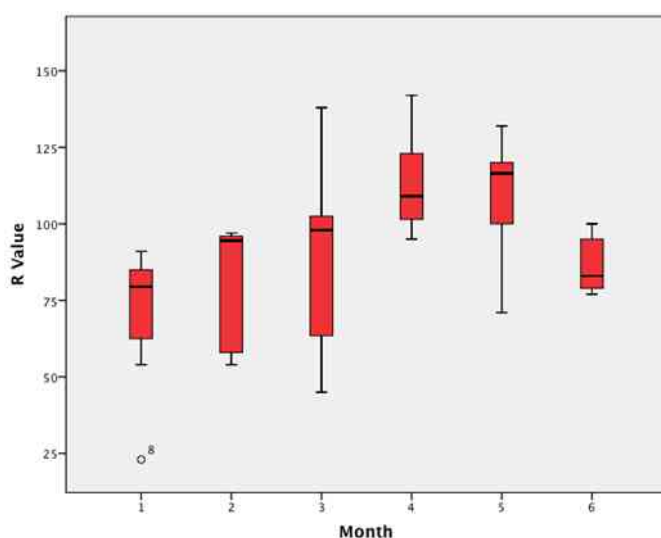


Figure 262 Box plot distributions of R values for stains generated on paper surfaces across monthly sample sets

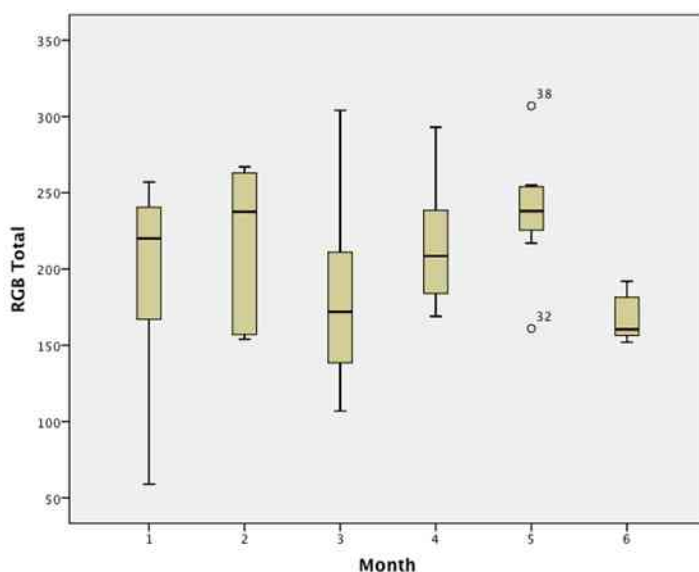


Figure 263 Box plot distributions of RGB totals for stains generated on paper surfaces across monthly sample sets

Results indicated that R (*figure 262*), G (*appendix 2*), B values (*appendix 2*) and RGB totals (*figure 263*) demonstrated minimal variability between all monthly sets, with a maximum range of 42 (mean R-values), 28.8 (mean G-values), 23.6 (mean B-values) and 70.3 (mean RGB total) between all monthly sets. This suggests that for paper stains, monthly variations in climatic characteristics (over the course of experimental stage 2) did not significantly influence stain colour, which was supported by observation of stain colours in *figure 259*. To determine whether variability observed in R, G, B values and RGB totals was linked to individual climatic characteristics (temperature, humidity, precipitation), the influence of each of these characteristics on stain colour was also examined.

#### **7.3.2.2.b Temperature**

*Figures 264 & 265* outline distributions of R-values and RGB totals for stains generated on paper surfaces, which were exposed to different temperatures according to monthly sample set.

*Figure 264* outlines the distribution of R-values for replicate stains ( $n = 8$ ) generated in each monthly sample set and exposed to different average temperatures. The minimum R-value for this range was 79.5 (17°C) and the maximum 116.5 (9°C). Results indicate that there is no clear relationship between increases in temperature and median R-values for stains generated on paper.

There were considerable ranges between minimum and maximum R-values were exhibited by sample sets exposed to temperatures of 9°C (61) and 15°C (93), 17°C (68). This suggests that R-value distributions for paper stains are variable across sample sets.

Figure 264 Box plot distributions of R values for stains generated on paper surfaces exposed to different temperature averages

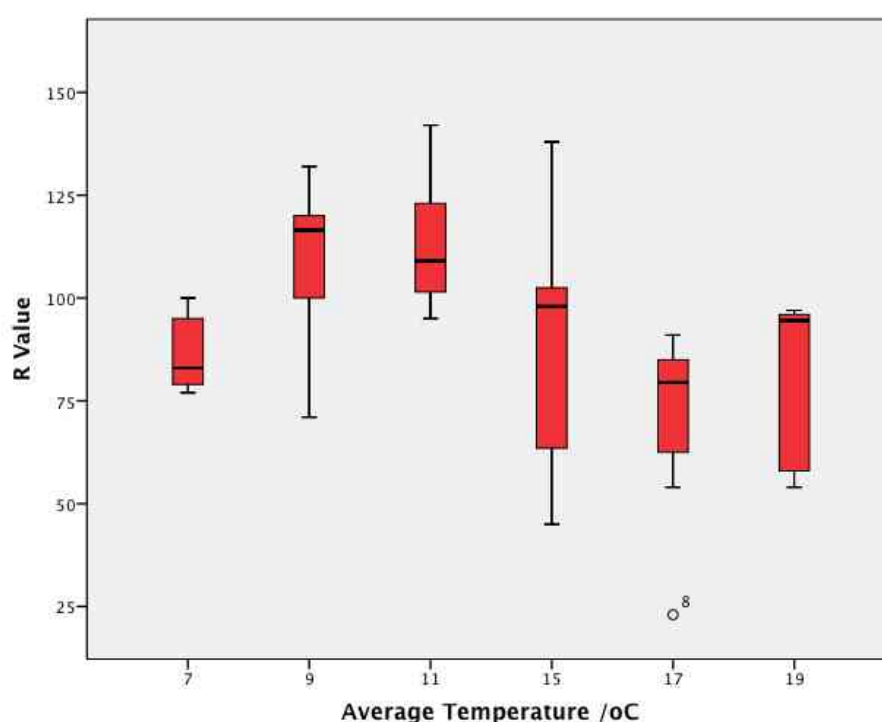
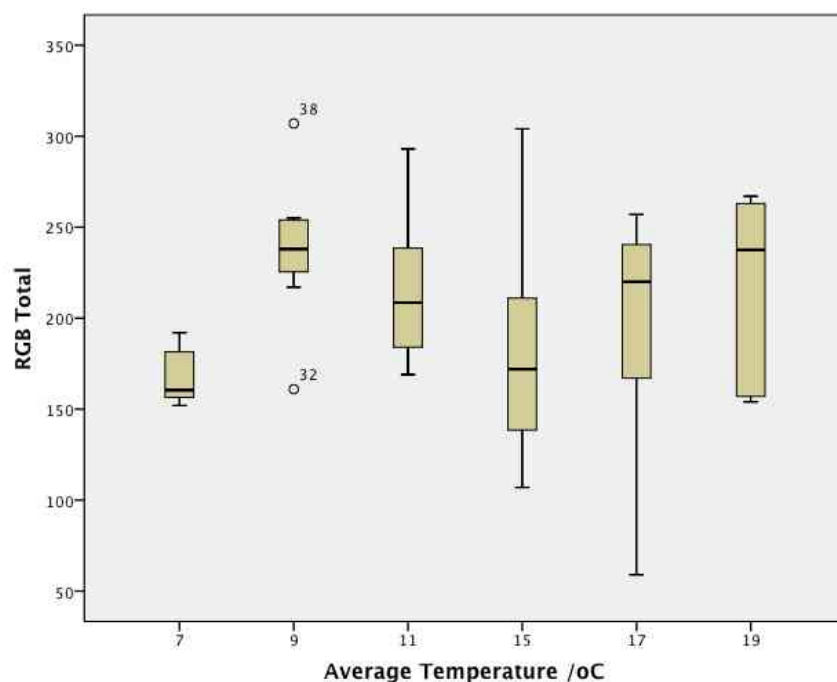


Figure 265 outlines the distribution of RGB totals for replicate stains exposed to different average temperatures. Stains exposed to the lowest temperature (7°C) exhibited the lowest median RGB total of 160.5. As temperature increased to 19°C, median RGB totals increased to a high of 237.5. This indicates that as temperature increases from 7°C to 11°C, RGB totals of stains generated on paper generally increased. Significant ranges between minimum and maximum RGB totals were exhibited by sample sets exposed to temperatures of 11°C (124), 15°C (197) and 17°C (198), indicating variability for the RGB total distributions for paper stains across sample sets.

Figure 265 Box plot distributions of RGB Totals for stains generated on paper surfaces exposed to different temperature averages



Across all distributions general trends between mean monthly temperature, R, G, B values and RGB totals was identified. As temperature increased from 7°C to 19°C, G-values (*appendix 2*), B-values (*appendix 2*) and RGB totals (*figure 265*) increased. The relationship between temperature and R-values (*figure 264*) was not so clear.

### 7.3.2.2.c Humidity

Figures 266 & 267 outline distributions of R-values and RGB totals for stains generated on paper surfaces exposed to different average humidity levels across monthly sample sets.

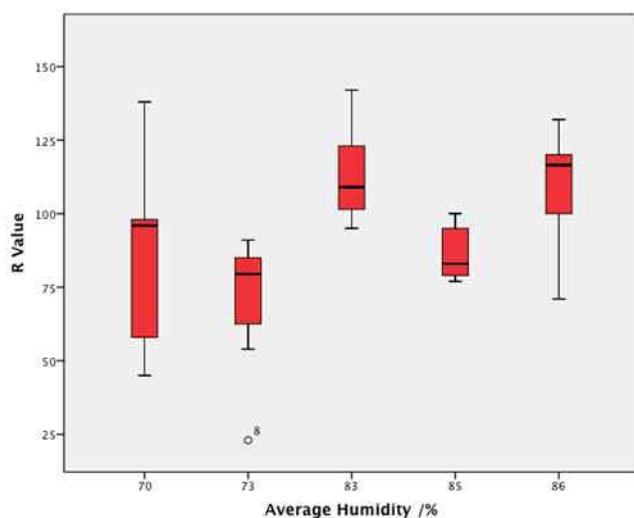


Figure 266 Box plot distributions of R values for stains generated on paper surfaces exposed to different humidity averages

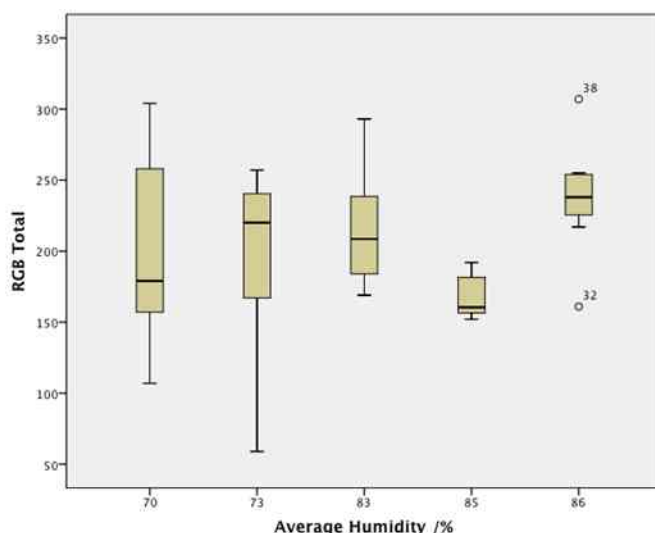


Figure 267 Box plot distributions of RGB totals for stains generated on paper surfaces exposed to different humidity averages

Across all distributions, trends between increases in average humidity and R-values (*figure 266*), humidity and G-values (*appendix 2*), humidity and B-values (*appendix 2*) and humidity and RGB totals (*figure 267*) were not identified.

#### **7.3.2.2.d Precipitation**

*Figures 268, 269, 270 & 271* outline distributions of R, G and B-values and RGB totals for stains generated on paper surfaces exposed to different volumes of precipitation across monthly sample sets.

Figure 268 outlines the distribution of R-values for replicate stains exposed to different volumes of precipitation. Median R-values appear to be randomly distributed between a range of values. The minimum R-value for this range was 79.5 (for stains exposed to 129mm) and the maximum 116.5 (for stains exposed to 101mm). Results support the suggestion that there is no clear relationship between exposure of stains to different volumes of precipitation and median R-values for stains generated on paper.

Considerable ranges between minimum and maximum R-values were exhibited by sample sets exposed to 60mm precipitation (93), 101mm precipitation (61) and 112mm precipitation (47). The presence of significant ranges suggests that R-value distributions for paper stains are variable across sample sets.



Figure 268 Box plot distributions of R values for stains generated on paper surfaces and exposed to different volumes of precipitation

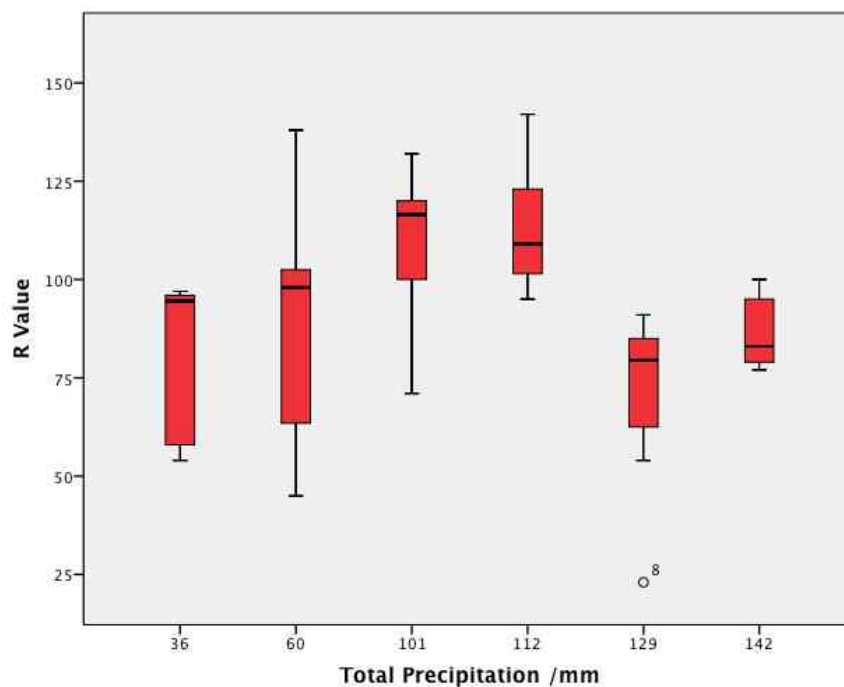


Figure 269 outlines the distribution of G-values for replicate stains exposed to different volumes of precipitation. Stains exposed to the smallest volume (36mm) exhibited the highest median G-value of 79.5. As volume of precipitation increased to 142mm, median G-values decreased to 43.5. This indicates that as the volume of precipitation that stains are exposed to increases from 36mm to 142mm, G-values of stains generated on paper generally decrease. G-values recorded for stains exposed to 60mm and 129mm appear anomalous to this general trend. They respectively exhibited median G-values of 44.5 and 75.5, which appears anomalous alongside decreasing G-values recorded for increases in volume between 36mm (79.5), 101mm (73.5), 112mm (61.0) and 142mm (43.5).

Considerable ranges between minimum and maximum G-values were exhibited by sample sets exposed to volumes of 60mm (67) and 129mm (69). The presence of significant ranges at these sample sets suggests that R-value distributions for paper stains were highly variable at 60mm and 129mm. This explains the observation of seemingly anomalous median values at these temperatures and supports the identification of a trend between decreases in G-values and increases in precipitation volumes.

Figure 269 Box plot distributions of G values for stains generated on paper surfaces and exposed to different volumes of precipitation

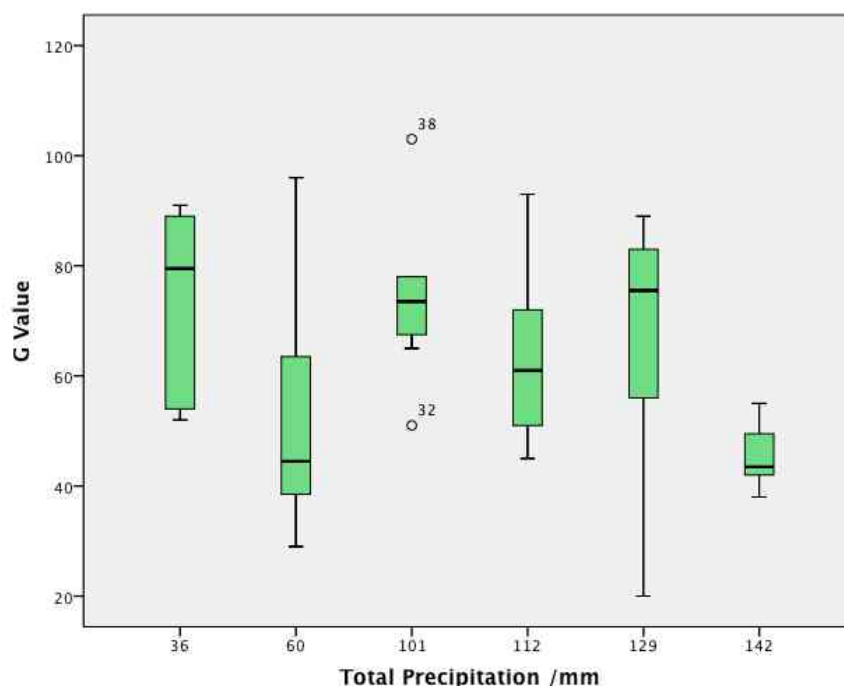


Figure 270 outlines the distribution of B-values for replicate stains exposed to different volumes of precipitation. Stains exposed to the smallest volume (36mm) exhibited a high median B-value of 63.5. As volume of precipitation increased to 142mm, median B-values decreased to 36.0. This supports a suggestion that as volume of precipitation stains are exposed to increases from 36mm to 142mm, B-values of stains generated on paper generally decrease. B-values recorded for stains exposed to 60mm, 112mm and 129mm appear anomalous to this general trend. They respectively exhibited median B-values of 35.5, 36.5 and 75.5, which appears anomalous to the trend in decreasing B-values recorded for increases in volume between 36mm (63.5), 101mm (54.0) and 142mm (36.0).

Significant ranges between minimum and maximum B-values were exhibited by sample sets exposed to volumes of 60mm (46) and 129mm (61). The presence of significant ranges at these sample sets suggests that B-value distributions for paper stains were highly variable at 60mm and 129mm. This explains the observation of seemingly anomalous median values at these temperatures and supports the identification of a trend between decreases in B-values and increases in precipitation volumes.

Figure 270 Box plot distributions of B values for stains generated on paper surfaces and exposed to different volumes of precipitation

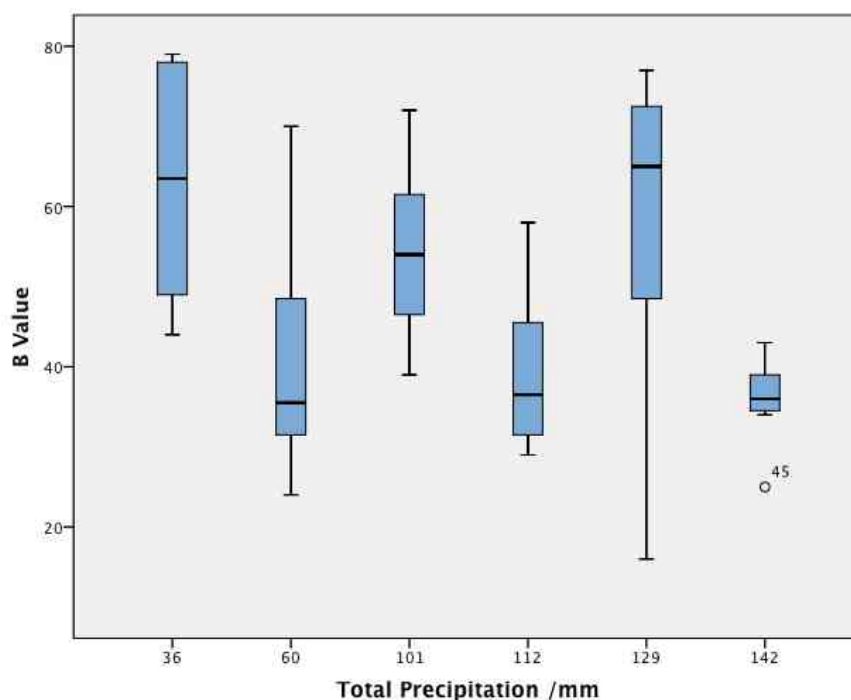
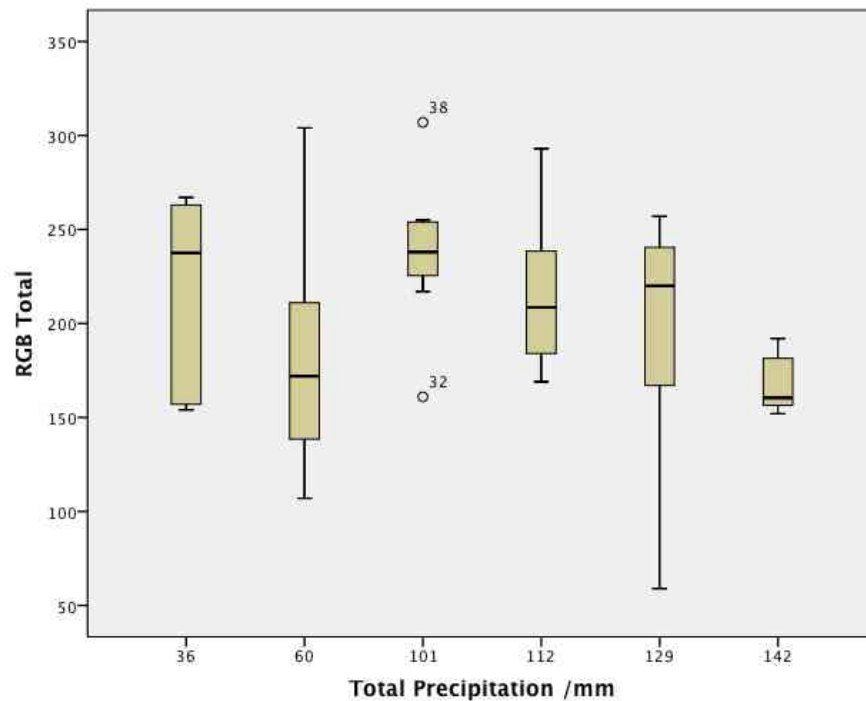


Figure 271 outlines the distribution of RGB totals for replicate stains exposed to different volumes of precipitation. Stains exposed to the smallest volume (36mm) exhibited a high median RGB total of 237.5. As volume of precipitation increased to 142mm, median RGB totals decreased to 160.5. This supports a suggestion that as volume of precipitation stains are exposed to increases from 36mm to 142mm, RGB total values of stains generated on paper generally decrease. RGB totals recorded for stains exposed to 60mm and 129mm appear anomalous to this general trend. They respectively exhibited median RGB totals of 172.0 and 220.0, which appears anomalous to the trend in decreasing RGB totals recorded for increases in volume between 36mm (237.5), 101mm (238.0), 112mm (208.5) and 142mm (160.5).

Significant ranges between minimum and maximum RGB totals were exhibited by sample sets exposed to volumes of 60mm (197) and 129mm (198). The presence of significant ranges at these sample sets suggests that RGB total distributions for paper stains were highly variable at 60mm and 129mm. This explains the observation of seemingly anomalous median values at these temperatures and supports the identification of a trend between decreases in RGB totals and increases in precipitation volumes.

Figure 271 Box plot distributions of RGB totals for stains generated on paper surfaces and exposed to different volumes of precipitation



Across all four distributions general trends between volume of precipitation, R, G, B values and RGB totals were identified. As volume increased from 36mm to 142mm, G-values (*figure 269*), B-values (*figure 270*) and RGB totals (*figure 271*) decreased. The relationship between volume and R-values (*figure 268*) was not so clear.

### 7.3.2.3 Stains generated in monthly glass sample sets

The measurements derived for stains on glass surfaces from monthly sample sets are presented in *figure 272*. Descriptive statistics are then presented in *figures 273* and *274*.

Figure 272 Table of measurements recorded for stains generated on glass surfaces in monthly sample sets

Stain ID	Surface	Month	Average Temperature /°C	Average Humidity /%	Total Precipitation /mm	R Value	G Value	B Value	RGB Total	Hex	Hex Colour
C009	Glass	1	17.4	73	129.0	86	59	40	185	563e2d	
C010	Glass	1	17.4	73	129.0	78	60	48	186	4e3b2f	
C011	Glass	1	17.4	73	129.0	91	69	57	217	5b4539	
C012	Glass	1	17.4	73	129.0	98	66	55	219	624236	
C013	Glass	1	17.4	73	129.0	89	78	68	235	594e43	
C014	Glass	1	17.4	73	129.0	75	57	46	178	4b392d	
C015	Glass	1	17.4	73	129.0	81	61	52	194	513e35	
C016	Glass	1	17.4	73	129.0	101	67	56	224	654338	
C031	Glass	2	19.3	70	35.9	228	227	200	655	e4e3c8	
C032	Glass	2	19.3	70	35.9	238	239	214	691	eeefd6	
C033	Glass	2	19.3	70	35.9	231	230	204	665	e7e6cc	
C034	Glass	2	19.3	70	35.9	197	191	158	546	c5bf9e	
C035	Glass	2	19.3	70	35.9	244	247	230	721	f4f7e6	
C036	Glass	2	19.3	70	35.9	241	244	222	707	f1f4e0	
C037	Glass	2	15.3	70	60.2	227	225	197	649	e3e1c5	
C038	Glass	2	15.3	70	60.2	250	251	237	738	eedd8	
C054	Glass	3	15.3	70	60.2	107	64	60	231	6b403c	
C055	Glass	3	15.3	70	60.2	110	58	54	222	6e3a36	
C056	Glass	3	15.3	70	60.2	102	54	50	206	663632	
C057	Glass	3	15.3	70	60.2	119	64	59	242	77403b	
C058	Glass	3	15.3	70	60.2	94	57	53	204	5e3935	
C059	Glass	3	15.3	70	60.2	107	60	56	223	6b3c38	
C060	Glass	3	11.3	83	112.0	112	62	57	231	703e39	
C077	Glass	4	11.3	83	112.0	125	71	44	240	7d472c	
C078	Glass	4	11.3	83	112.0	103	44	21	168	672c15	
C079	Glass	4	11.3	83	112.0	163	130	106	399	a3826a	
C080	Glass	4	11.3	83	112.0	136	82	45	263	88522d	
C081	Glass	4	11.3	83	112.0	174	135	97	406	ae8761	
C082	Glass	4	11.3	83	112.0	164	126	85	375	a47e55	
C083	Glass	4	11.3	83	112.0	206	188	159	553	cebc9f	
C084	Glass	4	8.6	86	100.8	180	152	116	448	b49874	
C101	Glass	5	8.6	86	100.8	113	83	69	265	715345	
C102	Glass	5	8.6	86	100.8	105	62	43	210	693e2b	
C103	Glass	5	8.6	86	100.8	117	73	49	239	754931	
C104	Glass	5	8.6	86	100.8	144	104	69	317	906845	
C105	Glass	5	8.6	86	100.8	114	58	36	208	723a24	
C106	Glass	5	8.6	86	100.8	115	71	50	236	734732	
C107	Glass	5	8.6	86	100.8	126	88	63	277	7e583f	
C108	Glass	5	6.5	85	142.0	129	78	52	259	814e34	
C125	Glass	6	6.5	85	142.0	79	26	16	121	4f1a10	
C126	Glass	6	6.5	85	142.0	84	25	16	125	541910	
C127	Glass	6	6.5	85	142.0	80	27	17	124	501b11	
C128	Glass	6	6.5	85	142.0	79	26	16	121	4f1a10	
C129	Glass	6	6.5	85	142.0	76	22	13	111	4c160d	
C130	Glass	6	6.5	85	142.0	77	30	21	128	4d1e15	
C131	Glass	6	6.5	85	142.0	81	29	19	129	511d13	
C132	Glass	6	6.5	85	142.0	82	31	22	135	521f16	

Figure 273 outlines mean R, G, B values and RGB totals calculated from replicate stains (n = 8) in each of 6 monthly sample sets. In each monthly sample set R-values were greater or equal to G and B-values. G and B-values recorded for each sample set were also high however, which meant for some sample sets R-values were only slightly higher or equal to G and B values. For example, in the M2 sample set the average R-value was 232.0, average G-value was 232.0 and average B-value was 208.0.

R-values for all sample sets fell between a low of 87.4 (M1) and a highest value of 232.0 observed for the M2 sample set. G-values across all sample sets fell between a recorded low of 27.0 (M6) and a high of 232.0 (M2). B-values were recorded between a low of 17.5 (M6) and a high of 208.0 (M2). Results demonstrate that whilst R, G and B-values were represented in similar levels in each sample set, for each sample set R-values represented the highest colour component, followed by G-values and finally B-values which represented the lowest individual colour component. The dominance of R-values suggests stains generated on glass and exposed to a range of monthly periods are all coloured towards red, rather than green or blue hues of colour and confirm the visual observations of a brown colour of stains (figure 272). An RGB triplet for brown colours is typically represented by similar figures in each of R, G and B values. Very high levels of R (232), G (232) and B (208) values support observations of a white, beige colour of stains in sample set M2 (figure 272). An RGB triplet for white is typically expressed as (R255, G255, B255). Stains in sample set M1 appear to have a dark intensity of colours, typically expressed by low values of R, G and B.

Figure 273 Descriptive statistics recorded for stains generated on glass surfaces in monthly sample sets

Sample Set		R Value	G Value	B Value	RGB Total
<b>M1</b>	Mean	87.4	64.6	53.0	204.8
	Std. Deviation	9.2	6.8	8.4	21.4
<b>M2</b>	Mean	232.0	232.0	208.0	671.5
	Std. Deviation	16.3	19.0	24.6	60.0
<b>M3</b>	Mean	107.3	60.0	55.6	222.7
	Std. Deviation	7.8	3.8	3.5	13.8
<b>M4</b>	Mean	156.4	116.0	84.1	356.5
	Std. Deviation	33.1	47.1	45.3	125.0
<b>M5</b>	Mean	120.4	77.1	53.9	251.4
	Std. Deviation	12.2	15.0	12.1	36.2
<b>M6</b>	Mean	80.0	27.0	17.5	124.3
	Std. Deviation	2.6	3.0	3.0	7.1

Figure 274 sets out average colour values for all glass stains. Average R, G and B values were calculated between all replicate stains (n = 47) from monthly sample sets. Mean values for stains generated on denim were R (131.02), G (96.83) and B (79.09) and stains exhibited a high ratio of R (to G and B) colour components with stains coloured towards a red rather than green or blue hue. Average levels of R, G and B values were low (below 100), which corresponds to the dark intensities of colour in monthly stains generated on glass (figure 272). Levels of R, G and B values were relatively low which corresponds to the low to medium intensity observed in monthly stains generated on glass (figure 272). The combination of a slight orientation towards red hues of colour and a low to medium intensity of colour indicate that stains generated on glass, on average, were characterised by a light brown colouring.

Figure 274 Mean R, G and B values for all monthly stains generated on glass

	N	Minimum	Maximum	Mean	Std. Deviation
R Value	47	75	250	131.02	55.054
G Value	47	22	251	96.83	70.493
B Value	47	13	237	79.09	65.573
Valid N (listwise)	47				

### 7.3.2.3.a Sample Sets

Figures 275 & 276 outline distributions of R-values and RGB totals for stains generated on glass surfaces across monthly sample sets. Distributions across monthly sample sets were compared to establish whether there were any differences between stains exposed to months characterised by different climatic characteristics (temperature, humidity and precipitation).

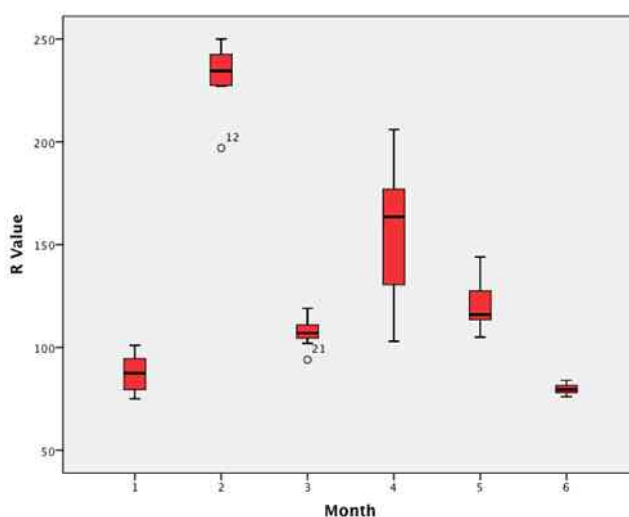


Figure 275 Box plot distributions of R values for stains generated on glass surfaces across monthly sample sets

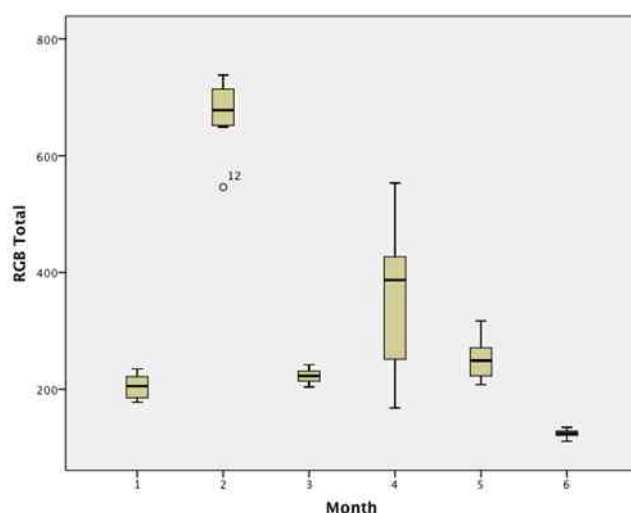


Figure 276 Box plot distributions of RGB totals for stains generated on glass surfaces across monthly sample sets

Results indicated that R (*figure 275*), G (*appendix 2*), B values (*appendix 2*) and RGB totals (*figure 276*) demonstrated variability between all monthly sets, with a maximum range of 152.3 (mean R-values), 205.0 (mean G-values), 190.3 (mean B-values) and 547.3 (mean RGB total) between all monthly sets. This suggests that for glass stains, monthly variations in climatic characteristics (over the course of experimental stage 2) did influence stain colour, which was supported by observation of stain colours in *figure 272*. To determine how variability observed in R, G, B values and RGB totals was linked to individual climatic characteristics (temperature, humidity, precipitation), the influence of each of these characteristics on stain colour was also examined.

#### **7.3.2.3.b Temperature**

*Figures 277 & 278* outline distributions of R-values and RGB totals for stains generated on glass surfaces, which were exposed to different temperatures according to monthly sample set.



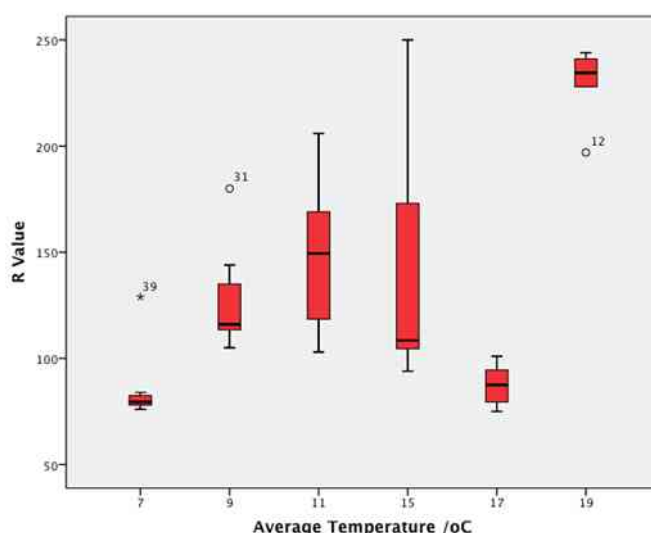


Figure 277 Box plot distributions of R values for stains generated on glass surfaces exposed to different temperature averages

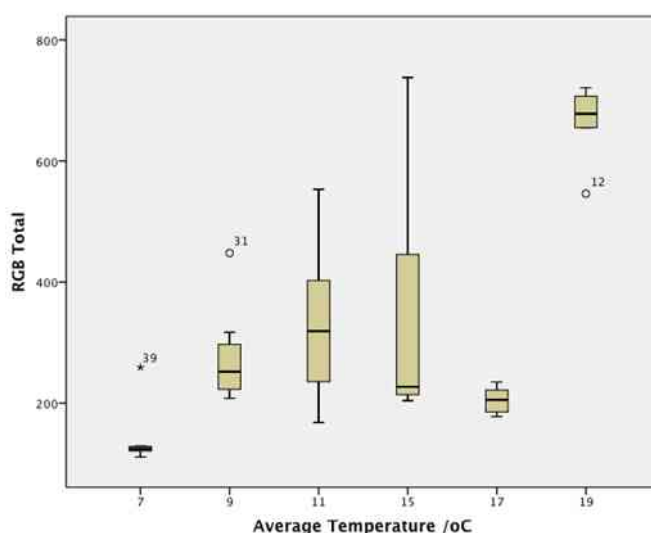


Figure 278 Box plot distributions of RGB Totals for stains generated on glass surfaces exposed to different temperature averages

Across all distributions, general trends between increases in average temperature and R-values (*figure 277*), humidity and G-values (*appendix 2*), humidity and B-values (*appendix 2*) and humidity and RGB totals (*figure 278*) were not identified.

### 7.3.2.3.c Humidity

*Figures 279 & 280* outline distributions of R-values and RGB totals for stains generated on glass surfaces exposed to different average humidity levels across monthly sample sets.

*Figure 279* outlines the distribution of R-values for replicate stains exposed to different humidity averages. Stains exposed to the lowest humidity (70%) exhibited the highest median R-value of 212.0 and vice versa (humidity 86%; lowest median

R-value 116.0). This indicates that as the average humidity level stains are exposed to increase, R-values of stains generally decreased.

Considerable ranges were exhibited between minimum and maximum R-values for stains generated at 70% humidity (156) and 83% humidity (103). The presence of significant ranges suggests that R-value distributions for glass stains are variable across humidity levels.

Figure 279 Box plot distributions of R values for stains generated on glass surfaces exposed to different humidity averages

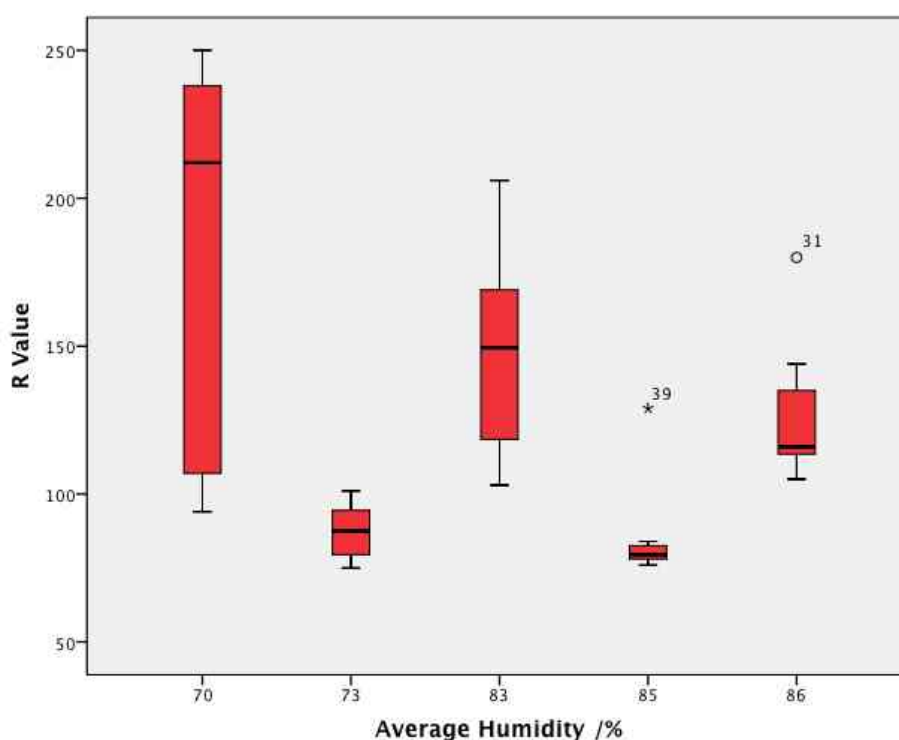
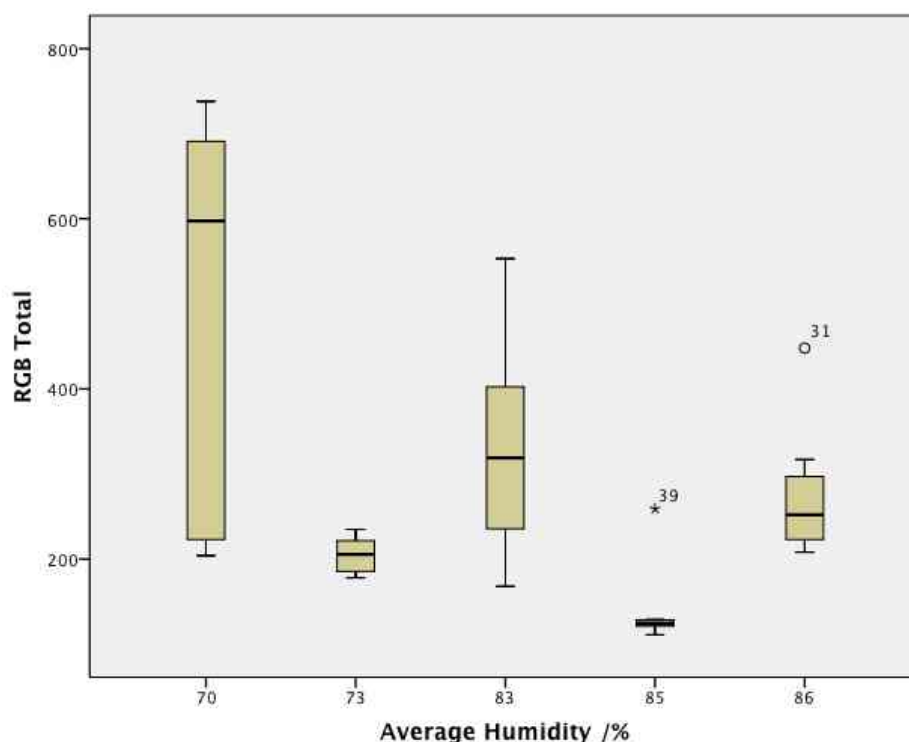


Figure 280 outlines the distribution of RGB totals for replicate stains exposed to different humidity averages. Stains exposed to the lowest humidity (70%) exhibited the highest median RGB total of 597.5. Stains exposed to the highest humidity (86%) exhibited the lowest median RGB total of 252.0. This indicates that as average humidity stains were exposed to increase, RGB totals of stains generally decreased.

Significant ranges were exhibited between minimum and maximum RGB totals for stains generated at 70% humidity (534) and 83% humidity (385). The presence of significant ranges suggests that RGB total distributions for glass stains are variable across humidity levels.

Figure 280 Box plot distributions of RGB totals for stains generated on glass surfaces exposed to different humidity averages



Across all distributions a general trend between average humidity, R, G, B values and RGB totals was identified. As humidity increased from 70% to 86%, R-values (figure 279), G-values (appendix 2), B-values (appendix 2) and RGB totals (figures 280) generally decreased.

#### **7.3.2.3.d Precipitation**

Figures 281 & 282 outline distributions of R-values and RGB totals for stains generated on glass surfaces exposed to different volumes of precipitation across monthly sample sets. Stains exposed to the lowest volume of precipitation (36mm) exhibited the highest median R-value of 234.5. Stains exposed to the highest volume of precipitation (142mm) exhibited the lowest median R-value of 79.5. This indicates that as the volume of precipitation stains are exposed to increases, R-values of stains decrease. Sizeable ranges were exhibited between minimum and maximum R-values at 60mm (156) and 112mm (103), which suggests that R-value distributions for glass stains were more variable at 60mm and 112mm. This explains the observation of seemingly anomalous median values at these temperatures and supports the identification of a trend between decreases in R-values and increases in precipitation volumes.

Figure 281 Box plot distributions of R values for stains generated on glass surfaces and exposed to different volumes of precipitation

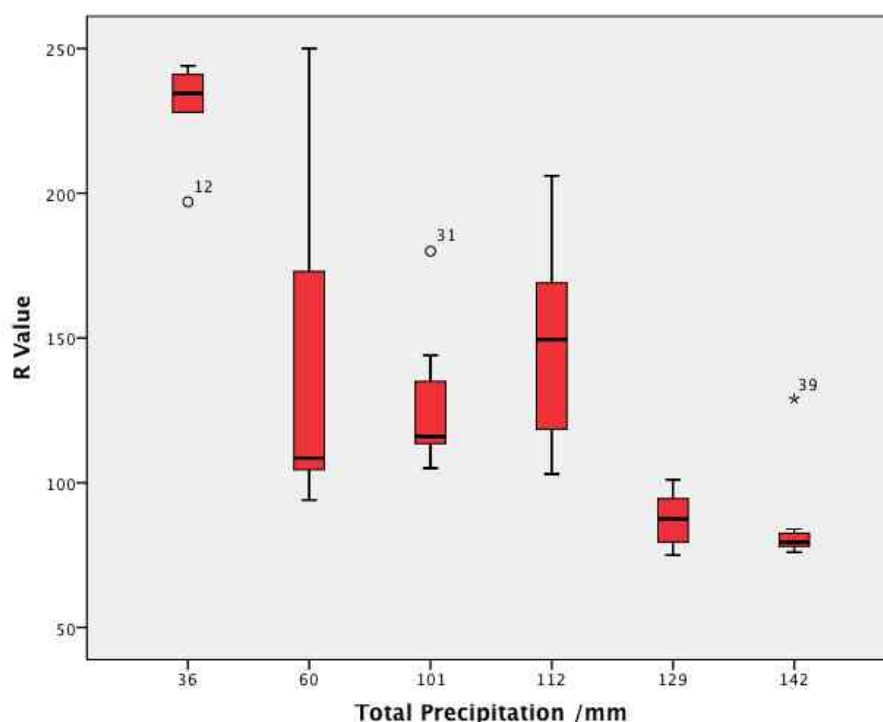
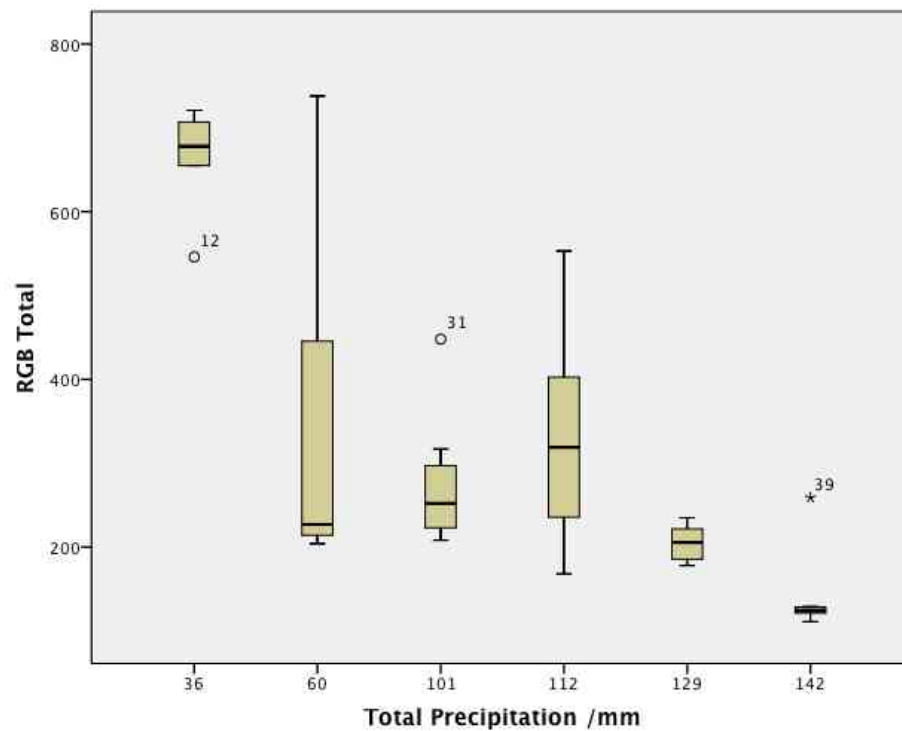


Figure 282 outlines the distribution of RGB totals for replicate stains generated in monthly sample sets that were exposed to different volumes of precipitation. Trends in RGB totals and precipitation were similar to those observed between R-values and precipitation. Stains exposed to the lowest volume of precipitation (36mm) exhibited the highest median RGB total of 678.0. Stains exposed to the highest volume of precipitation (142mm) exhibited the lowest median RGB total of 124.5. This supports a suggestion that as volume of precipitation stains are exposed to increases, RGB totals of stains decrease.

Similar to ranges observed for R-values (*figure 281*) sizeable ranges were exhibited between minimum and maximum RGB totals at 60mm (534) and 112mm (385). The presence of significant ranges at these sample sets suggests that RGB total distributions for glass stains were variable at 60mm and 112mm. This supports the identification of a trend between decreases in RGB totals and increases in precipitation volumes.

Figure 282 Box plot distributions of RGB totals for stains generated on glass surfaces and exposed to different volumes of precipitation



Across all distributions a general trend between total volume of precipitation, R, G, B values and RGB totals was identified. As precipitation totals increased from 36mm to 142mm, R-values (*figure 281*), G-values (*appendix 2*), B-values (*appendix 2*) and RGB totals (*figures 282*) decreased.

### **7.3.3 Monthly stain colour analysis – surface comparison**

Once the results of stain colour analyses and trends had been identified for each surface individually, trends and results observed for these surfaces were compared to assess stains generated under the same conditions, on different surfaces. Colours of stains generated on the three different surfaces (paper, glass and denim) were compared visually and through quantitative analysis.

#### **7.3.3.1 Colour ribbon comparison**

To facilitate visual comparison of colours of stains exposed to a temperate climate for different monthly periods, colour ribbons were compiled. Blocks of hexadecimal colour corresponding to individual stain were aligned into longitudinal ribbons according to numerical order of months of stain exposure (*figure 283*).

*Figure 283* provides a visual overview of changes in stain colour between different periods of monthly exposure for each surface and how colours of stains compare between denim, paper and glass overall. An initial observation related to a comparison of stain colours between surfaces. As all surfaces were stained under the same conditions and from the same blood source, a reasonable expectation follows that stains might therefore be generally similar in colour. Observations from *figure 283* indicated however that stains generated on denim, paper and glass surfaces vary in colour. Stains generated on denim surfaces generally appear a light tan-brown or beige colour. Stains generated on paper surfaces generally appear a varied range of much darker hues of brown, grey and even black. Stains generated on glass surfaces generally also appear as a range of colours, including hues of white-beige, brown and pink-grey. A quantitative confirmation of this difference is set out in 7.9.2 and 7.9.3 through comparisons of R, G, B values and RGB totals for all three surfaces.

Figure 283 Colour ribbons for stains generated on denim, paper and glass and exposed to a temperate climate across 6 different monthly periods



### 7.3.3.2 Comparison of RGB totals between surfaces

RGB totals were calculated by adding together R, G and B values recorded for individual replicate stains. RGB totals for individual stains were then averaged between replicate stains in each monthly sample set and across all sample sets to generate an overall mean RGB total for stains generated on each surface, as outlined in *figures 284 and 285*.

*Figure 284* outlines descriptive statistics for RGB totals calculated from all stains generated on denim, glass and paper. A comparison of mean RGB totals indicates the comparative intensity of stains between denim, glass and paper surfaces, following exposure to a temperate climate for 6 different monthly periods. Stains generated on denim in months 1, 3, 4, 5 and 6 exhibited higher RGB totals than stains generated on paper and glass. Thus, for months 1, 3, 4, 5 and 6 denim stains were characterised by lighter intensities of colour than glass and paper stains as shown in the colour ribbons (*figure 283*).



Figure 284 Descriptive statistics for RGB totals calculated from all stains generated on denim, glass and paper







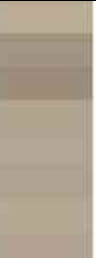




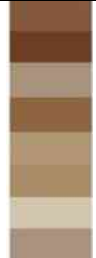


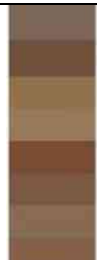



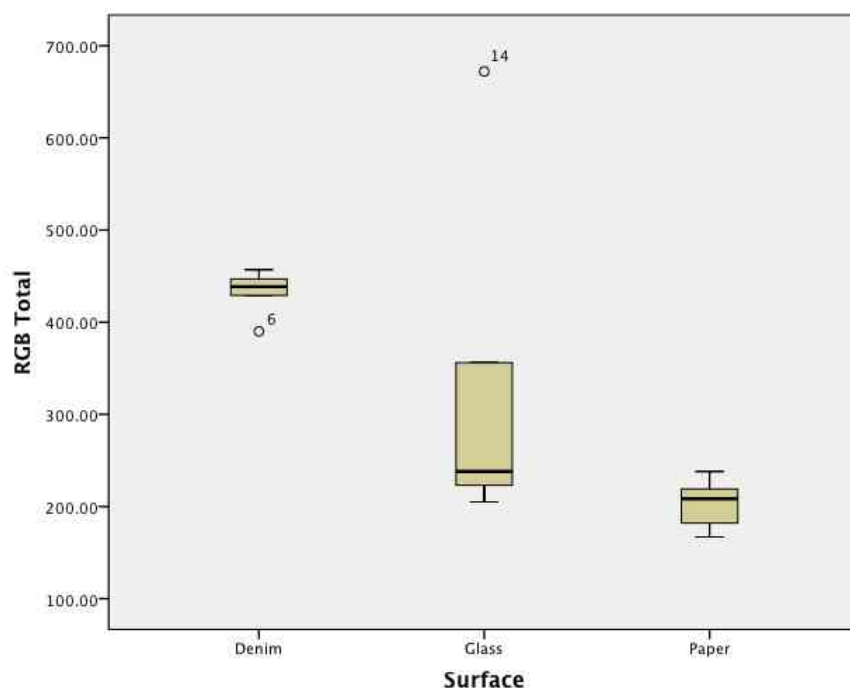
	Denim	Paper	Glass		Denim	Paper	Glass
<b>Month 1</b>				<b>Month 2</b>			
Average R, G & B values	R 173 G 150 B 124	R 71 G 67 B 58	R 87 G 65 B 53	Average R, G & B values	R 168 G 150 B 127	R 82 G 74 B 63	R 232 G 232 B 208
Average RGB total	447	202	205	Average RGB total	445	219	672
<b>Month 3</b>				<b>Month 4</b>			
Average R, G & B values	R 165 G 145 B 122	R 89 G 52 B 41	R 107 G 60 B 56	Average R, G & B values	R 177 G 154 B 126	R 113 G 63 B 39	R 156 G 116 B 84
Average RGB total	432	182	223	Average RGB total	457	215	356
<b>Month 5</b>				<b>Month 6</b>			
Average R, G & B values	R 169 G 144 B 116	R 110 G 74 B 54	R 120 G 77 B 54	Average R, G & B values	R 158 G 130 B 102	R 86 G 45 B 36	R 80 G 27 B 18
Average RGB total	429	238	251	Average RGB total	390	167	225

Figure 285 demonstrates average RGB totals for denim, glass and paper surfaces, which reflect lightness or darkness of stain intensity on each surface. Denim stains exhibit the lightest intensity, followed by glass stains and finally paper stains, which exhibit the darkest intensity of colours.

Figure 285 Box plot distributions of average RGB totals for stains generated on denim, glass and paper surfaces



### 7.3.3.3 Comparison of ratios of R, G and B values between months and surfaces

As outlined in chapter 3 (*section 3.4.4.1*), RGB totals give a measure of intensity of overall stain colour but ratios of R to G and B values give an indication of the significance or strength of colour orientation towards a particular component. Average ratios of R, G and B values were calculated (*figures 286, 287 - 292*) to allow comparison of the colouration of stains between surfaces during different months.

Figure 286 Average R, G and B values for all stains generated across monthly sample sets on denim, glass and paper

Denim				Paper				Glass					
M1	R	173	R	71	R	87	M2	R	168	R	82	R	232
	G	150	G	67	G	65		G	150	G	74	G	232
	B	124	B	58	B	53		B	127	B	63	B	208
M3	R	165	R	89	R	107	M4	R	177	R	113	R	156
	G	145	G	52	G	60		G	154	G	63	G	116
	B	122	B	41	B	56		B	126	B	39	B	84
M5	R	169	R	110	R	120	M6	R	158	R	86	R	80
	G	144	G	74	G	77		G	130	G	45	G	27
	B	116	B	54	B	54		B	102	B	36	B	18

Figures 287 - 292 illustrate the ratio of average R to G and B values generated across monthly sample sets on denim, paper and glass. The largest single component of RGB totals for denim, paper and glass stains generated in every monthly sample set was R-values. With the exception of paper stains in M4 and M6 and glass stains in M6, R-values accounted for less than half of RGB totals in every monthly sample set. Levels of G and B values were therefore significant in all stains on all surfaces in all sample sets. On average R-values accounted for between 36.2% (paper M1) – 64% (glass M6), G-values accounted for between 21.6% (glass M6) – 33.8% (paper M2) and B-values accounted for between 14.4% (glass M6) – 31% (glass M2) of RGB totals.

This suggests that across all monthly sample sets, stains on any surface are characterised by relatively balanced representations of R, G and B values with slight orientations towards red hues of colour. This was reflected in observations of a variety of grey and brown hues, of varying intensities, of stain colour for monthly stains, confirmed in stain images and colour ribbons in *figure 284*.

Figure 287 Representation of average ratios of R to G and B values for M1 stains

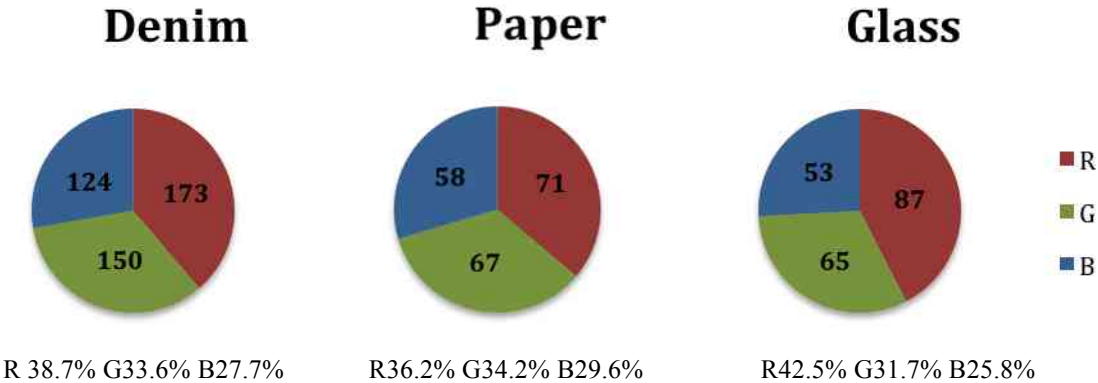


Figure 288 Representation of average ratios of R to G and B values for M2 stains

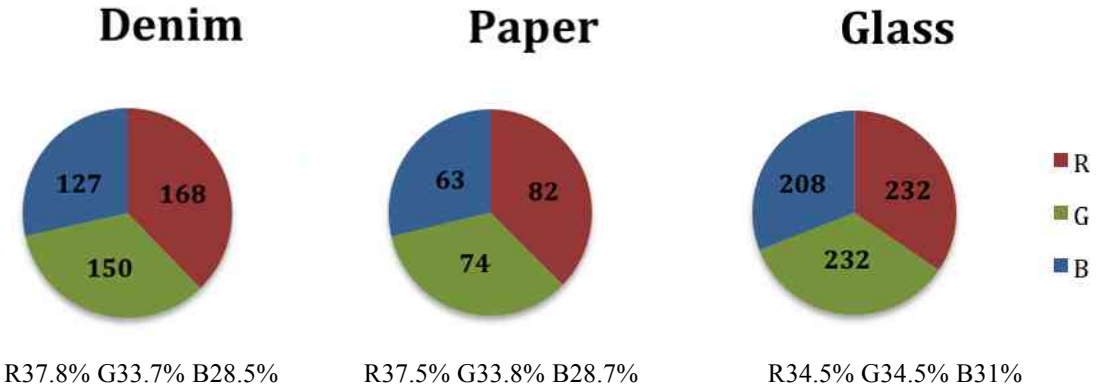


Figure 289 Representation of average ratios of R to G and B values for M3 stains

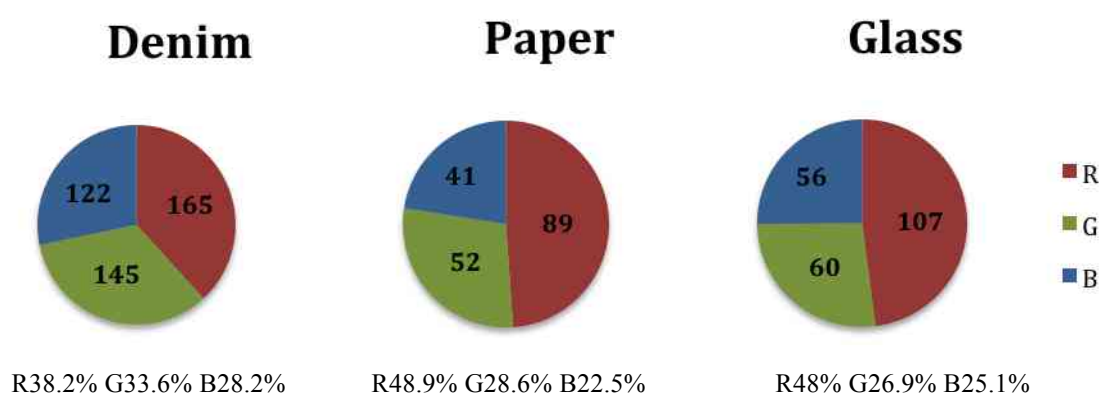


Figure 290 Representation of average ratios of R to G and B values for M4 stains

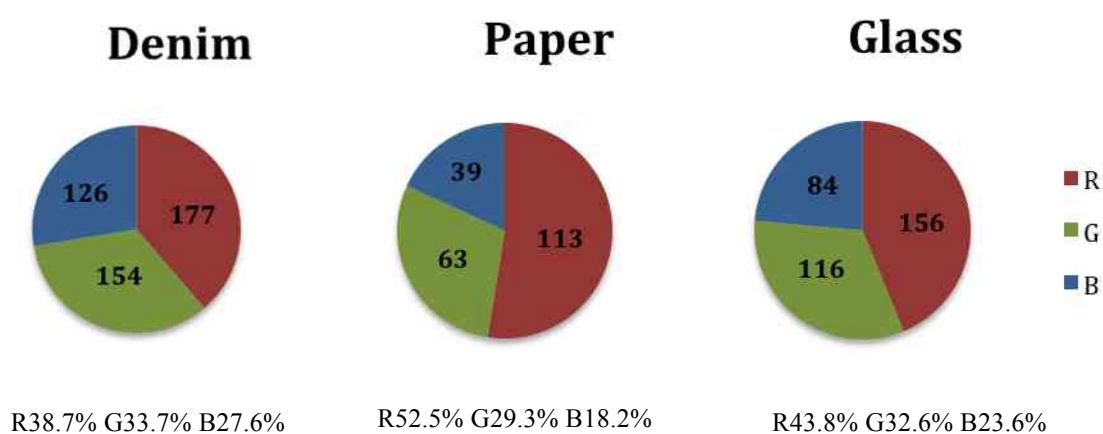


Figure 291 Representation of average ratios of R to G and B values for M5 stains

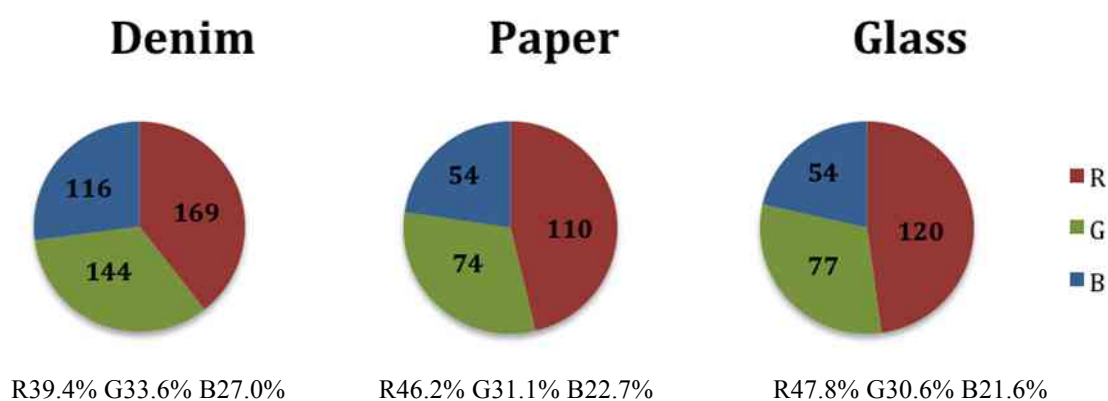
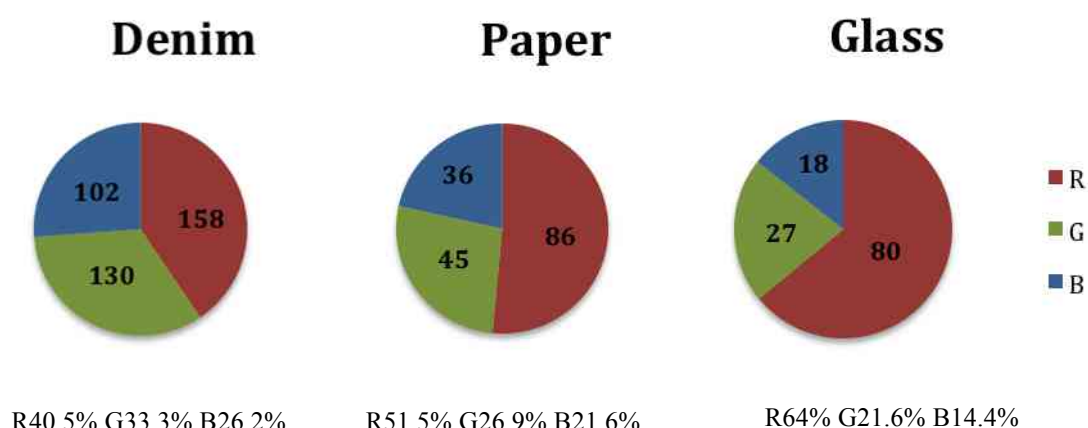


Figure 292 Representation of average ratios of R to G and B values for M6 stains



Variations in intensity and strength of colouring of stains may affect interpretation of bloodstain evidence by altering the ease with which analysts identify bloodstains. Experimental stage 2 demonstrated that exposing stains to the environment for periods of at least one month, influences stain appearance. This has implications for the analysis of bloodstains at a crime scene and in particular, analysis of stains at scenes located outdoors, in exposed locations or which are not 'fresh'. Results also indicated that discolouration of stains caused by environmental exposure, varied according to the nature of surface stained. This has implications for identification and analysis of stains recovered from a range of surface types at environmentally exposed crime scenes. The implications of results of experimental stage 2 for bloodstain pattern analysis and the subsequent process of crime scene reconstruction are discussed in *chapter 13*.

## **8. Experimental Stage 3 – Exploration of environmental influences on bloodstain identification (Extreme conditions)**

### **8.1 Overview**

Experimental stage 3 consisted of a series of different experiments in which bloodstains, on a variety of surfaces, were exposed to extreme environmental conditions. Conditions stains were exposed to included:

- freeze thaw mechanisms,
- exposure to extreme heat,
- exposure to extreme cold,
- exposure to snow and
- exposure to fire (burning).

Once stains had been exposed to these extreme environmental conditions they were immediately subjected to visual analysis and chemical identification tests. This was in order to assess the effects of exposure on both stain appearance and internal composition of stains. Exposure to extreme environmental conditions can significantly alter the appearance or behaviour of a bloodstain (*Lovelock. 1953. Paonessa. 2005. Leak. 2006. Morris. 2010. Leak. 2010*), which can subsequently complicate identification, analysis and interpretation of the stain. This may reduce the ability of analysts to include stains that have experienced these alterations from crime scene reconstructions. In order to prevent exclusion of these stains from reconstructions and bloodstain pattern analysis, quantitative measures of the nature and order of environmentally charged alterations need to be recorded, to assist in the identification, analysis and interpretation of these stains.

The primary objective of stage 3 therefore was to explore the effects of extreme environmental conditions, more extreme than those explored in stages 1 & 2, on two aspects of bloodstain analysis: visual and chemical identification. Observations regarding the effects of extreme environmental conditions on bloodstains suggest that stains respond to extremes of temperature or exposure to snow and fire by exhibiting significant alterations to their appearance and behaviour. In certain forensic scenarios this can complicate and mislead stain analysis and subsequent

crime scene reconstructions from bloodstains. A real case scenario (*Morris. 2010*) illustrates this potential for environmental conditions to mislead crime scene investigation by causing alterations to bloodstain evidence. Bloodstains generated on frozen surfaces outdoors in an extremely cold climate were observed to exhibit a pink, puffy discolouration that led to them initially being identified as brain tissue (*Morris. 2010*). The investigative repercussions in this scenario were quite significant, leading to an inaccurate identification of brain tissue at a scene and through identification of bloodstains as brain tissue; an incomplete analysis of blood evidence at the scene. Although the evidence was eventually identified as bloodstain evidence, the unfamiliar presence of environmentally altered bloodstains could have resulted in an inaccurate interpretation of evidence and inaccurate crime scene reconstruction. Despite observations of the influence of extreme environmental conditions on bloodstain appearance and behaviour and the gravity of their consequences for accurate interpretation of stains recovered from environmentally exposed crime scenes, observations regarding them remain in some respects anecdotal. By establishing quantitative relationships between environmental extremes and stain appearance and behaviour, experimental stage 3 aimed to examine the nature of these relationships more robustly and empirically. Results will then inform the identification, analysis and interpretation of stains recovered in these scenarios and improve the accuracy of their incorporation into scene analysis. A secondary element of the experimental stage was to allow comparisons to be made between stains exposed to extreme conditions (stage 3) and those exposed to more benign environmental conditions (stages 1 & 2). This has a major forensic implication in enabling analysts to determine when stains have been exposed to extreme conditions, that are unlikely to have occurred naturally, and may therefore be the result of evasive actions taken by a suspect. For example, setting fire to a crime scene to destroy evidence.

The experimental methodologies adopted for the different sections of experimental stage 3 leant heavily upon the methodologies designed for stages 1 and 2. Due however to the inherently destructive nature of some of the extreme conditions and difficulties in handling some of the materials used, some adaptations and variations in experimental methodology were necessary. This meant that the stage was subsequently considered more of an exploratory and preliminary examination of the

effects of extreme environmental conditions on bloodstains. Methodological limitations for each section of experimental stage 3 are outlined within the relevant sections.

## 8.2 Materials

The materials utilised for the experimental work in this chapter are set out in *figure 293*.

Experimental equipment	Additional specifications
<b>100ml Whole Ovine Blood</b>	With Alsever's solution
<b>Paper</b>	Ryman's A4 white laid paper, 100gm <sup>2</sup>
<b>Glass microscope slides</b>	CellPath. 90° ground edges. 25.4 x 76.2 mm. Thickness 1.0-1.2mm
<b>White denim cloth</b>	100% cotton. Weight: 345g/metre
<b>Plain white record cards</b>	Ryman's Silvine 127x77mm
<b>Thermo Scientific Finnpiquette® F1 Variable Volume Single Channel Pipette</b>	1-10µl
<b>Biological waste disposal unit</b>	
<b>Temperature &amp; Relative Humidity data logger</b>	Ebro. VWR. EBI 20-TH1
<b>Plastic tray</b>	
<b>Plastic tub</b>	H12cm x L30cm x W18cm
<b>MESM Portable laboratory refrigerator</b>	Temperature range: -10°C → 60°C
<b>Metal baking tray</b>	Fan-assisted, temperature range: 0-250°C
<b>Oven</b>	
<b>Charcoal barbecue</b>	
<b>Kastle-Meyer testing kit</b>	SceneSafe. Product code K160
<b>Hemastix® testing kit</b>	SceneSafe. Product code K162
<b>Bluestar testing kit</b>	SceneSafe. Product code K285
<b>Digital scanner</b>	HP Scanjet G2710
<b>Digital camera</b>	Panasonic Lumix FS30 Digital Camera (14.1MP, 8x Optical Zoom)

Figure 293 Table of materials used in experimental stage 3 (Author. 2012)

Justification for the selection of presumptive tests is provided in *section 3.4.3*.

## 8.3 Methodologies

There were five different extreme conditions to which stains were exposed. These five conditions were exposure to: snow, freeze thaw mechanisms, freezing, extreme heat and fire. Across these five, conditions could be broadly categorised as either cold or hot extremes (*figure 294*).



Extreme	Condition	Method	Overview	Methods of stain analysis
Cold	Snow	1	Stains were generated directly onto snow	Visual (digital camera)
		2	Stains were generated on glass microscope slides which were positioned on snow	Visual (digital camera)
		3	Multi-drop stains were generated directly onto snow	Visual (digital camera)
	Freeze-thaw	1	Stains were generated on glass microscope slides, which were then exposed to freeze thaw mechanisms overnight	Visual (digital camera) Chemical identification tests
		1	Stains were generated onto room temperature surfaces	Visual (digital camera & scanner) Chemical identification tests
	Freezing conditions	2	Stains were generated onto frozen paper, glass and denim surfaces	Visual (digital camera & scanner) Chemical identification tests
		3	Stains were generated directly onto ice	Visual (digital camera) Chemical identification tests
	High temperatures	1	Stains were generated on paper, glass and denim surfaces, which were at room temperature – and then dried at 100°C, 150°C, 200°C & 250°C	Visual (digital scanner) Chemical identification tests
		2	Stains were generated on paper, glass and denim surfaces which had been heated, prior to staining, to 100°C, 150°C, 200°C & 250°C	Visual (digital scanner) Chemical identification tests
Hot	Fire	1	Stains were generated on glass microscope slides that were placed in a charcoal-fuelled fire.	Visual (digital scanner) Chemical identification tests

Figure 294 Table listing the extreme conditions stains were exposed to during experimental stage 3, broadly categorised between extremes of cold/hot, and descriptive overviews of each condition

For some of the conditions there were different ways in which bloodstains could be exposed or introduced to the environmental extremes being explored. For these conditions, several methods of exposure were designed. For example three different experimental methods were designed to explore the effects of stain deposition on snow (*figure 294*). Individual methodologies designed for each condition are outlined in **8.4 – 8.8**.

## 8.4 Exposure of stains to snow

### 8.4.1 Establishing experimental conditions

These experiments were designed to explore the behaviour of bloodstains generated on snow. A period of snowfall and sustained groundcover was therefore a prerequisite to experimentation. Following a period of snowfall, stains were generated and deposited onto snow, in a variety of ways. Observations were then

made about their responses to snow exposure. Three different methods were designed to generate and deposit bloodstains on snow:

*Method 1: Generation of single-drop stains directly onto snow*

*Method 2: Generation of single-drop stains directly onto glass slides on top of snow*

*Method 3: Generation of multi-drop stain directly onto snow*

In order to establish experimental consistency, as far as possible, between methods – a large, clean, fresh area of snow was chosen for experimentation. The snow was located on a flat roof with limited access. The flat roof meant that the snowfall had settled with a uniformly flat surface and was of a consistent depth (approximately 2 inches). The limited access to the roof ensured that it had not been disturbed prior to experimentation.

#### **8.4.2 Method 1 stain generation**

A clean fresh area of snow measuring approximately 100cm x 75cm was identified (*figure 295*). Using a fixed 10 $\mu$ l volume pipette, a series of Ovine bloodstains were deposited from a height of 10cm onto the snow. Each stain was generated from a single drop of blood, of 10 $\mu$ l volume and twenty-four separate replicate stains were generated (*figure 296*).



Figure 295 Clean area of snow for experimentation

(*Author. 2012*)

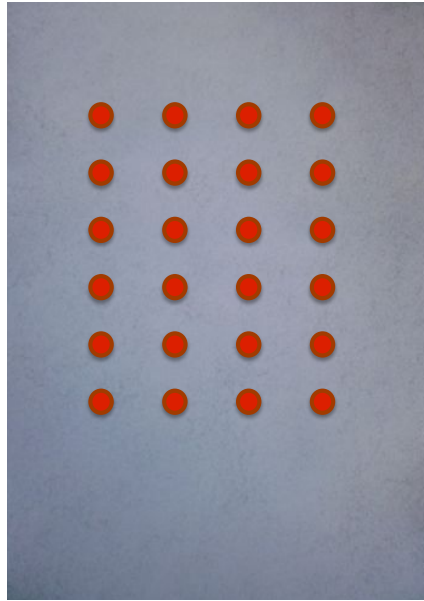


Figure 296 24 single-drop replicate stains generated on snow

*(Author, 2012)*

A digital camera was used to take photographs of stains at various time intervals following generation. Photographs were taken 5, 15, 30, 45 and 60 minutes after stain generation. These photographs were then used to observe how appearance of single-drop stains, generated directly onto snow, altered over time. The aim of this method of stain generation was to allow observations to be made regarding how the appearance of single drops of blood generated directly onto snow is influenced by this exposure to snow.

#### **8.4.3 Method 2 stain generation**

A clean fresh area of snow measuring approximately 100cm x 75cm was identified (*figure 297*). Twelve clean glass microscope slides were arranged on top of the snow's surface and left lying on the snow for 2 hours to allow them to adjust to the same temperature as the snow. Once slides had acclimatised to the temperature of the snow's surface, bloodstains were generated onto them. Using a fixed 10 $\mu$ l volume pipette, a series of Ovine bloodstains were deposited from a height of 10cm onto slides. Each stain was generated from a single 10 $\mu$ l volume drop, on a separate slide (*figure 298*).



Figure 297 Clean area of snow for experimentation

*(Author. 2012)*

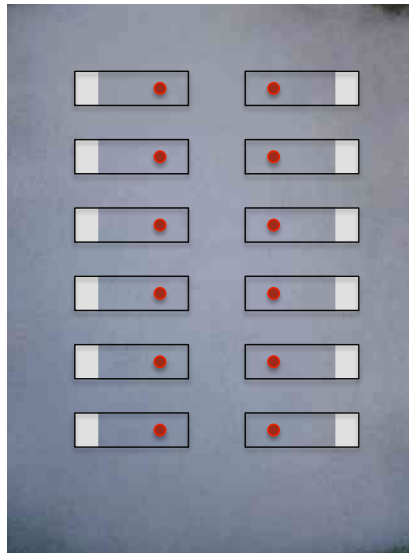


Figure 298 12 replicate stains generated on glass microscope slides, on snow

*(Author. 2012)*

A digital camera was used to take photographs of stains at various time intervals following generation. Photographs were taken 5, 15, 30, 45 and 60 minutes after stain generation. These photographs were then used to observe how the appearance of stains generated on glass slides, which were in contact with snow, altered over time.

The aim of this method of stain generation was to allow observations to be made regarding how the appearance of single drops of blood generated on glass slides, in contact with snow, were influenced by this exposure. Observations could also be made comparing the appearance of stains generated on slides in contact with snow, with the appearance of stains generated directly onto snow.

#### 8.4.4 Method 3 stain generation

A clean fresh area of snow measuring approximately 100cm x 75cm was identified (*figure 299*). Using a fixed 10 $\mu$ l volume pipette, an Ovine bloodstain was deposited from a height of 10cm onto the snow. The stain was generated by depositing multiple drops of blood in the same area, generating one large multi-drop stain (*figure 300*). 20 drops, each of 10 $\mu$ l volume, were deposited to form this stain.



Figure 299 Clean area of snow for experimentation

(*Author. 2012*)



Figure 300 Multi-drop stain generated on snow

(*Author. 2012*)

A digital camera was used to take photographs of the stain at various time intervals following generation. Photographs were taken 5, 15, 30, 45 and 60 minutes after

stain generation. These photographs were then used to observe how the appearance of a multi-drop stain, generated directly onto snow, altered over time.

The aim of this method of stain generation was to allow observations to be made regarding how the appearance of a multi-drop bloodstain generated directly onto snow is influenced by this exposure to snow.

#### **8.4.5 Methodological limitations**

For all methodologies involving exposure of bloodstains to snow certain experimental limitations had to be taken into account. In experimental stages 1 and 2 a flatbed scanner was used to capture digital images of generated stains, under uniform lighting and resolution conditions. For stains generated on snow however this method of image capture was impossible. A decision was therefore made to use a digital camera instead. Efforts were made to maintain as much consistency in lighting levels and distance of camera from stains when taking photographs of stains at different time intervals. This included conducting the experiments as close to the middle of the daylight hours as possible – to ensure changes in light levels were minimised - and taking all photographs at a height, directly above stains, of not more than 50cm.

In experimental stages 1 and 2 bloodstains were generated on paper, glass and denim fabric surfaces. For stains generated on snow, the use of paper and denim surfaces was thought to be experimentally problematic. Therefore only glass surfaces, mounted on snow, were stained. In experimental stages 1 and 2 chemical identification tests were conducted on generated stains. For stains generated on snow however these tests were considered extremely difficult to carry out. This meant that no chemical analysis of stains generated on snow was conducted. These limitations were considered during interpretation and analysis of results generated during experiments outlined in *section 8.4* and particularly when comparing these results to results generated through other experimental methodologies and sections.

## 8.5 Exposure of stains to freeze-thaw

### 8.5.1 Establishing experimental conditions

The experiment was designed to explore the behaviour of bloodstains subjected to freeze-thaw mechanisms overnight. For the purposes of ensuring stains were exposed to freeze-thaw mechanisms, a night where temperatures were forecast below 0°C was identified for experimentation.

An outdoor location, where stains could be left undisturbed overnight was identified as the experimental site. The location chosen was a walled balcony located on the 3<sup>rd</sup> floor of a building's exterior. This choice of experimental site offered stains physical protection from any possible animal or human interferences whilst ensuring they were exposed to true environmental conditions and fluctuations.

In order to generate a record of temperature fluctuations overnight, a digital temperature and humidity data logger (*figure 301*) was placed at the experimental site. The logger was programmed to record temperature and humidity levels at 5-minute intervals throughout the experiment. Stains were generated on glass surfaces and then left, exposed, overnight in temperatures below 0°C. The next day, once temperatures had risen above 0°C, observations were made about stains generated.



Figure 301 Digital temperature and humidity data logger, attached at experimental site

(Author. 2012)

### 8.5.2 Stain generation

Ten clean glass microscope slides were arranged on a plastic tray. The tray was then placed at the experimental location, on top of a raised brick shelf, which formed the lower half of the balcony wall at the experimental site. Using a fixed volume pipette, a series of Ovine bloodstains were deposited from a height of 10cm onto the slides. Each stain was generated from a single 10µl volume drop. In total 16 stains were generated (*figure 302*). Stains were generated at 22:00h, when the outside temperature was -3°C.



Figure 302 Stains generated on glass microscope slides, on brick wall at experimental site, located next to digital temperature and humidity data logger

(Author. 2012)

A digital camera was used to take photographs of stains at various time intervals following generation. Photographs were taken immediately after stains had been generated, some time after generation and at the end of the experiment. These photographs were then used to make observations about the appearance of stains, which had been exposed to freeze-thaw mechanisms. These observations were then compared to observations made from stains exposed to other environmental conditions or extremes. Once photographs of stains had been taken at the end of the experiment, stains were immediately subjected to chemical identification tests, as outlined in *sections 3.4.4 – 3.4.6*.

### 8.5.3 Methodological limitations

In experimental stages 1 and 2 a flatbed scanner was used to capture digital images of generated stains. Although this could have been used to image stains exposed to freeze-thaw mechanisms, in order to allow comparisons to be made between stains generated in *sections 8.4* (stains generated on snow) and **8.5** (stains exposed to



freeze-thaw) a digital camera was once again used. Photographs were taken at a fixed distance from stains. It was impossible to maintain a consistent natural lighting level as photographs of stains were taken at different times of day and night. This presented a limitation during interpretations of images of stains, based on colour analysis.

## 8.6 Exposure of stains to freezing conditions

### 8.6.1 Establishing experimental conditions

The experiment was designed to examine the behaviour of bloodstains generated on frozen surfaces and ice in freezing conditions. Observations were then made about stain appearance and behaviour, following their exposure to these surfaces and conditions. Three different methods were designed to generate and expose bloodstains to freezing surfaces and conditions.

*Method 1: Generation of single-drop stains onto room-temperature surfaces (paper, glass, denim)*

*Method 2: Generation of single-drop stains onto frozen surfaces (paper, glass, denim)*

*Method 3: Generation of single-drop stains directly onto ice*

In order to establish experimental consistency between methods, the frozen environment and conditions stains were exposed to were maintained with the use of a portable freezer (*figure 303*). The freezer temperature was set to  $-5^{\circ}\text{C}$  and a digital thermometer placed inside the freezer to indicate when that target temperature had been reached.



Figure 303 Portable freezer (*Author. 2012*)

### 8.6.2 Method 1 stain generation

In method 1, stains were generated on surfaces (at room temperature) and then housed in freezing conditions, on top of an ice surface. A plastic tub ( $H12\text{cm} \times L30\text{cm} \times W18\text{cm}$ ) was filled with water, to a depth of 3cm (*figure 304*). With the temperature in the experimental freezer fixed at  $-5^{\circ}\text{C}$ , the plastic tub was placed in the freezer and left for 24 hours. After a period of 24 hours, the water in the tub was frozen – providing a frozen ice surface for bloodstains to be generated either directly onto, or on surfaces lying on the ice surface.



Figure 304 Plastic tub filled with water to a depth of 3cm

(Author. 2012)

Using a fixed  $10\mu\text{l}$  volume pipette, a series of Ovine bloodstains were deposited from a height of 10cm onto paper, glass microscope slides and denim fabric. Each stain was generated from a single  $10\mu\text{l}$  volume drop of blood and 6 replicate stains were generated on each surface. Once stains had been generated, the surfaces were placed on top of the frozen ice surface, in the freezer (*figure 305*).



Figure 305 Bloodstains generated on paper (top left), glass microscope slides (right) and denim fabric (bottom left) surfaces, which were then placed on top of a frozen ice surface after generation

(Author. 2012)

Stains were left in the freezer for a period of 24 hours. Following this period of time, two methods of visual analysis were conducted on stains. First, a digital camera was used to take photographs of the stains. This allowed comparison of stains generated on surfaces at room temperature and subsequently exposed to freezing conditions to stains generated on snow (8.4) and those subjected to freeze-thaw mechanisms (8.5), which due to experimental limitations had also been photographed for visual analysis. The surfaces on which stains had been generated were then removed from the freezer and subjected to a secondary method of visual analysis (outlined in *section 3.4.7*) with the use of a flatbed scanner. This secondary method of visual analysis was used in experimental stages 1 and 2 and use of it in the analysis of stains generated in freezing conditions allowed comparisons to be made between stains generated across all three experimental stages. Once visual analysis of stains had been completed, stains were immediately subjected to chemical identification tests, as outlined in *sections 3.4.4 – 3.4.6*.

The aim of this method of stain generation was to allow observations to be made regarding the appearance and behaviour of bloodstains (generated on unfrozen surfaces) when exposed to a freezing environment. This mimics forensic scenarios where stains have been generated on surfaces at temperatures above 0°C and then exposed to freezing conditions. This can make identification and analysis of stains difficult as significant alterations to stain colour and behaviour can be caused by exposure to extreme cold. An example of when this might be encountered is in cold climates, where temperatures naturally drop below freezing overnight, if a stain was generated during a crime event occurring in the day and not discovered or analysed until the next day. Collecting observations about the nature of these alterations to appearance and behaviour of stains informs future analysis and interpretation of stains exposed to this type of scenario.

### **8.6.3 Method 2 stain generation**

In method 2, stains were generated on frozen surfaces, in freezing conditions. A frozen ice surface was generated according to the method set out in *section 8.6.2*. Swatches of paper, denim fabric and glass microscope slides were placed on top of

the ice and left for 24 hours to ensure they were adjusted to the frozen conditions of the underlying ice surface (*figure 306*).

Figure 306 Plastic tub filled with ice (to an approximate depth of 3cm) containing swatches of paper, denim fabric and glass microscope slides following 24 hours exposure to freezing conditions

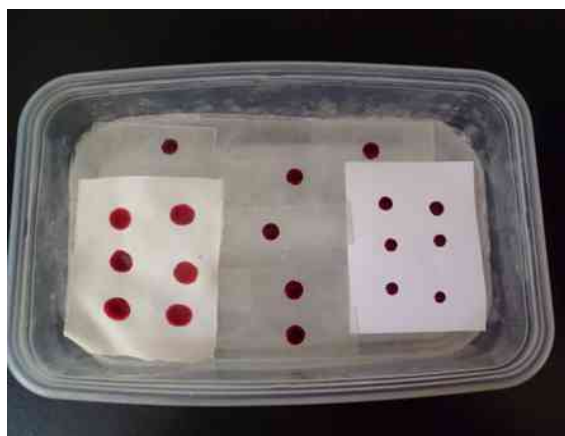
(*Author. 2012*)



Using a fixed 10 $\mu$ l volume pipette, a series of Ovine bloodstains were generated onto these frozen surfaces. For each surface (paper, glass, denim) 6 replicate stains, each of 10 $\mu$ l volume, were generated from a height of 10cm (*figure 307*).

Figure 307 18 bloodstains generated onto frozen surfaces (paper, glass, denim) from a height of 10cm

(*Author. 2012*)



Stains were left in the freezer for a period of 24 hours. Following this 24-hour period, two methods of visual analysis were conducted on stains. A digital camera was initially used to capture images of stains generated. This allowed comparison of stains generated on frozen surfaces and subsequently exposed to freezing conditions to stains generated on snow (8.4) and those subjected to freeze-thaw mechanisms (8.5), which had both also been captured for visual analysis by digital camera. The surfaces on which stains were generated were then removed from the freezer and subjected to a secondary method of visual analysis (outlined in *section 3.4.7*). This secondary method allowed comparisons to be made between stains generated in

experimental stages 1, 2 and those generated in experimental stage 3 which were capable of being imaged in this way.

Once visual analysis of stains had been completed, stains were immediately subjected to chemical identification tests, as outlined in **sections 3.4.4 – 3.4.6**. The aim of this method of stain generation was to allow observations to be made regarding the appearance and behaviour of bloodstains (generated on frozen surfaces) when exposed to a freezing environment.

#### 8.6.4 Method 3 stain generation

In method 3, stains were generated directly onto an ice surface. A plastic tub (*H12cm x L30cm x W18cm*) was filled with water, to a depth of 3cm. A frozen ice surface was generated according to the method set out in *section 8.6.2 (figure 308)*.



Figure 308 Plastic tub filled with ice (to a depth of approximately 3cm) (*Author. 2012*)

Using a fixed 10 $\mu$ l volume pipette, a series of Ovine bloodstains were generated directly the ice surface. 24 replicate stains, each of 10 $\mu$ l volume, were generated from a uniform height of 10cm (*figure 309*).

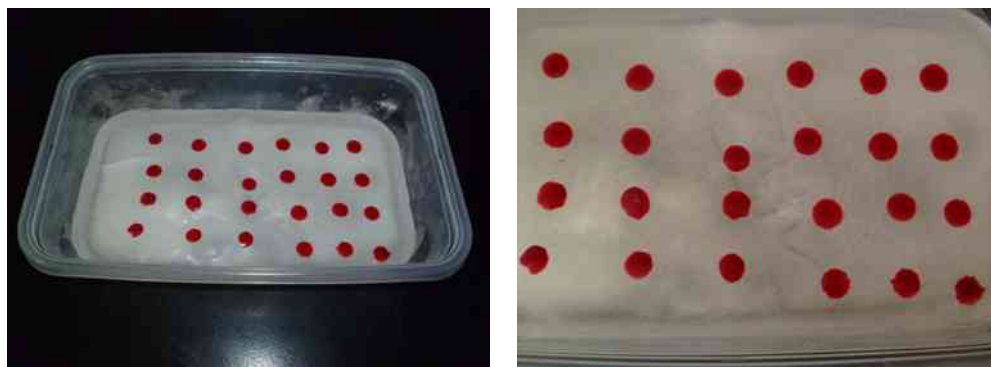


Figure 309 24 bloodstains generated directly onto ice from a height of 10cm (*Author. 2012*)

Once stains had been generated, they were left in the freezer for 24 hours. Following this period of 24 hours, visual and chemical analysis of stains was carried out. For visual analysis a digital camera was used to photograph stains. This allowed for a visual comparison of images of stains generated directly onto ice and stains generated on snow (8.4), subjected to freeze-thaw mechanisms (8.5) and other stains generated in freezing conditions (8.6.2 & 8.6.3). Once visual analysis of stains had been completed stains were immediately subjected to chemical identification tests, as outlined in *sections 3.4.4 – 3.4.6*.

The aim of this method of stain generation was to allow observations to be made regarding the appearance and behaviour of bloodstains generated directly on ice and further exposed to a freezing environment. This mimics forensic scenarios where stains are generated on frozen surfaces and remain exposed to freezing conditions. An example of when this might be encountered is in instances where stains are generated during crime events located outdoors onto frozen groundcover, for example snow, ice or permafrost. In these scenarios identification and analysis of stains can become difficult as significant alterations to stain colour and behaviour can occur. Collecting observations about the nature of these alterations to appearance and behaviour of stains informs future analysis and interpretation of stains generated on frozen surfaces and exposed to freezing conditions up to analysis.

#### **8.6.5 Methodological limitations**

In experimental stages 1 and 2 a flatbed scanner was used to conduct visual analysis of generated stains. Both experimental methods 1 and 2, exploring stains exposed to freezing conditions, involved the generation of stains on surfaces that could be removed from the freezing conditions and scanned. In method 3 however stains were generated directly onto ice, which could not be scanned. Visual analysis of stains generated on ice was therefore limited to analysis of digital photographs of stains. This presented a limitation to be considered in the interpretation and analysis of images of stains generated.

For stains generated, in method 2, on frozen surfaces, another experimental limitation presented itself. The stained surfaces (paper, glass and denim) were all placed onto ice and exposed to freezing conditions for 24 hours before they were stained. The rationale in doing so was to freeze the surfaces themselves prior to stain generation. As the surfaces froze they became attached to the ice underneath. Once stains had been generated and left in the freezer for 24 hours they were then removed for analysis. Detaching surfaces from the ice was achieved with some difficulty for both glass microscope slides and denim, however it was impossible to detach the stained paper from the ice without completely disintegrating the surface. In the case of stains generated on paper in method 2 therefore visual analysis was limited to analysis of photographs of stains. To compensate for the limitation that some stains could not be visually imaged with a digital scanner, all stains were also photographed. This allowed comparisons to be made between photographs of all stains generated in *sections 8.4, 8.5 and 8.6*. Where it was possible to analyse stains with the scanner, more methodologically robust comparisons could be made between stains generated in experimental stages 1, 2 and 3.

## **8.7 Exposure to high temperatures**

### **8.7.1 Establishing experimental conditions**

The experiment was designed to explore the behaviour of bloodstains exposed to high temperatures. Stains were generated on a range of surfaces (paper, glass, denim) and exposed to temperatures of 100, 150, 200 or 250°C. Temperatures were chosen to mimic a range of temperatures stains might be exposed to at different proximities away from the centre of a fire (*Tontarski et al. 2009*). This was to simulate forensic scenarios where stains are recovered following attempts by a suspect to obscure or obliterate evidence by setting fire to the scene. Observations were made about the responses of stains exposed to such high temperatures, through visual and chemical analysis. Two different methods were designed to generate and expose bloodstains to high temperatures.

**Method 1:** *Generation of single-drop stains onto room-temperature surfaces (paper, glass, denim)*

**Method 2:** *Generation of single-drop stains onto heated surfaces (paper, glass, denim)*

To achieve the high temperatures required an oven, capable of a top temperature of 250°C was selected for experimental purposes. A fan-assisted oven was chosen due to its ability to distribute air in the oven evenly, achieving a relatively consistent temperature throughout. To achieve further experimental consistency between stain samples, all samples were placed on a shelf located in the middle of the oven during experimentation.

As one oven was used for all samples a sampling order was required to ensure temperature in the oven did not exceed the target temperature for each sample. The sampling order was aligned with increases in temperature. Stain samples were generated at 100°C first, then 150°C, 200°C and finally 250°C.

### 8.7.2 Method 1 stain generation

In method 1, stains were generated on a range of surfaces (at room temperature) and exposed to a range of high temperatures. 100°C was the first temperature stains were exposed to. The oven was set to 100°C and left for 15 minutes to achieve this temperature throughout. In the meantime three different surfaces (paper, glass, denim) were prepared for staining. To prepare paper and denim surfaces for staining, rectangular swatches were cut of both. Glass microscope slides were mounted onto plain white record cards and attached with lengths of sellotape at both ends (*figure 310*).

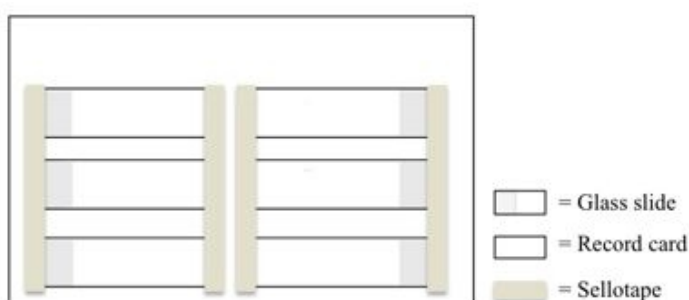


Figure 310 Glass microscope slides mounted on white record cards

(Author. 2012)

Using a fixed 10µl volume pipette, a series of Ovine bloodstains were deposited from a height of 10cm onto the paper, glass slides and denim fabric. Each stain was



generated from a single 10µl volume drop of blood and 6 replicate stains were generated on each surface. Once stains had been generated, the surfaces were placed onto a shelf located in the middle of the oven (*figure 311*).



Figure 311 Stains on middle shelf of fan-assisted oven (*Author. 2012*)

Stains were left in the oven at 100°C for 30 minutes, then removed and subjected to visual and chemical analysis. Visual analysis was conducted by using a flatbed scanner to capture digital images of generated stains (as outlined in **section 3.4.7**). This allowed comparison of stains generated at high temperatures with stains generated in experimental stages 1, 2 and others generated in experimental stage 3. Once visual analysis of stains had been completed, stains were subjected to chemical identification tests, as outlined in *sections 3.4.4 – 3.4.6*.

The temperature of the oven was then adjusted to the next experimental temperature, 150°C, and left for 15 minutes to achieve this temperature throughout. The process of stain generation, as described above, was then reproduced to generate a set of stains at 150°C. The entire process was then replicated identically for temperatures of both 200°C and 250°C.

### **8.7.3 Method 2 stain generation**

In method 2, stains were generated on a range of heated surfaces and exposed to a range of high temperatures. Paper swatches, denim fabric and glass microscope slides, prepared for staining, were placed on a shelf located in the middle of the oven. To prepare materials for staining, rectangular swatches of paper and denim were cut and 6 clean microscope slides were mounted onto plain white record cards (*figure*

310). 100°C was the first temperature stains were exposed to so the oven was set to 100°C and left for 15 minutes to achieve this temperature throughout.

Using a fixed 10µl volume pipette, a series of Ovine bloodstains were deposited from a height of 10cm onto the paper, glass slides and denim fabric. Each stain was generated from a single 10µl volume drop of blood and 6 replicate stains were generated on each surface. Once stains had been generated, the surfaces were returned to their previous location, on the middle shelf of the oven (*figure 311*).

Stains were left in the oven at 100°C for 30 minutes, then removed and subjected to visual and chemical analysis. Visual analysis was conducted by using a flatbed scanner to capture digital images of generated stains (as outlined in *section 3.4.7*). This allowed comparison of stains generated at high temperatures with stains generated in experimental stages 1, 2 and others generated in experimental stage 3. Once visual analysis of stains had been completed, stains were subjected to chemical identification tests, as outlined in *sections 3.4.4 – 3.4.6*.

Once visual and chemical analysis had been carried out, new unstained swatches of paper, denim fabric and glass slides were placed on the middle shelf of the oven and the temperature was adjusted to the next experimental temperature: 150°C. The oven was left for a period of 15 minutes until the temperature had been achieved throughout and then the process of stain generation was identically replicated to generate a set of stains at 150°C. The entire process was then replicated identically for temperatures of both 200°C and 250°C.

#### **8.7.4 Methodological limitations**

In previous experimental stages white or clear surfaces were stained in order to provide a ‘control’ background colour, against which colour analysis and comparisons of stains could be reliably made. In experiments examining the effects of extreme heat on stains, the surfaces that were stained were themselves significantly discoloured through exposure to heat. This had the effect of darkening the appearance and original colours of the white (paper, denim) and clear (glass)

surfaces. This darkening and discolouration of surfaces exposed to extreme heats had to be considered during colour analysis of stains generated on them.

As colour analysis of bloodstains generated in other experimental stages was not influenced by this discolouration effect, when comparing stains generated in experimental stages 1, 2 and other sections of stage 3 with stains generated at extremely heat temperatures, this was also a necessary consideration.

## **8.8 Exposure to fire (burning)**

### **8.8.1 Establishing experimental conditions**

The experiment was designed to explore the behaviour of bloodstains exposed to fire (burning environment). An outdoors location, which was well ventilated and where a controlled fire could be set up was chosen for experimentation. This simulated a forensic scenario where suspects may have attempted to destroy evidence by intentionally setting fire to a scene. Exposure to fire has been shown to alter the appearance and behaviour of bloodstains and observations of the nature of these alterations could assist with future analysis of stains recovered in these scenarios. In order to ensure maximum control over the experimental environment a decision was made to use a small charcoal barbecue as the source of fire. The barbecue consisted of a foil tray filled with approximately 700 grams of charcoal briquettes, with an inbuilt steel mesh grill suspended above the charcoal. The mesh grill was particularly important for experimental purposes. Stain samples could be rested on it, affording stains exposure to the centre of the burning environment, so that they were completely surrounded by fire. Stains were generated on glass microscope slides, on top of the grill, and then the unit was set on fire. Once the fire had burnt out and the slides cooled down sufficiently to handle, observations were made about stains generated.

### **8.8.2 Stain generation**

Eight clean glass microscope slides were arranged on top of the mesh grill of the unlit barbecue (*figure 312*).



Figure 312 Eight glass microscope slides arranged on mesh grill of unlit charcoal barbecue (slide circled in photo on left) (Author. 2012)

Using a fixed 10 $\mu$ l volume pipette, a series of Ovine bloodstains were deposited from a height of 10cm onto the slides. One stain was generated on each slide and each stain was generated from a single 10 $\mu$ l volume drop. In total 8 stains were generated (*figure 313*).

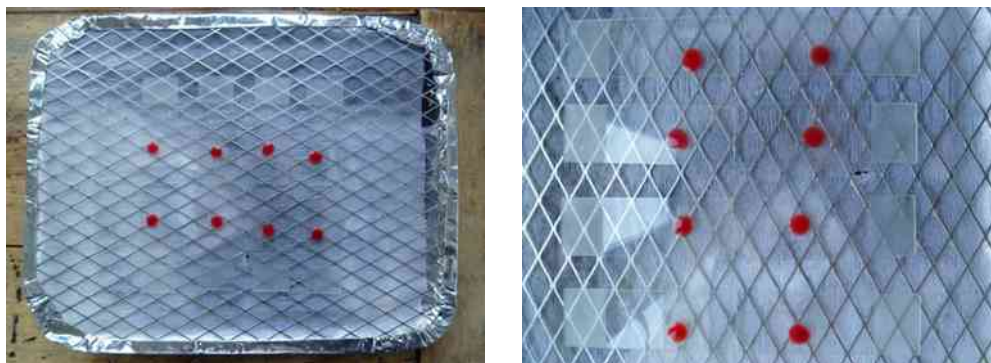


Figure 313 Eight bloodstains generated on glass microscope slides from a height of 10cm (Author. 2012)

The barbecue was then moved outdoors, gently placed on a fire-resistant surface and ignited (*figure 314*).



Figure 314 Blood-stained slides on the barbecue, immediately after charcoal was ignited

(Author. 2012)

Ignition continued until all charcoal, spread throughout the tray, was alight (*figure 315*). As the fire then continued to burn photographs of the stains were taken and observations made about their responses to fire exposure, the burning process and associated heat.



Figure 315 Tray barbecue following completion of the ignition process, when charcoal throughout the tray was alight (*Author. 2012*)

The charcoal fire was left to burn itself completely out. Once the fire had ceased and the tray cooled sufficiently to touch, microscope slides were retrieved from the mesh grill. Stains were then subjected to visual and chemical analysis. Visual analysis was carried out with the use of a flatbed scanner (as outlined in **section 3.4.7**). This allowed comparison of stains exposed to fire, the burning process and associated heat with stains generated in experimental stages 1, 2 and others generated in stage 3. Once visual analysis of stains was completed, stains were subjected to chemical identification tests, as outlined in *sections 3.4.4 – 3.4.6*.

### **8.8.3 Methodological limitations**

In experimental stages 1 and 2 stains were generated on paper, glass and denim fabric surfaces. Experiments exploring the effects on bloodstains of exposure to fire and burning processes required stains to be exposed to fire. In these experiments, paper and denim surfaces had to be excluded due to the likelihood of these surfaces being completely destroyed in the burning process. In forensic reality, destruction of any surfaces at a scene means that any evidence present on these surfaces would not be expected to survive exposure to fire and burning either. Attempting to develop methods to analyse stains generated on combustible surfaces has no practical investigative use. This meant that stains generated on glass were the only stains

exposed to fire. This methodological limitation restricted observations about and comparisons of stains exposed to fire and burning processes to stains exposed to other environmental conditions.

In previous experimental stages, as described in *section 8.7.4*, white or clear surfaces were stained in order to facilitate colour comparisons between different stain samples. In experiments examining effects of stain exposure to fire, smoke from the fire caused significant discolouration of the underside of stained slides. This had the effect of darkening the appearance of their originally clear glass surfaces. Awareness of this effect was incorporated into subsequent analysis of stains generated under these conditions and comparison of them to stains generated on unaltered glass slides in other experimental stages.

## 9. Experimental Stage 3 – Results

### 9.1 Responses of samples to chemical identification tests

Figure 316 presents the results of chemical identification tests performed on bloodstains generated under extreme environmental conditions. Presumptive tests conducted included the Kastle-Meyer, Hemastix and Bluestar tests. Results indicate that all stains exposed to environmental conditions B (freeze-thaw), C (freezing), D (high temperatures) and E (fire) tested presumptive positive for blood.

Environmental condition A (Snow)			Environmental condition B (Freeze-thaw)		
No chemical identification tests completed *			Denim	KM	+ive
				Hemastix	+ive
				Bluestar	+ive
			Glass	KM	+ive
				Hemastix	+ive
				Bluestar	+ive
			Paper	KM	+ive
				Hemastix	+ive
				Bluestar	+ive
Environmental condition C (Freezing)			Environmental condition D (High temperatures)		
Denim	KM	+ive	Denim	KM	+ive
	Hemastix	+ive		Hemastix	+ive
	Bluestar	+ive		Bluestar	+ive
Glass	KM	+ive	Glass	KM	+ive
	Hemastix	+ive		Hemastix	+ive
	Bluestar	+ive		Bluestar	+ive
Paper	KM	+ive	Paper	KM	+ive
	Hemastix	+ive		Hemastix	+ive
	Bluestar	+ive		Bluestar	+ive
Environmental condition E (Fire)			*Stains generated on snow were not subjected to chemical testing due to experimental limitations.		
Denim	KM	+ive			
	Hemastix	+ive			
	Bluestar	+ive			
Glass	KM	+ive			
	Hemastix	+ive			
	Bluestar	+ive			
Paper	KM	+ive			
	Hemastix	+ive			
	Bluestar	+ive			

Figure 316 Checklist of responses recorded for stains generated across five different extreme environmental conditions (& multiple methods) to presumptive chemical tests

Photographic examples of presumptive positive tests for stains generated in experimental stage 3 are set out in *figures 317 – 324*.



*Figure 317*

*Figure 317* illustrates an example of a stain on glass responding positively to a presumptive Hemastix test through observation of a green colouring of the Hemastix test stick. The stain shown was a stain exposed to environmental condition D (high temperatures).



*Figure 318*

*Figure 318* illustrates an example of a stain on denim responding positively to the Kastle-Meyer (KM) presumptive test through observation of a pink colouration. The stain shown was a stain exposed to environmental condition D (high temperatures).

*Figures 319 & 320* illustrate an example of a stain generated directly on ice responding positively to the Kastle-Meyer (KM) presumptive test through observation of a pink colouration.

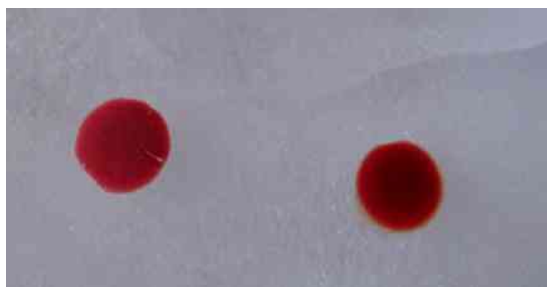


Figure 319 Stains pictured following application of Kastle-Meyer solution



Figure 320 Stains pictured following application of Hydrogen Peroxide solution

*Figures 321 & 322* illustrate an example of a stain generated directly on ice responding positively to Bluestar luminol testing through the emission of chemiluminescence.





Figure 321 Stains pictured in normal light

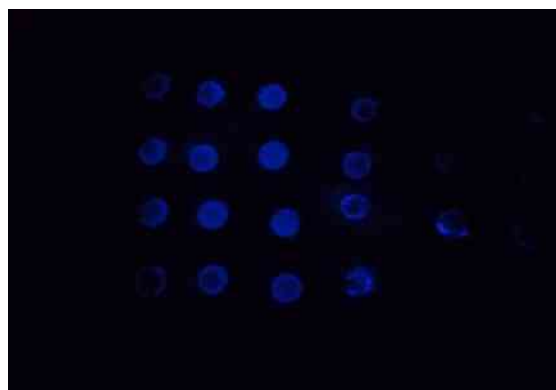


Figure 322 Stains pictured following application of Bluestar Luminol solution (in darkness)

*Figures 323 & 324* illustrate an example of a stain generated on glass and exposed to fire responding positively to Bluestar luminol testing through the emission of chemiluminescence.



Figure 323 Stains pictured in normal light

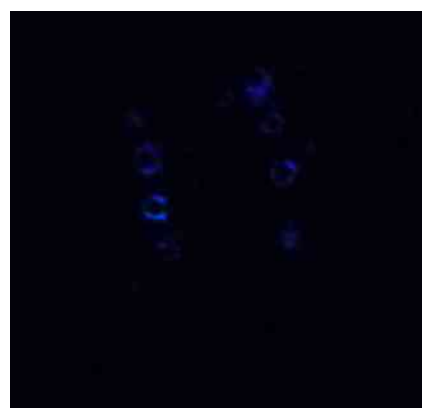


Figure 324 Stains pictured following application of Bluestar Luminol solution (in darkness)

An observation of presumptive positive chemical test results for stains exposed to the range of environmental conditions B-E has implications for the future identification of stains at crime scenes associated with exposure to these conditions. Results contradict previous suggestions that mechanisms such as burning (*Paonessa. 2005*) and freeze-thaw (*Lovelock. 1953*) present a barrier to positive chemical identification of stains and indicate that tests can continue to be used, with confidence, to identify stains in scenes which have been exposed to extreme conditions (B-E).

## **9.2 Environmental condition A (stains exposed to snow)**

Images and analysis of stains generated in environmental condition A are presented in *section 9.2*.

### **9.2.1 Images of stains generated**

Images of individual stains exposed to environmental condition A were captured using a digital camera and observations about stain appearance and behaviour were made from digital photographs. It was not possible to maintain comparable light conditions between photographs taken at different times and therefore RGB analysis conducted from photographs of stains was only considered rudimentary. Due to experimental limitations it was not possible to capture images of stains by digitally scanning them. Stains are presented in groups according to method of generation.

**9.2.1.1 Method 1**

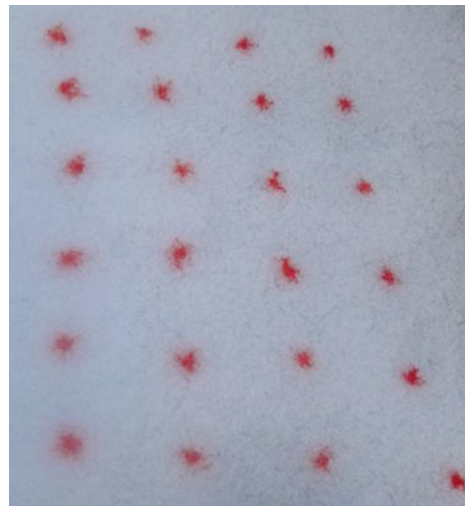
The images captured (as described in *section 9.2.1*) from single-drop stains generated directly onto snow are presented in *figure 325*. *Figure 325* shows stains at 00:05, 00:15, 00:30, 00:45 and 01:00 hours after stains were deposited on snow. As time increased, a general observation was made that stains appeared lighter in colour, more faint and diffuse. This observation was confirmed through visual examination of individual stains. Examination of a representative stain is presented in *figure 326*.

Figure 325 Overall images of 24 single drop stains generated directly onto snow taken at time intervals of +00:05, +00:15, +00:30, +00:45 and +01:00 hours

**Time since deposition /hours**

**Images of stains**

**+00:05**



**+00:15**



**+00:30**



**+00:45**



**+01:00**



Figure 326 Images of one particular single drop stain generated directly onto snow taken at time intervals of +00:05, +00:15, +00:30, +00:45 and +01:00 hours

**Time since deposition /hours**

**Images of stain**

**+00:05**



**+00:15**



**+00:30**



**+00:45**



**+01:00**



Quantitative RGB analysis of stains, from digital photographs, was carried out. As stain images were captured with a digital camera, under varying light conditions however, analysis was considered basic and only a summary of results is provided here (*figure 327*). Full results are set out in *appendix 3*. Although variations in light conditions were not recorded, light was fading and so it was thought they might exert some effect on stain colour readings by darkening the overall recorded colour intensity of stains. Varying light conditions have implications for capturing images of bloodstain evidence in real-life forensic scenarios and should be considered in any subsequent analysis of stain appearance, when it has not been possible to ensure a uniform method or light conditions whilst capturing images of stains.

*Figure 327* outlines average R, G, B values and RGB totals for stains generated directly onto snow. Results indicate that at each time interval R-values were higher than G or B values, which supports the observation that stains were orientated towards red, rather than green or blue, colour hues. Between 00:05 and 01:00 significant changes in colour values were noted. At 00:05 R-values were significantly higher (149) than G (45) or B (62) values. This suggests stains exhibited a strong red colour at 00:05. At 01:00 R-values had decreased slightly to 146 (from 149 at 00:05) whilst G (84) and B (122) values had almost doubled from 45 (G-value) and 62 (B-value) respectively at 00:05. This indicates that stains at 01:00 were coloured less intensely towards red than stains at 00:05. R-values were still dominant at 01:00, which means stains were still orientated towards a red colour but less intensely than at 00:05. This resulted in a lighter red, pink colouration in stains at 01:00 (*figure 326*). RGB totals also varied between 00:05 (256) and 01:00 (352), increasing by 96. Therefore stains were observed to become lighter in colour as time since deposition increased. Quantitative results support observations in *figure 326* that stains generated directly onto snow become less intensely red, lighter and pink in colour as time following deposition increases. Caution in any further interpretation of results is necessary however, considering the method of digital image capture. In forensic reality, when methods of capturing images of bloodstains on snow are restricted to digital photography under variable light conditions, similar caution should be exercised.

Time /hours	Average R Value	Average G Value	Average B Value	Average RGB Total
00:05	149	45	62	256
00:15	136	77	98	312
00:30	130	80	103	314
00:45	141	84	107	332
01:00	146	84	122	352

Figure 327 Average R, G, B values and RGB totals for single drop stains generated directly onto snow

### 9.2.1.2 Method 2

The images captured (as described in *section 9.2.1*) from single-drop stains generated onto glass slides on snow are presented in *figure 328*. Images support an observation made that stains generated onto glass slides on snow did not appear to vary in colour following their deposition. Examination of a representative stain is presented in *figure 329*.

Figure 328 Overall images of single drop stains generated onto glass slides on snow taken at time intervals of +00:15, +00:30, +00:45 and +01:00 hours

**Time since deposition /hours**

**Images of stains**

**+00:15**



**+00:30**



**+00:45**



**+01:00**





Figure 329 Images of one particular single drop stain generated onto glass slides on snow taken at time intervals of +00:15, +00:30, +00:45 and +01:00 hours

**Time since deposition /hours**

**Images of stain**

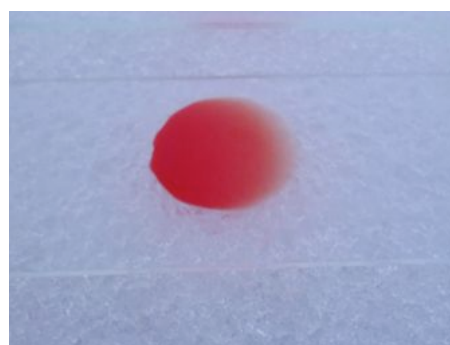
**+00:15**



**+00:30**



**+00:45**



**+01:00**



*Figure 330* outlines average R, G, B values and RGB totals for stains generated onto glass slide on snow. Full results are set out in *appendix 3*. Results indicate that at each time interval R-values were significantly higher than G or B values, which supports the observation, that stains were strongly orientated towards red hues of colour (*figures 328 and 329*). Between 00:15 and 01:00 sizeable alterations in colour

values were not observed. Between 00:15 and 01:00, values demonstrated minimal ranges of 17 (R-values), 8 (G-values) and 20 (B-values). This confirmed visual observations that stains generated on glass slides on snow do not exhibit considerable alterations in colour with increases in time following deposition.

Time /hours	Average R Value	Average G Value	Average B Value	Average RGB Total
00:15	132	19	46	197
00:30	133	24	54	211
00:45	146	26	54	226
00:50	149	27	66	242

Figure 330 Average R, G, B values and RGB totals for single drop stains generated directly onto snow

### 9.2.1.3 Method 3

The images captured (as described in *section 9.2.1*) from a multi-drop stain generated directly onto snow are presented in *figure 331*. Images support an observation that intensity and colour of stains generated on snow appears to vary following deposition.

*Figure 331* shows a multi-drop stain at 00:05, 00:15, 00:30, 00:45 and 01:00 hours after it was deposited on snow. As time increased, an observation was made that the stain appeared to fade in colour intensity. At 00:05 the stain appeared a vibrant red colour with a relatively clear margin. As time increased to 01:00 the stain appeared a less vibrant shade of red and closer in colour to pink. The stain also appeared to diffuse through the snow over the course of the hour, with the margin of the stain becoming less defined within 00:15 minutes of deposition. Diffusion of the stain is also demonstrated by the observation, from 00:15, of a line of blood that appears to extend from the bottom right hand corner of the main body of the stain.

Figure 331 Images of multi-drop stain generated directly onto snow taken at time intervals of +00:05, +00:15, +00:30, +00:45 and +01:00 hours

**Time since deposition /hours**

**Images of stain**

**+00:05**



**+00:15**



**+00:30**



**+00:45**



**+01:00**



*Figure 332* outlines average R, G, B values and RGB totals for a multi-drop stain generated directly on snow. Full results are set out in *appendix 3*. Results indicate that at each time interval R-values were significantly higher than G or B values, which supports the observation, that stains were strongly orientated towards red hues of colour (*figure 331*). Between 00:05 and 00:45 alterations in colour values were noted. At 00:05 R-values were significantly higher (159) than G (20) or B (41) values. This suggests stains exhibited a strong red colour at 00:05. At 00:45 R-values were approximately unaltered (158) whilst G values (63) had tripled and B values (84) values had doubled. This accounts quantitatively for the observation that stains at 00:45 were coloured less intensely red than stains at 00:05 and resulted in a lighter red, pink colouration of stains at 00:45 (*figure 331*). RGB totals between 00.05 (220) and 00:45 (305) increased by 85, supporting the suggestion that a multi-drop stain generated directly onto snow becomes lighter in colour as time from deposition increases. Results for colour values at 01:00 appear to counter this observation but appearances of varying light levels (*figure 331*) between stain photographs suggests measurements recorded for stain are likely to be somewhat inaccurate. Quantitative results indicate that stains generated directly onto snow become less intensely red, lighter and pink in colour as time following deposition increases. Caution in the interpretation of results further is a necessary consideration however, considering the method of digital image capture.

Time /hours	Average R Value	Average G Value	Average B Value	Average RGB Total
00:05	159	20	41	220
00:15	157	57	70	284
00:30	148	63	83	294
00:45	158	63	84	305
01:00	137	36	66	239

Table 332 Average R, G, B values and RGB totals for single drop stains generated directly onto snow

Analysis of stains exposed to environmental condition A (snow) has implications for future interpretations and analyses of bloodstains exposed to snow in real forensic scenarios. Results appear to support previous case-specific observations of bloodstains on snow exhibiting unusual appearances and pink colouring (*Leak. 2006. Morris. 2010*). As length of exposure to snow increased, single- and multi-drop

stains appeared to diffuse, become less intense shades of red and more pink in colour. Previously, observations of this were limited to a few case-specific scenarios with results in *section 9.2* representing the first experimental replication of observations. Discolouration of stains has implications for source level identification of bloodstains at a scene as it can lead to misidentification of stains as other types of physical evidence (*Morris. 2010*), leading to inaccurate stain analysis and crime scene reconstructions. Results also provide evidence for the possible cause of stain discolourations in stains generated on snow. Observations of minimal changes in colour for stains insulated from direct contact with snow by a glass slide support a suggestion that direct contact with snow causes discolouration, rather than exposure solely to associated temperatures. Implications of results for bloodstain pattern analysis mainly resonate for analysis of outdoors crime scenes involving snow. Awareness of the characteristic nature and unusual colouring of bloodstains deposited directly on snow should be incorporated into identification, interpretation and subsequent analysis of any evidence on snow-covered areas. Implications of results for bloodstain pattern and crime scene analysis are discussed further in *chapter 13*.

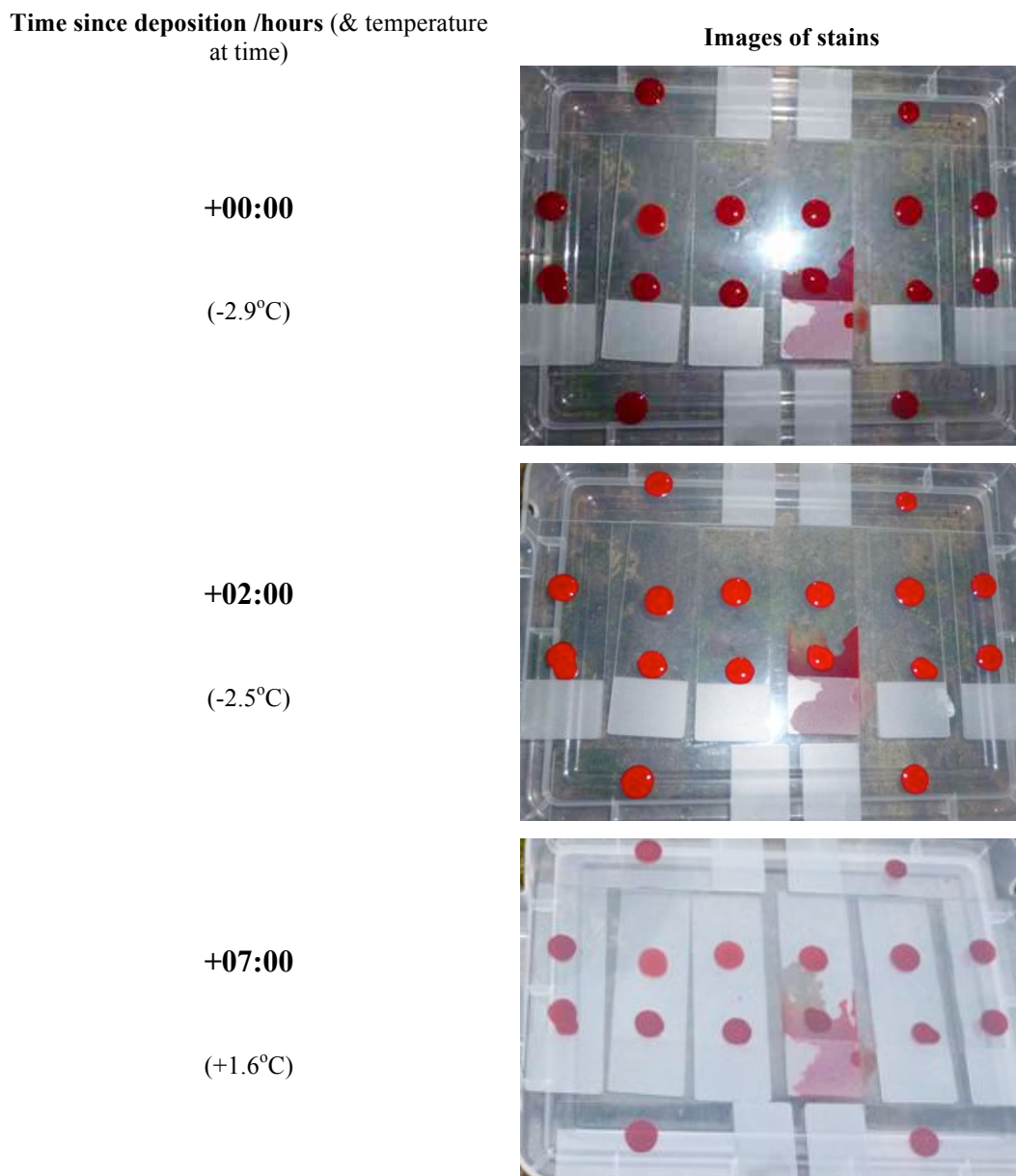
### **9.3 Environmental condition B (stains exposed to freeze-thaw)**

Images and analysis of stains generated in environmental condition B are presented in *section 9.3*.

#### **9.3.1 Images of stains generated**

*Figure 333* shows stains at 00:00, 02:00 and 07:00 hours after stains were deposited on glass slides in sub-zero temperatures and exposed to freeze-thaw mechanisms. Stains at +02:00 hours are still liquid and appear a brighter red than stains at 00:00 hours. Stains were left overnight and examined again at +07:00 hours, when they had dried and appeared a darker red than stains at +02:00 hours. An observation regarding the variability of stains exposed to identical environmental conditions was made from visual analyses (*figure 334*).

*Figure 333 Overall images of stains generated onto glass slides and exposed to freeze-thaw mechanisms*



*Figure 334* is comprised of two stains generated on one glass slide under identical environmental conditions. The stains significantly differ in appearance. The stain on the left (stain A) appears a much darker red colour than the stain on the right (stain B). Stain A also appears to exhibit some linear fractures across the surface of the stain whilst stain B appears a smooth disc. Visual observations appear to support a suggestion that stains generated on glass slides and subsequently exposed to freeze-thaw mechanisms demonstrate high variability.

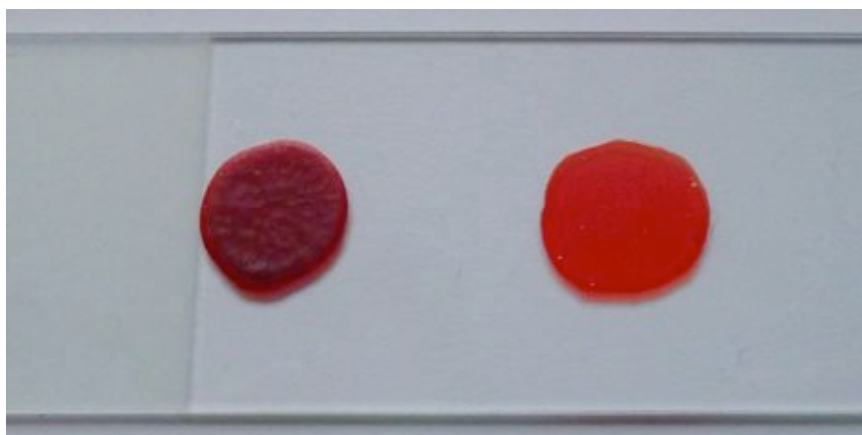


Figure 334 Two stains generated on a glass slide and exposed to identical environmental conditions

Observations of visible variability in stains simultaneously exposed to freeze-thaw mechanisms imply that in forensic reality, analysis of stain appearance for stains exposed to these mechanisms is complicated, as the cause of variability identified in section 9.3 was not identified.

## **9.4 Environmental condition C (stains exposed to freezing)**

Images and analysis of stains generated in environmental condition C are presented in *section 9.4*.

### **9.4.1 Images of stains generated**

Images of individual stains exposed to environmental condition are set out in sections 9.4.3, 9.4.4 and 9.4.6. Images were generated by digitally scanning stains immediately following their removal from experimental conditions, where possible. Due to experimental limitations it was not possible to capture images of stains generated directly onto ice by digitally scanning them. For these stains a digital camera was used and basic RGB analysis and observations about stain appearance and behaviour were made from digital photographs.

Stains are presented in groups according to method of generation. Stains generated in staining methods 1 (9.4.3) and 2 (9.4.4) are presented in groups of six, representing groups of 6 replicate stains generated on three different surfaces (denim, paper, glass). Stains generated in staining method 3 are presented in section 9.4.6.

### **9.4.2 Stain colour analysis**

Once stains had been digitally scanned, images were imported into colour analysis software to extract quantitative information about stain colour from the images. Each stain was analysed individually. Measurements from analysis are set out in results tables (*figures 336 and 339*). Statistical tests of comparison were conducted on results of stain colour analysis for staining methods 1 and 2 (section 9.4.5).

### **9.4.3 Staining method 1**

The images captured (as described in *section 9.4.1*) from stains generated on surfaces at room temperature and exposed to freezing conditions are presented in *figure 335*.

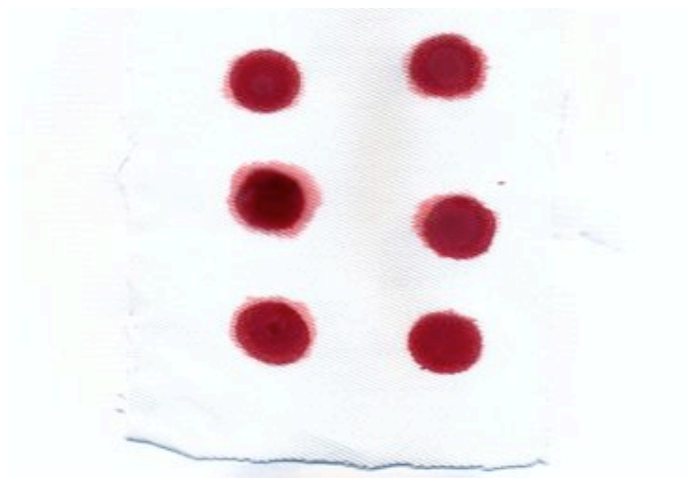


Figure 335 Images of stains generated on room temperature denim, paper and glass surfaces and exposed to freezing conditions

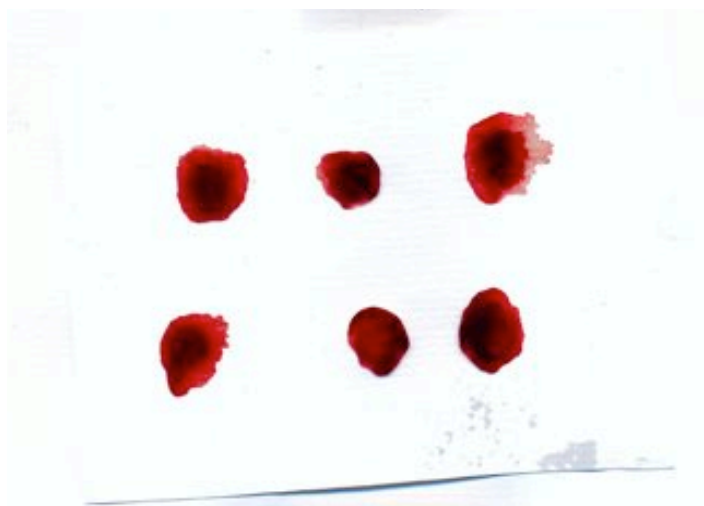
**Surface**

**Images of stains**

**Denim**



**Paper**



**Glass**



Figure 336 Table of measurements recorded for stains generated and exposed to environmental condition C via staining method 1





































Staining method 1							
Surface	R Value	G Value	B Value	RGB Total	Hex code	Stain	Hex colour
Denim	149	19	45	213	95132d		
Denim	145	29	52	226	911d34		
Denim	93	0	13	106	5d000d		
Denim	141	30	53	224	8d1e35		
Denim	140	14	38	192	8c0e26		
Denim	144	11	38	193	900b26		
Paper	104	0	6	110	680006		
Paper	87	6	13	106	57060d		
Paper	109	3	9	121	6d0309		
Paper	126	1	10	137	7e010a		
Paper	121	2	6	129	790206		
Paper	84	1	6	91	540106		
Glass	247	11	23	281	F70b17		
Glass	254	6	12	272	Fe060e		
Glass	253	3	21	277	Fd0315		
Glass	254	2	13	269	Fe020d		
Glass	251	4	15	270	Fb040f		
Glass	254	3	10	267	Fe030a		

Figure 337 sets out average R, G and B values calculated from replicate stains (n = 6) generated on denim, paper and glass surfaces and exposed to freezing conditions in addition to the percentage ratio of each component value for RGB totals. At each temperature interval R-values for stains were significantly higher than G and B-values. Stains therefore appeared strongly coloured towards a red rather than green

or blue hue. This was confirmed through observations of red stain colours in *figure 336*. Average measurements of R-values for surfaces were 135 (denim), 105 (paper) and 252 (glass). R-values can range between a minimum of 000 and a maximum of 255, representing darkest (000) or lightest (255) intensities of colour. Denim and paper stains exhibited medium intensities of red colour (135 & 105 respectively) whilst glass stains exhibited extremely strong intensities of red (252). This supports the observation in *figure 336* of medium intensities of colour in stains generated on denim and paper and extremely light intensity of colour in glass stains. This suggests, for stains exposed to freezing conditions through staining method 1, that glass stains appear a brighter, more vibrant red colour than denim or paper stains.

Surface	R Value	R %	G Value	G %	B Value	B %	RGB Total
<b>Denim</b>	135	70	17	9	40	21	192
<b>Paper</b>	105	90	2	1	8	9	116
<b>Glass</b>	252	92	5	2	16	6	273

Figure 337 Average R, G, B values and RGB Totals for denim, paper and glass stains exposed to condition C via staining method 1

Calculation of ratios of R to G and B values at each temperature gives an indication of strength of expression of each colour component across surfaces. Proportions of RGB totals of R-values ranged from 70% (denim) to 92% (glass), of G values ranged from 1% (paper) to 9% (denim) and B values ranged from 6% (glass) to 21% (denim). This meant that proportions of RGB totals comprised of R-values were greatest for glass stains (92%) and lowest for denim stains (70%). Results suggest that all stains exposed to freezing conditions were characterised by a red colouring but exhibited slight differences in colour, according to surface type.

#### 9.4.4 Staining method 2

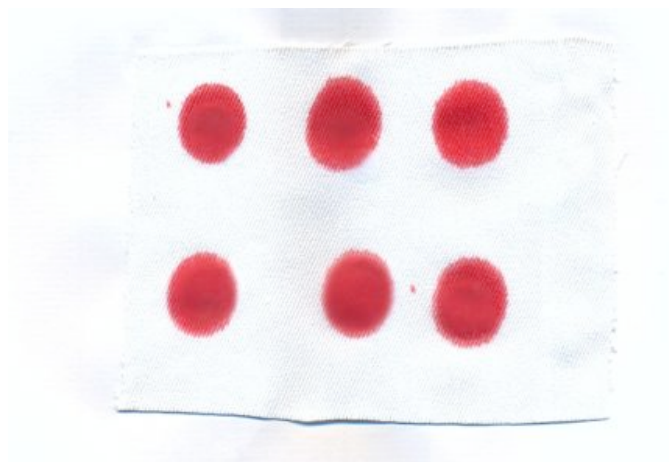
The images captured (as described in *section 9.4.1*) from stains generated on frozen surfaces and exposed to freezing conditions are presented in *figure 338*.

Figure 338 Images of stains generated on frozen denim, paper and glass surfaces and exposed to freezing conditions

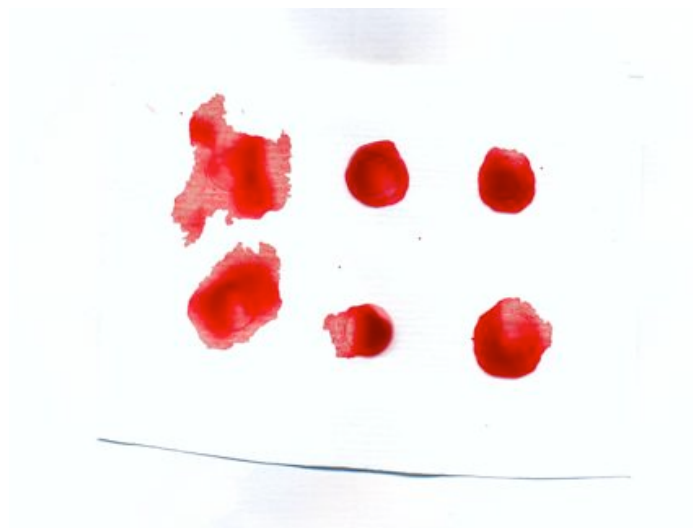
**Surface**

**Images of stains**

**Denim**



**Paper**



**Glass**

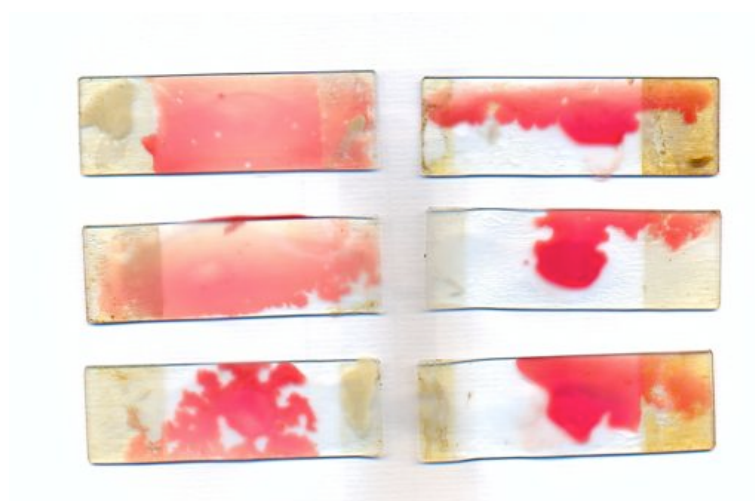


Figure 339 Table of measurements recorded for stains generated exposed to environmental condition C via staining method 2

Staining method 2





































Surface	R Value	G Value	B Value	RGB Total	Hex code	Stain	Hex colour
Denim	207	61	79	347	Cf3d4f		
Denim	197	50	69	316	C53245		
Denim	211	44	66	321	D32c42		
Denim	206	57	77	340	Ce394d		
Denim	205	52	73	330	Cd3449		
Denim	212	59	77	348	D43b4d		
Paper	227	7	16	250	E30710		
Paper	200	3	11	214	C8030b		
Paper	178	1	4	183	B20104		
Paper	223	10	18	251	Df0a12		
Paper	194	24	30	248	C2181e		
Paper	209	8	18	235	D10812		
Glass	255	154	156	565	Ff9a9c		
Glass	252	52	93	397	Fc345d		
Glass	255	147	149	551	Ff9395		
Glass	238	3	75	316	Ee034b		
Glass	254	78	113	445	Fe4e71		
Glass	251	28	87	366	Fb1c57		

Figure 340 sets out average R, G and B values calculated from replicate stains (n = 6) generated on denim, paper and glass surfaces and exposed to freezing conditions. The percentage ratio of each component value for RGB totals is also outlined. At each temperature interval R-values for stains were higher than G and B-values. Stains therefore appeared strongly coloured towards a red rather than green or blue

hue. This was confirmed through observations of red and pink stain colours in *figure 339*. Average measurements of R-values for surfaces were 206 (denim), 205 (paper) and 251 (glass). R-values can range between a minimum of 000 and a maximum of 255, representing darkest (000) or lightest (255) intensities of colour. Denim and paper stains exhibited strong intensities of red colour (206 & 205 respectively) whilst glass stains exhibited extremely strong intensities of red (251). This supports observations in *figure 339* of strong intensities of red colour in stains on all surfaces. This suggests, for stains exposed to freezing conditions through staining method 2, stains on all surfaces appear a bright red or pink colour.

Surface	R Value	R %	G Value	G %	B Value	B %	RGB Total
<b>Denim</b>	206	62	54	16	74	22	334
<b>Paper</b>	205	89	9	4	16	7	230
<b>Glass</b>	251	57	77	18	112	25	440

Figure 340 Average R, G, B values and RGB Totals for denim, paper and glass stains exposed to condition C via staining method 2

Calculation of ratios of R to G and B values at each temperature gives an indication of strength of expression of each colour component across surfaces. Proportions of RGB totals of R-values ranged from 57% (glass) to 89% (paper), of G values ranged from 4% (paper) to 18% (glass) and B values ranged from 7% (paper) to 25% (glass). This meant that proportions of RGB totals comprised of R-values were greatest for paper stains (89%) and lowest for glass stains (57%). Results may have been affected by observations of glass stains (*figure 338*) which demonstrate that stains formed on glass froze during the experiment, melting and becoming dilute as soon as they were removed from the experimental environment for colour analysis. Results indicate that all stains exposed to freezing conditions were characterised by a red colouring but exhibited slight differences in colour, according to surface type.

#### 9.4.5 Statistical tests of comparison

Statistical tests of comparison were conducted to statistically compare the distribution of R, G, B and RGB-values between stains generated according to methods 1 & 2 and between stains generated on different surfaces.

#### 9.4.5.1 Comparison of means between staining methods 1 & 2

To compare distributions of R, G, B values and RGB totals of stains generated in methods 1 and 2, a Kruskal-Wallis test was conducted. For stains generated in methods 1 and 2, results of the test indicated whether staining method had a significant effect on stain colour. *Figure 341* presents the results of the Kruskal-Wallis test carried out on stains generated. The results indicated that the null hypotheses should be rejected as  $p < 0.05$  in all scenarios indicating that the distribution of R, G, B values and RGB totals of stains generated by different staining methods (SM 1 and 2) were statistically different at the 95% significance level. Respective denim, paper and glass stains generated in method 1 were not statistically similar to the denim, paper and glass stains generated in method 2. This suggests that the different methods used to generate and expose stains to freezing conditions have an influence on stain appearance.

1	The distribution of R Value is the same across categories of Staining Method.	Independent-Samples Kruskal-Wallis Test	.019	Reject the null hypothesis.
2	The distribution of G Value is the same across categories of Staining Method.	Independent-Samples Kruskal-Wallis Test	.001	Reject the null hypothesis.
3	The distribution of B Value is the same across categories of Staining Method.	Independent-Samples Kruskal-Wallis Test	.001	Reject the null hypothesis.
4	The distribution of RGB Total is the same across categories of Staining Method.	Independent-Samples Kruskal-Wallis Test	.000	Reject the null hypothesis.

Asymptotic significances are displayed. The significance level is .05.

Figure 341 Kruskal-Wallis test comparing distributions of R, G, B values and RGB totals between staining methods 1 and 2

#### 9.4.5.2 Comparison of means between surfaces

To compare distributions of R, G, B values and RGB totals of stains generated on different surfaces, a Kruskal-Wallis test was conducted to test the null hypothesis that three unrelated (independent) sets of data have the same distribution. Therefore, for stains generated in methods 1 and 2, results of the test indicated whether surface



(denim, glass, paper) had a significant effect on stain colour (see *figure 342*).

1	The distribution of R Value is the same across categories of Surface.	Independent-Samples Kruskal-Wallis Test	.000	Reject the null hypothesis.
2	The distribution of G Value is the same across categories of Surface.	Independent-Samples Kruskal-Wallis Test	.004	Reject the null hypothesis.
3	The distribution of B Value is the same across categories of Surface.	Independent-Samples Kruskal-Wallis Test	.000	Reject the null hypothesis.
4	The distribution of RGB Total is the same across categories of Surface.	Independent-Samples Kruskal-Wallis Test	.000	Reject the null hypothesis.

Asymptotic significances are displayed. The significance level is .05.

Figure 342 Kruskal-Wallis test comparing distributions of R, G, B values and RGB totals between surfaces

The results indicated that  $p < 0.05$  for each test and therefore, the null hypotheses is rejected demonstrating that R, G, B values and RGB totals for stains generated on different surfaces (denim, glass, paper) can be considered to be statistically different at the 95% significance level. Denim stains, for example, were statistically distinct from glass or paper stains. This suggests, for stains exposed to freezing conditions that different surfaces stains were generated on had an influence on stain appearance.

Results of statistical tests (*figures 341 and 342*) conducted on stains exposed to environmental condition C confirmed that method of staining and surface stains were generated on significantly influenced stain colour. These results confirmed visual observations discussed in *sections 9.4.3 and 9.4.4*.

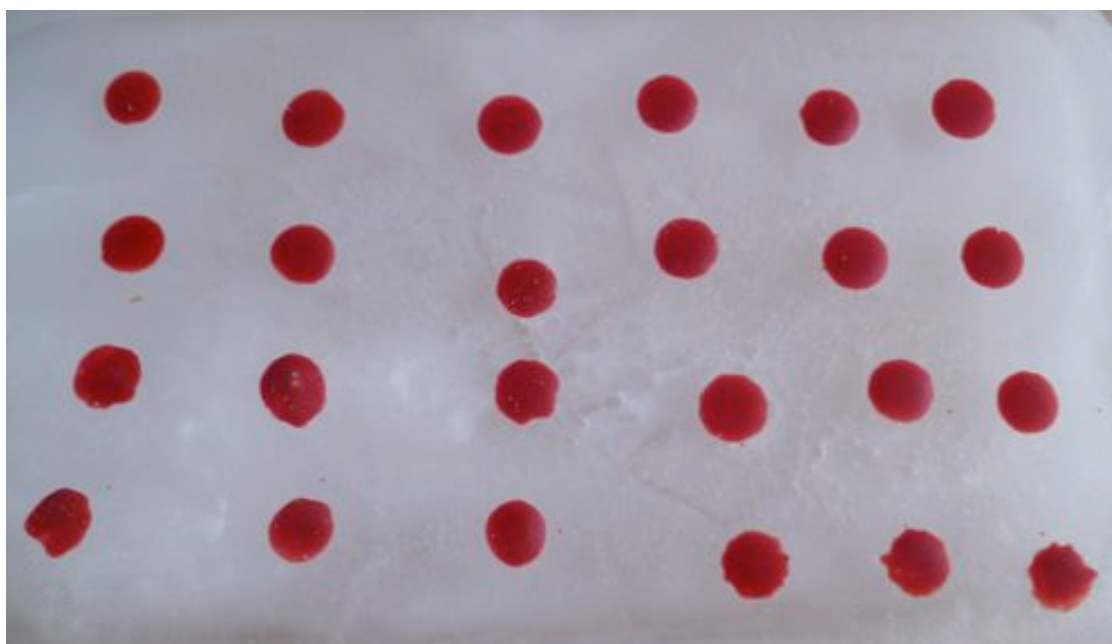
### 9.4.6 Staining method 3

Due to experimental limitations, images of stains generated in staining method 3 were captured by digital camera. Digital images of stains (*figure 343*) were imported into colour analysis software to extract quantitative information about stain colour from the images. Each stain was analysed individually and the measurements from the analysis are set out in *figure 344*.



Individual results set out in *figure 344* were used to calculate average colour values for stains generated directly on ice and exposed to freezing conditions. Stains on average exhibited an R-value of 115, G-value of 14 and B-value of 28, which meant that R-values for stains were significantly higher than G and B values. This supports observations of stains strongly coloured red in *figure 343*. RGB total is a measure of overall intensity of colour. The highest possible RGB total for the lightest intensity of all colour components (R255, G255, B255) is 765. For stains generated directly onto ice the average RGB total was 158, which was significantly lower than 765. This suggests stains were relatively dark in intensity. The experimental limitation of using a digital camera rather than scanner to capture images of stains may have influenced true colour values recorded and was considered in the interpretation of stains. Limited results presented suggest that stains deposited directly onto ice and exposed to freezing conditions in staining method 3 were characterised by red colourings and appear to exhibit consistency in colour.

Figure 343 Images of stains generated directly onto ice and exposed to freezing conditions



Stain	R Value	G Value	B Value	RGB Total
1	106	11	19	136
2	111	8	20	139
3	115	9	24	148
4	117	12	28	157
5	120	19	36	175
6	117	18	34	169
7	106	4	14	124
8	111	8	20	139

<b>9</b>	117	15	30	162
<b>10</b>	116	13	29	158
<b>11</b>	120	18	35	173
<b>12</b>	119	19	33	171
<b>13</b>	104	8	19	131
<b>14</b>	117	23	37	177
<b>15</b>	114	13	29	156
<b>16</b>	122	12	28	162
<b>17</b>	122	21	37	180
<b>18</b>	125	22	37	184
<b>19</b>	104	15	24	143
<b>20</b>	114	14	27	155
<b>21</b>	116	15	29	160
<b>22</b>	112	8	21	141
<b>23</b>	119	18	34	171
<b>24</b>	117	21	34	172

Figure 344 R, G, B values and RGB totals calculated for stains (n = 24) generated directly on ice and exposed to freezing conditions.

Analysis of stains exposed to environmental condition C (freezing conditions) has implications for future forensic interpretations and analyses of bloodstains exposed to these conditions. Despite previous anecdotal observations of stains exposed to extremely cold temperatures exhibiting bright, intense red and pink colours (*Brady et al. 2002. Morris. 2010*) results in *section 9.4* present the first experimental confirmation of these observations. Discolouration of stains has implications for source level identification of bloodstains at a scene as it may lead to incomplete identification of bloodstain evidence or inaccurate stain analysis and crime scene reconstructions. Awareness of the range of colours expected of bloodstains exposed to freezing conditions should be incorporated into identification, interpretation and subsequent analysis of any evidence recovered in scenes exposed to these conditions. Results indicated that stains exposed to freezing conditions via different staining methods could be differentiated between those deposited on frozen surfaces and those deposited on surfaces that were subsequently frozen. This has implications for constructing inferences about possible stain deposition times in certain scenarios. In an environment where surface conditions are only frozen overnight for example, being able to determine that stains were deposited on frozen surfaces (overnight) or unfrozen surfaces (daytime) may assist in isolating possible windows for stain deposition. Observations presented in *section 9.4* can be extrapolated to increase accuracy in the identification and interpretation of stains exhibiting signs of exposure to freezing conditions. Implications of results for bloodstain pattern and crime scene analysis are discussed further in *chapter 13*.

## **9.5 Environmental condition D (stains exposed to high temperatures)**

Images and analysis of stains generated in environmental condition D are presented in *section 9.5*.

### **9.5.1 Images of stains generated**

Images of individual stains exposed to environmental condition D are set out in sections 9.5.3 & 9.5.4. Images were generated by digitally scanning stains immediately following their removal from the experimental oven. Stains are presented in groups of six, representing groups of 6 replicate stains generated on three different surfaces (denim, paper, glass) at each of four different temperature intervals (100°C, 150°C, 200 °C and 250 °C). Experiments involved two different staining methods, which are discussed in *sections 9.5.3 and 9.5.4* respectively.

Comparisons of characteristics of stains generated on different surfaces (denim, paper, glass) and different staining methods are provided after individual analyses in *section 9.5.5*.

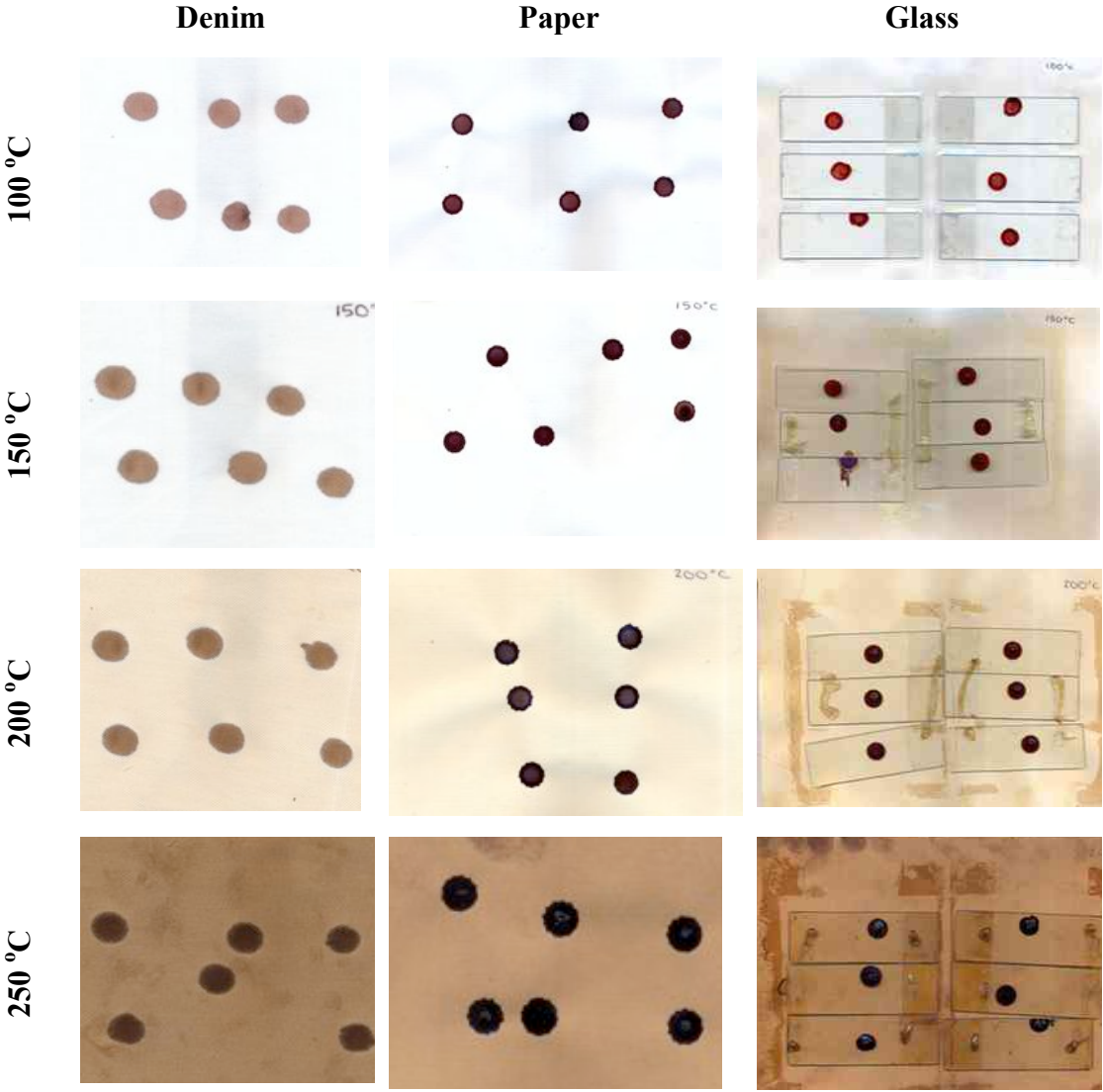
### **9.5.2 Stain colour analysis**

Once stains had been digitally scanned, images were imported into colour analysis software to extract quantitative information about stain colour from the images. Each stain was analysed individually. Measurements from analysis are set out in results tables (*figures 346 - 351*). Images of individual stains and blocks of corresponding hexadecimal colour for each stain are also included.

### **9.5.3 Staining method 1**

The images captured (as described in *section 9.5.2*) from each stain generated on surfaces at room temperature and exposed to high temperatures are presented in *figure 345*.

Figure 345 Images of stains generated on denim, paper and glass surfaces and exposed to temperatures of 100°C, 150°C, 200°C and 250°C



### 9.5.3.a Denim surfaces

Figure 346 Table of measurements recorded for stains generated on denim surfaces from 100°C to 250°C











Temperature /°C	R value	G value	B value	RGB Total	Hex	Stain	Hex Colour
100	167	126	116	409	A77e74		
100	160	117	106	383	A0756a		
100	159	117	108	384	9f756c		
100	165	121	111	397	A5796f		
100	133	91	85	309	855b55		
100	162	119	108	389	A2776c		
150	148	111	88	347	946f58		
150	144	106	82	332	906a52		
150	147	111	88	346	936f58		
150	150	115	92	357	96735c		
150	149	112	87	348	957057		
150	154	118	94	366	9a765e		
200	134	96	67	297	866043		
200	131	92	62	285	835c3e		
200	137	99	69	305	896345		
200	134	97	69	300	866145		
200	127	90	62	279	7f5a3e		
200	140	102	72	314	8c6648		
250	63	38	26	127	3f261a		
250	55	32	21	108	372015		
250	62	39	28	129	3e271c		
250	62	38	26	126	3e261a		
250	56	34	25	115	382219		
250	61	38	27	126	3d261b		

Figure 347 outlines average R, G, B values and RGB totals calculated from 6 replicate stains at each temperature. The percentage ratio of each component value for RGB totals is also presented. At each temperature interval R-values for stains were higher than G and B-values. Stains therefore appeared coloured towards a red

rather than green or blue hue. This was confirmed through observations of pink and brown stain colours in *figure 346*. As temperature increased from 100°C to 250°C R, G, B values and RGB totals decreased from 379 (100°C) to 122 (250°C) indicating that denim stains exhibited darker intensities of colour as temperature increased, as illustrated in *figure 346*.

A decrease in RGB totals from 379 (100°C) to 122 (250°C) supports observations that as temperature increased, denim stains exhibited darker intensities of colour. This was confirmed through observations of stain colours in *figure 346*, which were pink at 100°C before transitioning through shades of lighter and then darker brown at 150°C and 200°C to a very dark brown colour at 250°C.

Figure 347 Descriptive statistics recorded for stains generated on denim surfaces from 100°C to 250°C

Temperature /°C	R Value	R %	G Value	G %	B Value	B %	RGB Total
<b>100</b>	158	42	115	30	106	28	379
<b>150</b>	149	43	112	32	89	25	349
<b>200</b>	134	45	96	32	67	23	297
<b>250</b>	60	49	37	30	26	21	122

Calculation of ratios of R to G and B values at each temperature gives an indication of changes in each colour component across temperatures. R-values ranged from 42% (100°C) to 49% (250°C), G values ranged from 30% (100°C) to 30% (250°C) and B values ranged from 28% (100°C) to 21% (250°C). This meant that proportions of RGB totals comprised of R-values and G-values increased as temperature increased, whilst proportion of B-values decreased. Results suggest that as stains on denim are exposed to increases in extreme temperatures they exhibit significant alterations in stain colour, slightly increasing their orientation towards red hues and becoming increasingly characterised by darker intensities of colour.

### 9.5.3.b Paper surfaces

Figure 348 Table of measurements recorded for stains generated on paper surfaces from 100°C to 250°C

Temperature /°C	R value	G value	B value	RGB Total	Hex	Stain	Colour
100	91	43	53	187	5b2b35		
100	34	16	31	81	22101f		
100	67	31	44	142	431f2c		
100	81	29	40	150	511d28		
100	83	32	43	158	53202b		
100	77	33	46	156	4d212e		
150	55	16	28	99	37101c		
150	54	12	23	89	360c17		
150	52	13	20	85	340d14		
150	56	14	25	95	380e19		
150	49	6	17	72	310611		
150	57	25	26	108	39191a		
200	51	33	44	128	33212c		
200	48	33	47	128	30212f		
200	64	42	48	154	402a30		
200	55	36	46	137	37242e		
200	44	21	29	94	2c151d		
200	46	14	11	71	2e0e0b		
250	18	12	16	46	120c10		
250	16	11	15	42	100b0f		
250	12	8	11	31	0c080b		
250	17	13	16	46	110d10		
250	7	4	5	16	070405		
250	16	10	14	40	100a0e		

Figure 349 outlines average R, G, B values and RGB totals calculated from 6 replicate stains on paper at each temperature, in addition to the percentage ratio of each component value for RGB totals. At each temperature interval R-values for stains were higher than G and B-values. Stains therefore appeared coloured towards



a red rather than green or blue hue. This was confirmed through observations of red, purple and brown stain colours in *figure 348*. As temperature increased from 100°C to 250°C R values and RGB totals decreased. The decrease in RGB totals from 146 (100°C) to 37 (250°C) supports observations that as temperature increased, paper stains exhibited darker intensities of colour. This was confirmed through observations of stain colours in *figure 348*, which were dark pink at 100°C before transitioning through shades of maroon and purple-brown at 150°C and 200°C to extremely dark brown-black colours at 250°C.

Figure 349 Descriptive statistics recorded for stains generated on paper surfaces from 100°C to 250°C

Temperature /°C	R Value	R %	G Value	G %	B Value	B %	RGB Total
<b>100</b>	72	49	31	21	43	30	146
<b>150</b>	54	59	14	16	23	25	91
<b>200</b>	51	43	30	25	38	32	119
<b>250</b>	14	38	10	27	13	35	37

Calculation of ratios of R to G and B values at each temperature gives an indication of changes in each colour component across temperatures. R-values ranged from 49% (100°C) to 38% (250°C), G values ranged from 21% (100°C) to 27% (250°C) and B values ranged from 30% (100°C) to 35% (250°C). This meant that proportions of RGB totals comprised of R-values decreased, whilst proportions of G and B-values increased, which suggests that paper stains became less strongly orientated to red hues as temperature increased. Results suggest that as stains on paper are exposed to increases in extreme temperatures they exhibit significant alterations in stain colour, becoming characterised by extremely dark intensities of colour. The average RGB triplet at 250°C was (R14, G10, B13), which is very close to the triplet typical triplet for 'black' (R000, G000, B000).



9.5.3.c Glass surfaces

Figure 350 Table of measurements recorded for stains generated on glass surfaces from 100°C to 250°C





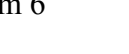
Temperature /°C	R value	G value	B value	RGB Total	Hex	Stain	Colour
100	149	35	29	213	95231d		
100	114	33	36	183	722124		
100	150	45	36	231	962d24		
100	138	37	33	208	8a2521		
100	111	22	25	158	6f1619		
100	123	21	21	165	7b1515		
150	97	19	5	121	611305		
150	92	15	8	115	5c0f08		
150	76	16	23	115	4c1017		
150	72	11	18	101	480b12		
150	82	50	86	218	523256		
150	90	15	8	113	5a0f08		
200	63	20	25	108	3f1419		
200	65	17	15	97	41110f		
200	65	24	25	114	411819		
200	62	16	18	96	3e1012		
200	62	16	20	98	3e1014		
200	61	20	24	105	3d1418		
250	38	36	45	119	26242d		
250	29	23	28	80	1d171c		
250	28	21	27	76	1c151b		
250	14	7	8	29	0e0707		
250	30	28	34	92	1e1c22		
250	32	27	31	90	201b1f		

Figure 351 outlines average R, G, B values and RGB totals calculated from 6 replicate stains on glass at each temperature. The percentage ratio of each component value for RGB totals is also outlined. At each temperature interval R-values for stains were higher than G and B-values, with the exception of average R and G values of stains at 250°C, which were equal (29). Stains therefore appeared coloured

towards a red rather than green or blue hue. This was confirmed through observations of red and maroon stain colours in *figure 350*. As temperature increased from 100°C to 250°C R, G, B values and RGB totals decreased. The decrease in RGB totals from 193 (100°C) to 81 (250°C) supports observations that as temperature increased, glass stains exhibited darker intensities of colour. This was confirmed through observations of a dramatic range of stain colours in *figure 350*, which were red at 100°C before transitioning through dark red and red-brown at 150°C and 200°C to a dark purple, black colour at 250°C.

Figure 351 Descriptive statistics recorded for stains generated on glass surfaces from 100°C to 250°C

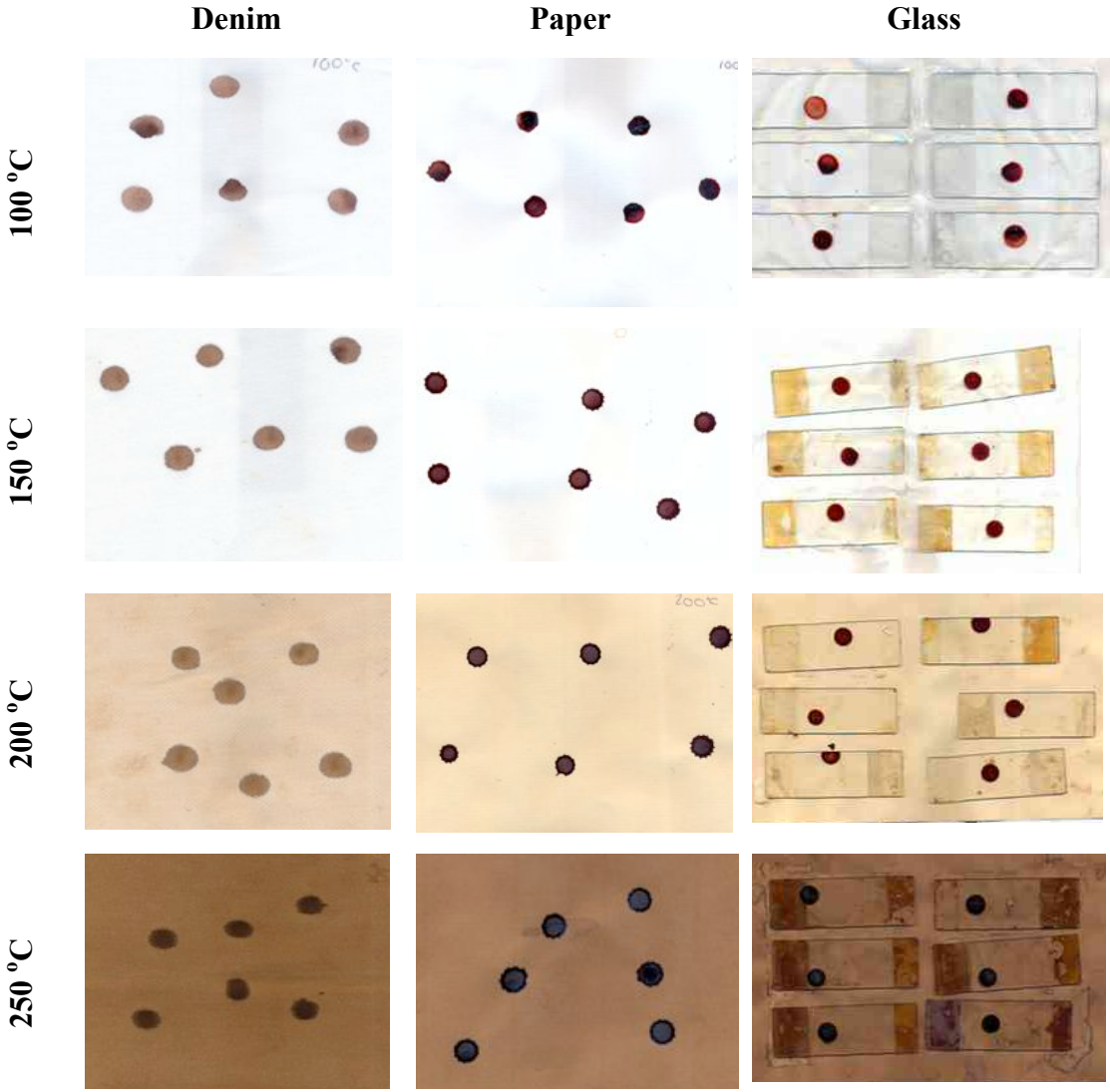
Temperature /°C	R Value	R %	G Value	G %	B Value	B %	RGB Total
<b>100</b>	131	68	32	17	30	15	193
<b>150</b>	85	65	21	16	25	19	131
<b>200</b>	63	61	19	19	21	20	103
<b>250</b>	29	36	24	29	29	35	81

Calculation of ratios of R to G and B values at each temperature gives an indication of changes in each colour component across temperatures. R-values ranged from 68% (100°C) to 36% (250°C), G values ranged from 17% (100°C) to 29% (200°C) and B values ranged from 15% (100°C) to 35% (250°C). This meant that proportions of RGB totals comprised of R-values decreased significantly, whilst proportions of G and B-values increased, which suggests that glass stains became less strongly orientated to red hues as temperature increased. Results suggest that as stains on glass are exposed to increases in extreme temperatures they exhibit significant alterations in stain colour, decreasing their orientation towards red hues and becoming increasingly characterised by darker intensities of colour.

#### 9.5.4 Staining method 2

The images captured (as described in *section 9.5.2*) from each stain generated on heated surfaces and exposed to high temperatures are presented in *figure 352*. Results from staining method 2 were very similar to results generated by staining method 1. This was confirmed by a statistical test of comparison presented in *section 9.5.5*.

Figure 352 Images of stains generated on denim, paper and glass surfaces and exposed to temperatures of 100°C, 150°C, 200°C and 250°C



#### 9.5.4.a Denim surfaces

Figure 353 Table of measurements recorded for stains generated on denim surfaces from 100°C to 250°C








































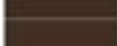

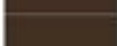




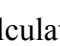
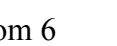
Temperature /°C	R value	G value	B value	RGB Total	Hex	Stain	Colour
100	111	75	71	257	6f4b47		
100	160	121	109	390	a0796d		
100	140	102	96	338	8c6660		
100	165	126	116	407	a57e74		
100	114	78	72	264	724e50		
100	152	113	105	370	987169		
150	144	106	85	335	906a55		
150	147	109	87	343	936d57		
150	123	88	75	286	7b584b		
150	144	106	86	336	906a56		
150	141	103	83	327	8d6753		
150	142	106	89	337	8e6a59		
200	138	102	71	311	8a6647		
200	134	96	64	294	866040		
200	140	103	71	314	8c6747		
200	138	101	69	308	8a6545		
200	138	100	67	305	8a6443		
200	139	101	69	309	8b6545		
250	56	32	20	108	382014		
250	52	30	17	99	341e11		
250	52	30	19	101	341e13		
250	53	30	19	102	351e13		
250	53	31	19	103	351f13		
250	45	26	18	89	2d1a12		

Figure 354 outlines average R, G, B values and RGB totals calculated from 6 replicate stains on denim at each temperature and the percentage ratio of each component value for RGB totals. At each temperature interval R-values for stains were higher than G and B-values. Stains therefore appeared coloured towards a red rather than green or blue hue. This was confirmed through observations of pink and

brown stain colours in *figure 353*. As temperature increased from 100°C to 250°C R, G, B values and RGB totals decreased. The decrease in RGB totals from 338 (100°C) to 100 (250°C) supports observations that as temperature increased, denim stains exhibited darker intensities of colour. This was confirmed through observations of stain colours in *figure 353*, which were pink-brown at 100°C, transitioning through shades of light-tan brown at 150°C and 200°C to a very dark brown colour at 250°C.

Figure 354 Descriptive statistics recorded for stains generated on denim surfaces from 100°C to 250°C

Temperature /°C	R Value	R %	G Value	G %	B Value	B %	RGB Total
<b>100</b>	140	41	103	31	95	28	338
<b>150</b>	140	43	103	31	84	26	327
<b>200</b>	138	45	101	33	69	22	307
<b>250</b>	52	52	30	30	19	19	100

Calculation of ratios of R to G and B values at each temperature gives an indication of changes in each colour component across temperatures. R values ranged from 41% (100°C) to 52% (250°C), G values ranged from 31% (100°C) to 30% (250°C) and B values ranged from 28% (100°C) to 19% (250°C). This meant that proportions of RGB totals comprised of R-values increased as temperature increased, whilst proportion of G and B-values decreased slightly. Results suggest that as stains on denim are exposed to increases in extreme temperatures they exhibit alterations in stain colour, slightly increasing their orientation towards red hues and becoming increasingly characterised by darker intensities of colour.

### 9.5.4.b Paper surfaces

Figure 355 Table of measurements recorded for stains generated on paper surfaces from 100°C to 250°C
























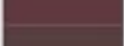











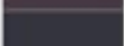

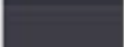

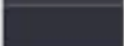



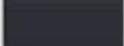

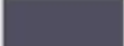


Temperature /°C	R value	G value	B value	RGB Total	Hex	Stain	Colour
100	82	38	46	166	52262e		
100	27	9	18	54	1b0912		
100	29	20	33	82	1d1421		
100	70	18	35	123	461223		
100	53	21	37	111	351525		
100	41	25	46	112	29192e		
150	74	26	33	133	4a1a21		
150	86	40	47	173	56282f		
150	75	29	39	143	4b1d27		
150	70	22	30	122	46161e		
150	83	36	42	161	53242a		
150	81	36	47	164	51242f		
200	73	44	45	162	492c2d		
200	66	41	47	154	42292f		
200	55	28	39	122	371c27		
200	51	23	28	102	33171c		
200	66	38	43	147	42262b		
200	58	36	48	142	3a2430		
250	34	34	45	113	22222d		
250	43	42	52	137	2b2a34		
250	32	32	44	108	20202c		
250	15	14	24	53	0f0e18		
250	28	28	39	95	1c1c27		
250	40	41	55	136	282937		

Figure 356 outlines average R, G, B values and RGB totals calculated from 6 replicate stains at each temperature. The percentage ratio of each component value for RGB totals is also outlined. At each temperature interval R-values for stains were higher than G and B-values, with the exception of stains at 250°C, which exhibited higher B-values than R or G values. With the exception of these stains, stains

therefore appeared coloured towards a red rather than green or blue hue. This was confirmed through observations of red, purple and brown stain colours in *figure 355*.

Figure 356 Descriptive statistics recorded for stains generated on paper surfaces from 100°C to 250°C

Temperature /°C	R Value	R %	G Value	G %	B Value	B %	RGB Total
<b>100</b>	50	46	22	20	36	33	108
<b>150</b>	78	52	32	21	40	27	149
<b>200</b>	62	45	35	25	42	30	139
<b>250</b>	32	30	32	30	43	40	107

RGB totals were lowest at 100°C (108) and 250°C (107) and highest at 150°C and 200°C. This supports an observation that paper stains exhibited darker intensities of colour at 100°C and 250°C. This was confirmed through observations of stain colours in *figure 355*, which were dark black, purple and grey at 100°C and 250°C and lighter shades of red and purple at 150°C and 200°C. Calculation of ratios of R to G and B values at each temperature gives an indication of changes in each colour component across temperatures. R values ranged from 46% (100°C) to 30% (250°C), G values ranged from 20% (100°C) to 30% (250°C) and B values ranged from 33% (100°C) to 40% (250°C). This meant that proportions of RGB totals comprised of R-values decreased, whilst proportions of G and B-values increased, which suggests that paper stains became less strongly orientated to red hues as temperature increased. Results suggest that as stains on paper are exposed to increases in extreme temperatures they exhibit alterations in stain colour and are characterised by extremely dark intensities of colour.



### 9.5.4.c Glass surfaces

Figure 357 Table of measurements recorded for stains generated on glass surfaces from 100°C to 250°C

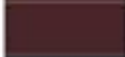
Temperature /°C	R value	G value	B value	RGB Total	Hex	Stain	Colour
100	149	35	29	213	95231d		
100	114	33	36	183	722124		
100	150	45	36	231	962d24		
100	138	37	33	208	8a2521		
100	111	22	25	158	6f1619		
100	123	21	21	165	7b1515		
150	97	19	5	121	611305		
150	92	15	8	115	5c0f08		
150	76	16	23	115	4c1017		
150	72	11	18	101	480b12		
150	82	50	86	218	523256		
150	90	15	8	113	5a0f08		
200	82	11	4	97	3f1419		
200	68	8	13	89	41110f		
200	87	17	6	110	411819		
200	80	12	13	105	3e1012		
200	87	23	11	121	3e1014		
200	72	6	7	85	3d1418		
250	20	15	20	55	26242d		
250	17	13	17	47	1d171c		
250	29	26	31	86	1c151b		
250	22	19	25	66	0e0707		
250	19	14	18	51	1e1c22		
250	11	4	4	19	201b1f		

Figure 358 outlines average R, G, B values and RGB totals calculated from 6 replicate stains at each temperature. The percentage ratio of each component value for RGB totals is also outlined. At each temperature interval R-values for stains were higher than G and B-values. Stains therefore appeared coloured towards a red rather than green or blue hue. This was confirmed through observations of red and maroon



stain colours in *figure 357*. As temperature increased from 100°C to 250°C R, G, B values and RGB totals decreased.

Figure 358 Descriptive statistics recorded for stains generated on glass surfaces from 100°C to 250°C

Temperature /°C	R Value	R %	G Value	G %	B Value	B %	RGB Total
<b>100</b>	96	62	28	18	32	20	156
<b>150</b>	102	79	13	10	15	11	129
<b>200</b>	79	78	13	13	9	9	101
<b>250</b>	20	37	15	28	19	35	54

A decrease in RGB totals from 156 (100°C) to 54 (250°C) supports observations that as temperature increased, glass stains exhibited darker intensities of colour. This was confirmed through observations of a dramatic range of stain colours in *figure 357*, which were dark red at 100°C, transitioning through shades of dark red and maroon at 150°C and 200°C to a dark grey, black colour at 250°C. Calculation of ratios of R to G and B values at each temperature gives an indication of changes in each colour component across temperatures. R values ranged from 62% (100°C) to 37% (250°C), G values ranged from 18% (100°C) to 28% (200°C) and B values ranged from 20% (100°C) to 35% (250°C). This meant that proportions of RGB totals comprised of R-values decreased significantly, whilst proportions of G and B-values increased, which suggests that glass stains became less strongly orientated to red hues as temperature increased. Results suggest that as stains on glass are exposed to increases in extreme temperatures they exhibit significant alterations in stain colour, decreasing their orientation towards red hues and becoming increasingly characterised by darker intensities of colour.

### 9.5.5 Comparison of stains between surfaces and staining methods

Once results of stain colour analyses had been collected for stains generated on each surface and across both staining methods, results were compared. *Figures 359 and 360* provide a visual overview of changes in stain colours between 100°C and 250°C for surfaces stained in staining methods 1 and 2. Comparison of colour ribbons in terms of the visible difference in colours of stains between surfaces was undertaken. Ribbons were characterised by different colours. Ribbons of denim stains included

tan-brown, pink and dark brown colours. Ribbons of paper stains included dark red, maroon, dark brown, grey and black colours. Ribbons of glass stains included red, maroon and black colours. Stains generated on glass appear most instantly recognisable as bloodstains, coloured in hues of red most commonly associated with blood.

A secondary observation related to alterations in bloodstain colour as temperature increased from 100°C to 250°C. Comparison of stain colours at 100°C and 250°C, across all surfaces and both staining methods indicate a significant darkening of stain colours. This alteration appears more prominently in paper (staining method 1) and glass stains (staining methods 1 & 2) and to a lesser extent in denim stains. Visual observations were explored further through a quantitative analysis of measures of colour recorded for stains (*sections 9.5.5.1 and 9.5.5.2*).

Figure 359 Longitudinal colour ribbons for stains generated on denim, paper and glass between 100°C and 250°C (staining method 1)

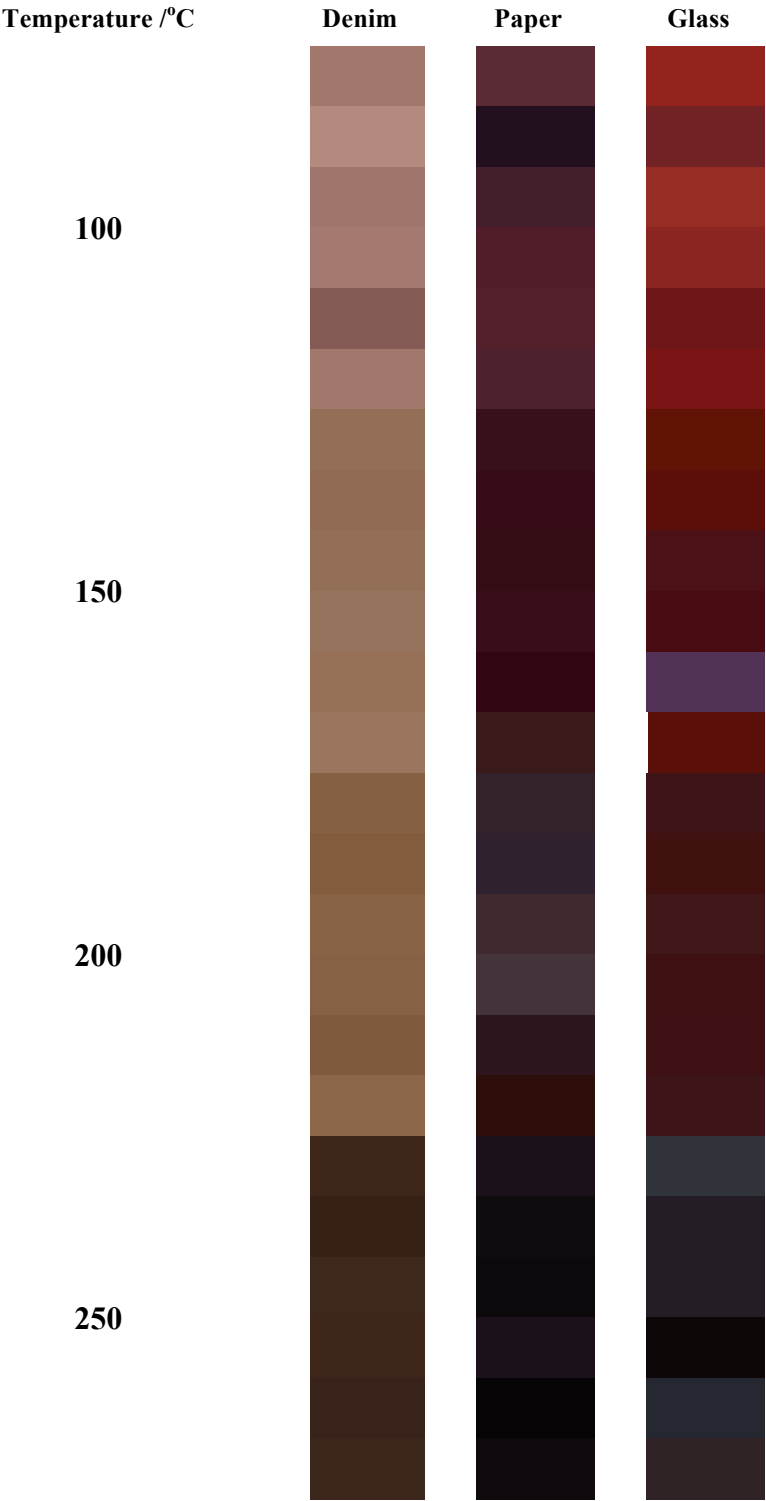
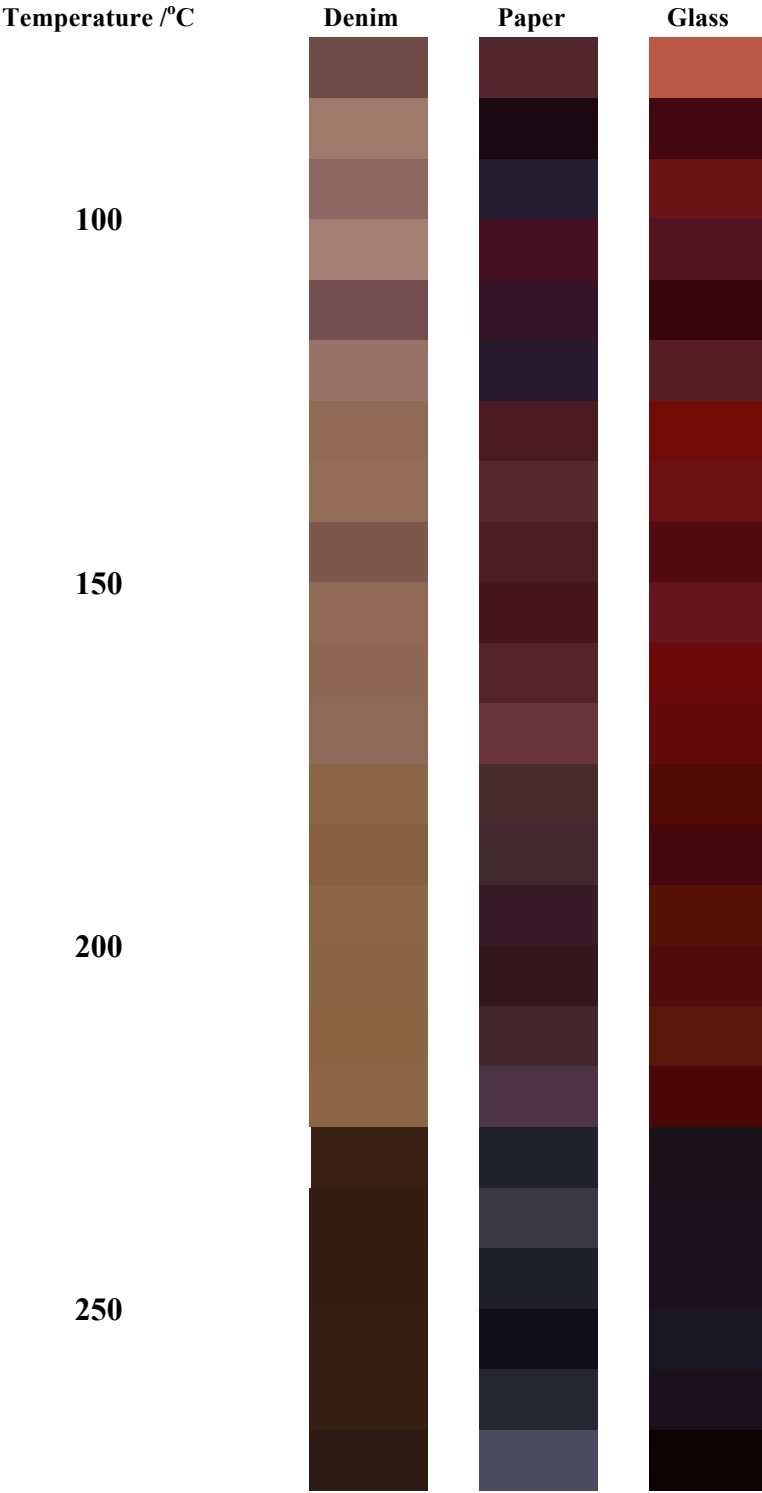


Figure 360 Longitudinal colour ribbons for stains generated on denim, paper and glass between 100°C and 250°C (staining method 2)



### 9.5.5.1 Comparison of means between staining methods 1 & 2

To compare distributions of R, G, B values and RGB totals of stains generated in methods 1 and 2, a Mann Whitney test was conducted to test the null hypothesis that two unrelated (independent) sets of data have the same distribution. For stains generated in methods 1 and 2, results of the test indicated whether staining method had a significant effect on stain colour. Results are set out in *figure 361*.

	Null Hypothesis	Test	Sig.	Decision
1	The distribution of R is the same across categories of SM.	Independent-Samples Mann-Whitney U Test	.951	Retain the null hypothesis.
2	The distribution of G is the same across categories of SM.	Independent-Samples Mann-Whitney U Test	.767	Retain the null hypothesis.
3	The distribution of B is the same across categories of SM.	Independent-Samples Mann-Whitney U Test	.974	Retain the null hypothesis.
4	The distribution of RGB Total is the same across categories of SM.	Independent-Samples Mann-Whitney U Test	.878	Retain the null hypothesis.

Asymptotic significances are displayed. The significance level is .05.

Figure 361 Mann Whitney test comparing distributions of R, G, B values and RGB totals between staining methods 1 and 2

The results indicated that the null hypotheses should be accepted with values of  $p > 0.05$ , thus, R, G, B values and RGB totals of stains generated by different staining methods (SM 1 and 2) were statistically similar. Denim, paper and glass stains generated in method 1 were statistically similar to the corresponding denim, paper and glass stains generated in method 2. This suggests that the different methods used to generate and expose stains to extreme temperatures between 100°C – 250°C did not have an influence on stain appearance.

### 9.5.5.2 Comparison of means between surfaces

A further Kruskal-Wallis test was undertaken to compare distributions of R, G, B values and RGB totals of stains generated on different surfaces. The analysis tested

a null hypothesis that three unrelated (independent) sets of data have the same distribution. For stains generated in methods 1 and 2, results of the test indicated whether surface (denim, glass, paper) had a significant effect on stain colour. Results are set out in *figure 362*.

	Null Hypothesis	Test	Sig.	Decision
1	The distribution of R is the same across categories of Surface.	Independent-Samples Kruskal-Wallis Test	.010	Reject the null hypothesis.
2	The distribution of G is the same across categories of Surface.	Independent-Samples Kruskal-Wallis Test	.001	Reject the null hypothesis.
3	The distribution of B is the same across categories of Surface.	Independent-Samples Kruskal-Wallis Test	.009	Reject the null hypothesis.
4	The distribution of RGB Total is the same across categories of Surface.	Independent-Samples Kruskal-Wallis Test	.022	Reject the null hypothesis.

Asymptotic significances are displayed. The significance level is .05.

Figure 362 Kruskal-Wallis test comparing distributions of R, G, B values and RGB totals between surfaces

The results indicated that the null hypotheses should be rejected with  $p < 0.05$ , indicating the R, G, B values and RGB totals for stains generated on different surfaces (denim, glass, paper) were not statistically similar. Denim stains, for example, were not statistically similar to glass or paper stains. This suggests, for stains exposed to temperatures between 100°C and 250°C that different surfaces stains were generated on had a statistically significant influence on stain appearance at the 95% significance level.

Results of statistical tests (*figures 361 and 362*) conducted on stains exposed to environmental condition D confirmed that method of staining did not significantly influence stain colour but that surface stains were generated on did. These results confirmed visual observations discussed in *section 9.5.5*.

Analysis of stains exposed to environmental condition D (exposure to high temperatures) has implications analysis of stains located in proximity to burning

events. Results indicated that, high temperatures are associated with dark intensities of stain colour. This may complicate or obscure identification of bloodstains at a crime scene where a fire has occurred. Stains generated on paper and glass exhibited particularly dark colours when exposed to high temperatures, whilst stains generated on denim retained lighter tan-brown colouring when exposed to the same temperatures. This suggests in the analysis of scenes surrounding a fire, stains generated on denim may be easiest to initially identify whilst identification of paper and glass stains will be considerably more difficult. Discolouration of stains, to the extent observed in stains set out in *section 9.5*, may have implications for identification of bloodstains at a scene. Awareness of the potential colours expected of stains exposed to high temperatures (i.e. proximity to a fire) can increase accuracy and confidence of identification, interpretation and subsequent analysis of evidence recovered in scenes exposed to these conditions. Implications of results for bloodstain pattern and crime scene analysis are discussed further in *chapter 13*.

## **9.6 Environmental condition E (stains exposed to fire)**

Images and analysis of stains generated in environmental condition E are presented in *section 9.6*.

### **9.6.1 Images of stains generated**

Images of individual stains exposed to environmental condition E are set out in *figure 363*. Images were generated by digitally scanning stains immediately following their removal from fire. Due to experimental limitations, stains were only generated on glass microscope slides. Eight stains were generated on slides and exposed to fire.

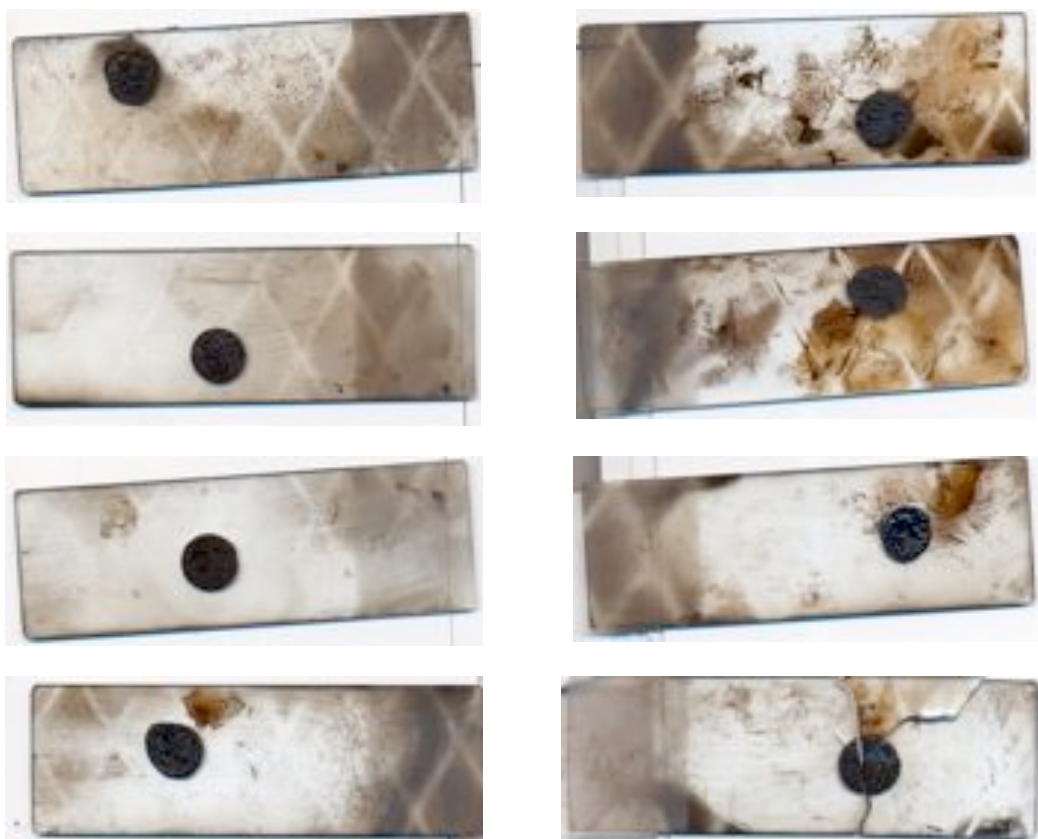


Figure 363 Images of stains exposed to environmental condition E

### 9.6.2 Stain colour analysis

Once stains had been digitally scanned, images were imported into colour analysis software to extract quantitative information about stain colour from the images. Each stain was analysed individually. Measurements from analysis are set out in *figure 364*. Images of individual stains and blocks of corresponding hexadecimal colour for each stain are also included.

*Figure 364* outlines R, G and B values calculated from replicate stains ( $n = 8$ ) generated and exposed to fire. R, G and B values were recorded below 50 for all stains. R, G and B values can range between a minimum of 000 and a maximum of 255 so measurements below 50 are therefore very low. Measures of 000 represent the darkest possible intensity (black) for colour values and measures of 255 represent the lightest possible intensity (white). As R, G and B values were all recorded below 50 this supports the observation in *figure 364* of very dark intensities of colour in stains exposed to fire. Calculation of RGB totals confirmed the dark intensity of stains,



ranging from 74 – 126, out of a possible maximum RGB total of 765 (R255, G255, B255). This supports the observation that stains exposed to fire are significantly closer to an RGB expression of a black colour (R000, G000, B000) than a white colour (R255, G255, B255).

Figure 364 Table of measurements recorded for stains generated on glass slides and exposed to environmental condition E (fire)

Stain Number	R Value	G Value	B Value	RGB Total	Hex Code	Stain	Hexadecimal Colour
1	32	27	28	87	201b1c		
2	37	37	45	119	25252d		
3	32	27	28	87	201b1c		
4	38	35	39	112	262327		
5	30	23	21	74	1e1715		
6	26	30	39	95	1a1e27		
7	31	31	35	97	1f1f23		
8	41	40	45	126	29282d		

*Figure 365* sets out the average ratio of R (33) to G (31) and B (35) values in stains exposed to fire. Results indicate that B values represented a slightly dominant component of RGB totals but that all colour values were expressed in relatively equal proportions. This suggests stains exposed to fire were not significantly orientated towards any particular R, G or B colour component and will appear grey in colour. Ratios of R, G and B values for the colour grey are typically expressed by fairly equal measures of R, G and B values as observed in stains exposed to fire (*figure 364*). Results indicate that stains exposed to fire will be characterised by dark grey colours.

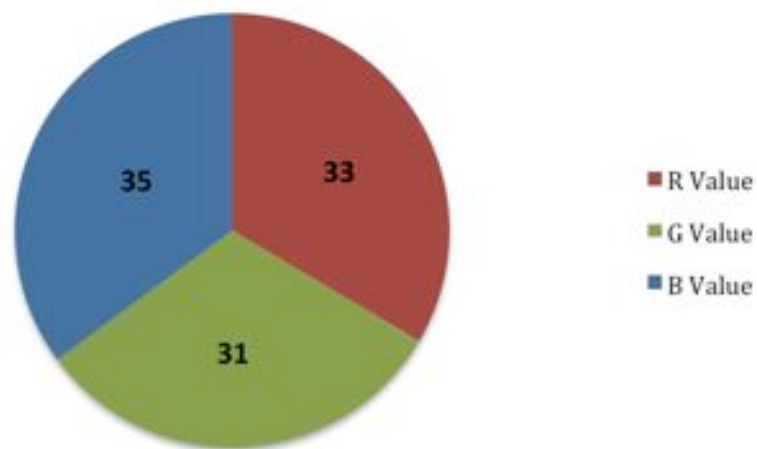


Figure 365 Average ratio of R to G to B values for stains exposed to fire

Observations of stains exposed to environmental condition E (fire) has implications on the analysis of stains recovered from burning events. Results indicated that stains exhibited considerable discolourations following exposure to fire, exhibiting extremely dark shades of grey. Whilst previous observations on the effects of fire on bloodstains (*Paonessa. 2005*) focused on the reaction of stains chemically to fire exposure, results presented here form the first experimental analysis of the effects of fire on stain appearance. Results indicate visual identification of stains at a crime scene where a fire has occurred may be prevented or misled due to the considerable alterations observed in stain appearance. This should be considered in the analysis of scenes where burning events may have occurred. Observations may have an additional implication for crime scene reconstruction in the identification of ‘misfit’ stains. If stains exhibit colours normally associated with exposure to fire are recovered on objects in a location where there is no evidence of fire or a burning

event having taken place, stains may be identified as ‘misfit’ stains. This may mean the objects they are recovered from were previously located at the scene of a burning event and subsequently removed from their original location. An example of when this might occur is if a suspect took evasive action by setting fire to evidence at a scene but then returned to recover a particular item of evidence later, for example a bloodstained knife. Observations presented in *section 9.6* can increase awareness and accuracy of identifying and interpreting stains in scenes that have been exposed to burning events. Implications of results for bloodstain pattern and crime scene analysis are discussed further in *chapter 13*.

Observations from results generated across experimental stage 3 enhance and increase knowledge about the nature of stains exposed to a range of environmentally extreme conditions. Given the frequency of encountering crime scenes located outdoors (*Cox. 1990*) expanding an understanding of the natures of stains found in unusual or extreme environments is important. The most important observation from experimental stage 3 related to the range of colours observed for stains exposed to different environmental conditions. A comparison of these is discussed in *chapter 10*. Overall, observations demonstrated the influence of extreme environmental conditions on stain appearance, exposure to which caused variations on colour and intensity of stains. Variations in intensity and strength of colour may affect the interpretation of bloodstain evidence and increasing familiarity with the type of variations and associated conditions in which they might be encountered is important for increasing the accuracy of bloodstain pattern analysis. The implications of results of experimental stage 3 for bloodstain pattern analysis and the subsequent process of crime scene reconstruction are discussed in *chapter 13*.

## 10. Synthesis of results of experimental stages 1, 2 & 3

### 10.1 Calculation of mean R, G, B values and RGB total values

Mean R, G, B and RGB total values were calculated from all stains generated in experimental stages 1, 2 and 3. Means were calculated for groups of stains according to environmental effects they had been exposed to. These effects were coded:

- A. Controlled temperature variations between -10°C and 50°C
- B. Natural climatic variations
- C. Exposure to snow
- D. Exposure to freezing conditions
- E. Exposure to ice
- F. Exposure to high temperatures between 100°C and 250°C
- G. Exposure to fire and burning

Calculation of these mean values allowed general comparisons to be made between characteristics of stains exposed to different environmental conditions. It also produced an indication of the variability of stains exposed to each environmental condition and allowed identification of any overlaps in stain characteristics between stains exposed to different conditions. Mean values calculated for all stains exposed to each environmental condition are set out in *figure 366*.

Stain Code	Environmental Effect	Experimental Stage	R Value	G Value	B Value	RGB Total
A	Temperature	1	211	50	68	329
B	Natural climate	2	124	101	82	306
C	Snow	3	139	61	75	274
D	Freezing	3	192	27	44	264
E	Ice	3	115	14	28	158
F	High temperatures	3	83	44	42	169
G	Fire	3	33	31	35	100

Figure 366 Table of mean R, G, B and RGB total values calculated

## 10.2 Comparison of mean R, G, B and RGB total values

*Figure 367* provides a comparison of R, G, B and RGB total value means calculated (*figure 366*) for stains according to conditions of environmental exposure.

Results indicate that the range of mean R and RGB total values calculated between stains exposed to different environmental conditions was considerable. This suggests that environmental conditions exert an observable influence on stain appearance. The implication of results for bloodstain pattern analysis is that environmental conditions at a scene and surrounding bloodstain generation should be considered during stain analysis. By altering stain appearance environmental conditions may influence the identification of bloodstains at a scene, leading to possible misidentification of stains or obscuring identification completely. This may lead to incomplete evidence recovery and subsequently inaccurate reconstructions of circumstances surrounding a bloodletting event.

The maximum RGB total calculated was 329 for stains exposed to controlled temperature variations and the minimum RGB total calculated was 100, for stains exposed to fire and burning conditions. This indicated a range of 229 for mean RGB totals, which totals calculated for stains exposed to natural climatic variations (306), snow (274), freezing (264), ice (158) and high temperatures (169) all fell within. RGB totals are an indication of the intensity of stain colour with dark intensities characterised by low RGB totals and light intensities characterised by high RGB totals. Comparison of mean RGB totals indicated that stains exposed to controlled (A) and naturally occurring (B), relatively benign variations in environmental conditions exhibited lighter colour intensities than stains exposed to more extreme environmental conditions (C, D, E, F & G). Amongst stains exposed to extreme environmental conditions a further distinction between RGB totals was observed. Stains exposed to extremes of heat; high temperatures and fire (F & G) exhibited darker intensities than stains exposed to extremes of cold; snow, freezing conditions and ice (C, D & E). In forensic reality, these observations have implications for bloodstain analysis and investigation of crime scenes. In particular, awareness of the possible ranges in stain appearance and caution should be taken when attempting visual identification of stains at scenes located outdoors, or otherwise exposed to

environmental conditions. When encountering scenes exhibited signs of exposure to extreme environmental conditions, an awareness of type of exposure (whether cold or hot) can be cross-referenced with observations from experimental stages 1, 2 and 3 to inform analysts of the order of alterations stains are likely to exhibit. Observations will improve accuracy of stain identification across environmentally exposed scenes.

The maximum R-value calculated was 211 for stains exposed to controlled temperature variations (A) and the minimum R-value calculated was 33, for stains exposed to fire and burning conditions (G). This indicated a range of 178 for mean R-values, which values calculated for stains exposed to natural climatic variations (124), snow (139), freezing (192), ice (115) and high temperatures (83) all fell within. Ranges of G and B values between stains exposed to different environmental conditions were smaller than ranges of R-values. Maximum G-value calculated was 101 for stains exposed to natural climatic variations (B) and the minimum G-value calculated was 14 for stains exposed to ice (E), indicating a range of 87 in G-values. Maximum B-value calculated was 82 for stains exposed to natural climatic variations (B) and the minimum B-value calculated was 28 for stains exposed to ice (E), indicating a range of 54 in B-values. Results indicate that across stains exposed to different environmental conditions, B and G values were lower in value and were less variable than R-values. This indicates that for stains exposed to all environmental conditions examined in experimental stages 1, 2 and 3, red colours were dominant. This has implications for forensic interpretations of suspected stains as bloodstains should retain and exhibit a dominance of R-values, regardless of environmental conditions they have been exposed to. The strength of orientation towards a red colour however varied between stains and this may also have implications for stain analysis. Ratios of R to G and B values give an indication of the strength of orientation or dominance of red colouring of stains. Visual comparison of ratios *from figure 367* demonstrate that stains exposed to controlled temperature variations (A) and freezing conditions (D) exhibited the highest ratios of R to G and B values. The ratio of stains exposed to A was R211: G50: B68 and the ratio of stains exposed to D was R192: G27: B44. Stains exposed to these conditions were heavily dominated by R-values to the order of 143 (A) and 148 (D) respectively, indicating stains were strongly orientated towards red colours. Visual

comparison of ratios from *figure 367* demonstrate that stains exposed to fire (G) exhibited the lowest ratio of R to G and B values; R33: G31: B35. Stains exposed to these conditions were not dominated by R-values, indicating stains were not orientated towards red colour. Implications of these observations in forensic reality are that differences in colour of stains are likely to be observed at scenes exposed to different environmental conditions, which may influence their identification. For example, stains exposed to fire and burning conditions will be least recognizable as red bloodstains. This could make identification of stains at scenes associated with fires more difficult than identification of stains at scenes involving freezing conditions, where stains are likely to be a more recognizable red colour.

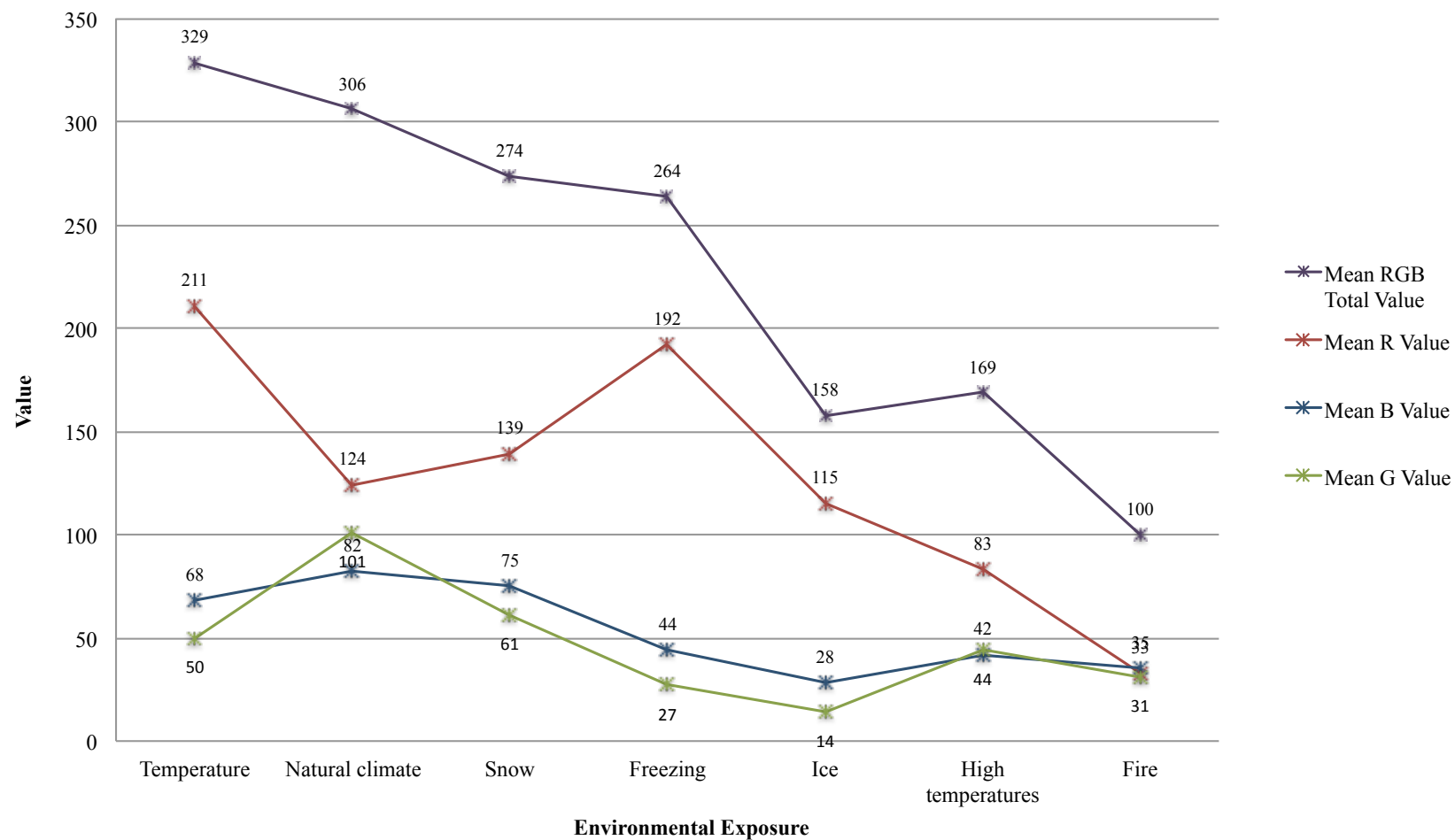


Figure 367 Comparison of mean R, G, B and RGB total values calculated for stains according to environmental exposure, including ‘Temperature’ (stain code A), ‘Natural Climate’ (stain code B), ‘Snow’ (stain code C), ‘Freezing’ (stain code D), ‘Ice’ (stain code E), ‘High temperatures’ (stain code F) and ‘Fire’ (stain code G)



Figure 368 presents the results of a Kruskal-Wallis test carried out on distributions of R, G, B and RGB total values across stains exposed to different environmental conditions to assess whether there was a significant effect of environmental condition on stain appearance. The results indicated that the null hypotheses should be retained ( $p > 0.05$  for each test) for distributions of G, B and RGB total values but rejected ( $p < 0.05$ ) for distributions for R-values. There is therefore a significant difference between R-values recorded in stains exposed to different environmental conditions at the 95% significance level. Results confirm that visual observations of variations in dominance of R-values and strengths of red colouring between stains (figure 367) are significant.

Figure 368 Kruskal-Wallis test for comparison between distributions of R, G, B and RGB total values for 'stain codes' (categories of stains exposed to different environmental conditions)

	Null Hypothesis	Test	Sig.	Decision
1	The distribution of R Value is the same across categories of Stain Code.	Independent-Samples Kruskal-Wallis Test	.019	Reject the null hypothesis.
2	The distribution of G Value is the same across categories of Stain Code.	Independent-Samples Kruskal-Wallis Test	.294	Retain the null hypothesis.
3	The distribution of B Value is the same across categories of Stain Code.	Independent-Samples Kruskal-Wallis Test	.353	Retain the null hypothesis.
4	The distribution of RGB Total is the same across categories of Stain Code.	Independent-Samples Kruskal-Wallis Test	.179	Retain the null hypothesis.

Asymptotic significances are displayed. The significance level is .05.

Variations in intensity and strength of colouring of stains may affect interpretation of bloodstain evidence by altering the ease with which analysts identify bloodstains. Comparison of results from experimental stages 1, 2 and 3 demonstrated that type of environmental condition stains are exposed to influences stain appearance. This has implications for the analysis of bloodstains at a crime scene and in particular, analysis of stains at scenes located outdoors and in other exposed locations. Implications of results for bloodstain pattern analysis and the subsequent process of crime scene reconstruction are discussed in *chapter 13*.

## **11. Experimental Stage 4 – Examining environmental influences on bloodstain drying time (under laboratory controlled conditions)**

### **11.1 Overview**

Experimental stage 4 consisted of a series of drying experiments designed to identify the strengths of influences on bloodstain drying time. The main influences on drying time are temperature, humidity, stained surface characteristics, blood volume and surface area of stain. The main focus of experimental stage 4 was examining the relationship between temperature and drying time. Bloodstains were generated on a variety of surfaces (paper, glass, denim fabric) and dried at the following temperature intervals: -10, 5, 0, 5, 10, 15, 20, 25, 30, 35, 40, 45 and 50°C. All other influences on drying time were closely controlled through experimental design, with the exception of humidity, which was impossible to control with the available equipment. Stains were observed regularly and temperature and humidity recorded at each observation. Once dry their drying times were recorded. The primary objective of stage 4 was to establish the influence of a) temperature on drying time with secondary objectives of exploring relationships between b) humidity and drying time and c) surface type and drying time.

### **11.2 Materials**

The materials utilised for the experimental work in this chapter are set out in *figure 369*.

Experimental equipment	Additional specifications
100ml whole Ovine blood	With Alsever's solution
MESM Portable laboratory refrigerator	With temperature range -10°C to 60°C
Temperature & relative humidity data logger	Ebro. VWR. EBI 20-TH1
Paper	Ryman's A4 white laid paper, 100 gm <sup>2</sup>
Glass microscope slides	CellPath. 90° ground edges. 25.4 x 76.2 mm. Thickness 1.0-1.2mm
White denim cloth	100% cotton. Weight: 345g/metre
Plain white record cards	Ryman's Silvine 127x77mm
Thermo Scientific Finnpiquette® F1 Variable Volume Single Channel Pipette	Volume range between 1-10µl
Plastic pipettes	10ml volume
Biological waste disposal unit	
Digital timer	

Figure 369 Table of materials used in experimental stage 4 (Author. 2012)

## 11.3 Methodology

### 11.3.1 Pre-experimental fridge set up

Prior to experimentation, the fridge was placed on its end, with the door opening towards the experimenter. This arrangement allowed horizontal shelves to be fixed within the fridge (*figure 370*), maximising the number of stain sets that could be simultaneously placed in the fridge. Pieces of polystyrene, cut to size, were used as shelves. The decision to use polystyrene was due to its insulating nature, which would ensure the shelves maintained a relatively stable temperature in comparison to the metallic interior of the fridge. With the addition of shelves, the fridge could house 3 stain sets at a time. As there were three different surfaces to be stained at each temperature, stain sets for each surface were simultaneously dried according to temperature intervals.



Figure 370 Photograph of experimental fridge set-up

(Author. 2012)

### 11.3.2 Controlling stained surface characteristics

Characteristics of surfaces that are stained are likely to influence drying time. During experimentation three surfaces were stained: paper, glass and denim fabric. Surfaces were purposefully chosen for their different characteristics. Throughout experimentation consistency within surface type was maintained by using exactly the same source and specification of paper type, glass microscope slides and denim fabric for each set of stains.

In order to measure differences in surface roughness between the three surfaces, each surface was analyzed through Atomic Force Microscopy (AFM). Atomic force microscopy is a high-resolution scanning and imaging process during which a microscopic cantilever is run across the surface of a material (*figure 371*). As the cantilever traverses the surface an interaction occurs between the cantilever tip and surface, causing the cantilever to move up or down. Over the course of scanning an entire surface these interactions result in oscillations of the cantilever. These oscillations are measured by laser reflection. A laser is aimed at and subsequently reflected off the end of the cantilever and as reflections vary according to cantilever oscillation, their variance is detected and interpreted to produce an image of surface features.

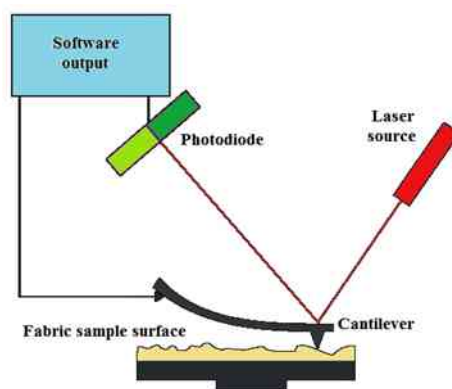


Figure 371 Sketch diagram of AFM set-up  
(Author. 2011)

AFM gives an assessment of surface roughness of surfaces scanned by calculating a roughness average ( $R_a$ ) and ratio of surface area to projected surface area. The roughness average gives an indication of surface roughness by calculating the average size of peaks and valleys in the fabric surface. The higher the  $R_a$  value the higher the surface roughness. Calculated ratios of surface area to projected surface area can also give an indication of surface roughness. The ratio calculated of surface area to projected surface area compares the surface area of the scanned sample, taking into account all peaks and valleys with the projected fixed area displayed by the scan output image. For example a rough surface with multiple peaks and valleys may have a surface area

To prepare surfaces for AFM 1cm<sup>2</sup> pieces of denim fabric and paper were selected and mounted onto ½-inch scanning electron microscope (SEM) stubs. The stubs were then placed into the AFM chamber and the mounted surfaces were then imaged. To image the glass surface no preparation was required and a new, clean, glass microscope slide was directly scanned by AFM.

### 11.3.2 Controlling temperature

Observations were primarily made during experimental stage 4 regarding stain drying time at a range of temperatures. Temperature was therefore the main independent variable and had to be closely controlled.

Drying time was examined across a temperature range that was considered to be climatologically natural. The chosen range minimum was  $-10^{\circ}\text{C}$  to mimic a possible night time low and the chosen range maximum was  $50^{\circ}\text{C}$  to mimic a maximum day-time high. Experimental temperatures were incrementally increased between the minimum ( $-10^{\circ}\text{C}$ ) and maximum temperature ( $50^{\circ}\text{C}$ ) through 5-degree intervals. This generated a set of stains dried at the following temperatures:  $-10^{\circ}\text{C}$ ,  $-5^{\circ}\text{C}$ ,  $0^{\circ}\text{C}$ ,  $5^{\circ}\text{C}$ ,  $10^{\circ}\text{C}$ ,  $15^{\circ}\text{C}$ ,  $20^{\circ}\text{C}$ ,  $25^{\circ}\text{C}$ ,  $30^{\circ}\text{C}$ ,  $35^{\circ}\text{C}$ ,  $40^{\circ}\text{C}$ ,  $45^{\circ}\text{C}$  and  $50^{\circ}\text{C}$ . Temperature was increased by incremental intervals, as had also been done during experimental stage 1 (*chapter 4*), in order to maintain an experimental consistency between stages. Temperature was controlled throughout experimentation by drying stains in a portable laboratory refrigerator (*figure 372*), chosen for its ability to individually reach and sustain all designated temperature intervals within the chosen experimental range ( $-10^{\circ}\text{C}$  to  $50^{\circ}\text{C}$ ).



Figure 372 Images of portable laboratory refrigerator (*Author. 2011*)

To monitor temperature precisely within the refrigerator whilst stains were being dried and in order to record any potential temperature fluctuations during experimentation a digital thermometer and data logger was placed in the middle of the refrigerator. Prior to drying stains at each temperature interval the refrigerator was set to the required temperature and left for 2-3 hours to achieve the target temperature throughout. Stains were not generated and placed in the refrigerator until the digital thermometer indicated that each target temperature had been reached. Once stains had been placed in the refrigerator the digital thermometer was checked whenever stain observations were made to confirm the temperature was still at the target temperature.

### **11.3.3 Controlling humidity**

Within the experimental refrigerator, in which stains were dried, it was impossible to control humidity. Humidity levels fluctuated according to the range of temperatures stains were dried at, as well as during the course of a stain's drying time at a particular temperature. Stains dried at different temperatures were exposed to different humidity levels whilst drying. In addition, several replicate experimental runs were conducted for each temperature which meant that stains dried across replicate runs at the same temperature, also experienced differences in humidity levels, between runs, whilst drying.

Whilst the experimental focus of stage 4 was the relationship between temperature and drying, as exposure of stains to fluctuating humidity values was experimentally unavoidable – the influence of humidity on drying time had to be considered alongside the influence of temperature.

In order to allow humidity values to be incorporated into analysis of stain drying time, records of humidity values and fluctuations were made throughout experimentation. A digital relative humidity data logger was placed in the middle of the experimental refrigerator in order to do so. Humidity was recorded a) when stains were initially placed into the refrigerator, b) whenever stain observations were made and c) when a stain was observed to be dry. All humidity values recorded for a stain were then used to calculate an 'average' humidity that that particular stain had been exposed to whilst drying.

### **11.3.4 Controlling blood drop volume**

Volume of blood contained in a stain is a variable of influence on stain drying time. With the focus of stage 4 on examining the influences of the variables temperature (and humidity) on drying time however, the volume of blood used to generate each individual stain had to be controlled and kept consistent. In order to experimentally control the volume of blood in each stain a fixed volume pipette was used to generate bloodstains. The fixed drop volume was set to 10 $\mu$ l. A set of experimental runs was then conducted to observe drying times for stains of 10 $\mu$ l volume.

In order to allow some assessment of the order of influence of drop volume on stain drying time to be made a secondary set of experimental runs were conducted for stains generated from a different volume of blood. Stains dried in this secondary set were generated by plastic pipette with an average volume of 45 $\mu$ l.

### 11.3.5 Controlling stain size

Surface area of stain is another variable of influence on stain drying time. In order to experimentally control surface size of stains across all experimental runs stains were consistently generated onto surfaces from a height of 10cm. The tips of pipettes used to release blood drops to form stains were aligned to exactly 10cm above the upper side of each surface to be stained.

### 11.3.6 Stain sets

At each temperature interval a series of stain sets were generated across three different surfaces (paper, glass, denim fabric). Each stain set contained 6 replicate stains. This allowed any variability in drying times expressed across stains dried on a certain surface at the same temperature, to be identified. At each temperature interval three stains sets, each consisting of 6 replicate stains were generated (*figure 373*).

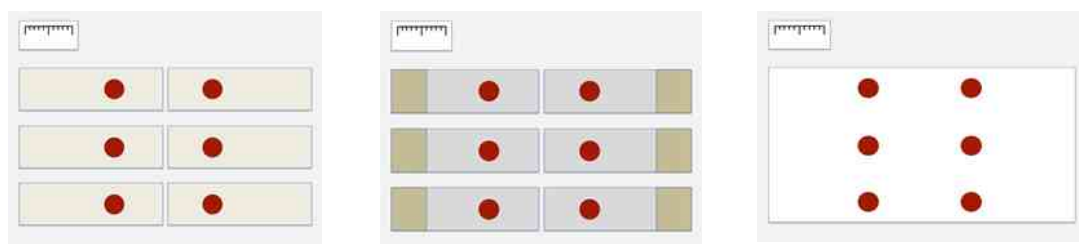


Figure 373 Sketches of 6 replicate stains on a) paper slips b) glass slides & c) denim fabric (L-R) generated for drying at each temperature interval (Author. 2012)

In total 234 individual bloodstains were generated in each experimental run, accounted for by 3 sets of 6 replicate stains at 13 temperature intervals. For each drop volume (10 $\mu$ l and 45 $\mu$ l) multiple experimental runs were completed. For stains generated from drops of 10 $\mu$ l volume five experimental runs were completed and for



stains generated from drops of 45µl volume two experimental runs were completed. This generated a total of 1170 individual bloodstains from 10µl drops and 468 individual bloodstains from 45µl drops (*figures 374 & 375*).

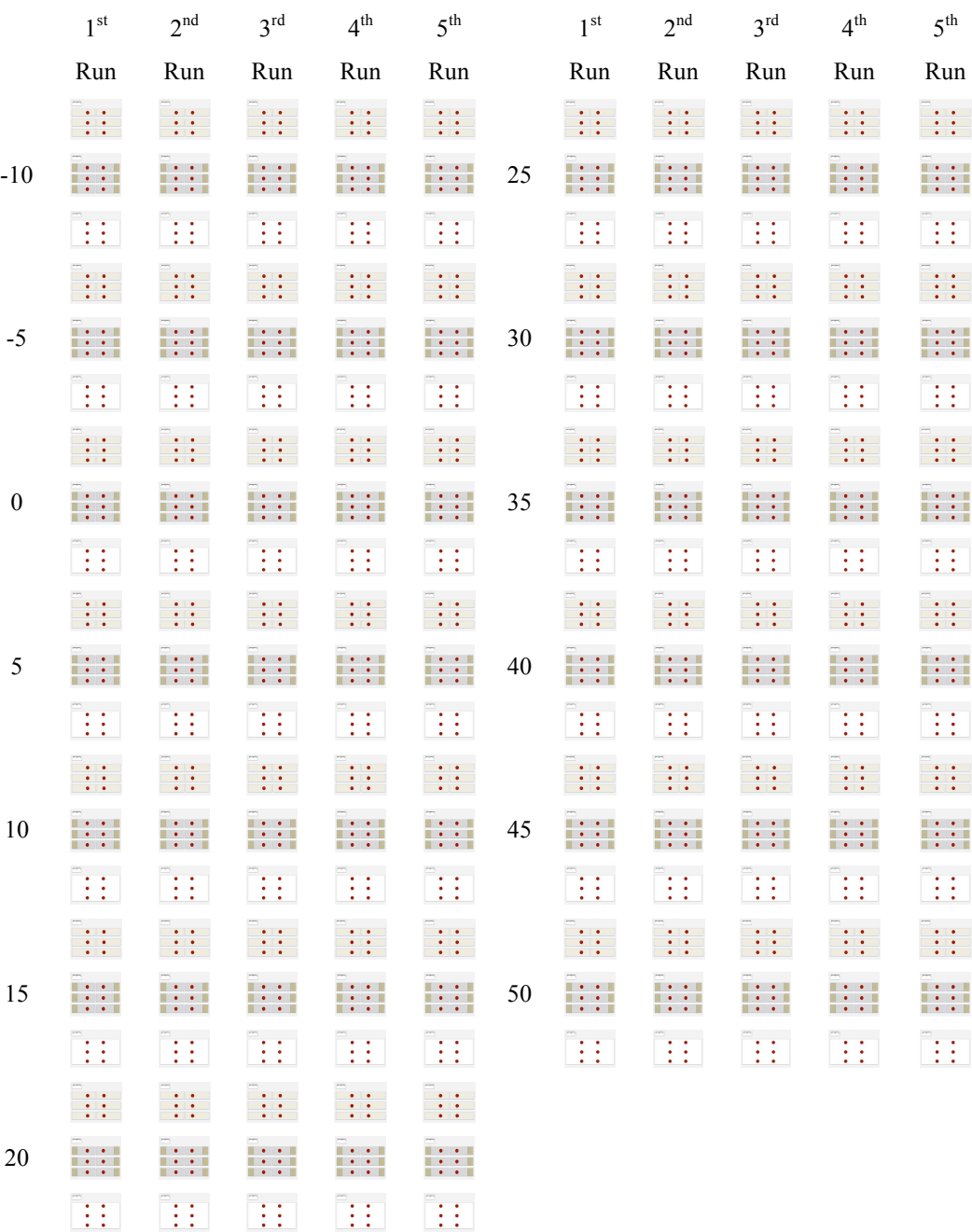


Figure 374 1170 individual bloodstains generated from 10µl drops (*Author. 2012*)

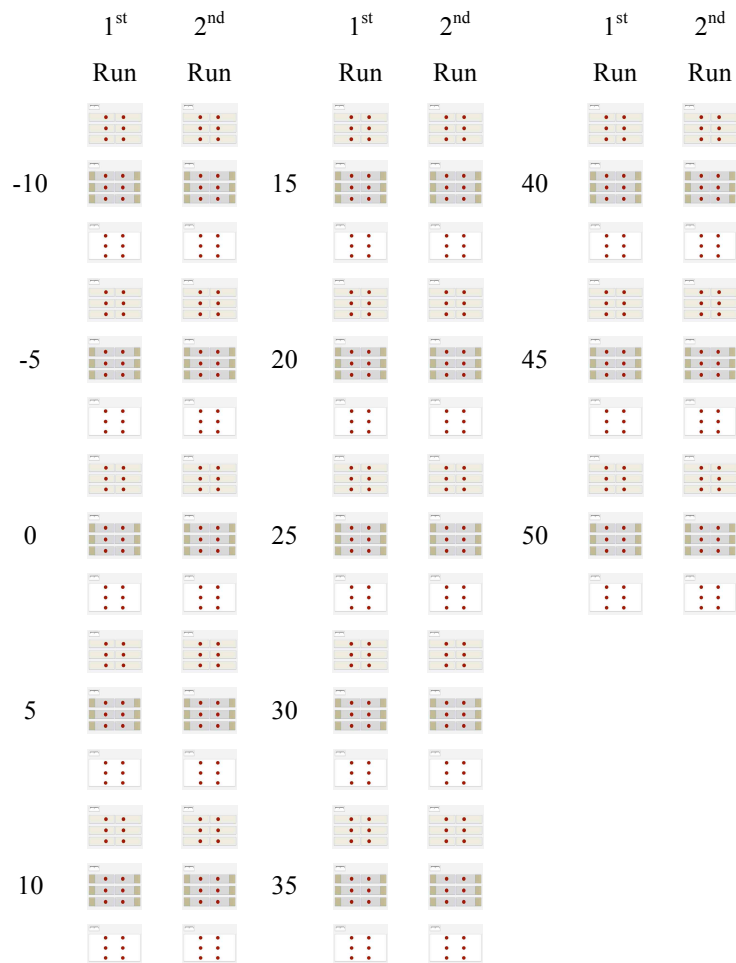


Figure 375 468 individual bloodstains generated from 45µl drops  
(Author. 2012)

### 11.3.7 Stain generation

To generate the first set of stains the temperature of the fridge was adjusted to the first experimental temperature. A thin piece of insulating material was placed into the open side of the inner compartment of the fridge. The door was then shut and the fridge left for 2-3 hours to adjust to the target temperature. In the meantime, the surfaces to be stained were prepared for staining. This involved cutting rectangular swatches of paper and denim fabric and mounting glass microscope slides onto white record cards (*figure 376*).

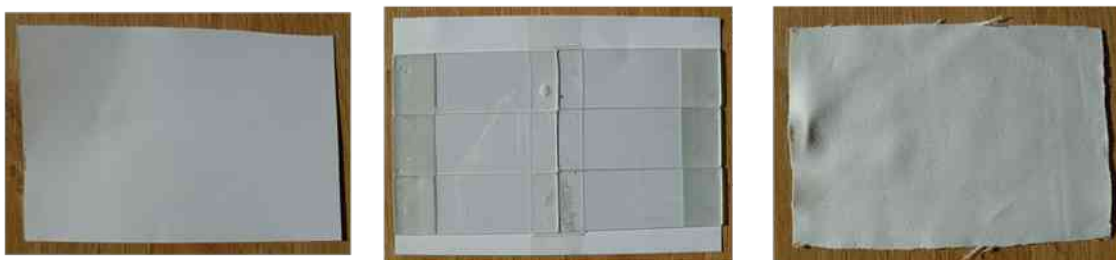


Figure 376 Surfaces to be stained prepared for experimentation (Paper/Glass/Denim from L-R)  
(Author. 2012)

After 2-3 hours, the fridge was re-opened and the data logger checked to ascertain that the target temperature interval had been reached. Stains could then be generated. Whilst preparing the stains, the fridge was reclosed, to prevent any alteration in temperature.



Figure 377 Fixed volume pipette set to deliver drops of 10µl volume  
(Author. 2012)

Using either a fixed volume (*figure 377*) or plastic pipette, a series of Ovine blood drops were deposited onto the paper, denim fabric and glass microscope slides from a height of 10cm to form six separate replicate stains on each. Fixed volume pipettes were used to generate 10µl volume stains and plastic pipettes were used to generate 45µl volume stains. Once bloodstains had been generated, the remaining Ovine blood was returned to storage at a refrigerated 4°C. Generated stain sets were then placed in the experimental refrigerator.

The time at which stains were placed in the fridge was noted and a digital timer set off to measure drying time of stains. The relative humidity and temperature were also recorded. The refrigerator was then closed and the stains left to dry. Stains were then observed at regular intervals until they were observed to be dry.

Measurements of relative humidity were taken whenever stain observations were made. As soon as a stain was observed to have dried the digital timer was consulted to record a total 'drying time' for each stain. Relative humidity measurements recorded during the course of each stain's 'drying time' were then averaged to calculate the average humidity level each stain was dried at.

Once stain sets had all dried at a certain temperature and final measurements of relative humidity and drying times had been recorded, the refrigerator was adjusted to the next experimental temperature and left for 2-3 hours to achieve that temperature throughout. Once the temperature had been reached, the process of stain generation was then repeated. This process was repeated to generate stain sets at all experimental temperature intervals: -10°C, -5°C, 0°C, 5°C, 10°C, 15°C, 20°C, 25°C, 30°C, 35°C, 40°C, 45°C and 50°C, across multiple experimental runs, for stains of both 10µl and 45µl volumes.

#### **11.3.8 Stain generation order**

The logistics and costs of sourcing blood from an external supplier presented certain experimental limitations. It was necessary to incorporate these limitations into the process of experimental design, the order in which stains were generated and dried at different temperatures and subsequently too in the analysis of results. As blood was sourced from an external supplier there was inevitably some length of time between it being sampled from a donor animal and its delivery. In order for blood to remain experimentally viable over this time it was necessary to add a preservative (Alsevers) to it. Alsevers solution is an isotonic, balanced salt solution which when added to whole blood acts as a preservative.

The addition of Alsevers extended the experimental shelf life of blood samples for up to 14-16 days. This was vital for experimental purposes as it was not possible, financially or logistically, to receive daily deliveries of fresh blood. The addition of Alsevers however introduced two vital extra considerations to the experimental design. Firstly, acting as a preservative, the addition of Alsevers to blood was expected to have a significant influence on bloodstain drying time. Secondly, by extending the shelf life of blood, throughout the course of experimental runs blood

used would vary in age. Both of these effects had to be considered during the design of experimental stage 4.

When considering the effects of Alsevers, as a preservative, on lengthening stain drying time – although thought to be a significant influence, it was also thought that as all blood used contained Alsevers, the effect could be considered to be consistent across stain generation and throughout experimental runs. The effects of Alsevers on stain drying time could therefore be dealt with in discussion during the analysis of all results. The effects of bloodstains dried at different temperature intervals and experimental runs varying in age was dealt with through experimental design. The order in which temperature intervals were used to dry stains was varied within each experimental run (*figure 378*).

Temperature	10µl volume stains					45µl volume stains	
	1 <sup>st</sup> run	2 <sup>nd</sup> run	3 <sup>rd</sup> run	4 <sup>th</sup> run	5 <sup>th</sup> run	1 <sup>st</sup> run	2 <sup>nd</sup> run
<b>-10</b>	2	13	13	6	15	14	1
<b>-5</b>	5	12	14	13	14	2	2
<b>0</b>	6	9	7	5	13	7	3
<b>5</b>	9	8	4	8	12	8	4
<b>10</b>	10	6	2	12	11	6	7
<b>15</b>	11	6	15	3	10	8	8
<b>20</b>	12	5	10	4	7	8	9
<b>25</b>	13	5	9	12	7	9	2
<b>30</b>	14	5	10	7	5	10	3
<b>35</b>	14	4	7	12	5	11	3
<b>40</b>	16	4	15	9	5	11	4
<b>45</b>	16	3	10	9	3	14	4
<b>50</b>	16	3	7	9	7	14	4

*Figure 378* Table outlining age of blood (in days) used to generate stains at each temperature interval, across the 5 experimental runs completed for 10µl volume stains and the 2 experimental runs completed for 45µl volume stains

In the first experimental run for 10µl volume stains for example temperature was increased linearly in order from low to high (-10, -5, 0, 5, 10, 15, 20, 25, 30, 35, 40, 45 & 50°C) so that -10°C was the first temperature stains were dried at and 50°C the last. This meant that blood used at the lower temperatures was ‘fresher’ and ‘younger’ in age than blood used at the higher temperatures. For the next experimental run for 10µl volume stains this order was reversed so that temperature

intervals were decreased linearly in order from high to low (50, 45, 40, 35, 30, 25, 20, 15, 10, 5, 0, -5, -10°C) so that 50°C was the first temperature stains were dried at and -10°C was the last. For this second experimental run, this order of staining meant that blood used at the higher temperatures was 'fresher' and 'younger' in age than blood used at the lower temperatures. Three further experimental runs were completed for 10µl volume stains and in them the order in which different temperature intervals were set for stains to be dried at was randomised. A randomised order for generating stains was also applied to the two experimental runs completed for 45µl volume stains. Over the course of all experimental runs, by incorporating this ordering variability into the experimental design, it was thought that the effects of age of blood on stain drying time would be normalised.

#### **11.3.6 Drying time measurement**

Drying time was measured by recording the time at which stains were placed in the experimental refrigerator, immediately following their generation, and the time at which they were deemed to be dry. As even approximate drying times for stains at different temperatures were unknown prior to experimentation stains had to be checked at regular time intervals throughout the entire drying process, until they were observed to be dry. The intervals at which stains were checked varied for stains drying at different temperature intervals and according to observations made during these interval checks.

For some temperatures, where drying time was expected to be long, perhaps in excess of 24 hours, there was no experimental logic for checking the state of stains every 5 minutes for example. Similarly, for temperatures where drying time was expected to be short, of an order of minutes, there was no experimental sense in only checking whether stains were dry after a couple of hours. As demonstrated through both of these scenarios, some method of roughly outlining suitable time intervals, for each temperature, to make regular observations at was therefore required.

A series of four preliminary experimental runs, the results of which were not included in the final set of results collected or analysis of those results, were run to

establish very approximate drying times for stains at different temperatures. The results of these runs allowed estimates of sensible time intervals for checking and making observations about drying stains at different temperatures to be made. For example, for stains dried at 50°C an average drying time of 10-20 minutes was observed, during the full experimental runs therefore stains dried at 50°C were checked every 3-4 minutes. For another example, stains dried at -10°C were observed to take in excess of 24-36 hours to dry, so during the full experimental runs therefore, stains dried at -10°C were checked every 2-3 hours. The early results indicated by the preliminary runs ensured that, for each temperature interval, a set of routine observations to be made at regular and intelligently spaced time intervals could be prescribed.

In addition to checking stains at regular time intervals, a further measure was incorporated into drying time measurement in order to increase the accuracy as of estimates as much possible.

For temperatures where stains were only being checked regularly every couple of hours, observations had to be made regarding levels of stain dryness. If a stain was observed to be almost dry during a 'routine' observation, further observations were continued at more discrete time intervals (e.g. 15-30 minutes) until the stain was observed to be dry.

#### **11.4 Methodological limitations**

Drying time was estimated by observation, which meant that there was some inherent subjectivity in its estimation. The preliminary runs allowed practice observations to be made to increase accuracy in estimating when stains were fully dry. During preliminary runs, when some stains appeared from observation to be dry they were touch tested and smearing of the stains was attempted. On glass and paper surfaces it was observed that occasionally stains which appeared dry would minimally smear – suggesting that although they were extremely close to being completely dry, the process was not entirely complete. For the majority of stains, which were touched once it had been observed that they appeared to be dry, no smearing was observed or moistness detected. This meant that although the

subjectivity of the observation method was taken into account during the analysis and interpretation stages of examining results – for the purposes of experimentation, it was thought to be a sufficiently reliable method of estimating when stains were dry.

It was not possible to attempt to touch test stains during the actual experimental runs to provide a secondary measure of testing whether they were dry or not – as any smearing of stains would have increased their surface area and influenced drying time. When interpreting drying times for denim stains it was also taken into account that the nature of the fabric meant that blood moved down into the fabric following impact and therefore only the dryness of blood on the upper and lower surface of the fabric could be assessed during the experiments.



## 12. Experimental Stage 4 – Results & Analysis

### 12.1 Results tables

Stains were generated from deposition of 10µl or 45µl volume blood drops onto a range of surfaces (paper, glass, denim) at a range of temperatures (-10°C, -5°C, 0°C, 5°C, 10°C, 15°C, 20°C, 25°C, 30°C, 35°C, 40°C, 45°C & 50°C). Stains were generated in experimental runs. In each experimental run, six replicate stains were generated on each surface at each temperature, generating a total of 234 stains in an experimental run (78 stains per surface). Five separate experimental runs were conducted for 10µl stains and two separate experimental runs were conducted for 45µl stains. This generated a total of 1170 individual 10µl stains (390 on each surface) and 468 individual 45µl stains (156 on each surface). Results for these individual stains are set out in *appendix 4*.

For the purposes of analysis, a mean value was calculated from replicate stains (n = 6) for each surface and temperature, within each run. Means calculated are presented in *figures 379 – 385*. Analysis of results generated during experimental stage 4 was based on these means.

### 12.1.1 Figure 379 Mean drying time results for 10µl stains (1<sup>st</sup> experimental run)

Surface	Temperature /°C	Age of Blood /days	Diameter of Dried Stain /mm	Drying Time /mins	Highest Humidity /Rh	Lowest Humidity /Rh	Average Humidity /Rh
Denim	-10	2	11.5	540	96.9	78.8	86.3
Glass	-10	2	10.0	990	96.9	78.8	86.2
Paper	-10	2	8.5	1055	96.9	78.8	86.0
Denim	-5	5	10.0	420	90.2	87.5	88.9
Glass	-5	5	10.0	615	91.0	85.7	88.9
Paper	-5	5	8.5	938	91.0	82.0	86.6
Denim	0	6	11.0	240	98.3	88.0	91.0
Glass	0	6	9.5	810	98.3	84.7	89.8
Paper	0	6	9.5	1560	98.3	83.5	89.7
Denim	5	9	11.0	210	94.6	90.8	93.0
Glass	5	9	10.0	730	94.6	90.8	93.0
Paper	5	9	9.0	1290	94.6	90.7	92.7
Denim	10	10	12.0	315	98.9	94.4	96.0
Glass	10	10	9.5	530	98.9	94.1	96.0
Paper	10	10	9.0	1035	98.9	93.7	95.9
Denim	15	11	9.5	180	100.0	99.4	99.7
Glass	15	11	9.5	510	100.0	99.4	99.6
Paper	15	11	8.0	780	100.0	99.0	99.5
Denim	20	12	10.0	330	100.0	100.0	100.0
Glass	20	12	10.0	690	100.0	100.0	100.0
Paper	20	12	9.5	1440	100.0	100.0	100.0
Denim	25	13	9.0	150	100.0	94.2	97.1
Glass	25	13	9.0	250	100.0	88.3	93.6
Paper	25	13	8.0	297	100.0	87.1	92.1
Denim	30	14	10.0	90	79.6	56.6	69.5
Glass	30	14	10.0	100	79.6	56.6	69.4
Paper	30	14	8.5	120	79.6	56.6	69.3
Denim	35	14	10.0	50	59.6	49.1	54.4
Glass	35	14	10.0	70	59.6	49.1	53.9
Paper	35	14	9.0	75	59.6	49.1	53.3
Denim	40	16	10.0	25	37.9	31.4	35.6
Glass	40	16	9.0	37	38.4	31.4	36.1
Paper	40	16	8.0	35	38.4	31.4	36.3
Denim	45	16	10.0	20	37.3	30.6	34.0
Glass	45	16	10.0	32	37.3	30.2	33.3
Paper	45	16	9.0	32	37.3	30.2	33.3
Denim	50	16	10.0	15	34.7	22.6	28.7
Glass	50	16	10.5	25	34.7	22.6	29.5
Paper	50	16	9.5	25	34.7	22.6	29.5

### 12.1.2 Figure 380 Mean drying time results for 10µl stains (2<sup>nd</sup> experimental run)

Surface	Temperature °C	Age of Blood /days	Diameter of Dried Stain /mm	Drying Time /mins	Highest Humidity /Rh	Lowest Humidity /Rh	Average Humidity /Rh
Denim	-10	13	10.5	480	94.6	87.5	91.1
Glass	-10	13	10.5	584	94.6	87.3	89.3
Paper	-10	13	9.0	990	94.6	85.6	88.8
Denim	-5	12	10.5	450	95.0	91.7	93.4
Glass	-5	12	9.5	585	95.0	85.7	90.2
Paper	-5	12	9.0	900	95.0	85.7	89.0
Denim	0	9	10.5	465	93.1	86.2	89.7
Glass	0	9	10.0	720	93.1	84.9	88.0
Paper	0	9	9.5	940	93.1	84.9	89.0
Denim	5	8	10.5	465	100.0	91.3	96.0
Glass	5	8	10.5	525	100.0	91.3	95.6
Paper	5	8	8.5	855	100.0	91.3	94.8
Denim	10	6	10.0	395	94.5	86.0	91.1
Glass	10	6	10.0	534	94.8	86.0	91.3
Paper	10	6	9.0	780	95.0	86.0	91.9
Denim	15	6	10.0	300	96.0	84.4	91.0
Glass	15	6	10.0	375	96.0	84.4	90.5
Paper	15	6	8.5	494	98.0	84.4	92.1
Denim	20	5	10.5	105	79.8	64.7	73.6
Glass	20	5	10.0	230	83.0	64.7	78.6
Paper	20	5	9.0	300	83.0	64.7	78.8
Denim	25	5	10.0	95	78.3	62.4	70.2
Glass	25	5	10.0	120	78.3	59.9	68.2
Paper	25	5	9.0	145	78.3	59.9	66.8
Denim	30	5	10.0	50	72.9	71.1	72.0
Glass	30	5	9.0	80	72.9	58.7	66.7
Paper	30	5	8.5	85	72.9	54.2	64.6
Denim	35	4	9.0	45	56.2	35.9	46.1
Glass	35	4	9.5	65	60.5	35.9	50.0
Paper	35	4	9.0	65	60.5	35.9	50.0
Denim	40	4	10.0	30	45.8	41.6	44.2
Glass	40	4	10.0	45	45.8	33.0	41.4
Paper	40	4	9.0	45	45.8	33.0	41.4
Denim	45	3	11.0	25	41.1	23.7	30.7
Glass	45	3	10.0	39	44.9	23.7	34.7
Paper	45	3	10.0	40	44.9	23.7	33.7
Denim	50	3	10.0	15	30.7	20.9	25.8
Glass	50	3	9.0	28	36.6	20.9	28.8
Paper	50	3	8.0	25	30.7	20.9	26.8

### 12.1.3 Figure 381 Mean drying time results for 10µl stains (3<sup>rd</sup> experimental run)

Surface	Temperature /°C	Age of Blood /days	Diameter of Dried Stain /mm	Drying Time /mins	Highest Humidity /Rh	Lowest Humidity /Rh	Average Humidity /Rh
Denim	-10	13	9.5	510	86.7	83.5	85.1
Glass	-10	13	10.0	765	89.1	83.5	86.3
Paper	-10	13	9.5	1040	91.7	83.5	86.7
Denim	-5	14	11.0	600	86.1	69.7	77.9
Glass	-5	14	10.5	1118	87.7	69.7	82.6
Paper	-5	14	9.5	930	87.7	69.7	82.2
Denim	0	7	10.5	345	100.0	77.8	86.8
Glass	0	7	10.0	555	100.0	77.8	85.0
Paper	0	7	9.5	760	100.0	77.8	85.3
Denim	5	4	11.0	450	96.0	93.0	94.5
Glass	5	4	10.5	550	96.0	89.8	92.7
Paper	5	4	9.0	825	96.0	89.4	91.7
Denim	10	2	10.0	380	93.2	84.6	90.0
Glass	10	2	10.0	510	93.2	84.6	90.4
Paper	10	2	9.5	760	93.2	84.6	91.0
Denim	15	15	11.5	240	100.0	98.5	99.3
Glass	15	15	10.5	675	100.0	96.9	98.6
Paper	15	15	9.7	715	100.0	96.8	98.6
Denim	20	10	10.5	210	94.3	93.7	94.0
Glass	20	10	11.0	455	94.3	89.1	92.0
Paper	20	10	9.5	355	94.3	89.8	92.6
Denim	25	9	12.0	105	100.0	93.9	96.7
Glass	25	9	10.0	210	100.0	94.7	97.6
Paper	25	9	9.0	300	100.0	94.3	97.0
Denim	30	10	11.0	60	67.7	37.8	55.3
Glass	30	10	10.5	95	67.7	37.8	55.3
Paper	30	10	9.5	108	67.7	37.8	55.5
Denim	35	7	10.5	55	100.0	46.5	82.1
Glass	35	7	10.0	88	100.0	46.5	87.5
Paper	35	7	8.5	94	100.0	46.5	88.3
Denim	40	15	10.0	35	56.3	49.2	52.8
Glass	40	15	9.5	40	56.3	49.2	52.2
Paper	40	15	9.0	50	56.3	49.2	51.8
Denim	45	10	11.0	35	59.3	36.6	44.4
Glass	45	10	10.0	38	59.3	34.3	42.5
Paper	45	10	10.0	41	59.3	33.6	41.5
Denim	50	7	11.5	20	100.0	100.0	100.0
Glass	50	7	10.5	29	100.0	100.0	100.0
Paper	50	7	9.5	30	100.0	100.0	100.0

#### 12.1.4 Figure 382 Mean drying time results for 10µl stains (4<sup>th</sup> experimental run)

Surface	Temperature /oC	Age of Blood /days	Diameter of Dried Stain /mm	Drying Time /mins	Highest Humidity /Rh	Lowest Humidity /Rh	Average Humidity /Rh
Denim	-10	6	10.0	480	92.3	90.7	91.5
Glass	-10	6	10.0	690	92.3	88.7	90.6
Paper	-10	6	9.0	1080	92.3	87.3	90.2
Denim	-5	13	11.0	540	87.7	84.1	85.9
Glass	-5	13	10.0	660	87.7	84.1	85.9
Paper	-5	13	9.0	945	88.0	84.1	86.4
Denim	0	5	10.5	360	93.8	87.1	90.5
Glass	0	5	10.0	690	93.8	87.1	89.9
Paper	0	5	9.0	960	93.8	87.1	89.4
Denim	5	8	11.0	405	91.1	88.8	90.2
Glass	5	8	10.0	655	91.8	88.8	90.7
Paper	5	8	8.5	855	91.8	88.8	90.7
Denim	10	12	10.0	360	96.7	59.1	83.0
Glass	10	12	10.0	435	96.7	59.1	86.1
Paper	10	12	9.0	565	96.7	59.1	86.8
Denim	15	3	10.5	280	100.0	95.0	97.5
Glass	15	3	10.0	463	100.0	95.0	98.1
Paper	15	3	8.5	610	100.0	94.0	97.8
Denim	20	4	10.5	465	100.0	100.0	100.0
Glass	20	4	10.0	1200	100.0	100.0	100.0
Paper	20	4	9.0	1560	100.0	100.0	100.0
Denim	25	12	11.0	100	85.8	57.6	74.8
Glass	25	12	10.0	175	85.8	57.6	78.4
Paper	25	12	9.0	190	87.1	57.6	77.9
Denim	30	7	11.0	120	100.0	100.0	100.0
Glass	30	7	10.0	150	100.0	93.2	98.3
Paper	30	7	9.0	195	100.0	89.4	96.5
Denim	35	12	10.0	45	68.9	44.1	59.2
Glass	35	12	10.5	65	68.9	44.1	60.5
Paper	35	12	8.0	80	68.9	44.1	59.4
Denim	40	9	10.0	33	100.0	59.1	84.8
Glass	40	9	10.0	45	100.0	48.2	74.2
Paper	40	9	9.0	50	100.0	47.8	71.1
Denim	45	9	10.0	25	52.3	37.0	44.0
Glass	45	9	10.0	40	52.3	37.0	42.7
Paper	45	9	9.0	43	52.3	35.4	41.8
Denim	50	9	10.0	15	48.6	36.9	42.2
Glass	50	9	10.0	29	48.6	29.4	38.5
Paper	50	9	9.0	30	48.6	27.5	37.6

### 12.1.5 Figure 383 Mean drying time results for 10µl stains (5<sup>th</sup> experimental run)

Surface	Temperature /°C	Age of Blood /days	Diameter of Dried Stain /mm	Drying Time /mins	Highest Humidity /Rh	Lowest Humidity /Rh	Average Humidity /Rh
Denim	-10	15	10.0	495	85.8	82.0	83.9
Glass	-10	15	10.0	670	95.8	85.8	88.0
Paper	-10	15	9.0	725	95.8	82.0	89.4
Denim	-5	14	10.5	410	83.6	81.9	82.7
Glass	-5	14	10.0	562	85.4	81.9	85.1
Paper	-5	14	9.0	605	88.2	81.9	84.7
Denim	0	13	11.0	390	96.3	87.8	93.4
Glass	0	13	10.0	570	96.3	87.8	94.0
Paper	0	13	10.0	750	96.3	83.1	91.5
Denim	5	12	10.0	500	92.3	82.8	89.4
Glass	5	12	11.0	680	92.3	82.8	88.9
Paper	5	12	9.0	810	92.6	82.8	89.5
Denim	10	11	11.0	435	100.0	96.9	98.5
Glass	10	11	10.0	600	100.0	85.9	94.3
Paper	10	11	9.0	810	100.0	85.9	96.0
Denim	15	10	10.0	135	99.1	93.9	96.3
Glass	15	10	10.0	365	100.0	93.5	96.4
Paper	15	10	9.0	570	100.0	93.5	96.6
Denim	20	7	10.0	185	93.0	83.6	86.9
Glass	20	7	10.0	218	93.0	83.6	87.6
Paper	20	7	9.0	236	93.0	83.6	88.0
Denim	25	7	10.5	120	89.2	77.3	84.4
Glass	25	7	10.0	165	89.2	77.3	84.2
Paper	25	7	9.0	165	89.2	77.3	84.2
Denim	30	5	10.0	85	79.5	48.3	67.8
Glass	30	5	10.0	105	79.5	48.3	69.2
Paper	30	5	9.0	120	79.5	48.3	69.3
Denim	35	5	10.0	50	77.0	56.0	66.5
Glass	35	5	10.0	75	77.0	56.0	65.7
Paper	35	5	9.0	83	77.0	56.0	65.1
Denim	40	5	10.0	45	69.3	56.4	63.0
Glass	40	5	10.0	55	69.3	56.4	63.6
Paper	40	5	9.0	65	69.3	48.9	60.0
Denim	45	3	9.5	23	67.7	48.8	55.4
Glass	45	3	10.0	33	67.7	35.5	48.5
Paper	45	3	9.0	32	67.7	36.3	49.0
Denim	50	7	10.0	15	68.0	43.0	55.5
Glass	50	7	10.5	28	68.0	33.5	44.6
Paper	50	7	9.0	28	68.0	33.5	44.7

**12.1.6 Figure 384 Mean drying time results for 45µl stains (1<sup>st</sup> experimental run)**

Surface	Temperature °C	Age of Blood /days	Drying Time /mins	Highest Humidity /Rh	Lowest Humidity /Rh	Average Humidity /Rh
Denim	-10	14	660	75.4	68.1	71.8
Glass	-10	14	960	86.2	68.1	74.6
Paper	-10	14	880	82.6	68.1	73.6
Denim	-5	2	420	73.0	69.1	71.1
Glass	-5	2	1100	73.0	65.6	69.9
Paper	-5	2	1680	73.0	63.4	68.9
Denim	0	7	630	69.7	61.2	66.5
Glass	0	7	915	79.3	61.2	69.2
Paper	0	7	1320	98.4	61.2	73.6
Denim	5	8	660	93.5	83.6	85.8
Glass	5	8	1200	93.5	83.0	85.2
Paper	5	8	1320	93.5	83.0	85.2
Denim	10	6	570	92.7	91.0	92.0
Glass	10	6	960	92.7	88.9	91.2
Paper	10	6	1380	94.3	88.9	92.0
Denim	15	8	540	89.0	88.3	88.7
Glass	15	8	780	91.6	88.3	89.6
Paper	15	8	870	91.6	88.3	89.4
Denim	20	8	560	97.2	91.3	94.8
Glass	20	8	920	97.2	91.3	95.0
Paper	20	8	950	98.0	91.3	95.6
Denim	25	9	480	99.0	97.2	98.0
Glass	25	9	1380	99.8	95.7	98.0
Paper	25	9	910	99.8	95.7	98.0
Denim	30	10	285	92.7	79.2	86.0
Glass	30	10	315	92.7	69.7	82.0
Paper	30	10	390	92.7	69.7	82.0
Denim	35	11	150	60.9	42.7	54.0
Glass	35	11	190	60.9	42.7	54.0
Paper	35	11	163	60.9	42.7	54.2
Denim	40	11	60	51.0	33.7	43.0
Glass	40	11	70	51.0	33.1	43.0
Paper	40	11	80	51.0	32.4	41.2
Denim	45	14	50	34.1	25.5	31.0
Glass	45	14	65	34.1	25.5	31.0
Paper	45	14	65	34.1	25.5	31.0
Denim	50	14	30	31.1	16.5	24.9
Glass	50	14	43	31.1	16.5	23.5
Paper	50	14	50	31.1	16.5	23.2

12.1.7 Figure 385 Mean drying time results for 45µl stains (2<sup>nd</sup> experimental run)

Surface	Temperature °C	Age of Blood /days	Drying Time /mins	Highest Humidity /Rh	Lowest Humidity /Rh	Average Humidity /Rh
Denim	-10	1	840	97.5	67.6	82.0
Glass	-10	1	900	97.5	67.6	82.0
Paper	-10	1	995	97.5	67.6	78.8
Denim	-5	2	1000	98.5	64.7	82.0
Glass	-5	2	1113	98.5	64.7	81.0
Paper	-5	2	1245	98.5	64.7	80.0
Denim	0	3	945	87.7	84.3	86.0
Glass	0	3	1090	86.3	84.3	85.1
Paper	0	3	1080	87.1	84.9	86.0
Denim	5	4	480	87.7	79.9	83.5
Glass	5	4	1255	87.7	79.9	83.4
Paper	5	4	1335	87.7	79.9	83.4
Denim	10	7	480	87.1	83.3	85.2
Glass	10	7	1075	91.2	83.3	87.3
Paper	10	7	1080	91.4	83.3	88.0
Denim	15	8	435	91.7	91.4	91.5
Glass	15	8	1010	91.7	87.1	89.8
Paper	15	8	1200	91.7	83.7	89.3
Denim	20	9	495	99.3	93.5	97.1
Glass	20	9	1113	99.3	93.5	96.7
Paper	20	9	1035	99.3	93.5	97.1
Denim	25	2	555	89.1	60.6	76.0
Glass	25	2	613	89.1	60.6	77.6
Paper	25	2	630	89.1	60.6	78.1
Denim	30	3	195	84.6	50.1	66.4
Glass	30	3	255	84.6	50.1	70.0
Paper	30	3	285	84.6	50.1	70.0
Denim	35	3	150	78.8	30.1	54.5
Glass	35	3	180	78.8	30.1	60.4
Paper	35	3	210	78.8	30.1	60.4
Denim	40	4	70	65.6	30.6	48.2
Glass	40	4	80	65.6	30.6	47.8
Paper	40	4	125	67.0	30.6	48.8
Denim	45	4	60	69.8	30.1	50.0
Glass	45	4	80	69.8	30.1	49.2
Paper	45	4	88	69.8	30.1	47.1
Denim	50	4	30	51.4	16.0	33.7
Glass	50	4	37	51.4	16.0	31.0
Paper	50	4	49	51.4	16.0	28.3



## 12.2 Descriptive Statistics

Results (set out in *sections 12.1.1 – 12.1.7*) were averaged across experimental runs to calculate single measurements of age of blood, stain diameter, drying time and humidity for each volume of bloodstain (10 $\mu$ l & 45 $\mu$ l), surface (denim, glass and paper) and temperature. An overall measure of mean drying time was also calculated for each stain volume and surface, to allow comparisons of the dependent variable (drying time) to be made between stains on all surfaces (*section 12.3*).

### 12.2.1 10 $\mu$ l stains on Denim

*Figure 386* sets out mean measurements for 10 $\mu$ l stains on denim, across 13 temperature intervals. Measurements at each temperature interval were calculated by averaging measurements recorded for 6 replicate stains at each temperature interval across 5 experimental runs; a total of 30 stains. Variables that exhibited the largest variations between temperature intervals were drying time and humidity. As temperature incrementally increased from -10°C to 50°C, drying time (minutes) decreased from 493 to 16 minutes and humidity decreased from 87.8 to 54.9%. Results indicated that for 10 $\mu$ l stains on denim, as temperature increased, humidity and drying time decreased considerably. Rates of decreases in humidity and drying time differed.

For decreases in drying time, three distinct periods of change were identified. As temperature increased between -10°C and 10°C (5 intervals) drying time decreased by 103 minutes, between 10°C and 25°C (4 intervals) drying time decreased by 283 minutes and between 25°C and 50°C (6 intervals) drying time decreased by 91 minutes. Results indicate that the largest decrease in drying time occurred between 10°C and 25°C, over the shortest number of temperature intervals. This observation supports a suggestion that temperature increases between 10°C and 25°C have a considerable effect on drying time, for 10 $\mu$ l stains on denim. Trends in decreasing humidity levels were more complicated to define. As temperature increased from -10°C to 15°C, humidity fluctuated within a relatively high range between 85.1 (-5°C) and 96.2 (15°C). Fluctuations in humidity within this range broadly increased as

temperature increased. Between 20°C and 50°C, humidity was lower, decreasing from 89.0 (20°C) and 54.9 (50°C). Results appeared to suggest that alterations in temperature had a more consistent and therefore considerable effect on drying time than alterations in humidity.

Temperature /°C	Age of blood /days	Blood Volume /µl	Stain Diameter /mm	Drying Time /Mins	Drying Time /hrs	Maximum Humidity /%	Minimum Humidity /%	Average Humidity /%
-10	11	10	10	493	8.2	90.1	85.7	87.8
-5	13	10	11	497	8.3	88.2	82.0	85.1
0	8	10	11	385	6.4	95.9	84.8	90.1
5	8	10	11	447	7.4	94.8	89.0	92.5
10	8	10	10	390	6.5	96.2	82.1	90.8
15	9	10	10	237	4.0	98.8	93.2	96.2
20	7	10	10	244	4.1	92.1	86.0	89.0
25	8	10	11	107	1.8	88.7	73.5	82.1
30	7	10	10	79	1.4	80.0	64.0	73.6
35	7	10	10	49	0.8	75.0	45.7	63.2
40	9	10	10	35	0.6	66.8	50.9	60.3
45	7	10	10	27	0.5	54.5	36.3	43.3
50	7	10	10	16	0.3	60.9	49.2	54.9

Figure 386 Results for 10µl stains on denim, averaged from replicates (n = 30) at each temperature interval and across 5 experimental runs

Figure 387 sets out a calculation of mean drying time for all 10µl stains on denim. Mean drying time was calculated as 231 minutes, with a minimum of 16 minutes and a maximum of 497 minutes across all 13 temperature intervals.

	N	Minimum	Maximum	Mean	Std. Deviation
Drying time /mins	13	16	497	231	189.982
Valid N (listwise)	13				

Figure 387 Calculation of minimum, maximum and mean drying time for 10µl stains on denim

### 12.2.2 10µl stains on Glass

Figure 388 sets out mean measurements for 10µl stains on glass, across 13 temperature intervals. Measurements at each temperature interval were calculated as described in section 12.2.1. Variables that exhibited the largest variations between temperature intervals were drying time and humidity. As temperature incrementally

increased from -10°C to 50°C, drying time (minutes) decreased from 688 to 28 minutes and humidity decreased from 88.5 to 52.2%. Results indicated that for 10µl stains on glass, as temperature increased, humidity and drying time decreased considerably. Rates of decreases in humidity and drying time differed.

For decreases in drying time, two distinct periods of change were identified. As temperature increased between -10°C and 20°C (7 intervals) drying time decreased by 159 minutes, between 20°C and 50°C (7 intervals) drying time decreased by 501 minutes. Results indicate that whilst drying time decreased as temperature increased between -10°C and 20°C, the largest decrease in drying time occurred between 20°C and 50°C. This observation supports a suggestion that temperature increases between -10°C and 50°C and particularly between 20°C and 50°C have an observable effect on drying time, for 10µl stains on glass. Trends in decreasing humidity levels were more complicated to define. As temperature increased from -10°C to 15°C, humidity fluctuated within a relatively high range between 82.4 (25°C) and 96.0 (15°C). Fluctuations in humidity within this range broadly increased as temperature increased. Between 20°C and 50°C, humidity was lower, decreasing from 89.8 (20°C) and 52.2 (50°C). Results appeared to suggest that alterations in temperature had a more consistent and therefore considerable effect on drying time than alterations in humidity.

Temperature /°C	Age of blood /days	Blood Volume /µl	Stain Diameter /mm	Drying Time /Mins	Drying Time /hrs	Maximum Humidity /%	Minimum Humidity /%	Average Humidity /%
-10	11	10	10	688	11.5	93.1	86.1	88.5
-5	13	10	10	727	12.1	89.0	80.5	86.0
0	8	10	10	640	10.7	95.9	84.4	89.2
5	8	10	10	607	10.1	95.0	88.3	92.0
10	8	10	10	520	8.7	96.3	79.4	90.7
15	9	10	10	471	7.9	99.1	92.7	96.0
20	7	10	10	529	8.9	92.8	84.8	89.8
25	8	10	10	171	2.9	88.7	72.9	82.4
30	7	10	10	107	1.8	80.0	59.6	72.4
35	7	10	10	73	1.2	76.0	45.7	65.5
40	9	10	10	46	0.8	66.8	46.2	57.1
45	7	10	10	37	0.6	55.4	32.5	41.8
50	7	10	10	28	0.5	62.3	45.1	52.2

Figure 388 Results for 10µl stains on glass, averaged from replicates (n = 30) at each temperature interval and across 5 experimental runs

*Figure 389* sets out a calculation of mean drying time for all 10µl stains on glass. Mean drying time was calculated as 357 minutes, with a minimum of 28 minutes and a maximum of 727 minutes across all 13 temperature intervals.

	N	Minimum	Maximum	Mean	Std. Deviation
Drying time /mins	13	28	727	357	280.374
Valid N (listwise)	13				

Figure 389 Calculation of minimum, maximum and mean drying time for 10µl stains on glass

### 12.2.3 10µl stains on Paper

*Figure 390* sets out mean measurements for 10µl stains on paper, across 13 temperature intervals. Measurements at each temperature interval were calculated as described in *section 12.2.1*. Variables that exhibited the largest variations between temperature intervals were drying time and humidity. As temperature incrementally increased from -10°C to 50°C, drying time (minutes) decreased from 962 to 28 minutes and humidity decreased from 88.7 to 51.5%. Results indicated that for 10µl stains on paper, as temperature increased, humidity and drying time decreased considerably. Rates of decreases in humidity and drying time differed.

For decreases in drying time, two distinct periods of change were identified. As temperature increased between -10°C and 20°C (7 intervals) drying time decreased by 321 minutes, between 20°C and 50°C (7 intervals) drying time decreased by 613 minutes. Results indicate that whilst drying time decreased as temperature increased between -10°C and 20°C, the biggest decrease in drying time occurred between 20°C and 50°C. This observation supports a suggestion that temperature increases between -10°C and 50°C have an effect of drying time, for 10µl stains on paper. Between 20°C and 25°C the largest single decrease in drying time (438 minutes) between two adjacent temperature intervals was recorded. This observation supports a suggestion that the most observable alterations in drying time occur as temperature increases above 20°C, for 10µl stains on paper. Trends in decreasing humidity levels were more complicated to define. As temperature increased from -10°C to 25°C, humidity fluctuated within a relatively high range between 81.8 (25°C) and 96.4 (15°C).

Fluctuations in humidity within this range did not appear to follow a general rule. Between 30°C and 50°C, humidity was lower, decreasing from 71.4 (30°C) to 41.2 (45°C). Results appeared to suggest that alterations in temperature had a more consistent and therefore considerable effect on drying time than alterations in humidity.

Temperature °C	Age of blood /days	Blood Volume /µl	Stain Diameter /mm	Drying Time /Mins	Drying Time /hrs	Maximum Humidity /%	Minimum Humidity /%	Average Humidity /%
-10	11	10	9	962	16.0	93.7	84.4	88.7
-5	13	10	9	848	14.1	89.8	80.4	85.6
0	8	10	10	877	14.6	95.9	83.2	88.8
5	8	10	9	853	14.2	95.1	88.2	91.7
10	8	10	9	739	12.3	96.3	79.4	91.6
15	9	10	9	604	10.1	99.5	92.4	96.4
20	7	10	9	641	10.7	92.8	85.1	90.2
25	8	10	9	203	3.4	89.0	72.8	81.8
30	7	10	9	127	2.1	80.0	57.4	71.4
35	7	10	9	80	1.3	76.0	45.7	65.2
40	9	10	9	52	0.9	66.8	44.3	55.4
45	7	10	9	39	0.6	55.4	32.2	41.2
50	7	10	9	28	0.5	60.9	44.7	51.5

Figure 390 Results for 10µl stains on paper, averaged from replicates (n = 30) at each temperature interval and across 5 experimental runs

*Figure 391* sets out a calculation of mean drying time for all 10µl stains on paper. Mean drying time was calculated as 465 minutes, with a minimum of 28 minutes and a maximum of 962 minutes across all 13 temperature intervals.

	N	Minimum	Maximum	Mean	Std. Deviation
Drying time /mins	13	28	962	465	377.876
Valid N (listwise)	13				

Figure 391 Calculation of minimum, maximum and mean drying time for 10µl stains on paper

#### 12.2.4 45µl stains on Denim

*Figure 392* sets out mean measurements for 45µl stains on denim, across 13 temperature intervals. Measurements at each temperature interval were calculated by

averaging measurements recorded for 6 replicate stains at each temperature interval across 2 experimental runs; a total of 12 stains. Variables that exhibited the largest variations between temperature intervals were drying time and humidity. As temperature incrementally increased from -10°C to 50°C, drying time (minutes) decreased from 818 to 30 minutes and humidity decreased from 80.7 to 32.6%. Results indicated that for 45µl stains on denim, as temperature increased, humidity and drying time decreased considerably. Rates of decreases in humidity and drying time differed.

For decreases in drying time, three distinct periods were identified, between -10°C and 0°C, 5°C and 25°C and 30°C and 50°C. Between -10°C and 0°C drying times were high, fluctuating between 818 minutes (-10°C) and 928 minutes (-5°C). A large decrease of 403 minutes in drying time was recorded between 0°C and 5°C. Between 5°C and 25°C drying time fluctuated between 503 minutes (5°C) and 546 minutes (25°C). Another large decrease in drying time was also recorded between 25°C and 30°C of 340 minutes. Between 30°C and 50°C drying time was decreased by 176 minutes. Results indicate that as temperature increased between -10°C and 50°C, drying time for 45µl stains on denim decreased, with two observable decreases in drying time occurring between 0°C and 5°C and 25°C and 30°C. Trends in decreasing humidity levels were more complicated to define. As temperature increased from -10°C to 20°C, humidity fluctuated within a relatively high range between 80.6 (-5°C) and 96.8 (20°C). Fluctuations in humidity within this range increased as temperature increased. Between 25°C and 50°C humidity was lower, decreasing from 78.8 (25°C) to 32.6 (50°C). Results appeared to suggest that alterations in temperature had a more consistent and therefore considerable effect on drying time than alterations in humidity.

Temperature °C	Age of blood /days	Blood Volume /µl	Drying Time /Mins	Drying Time /hrs	Maximum Humidity /%	Minimum Humidity /%	Average Humidity /%
-10	3	45	818	13.6	94.7	67.7	80.7
-5	2	45	928	15.5	95.3	65.3	80.6
0	4	45	906	15.1	85.5	81.4	83.6
5	5	45	503	8.4	88.4	80.4	83.8
10	7	45	491	8.2	87.8	84.3	86.1
15	8	45	448	7.5	91.4	91.0	91.2
20	9	45	503	8.4	99.0	93.2	96.8
25	3	45	546	9.1	90.3	65.2	78.8
30	4	45	206	3.4	85.6	53.7	72.0
35	4	45	150	2.5	76.6	31.7	54.4
40	5	45	69	1.2	63.8	31.0	47.6
45	5	45	59	1.0	65.3	29.5	47.6
50	5	45	30	0.5	48.9	16.1	32.6

Figure 392 Results for 45µl stains on denim, averaged from replicates (n = 30) at each temperature interval and across 2 experimental runs

Figure 393 sets out a calculation of mean drying time for all 45µl stains on denim. Mean drying time was calculated as 435 minutes, with a minimum of 30 minutes and a maximum of 928 minutes across all 13 temperature intervals.

	N	Minimum	Maximum	Mean	Std. Deviation
Drying time /mins	13	30	928	435	317.474
Valid N (listwise)	13				

Figure 393 Calculation of minimum, maximum and mean drying time for 45µl stains on denim

### 12.2.5 45µl stains on Glass

Figure 394 sets out mean measurements for 45µl stains on glass, across 13 temperature intervals. Measurements at each temperature interval were calculated as described in section 12.2.4. Variables that exhibited the largest variations between temperature intervals were drying time and humidity. As temperature incrementally increased from -10°C to 50°C, drying time (minutes) decreased from 908 to 37 minutes and humidity decreased from 81.1 to 30.0%. Results indicated that for 45µl stains on glass, as temperature increased, humidity and drying time decreased

considerably. Rates of decreases in humidity and drying time differed.

For decreases in drying time, three distinct periods of change were identified, between -10°C and 20°C, 20°C and 30°C and 30°C and 50°C. As temperature increased between -10°C and 20°C drying times were high, fluctuating between 908 (-10°C) and 1248 (5°C). Large decreases in drying time were recorded between 20°C and 25°C (380 minutes) and 25°C and 30°C (445 minutes), indicating a total decrease in drying time between 20°C and 30°C of 825 minutes. Between 30°C and 50°C drying times decreased from 263 minutes (30°C) and 37 minutes (50°C). Results indicate that as temperature increased between -10°C and 50°C, drying time for 45µl stains on glass decreased, with the largest decreases in drying time occurring between 20°C and 30°C. Trends in decreasing humidity levels were more complicated to define. As temperature increased from -10°C to 20°C, humidity fluctuated within a relatively high range between 79.6 (-5°C) and 96.5 (20°C). Fluctuations in humidity within this range broadly increased as temperature increased. Between 20°C and 50°C, humidity was lower, decreasing from 80.2 (20°C) to 30.0 (50°C). Results appeared to suggest that alterations in temperature had a more consistent and therefore considerable effect on drying time than alterations in humidity.

Temperature °C	Age of blood /days	Blood Volume /µl	Drying Time /Mins	Drying Time /hrs	Maximum Humidity /%	Minimum Humidity /%	Average Humidity /%
-10	3	45	908	15.1	96.1	67.7	81.1
-5	2	45	1111	18.6	95.3	64.8	79.6
0	4	45	1068	17.8	85.4	81.4	83.2
5	5	45	1248	20.8	88.4	80.3	83.6
10	7	45	1061	17.7	91.3	84.0	87.8
15	8	45	981	16.4	91.7	87.3	89.8
20	9	45	1088	18.2	99.0	91.8	96.5
25	3	45	708	11.8	90.4	65.0	80.2
30	4	45	263	4.4	85.6	52.6	71.6
35	4	45	177	3.0	76.6	31.7	59.6
40	5	45	79	1.4	63.8	30.9	47.1
45	5	45	78	1.3	65.3	29.5	46.9
50	5	45	37	0.7	48.9	16.1	30.0

Figure 394 Results for 45µl stains on glass, averaged from replicates (n = 30) at each temperature interval and across 2 experimental runs



*Figure 395* sets out a calculation of mean drying time for all 45µl stains on glass. Mean drying time was calculated as 677 minutes, with a minimum of 37 minutes and a maximum of 1248 minutes across all 13 temperature intervals.

	N	Minimum	Maximum	Mean	Std. Deviation
Drying time /mins	13	37	1248	677	472.387
Valid N (listwise)	13				

Figure 395 Calculation of minimum, maximum and mean drying time for 45µl stains on glass

### 12.2.6 45µl stains on Paper

*Figure 396* sets out mean measurements for 45µl stains on paper, across 13 temperature intervals. Measurements at each temperature interval were calculated as described in *section 12.2.4*. Variables that exhibited the largest variations between temperature intervals were drying time and humidity. As temperature incrementally increased from -10°C to 50°C, drying time (minutes) decreased from 981 to 49 minutes and humidity decreased from 78.2 to 27.7%. Results indicated that for 45µl stains on paper, as temperature increased, humidity and drying time decreased considerably. Rates of decreases in humidity and drying time differed.

For decreases in drying time, two distinct periods were identified, between -10°C and 20°C and 20°C and 50°C. As temperature increased between -10°C and 20°C drying times were high, fluctuating between 981 (-10°C) and 1333 (5°C). A significant decrease in drying time was recorded between 20°C and 25°C (359 minutes). Between 25°C and 50°C drying times decreased from 665 minutes (25°C) to 49 minutes (50°C). Results indicate that as temperature increased between -10°C and 50°C, drying time for 45µl stains on paper decreased, with the largest decreases in drying time occurring between 20°C and 25°C. Trends in decreasing humidity levels were more complicated to define. As temperature increased from -10°C to 20°C, humidity fluctuated within a relatively high range between 78.2 (-10°C) and 96.9 (20°C). Fluctuations in humidity within this range broadly increased as temperature increased. Between 25°C and 50°C, humidity was lower, decreasing from 80.6

(20°C) to 27.7 (50°C). Results appeared to suggest that alterations in temperature had a more consistent and therefore considerable effect on drying time than alterations in humidity.

Temperature /°C	Age of blood /days	Blood Volume /µl	Drying Time /Mins	Drying Time /hrs	Maximum Humidity /%	Minimum Humidity /%	Average Humidity /%
-10	3	45	981	16.3	95.6	67.7	78.2
-5	2	45	1299	21.8	95.3	64.5	78.6
0	4	45	1110	18.5	88.5	81.9	84.5
5	5	45	1333	22.2	88.4	80.3	83.6
10	7	45	1118	18.6	91.8	84.0	88.5
15	8	45	1159	19.3	91.7	84.3	89.3
20	9	45	1024	17.0	99.1	93.2	96.9
25	3	45	665	11.1	90.4	65.0	80.6
30	4	45	298	5.0	85.6	52.6	71.6
35	4	45	204	3.4	76.6	31.7	59.6
40	5	45	119	2.0	65.0	30.8	48.0
45	5	45	85	1.4	65.3	29.5	45.1
50	5	45	49	0.8	48.9	16.1	27.7

Figure 396 Results for 45µl stains on paper, averaged from replicates (n = 30) at each temperature interval and across 2 experimental runs

Figure 397 sets out a calculation of mean drying time for all 45µl stains on paper. Mean drying time was calculated as 726 minutes, with a minimum of 49 minutes and a maximum of 1333 minutes across all 13 temperature intervals.

	N	Minimum	Maximum	Mean	Std. Deviation
Drying time /mins	13	49	1333	726	503.013
Valid N (listwise)	13				

Figure 397 Calculation of minimum, maximum and mean drying time for 45µl stains on paper

## 12.3 Exploration of relationships between variables

Once descriptive statistics for each volume of stains on each surface had been outlined, relationships between independent variables (temperature, humidity, age of blood, stain volume and surface) and the dependent variable (drying time) were examined collectively for all stains. The relationship between temperature and humidity was also examined.

### 12.3.1 Temperature and drying time

*Figure 398* outlines the relationship between temperature and drying time for all stains on all surfaces. For all groups of stains, as temperature increased drying time decreased. As temperature increased, the range of drying times between groups of stains also decreased. For stains generated between  $-10^{\circ}\text{C}$  and  $25^{\circ}\text{C}$  ranges of drying times exhibited by different groups of stains at the same temperature interval were sizeable, with a maximum range of 922 minutes ( $15^{\circ}\text{C}$ ) and a minimum range of 488 minutes ( $-10^{\circ}\text{C}$ ). For stains generated between  $30^{\circ}\text{C}$  and  $50^{\circ}\text{C}$  these ranges were much smaller, with a maximum range of 219 minutes ( $30^{\circ}\text{C}$ ) and a minimum range of 33 minutes ( $50^{\circ}\text{C}$ ) between drying times at each temperature interval. At temperatures between  $30^{\circ}\text{C}$  and  $50^{\circ}\text{C}$  mean drying times for groups of stains maintained the same order. This order, from shortest to longest length of drying time was: 10 $\mu\text{l}$  stains on denim, 10 $\mu\text{l}$  stains on glass, 10 $\mu\text{l}$  stains on paper, 45 $\mu\text{l}$  stains on denim, 45 $\mu\text{l}$  stains on glass and 45 $\mu\text{l}$  stains on paper.

Observations offer confirmation of two relationships between temperature and drying time for stains generated in experimental stage 4. Firstly, results support a suggestion that as temperature increased between  $-10^{\circ}\text{C}$  and  $50^{\circ}\text{C}$ , across all surfaces stain drying time decreased. Secondly, results suggest that at temperatures above  $30^{\circ}\text{C}$ , the influence of temperature on stain drying time increased considerably.

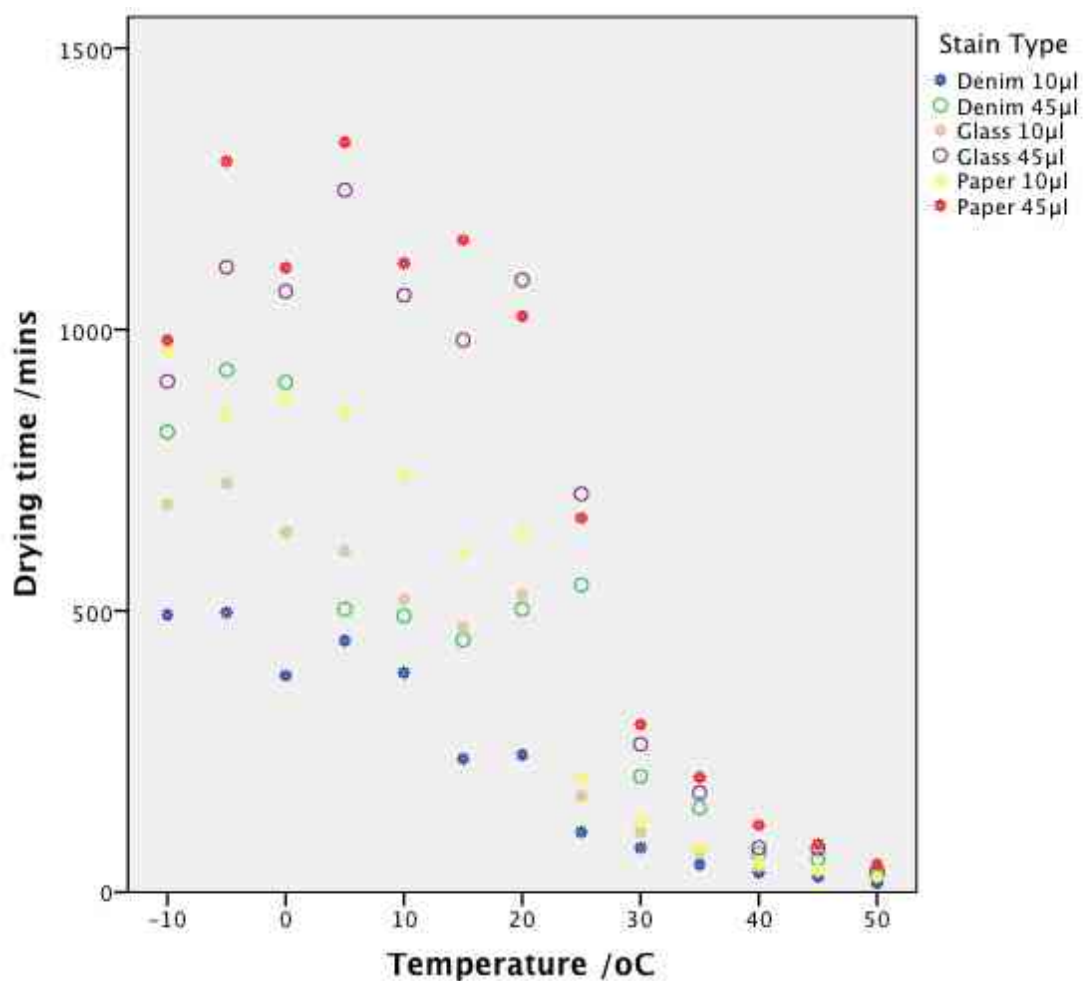


Figure 398 Relationship between temperature (°C) and stain drying time (minutes) for all stains

Figure 399 presents the results of the Kruskal-Wallis test carried out on stains generated. The Kruskal-Wallis test is a non-parametric statistical method that tests a null hypothesis that three or more unrelated (independent) sets of data have the same distribution (*Laerd Statistics. 2013*). A non-parametric test was used as normality tests conducted on data from experimental stage 4 indicated strongly that datasets were not normally distributed (normality tests are included in *appendix 4*). For stains generated, results of the test indicated whether temperatures had a significant effect on drying times. Results indicated that the null hypothesis should be rejected. There is therefore a statistically significant difference between stain drying times at different temperatures, at the 99% significance level ( $p < 0.01$ ). This confirms that temperature had a significant influence on stain drying time.

	Null Hypothesis	Test	Sig.	Decision
1	The distribution of Drying time /mins is the same across categories of Temperature /oC.	Independent-Samples Kruskal-Wallis Test	.000	Reject the null hypothesis.

Asymptotic significances are displayed. The significance level is .05.

Figure 399 Kruskal-Wallis test for comparison between distributions of drying time across temperature intervals

Empirical confirmation of the significance of influence of temperature on drying time substantially expands current understanding of influences on bloodstain drying time, which has implications for bloodstain pattern analysis and crime scene reconstruction in the future. Knowledge about influences on drying time had previously been limited to general acceptance of the influence of temperature on drying time (*Laber. Epstein. 1983. Peschel et al. 2011*) and two experimental attempts to verify the nature of this influence (*Brady et al. 2002. Ramsthaler et al. 2012*). In both experimental studies, observations were limited to drying times recorded at three temperature intervals with results generally indicative of negative correlations between temperature and drying time. In one study (*Brady et al. 2002*), drying times were recorded at -3°C (87 minutes), 22°C (8 minutes) and 45°C (13 minutes). Comparison of drying times at -3°C and 45°C supported a hypothesis that drying times are shorter at higher temperatures. Observation of a lower drying time at 22°C than at 45°C however confused conclusions about the temperature and drying time. With observations limited to three temperatures in the study it was consequently difficult to draw conclusions about the precise nature of the relationship between temperature and drying time. In the other study (*Ramsthaler et al. 2012*) observations were limited to measurements of drying time at 15°C (75-90 minutes), 20°C (60-75 minutes) and 24°C (30 minutes). Although observations over this range clearly indicated a negative relationship between increases in temperature and decreases in drying time, they are limited in their extrapolation to a relatively small temperature range (range: 9°C).

Results presented here represent the first empirical confirmation of a negative correlation between temperature and drying time, across such a large range of temperatures (-10°C to 50°C). They also present the first empirical confirmation that stains generated across a range of surfaces replicate this relationship. Results have

implications for future stain analysis and in particular, estimations of drying time for incorporation into crime scene reconstructions. An important aspect of crime scene reconstruction is to chronologically reconstruct the most probable sequence or circumstances surrounding generation of evidence during a bloodletting event. Being able to estimate time of stain deposition can assist in identifying the time a bloodletting event occurred, which may have consequences for other aspects of an investigation, or establishing the chronological order of different phases associated with multiple patterns identified within a complex bloodletting event. Empirical confirmation of the relationship between temperature and drying time through results generated in experimental stage 4 ultimately mean that temperatures recorded at a scene can be used to inform, with much greater accuracy than historically possible, estimated times of stain deposition. For example, consultation of results generated can provide analysts with an estimated drying time for a stain deposited on a particular surface at a particular temperature, within the limits of surfaces examined (paper, glass, denim) and as long as temperature at a scene is known. This will subsequently increase accuracy of temporal reconstructions of bloodletting events.

### **12.3.2 Humidity and drying time**

*Figure 400* outlines the relationship between humidity and drying time for all stains on all surfaces. As humidity increased drying time broadly increased. A significant difference in drying times was observed between humidity levels below and above 80%. At humidity measures of below 80%, average drying times for all stains did not exceed 298 minutes (45µl stains on paper at 71.6% humidity). At humidity measures of above 80%, the majority of stains exhibited drying times in excess of 500 minutes, with a maximum of 1333 minutes (45µl stains on paper at 83.6% humidity). As humidity increased, the range of drying times between groups of stains also increased. For stains generated at humidity levels below 80%, ranges of average drying times exhibited by different groups of stains at the same humidity level were limited. The maximum range in drying time between stains dried at the same humidity was 171 minutes at 71% humidity (45µl stains on paper dried at 71.6%: drying time of 298 minutes, 45µl stains on glass dried at 71.6%: drying time of 263

minutes and 10 $\mu$ l stains on paper dried at 71.4%: drying time of 127 minutes). For stains generated at humidity levels above 80%, ranges of drying times exhibited by different groups of stains at the same humidity were considerable. The maximum range in drying time between stains dried at the same humidity was 915 minutes at 89% humidity (10 $\mu$ l stains on glass dried at 89.8%: drying time of 529 minutes, 10 $\mu$ l stains on denim dried at 89.0%: drying time of 244 minutes, 10 $\mu$ l stains on glass dried at 89.2%: drying time of 640 minutes, 45 $\mu$ l stains on glass dried at 89.8%: drying time of 981 minutes and 45 $\mu$ l stains on paper dried at 89.3%: drying time 1159 minutes). The presence of such a range of drying times between groups of stains dried at the same humidity supports a suggestion that although humidity appeared to influence drying time, it did not appear to be the most influential variable on stain drying time. Other measurements of drying time between stains dried at the same humidity support this conclusion. For example for 10 $\mu$ l stains on denim and 45 $\mu$ l stains on glass both dried at 87.8% humidity, average drying times were 493 minutes and 1061 minutes respectively, a considerable difference of 568 minutes. This particular example highlights the stronger influence volume of blood and surface type appears to exert on drying time over the influence of humidity. Two observations could be made regarding the relationship between humidity and drying time for stains generated in experimental stage 4. First, results appeared to support a suggestion that as humidity increased stain drying time increased. Secondly however, results also suggested, through analysis of drying times at the same humidity, that other variables may act as stronger influences on drying time than humidity.

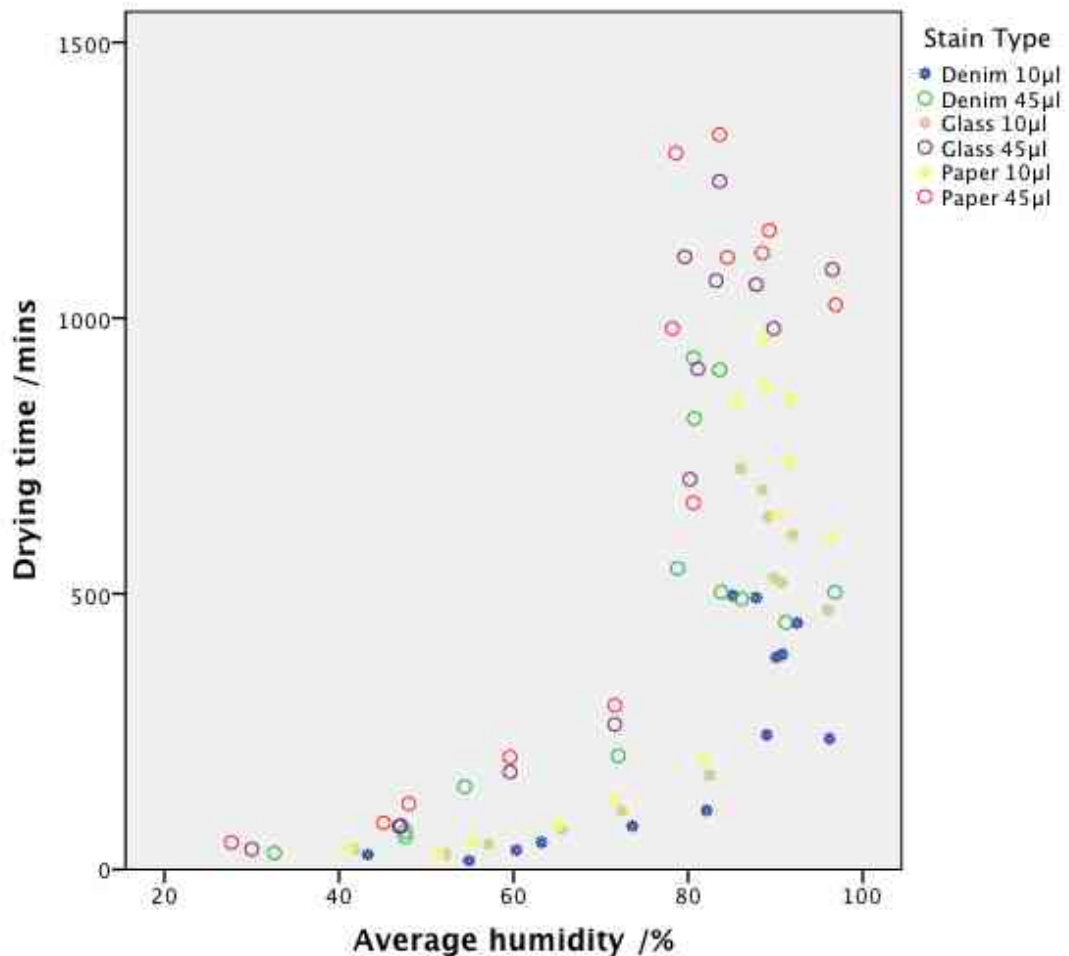


Figure 400 Relationship between humidity (%) and stain drying time (minutes) for all stains

Observations of the influence of humidity on stain drying time supports current acceptance of the general influence of humidity on bloodstain drying time (*Laber. Epstein. 1983. Peschel. 2010*). Results support a suggestion that whilst humidity does appear to influence drying time it does not appear to be as dominant an influence on drying time as other variables such as temperature, stain volume or surface type. This has implications for interpretations of drying time in forensic reality by indicating that whilst humidity should still be considered as a contributory influence on estimations of drying time, estimations should not be led by measurements of humidity.



### 12.3.3 Age of blood and drying time

Figure 401 outlines the relationship between age of blood and drying time for all stains on all surfaces. Across data from all groups of stains, there does not appear to be any correlation between age of blood and drying time. This suggests that use of blood of different ages in experimental stage 4 did not influence drying time.

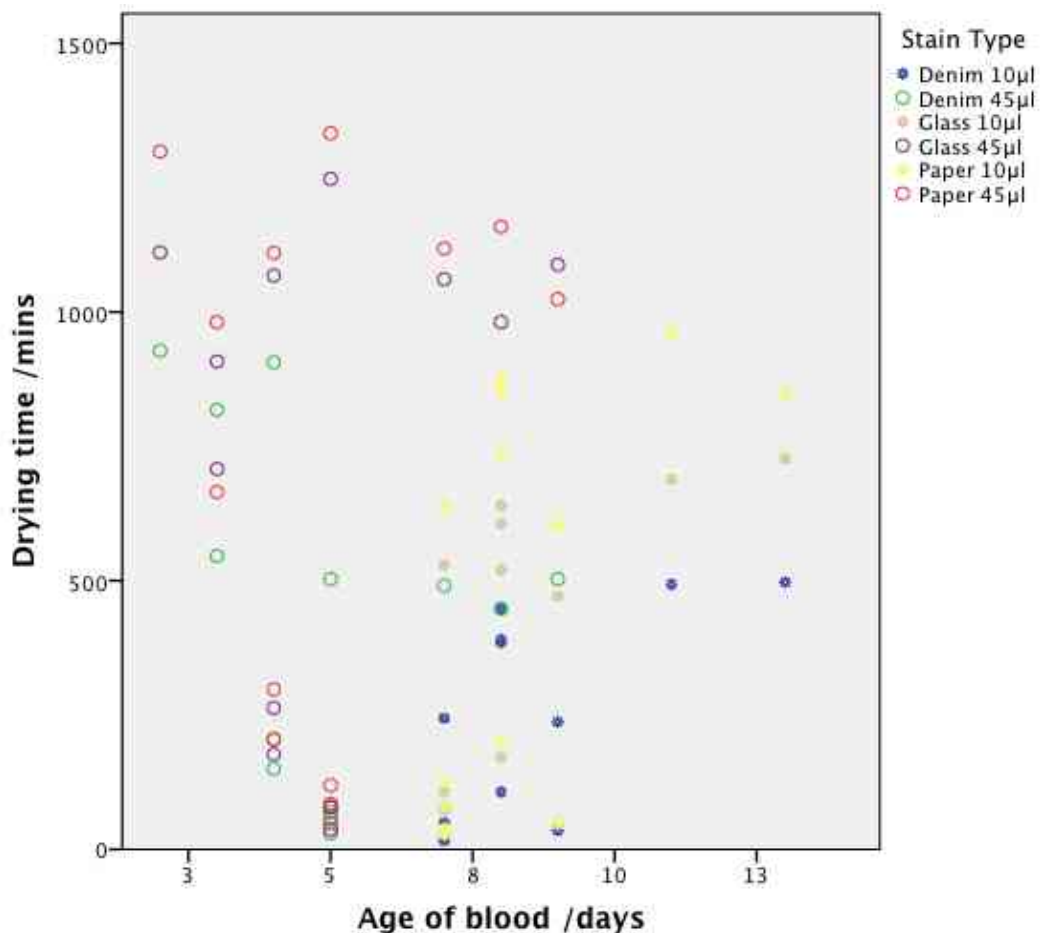


Figure 401 Relationship between age of blood (days) and stain drying time (minutes) for all stains

No previous experimental studies have examined the influence of age of blood on drying time. In forensic reality it would be highly unusual to encounter blood that was aged, i.e. not fresh, however, results of experimental stage 4 indicate that in specific cases where age of blood may be a consideration, it is unlikely to affect drying time. Age of blood should not therefore be considered during estimations of stain drying time for crime scene reconstruction.

#### 12.3.4 Volume of blood and drying time

Figure 402 outlines the distributions of mean drying times for 10 $\mu$ l and 45  $\mu$ l volume stains. Stains generated from 45 $\mu$ l volumes exhibit longer drying times than stains generated from 10 $\mu$ l. Comparison of the lowest, median and highest drying times for each volume confirms this. Stains generated from 10 $\mu$ l volumes, on average, exhibited a shortest drying time of 16 minutes, a median drying time of 351 minutes and a longest drying time of 962 minutes. Stains generated from 45 $\mu$ l volumes, on average, exhibited a shortest drying time of 30 minutes, a median drying time of 613 minutes and a longest drying time of 1333 minutes. Although measures of drying time for 45 $\mu$ l volume stains are greater than comparable measures for 10 $\mu$ l volume stains, there was a considerable overlap in drying times between different stains of both volumes. This indicated that volume of blood was not the sole influence on stain drying time and there was variability, caused by the influence of other variables, in drying times for stains of either volume.

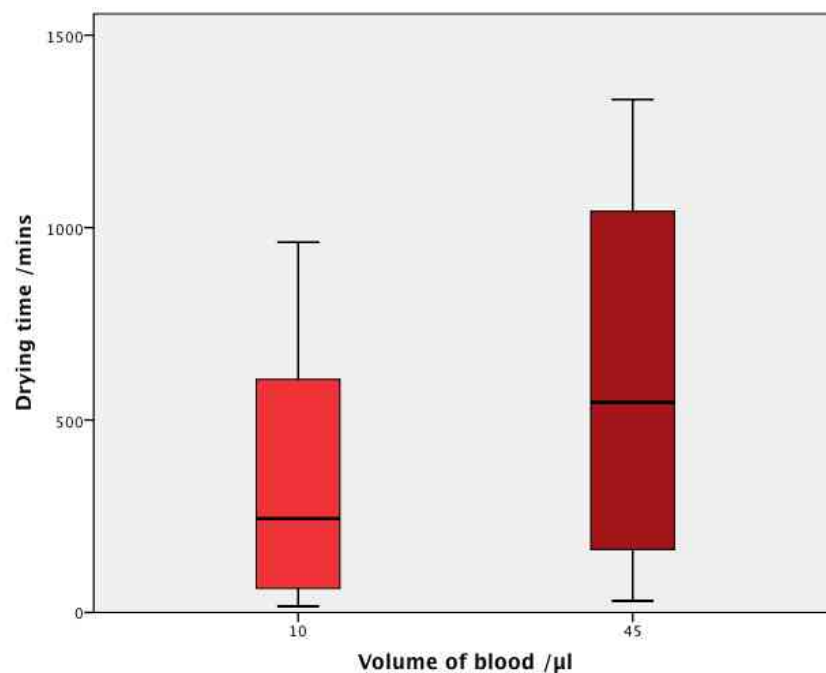


Figure 402 Relationship between volume of blood ( $\mu$ l) and drying time (minutes) for all stains

Figure 403 presents the results of a Mann-Whitney test carried out on stains generated. The Mann-Whitney test is a non-parametric statistical method that tests a null hypothesis that two unrelated (independent) sets of data have the same distribution (*Laerd Statistics. 2013*). A non-parametric test was used as normality

tests conducted on data from experimental stage 4 indicated strongly that datasets were not normally distributed (normality tests are included in *appendix 4*). For stains generated, results of the test indicated whether volume of blood had a significant effect on drying times. The results indicated that the null hypotheses should be rejected. There is therefore a statistically significant difference between stain drying times for different volumes of blood, at the 99% significance level ( $p < 0.01$ ). This confirms that volume of blood had a significant influence on stain drying time.

	Null Hypothesis	Test	Sig.	Decision
1	The distribution of Drying time /mins is the same across categories of Volume of blood / $\mu$ l.	Independent-Samples Mann-Whitney U Test	.004	Reject the null hypothesis.

Asymptotic significances are displayed. The significance level is .05.

Figure 403 Mann-Whitney test for comparison between distributions of drying time across temperature intervals

Although it is generally accepted that volume of blood is an influence on drying time (*Laber. Epstein. 1983*) results presented in *section 12.3.4* represent the first empirical confirmation of the relationship between increases in stain volume and increases in drying time. In forensic reality, implications of observations are limited as it is not currently possible to calculate the volume of blood contained in stains. Development of a method of accurately estimating volumes of blood at a scene would increase the implications of observations of influence of stain volume on drying time.

### 12.3.5 Surface type and drying time

*Figure 404* sets out the relationship between stain type and drying time. Stains generated were classified according to volume and surface to allow comparison of distributions of drying time between surface types. Results indicate that for both volumes (10 $\mu$ l and 45 $\mu$ l) of stains denim stains exhibit the shortest drying times, then glass stains and finally paper stains which exhibit the longest drying times. Median drying times for 10 $\mu$ l stains increase from 237 minutes (denim) to 471 (glass) to 604 (paper). Median drying times for 45 $\mu$ l stains increase from 491 (denim) to 908 (glass) to 981 (paper). The trend indicated in *figure 404* that denim stains exhibited

the shortest drying times, glass stains the medium length of drying times and paper stains the longest drying times is confirmed in *figure 405*, which outlines distributions of drying time for denim, glass and paper surfaces combined for 10 $\mu$ l and 45 $\mu$ l volume stains.

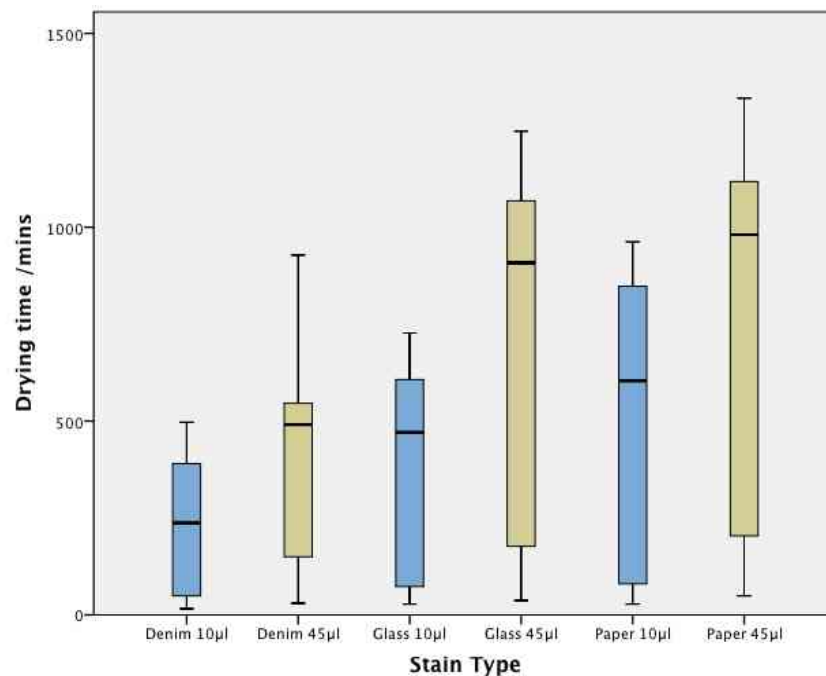


Figure 404 Relationship between stain type and drying time (minutes)

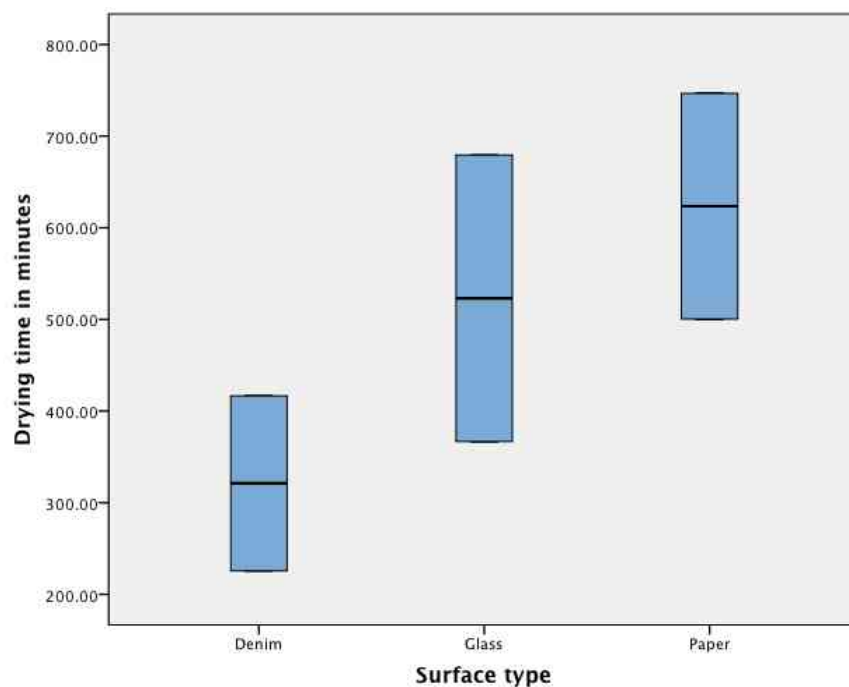


Figure 405 Distributions of drying time (minutes) for denim, glass and paper surfaces, combined for 10 $\mu$ l and 45 $\mu$ l volume stains

Figure 406 presents the results of the Kruskal-Wallis test carried out on stains generated to assess whether stain type (and therefore surface) had a significant effect on drying times. Results indicated that the null hypotheses should be rejected. There is therefore a significant difference between drying times recorded for different surfaces at the 95% significance level ( $p < 0.05$ ). This confirms that surface type had a significant influence on stain drying time.

	Null Hypothesis	Test	Sig.	Decision
1	The distribution of Drying time /mins is the same across categories of Stain Type.	Independent-Samples Kruskal-Wallis Test	.017	Reject the null hypothesis.

Asymptotic significances are displayed. The significance level is .05.

Figure 406 Kruskal-Wallis test for comparison between distributions of drying time and stain type

Empirical confirmation of the influence of surface type and characteristics on drying time enhances current understanding of influences on bloodstain drying time, which has implications for bloodstain pattern analysis and crime scene reconstruction in the future. Previous understanding of the influence of surface characteristics had been limited to general acknowledgment of their expected influence on stain drying time (*Laber. Epstein. 1983. Peschel et al. 2011*). Results presented in section 12.3.5 represent therefore the first empirical confirmation of the influence of surface characteristics on bloodstain drying time. They demonstrated that amongst experimental surfaces, drying times varied significantly for stains generated on denim, glass and paper surfaces. This has implications in forensic reality for incorporating estimations of drying times for stains on different surfaces into chronological crime scene reconstructions. For example, bloodstains may be simultaneously deposited on both denim and paper surfaces at a scene. During interpretation of stains, if one stain (paper) is observed to still be wet whilst the other stain (denim) appears dry an inference may be made that the stain on denim was deposited prior to the stain on paper. Results demonstrate however that differential drying rates might be an influence of surface type, rather than order of deposition. Without taking into account surface type, comparisons of estimated drying times for stains generated on different surfaces for the purposes of reconstructing a chronology of staining events are therefore likely to be erroneous.

Empirical confirmation of the relationship between surface type and drying time underlines the importance of incorporating considerations about surface characteristics into estimations of drying time. Doing so will subsequently increase the accuracy of estimations of drying time and temporal reconstructions of bloodletting events.

#### **12.3.5.1 AFM images of surfaces for comparison of surface roughness**

Atomic Force Microscope imaging was used to calculate a measure of surface roughness (roughness average: Ra) for each surface used in experimental stage 4 (denim, glass, paper). This was conducted to test for possible correlations between surface roughness and trends in stain drying time for different surfaces. *Figures 407, 408 & 409* outline AFM images and measures of surface roughness recorded for denim, glass and paper surfaces used in experimental stage 4. Results indicate that paper surfaces exhibited the highest surface roughness (338nm) whilst glass surfaces exhibited the lowest surface roughness (2.38nm). Drying time averages indicated that paper stains demonstrated the longest drying times, which supports a suggestion that surfaces with higher surface roughness exhibit longer stain drying times. Results of surface roughness for glass surfaces however contradict this rule. The roughness average measured for glass surfaces (2.38nm) was considerably lower than the roughness average for denim surfaces (158nm). If there was a relationship between surface roughness and drying time, denim stains should exhibit longer drying times than glass stains. Results in *figures 404 & 405* demonstrate that this was not so, as there does not appear to be any clear relationship, in results recorded during experimental stage 4, between surface roughness and drying time.

#### 12.3.5.1.a Denim – Roughness average (Ra): 158nm

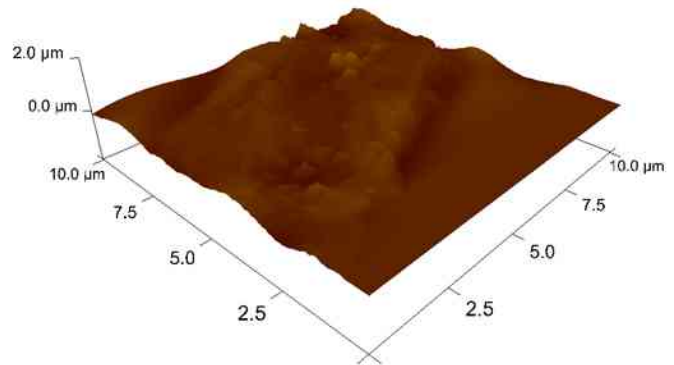
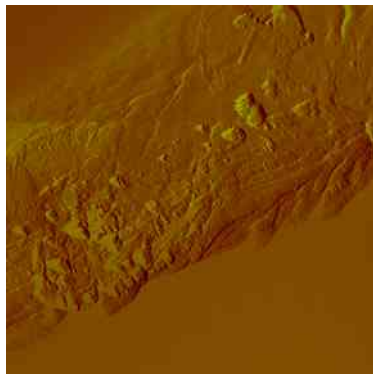


Figure 407 AFM images of denim surfaces generated during calculation of surface roughness average (Ra)

#### 12.3.5.1.b Glass – Roughness average (Ra): 2.38nm

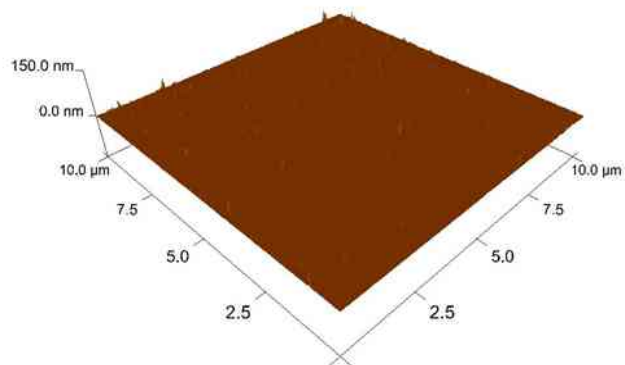


Figure 408 AFM images of glass surfaces generated during calculation of surface roughness average (Ra)

#### 12.3.5.1.c Paper – Roughness average (Ra): 338nm

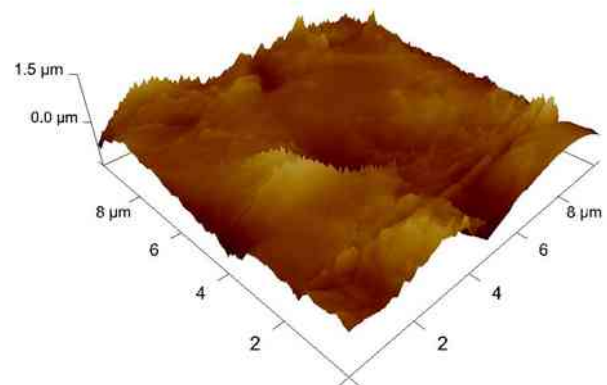
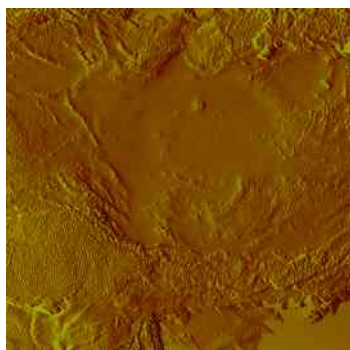


Figure 409 AFM images of paper surfaces generated during calculation of surface roughness average (Ra)

### 12.3.6 Temperature and humidity

Figure 410 outlines the relationship between temperature intervals and humidity levels recorded during experimental stage 4. A relationship appears to be demonstrated between temperature and humidity. Between  $-10^{\circ}\text{C}$  and  $20^{\circ}\text{C}$ , increases in temperature appeared to be associated with increases in humidity. Between  $20^{\circ}\text{C}$  and  $50^{\circ}\text{C}$  further increases in temperature appeared to be associated with more significant decreases in humidity. As it was not possible to control humidity during experimentation this relationship was an uncontrollable aspect of the experiment and interpretation of the separate relationships between temperature and drying time and humidity and drying time should consider the intrinsic relationship between temperature and humidity.

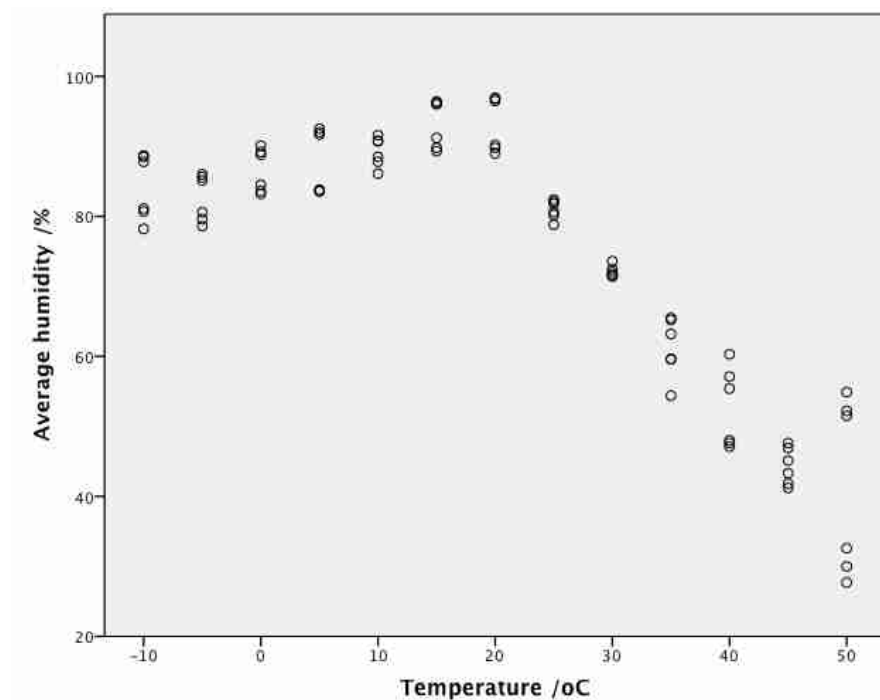


Figure 410 Relationship between temperature intervals and humidity recorded during experimental stage 4

Being able to conduct accurate estimations of stain drying time has considerable investigative use for reconstructing temporal aspects of bloodletting events. Estimations can assist with identification of approximate stain deposition times, which infer times associated with bloodletting events. They can also assist with developing chronologies for generation of individual stain patterns within a complex



crime scene. Increasing an understanding of influences on drying time improves the accuracy with which analysts can make drying time estimations. Observations from experimental stage 4 provided empirical confirmation of relationships between particular variables of influence and drying time, which can be used to inform and improve the accuracy of drying time estimations. Improving accuracy of drying time estimates will also increase the confidence that can be attached when extrapolating estimates to broader inferences about timings associated with events occurring at a crime scene. Implications of results for bloodstain pattern analysis and the subsequent process of crime scene reconstruction are discussed in *chapter 13*.

### **Section 3**

## **13. Discussion and Synthesis**

### **13.1 Answering experimental hypotheses**

Hypotheses were developed to examine certain empirically unsubstantiated observations relating to physically altered bloodstains. The context for exploring these hypotheses was to enhance the scope for analysis and interpretation of physically altered bloodstain patterns and increasing incorporation of these stains into crime scene reconstruction. Informed by literature review a series of hypotheses were developed within three thematic groups. These groups broadly corresponded to investigating the influence of temperature on identification of bloodstains (A), the influence of a wider range of environmental variables on identification of bloodstains (B) and influences on drying time. Presentation and analysis of results from all four experimental stages, set out in section 2, allows for answering and discussion of specific hypotheses within each of these groups.

#### **13.1.1 Group A**

Hypotheses in group A specifically focused on exploring the relationship between temperature and chemical and visual identification of bloodstains. The relevance of this relationship to crime scene reconstruction resonates at both source and activity level levels of evidence interpretation.

##### **13.1.1.1 Source level interpretations of Bloodstain Pattern evidence**

Source level interpretations of Bloodstain Pattern evidence involve the identification and confirmation of the presence of blood at a scene. This provides investigators with an indication of involvement of stained objects, individuals or locations with a bloodletting event.

Identification and confirmation of bloodstains at a scene is conducted via a two-step process of visual, then chemical identification. The implications of anything inhibiting or obscuring either visual or chemical identification are in the subsequent

risks of incomplete collection of evidence and misinterpretation or misidentification of blood evidence. Incomplete collection or misinterpretations of evidence are significant evidentiary issues as they may influence initial inferences of levels of “involvement” and mislead scrutiny of an investigation towards less directly involved parties. If considered within the more holistic context of the ‘forensic process’ the implications become even greater. Accurate identification of evidence serves as perhaps the most crucial investigative step, providing the point of entry for evidence into this process from which the investigative stages of evidence analysis, interpretation and ultimately presentation to court follow.

The investigative importance of source level interpretations of blood pattern evidence emphasizes the vital importance of increasing awareness and understanding of any mechanisms that may inhibit or obscure the visual and/or chemical identification of bloodstains.

#### **13.1.1.2 Temperature and source level interpretations of Bloodstain Pattern evidence**

A limited number of experimental studies have commented on the influence of temperature on visual identification of bloodstains. In particular, observations focused on the perceived effects of cold temperatures on stain appearance (*Brady et al. 2002. Leak. 2006. 2010. Morris. 2010*). Discolourations observed in stains occurred to such a degree that initial interpretations of evidence as bloodstain patterns were prevented. If upheld, observations have obvious repercussions for the visual identification of bloodstains. In addition, a number of experimental observations have been made regarding the influence of temperature on chemical identification. The possibility of variations in temperature weakening stain responses to chemical tests (*Lee. De Forest. 1976*) and stimulating denaturing of internal components which may limit positive responses to chemical tests (*Lovelock. 1953*) have been noted.

Hypotheses in group A were set out to test and develop observations regarding the influence of temperature on stain appearance and identification tests, from results generated in experimental stage 1. Results indicated that stains generated on denim,

paper and glass surfaces and dried at temperatures between -10°C and 50°C were all positively identified by Bluestar, Kastle-Meyer and Hemastix presumptive chemical tests. Exposing stains to temperatures within that range did not therefore appear to obscure chemical identification of bloodstains. Temperature did however influence stain appearance, causing visible alterations in colour. This means that for stains generated on paper, denim and glass at temperatures between -10°C and 50°C analysts can determine, from quantitative measures of colour the temperature at which stains were formed. At all temperatures the hypothesis that stains would exhibit higher R (red) values than G (green) or B (blue) values was supported. This meant that all stains retained a dominant hue of red. As temperature increased from -10°C to 50°C however R-values and RGB totals decreased, indicating that stains at higher temperatures were characterised by much darker intensities of overall colour. Significantly, a large decrease in R-values was observed between the particular temperature intervals of 25°C and 30°C. This trend was observed in stains on each surface, denim, paper and glass.

Source level implications of observations from stains generated in experimental stage 1 are that variations in temperature between -10°C and 50°C exert a significant influence on stain appearance. This may complicate or obscure visual identification of bloodstains generated within this range. Temperature should therefore be considered when conducting visual searches for bloodstains, particularly when the ambient temperature at a scene is in excess of 25°C, where stain appearance is altered most dramatically. Variations in temperature between -10°C and 50°C did not influence chemical identification of stains and do not need to be considered when conducting chemical searches for bloodstains, when the temperature is between -10°C and 50°C.

#### **13.1.1.3 Temperature and activity level interpretations of Bloodstain Pattern evidence**

Activity level interpretations of Bloodstain Pattern evidence provides investigators with an indication or inference of the mechanisms and circumstances by which blood evidence has been generated and deposited at a scene. The principles of evidence dynamics are applied to physical evidence to generate activity level interpretations.

Evidence dynamics refers to any activity or “influence that changes, relocates, obscures, or obliterates physical evidence, regardless of intent” (*Chisum. Turvey. 2000*) between point of deposition and interpretation. Temperature conditions at a crime scene should be included in discussions on evidence dynamics and activity level propositions because as demonstrated by the results of experimental stage 1, they exert an influence on stain colour that changes and may obscure bloodstain evidence. This may complicate the process of interpreting and analysing bloodstains and contextualising their presence at a crime scene.

Alteration of stain colour caused by temperature variations has two major activity level implications. It may lead to misidentification of bloodstains as other physical evidence or alternatively lead to complete lack of identification of stains. An illustration of the activity level implications of misidentification of stains is provided by a case example of stains observed in an extremely cold environment (*Morris. 2010*). Stains had undergone such discolouration that they were ‘initially misidentified as brain tissue by first responders’ (*Morris. 2010*) (*figure 411*).



Figure 411 Image of bloodstains observed in a cold environment that were initially misidentified as brain tissue on account of their pink puffy appearance (*Morris. 2010*)

By identifying bloodstains as another type of physical evidence they will be excluded, at least initially, from bloodstain pattern analysis conducted at a scene. The investigative implications of mistakenly excluding bloodstain evidence from pattern analysis are significant. Bloodstain patterns correspond to particular bloodletting mechanisms or indicate movement of involved parties at a scene. Excluding a valid pattern from an investigation therefore results in an incomplete analysis of a crime

scene and risks leading to partial analysis of events and circumstances surrounding the presence of blood. A secondary implication of mistakenly identifying bloodstain evidence as another physical evidence, for example brain tissue, is that incorrect inferences will have to be made to explain the presence of the alternative evidence. In the particular example given (*Morris. 2010*) misidentification of bloodstains as brain tissue, due to temperature-led discolouration, would have led investigators to infer that a severe head injury had occurred. This is a prime example of how incorrect activity level interpretations, led by misidentifications of bloodstains due to temperature-induced alterations in colour, can mislead and confuse an investigation.

Discolouration of stains, which results in a complete lack of identification of bloodstains as any type of evidence at all, also has implications for activity level interpretations of evidence. If recovery of blood evidence is incomplete, any evidence that is not identified cannot be incorporated into later evidential considerations. If for example bloodstains are generated by a particular mechanism and not recovered, investigators may not identify the involvement of that mechanism, if no other evidence of that mechanism occurring is collected from a scene. It is difficult to provide specific case-examples to demonstrate the scope of these implications, as the investigative repercussions are a complete lack of identification of any bloodstains at a scene, as blood or any other evidence. It is inherently difficult to estimate the number of instances when evidence has been 'missed' and evidence retrieval has been incomplete. Being able to determine the temperature stains were formed at, from quantitative measures of colour, allows analysts to reconstruct the time at which stains were generated, as long as temperature records for the period concerned are known. This demonstrates another activity level interpretation that is possible with knowledge of the influence of temperature on stain colour.

The results of experimental stage 1 demonstrate the influence variations in temperature between a relatively limited range (-10°C to 50°C) had on bloodstain evidence. Extrapolating experimental findings to a case-scenario, temperature will therefore have an affect on source and activity level interpretations of bloodstain pattern evidence and temperature should therefore be an important consideration when conducting investigation and identification of stains at a scene.

### **13.1.2 Group B**

Hypotheses in group B specifically focused on exploring the relationship between exposure to a range of environmental conditions and chemical and visual identification of bloodstains from the results of experimental stages 1, 2 and 3. The relevance of these relationships impacts on both source and activity level interpretations of Bloodstain Pattern evidence, used in crime scene reconstruction.

#### **13.1.2.1 Exposure to environmental conditions and source level interpretations of Bloodstain Pattern evidence**

Section 13.1.1.1 emphasized the investigative importance of source level interpretations of blood pattern evidence and increasing awareness and understanding of any mechanisms that may inhibit or obscure the visual and/or chemical identification of bloodstains. Having established the effects of temperature on chemical and visual identification of bloodstains, hypotheses in group B focused on exploring the relationship between a wider range of environmental conditions and chemical and visual identification of bloodstains.

A number of experimental studies have commented on the effects of exposing bloodstains to a range of environmental conditions on chemical identification of stains. Observations focused on the persistence of chemical identification tests in identifying stains, which have been exposed to extreme environmental conditions. Results of studies indicated that presumptive positive identifications of stains were not inhibited by exposures to long periods of environmental fluctuations (*Lee. De Forest. 1976. Gurfinkel. Franklin. 1987. Waldoch. 1996. Adair et al. 2008*), ‘washing’ or soaking in water (*Jain. Singh. 1984*), fire and burning (*Paonessa. 2005. Tontarski et al. 2009*) or extreme heat (*Lee. De Forest. 1976. Tontarski et al. 2009. Quickenden et al. 2004*). These observations were upheld by results of experimental stages 2 and 3, in which stains were exposed to a range of similar environmental conditions. Conditions included longitudinal exposures to naturally variable environmental fluctuations, freeze-thaw mechanisms, snow and freezing conditions, high temperatures and fire. The implications for crime scene investigators is that



these environmental conditions do not need to be considered an obstacle to presumptive positive chemical identification of bloodstains at scenes where environmental conditions are variable and possibly extreme in nature.

A limited number of experimental studies have commented on the influence of exposing bloodstains to a range of environmental conditions on visual identification of bloodstains. Observations of the effects of longitudinal exposure to natural occurring environmental fluctuations (*Cox. 1990. Anderson et al. 2005. Leak. 2010*) indicated that exposure might cause discolouration of stains and removal or obscuring of stains due to the effects of prolonged exposure to precipitation. If upheld, observations have repercussions for the visual identification of bloodstains exposed to such conditions. Observations of the effects of freezing temperatures on stain appearance (*Eckert. James. 1993. Brady et al. 2002. Morris. 2010*) indicated that discolourations in stains occurred to such an extent that initial identifications of bloodstains were prevented. Again, if upheld, observations have repercussions for the visual identification of bloodstains. Observations of the effects of burning on stain appearance (*Eckert. James. 1993. Paonessa. 2005*) indicated that burning can cause significant discolouration of stains, which if upheld by observations from experimental stage 3 would have repercussions for visual identifications of stains exposed to such conditions. The effects of freeze-thaw mechanisms and extreme heat on stain appearance have not previously been studied but were also included in experimental stage 3 as it was thought they might also affect stain appearance.

Hypotheses in group B were set out to test and develop observations regarding the influence of these environmental conditions on stain appearance, from results generated in experimental stages 2 and 3. Results indicated that stains generated on denim, paper and glass surfaces and exposed to naturally variable environmental conditions for different longitudinal periods exhibited significant differences in colour to stains generated in laboratory-controlled conditions. Although stains did not differ significantly according to average RGB totals, stains exposed to natural climate variations were characterised by much lower R-values and higher G and B values than laboratory generated stains. This meant that stains generated in experimental stage 2 were much closer to grey and brown colours than the red colours demonstrated by stains generated in laboratory conditions. This has source

level implications for the identification of stains exposed to the environment for any length of time.

Results indicated that the appearance of stains generated on denim, paper and glass surfaces and exposed to extreme environmental conditions (freeze-thaw, freezing, snow, high temperatures and fire) varied according to environmental conditions. Stains exposed to cold extremes (freezing and snow) exhibited very high R (red) values and very high ratios (60-90%) of R (red) to G (green) and B (blue) values. The ratios observed for R to G and B values, for stains exposed to freezing conditions, were the highest ratios recorded amongst stains exposed to the range of environmental conditions outlined in experimental stage 1 (temperatures between -10°C and 50°C), experimental stage 2 (longitudinal exposure to environmental fluctuations) and experimental stage 3 (freeze-thaw, high temperatures and fire). This supported the hypotheses that stains exposed to snow and freezing conditions would exhibit significant differences in colour to stains generated in laboratory-controlled or exposed for prolonged periods to natural climatic fluctuations. Confirmation of strong orientations in stain colour in freezing conditions towards the brightest, most vivid hues of red observed across stains exposed to a range of environmental conditions supports prior observations of the effects of freezing temperatures on stain appearance (*Eckert. James. 1993. Brady et al. 2002. Morris. 2010*). Source level implications of observations are that exposure to freezing conditions exerts a significant influence on stain appearance. This may complicate or obscure visual identification of bloodstains generated in these circumstances. Temperature should therefore be considered when conducting visual searches for bloodstains, particularly in outdoor scenes where surfaces may be frozen, as stain appearance may be altered dramatically. For stains generated on snow, changes in colour were recorded over time and stains became pinker, appearing to dissipate through the snow. This confirmed previous observations of pink colouring in stains on snow (*Leak. 2006. Morris. 2010*) and has source level implications by potentially obscuring identification of stains on snow.

Stains exposed to hot extremes (high temperatures and burning) exhibited low R (red) values and very low ratios of R (red) to G (green) and B (blue) values. The ratios observed for R to G and B values, for stains exposed to hot environmental

conditions, were the lowest ratios (average R %: 49%) recorded amongst stains exposed to the range of environmental conditions outlined in experimental stage 1 (temperatures between -10°C and 50°C), experimental stage 2 (longitudinal exposure to environmental fluctuations) and experimental stage 3 (freeze-thaw, high temperatures and fire). This supported the hypotheses that stains exposed to high temperatures and burning conditions would exhibit significant differences in colour to stains generated in laboratory-controlled or exposed for prolonged periods to natural climatic fluctuations. Confirmation of strong orientations in stain colour in extreme conditions of heat towards the darkest hues of red, brown and black observed across stains exposed to a range of environmental conditions supports prior observations of the effects of hot temperatures on stain appearance (*Eckert. James. 1993. Paonessa. 2005*). Source level implications of observations are that exposure to hot temperatures and fire exerts a significant influence on stain appearance. This may complicate or obscure visual identification of bloodstains generated in these circumstances. Temperature should therefore be considered when conducting visual searches for bloodstains, particularly at scenes where temperatures have been high or where there is evidence of accidental or intentional burning, as stain appearance may be altered dramatically. Results across experimental stages 1-3 indicated that whilst stains generated on all surfaces exhibited higher R values than G or B values, within each environmental condition the intensity of red colouring varied between paper, denim and glass. This has source level implications for identification of stains across a range of surfaces.

#### **13.1.2.2 Exposure to environmental conditions and activity level interpretations of Bloodstain Pattern evidence**

Section 13.1.1.3 emphasized the investigative importance of activity level interpretations of blood pattern evidence and increasing awareness and understanding of any mechanisms that may inhibit or obscure the visual and/or chemical identification of bloodstains. Environmental conditions at a crime scene should be included in discussions on evidence dynamics and activity level propositions because as demonstrated by the results of experimental stages 2 and 3, they exert an influence on stain colour that changes and may obscure bloodstain

evidence. This may complicate the process of interpreting and analysing bloodstains and contextualising their presence at a crime scene.

Alteration of stain colour caused by different environmental conditions has activity level implications. It may lead to misidentification of bloodstains as other physical evidence or alternatively lead to complete lack of identification of stains, if for example stains are removed. An illustration of the activity level implications of misidentification of stains is provided by a case example of stains observed in an extremely cold environment (*Morris. 2010*) described in 13.1.1.3. By misidentifying bloodstains they may be excluded, at least initially, from bloodstain pattern analysis conducted at a scene. Excluding a pattern or set of stains from an investigation results in an incomplete analysis of a crime scene and risks leading to partial analysis of events and circumstances surrounding the presence of blood. A lack of identification of bloodstains as any type of evidence at all, also has implications for activity level interpretations of evidence. If recovery of evidence is incomplete, any evidence that is not identified cannot be incorporated into later evidential considerations.

In experimental stage 2 several findings have particular relevance for activity level interpretations of bloodstain evidence. Results confirmed the hypothesised ability to quantitatively distinguish stains that have been exposed to natural environmental fluctuations for a minimum of a month from stains that have been freshly generated, on the basis of colour. This has particular importance for activity level interpretations. It allows analysts to determine whether stains are fresh or not, which can be used to infer and reconstruct temporal aspects surrounding a bloodletting event. There were no significant differences recorded between stains exposed to different periods of climatic conditions, or between stains exposed for different lengths of time. This means for stains generated on denim, paper and glass it is not possible to determine quantitatively, on the basis of colour, how old stains are. Certain results of experimental stage 3 also have implications for activity level interpretations of evidence. For stains exposed to freezing conditions the colour of stains generated on room temperature surfaces and then exposed to freezing conditions was significantly different to the colour of stains generated on frozen

surfaces. An example of how this could influence activity level interpretations can be illustrated by a hypothetical scenario of interpretation of stains at a scene located outdoors to infer time of deposition. In this hypothetical scenario, add the consideration that the ambient temperature only dips below freezing overnight. Through an analysis of the colour of stains identified at the scene it would be possible to infer whether stains were deposited whilst stained surfaces were above (daytime) or below (night-time) freezing. Observations of the distinctive nature of stains exposed to burning conditions also can assist with activity level interpretations. Identification of stains exposed to burning can be used to infer, in instances where fire is not expected to have occurred naturally, post bloodletting actions of a suspect attempting to remove evidence from a scene.

The results of experimental stages 2 and 3 demonstrate the influence a variety of environmental conditions had on bloodstain evidence. Extrapolating experimental findings to a case-scenario, environmental conditions can be observed to have an affect on both source and activity level interpretations of bloodstain pattern evidence and should therefore be an important consideration when conducting investigation and identification of stains at a scene.

### **13.1.3 Group C**

Hypotheses in group C focused on determining the relationships between temperature, humidity, drop volume, surface characteristics and bloodstain drying time. The relevance of these relationships to crime scene reconstruction is demonstrated during activity level interpretations of evidence.

#### **13.1.3.1 Influences on activity level interpretations of drying time**

Activity level interpretations of bloodstain drying time provide investigators with an indication of the circumstances and specifically chronology associated with bloodletting events. This assists with temporal aspects of crime scene reconstruction, which include making inferences about the order in which different stain patterns were generated and establishing an estimated time of blood deposition. A

hypothetical scenario demonstrates the investigative advantage of being able to determine a chronological order for different stain patterns. In a case where a suspect claims he attacked a victim in self-defence and bloodstains from both the victim and suspect are identified at an associated scene, determining that blood shed by the suspect was deposited some significant time after blood deposited by the victim may cast reasonable doubt on this defence. Activity level implications of being able to accurately estimate stain drying time is that an estimation can then be made, for stains which are still wet, as to the upper possible limit of time of blood deposition. This allows investigators to identify windows of time when bloodletting events are most likely to have occurred. Knowledge of these windows can then be used to corroborate or refute suspect and alibi witness testimonies centred on particular timings associated with a crime event. If stain-drying time is inherently variable due to an interaction of a range of influences, in order to still accurately incorporate drying time estimates into activity level interpretations of deposition times, the nature of these influences needs to be empirically established.

A limited number of experimental studies have explored a range of influences, including temperature, humidity, stain volume and surface characteristics on bloodstain drying time. Studies have particularly focused on the influence of temperature on drying time (*Brady et al. 2002. Peschel et al. 2011. Gardner. Griffin. 2010. Laber. Epstein. 1983. Ramsthaler et al. 2012*). Only two of these studies (*Brady et al. 2002. Ramsthaler et al. 2012*) attempted to empirically examine variations in drying time with both observing that as temperature increased, drying time decreased and that the relationship was consistent across a range of stained surfaces. Both studies were limited however in their comparisons of drying time at three random temperatures and did not attempt to examine drying times variations across consistently incremental increases in temperature. Others studies have posited the influence of temperature on drying time more generally (*Peschel et al. 2011. Laber. Epstein. 1983. Gardner. Griffin. 2010*). If upheld, these observations have repercussions for the use of estimated stain drying times in activity level interpretations of evidence. Observations about the influence of other variables such as humidity, stain volume and surface characteristics on stain drying time have also been reported. An understanding of the nature of influence of each on stain drying time has implications for the integration of stain drying time into activity level

interpretations. In large, these observations were limited to general observations of influence (*Peschel et al. 2011. Laber. Epstein. 1983*) and did not empirically establish the significance or direction of influence of each on drying time, with the exception of observations regarding stain volume where it was noted that ‘larger [volume] stains dried faster than smaller stains’ (*Gardner. Griffin. 2010: 258*).

#### **13.1.3.2 Temperature and activity level interpretations of drying time**

Hypotheses in group C were set out to test and develop these observations, from results generated in experimental stage 4. Results indicated that for stains generated and dried on denim, paper and glass surfaces at temperature intervals between -10°C and 50°C, there was a statistically significant negative correlation between increases in temperature and decreases in drying time. Confirmation of variations in stain drying time caused by variations in temperature has a major activity level implication. If stain-drying times were universal, observation of a wet stain at a scene would indicate that the stain was deposited within the limits of the known drying time, regardless of the ambient temperature. Results from experimental stage 4 confirmed however that at each temperature interval this drying time limit varies. Analysis of a stain to estimate drying time and possible time of deposition should therefore only be carried out if the ambient temperature is also considered.

The negative correlation observed between temperature and drying time supports a suggestion that if wet stains are observed at a hot temperature, time between deposition and identification is short, e.g. 15 minutes. Conversely, if wet stains are observed at a cold temperature, time between deposition and identification is longer, e.g. 500 minutes. At temperatures between -10°C and 50°C average and upper drying time limits were calculated for each temperature interval and a range of surfaces at each temperature. Even relatively small variations in temperature at a scene significantly influenced drying times. This is the first instance of drying times being empirically established across this temperature range. Calculation of these limits has implications for activity level interpretations, whereby as long as ambient temperature is known, investigators can now make discrete predictions of stain drying time for stains generated on denim, paper and glass surfaces. For example, if ambient temperature at a scene is measured as -10°C, consultation of results from

experimental stage 4 indicate that at  $-10^{\circ}\text{C}$  a  $10\mu\text{l}$  stain on denim takes on average 500 minutes to dry. Discovery of wet stains on denim at the scene therefore indicates that stains were deposited no longer than 500 minutes prior to discovery. Discovery of dry stains on denim at the scene indicates that stains were deposited longer than 500 minutes prior to discovery. Results confirm it is possible to conduct these activity level interpretations at all temperatures between  $-10^{\circ}\text{C}$  and  $50^{\circ}\text{C}$ , for stains generated on paper, denim and glass surfaces. This is the first time the possibility of doing so has been empirically established. Overall, results indicate that calculations of stain drying times can and should be adjusted according to ambient temperature at a scene to achieve accurate quantitative estimations of temperature-specific upper drying time limits, which can be used to infer activity level interpretations of time of stain deposition.

Further observations of the influence of temperature on drying time demonstrated that within the temperature range  $-10^{\circ}\text{C}$  to  $50^{\circ}\text{C}$ , significant changes in drying time were associated with particular temperature intervals. Drying times between  $-10^{\circ}\text{C}$  and  $25^{\circ}\text{C}$  exhibited greater variability than drying times between  $30^{\circ}\text{C}$  and  $50^{\circ}\text{C}$ . Calculations of drying time at temperatures below  $25^{\circ}\text{C}$  for the purposes should therefore be interpreted as slightly more indicative than exacting calculations of drying time, compared to calculations of drying time at temperatures above  $30^{\circ}\text{C}$ .

#### **13.1.3.3 Humidity and activity level interpretations of drying time**

Observations from experimental stage 4 appeared to support suggestions that humidity is a general influence on drying time (*Peschel et al. 2011. Gardner. Griffin. 2010. Laber. Epstein. 1983*). As humidity increased drying time appeared to increase, however the influence of humidity on drying time did not appear as strong as the influence of temperature on drying time. Drying times were more variable at specific humidity levels than they were at specific temperature intervals. It was also noted that humidity and temperature variables were closely related. To a certain extent it was therefore difficult to determine the order of influence humidity exerts on stain drying time compared to the influence of temperature. Overall comparison of the strength of relationships between temperature and drying time and humidity and drying time however supports a suggestion that whilst humidity should be



considered during activity level interpretations of drying time it does not appear as dominant an influence on drying time as temperature.

#### **13.1.3.4 Surface characteristics and activity level interpretations of drying time**

Observations from experimental stage 4 support previously unproven suggestions (*Peschel et al. 2011. Gardner. Griffin. 2010. Laber. Epstein. 1983*) that drying times vary significantly according to surface type stained. When all other variables are consistent, stains deposited on paper surfaces exhibited the longest drying times, then stains on glass surfaces and finally stains deposited on denim surfaces that exhibited the shortest drying times. Use of a stain to estimate possible time of deposition must therefore take account of the types of surface stained at a scene. In the context of attempting to analyse multiple stains at a scene to infer a chronology of bloodletting events, this is a particularly pertinent result. When equal volumes of blood are simultaneously deposited on different surfaces at the same temperature, after some time whilst stains on one surface may be dry, on another surface they may remain wet. Without knowledge of the significant influence of surface characteristics on drying time, a temptation is presented to infer that the stain that is still wet was deposited after the stain that was dry. Results of experimental stage 4 indicate that this would be an incorrect inference to make without considering the influence of surface characteristics on drying time. When attempting to reconstruct the chronology of bloodletting mechanisms at a scene, investigators must incorporate an awareness of differential rates of drying between surfaces into their reconstructions. There was no indication of a relationship between surface roughness and drying times between paper, denim and glass surfaces. Further experimental work must be conducted to identify the characteristics of a surface, which significantly influence differential stain drying times.

#### **13.1.3.5 Stain volume and activity level interpretations of drying time**

Observations from experimental stage 4 support previous observations of a positive correlation between stain volume and drying time (*Gardner. Griffin. 2010*). However, as it is not possible to establish volume of stains at a scene, the scope for incorporating observations of stain volume into activity level interpretations of drying time is extremely limited.

Results from experimental 4 and answering of hypotheses in group C demonstrate that when stains are analysed for the purposes of estimating drying time and subsequently providing temporal activity level reconstructions, the influence of several variables must be incorporated into calculations. These variables include ambient temperature, humidity, surface characteristics and stain volume.

Results indicate that measurements of ambient temperature provide the strongest individual prediction variable for stain drying time. A quantitative method of predicting drying time from ambient temperatures between -10°C and 50°C was produced and can be used in the future analysis of stains generated on paper, glass or denim surfaces to inform activity level interpretations of blood evidence. It is not sufficient however to base a reconstruction of stain deposition time at a scene purely on the basis of ambient temperature and each contributing variable must still be considered and incorporated into any predictions of drying time.

### **13.2 Implications of results for Bloodstain Pattern Analysis (BPA)**

Experimental results and answering of hypotheses demonstrate that it is possible to identify a series of objective criteria for the identification, analysis and interpretation of physically altered bloodstains (PABs). The development of such criteria is based on the discovery that blood, once exposed to environmental conditions, reacts to the influences it encounters in a predictable and quantifiable manner. These reactions were measured through alterations to stain appearance and behaviour, two characteristics instrumental to the identification and interpretation of stains (*Wonder. 2001*). This had not been established previously for bloodstains and the implication of results therefore is that they significantly enhance the possibility of including considerations of environmental influence in source and activity level interpretations of bloodstain evidence and subsequent crime scene reconstructions. The aim of crime scene reconstruction is to create an accurate and objective account of the presence and circumstances surrounding the generation of evidence (*Chisum. Turvey. 2000. Fratini et al. 2006*). The development and extension of objective criteria to new

aspects of bloodstain pattern analysis increases the scope for conducting accurate and objective crime scene reconstructions from bloodstain evidence.

The implications of results for BPA resonate particularly in two specific aspects of bloodstain pattern analysis, in source and activity level interpretations of stains based on appearance and in activity level interpretations of stains based on behaviour.

### **13.2.1 Implications of results for analysis of stain appearance**

Visual identification of bloodstains is often the initial step in confirming the presence of bloodstains at a scene (*Wonder. 2001*), which all other stages of analysis and interpretation follow. Results impact on visual identifications (source level analysis) of stains by demonstrating the variety of stain colours that may be encountered across environmental conditions. This should be considered by analysts conducting visual searches for bloodstain evidence at any scene but particularly at scenes where environmental conditions are extreme or there is evidence that they may have been extreme at some stage. Examples of these stains being encountered in the past (*Brady et al. 2002. Morris. 2010*) indicated that a lack of empirical knowledge and subsequent failure in recognising environment-led variability of stain appearance led to misidentification of bloodstains. As outlined in 13.1.1.1 misidentification or lack of identification of stains has significant repercussions for both source and subsequently activity level interpretations of evidence and therefore the entire process of crime scene reconstruction. Developing methods of enhancing the identification of stains is demonstrably vitally important. It is impossible to estimate how many other similar alterations to stain appearance may have led to incomplete or inaccurate source level interpretations of bloodstains in the past but results set out here can be used to minimise the risks of inaccurate interpretations in the future.

Results comprise the first quantitative method of analysing stains generated at different temperatures according to colour and R, G and B values. In a recent experimental study (*Thanakiatkrai et al. 2013*) an attempt was made to similarly quantify colours of ageing stains for development as a smartphone application as a tool for estimating the age and therefore time of deposition of a stain. The implications of the discovery of a significant relationship between temperature and

quantitative measures of stain colour, in research presented here, are that these results too could be incorporated in the future into a smartphone application (*figure 412*). This application would have to incorporate methods of digitally capturing and analysing bloodstains in order to derive numerical values of their ‘colour’ with a calibration tool for taking into account the background colour of a stained surface.



Figure 412 Mock-up of possible smartphone application designed for rapid quantitative colour analysis of bloodstains  
(*Author. 2013*)

Development of such an application would offer a quantitatively robust, relatively cheap, easy-to-use and portable tool for identifying physically altered bloodstains. This would facilitate at least two possible extrapolations of results to future source (1) and activity (2) level interpretations of stains based on appearance. First, when encountering a suspected bloodstain that exhibits significant discolouration to obscure initial identification as a bloodstain, inputting ambient temperature and environmental factors recorded at a scene alongside quantitative measures of colour would allow the colour of the suspected stain to be quantitatively compared to expected colour values for the input conditions. This has implications for future source level analyses by providing analysts with a quick tool for verifying whether a suspect stain is likely to be blood or not, given associated environmental conditions. Secondly, inputting an image of a stain and quantitative measures of the colour of that stain would allow a calculated identification of the temperature stains of that colour are expected at. This has implications for activity level analyses by providing analysts with an indication of the environmental circumstances the stain was deposited in. If those environmental circumstances do not approximate the conditions at time of identification, analysts may be able to identify time of deposition with knowledge of environmental conditions and fluctuations in these conditions over time prior to stain identification. This could contribute significantly

to temporal reconstructions of bloodletting events. A further implication of results to activity level interpretations of physically altered bloodstains is provided by the finding that stains exposed to extreme conditions, such as fire, freezing and longitudinal periods of exposure, can be quantitatively distinguished from stains exposed to more benign environmental conditions. As extreme conditions, in many cases where these conditions are observed they are unlikely to have occurred naturally and may therefore result from a suspect purposefully attempting to remove or obscure evidence (*Pye. 2004*). By enhancing quantitative information available to analysts to allow them to determine whether stains have been exposed to extreme or natural environmental conditions, results have implications for inferring post-event suspect activity.

### **13.2.2 Implications of results for analysis of stain behaviour**

Analysis of stain behaviour, in particular drying time, can assist investigators in establishing and reconstructing temporal circumstances surrounding stain generation (*Ramsthaler et al. 2012. Nakao et al. 2013*). Experimental work conducted in research established quantitative measures of drying time for stains generated on three surfaces (glass, paper and denim) at temperatures between -10°C and 50°C. Although several studies had previously empirically established drying times at a number of temperatures (*Brady et al. 2002. Ramsthaler et al. 2012*) these studies were somewhat limited by number and range of temperatures they examined drying time at. Results generated in experimental stage 4 therefore represent the most thorough examination of drying time and environmental influences on drying time conducted to date. The implication of establishing these results for the process of BPA is that they can now significantly enhance the reconstruction of temporal aspects of a bloodletting event, from stain analysis. By establishing drying times at particular temperatures and for the range of surfaces tested, results allow analysts, with knowledge of ambient temperature at a scene to make activity level interpretations upon discovery of either wet or dry stains at a scene. A basic illustration follows that discovery of a wet stain indicates the stain was deposited within a window of time lower than the known drying time for the specific surface and ambient temperature. Discovery of a dry stain indicates the stain was deposited within a window of time higher than the known drying time for the specific surface

and ambient temperature. The implications of empirically establishing the relationships between temperature, surface type and quantitative measures of drying time are that these results could be incorporated in the future into a predictive tool for estimations of stain deposition time or age, which would significantly increase the accuracy with which analysts make these estimations.

With relevance for both source and activity interpretations, investigative implications of results will be demonstrated across all stages of the 'forensic process', from crime scene to court room. Source level interpretations will impact directly on stages of evidential preservation, collection, validation and identification and indirectly (by dictating levels of evidence recovery) on the limits of subsequent activity level interpretations in stages of evidential analysis, interpretation and presentation.

### **13.3 Limitations of results**

Despite the likelihood of encountering physically altered bloodstains at a crime scene, they have historically not formed the focus for empirical development within the discipline of BPA. Results generated by experimental research demonstrate however that there is significant potential for further incorporating quantitative analysis and interpretation of PABs into BPA and crime scene reconstruction. Despite the obvious implications of results for the potential expansion and enhancement of certain aspects of BPA, it should be acknowledged however that there were significant limitations inherent to the experimental design that may prevent the immediate extrapolation of findings to real-life analyses.

One of the major limitations of observations regarding the influence of environmental conditions on stain appearance is that experimental surfaces were somewhat 'ideal' in their unstained states. Paper and denim surfaces were white in colour whilst glass slides were transparent, mounted on white card. The use of white backgrounds facilitated the quantitative analysis of subtle variations in stain colours between environmental conditions. In real forensic scenarios it more likely that stains will be encountered on a range of coloured surfaces than on white or clear surfaces,

which undoubtedly should be considered in any subsequent interpretations of stain colour. In order to validate relationships observed for ‘ideal’ surfaces between stain appearance and environmental conditions, further experimental work must be conducted on the effects of environmental conditions on the appearance of stains on coloured surfaces. It has been suggested it may be possible to overcome the interference of underlying surface colour with measurements of the colour of stains generated on them by extracting bloodstains from the surface to performing remote colour analysis (*Thanakiatkrai et al. 2013*). Whilst this may offer a solution in the future to overcome the problem of currently being limited to extrapolating results to white and clear surfaces, further experimental work is undoubtedly required before the colour of stains generated on coloured surfaces can be interpreted in the same manner.

Although three distinct experimental stages were designed to provide exposure of stains to as broad and varied a range of environmental variables as possible, mimicking a number of scenarios that stains might be encountered in, and including the sheer complexity of potential combinations of variables presenting themselves in forensic reality, placed a certain restriction on experimental design. Within any individual scene there may also be scene-specific variations to consider, for example the presence of a radiator or air-conditioning unit within a room may generate a microclimatic effect, exerting a particular influence on bloodstains in the room according to their proximity to them. Within the scope of the experimental work presented in this study it was not possible to examine the complete range of potential environmental scene variables or examine the interactions of microclimatic features with bloodstains across a scene. Future extrapolation of observations and results presented in this study must simultaneously take account of specific variables presenting themselves in association with individual scenes.

Several limitations presented themselves during the imaging and measurement of stain colour. These limitations concerned a lack of uniformity and unexpected physical alterations observed in stains exposed to certain environmental conditions, and how these influenced the accuracy of measuring average values of stain colour. The experimental method outlined for capturing average colour values for stains was limited in the extent to which it could incorporate these effects.

Stains generated on glass in experimental stage 2 (both longitudinal and monthly samples) showed evidence of physically cracking, during exposure to environmental conditions, resulting in a ‘crazed’ appearance (*figures 170 & 246*). The extent of cracking varied between sets of glass stains but was not observed in stains generated on paper and denim or in stains generated on glass and exposed to other environmental conditions. Where blood stains exhibited this effect, the formerly continuous body became fractured, exposing cracks through which the white background emerged. According to the chosen experimental stain imaging method, these areas or white colour were included in the fixed area sampled for stain colour averages, artificially lowering the colour average of glass stains generated in stage 2. Within the limitations of the experimental work conducted it was not possible to adjust the imaging method to exclude white areas from affected stains. Whilst therefore the effect and its potential effect on colour averages for these stains was acknowledged, development of a method of imaging crazed stains to obtain the most accurate quantitative measures of colour should be reserved for future studies.

Other stains demonstrated a lack of uniformity that may have limited the accuracy of calculating stain colour values. Certain stains generated in experimental stage 1, on glass slides, exhibited evidence of blood spilling between slides onto the background card slides were mounted on (*figures 61, 67, 73, 79, 91, 94 & 97*). The effect of this spilling meant that in some stains there was a risk that dried blood on the background would increase colour averages measured for these stains, as background colour effectively contributed to producing a measurement of the colour of two overlapping stains. The risk of this lack of uniformity affecting colour measurements was minimised by generating six replicate stains in each sample set and utilising an average colour value (from replicates) in subsequent analysis and interpretation. The maximum number of stains affected by this overlapping effect, in any one sample set, was two stains. It was felt that this was a relatively small number that would not substantially influence average colour values calculated from a minimum of 6 stains.

Further experimental limitations related to observations of stain drying time and should be included when considering the extrapolation of results to real forensic scenarios. Drying time measurements were limited by two factors, the inclusion of a



preservative in experimental blood sourced and measurement of stain drying times across only three surfaces (paper, denim and glass). Although not empirically established prior to experimentation, it was expected that the addition of a preservative to blood would lengthen stain-drying time to some extent. Due to experimental limitations it was not possible to perform a comparative experimental run with fresh blood to establish any difference, in drying times, caused by addition of a preservative. Further comparative experimental runs will be necessary therefore before drying time measurements for each surface and temperature can be verified for extrapolation to real forensic scenarios. The limitations of restricting observations of drying time to three surfaces can be overcome by replication of the experimental methods to a wider range of surfaces and on a case-specific basis (*Peschel et al. 2011*). For example, if estimating stain drying times in a hypothetical case involving stains generated on a wooden table, broad information on drying times for wooden surfaces as well as drying times for the specific wood, polish, varnish etc involved in the case in question could be used in combination to estimate drying time and time of deposition. The broader estimates of stain drying times on wood could be used to infer an estimated drying time until a case-specific examination could be conducted to more narrowly estimate drying times in the case-specific scenario.

### **13.4 The “path forward” for BPA research**

The importance of conducting experimental studies in bloodstain pattern analysis, in order to identify objective methods and criteria for furthering the discipline’s development has been reiterated in the aftermath of the 2009 NAS report. Criticism levelled at the discipline in the report focused on querying the scientific foundations of the discipline (*Mnookin et al. 2011*) and the purported emphasis on ‘*experience over scientific foundation*’ (*NAS. 2009: 178*). Whilst it has since been acknowledged that certain aspects of this criticism appear contradictory and inaccurate, in response the discipline must nonetheless endeavour to demonstrate and reinforce the robust, replicable scientific principles which guide practitioners in aspects of bloodstain pattern analysis. The discipline should seize the opportunity to answer these criticisms now, to prevent repetitions of them in the future.

Results presented in experimental research conducted here on physically altered bloodstains demonstrate the possibility of establishing new objective criteria for stain analysis in a commonly encountered but problematic area of BPA. Results, once subjected to peer-review and close scrutiny by the more general ‘scientific community’ will form the foundations for further, more complex and case-specific work in this field. This is the direction the development of the discipline needs to continue in, empirically examining the underlying scientific principles in question first before layering analysis and development of techniques, through experimental work, to add the case-specific relevance required by individual scenarios. At both levels of development, criteria must be subjected to peer-review, in both academic and practitioner-based environments. Ensuring practising analysts are proficient and universally accept with these criteria is essential to success of their future application across the discipline.

Areas of the discipline for which objective criteria are currently lacking, or are in the process of development, should be identified and acknowledged as areas about which source & activity level propositions and crime scene reconstructions should be very cautiously, if at all, made.

## 14. Conclusions

### 14.1 Summary of research

The focus of research was to examine the potential to collect quantitative observations about bloodstains that have been physically altered through interactions with a range of environmental variables and conditions. These stains are identified as Physically Altered Bloodstains (PABs) (Gardner. Griffin. 2010). In the context of analysis of outdoor crime scenes and scenes that may have been intentionally interfered with, the likelihood of encountering stains which exhibit physical alterations is high (Pye. 2004. Bevel. Gardner. 2008).

The potential for environmentally forced interactions to alter the appearance and behaviour of bloodstains has implications for increasing the complexity of their identification and analysis. These implications are largely based on the principles of evidence dynamics and an appreciation that “*any influence that changes, relocates, obscures, or obliterates physical evidence, regardless of intent*” has a consequence for subsequent interpretation and analysis of that evidence (Chisum. Turvey. 2000). Alterations may, for example, obscure, prevent or mislead identification of stains, which limits further analysis of them as physical evidence associated with a bloodletting event. Improving the ability of analysts to identify and interpret physically altered evidence has important consequences therefore for increasing overall accuracy of evidence analysis. Amongst practitioners this has been recognised with calls for a much more concerted and focused effort to “*validate inclusion of [PABs] in source/activity level analysis*” (Gardner. Griffin. 2010). Despite the likelihood of encountering PABs in forensic reality and observations about the potential for alterations to obstruct or mislead analysis of bloodstains, attempts to develop empirical understandings of PABs have remained, historically, limited. Research presented in this thesis represents the first empirical attempt to substantially develop an understanding of the nature of PABs, their interactions with environmental variables and perhaps most importantly, the potential for extrapolating quantitative observations about PABs to future source and activity level interpretations of bloodstain pattern evidence.

Through a series of experimental stages, stains were exposed to a range of environmental conditions, of varying complexity, designed to reflect different forensic scenarios. Once stains had been exposed to environmental conditions, a series of quantitative observations regarding stain appearance and behaviour were made. Observations indicated that bloodstains respond in a predictable manner to environmental conditions they are exposed to. This has implications for Bloodstain Pattern Analysis (BPA) as it confirms the possibility and potential for developing quantitative methods for the identification, interpretation and analysis of PABs.

## **14.2 Empirical observations**

From empirical observations three main conclusions about PABs could be made:

- I. Environmental conditions influence bloodstain appearance in a predictable manner
- II. Environmental conditions influence bloodstain behaviour in a predictable manner
- III. Quantitative observations of environmental influences on bloodstain appearance and behaviour can be extrapolated to the identification, interpretation and analysis of PABs

### **I. Environmental influences on stain appearance**

Results of experimental research demonstrated that environmental conditions exert a considerable influence on bloodstain appearance and specifically colour of stains.

#### **I.i Temperature and stain appearance**

Observations indicated that temperature exerted a strong influence on bloodstain colour, which was observable between even relatively minor variations (5°C intervals) of temperature. When exposed to a range of controlled temperature

variations between -10°C and 50°C, stains generated on glass, paper and denim surfaces all retained red orientations of colour. However, depending on the temperature stains were exposed to stains varied considerably according to intensity and strength of red colouring. Low temperatures were associated with light intensities of bright red colours whilst high temperatures within the experimental range were associated more with darker intensities of red and red-brown colours. Observations also indicated that stain appearance was most dramatically altered at temperatures above 25°C. The temperature range over which alterations in stain colour occurred was not considered extreme (-10°C to 50°C) and encountering scenes exposed (naturally) to temperatures outside of this range would be considered rare in forensic reality. Results provide the first empirically established observations of variations of bloodstain colour according to temperature.

#### I.ii Longitudinal exposure to climatic variations and stain appearance

Observations following exposure of stains to natural climatic variations for longitudinal periods indicated exposure caused a marked alteration in stain appearance. Stains exposed to environmental fluctuations for a minimum period of one month were characterised by grey and brown colourings, compared to the red, red-brown colour of 'fresh' stains. This observation was consistent with previous observations recorded of ageing blood naturally progressing through a series of colour changes from red to reddish brown and eventually dark brown and black (*James et al. 2005*). As length of exposure was increased, stain colour did not appear to undergo further alterations however, which indicates it not possible to determine length of exposure from stain colour, beyond determining whether stains were 'fresh' or not. These results provide the first example of empirical support for the possibility of determining an estimation of whether an exposed stain is fresh or aged from quantitative measurements of stain colour.

#### I.iii Extreme environmental conditions and stain appearance

Observations indicated exposing stains to extreme environmental conditions (snow, fire, freezing conditions, high temperatures) caused significant alterations to stain colour. This represents the first empirical confirmation of previously anecdotal

suggestions of the influence of extreme conditions on stain appearance (*Morris. 2010*). Comparison of stains exposed to different conditions indicated that it was possible to approximately identify types of environmental conditions stains have been exposed to, on the basis of quantitative measures of colour. Results constitute the first empirical evidence of the effects of extreme environmental influences on bloodstains through quantitative measures of colour.

## **II. Environmental influences on stain behaviour**

Results of experimental explorations of environmental influences on stain drying time indicated that the main influences on drying time are temperature, surface characteristics and volume of blood. Whilst the influence of these variables on drying time is generally accepted, quantitative confirmation of the relationships between the main variables of influence and drying time has not previously been established. Experimental results presented represent only the third attempt to quantify influences on drying time and of those three, is the most complex in terms of the range of variables it incorporated into experimental design. Results indicate that the main variables of influence on drying time are temperature, surface characteristics and stain volume. Observations indicate it may be possible to develop quantitative estimates of drying time for stains generated at a particular temperature and on a particular surface.

## **III. Extrapolation of observations to the identification, interpretation and analysis of PABs**

Observations regarding the effects of environmental variables and conditions on bloodstain appearance and behaviour can be extrapolated and considered with relevance to their implications for the identification, interpretation and analysis of PABs.

### III.i Identification of Physically Altered Bloodstains (PABs)

The identification of bloodstain evidence at a crime scene is based, primarily, on visual identifications of bloodstains. As such, the identification of stains is ordinarily limited to source level interpretations of evidence, providing investigators with an indication of “*where a [bloodletting] incident*” occurred (Boonkhong *et al.* 2010). Observations of the influence of environmental conditions on stain appearance have implications for these source level interpretations as alterations to appearance may obscure or mislead visual identification of stains. Case-specific anecdotes demonstrate that in forensic reality, significant alterations in colour can lead to misidentification of bloodstain evidence (Morris. 2010) or may prevent its identification altogether. By establishing a quantitative record of alterations observed in stain colour following exposure to a range of environmental variables and conditions, the research presented here can be used to better inform predictions and expectations of stain colour, given the environmental conditions at a particular crime scene. The consequences will be an improvement in the accuracy of identification of physically altered bloodstains.

In addition, empirical observations also demonstrate that the identification of physically altered bloodstains can contribute to activity level interpretations of evidence. Observations indicated it is possible to differentiate stains exposed to different environmental conditions on the basis of quantitative measures of colour. This has implications for assisting in the identification of ‘misfit’ stains. For example, imagine the hypothetical identification of a stain on a surface, which quantitative analysis of colour demonstrates has been exposed to a particular environmental condition, e.g. burning. If the environmental conditions at the location in which it was recovered do not appear to mirror the environmental conditions expected, the stain may be identified as ‘misfit’ to its environmental surroundings. Inferences can then be made that the surface has been moved since staining and provide evidence of the presence of the stain (and stained surface) at a different location and environment. The suggestion, based on evidence presented in thesis, of the possibility of making these kinds of activity level inferences on the basis of quantitative analysis of bloodstain colour is completely novel.

### III.ii Interpretation and analysis of Physically Altered Bloodstains (PABs)

The interpretation and analysis of bloodstain evidence contributes an explanation of the activities and circumstances surrounding the generation and presence of evidence at a scene. Observations establishing the predictable nature of environmental influences on stain behaviour can be incorporated into the interpretation and analysis of PABs to increase the accuracy of these activity level interpretations of evidence.

In particular, observations regarding the influence of temperature on drying time can contribute to activity level interpretations. Estimations of drying time are particularly useful in assisting analysts to construct a depositional timeframe for bloodstain evidence identified at a scene, which can contribute significantly to making more general temporal inferences about a crime event. Empirical observations demonstrated that one of the strongest influences on drying time was temperature. Drying times for stains generated on paper, glass and denim were recorded at 5°C temperature intervals between -10°C and 50°C. These provide, for the first time, a range of surface-specific quantitative indications of bloodstain drying times at specific temperatures. The major implication of these measurements is that by extrapolation to a hypothetical crime scene, with knowledge of type of surface and ambient temperature, analysts can make more informed and accurate estimations of drying time.

Observations also indicate that interpretations of stain appearance can provide evidence of exposure of stains to particular environmental conditions and rough estimates of length of exposure, such as indicating whether a stain is 'fresh' or may have been exposed to environmental conditions for some length of time. An example of where being able to quantitatively identify when stains have been exposed to a particular environmental condition may become particularly relevant is inferring the involvement of particular evasive actions taken by a suspect to remove and obliterate evidence, for example by setting fire to a scene or item of evidence. This work presents, for the first time, evidence for the potentially successful extrapolation of quantitative measures of colour to activity level interpretations and inferences about suspect activity.



### 14.3 Conclusion

Despite the likelihood of analysts encountering Physically Altered Bloodstains and their potential investigative value, empirical understandings of PABs are currently significantly under-developed. This has implications for limiting the accuracy with which they can be identified, interpreted and analysed as well as limiting their potential contribution to source and activity level interpretations of evidence. Empirical research outlined in this thesis represents the first concerted attempt to derive and relate quantitative measures of environmentally forced alterations to stain appearance and behaviour to specific environmental variables and conditions. Observations made establish that physically altered bloodstains respond in predictable ways to environmental influences and that these responses can be quantitatively measured. The implication of this finding means that there is huge scope for developing predictive and interpretative tools based on the analysis of alterations in stain appearance and behaviour. It demonstrates that not only is increasing an awareness of the nature of PABs important for improving overall accuracies in identification, interpretation and analysis of bloodstains but that PABs can advance the complexity of activity level interpretations made from stain analysis.

Recent criticisms levelled at the discipline of BPA (and forensic science more generally) have focused on the perceived lack of empirical support for inferences and claims made by investigators, following their analysis of evidence. In order to reduce the vulnerability of the discipline to such criticisms, it is essential to promote and establish an empirical body of supportive evidence. At present, understanding of PABs in particular is limited to case-specific and anecdotal observations and as such inclusion of inferences based on PABs in scene analysis would be justifiably vulnerable to such criticisms. Identification, in this thesis, of quantitative relationships between environmental influences and stain characteristics demonstrates however how these criticisms can be undermined and overturned by undertaking experimental work which unequivocally demonstrates the rationale behind inferences made from stain analysis.

A final underlining of the importance of developing interpretations of PABs is consideration of stain interpretation within the context of the 'forensic process'. Successful progression of physical evidence from collection at a crime scene to presentation in a courtroom is dependent upon the chronological processing of evidence through a series of investigative stages. These stages are represented by preservation & collection, validation & identification, analysis, interpretation and finally presentation of evidence. With implications for source and activity level interpretations of evidence, physical altered bloodstains impact on multiple steps in this process. Most crucially perhaps, physical alterations to bloodstains may obscure their identification, which prevents subsequent analysis, interpretation and presentation of evidence. The importance of improving interpretations of PABs therefore resonates throughout the 'forensic process'.

## References

- Aalders. M. Bremmer. R. Edelman. G. 2010. "Reflectance spectroscopy for identification and ageing of bloodstains". Presentation at 3<sup>rd</sup> European IABPA conference, Lisbon, 2010.
- Adair. T. W. Shimamoto. S. Tewes. R. Gabel. R. 2008. "The use of luminol to detect blood in soil one year after deposition". *IABPA News*. September 2006.
- Ames. C. Turner. B. 2003. "Low temperature episodes in development of blowflies: implications for post-mortem interval estimation". *Medical and Veterinary Entomology*. 17: 178-186
- Ammer. K. Ring. E. F. J. 2005. "Application of thermal imaging in forensic medicine". *The Imaging Science Journal*. 53: 125-131
- Anderson. S. Howard. B. Hobbs. G. R. Bishop. C. P. 2005. "A method for determining the age of a bloodstain". *Forensic Science International*. 148: 37-45
- Atkinson. C. Silenieks. T. Pearman. C. 2003. "Validation of ABACard Hematrace KITS". *Evidence Recovery and Biology Analytical Groups – Summer Vacation Project*. Available at:  
[http://www.4n6shop.cz/static\\_pages\\_files/file/Hematrace\\_Forensic%20Science\\_Silenieks.pdf](http://www.4n6shop.cz/static_pages_files/file/Hematrace_Forensic%20Science_Silenieks.pdf) (Accessed: 22<sup>nd</sup> October 2013).
- Balthazard. V. Piedelievre. R. DeSoille. H. DeRobert. L. 1939. "Etude des Gouttes de Sang Projecte" (A study of projected drops of blood). 22<sup>nd</sup> Congress of Forensic Medicine. Paris. France.
- Barni. F. Lewis. S. W. Berti. A. Miskelly. G. M. Lago. G. 2007. "Forensic application of the luminol reaction as a presumptive test for latent blood detection". *Talanta*. 72(3): 896-913

*Baryumureeba. V. Tushabe. F. 2004. "The Enhanced Digital Investigation Process Model". Proceedings of the 4<sup>th</sup> Annual Digital Forensic Research Workshop (DFRWS) 2004.*

*Benecke. M. 2001. "A brief history of forensic entomology". Forensic Science International. 120: 2-14*

*Bevel. T. Gardner. R. M. 2008. Bloodstain Pattern Analysis: With an introduction to Crime Scene Reconstruction. CRC Press. 3<sup>rd</sup> Edition.*

*Bevel. T. Gardner. R. M. May 2012a. "A Methodology For Bloodstain Pattern Analysis – practical application of the scientific method to BPA". Advanced Bloodstain Pattern Analysis Course Notes. Bevel, Gardner & Associates.*

*Bevel. T. Gardner. R. M. May 2012b. "Bloodstain Pattern Taxonomy and Terminology". Advanced Bloodstain Pattern Analysis Course Notes. Bevel, Gardner & Associates*

*Bevel. T. Gardner. R. M. October 2013. Bloodstain Pattern Taxonomy Hierarchy, version 2.3. Advanced Bloodstain Pattern Analysis Course Notes. Bevel, Gardner & Associates.*

*Bluestar® Forensic, Ltd. 2006. "Bluestar Forensic – Latent bloodstain reagent. User's Manual. Bluestar® Forensic Kit". Available at: [http://www.bluestar-forensic.com/pdf/en/instructions\\_bluestar\\_kit.pdf](http://www.bluestar-forensic.com/pdf/en/instructions_bluestar_kit.pdf) (Accessed: May 2012).*

*Bluestar Forensics. 2011. "Hexagon OBTI – Immunochromatographic test for confirming the presence of human blood traces. User Manual. Available at: " [http://www.bluestar-forensic.com/gb/documentation\\_hexagon.php](http://www.bluestar-forensic.com/gb/documentation_hexagon.php) (Accessed: 21st September 2011).*

- Boonkhong. K. Karnjanadecha. M. Aiyara. P. 2010. "Impact angle analysis of bloodstains using a simple image processing technique". *Songklanakarin J. Sci. Technol.* 32 (2). 169-173.
- Brady. T. Tigmo. J. Graham. G. 2002. "Extreme temperature effects on bloodstain pattern analysis". *LABPA News*. 2002.
- Brehmer. B. 1980. "In one word: not from experience". *Acta Psychologica*. 45: 223-241
- Bright. D. A. Goodman-Delahunty. J. 2006. "Gruesome evidence and emotion: anger, blame, and jury decision-making". *Law and Human Behavior*. 30(2): 183-202
- Brown. C. Peckmann. T. 2014. "Decomposition rates and taphonomic changes associated with the estimation of time since death in a summer climate: a case study from urban Nova Scotia". *Canadian Society of Forensic Science Journal*. 46(4): 209-230
- Budowle. B. Leggitt. J. L. Defenbaugh. D. A. Keys. K. M. Malkiewicz. S. F. 2000. "The presumptive reagent fluorescein for detection of dilute bloodstains and subsequent STR typing of recovered DNA". *Journal of Forensic Science*. 45(5): 1090-1092
- Bull. P. A. Morgan. R. M. Sagovsky. A. Hughes. G. J. A. 2006. "The transfer and persistence of trace particulates". *Science & Justice*. 46: 185-195.
- Burnett. B. R. Orantes. J. M. Pierson. M. 1997. "An unusual bloodstain case". *Journal of Forensic Science*. 42(3): 519-523
- Bussmann. M. Mostaghimi. J. Chandra. S. 1999. "On a three-dimensional volume tracking model of droplet impact". *Physics of Fluids*. 11(6): 1406-1418

Castello. A. Frances. F. Verdu. F. 2009. "Bleach interference in forensic luminol tests on porous surfaces: More about the drying time effect". *Talanta*. 77(4): 1555-1557

Chisum. W. J. 2006. "Crime Reconstruction" In: Mozayani. A. Noziglia. C. eds. *The Forensic Laboratory Handbook – Procedures and Practice*. Humana Press, pp. 63 - 77

Chisum. W. J. Turvey. B. E. 2000. "Evidence Dynamics: Locard's Exchange Principle & Crime Reconstruction." *Journal of Behavioral Profiling*. 1 (1): 1-10

Chisum. W. J. Turvey. B. E. 2007. *Crime Reconstruction*. Burlington, MA: Elsevier Academic Press.

Christman. D. V. 1996. "A study to compare and contrast animal blood to human blood product". *IABPA News*. 12(2): 10-25

Cotton. E. A. Allsop. R. F. Guest. J. L. Frazier. R. R. E. Koumi. P. Callow. I. P. Seager. A. Sparks. R. L. 2000. "Validation of the AMPFISTR® SGM Plus™ system for use in forensic casework". *Forensic Science International*. 112: 151-161

Cox. M. 1990. "A Study of the sensitivity and specificity of four presumptive tests for blood." *Journal of Forensic Science*. 36(5): 1503-11

Creamer. J. I. Quickenden. T. I. Apanah. M. V. Kerr. K. A. Robertson. P. 2003. "A comprehensive experimental study of industrial, domestic and environmental interferences with the forensic luminol test for blood". *Luminescence*. 18(4): 193-198

Creamer. J. I. Quickenden. T. I. Crichton. L. B. Robertson. P. Ruhayel. R. A. 2005. "Attempted cleaning of bloodstains and its effects on the forensic luminol test". *Luminescence*. 20: 411 – 413

Cwiklik, C. 1999. "An evaluation of the significance of transfers of debris: criteria for association and exclusion". *Journal of Forensic Sciences*. 44 (6): 1136-1150

Dabbs, G. R. Martin, D. C. 2013. "Geographic variation in the taphonomic effect of vulture scavenging: the case for southern Illinois". *Journal of Forensic Science*. 58(51): 20-25

Dini, V. Bizhga, B. Zalla, P. Sotiri, E. 2011. "The influence of season and age in the hematologic parameters of sheep." *Scientific Papers: Series D, Animal Science-The International Session of Scientific Communications of the Faculty of Animal Science* 54.

Directorate of Forensic Science. Ministry of Home Affairs. Govt. Of India. "Procedure Manual on Forensic Biology". "1.0 Examination of Blood & Bloodstains". [http://dfs.gov.in/manuals\\_close/biologymanualedit.htm](http://dfs.gov.in/manuals_close/biologymanualedit.htm) Accessed 19th September 2011.

Dixon, T. R. Samudra, A. V. Stewart, W. D. Johari, O. 1976. "A scanning electron microscope study of dried blood". *Journal of Forensic Sciences*. 21(4): 797-803

Douglas, K. S. Lyon, D. R. Ogloff, J. R. P. 1997. "The impact of graphic photographic evidence on mock jurors' decisions in a murder trial: Probative or Prejudicial?" *Law and Human Behavior*. 21(5): 485-501

Dunn, M. A. Salovey, P. Feigenson, N. 2006. "The jury persuaded (and not): computer animation in the courtroom". *Law & Policy*. 28(2): 228-248

Elena, N. Mohamed, N. 2009. "Investigation of blood dynamics; surface flow and droplet stain morphology on fabrics". Thesis submitted in partial fulfilment of the requirements for the Master of Forensic Science degree at the Centre for Forensic Science, University of Western Australia. 1-147

Evelt, I. W. 1987. "Bayesian inference and forensic science: problems and perspectives". *Journal of the Royal Statistical Society. Series D (The Statistician)*. 36(2): 99-105.

Fechner, G. G. P. Gee, D. J. 1989. "Study on the effects of heat on blood and on the post-mortem estimation of carboxyhaemoglobin and methaemoglobin". *Forensic Science International*. 40: 63-67

Feigenson, N. Dunn, M. A. 2003. "New visual technologies in court: directions for research" *Law and Human Behavior*. 27(1): 109-126

Findley, J. Hopkins, C. 1984. "Reconstruction: An Overview". *Identification News*: 3-15

Fratini, P. Floris, T. Piemi, M. Talamelli, L. Garofano, L. 2006. "BPA analysis as a useful tool to reconstruct crime dynamics – Part I". *International Congress Series* 1288: 535-537

Fre'geau, C. J. Germain, O. Fournery, R. M. 2000. "Fingerprint enhancement revisited and the effects of blood enhancement chemicals on subsequent Profiler Plus<sup>TM</sup> fluorescent short tandem repeat DNA analysis of fresh and aged bloody fingerprints". *Journal of Forensic Science*. 45(2): 354-380

French, J. C. Morgan, R. M. Baxendell, P. Bull, P. A. 2012. "Multiple transfers of particulates and their dissemination within contact networks". *Science & Justice*, 52 (1): 33-41

Frueh, S. Yeibio, L. 2009. "Badly fragmented forensic science system needs overhaul; evidence to support reliability of many techniques is lacking." *NAS Press Release*. Available at:

<http://www8.nationalacademies.org/onpinews/newsitem.aspx?RecordID=12589>

(Accessed: 15<sup>th</sup> October 2013)



Fujimoto, H. Shiraishi, H. Hatta, N. 2000. "Evolution of liquid/solid contact area of a drop impinging on a solid surface". *International Journal of Heat and Mass Transfer*. 43: 1673-1677

Gallerani, M. Reverberi, R. Salmi, R. Smolensky, M. Manfredini, R. 2013. "Seasonal variation of platelets in a cohort of Italian blood donors: a preliminary report". *European Journal of Medical Research* 18: 31

Galloway, A. Brikby, W. H. Jones, A. M. Henry, T. E. Parks, B. O. 1989. "Decay rates of human remains in an arid environment". *Journal of Forensic Science*. 34(3): 607-616

Gardner, P. H. Berry, D. C. 1995. "The effect of different forms of advice on the control of a simulated complex system". *Applied Cognitive Psychology*. 9: S55-S79

Gardner, R. M. Griffin, T. 2010. "The foundations for the discipline of bloodstain pattern analysis – a response to the report by the National Academy of Sciences". *Journal of Forensic Identification*. 60 (4): 477-490

Garner, D. D. Cano, K. M. Peimer, R. S. Yeshion, T. E. 1976. "An evaluation of Tetramethyl Benzidine as a presumptive test for blood". *Journal of Forensic Sciences*. 21(4): 816-821

Gatowski, S. I. Dobbin, S. A. Richardson, J. T. Ginsburg, G. P. 2001. "Asking the gatekeepers: A national survey of judges on judging expert evidence in a post-daubert world". *Law and Human Behavior*. 25(5): 433-458

Gibson, C. 2006. "Case turned on 158 spots of blood". *BBC News*. Available at: [www.bloodspatter.com/News.htm](http://www.bloodspatter.com/News.htm) (Accessed: 29th July 2011)

Glaister, J. 1926. "The Kastle-Meyer test for the detection of blood". *The British Medical Journal*. 650-652

Grodsky. M. Wright. K. Kirk. P. L. 1951. "Simplified preliminary blood testing – an improved technique and a comparative study of methods". *Journal of Criminal Law and Criminological Political Science*. 42: 95-104

Gross. A. M. Harris. K. A. Kaldun. G. L. 1999. "The effect of luminol on presumptive tests and DNA analysis using the polymerase chain reaction". *Journal of Forensic Science*. 44(4): 837-840

Gurfinkel. D. M. Franklin. U. M. 1987. "A study of the feasibility of detecting blood residue on artifacts". *Journal of Archaeological Science*. 15(1): 83-97

Harlan Laboratories. 2013. "Whole Blood Information and Research Data" Harlan Laboratories Website, available at:  
[http://www.harlan.com/products\\_and\\_services/research\\_models\\_and\\_services/custom\\_antibody\\_production/europes\\_biological\\_products\\_and\\_services/whole\\_blood.html](http://www.harlan.com/products_and_services/research_models_and_services/custom_antibody_production/europes_biological_products_and_services/whole_blood.html)  
(Accessed: 25th April 2014)

Harvey. N. Harries. C. 2004. "Effects of judges' forecasting on their later combination of forecasts for the same outcomes". *International Journal of Forecasting*. 20: 391-409

Hermon. D. Shpitzen. M. Oz. C. Glattstein. B. Azoury. M. Gafny. R. 2003. "The use of the Hexagon OBTI test for detection of human blood at crime scenes and on items of evidence. Part I: Validation studies and Implementation". *Journal of Forensic Identification*. 53 (5): 566-575

Hicks. T. Schutz. F. Curran. J. M. Triggs. G. M. 2005. "A model for estimating the number of glass fragments transferred when breaking a pane: experiments with firearms and hammer". *Science & Justice*. 45(2): 65-74

Hochmeister. M. N. Budowle. B. Sparkes. R. Rudin. O. Gehrig. C. Thali. M. Schmidt. L. Cordier. A. Dirnhofer. R. 1999. "Validation studies of an Immunochromatographic 1-step test for the forensic identification of human blood". *Journal of Forensic Science*. 44(3): 597-602

Hochmeister. M. Sparkes. R. Rudin. O. Gehrig. C. Schmidt. L. Cordier. A. Dirnhofner. R. 1998. "Evaluation of an Immunochromatographic 1-step Test for the Forensic Identification of Human Blood". Presented as the 50<sup>th</sup> Annual meeting of the American Academy of Forensic Sciences. San Francisco, CA.

Houck. M. 2001. "Mute witness: trace evidence analysis". London: Academic Press, 2001.

Hulse-Smith. L. Mehdizadeh. N. Z. Chandra. S. 2005. "Deducing drop size and impact velocity from circular bloodstains". *Journal of Forensic Science*. 50(1): 1-10

Hulse-Smith. L. Illes. M. 2005. "A blind trial evaluation of a crime scene methodology for deducing impact velocity and droplet size from circular bloodstains". *Journal of Forensic Science*. 52(1): 65-69

Hunt. A. C. Corby. C. Dodd. B. E. 1960. "The identification of human stains – a critical survey". *Journal Forensic Medicine*. 7: 112-130

Illes. M. B. Dalley. I. Kish. P. E. Taylor. M. C. 2010. "The use of blood and its substitutes for training". *IABPA News*.

Imwinkelried. E. J. 1983. "The standard for admitting scientific evidence: a critique from the perspective of juror psychology". *Villanova Law Review*. 28: 554-571

Ingham. J. 1932. "An improved and simplified benzidine test for blood in urine and other clinical material". *Biochemical Journal*. 26(4): 1124-1126

Jain. P. Singh. H. P. 1984. "Detection and origin of blood stains on various types of cloth immersed in water for a prolonged period". *Canadian Society of Forensic Science Journal*. 17 (2): 58-60

James. S. H. Eckert. W. G. 1999. *Interpretation of Bloodstain Evidence at Crime Scenes*. CRC Press. 2<sup>nd</sup> Ed.

James. S. H. Kish. P. E. Sutton. P. T. 2005. *Principles of Bloodstain pattern analysis: theory and practice*. CRC Press.

Jelinek. P. Illek. J. Helanova. I. Frajs. Z. 1984. "Biochemical and haematological values of the blood in rams during rearing" *Acta Vet Brno*, 3-4: 143-150

Johnston. E. Ames. C. E. Dagnall. K. E. Foster. J. Daniel. B. E. 2008. "Comparison of Presumptive Blood Test Kits including Hexagon OBTI". *Journal of Forensic Science*. 53(3): 687-689

Kang. B. S. Lee. D. H. 2000. "On the dynamic behaviour of a liquid droplet impacting upon an inclined heated surface". *Experiments in Fluids*. 29: 380-387

Karger. B. Nüsse. R. Schroeder. G. Wustenbecker. Brinkmann. B. 1996. "Backspatter from experimental close-range shots to the head. I. Macrobackspatter." *International Journal of Legal Medicine*. 109(2): 66-74

Karger. B. Nüsse. R. Troger. H. D. Brinkmann. B. 1997. "Backspatter from experimental close-range shots to the head. II. Microbackspatter and the morphology of bloodstains". *International Journal of Legal Medicine*. 110 (1): 27-30

Karger. B. Rand. S. P. Brinkmann. B. 1998. "Experimental bloodstains on fabric from contact and from droplets". *International Journal of Legal Medicine*. 111: 17-21

Karger. B. Nüsse. R. Bajanowski. T. 2002. "Backspatter on the firearm and hand in experimental close-range gunshots to the head." *American Journal of Forensic Medicine & Pathology*. 23(3): 211-213

Kasper. J. Mumm. R. Ruther. J. 2012. "The composition of carcass volatile profiles in relation to storage time and climate conditions". *Forensic Science International*. 223: 64-71

Kircher. T. 2013a. "David Camm Blog: Spatter or Transfer?" Available at: <http://www.wdrb.com/story/23544274/david-camm-blog-spatter-or-transfer> (Accessed: 8<sup>th</sup> October 2013).

Kircher. T. 2013b. "David Camm Blog: Tiny dots of blood..." Available at: <http://www.wdrb.com/story/23470475/david-camm-blog-tiny-dots-of-blood> (Accessed: 8th October 2013).

Kirk. P. 1974. *Crime Investigation*. Wiley & Sons. 2<sup>nd</sup> Ed.

Knock. C. Davison. M. 2007. "Predicting the position of the source of bloodstains for angled impacts". *Journal of Forensic Science*. 52(5): 1044-1049

Komar. D. A. 1998. "Decay rates in a cold climate region: a review of cases involving advanced decomposition from the medical examiner's office in Edmonton, Alberta". *Journal of Forensic Science*. 43(1): 57-61

Kozarovich. L. H. 2009. "State of Indiana vs. David Camm – a look at both sides". *News and Tribune*. Available at: <http://newsandtribune.com/clarkcounty/x519395825/State-of-Indiana-vs-David-Camm-a-look-at-both-sides> (Accessed: 8th October 2013)

Laber. T. L. Epstein. B. P. Taylor. M. C. 2008. "High speed digital video analysis of bloodstain pattern formation from common bloodletting mechanisms". Project report published in I.A.B.P.A. News June 2008: 4-8

Laerd Statistics. 2013. "Kruskal-Wallis H Test using SPSS" [Online] Available from: <https://statistics.laerd.com/spss-tutorials/kruskal-wallis-h-test-using-spss-statistics.php>. [Accessed: December. 2012]

Lagnado. D. Harvey. N. 2008. "The impact of discredited evidence". *Psychonomic Bulletin & Review*. 15(6): 1166-1173

Lane. A. G. Campbell. J. R. 1969. "Relationship of Hematocrit values to selected physiological conditions in dairy cattle" *Journal of Animal Science* (28): 508-511

Larkin. T. Gannicliffe. C. 2008. "Illuminating the health and safety of luminol". *Science & Justice*. 48(2): 71-75

Laurent. A. Durussel. J. J. Dufaux. J. 1999. "Effects of contrast media on blood rheology: comparison in humans, pigs and sheep". *Cardiovascular and interventional radiology*. 22(1): 62-66

Laville. S. 2006. "Case hinged on mist of blood found on clothes". *The Guardian*. February 10 2006. Available at: <http://www.theguardian.com/uk/2006/feb/10/ukcrime.sandralaville> (Accessed: 8th October 2013)

Leak. G. 2006. "An unusual altered bloodstain pattern". *IABPA News*. 2006.

Leak. G. 2010. "How confident are we that all bloodstains present on clothing relate to the scene?" Presentation at 3<sup>rd</sup> European IABPA Conference. Lisbon. 2010.

Lee. H. C. De Forest. P. R. 1976. "A precipitin-inhibition test on denatured bloodstains for the determination of human origin". *Journal of Forensic Science*. 21(4): 804-810

Lovelock. J. E. 1953. "The Haemolysis of human red blood-cells by freezing and thawing". *Biochim Biophys Acta*. 10(3): 414-426

Lowrie. C. N. Jackson. G. 1994. "Secondary transfer of fibres". *Forensic Science International*. 64: 73-82

Ma. M. Zheng. H. Lallie. H. 2010. "Virtual reality and 3D animation in forensic visualization". *Journal of Forensic Sciences*. In Press. doi: 10.1111/j.1556-4029.2010.01453.x

Macdonnell. H. 1982. "Bloodstain Pattern Interpretation". Corning, NY, USA.

Maes. M. Scharpe. S. Cooreman. W. Wauters. A. Neels. H. Verkerk. R. De Meyer. F. D'Hondt. P. Peeters. D. Cosyns. P. 1995. "Components of biological, including seasonal, variation in haematological measurements and plasma fibrinogen concentrations in normal humans" *Experientia*. 51 (2): 141 -149

Mann. R. W. Bass. W. M. Meadows. L. 1990. "Time since death and decomposition of the human body: variables and observations in case and experimental field studies". *Journal of Forensic Science*. 35(1): 103-111

McMurtrie. J. 2005. "The role of the social sciences in preventing wrongful convictions". *American Criminal Law Review*. 42: 1271-1288

Mehdizadeh N. Z. Chandra S. Mostaghimi. J. 2004. "Formation of fingers around the edges of a drop hitting a metal plate with high velocity". *Journal of Fluid Mechanics*. 510: 353–373

Miles. H. F. Morgan. R. M. Millington. J. E. 2014. "The influence of fabric surface characteristics on satellite bloodstain morphology". *Science & Justice*. *Science & Justice*. 54 (4): 262-266

Miller. L. B. 1969. "Hemochromogen crystal formation with minute amounts of blood". *Journal of Forensic Science Soc*. 9: 84-86

Millington. J. 2004. "Development of a synthetic blood substitute for use in forensic science teaching". *Final LTSN development project report published in LTSN Physical Sciences Newsletter*. 11: 3-22

Mnookin. J. L. Cole. S. A. Dror. I. E. Fisher. B. A. J. Houck. M. Inman. K. Kaye. D. H. Koehler. J. J. Langenburg. G. Risinger. D. M. Rudin. N. Siegel. J. Stoney. D. A. 2011. "The need for a research culture in the forensic sciences". *UCLA Law Review*. 58 (3): 725-79

Morgan. R. M. Cohen. J. McGookin. I. Murly-Gotto. J. O'Connor. R. Muress. S. Freudiger-Bonzon. J. Bull. P. A. 2009. "The relevance of the evolution of experimental studies for the interpretation and evaluation of some trace physical evidence". *Science & Justice*. 49: 277-285

Morris. J. 2010. "Unusual bloodstains in an extremely cold outdoor environment". *IABPA News*.

Moss. A. 1989. "Impact droplets and the protection of soils by plant covers". *Australian Journal of Soil Research*. 27 (1): 1 - 16

Myburgh. J. L'Abbe. E. N. Steyn. M. Becker. P. J. 2013. "Estimating the post-mortem interval (PMI) using accumulated degree-days (ADD) in a temperate region of South Africa". *Forensic Science International*. 229: 165-170

Nakao. K. I. Shimada. R. Hara. K. Kibayashi. K. 2013. "Experimental study on age estimation of bloodstains based on biological and toxicological analysis". *The Open Forensic Science Journal*. 6: 6-11

National Academies Press. 2009. *NAS, Strengthening Forensic Science in the United States: A Path Forward*, ed. C.o.A.a.T.S.N.R.C. Committee on Identifying the Needs of the Forensic Science Community. 2009, Washington, DC: The National Academy of Sciences.

Oliveira-Costa. J. Antunes de Mello-Patiu. C. 2004. "Application of forensic entomology to estimate the post-mortem interval (PMI) in homicide investigations by the Rio de Janeiro Police Department in Brazil". *Aggrawal's Internet Journal of Forensic Medicine and Toxicology*. 5(1): 40-44

Olson. R. D. 1985. "Sensitivity comparison of blood enhancement techniques". *Identification News*. Aug: 10-4

Paonessa. N. A. 2005. "Blood, fire and water: The murder of Isabella Cox". *Case Report*. *IABPA News*.



Parks. C. L. 2011. "A study of the human decomposition sequence in Central Texas". *Journal of Forensic Sciences*. 56(1): 19-22

Pennington. N. Hastie. R. 1992. "Explaining the evidence: tests of the story model for juror decision making". *Journal of Personality and Social Psychology*. 62(2): 189-206

Peschel. O. Kunz. S. N. Rothschild. M. A. Mutzel. E. 2011. "Blood Stain Pattern Analysis". *Forensic Science, Medicine and Pathology*. 7(3): 257-270

Piotrowski, E. 1895. "Uher Entstehung, Form, Richtung und Ausbreitung der Blutspat-en Nach Heibwunden der Kopfes" (Concerning the origin, shape, direction and distribution of the bloodstains following head wound caused by blows). K.K. Universitat, Wien.

Pizzamiglio. M. Fratini. P. Floris. T. Cappiello. A. Matassa. N. Festuccia. N. Garofano. L. 2006. "BPA analysis as a useful tool to reconstruct crime dynamics – Part II". *International Congress Series* 1288: 538-540

Pizzola. P. A. Roth. S. De Forest. P. R. 1986. "Blood Droplet Dynamics – I". *Journal of Forensic Sciences*. 31(3): 36-49

Ponce. A. C. Pascual. F. A. V. 1999. "Critical revision of presumptive tests for bloodstains". *Forensic Science Committee*. 1(2). Available at: <http://www.fbi.gov/hq/lab/fac/backissu/july1999/ponce.htm>

Pounds. C. A. Smalldon. K. W. 1975. "The transfer of fibres between clothing materials during simulated contacts and their persistence during wear. Part I – Fibre transference". *Journal of the Forensic Science Society*. 15: 17-27

Pounds. C. A. Smalldon. K. W. 1975. "The transfer of fibres between clothing materials during simulated contacts and their persistence during wear. Part II". *Journal of the Forensic Science Society*. 15: 29-37

Pounds. C. A. Smalldon. K. W. 1975. "The transfer of fibres between clothing materials during simulated contacts and their persistence during wear. Part III – a preliminary investigation of the mechanisms involved". *Journal of the Forensic Science Society*. 15: 197-207

Proescher. F. Moody. A.M. 1939. "Detection of blood by means of chemiluminescence". *Journal of Laboratory and Clinical Medicine*. 24: 1183-1189

Pye. K. Croft. D. J. 2004. "Forensic Geoscience: Principles, Techniques and Applications." Geological Society. London. *Special Publications*. 232: 1-5

Quickenden. T. I. Ennis. C. P. Creamer. J. I. 2004. "The forensic use of luminol chemiluminescence to detect traces of blood inside motor vehicles". *Luminescence*. 19: 271-277

Ramsthaler. F. Schmidt. P. Bux. R. Potente. S. Kaiser. C. Kettner. M. 2012. "Drying properties of bloodstains on common indoor surfaces". *International Journal of Legal Medicine*. 126: 739-746

Raymond. M. A. Smith. E. R. Liesegang. J. 1995. "The physical properties of blood – forensic considerations". *Science & Justice*. 36(3): 153-160

Raymond. M. A. Smith. E. R. Liesegang. J. 1996. "Oscillating blood droplets – implications for crime scene reconstruction". *Science & Justice*. 36(3): 161-171

Reynolds. M. 2004. "The ABACard® HemaTrace® - A Confirmatory Identification of Human Blood". *IABPA News*. June 2004. 4-11

Risinger. M. D. 2010. "Whose fault? – Daubert, The NAS report and the notion of error in forensic science". *Fordham Urban Law Journal*. 38 (2): 519 - 545

Ristenblatt. R. R. Shaler. R. C. 1995. "A bloodstain pattern interpretation in a homicide case involving an apparent 'stomping'". *Journal of Forensic Science*. 40(1): 139-145

Robertson. J. Grieve. M. C. 1999. *“The Forensic Examination of Fibres”*. London” Taylor and Francis.

Rowley. B. O. 1999. *Commentary on Hochmeister. M. N. Budowle. B. Sparkes. R. Rudin. O. Gehrig. C. Thali. M. Schmidt. L. Cordier. A. Dirnhofer. R.* 1999. *“Validation Studies of an Immunochromatographic 1-step Test for the Forensic Identification of Human Blood”*. *Journal of Forensic Science*. 44 (3): 597-601. In *Journal of Forensic Science* 44(6): 1323.

Saferstein. R. 1998. *“Criminalistics: An Introduction to Forensic Science”*. Prentice Hall. 6<sup>th</sup> Ed.

Saks. M. J. 1990. *“Expert witnesses, non-expert witnesses and non-witness experts”*. *Law and Human Behavior*. 14(4): 291-313

SceneSafe®, FSS Ltd. 2008. *“Guidelines for Use of the Kastle Meyer Kit – K160”* & *“Material Safety Data Sheet – Kastle Meyer Reagent (K160)”* & *“Material Safety Data Sheet – Hydrogen Peroxide (6%)”*

Shaffer. L. Roussel. J. D. Koonce. K. L. 1981. *“Effects of age, temperature-season and breed on blood characteristics of dairy cattle”*. *Journal of Dairy Science*. 64 (1): 62-70

Simmons. T. Cross. P. A. 2013. *“Forensic Taphonomy”* in *Encyclopedia of Forensic Sciences*, Academic Press. December 2013. Pg: 12

SWGSTAIN (Scientific Working Group on Bloodstain Pattern Analysis), 2009 *“Recommended Terminology”* *Forensic Science Communications*, 11(2).

SWGSTAIN (Scientific Working Group on Bloodstain Pattern Analysis): *Response to 2009 NAS Report (“Strengthening Forensic Science in the United States: A Path Forward”)*. Available at:

[http://www.theiai.org/current\\_affairs/SWGSTAIN\\_response.pdf](http://www.theiai.org/current_affairs/SWGSTAIN_response.pdf) (Accessed: August

2011)

Schofield. D. 2009. "Graphical evidence: forensic animations and virtual reconstructions". *Australian Journal of Forensic Sciences*. 41(2): 131-145

Shanteau. J. Weiss. D. J. Thomas. R. P. Pounds. J. 2003. "How can you tell if someone is an expert? Empirical assessment of expertise". *Emerging Perspectives on Decision Research*. Cambridge, UK. Cambridge University Press.

Sigma-Aldrich, Inc. 2011. "Alsever's solution, Product Number A3551 – Product Information".

Siemens Healthcare Diagnostics Inc. 2008. "HEMASTIX® Reagent Strips – Product Information".

Slemko. J. 2003. "Bloodstains on Fabrics". *IABPA News* 19 (4): 3-11

Spector. J. Von Gemmingen. D. 1971. "The effect of washing on the detection of blood and seminal stains". *Canadian Society of Forensic Science Journal*. 4: 3-9

Stedman's Medical Dictionary. 2005. 28<sup>th</sup> Edition. Lippincott Williams & Wilkins.

Stow. C. O. Hadfield. M. G. 1981. "An experimental investigation of fluid flow resulting from the impact of a water drop with an unyielding dry surface" *Proceedings of the Royal Society of London. Series A, Mathematical and Physical Sciences*. 373(1755): 419-441

Swander. C. J. Stites. J. G. 1998. "Evaluation of the ABACard HemaTrace for the forensic identification of human blood". *Midwestern Association of Forensic Scientists*. 1-5. Available at:

[http://www.4n6shop.cz/static\\_pages\\_files/file/Hematrace\\_Michigan%20State%20Police\\_Connie%20Swander\\_Jennifer%20Stites.pdf](http://www.4n6shop.cz/static_pages_files/file/Hematrace_Michigan%20State%20Police_Connie%20Swander_Jennifer%20Stites.pdf) (Accessed: 21<sup>st</sup> September 2011).

SWGANTH (Scientific Working Group for Forensic Anthropology). 2013. "Taphonomic observations in the post-mortem interval". Available at: <http://swganth.startlogic.com/Taphonomic%20Observations%20Rev0.pdf> (Accessed 29<sup>th</sup> April 2014)

SWGSTAIN Research Subcommittee. 2011. "Current Research Needs for Bloodstain Pattern Analysis". Available at: [www.swgstain.org/documents](http://www.swgstain.org/documents) (Accessed 2nd August 2011)

Taupin. J. M. 1996. "Hair and fiber transfer in an abduction case – evidence from different levels of trace evidence transfer". *Journal of Forensic Sciences*. 41 (4): 697-9

Thanakiatkrai. P. Yaodom. A. Kitpipit. T. 2013. "Age estimation of bloodstains using smartphones and digital image analysis". *Forensic Science International*. 233: 288-297

Thorne. D. 2006. "Constable helps clear British man accused of foster daughter's murder". *The Edmonton Journal*. February 12 2006. Available at: [www.bloodspatter.com/News.htm](http://www.bloodspatter.com/News.htm) (Accessed: 29th July 2011)

Thoroddsen. S. T. Sakakibara. J. 1998. "Evolution of the fingering pattern of an impacting drop". *Physics of Fluids*. 10(6): 1359-1374

Tobe. S. S. Nic Daeid. N. 2009. "Comparison of presumptive blood test kits including Hexagon OBTI". *Journal of Forensic Sciences*. 54(1): 239

Tobe. S. S. Watson. N. Nic Daeid. N. 2007. "Evaluation of six presumptive tests for blood, their specificity, sensitivity, and effect on high molecular-weight DNA". *Journal of Forensic Science*. 52(1): 102-109.

Tontarski. K. L. Hoskins. K. A. Watkins. T. G. Brun-Conti. L. Michaud. A. L. 2009. "Chemical enhancement techniques of bloodstain patterns and DNA recovery after fire exposure". *Journal of Forensic Science*. 54(1): 37-48

*Turchetto. M. Vanin. S. 2004. "Forensic entomology and climatic change". Forensic Science International. 146: 207-209*

*Turner. B. Wiltshire. P. 1999. "Experimental validation of forensic evidence: a study of the decomposition of buried pigs in a heavy clay soil". Forensic Science International. 101 (2): 113 - 122*

*Turvey. B. E. 1999. Criminal Profiling: An Introduction to Behavioural Evidence Analysis. London, UK. Academic Press.*

*Veldhoen. D. 2006. "Disposable mannequins – an alternative for clothing examination". IABPA News.*

*Waldoch. T. L. 1996. "Chemical detection of blood after dilution by rain over a 72 day period". Journal of Forensic Identification. 46(2): 173-177*

*Webb. J. L. Creamer. J. I. Quickenden. T. I. 2006. "A comparison of the presumptive luminol test for blood with four non-chemiluminescent forensic techniques". Luminescence. 21: 214-220.*

*White. B. 1986. "Bloodstains on Fabrics: the effect of drop volume, dropping height and impact angle". Canadian Society of Forensic Sciences Journal. 19 (1): 3-36*

*Woffinden. B. Jenkins. S. 2008. The Murder of Billie-Jo. Metro Books Ltd. John Blake Publishing, London. UK.*

*Wolff. M. Uribe. A. Ortiz. A. Duque. P. 2001. "A preliminary study of forensic entomology in Medellin, Colombia". Forensic Science International. 120: 53-59*

*Wolson. T. March. 2011. Pers. Comm.*

*Wonder. A. 2001. Blood Dynamics. Academic Press. London, UK.*

*Wonder, A. 2003. "Fact of fiction in bloodstain pattern evidence". Science & Justice. 43 (3): 166-168*

*Yen, K. Thali, M. J. Kneubuehl, B. P. Peschel, O. Zollinger, U. Dirnhofer, R. 2003. "Blood-spatter patterns: hands hold clues for the forensic reconstruction of the sequence of events". American Journal of Forensic Medicine and Pathology. 24 (2): 132 - 140*

## **Appendices**

Appendices are included in a CD inside the back cover of the thesis.

### **Appendix I:**

Method and application of the Hexagon OBTI confirmatory test for blood

### **Appendix II:**

G and B-value distribution data for stains generated in experimental stage 2

### **Appendix III:**

Dataset of results for Experimental stage 3

### **Appendix III:**

Dataset of results for Experimental stage 4